agriculture

Special Issue Reprint

Agricultural Crops Subjected to Drought and Salinity Stress

Edited by
Francisco Vanies Da Silva Sá, Alberto Soares De Melo and Miguel Ferreira Neto

mdpi.com/journal/agriculture

MDPI

Agricultural Crops Subjected to Drought and Salinity Stress

Agricultural Crops Subjected to Drought and Salinity Stress

Guest Editors

Francisco Vanies Da Silva Sá
Alberto Soares De Melo
Miguel Ferreira Neto

MDPI

Basel • Beijing • Wuhan • Barcelona • Belgrade • Novi Sad • Cluj • Manchester

Guest Editors

Francisco Vanies Da Silva Sá
Department of Agrarian and Exact Sciences
State University of Paraíba-UEPB
Catolé do Rocha
Brazil

Alberto Soares De Melo
Departamento de Biologia
Universidade Estadual da Paraíba
Campina Grande
Brazil

Miguel Ferreira Neto
Ciências Ambientais e Tecnológicas
Universidade Federal Rural Do Semi-Árido
Mossoró
Brazil

Editorial Office

MDPI AG
Grosspeteranlage 5
4052 Basel, Switzerland

This is a reprint of the Special Issue, published open access by the journal *Agriculture* (ISSN 2077-0472), freely accessible at: https://www.mdpi.com/journal/agriculture/special_issues/483RNMMLBN.

For citation purposes, cite each article independently as indicated on the article page online and as indicated below:

Lastname, A.A.; Lastname, B.B. Article Title. *Journal Name* **Year**, *Volume Number*, Page Range.

ISBN 978-3-7258-4565-1 (Hbk)
ISBN 978-3-7258-4566-8 (PDF)
https://doi.org/10.3390/books978-3-7258-4566-8

Contents

About the Editors . . . . . **vii**

Preface . . . . . **ix**

Maria Valdiglezia de Mesquita Arruda, Nildo da Silva Dias, Cynthia Cavalcanti de Albuquerque, Eduardo Cezar Medeiros Saldanha, Pedro Henrique de Araújo Gurgel, Marcondes Ferreira Costa Filho, et al.
Effects of the Arbuscular Mycorrhizal Fungus *Gigaspora albida* (Gigasporaceae) on the Physiology, Growth, and Na/K Balance of Creole Corn (Poaceae) Under Different Salinity Levels
Reprinted from: *Agriculture* **2025**, *15*, 660, https://doi.org/10.3390/agriculture15060660 . . . . . **1**

Tao Liu, Shuangshuang Li, Haoqiang Du, Jingnan Cui, Shanbin Xu, Jingguo Wang, et al.
The Identification of Drought Tolerance Candidate Genes in *Oryza sativa* L. ssp. *Japonica* Seedlings through Genome-Wide Association Study and Linkage Mapping
Reprinted from: *Agriculture* **2024**, *14*, 603, https://doi.org/10.3390/agriculture14040603 . . . . . **28**

José Orlando Nunes da Silva, Luiz Guilherme Medeiros Pessoa, Emanuelle Maria da Silva, Leonardo Raimundo da Silva, Maria Betânia Galvão dos Santos Freire, Eduardo Soares de Souza, et al.
Effects of Silicon Alone and Combined with Organic Matter and *Trichoderma harzianum* on Sorghum Yield, Ions Accumulation and Soil Properties under Saline Irrigation
Reprinted from: *Agriculture* **2023**, *13*, 2146, https://doi.org/10.3390/agriculture13112146 . . . . **43**

Muhammad Bilawal Junaid, Salah El-Hendawy, Ibrahim Al-Ashkar, Nasser Al-Suhaibani and Majed Alotaibi
Integrating Agro- Morpho-Physiological Traits and SSR Markers for Detecting the Salt Tolerance of Advanced Spring Wheat Lines under Field Conditions
Reprinted from: *Agriculture* **2023**, *13*, 2135, https://doi.org/10.3390/agriculture13112135 . . . . **66**

Patrícia Ferreira da Silva, Bárbara Davis Brito dos Santos, José Dantas Neto, Alberto Soares de Melo, Rigoberto Moreira de Matos, Semako Ibrahim Bonou, et al.
Effect of Electrical Conductivity Levels and Hydrogen Peroxide Priming on Nutrient Solution Uptake by Chives in a Hydroponic System
Reprinted from: *Agriculture* **2023**, *13*, 1346, https://doi.org/10.3390/agriculture13071346 . . . . **94**

Josinaldo Lopes Araujo, Jackson de Mesquita Alves, Railene Hérica Carlos Rocha, José Zilton Lopes Santos, Rodolfo dos Santos Barbosa, Francisco Marcelo Nascimento da Costa, et al.
Beneficial Microorganisms Affect Soil Microbiological Activity and Corn Yield under Deficit Irrigation
Reprinted from: *Agriculture* **2023**, *13*, 1169, https://doi.org/10.3390/agriculture13061169 . . . . **108**

Kleane Targino Oliveira Pereira, Salvador Barros Torres, Emanoela Pereira de Paiva, Tatianne Raianne Costa Alves, Maria Lilia de Souza Neta, Jefferson Bittencourt Venâncio, et al.
Discontinuous Hydration Cycles with Elicitors Improve Germination, Growth, Osmoprotectant, and Salt Stress Tolerance in *Zea mays* L.
Reprinted from: *Agriculture* **2023**, *13*, 964, https://doi.org/10.3390/agriculture13050964 . . . . . **127**

Gabriela Carvalho Maia de Queiroz, José Francismar de Medeiros, Rodrigo Rafael da Silva, Francimar Maik da Silva Morais, Leonardo Vieira de Sousa, Maria Vanessa Pires de Souza, et al.
Growth, Solute Accumulation, and Ion Distribution in Sweet Sorghum under Salt and Drought Stresses in a Brazilian Potiguar Semiarid Area
Reprinted from: *Agriculture* **2023**, *13*, 803, https://doi.org/10.3390/agriculture13040803 . . . . . **141**

Elias Ariel Moura, Vander Mendonça, Vladimir Batista Figueirêdo, Luana Mendes Oliveira, Marlenildo Ferreira Melo, Toni Halan Silva Irineu, et al.
Irrigation Depth and Potassium Doses Affect Fruit Yield and Quality of Figs (*Ficus carica* L.)
Reprinted from: *Agriculture* **2023**, *13*, 640, https://doi.org/10.3390/agriculture13030640 . . . . . **163**

Luca Nerva, Walter Chitarra, Gianni Fila, Lorenzo Lovat and Federica Gaiotti
Variability in Stomatal Adaptation to Drought among Grapevine Cultivars: Genotype-Dependent Responses
Reprinted from: *Agriculture* **2023**, *13*, 2186, https://doi.org/10.3390/agriculture13122186 . . . . **179**

About the Editors

Francisco Vanies da Silva Sá

Professor Dr. Francisco Vanies da Silva Sá holds PhDs in Agricultural Engineering and Agronomy; a Master's degree in Soil and Water Management; and a Bachelor's degree in Agronomy. He has a Post-Doc in Agricultural Engineering and in Soil and Water Management. He is a Professor at the State University of Paraíba, a Professor of the Postgraduate Program in Agrarian Science, and a Collaborating Professor of the Postgraduate Program in Soil and Water Management of the Federal Rural University of the Semi-Arid Region. He has experience in Agricultural Engineering and Agronomy.

Alberto Soares De Melo

Professor Dr. Alberto Soares De Melo is an Agronomist with a master's degree in Agricultural Sciences, a PhD in Natural Resources, and a Post-Doctorate in Agricultural Engineering. He is an Associate Professor at the State University of Paraíba and Coordinator of the Postgraduate Program in Agricultural Sciences at the Master's and Doctorate levels. He has experience in Agricultural Engineering/Agronomic Engineering.

Miguel Ferreira Neto

Professor Dr. Miguel Ferreira Neto is an agronomist with a master's degree in Agricultural Engineering, a Doctorate in Irrigation and Drainage, and a Post-Doctorate in Agricultural Engineering. He is a Full Professor at the Federal Rural University of the Semi-Arid Region and a professor of the Postgraduate Program in Soil and Water Management at the Master's and Doctoral levels. He has experience in Agricultural Engineering and Agronomy

Preface

Agriculture has historically been vital to the prosperity of civilizations and has withstood environmental pressure and population growth thanks to genetic improvement and plant management. Most crops are subject to environmental stresses such as drought and salinity, and in many cases, these stresses act together, limiting crop productivity. From this perspective, innovative management strategies can improve the productivity of crops subjected to such unfavorable environmental conditions.

This Special Issue focused on developing and evaluating management strategies for crops subjected to drought and salt stress, featuring interdisciplinary studies from research fields related to agriculture, including horticulture, genetics, plant ecophysiology, irrigation, soils, and plant nutrition. It featured 10 research papers that shed light on Agricultural Crops Subjected to Drought and Salinity Stress. The papers published in this Special Issue discuss the importance of using microorganisms for cultivation in irrigated areas with water deficits or brackish water, with some discussing the importance of advancing genetic improvement and enhancing tolerance to drought and salinity. In addition, this Special Issue presents information from the literature on managing stress attenuators in agriculture, from using fertilizers such as silicon and potassium to using phytohormones and growth regulators such as salicylic acid.

In summary, this Special Issue reflects the efforts of multiple researchers in the field of agricultural sciences to investigate Agricultural Crops Subjected to Drought and Salinity Stress, therefore encouraging the incorporation of scientific and technological knowledge in this field.

Francisco Vanies Da Silva Sá, Alberto Soares De Melo, and Miguel Ferreira Neto
Guest Editors

agriculture

MDPI

Article

Effects of the Arbuscular Mycorrhizal Fungus *Gigaspora albida* (Gigasporaceae) on the Physiology, Growth, and Na/K Balance of Creole Corn (Poaceae) Under Different Salinity Levels

Maria Valdiglezia de Mesquita Arruda [1], Nildo da Silva Dias [1,*], Cynthia Cavalcanti de Albuquerque [2], Eduardo Cezar Medeiros Saldanha [1], Pedro Henrique de Araújo Gurgel [1], Marcondes Ferreira Costa Filho [1], Matheus Henrique de Alencar Souza [2], Natanael da Silva Rodrigues [2], Marcelo Augusto Costa Lima [1], Maria Elisa da Costa Souza [1], Leonardo Ângelo Mendonça [1], Kleane Targino Oliveira Pereira [2], Rômulo Carantino Lucena Moreira [1], Micharlyson Carlos de Morais [1] and José Francismar de Medeiros [1]

[1] Soil and Water Salinity Laboratory, Federal Rural University of the Semi-Arid—UFERSA, Mossoró 59625-900, Brazil; valdigleziaarruda@yahoo.com.br (M.V.d.M.A.); eduardo.saldanha@riotinto.com (E.C.M.S.); pedro.gurgel@alunos.ufersa.edu.br (P.H.d.A.G.); marcondes.filho@alunos.ufersa.edu.br (M.F.C.F.); marcelo.lima@alunos.ufersa.edu.br (M.A.C.L.); maria.souza25244@alunos.ufersa.edu.br (M.E.d.C.S.); leonardo.mendonca@alunos.ufersa.edu.br (L.Â.M.); romulocarantino@gmail.com (R.C.L.M.); micharlyson.morais@alunos.ufersa.edu.br (M.C.d.M.); jfmedeir@ufersa.edu.br (J.F.d.M.)

[2] Plant Physiology and Biochemistry Laboatory, State University of Rio Grande do Norte—(UERN), Mossoró 59610-210, Brazil; cynthiacavalcanti@uern.br (C.C.d.A.); matheus-henrique14@live.com (M.H.d.A.S.); natanaelsr99@gmail.com (N.d.S.R.); kleane_rn@hotmail.com (K.T.O.P.)

* Correspondence: nildo@ufersa.edu.br

Abstract: Arbuscular mycorrhizal fungi (AMFs) can alleviate salt stress in plants by promoting growth. The mitigating effect of the AMF Gigaspora albida on the physiology, growth, and Na^+/K^+ balance in heirloom maize under different dilutions of saline wastewater was evaluated. The study was conducted in a greenhouse under a completely randomized design (CRD) in a 3 × 4 factorial scheme, with six replicates. The treatments consisted of three mycorrhizal conditions (M1—control plants without the AMF; M2—plants inoculated with G. albida; and M3—plants inoculated with G. albida plus the soil microbiota) and four levels of electrical conductivity (ECw): 0.5, 1.8, 3.1, and 4.4 dS m^{-1}. The results indicate that saline wastewater affects the physiology of heirloom maize. The symbiosis in M2 and M3 mitigated the stress in PSII by dissipating heat. The M3 treatment alleviated ionic stress in maize, reduced the Na^+/K^+ ratio in the aerial part, and increased the MSPA, MSRA, AP, and DC at EC_a levels of 1.8 and 3.1 dS m^{-1}. The M1 plants adapted by investing in root growth to tolerate the high salinity. In M2, the plant–AMF interaction did not mitigate the effects of high salinity, showing the worst growth performance. The saline wastewater reduced the percentage of *G. albida* colonization. An EC_a of 2.9 dS m^{-1} favored a high spore density.

Keywords: abiotic stress; attenuators; spore density; saline waste; mycorrhiza

1. Introduction

Water scarcity is a paramount global concern, which is particularly pronounced in regions like Brazil, where irrigation often becomes the sole recourse to ensure agricultural productivity, especially in hot, arid climates such as the semi-arid Northeast region [1]. The arid and semi-arid areas' scarcity underscores the imperative for sustainable water

management technologies, particularly in agriculture. Among these, water reuse emerges as a prevalent practice, notably through irrigation with saline water sourced from agricultural drainage wells and brackish water treatment plant effluents. When effectively implemented, this practice fulfills crop water requirements while reducing the demand for freshwater resources [2]. However, without proper management techniques, it poses a significant challenge for agriculture. High salt concentrations in reused water can severely limit agricultural outputs, reducing crop yields to economically unviable levels [3,4].

Restrictions on plant development stem from the osmotic and ionic stress induced by excessive salt levels, hindering water absorption, nutrient assimilation, and transport [5,6]. Osmotic stress, characterized by Na^+ and Cl^- accumulation in tissues, triggers nutritional stress and tissue cytotoxicity [7,8], disrupting metabolic, physiological, and biochemical pathways [9] and leading to a redox imbalance and biomolecule damage via lipid peroxidation [10].

Crop responses to salinity, in terms of sensitivity and tolerance, exhibit variability [11, 12]. Adaptation mechanisms include alterations in photosynthetic pathways, the synthesis of compatible osmolytes, the activation of enzymatic and non-enzymatic antioxidant systems, and selective ion absorption, enhancing plant survival in saline environments [13, 14].

Selective ion absorption is a crucial strategy in salinity tolerance, allowing plants to preferentially absorb essential nutrients even in the presence of higher concentrations of non-essential ions [15]. Simultaneously, it diminishes sodium uptake and accumulation in tissues [16], thus maintaining a favorable K^+/Na^+ ratio that is essential for sustained plant growth [17].

Among the strategies to utilize saline waste for irrigation, employing arbuscular mycorrhizal fungi (AMFs) has emerged as an effective approach to mitigate saline stress in plants [18–20]. Symbiosis with AMFs promotes the expression of osmoregulatory substances such as proline, glycine betaine, and polyamines, aiding in the regulation and maintenance of cellular water potential. This leads to improved water use efficiency, the maintenance of cell turgor, gas exchange, and subsequently, enhanced photosynthetic rates [21,22]. Nutritionally, this symbiosis promotes nutrient absorption and, under saline conditions, can reduce the uptake of toxic ions such as Na^+ and Cl^-, which compromise the ionic balance in photosynthetic tissues [23–25].

In this context, *Gigaspora albida*, an AMF belonging to the Gigasporaceae family [26], has been reported in the literature to enhance the growth of various crops. In a more recent study, *G. albida* improved the quality of *Dipteryx alata* seedlings by promoting increases in height, diameter, and dry biomass accumulation [27]. Under high salinity conditions (10, 15, and 20 dS m^{-1}), *G. albida* increased the tolerance of eucalyptus seedlings by maintaining the relative water content (RWC), enhancing nutrient uptake, particularly nitrogen, phosphorus, and potassium, and improving the K/Na ratio by reducing sodium accumulation [28]. For maize, although several studies in the literature highlighted the benefits of symbiotic relationships with AMFs, there is still a gap regarding the interaction of *Gigaspora albida*, associated with the original soil microbiota, with Creole maize varieties under saline stress.

The benefits of AMFs result from strengthening the plant's resistance to salinity, increasing the absorption area for nutrients and water, promoting the selective uptake of elements, enhancing the efficiency of the photosynthetic apparatus, and reinforcing antioxidant defense mechanisms [29,30]. However, the interaction between non-native AMFs and soil microbiota remains poorly understood. According to [31], native soil microorganisms have a greater potential to increase plant yield. This potential can be attributed to the bene-

ficial growth-promoting properties of these microorganisms, the harmonious symbiosis within the community, and their strong colonization ability compared to non-native ones.

AMFs and soil microbiota interact in complex ways that can enhance plant growth. Ref. [32] found that the interaction between AMFs and *Bacillus* spp. promotes greater phosphate solubilization and the absorption of phosphorus, zinc, and copper. Additionally, this interaction leads to an increased production of phytohormones that protect against biotic and abiotic stresses compared to isolated strains.

There is evidence that plant growth-promoting rhizobacteria stimulate the growth of AMFs. Among them, those in the genus *Pseudomonas* are more frequently found in the rhizosphere, while *Arthrobacter* and *Bacillus* are more common in the AMF hyphosphere. Some species of *Rhizobium* and *Pseudomonas* attach to fungal spores and hyphae; however, the colonization capacity varies considerably among different bacteria. Although AMFs can contribute to an increase in the nutritional status of the mycorrhizosphere by decomposing organic nitrogen (N_2) compounds, in the presence of nitrogen-fixing bacteria, there is a considerable increase in N_2 fixation, which is one of the main benefits of this interaction [33].

Under high salinity conditions, inoculation with endophytic *Bacillus subtilis*, both alone and in combination with AMFs, increased the levels of N, P, K, Mg, and Ca, as well as phosphatase activity in plant tissues. This confirmed that the enhanced nutrient uptake resulting from this interaction supports plant species development under salt stress. Additionally, reductions in Na^+ and Cl^- levels were observed, demonstrating mitigation of the deleterious effects of salts [34]. Thus, native soil microorganisms associated with AMFs can be used as an alternative to optimize production in agroecosystems affected by high salinity.

The improvement of soil physical properties through the addition of AMFs is primarily attributed to the production of organic acids and glomalin, which protect against soil erosion, chelate heavy metals, enhance carbon sequestration, and stabilize soil macroaggregation. By recruiting bacteria that produce alkaline phosphatase, an enzyme involved in soil mineralization and associated with organic phosphorus availability, AMFs also enhance the soil's chemical activity. Additionally, dead mycelia contribute to organic matter accumulation. AMFs influence the composition, diversity, and activity of soil microbial communities through antagonism or cooperation [29].

In the long term, the addition of AMFs can increase the organic carbon accumulation in agricultural soils; however, the successful establishment of AMFs depends on the soil properties, host plant, inoculum type, and experimental conditions [35]. The increased resistance of plants inoculated with AMFs to high salinity conditions can also be attributed to various biochemical and physiological mechanisms, which, according to [30], can be categorized into three groups: (1) enhanced nutrient uptake, maintenance of ionic homeostasis, improved water absorption, and osmotic balance; (2) increased photosynthetic efficiency and protection of the photosynthetic apparatus; and (3) modulation of the plant's hormonal profile and induction of the antioxidant system to prevent ROS-induced damage.

In this context, we hypothesized that combining the AMF *Gigaspora albida* with soil microbiota can ameliorate the effects of saline stress on the growth, physiology, and Na^+ and K^+ balance of Creole corn (Ibra variety) when irrigated with saline waste from reverse osmosis. Hence, this study aimed to assess the impact of the arbuscular mycorrhizal fungus (AMF) *Gigaspora albida* on the growth, physiology, and Na^+ and K^+ balance of Creole corn (Ibra variety) under various levels of electrical conductivity from saline waste.

2. Materials and Methods

2.1. Location and Characterization of the Area

The study was conducted at the Universidad Federal Rural do Semi-Árido (UFERSA) in Mossoró, Rio Grande do Norte/RN (5°12′2.03″ N and 37°19′36.32″ W). The experiment was carried out in a greenhouse environment, using pots, from January to March 2022. The greenhouse covered an area of 126 m^2, with a ceiling height of 4.0 m, and was constructed with a metallic frame and a transparent plastic cover, while the walls were shaded at 50%. The average maximum temperature recorded was 37.4 °C, with daytime fluctuations, and the average minimum temperature hovered around 31 °C. The average relative humidity (RH) was 97.7% with a standard deviation of 86%.

2.2. Experimental Design

The experimental design followed a completely randomized model, in a 3 × 4 factorial scheme, with six replications; the plots contained polyethylene pots with a capacity of 30 L, totaling 72 experimental units. The treatments consisted of three mycorrhizal conditions (M1—control plants without the fungal inoculum; M2—plants with the *G. albida* fungal inoculum; and M3—plants with the *G. albida* fungal inoculum plus soil microbiota) and saline waste with four electrical conductivity levels (EC_a): 0.5, 1.8, 3.1 and 4.4 dS m^{-1} (conductivity of 0.5 dS m^{-1} is from the supply water, which was used as the control). The saline concentrations of the irrigation water were established by diluting reverse osmosis saline waste with supply water from the Rio Grande do Norte Water and Sewage Company (CAERN), Mossoró, Brazil.

2.3. Soil, Saline Waste, Plant, and Mycorrhizal Materials

Soil material with a sandy texture was gathered from the upper soil layer, approximately 0–30 cm deep, at the Rafael Fernandes Experimental Farm of UFERSA, situated in the rural vicinity of Mossoró/RN. For physical–chemical characterization, disturbed samples were collected and subsequently analyzed using the Embrapa methodology [36], as detailed in Table 1.

Table 1. Physicochemical characterization of the eutrophic red Oxisol.

pH	CEes	OM	P	K^+	Na^+	Ca^{2+}	Mg^{2+}	Al^{3+}	H + Al	SB	t	CEC
(water)	dS m^{-1}	g/kg	———	mg/dm^3	———	———	———	———	cmolc/dm^3	———	———	———
7.4	0.80	31.9	112.2	791.7	160.1	6.5	4.8	0.0	0.0	14.0	14.56	14.0
V	m	ESP		Sand			Silt			Clay		
	——— % ———					———	———	(g kg^{-1})	———	———		
100	0.0	5.5		89.25			2.79			7.79		

The pH in water was determined using a soil–water ratio of 1:2.5. CEes is the electrical conductivity of the soil–water extract at a ratio of 1:2.5. The elements P, Na^+, and K^+ were extracted using a Mehlich-1 extractor at a soil–extractor ratio of 1:10. The elements Ca^{2+}, Mg^{2+}, and Al^{3+} were extracted with 1 mol/L KCl using a soil–extractant ratio of 1:10. H + Al is the potential acidity extracted with 0.5 mol/L calcium acetate using a soil–extractor ratio of 1:15. SB is the sum of bases. t is the effective CEC. CEC is the soil CEC or CEC at pH 7.0. V is the base saturation. m is the aluminum saturation. ESP is the percentage of exchangeable sodium.

The saline waste was obtained from the water treatment facility of the Jurema Rural Settlement, situated along the RN-012 highway, which links Mossoró to the municipality of Tibau, RN. The physicochemical attributes of both the saline waste and the supply water are outlined in Table 2.

Table 2. Physicochemical characteristics of the supply water (ABT) and the concentrated saline waste (RSC) used in the experiment.

	pH	**CE_{es}**	**K^+**	**Na^+**	**Ca_2^+**	**Mg_2^+**	**Cl**	**CO_3^{2-}**	**HCO_3^-**	**RAS**
	(H_2O)	(dS m^{-1})	----------mmol$_c$/L----------							
ABT	7.5	0.54	0.31	3.78	0.84	1.20	2.40	0.61	3.21	3.76
RSC	7.11	9.50	0.83	54.13	36.80	24.2	116	0	3.39	9.71

CEes—electrical conductivity of the soil saturation extract; RAS—sodium adsorption ratio.

Creole corn seeds, specifically of the Ibra variety, were procured from the 2021 harvest in the municipality of Umarizal. The *Gigaspora albida* arbuscular mycorrhizal fungi (AMF) inoculants were sourced from the Laboratory of Plant Physiology and Biochemistry (LFBP) at the State University of Rio Grande do Norte (UERN).

2.4. Experimental Stage

Soil Preparation, AMF Propagation, and Experimental Setup

To propagate the fungus, a substrate comprising soil and sand in a 3:1 (*v*/*v*) ratio was utilized; it was sterilized in an autoclave at 121 °C and 1 ATM for two hours, with a 24 h interval between successive autoclaving sessions. In a greenhouse, the sterilized substrate was transferred to polyethylene pots with an 8 L capacity, along with 8 g of inoculum soil containing fragments of colonized roots and propagules of the *G. albida* species. Subsequently, *Panicum milaceum* (millet) seeds were sown as trap plants to facilitate the proliferation of the AMF. After 60 days, soil portions weighing 1.5 kg containing the inoculum were collected and preserved in plastic bags at 4 °C for future use.

The substrate employed in the experiment was a blend of soil and organic compounds (0.7% (*w*/*w*) N, 0.5% (*w*/*w*) P2O5, 0.5% (*w*/*w*) K2O, maximum humidity of 50% (*w*/*w*), 15% (*w*/*w*) total organic carbon, CTC of 250, C/N (maximum) of 18, pH 8.0) in a 2:1 (*v*/*v*) ratio. This substrate underwent sterilization following the aforementioned protocol, except for the M3 treatment. Post-sterilization, the substrate was allocated into polyethylene pots with a 30 L capacity. Inoculation with 100 g of soil containing the AMF inoculum (675 spores/50 dm^3 of soil) was conducted prior to sowing, which was positioned approximately 3 cm below the seeds. To maintain uniform microbial populations across all treatments, each plot of non-mycorrhizal plants received 100 mL of crude soil filtrate devoid of AMF spores. This filtrate was obtained from a suspension of 50 dm^3 of soil, which was filtered through a sieve with pores measuring 0.053 mm in diameter, and subsequently filtered twice through qualitative filter paper to eliminate AMF propagules, as outlined in [37].

2.5. Irrigation and Fertilization

Irrigation was conducted on a daily basis to maintain a soil moisture close to its maximum retention capacity. Saline water irrigation commenced 20 days after thinning, in accordance with the electrical conductivity (EC_a) of each treatment. To induce salt stress, the diluted saline waste was progressively applied until the desired concentration was reached. The EC_a of the saline waste in each treatment was monitored using a portable conductivity meter (model Instrutherm CD-860) every two days. The irrigation was manually administered.

The daily irrigation depth (LD) was determined via drainage lysimetry, calculated every two days using lysimeters corresponding to each salinity level (average of two vessels). The calculation considered the volume applied (*Va*) via irrigation per vessel, which was obtained by subtracting the previous applied lamina (*La*) from the average drained volume (*Vd*), divided by the number of vessels (*n*), as per Equation (1). Table 3 presents the volumes of saline waste applied during cultivation.

$$Va = (La - Vd)/n \quad (1)$$

Table 3. Volumes of saline waste applied to Creole corn (*Zea mays* L.) plants under the influence of an AMF as a function of EC_a.

	V. Irrigation (L Plant^{-1})
EC_a (dS m^{-1})	**M1/M2/M3**
0.5	36,350
1.8	39,520
3.1	32,700
4.4	31,500

M1—control plants without fungal inoculum; M2—plants with fungal inoculum of *G. albida*; and M3—plants with fungal inoculum of *G. albida* plus soil microbiota.

To ensure adequate nutrition, two applications of Hoagland and Arnon's [38] solution, which is devoid of phosphorus, were administered at full concentration at 15-day intervals post-germination. At 34 days, fertigation as recommended in [39] was applied, which consisted of 72.73 kg of N ha^{-1} and 39.28 kg of KCl ha^{-1}, split into two fractions. The fertilizer sources utilized were urea (45% N) and potassium chloride (60% K_2O).

The saline treatment irrigation commenced on the 20th day after thinning. Growth analyses were conducted following the methodology outlined in [40] after 30 days. The plant height (AP) was measured, using a measuring tape, as the distance between the ground and the youngest leaf; the stem diameter (DC) was recorded with a digital caliper (Digital Caliper 150 mm model) using the first internode of the plant as the measurement point; the number of leaves (NF) was determined by counting the leaves with fully expanded limbs.

2.6. Plant Analyses

2.6.1. Gas Exchange and Chlorophyll Fluorescence

Physiological analyses were conducted at the onset of the bolting phase (50 days after sowing). The readings were obtained in the morning, between 7:00 am and 9:00 am, from the fully expanded third leaf of the apical meristem, using a portable infrared gas analyzer (IRGA), specifically the LCPro Portable Photosynthesis System (ADC BioScientific Limited, Hertfordshire, UK). The IRGA maintained a controlled temperature of 25 °C, irradiation of 1200 photomotonic m^{-2} s^{-1}, and an air flow of 200 mL min^{-1}. The quantified variables included transpiration (E) (mmol (H_2O) m^{-2} s^{-1}), stomatal conductance (gs) (mol (H_2O) m^{-2} s^{-1}), net assimilation rate (A), and leaf temperature (TI) (°C).

Subsequently, chlorophyll fluorescence readings were taken using a pulse-modulated fluorometer, specifically the OptiScience OS5p model (Marconi Manufacturer, Piracicaba, SP, Brazil. The Fv/Fm protocol was employed for assessments under dark conditions, following a 30 min dark adaptation of the leaves using accessory clips from the device to ensure that all reaction centers were open [41]. From these readings, the initial fluorescence (Fo), maximum fluorescence (FM), variable fluorescence (Fv = Fm − Fo), maximum quantum efficiency of photosystem II (PSII) (Fv/Fm), basal quantum yield of photochemical processes in PSII (Fo/Fm), and photochemical efficiency in PSII (Fv/Fo) were estimated.

The evaluations were conducted under light conditions utilizing the Yield protocol. The readings were taken by applying an actinic light source with a saturating multi-flash pulse that was connected to a clip for determining the active photosynthesis radiation (PAR-Clip). From these measurements, the following parameters were estimated: the initial fluorescence before the saturation pulse (F'), maximum fluorescence after adaptation to saturated light (Fm'), electron transport rate (ETR) (µmol (photons) m^{-2} s^{-1}), and quantum efficiency of photosystem II Y(II). Additionally, the minimum fluorescence of illuminated plant tissue (Fo') [42], photochemical extinction coefficient by the lake model (qL), regulated photochemical extinction yield (YNOP), and unregulated photochemical extinction yield (YNO) [43] were calculated from these data.

2.6.2. Growth Analysis

The leaf area (FA) was estimated by extracting leaf discs (area of 1.78 cm^2) from the basal portion of the leaf, leaving the central vein intact. Subsequently, both the leaf discs and the remaining leaf tissues were dried in a forced air circulation oven at 70 °C until a constant weight was reached. The leaf area was calculated using the formula AF = PF × AD/PD, where AF represents the estimated leaf area, PF is the dry mass of the leaf, AD is the area of the removed leaf disc (1.78 cm^2), and PD is the dry mass of the leaf discs, as per [44,45].

The dry matter of the shoot (MSPA) and root (MSR) was determined by dehydrating the fresh biomass in a forced air circulation oven at 70 °C until a constant weight was achieved. Prior to drying, a 1 g sample of fresh root was collected from each plot, washed, and preserved in an FAA solution (5% formaldehyde, 90% ethyl alcohol, and 5% acetic acid) for the subsequent analysis. Using the obtained dry mass data, the root-to-shoot ratio (R/PA) was calculated by dividing the dry mass of the root by the mass of the shoot, following the method described in [46].

2.6.3. Accumulation of Na and K in the Plant

The extraction of Na^+ and K^+ ions from the leaf, stem, and root tissues involved digesting 0.5 g of dry biomass in a muffle furnace at 500 °C. The biomass was combined with a nitric acid solution (containing nitric acid and 1 mol HCl) to produce an extract. The extract was then subjected to flame spectrophotometry to determine the concentrations of Na and K ions. Subsequently, the Na/K ratio was calculated based on the obtained Na and K concentrations, following the methodology described in [36].

2.6.4. Mycorrhizal Colonization Rate

The root colonization rate (TC) was assessed by examining roots that were diaphanized in 10% KOH, acidified with 1% HCl, and stained with 0.05% Trypan blue, following the protocol outlined in [47]. The percentage of root colonization was determined using the gridline intersection method on a checkered plate, using a binocular magnifying glass with a 40× magnification, as described in [48]. Roots were considered colonized by arbuscular mycorrhizal fungi (AMFs) if they exhibited at least one mycorrhizal structure (e.g., vesicles, arbuscules, or hyphae).

2.7. Variables Evaluated in the Soil

Soil Spore Density

The spore density in the soil was determined using the wet sieving method described in [49] for spore extraction. Following extraction, the spores were centrifuged in a 50% sucrose solution at 1106 g for three minutes, as outlined in [50]. The spore density per gram of soil was estimated from a diluted aliquot of the sample, which was then observed under a stereoscopic microscope (40×), Leica Microsystems manufacturer, Wetzlar, Germany, following the procedure described in [51].

2.8. Statistical Analysis

The results were subjected to analysis of variance using the F test. For the mycorrhizal condition factor, Tukey's test was applied at a 5% level of significance, and for the EC_a factor of saline waste, regression analysis was applied. Data that did not present a normal distribution were transformed into square roots (SQRTs). The analyses were carried out using the statistical software SISVAR, version: 5.6 [52].

3. Results

Salinity affected the photosynthesis and the symbiotic relationship between the plants and AMF. The association with the AMF reduced the damage to the photosystems. The interaction of the EC of the saline waste and AMF produced a significant difference in the electron transport rate ($p < 0.05$) and regulated photochemical quenching quantum yield ($p < 0.05$). The EC_a of the saline waste significantly affected the stomatal conductance ($p < 0.01$), transpiration ($p < 0.05$), leaf temperature ($p < 0.05$), CO_2 assimilation rate ($p < 0.05$), intrinsic water use efficiency ($p < 0.001$), minimum fluorescence of illuminated plant tissue ($p < 0.001$), PSII quantum efficiency ($p < 0.001$), and maximum PSII quantum efficiency ($p < 0.05$). The FMA condition was significant for sweating ($p < 0.05$). The unregulated photochemical quenching quantum yield was not significant for either factor (Table 4).

Table 4. Summary of analysis of variance for stomatal conductance (gs), transpiration (E), leaf temperature (Tl), CO_2 assimilation rate (A_N), intrinsic water use efficiency (A/gs), instantaneous water use efficiency (A/E), minimum fluorescence of illuminated plant tissue (Fo'), PSII quantum efficiency (Y), maximum PSII quantum efficiency (Fv/Fm), electron transport rate (ETR), photochemical quenching quantum yield regulated (YNPQ) and unregulated photochemical quenching quantum yield (YNO) of Creole corn plants as a function of EC_a and the AMF.

		Test F					
		Gas Exchange					
FV	**GL**	**gs** †	**E**	**Tl**	**A_N** †	**A/gs** †	**A/E**
AMF	2	1709 ^{ns}	5180 *	0.626 ^{ns}	1483 ^{ns}	0.653 ^{ns}	0.667 ^{ns}
EC_a (d Sm^{-1})	3	8569 **	3559 *	3141 *	3327 *	8929 ***	1131 ^{ns}
AMF × EC_a	6	0.809 ^{ns}	1372 ^{ns}	0.952 ^{ns}	2112 ^{ns}	1375 ^{ns}	1929 ^{ns}
		Chlorophyll fluorescence					
		Fo' †	**Y**	**Fv/FM**	**ETR †**	**Y(NPQ)**	**YNO**
AMF	2	0.180 ^{ns}	0.666 ^{ns}	2657 ^{ns}	1106 ^{ns}	0.701 ^{ns}	0.576 ^{ns}
EC_a (d Sm^{-1})	3	22.053 ***	22.569 ***	3339 *	6674 **	23.300 ***	2103 ^{ns}
AMF × EC_a	6	2103 ^{ns}	2643 ^{ns}	1258 ^{ns}	2427 *	2517 *	1503 ^{ns}

† Data transformed into square roots (SQRTs); FV—source of variation; GL—degrees of freedom; AMF—arbuscular mycorrhizal fungus; (EC_a)—electrical conductivity of saline wastewater; *** $p < 0.001$; ** $p < 0.01$; * $p < 0.05$; and ns—not significant.

The stomatal conductance (gs) of the irrigated corn exhibited a linear decrease in response to increasing electrical conductivity levels from the saline waste (EC_a). The highest and lowest values of corn gs were recorded as 0.631 and 0.414 mol (H_2O) m^{-2} s^{-1} at EC_a levels of 0.5 and 4.4 dS m^{-1}, respectively, representing a 34.38% decrease in gs (Figure 1A). When comparing the optimal gs results for corn, the plants irrigated with the saline waste demonstrated a reduction in gs of at least 24.4% when compared to those irrigated with freshwater.

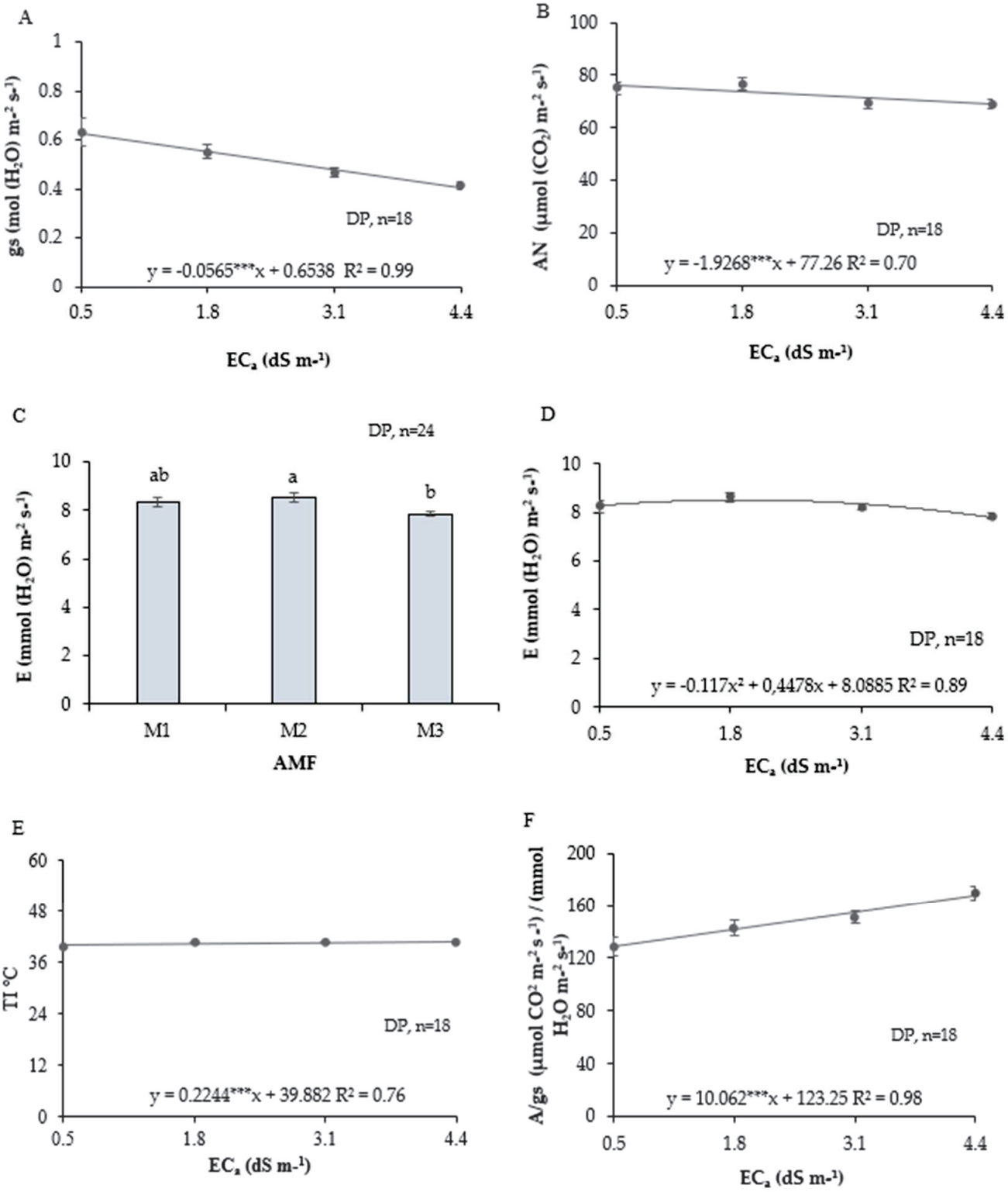

Figure 1. Representation of isolated factors. Regression for stomatal conductance (gs) (**A**), CO_2 assimilation rate (AN) (**B**), mean test and regression for transpiration (E) (**C**,**D**), regression for leaf temperature (Tl) (**E**), and intrinsic water use efficiency (A/gs) (**F**) of Creole corn plants as a function of EC_a (dS m^{-1}) and the AMF. (M1) control plants without fungal inoculum, (M2) plants with *G. albida* fungal inoculum, (M3) plants with *G. albida* fungal inoculum plus soil microbiota. Similar lowercase letters in columns (AMF) indicate no statistical difference according to Tukey's test ($p < 0.05$). *** $p < 0.001$ indicate significance for regression.

The transpiration rate (E) of the corn plants showed variability with changes in the electrical conductivity of the saline waste. At an EC_a level of 1.91 dS m^{-1}, the transpiration rate peaked at 8.52 mmol (H_2O) m^{-2} s^{-1}, representing a 3.4% increase compared to the 0.5 dS m^{-1} level (Figure 1B). Comparing the plants irrigated with an EC of 0.5 dS m^{-1} to those irrigated with the saline waste, the increase was 2.75%. When examining the average transpiration rates for the treatments with the AMF, the highest average was observed in the M2 plants, reaching 8.53 mmol (H_2O) m^{-2} s^{-1}, which was statistically different from the M3 treatment with a value of 7.86 mmol (H_2O) m^{-2} s^{-1}, representing a difference of 8.5% (Figure 1C). The transpiration rate of the M1 plants did not exhibit statistical differences compared to that of the M2 and M3 plants, with an average transpiration rate of 8.33 mmol (H_2O) m^{-2} s^{-1}.

The CO_2 assimilation rate (AN) of the corn plants decreased with increasing EC_a of the saline waste. The corn plants irrigated with an EC_a of 0.5 dS m^{-1} demonstrated a higher CO_2 assimilation rate compared to those irrigated with saline waste with a higher EC_a (Figure 1D). The difference was 5.938 µmol (CO_2) m^{-2} s^{-1} between the 0.5 dS m^{-1} level and the 4.4 dS m^{-1} level.

The leaf temperature (T_l) of the corn plants exhibited a linear increase with rising electrical conductivity of the saline waste. The difference in average Tl values between the corn plants at EC levels of 0.5 and 4.4 dS m^{-1} was 0.94 °C (Figure 1E).

The intrinsic water use efficiency (A/gs) increased linearly with the rise in EC_a of the saline waste, with a unit increase of 10.062 (µmol CO_2 m^{-2} s^{-1})/(mmol H_2O m^{-2} s^{-1}) (Figure 1F).

The minimum fluorescence of illuminated plant tissue (Fo') increased with higher EC_a levels of the saline waste, showing a unit increase of 0.6996 µmol (photons) m^{-2} s^{-1} (Figure 2A. Fo' increased by 63.93% at the 4.4 dS m^{-1} level compared to the EC_a level of 0.5 dS m^{-1} (Figure 2A).

The quantum efficiency of PSII (y) exhibited a linear reduction with the increase in electrical conductivity of the saline waste. At the 0.5 dSm^{-1} level, the average value was 0.504; when compared to the plants irrigated with saline waste with an EC of 4.4 dSm^{-1}, the reduction was 19.84% (Figure 2B). The maximum efficiency of photosystem II (Fv/FM) as a function of the increase in the electrical conductivity of the saline waste was fitted to a quadratic regression model, with its maximum point at an EC of 1.7 dS m^{-1}. Beyond this point, there was a reduction of 3.85% at the highest EC_a of the saline waste at 4.4 dS m^{-1} (Figure 2B).

The electron transport rate (ETR) of the corn plants in response to increasing EC_a levels in mycorrhizal treatments M1 and M2 was fitted to a quadratic regression model, (Figure 3C). The ETR results in the M1 and M2 plants were comparable, with their maximum points occurring around EC levels of 2.2 and 2.3 dS m^{-1}, reaching values of 86.03 and 94.76 µmol (photons) m^{-2} s^{-1}, respectively. In contrast, the ETR of the M3 plants at an EC level of 4.4 dSm^{-1} decreased by 26.96% compared to the control at 0.5 dSm^{-1} (Figure 2C). Among the mycorrhizal treatments, at an EC_a level of 0.5 dSm^{-1}, the M3 plants exhibited the highest ETR at 91.683 µmol (photons) m^{-2} s^{-1}, differing significantly from M2 by an average of 61.1 µmol (photons) m^{-2} s^{-1}, representing an increase of 33.35% (Figure 2C).

The quantum yield of regulated photochemical quenching (YNPQ) increased in all mycorrhizal treatments as the EC_a levels increased (Figure 2D). In treatment M1, the linear regression equation was not significant, yielding an average of 0.45 across all saline levels. The plants from the M2 and M3 groups at the highest EC_a level of 4.4 dSm^{-1} exhibited unit increases in YNPQ of 0.0672 and 0.0425, respectively. Among the highest averages, the M2 plants at an EC_a of 4.4 dS m^{-1} recorded an average of 0.608, which was statistically different from that of the M1 mycorrhizal plants (0.483). However, the YNPQ of the M3

plants did not differ significantly from that of the M1 and M2 plants, with an average value of 0.531.

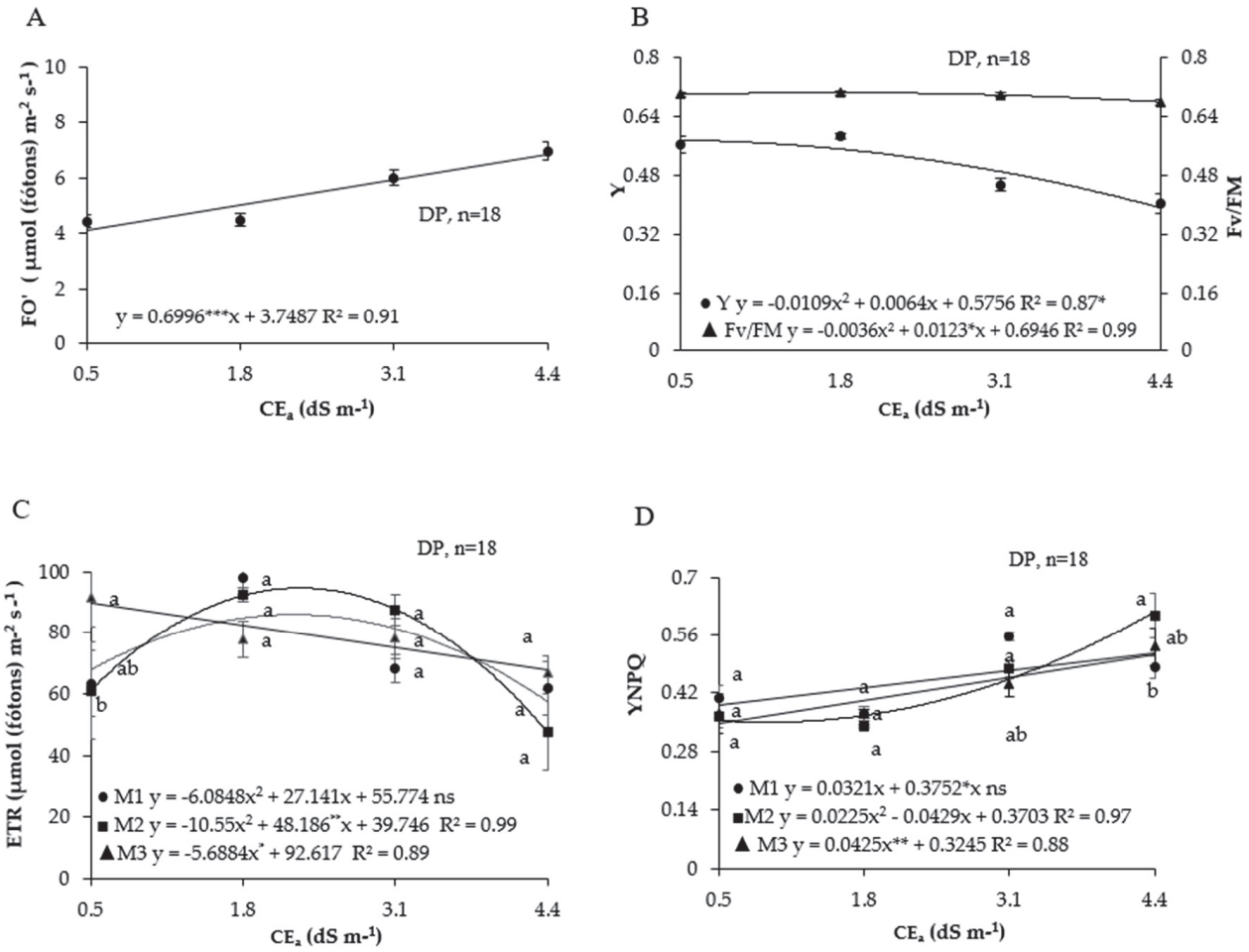

Figure 2. Regression analysis for minimum fluorescence of illuminated plant tissue (Fo') (**A**), quantum efficiency of PSII (Y), and maximum quantum efficiency of PSII (Fv/Fm) (**B**). Regression and mean comparison test for electron transport rate (ETR) (**C**) and quantum yield of regulated photochemical quenching (YNPQ) (**D**) in landrace maize plants as a function of ECa (dS m^{-1}) and the AMF. • M1—control plants without fungal inoculum; ■ M2—plants inoculated with *G. albida*; ▲ M3—plants inoculated with *G. albida* plus the native soil microbiota. Similar lowercase letters in columns (AMF) indicate no statistical difference according to Tukey's test ($p < 0.05$). *** $p < 0.001$; ** $p < 0.01$; * $p < 0.05$ indicate significance for regression and ns—not significant.

Salt stress significantly impacted the plant growth parameters. The interaction of salinity and the presence of the AMF resulted in significant differences ($p < 0.001$) in the growth parameters such as shoot dry matter (MSPA), root dry matter (MSR), and the root/shoot ratio (R/PA). Additionally, there was an of both factors on the plant height (AP) and number of leaves (NF), and an effect of mycorrhizal association (AMF) on the stem diameter (DC) ($p < 0.5$) (Table 5).

The dry mass of the aerial part (MSPA) of the corn plants exhibited variation across the different mycorrhizal conditions and electrical conductivity levels of the saline waste. In the M3 condition, the MSPA increased with the rise in EC_a, reaching its highest value at an EC_a of 2.5 dS m^{-1}, with an average of 120.92 g per plant (Figure 3A). Treatments M1 and M2 showed similar trends, following a quadratic regression model with their maximum points at EC_a levels of 1.4 and 1.9 dS m^{-1}, corresponding to 87.83 and 68.09 g per plant, respectively.

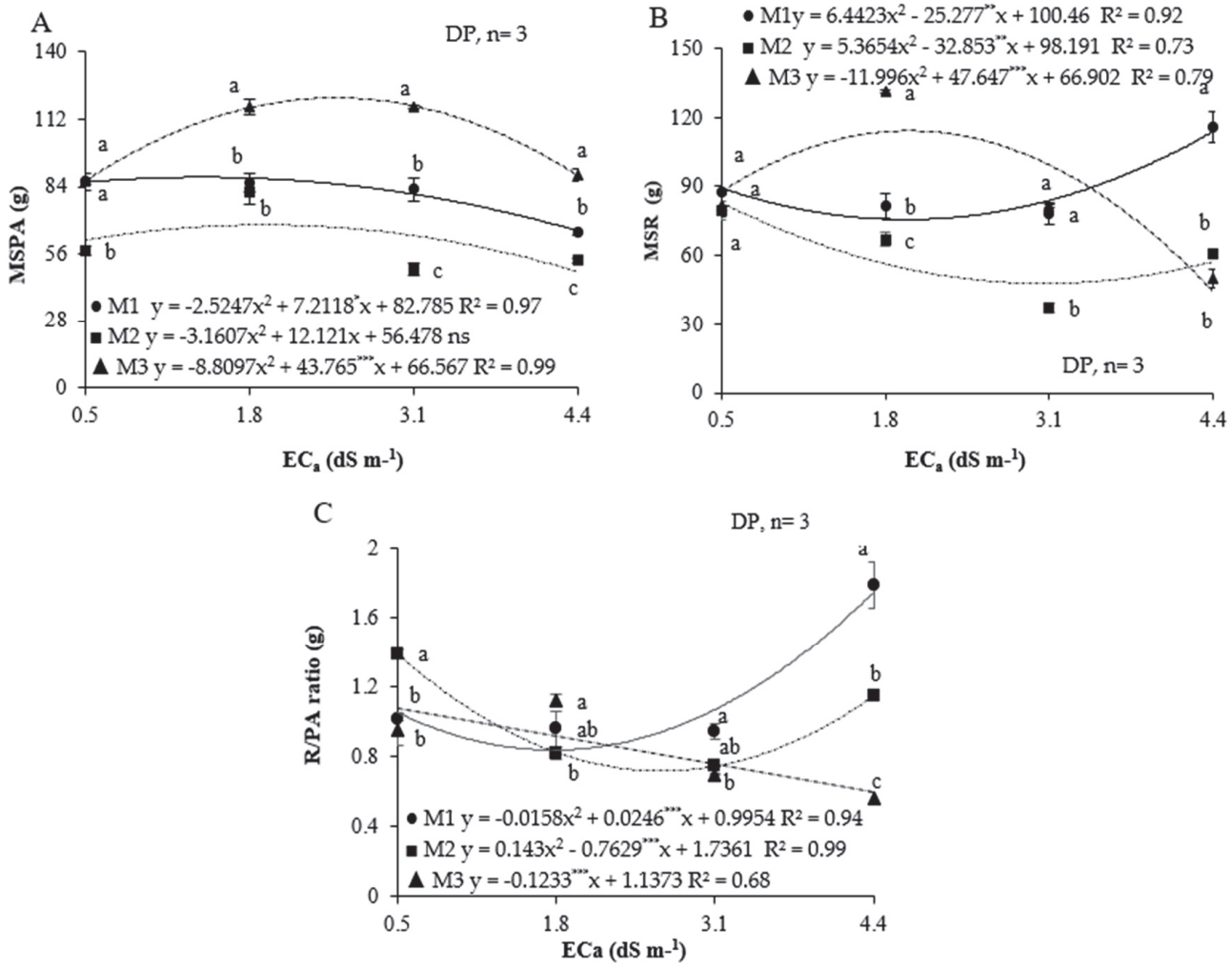

Figure 3. Regression analysis and test of means for shoot dry mass (MSPA) (**A**), root dry mass (MSRA) (**B**), root/shoot ratio (R/PA ratio) (**C**), and total dry mass (MST) (D) of Creole corn as a function of EC_a (d Sm^{-1}) and the AMF. • M1—control plants without fungal inoculum; ■ M2—plants with *G. albida* fungal inoculum; ▲ M3—plants with *G. albida* fungal inoculum and soil microbiota. Similar lowercase letters in columns (AMF) indicate no statistical difference according to Tukey's test ($p < 0.05$), *** $p < 0.001$; ** $p < 0.01$; * $p < 0.05$ indicate significance for regression and ns—not significant.

Table 5. Analysis of variance for the growth parameters shoot dry mass (MSPA), root dry mass (MSRA), root/shoot ratio (R/PA), total dry mass (MST), leaf area (AF), height of the plant (AP), stem diameter (DC), and number of leaves (NF) of Creole corn (v. Ibra) of Creole corn plants as a function of EC_a and the AMF.

		Teste *F*			
FV	**GL**	**MSPA**	**MSRA**		**R/PA**
AMF	2	185.42 ***	73.223 ***		32.513 ***
EC_a (d Sm^{-1})	3	38.69 ***	29.270 ***		22.963 ***
AMF × EC_a	6	13.16 ***	47.989 ***		32.555 ***
		AF	AP	DC	NF
AMF	2	1.385	3.414 *	4.514 *	4.333 *
EC_a (d Sm^{-1})	3	28.332 ***	5.393 **	2.394 ^{ns}	5.127 *
AMF × EC_a	6	6.469 **	1.371 ^{ns}	1.427 ^{ns}	0.841 ^{ns}

FV—source of variation; GL—degrees of freedom; AMF—arbuscular mycorrhizal fungus; EC_a—electrical conductivity of irrigation water; *** $p < 0.001$; ** $p < 0.01$; * $p < 0.05$; and ns—not significant.

When considering mycorrhizal conditions under the influence of the saline waste, significant differences were observed among treatments. Both the M1 and M3 treatments showed notable disparities from M2 (Figure 3A). At the highest EC_a level of 4.4 dS m^{-1}, M3 exhibited the highest MSPA at 88.57 g per plant, which was statistically different from that of M1 and M2, which had average values of 64.67 and 48.62 g per plant, respectively. This represents decreases of 26.98% and 45.11%, respectively, in comparison to M3 (Figure 3A).

The root dry mass (MSR) of the M3 plants exhibited a quadratic regression pattern, with its peak at an EC_a of 2.0 dS m^{-1}, averaging 114.2 g per plant (Figure 3B). In contrast, the plants from the M1 and M2 groups showed their highest MSR values at EC_a levels of 4.4 and 0.5 dS m^{-1}, respectively, with values of 113.96 and 83.10 g per plant (Figure 3B). At the highest EC_a level (4.4 dS m^{-1}), the corn plants under the different mycorrhizal conditions differed significantly: M1 had the highest value at 115.87 g per plant, followed by M2 with 61.05 g per plant, and M3 with 50.17 g per plant (Figure 3B).

Regarding the root/shoot ratio (R/PA ratio), it was higher in the plants from the M1 condition at an EC_a level of 4.4 dS m^{-1}, with an average of 1.78 (Figure 3C). However, in the M3 plants, the R/PA ratio decreased linearly with increasing EC_a of the saline waste, with a unit reduction of 3.16 g per plant. The difference between the highest and lowest EC_a levels (4.4 and 0.5 dS m^{-1}) was 41.09% (Figure 3C). For the corn plants irrigated with the water supply, the M2 plants had a higher R/PA ratio, averaging 1.39, statistically differing from the M1 and M3 plants. At the highest saline waste level (4.4 dS m^{-1}) among the mycorrhizal treatments, the M2 and M3 plants differed significantly, with a reduction in the R/PA ratio of 0.58 compared to M1 (Figure 3C).

The height of the corn plants (AP) decreased with increasing electrical conductivity levels of the saline waste, peaking at an EC_a of 1.8 dS m^{-1}, with an average of 191.14 cm (Figure 4A). Beyond this EC_a, there was a significant reduction in AP with increasing salinity, showing a difference of 10.91% (Figure 4A).

In terms of mycorrhizal treatments, the M3 plants exhibited greater height, averaging 189.23 cm, which was statistically different from that of M2 only, with a difference of 13.23 cm. The M1 plants had an average height of 184.03 cm, showing no statistical difference from that of the M2 plants (Figure 4B).

The response of the number of leaves (NF) of the corn plants to the increase in electrical conductivity fit a quadratic regression model, reaching an average of 14.41 leaves at its peak, which occurred at an EC_a of 2.3 dS m^{-1} (Figure 4C). In terms of mycorrhizal treatments, the M3 plants exhibited a higher NF, averaging 14.33 leaves, with no significant differences from that of the M1 plants (average of 14.25 leaves), but differing from M2 plants, where there was a reduction of 5.79%, equivalent to 0.83 leaves (Figure 4D).

The leaf area (FA) of the corn plants did not significantly differ between the mycorrhizal treatments in response to the increasing electrical conductivity of the saline waste, except at an EC_a of 3.1 dS m^{-1}, where M1 had the highest average FA of 1640.46 cm^2. Compared to the M2 and M3 treatments, this represented an increase of 29.58% and 23.97%, respectively (Figure 4E). The maximum leaf area of the corn plants in M2 at different EC_a levels of the saline waste was 1155.15 cm^2 at an EC_a of 2.1 dS m^{-1}, while in M3, it peaked at an EC_a of 2.4 dS m^{-1}, with an average leaf area value of 1247.19 cm^2.

The corn stalk diameter (DC) exhibited a similar trend to that of the AP and NF, with the M3 plants having higher values compared to the M2 plants but not differing from the M1 plants (Figure 4F). The M3 plants had an average DC of 2.4 mm, approximately 0.27 mm higher, representing an increase of 11.25% compared to the M2 plants (Figure 4F).

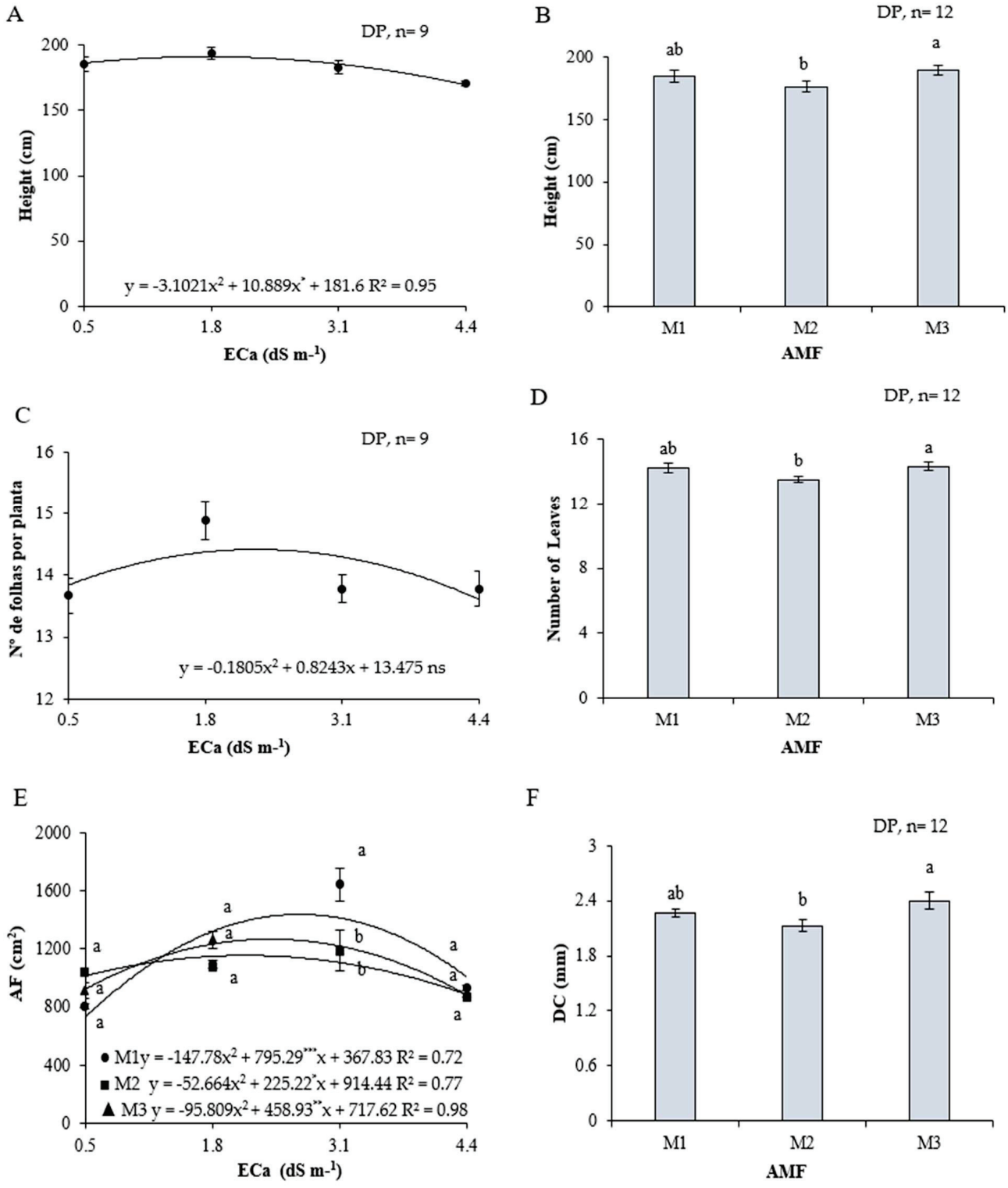

Figure 4. Regression and test of means of isolated factors for plant height PA (**A**,**B**), number of leaves NF (**C**,**D**), interaction of factors for leaf area AF (**E**), and stem diameter DC (**F**) of Creole corn as a function of EC_a (dS m^{-1}) and the AMF. ● M1—control plants without fungal inoculum; ■ M2—plants with *G. albida* fungal inoculum; ▲ M3—plants with *G. albida* fungal inoculum plus soil microbiota. Similar lowercase letters in columns (AMF) indicate no statistical difference according to Tukey's test ($p < 0.05$), *** $p < 0.001$; ** $p < 0.01$; * $p < 0.05$ indicate significance for regression and ns—not significant.

The interaction between the electrical conductivity of the irrigation water (EC_a dSm^{-1}) and the mycorrhizal condition significantly affected the sodium content in the leaf ($p < 0.05$), stem, and root ($p < 0.001$), as well as the potassium content in the stem and root ($p < 0.001$), and the sodium-to-potassium ratio in the leaf, stem, and root ($p < 0.01$). Additionally, there was an effect of the EC_a levels on the sodium-to-potassium ratio in the root ($p < 0.01$) (Table 6).

Table 6. Analysis of variance for the sodium (Na^+) and potassium (K^+) content in the leaf, stem, and root. Sodium and potassium ratio (Na/K) in the leaves, stems, and roots of Creole corn plants as a function of the EC_a of the saline waste and the AMF.

					Teste F	
FV	**GL**	**Na (folha)**	**Na (colmo)**		**Na (raiz)**	**Na/K (folha)** †
AMF	2	29.910 ***	86.367 ***		51.937 ***	1.617 ns
EC_a (d Sm^{-1})	3	65.373 ***	274.226 ***		229.684 ***	0.345 ns
AMF × EC_a	6	2.862 *	25.310 ***		21.147 ***	21.485 ***
		K (folha)	K (colmo)	K (raiz)	Na/K (colmo)	Na/K (raiz) †
AMF	2	7.683 *	17.578 ***	0.438 ns	68.526 ***	4.441 *
EC_a (d Sm^{-1})	3	7.094 **	23.352 ***	6.479 **	11.455 **	2.773 ns
AMF × EC_a	6	2.132 ns	40.669 ***	10.811 ***	51.162 ***	8.430 ***

† Data transformed into square roots (SQRTs). FV—source of variation; GL—degrees of freedom; AMF—arbuscular mycorrhizal fungus; EC_a—electrical conductivity of irrigation water; *** significant at 0.1% probability level ($p < 0.001$); ** significant at the 1% probability level ($p < 0.01$); * significant at the 5% probability level ($p < 0.05$) and ns—not significant.

The leaf sodium accumulation exhibited a linear increase with increasing EC_a, with the highest accumulations observed in the control plants (M1) at all studied levels. The highest concentration was 7.18 g kg^{-1} at an EC_a of 4.4 dS m^{-1}. In contrast, the plants from the M2 and M3 groups showed lower sodium accumulations at all levels compared to the M1 plants. The highest concentrations obtained were 5.19 g kg^{-1} and 4.180 g kg^{-1} for M3 and M2, respectively, at an EC_a of 4.4 dS m^{-1}. The corn plants under mycorrhizal influence (M2 and M3) reduced their leaf sodium accumulation by 41% and 28%, respectively, compared to M1 at the same EC_a of 4.4 dS m^{-1} (Figure 5A).

The sodium concentrations in the stalk increased with the EC_a of the saline waste. The plants from the M2 and M1 groups exhibited the highest accumulations at an EC_a of 4.4 dS m^{-1}, with averages of 24.13 g kg^{-1} and 23.12 g kg^{-1}, respectively (Figure 5B). The M1 plants differed from the M3 plants only at EC_a levels of 0.5, 3.1, and 4.4 dS m^{-1}. The M3 plants, at an EC_a of 3.1 dS m^{-1}, had a reduction in the sodium content in the stem of 62% and 52% compared to the M2 and M1 plants, respectively. At an EC_a of 4.4 dS m^{-1}, there was a reduction of 66% and 37% compared to M1 and M2, respectively, under the same EC_a condition (Figure 5B).

The sodium concentrations in the root increased linearly with the electrical conductivity levels. In the M1 and M3 plants, the highest sodium concentration of 21.0 g kg^{-1} and 21.8 g kg^{-1}, respectively, corresponded to the highest EC_a level of 4.4 dS m^{-1} (Figure 5C).

Among all treatments, the M2 plants accumulated less sodium in their roots. When comparing the plants from the M3 and M1 groups at the same level (EC 4.4 dS m^{-1}), there was a reduction of 18.4% and 15.2%, respectively, in the sodium content in their root. For the M3 plants, the lowest root sodium concentration (10.56 g kg^{-1}) occurred at the minimum point of the curve (1.9 dSm^{-1}), which was only statistically different compared to that of the M1 plants at the same saline level (Figure 5C).

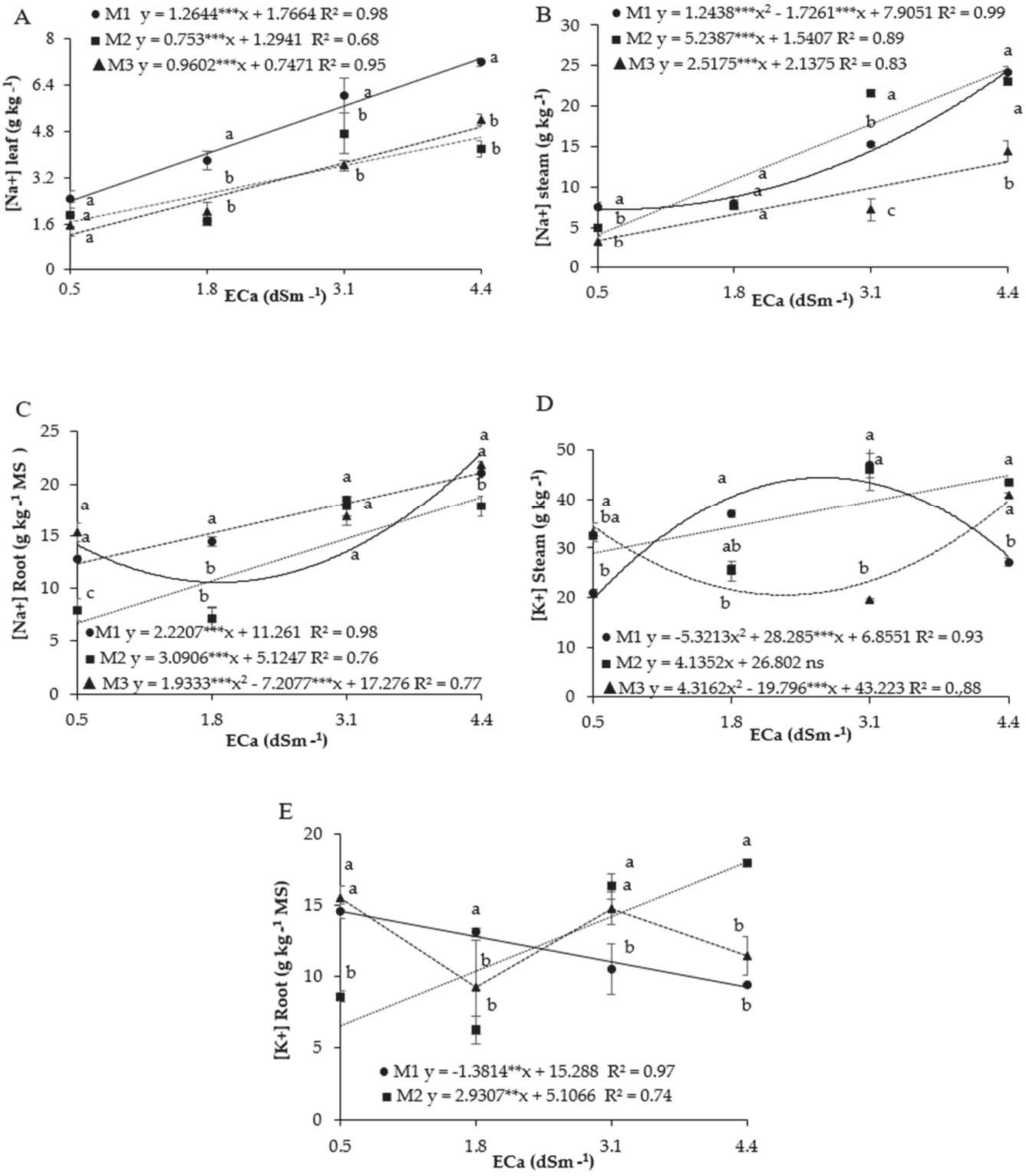

Figure 5. Sodium content in the leaf ($[Na^+]_{leaf}$) (**A**), stem ($[Na^+]_{stem}$) (**B**) and root ($[Na^+]_{Root}$) (**C**). Potassium content in the stem ($[K^+]_{Stem}$) (**D**) and in the root ($[K^+]_{Root}$) (**E**) of landrace corn (*Zea mays* L.) plants as a function of EC_a (dS m^{-1}) and the AMF. ● M1—control plants without fungal inoculum; ■ M2—plants with *G. albida* fungal inoculum; ▲ M3—plants with *G. albida* fungal inoculum plus soil microbiota. DP, $n = 3$. Similar lowercase letters in columns (AMF) indicate no statistical difference according to Tukey's test ($p < 0.05$). *** $p < 0.001$; ** $p < 0.01$ indicate significance for regression and ns—not significant.

The interaction of factors resulted in a higher potassium (K^+) content in the stem of the control plants (M1), which differed from that of the M2 and M3 plants only at the level of 1.8 dS m^{-1} (Figure 5D). The highest concentration in M1 was 44.43 g kg^{-1} at an EC_a of 2.7 dS m^{-1}. In the M2 plants, the potassium content increased with the EC_a levels, reaching the highest concentration of 43.53 g kg^{-1} at an EC_a of 4.4 dS m^{-1}, differing only from that of M1. In M3, the highest concentration occurred at the highest level (4.4 dS m^{-1}), reaching 40.93 g kg^{-1} of K^+ in the stem (Figure 5D). At the highest EC_a condition (4.4 dS m^{-1}), the M2 and M3 plants were more efficient in concentrating potassium in the stalk, with an increase of 60% and 50.6%, respectively, compared to the control.

The potassium accumulation in the roots of non-inoculated plants (M1) decreased with increasing EC_a levels. Among the mycorrhizal treatments, the highest concentration (14.56 g kg^{-1}) occurred at an EC_a of 0.5 dS m^{-1}, which was statistically different from that of M2 under the same condition (Figure 5E). The M2 plants increased their root potassium content with increasing EC_a levels, with the largest accumulation (17.94 g kg^{-1}) occurring at an EC_a of 4.4 dS m^{-1} (Figure 5E). For the potassium accumulation in M3, no regression models were fitted; the plants had an average of 11.90 g kg^{-1} of potassium at all EC_a levels. The M2 plants showed the best results for K^+ accumulation, increasing their root potassium content by 90% and 56%, respectively, compared to the M1 and M3 plants (Figure 5E).

The leaf potassium (K^+) concentration decreased quadratically with increasing EC_a (Figure 6A).

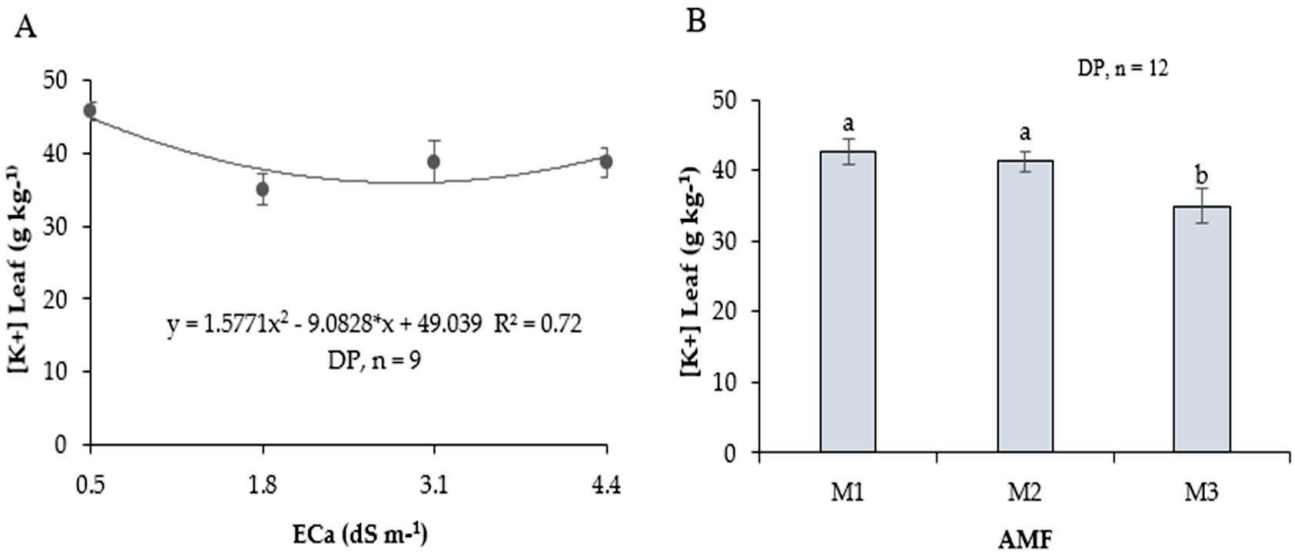

Figure 6. Potassium accumulation ($[K^+]_{Leaf}$) (**A**,**B**) of landrace corn plants as a function of EC_a (dSm^{-1}) and the AMF. M1—control plants without fungal inoculum; M2—plants with fungal inoculum of *G. albida*; M3—plants with fungal inoculum of *G. albida* plus soil microbiota. Similar letters in rows (EC_a) and columns (AMF) are not statistically different according to the Tukey test ($p < 0.05$), * $p < 0.05$ indicate significance for regression.

The lowest accumulation occurred at an EC_a of 2.9 dS m^{-1}, corresponding to 36 g kg^{-1} of potassium in the leaf (Figure 6A). For the AMF treatments, the highest concentration of K^+ occurred in the M1 and M2 plants, with an average of 42.0 g kg^{-1}, compared to the M3 plants, which obtained an average of 35.0 g kg^{-1} (Figure 6B). The increase in M1 and M2 was 20% compared to M3 (Figure 6B).

The sodium to potassium ratio in the M1 corn leaves (Na^+/K_{leaf}^+) increased quadratically as a function of the EC_a level. The highest (0.16) and lowest (0.03) ratios occurred at EC_a levels of 2.3 and 4.4 dS m^{-1}, respectively, representing a decrease of 76.2% in the

Na^+/K^+_{leaf} ratio at the highest level (Figure 7A). For the M2 plants, the Na^+/K^+_{leaf} ratio did not differ between the EC_a levels, with an average of 0.08 (Figure 7A). The Na^+/K^+_{leaf} ratio in the M3 plants was fitted to a quadratic regression model. The highest and lowest ratios (0.16 and 0.04) occurred at EC_a levels of 4.4 and 2.4 dS m^{-1}, respectively, representing an increase of 284.6% at the highest level and a reduction of 74% at an EC_a level of 2.5 dS m^{-1}. Among plants, the highest Na^+/K^+_{leaf} ratio occurred at the 4.4 dS m^{-1} level in the M3 plants, corresponding to an increase of 231.4% and 97% compared to the M1 and M2 plants, respectively (Figure 7A).

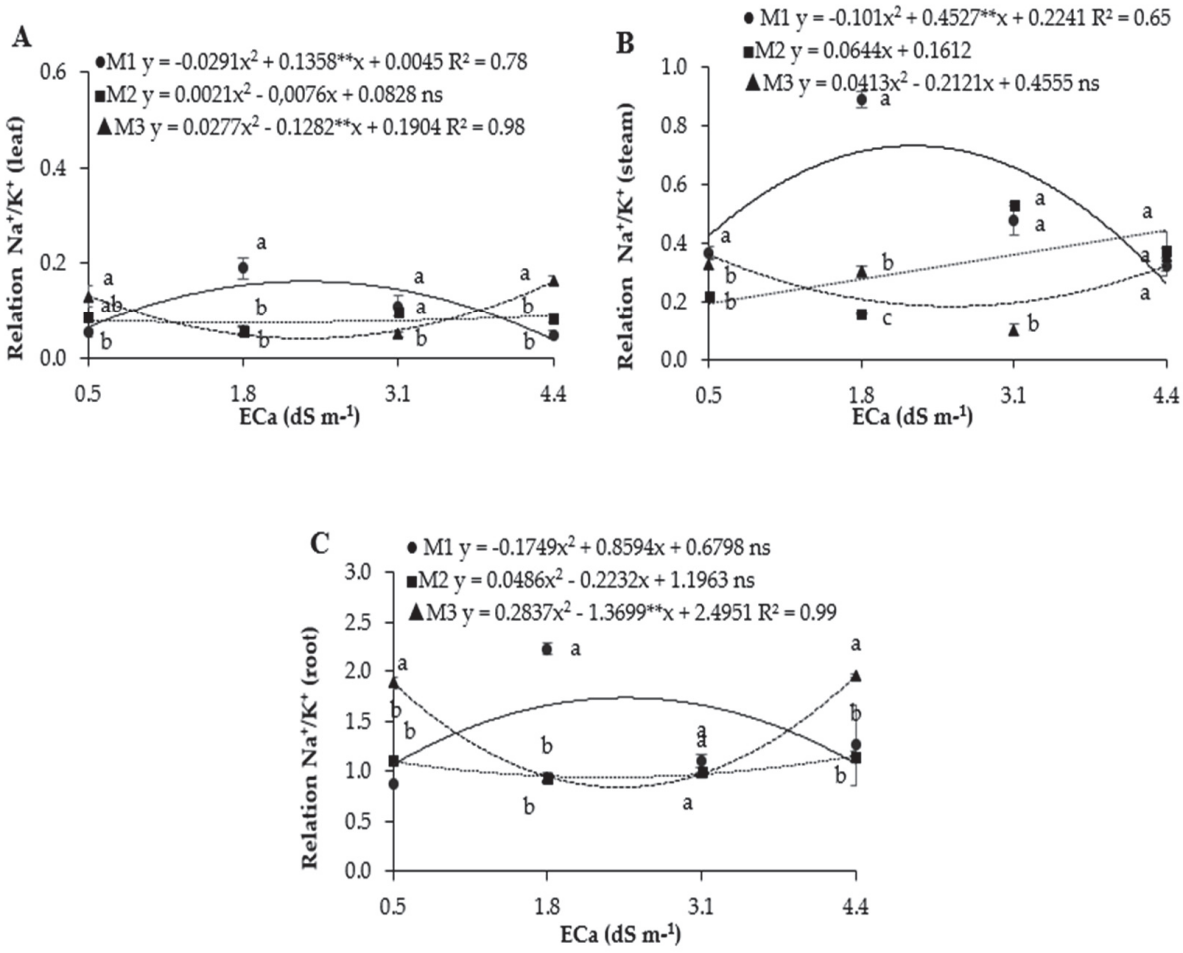

Figure 7. Relation of sodium and potassium in the leaf (Na/K_{leaf}) (**A**), in the stem (Na/K_{culm}) (**B**), and in the root (Na/K_{root}) (**C**) of Creole corn plants as a function of EC_a (d Sm^{-1}) and the AMF. • M1—control plants without fungal inoculum; ■ M2—plants with *G. albida* fungal inoculum; ▲ M3—plants with *G. albida* fungal inoculum plus soil microbiota. Similar lowercase letters in columns (AMF) indicate no statistical difference according to Tukey's test ($p < 0.05$), ** $p < 0.01$ indicate significance for regression and ns—not significant.

The relationship of sodium and potassium in the M1 corn stalks (Na/K_{culm}) was fitted to a quadratic regression model, with the highest and lowest ratios being 0.73 and 0.26 at EC_a levels of 2.3 and 4.4 dS m^{-1}, respectively, representing a reduction of 64.3% (Figure 7B). The Na/K_{culm} ratio in the M2 plants could not be fitted to any of the tested regression models; it showed an average of 0.31 for all EC_a levels (Figure 7B). The Na/K_{culm} ratio in M3 showed a quadratic behavior but it was not significant based on the regression analysis, it showed an average of 0.27 for all levels. The highest ratio (0.71) was observed in the M1 plants at the 1.8 dS m^{-1} level, corresponding to increases of 359% and 134% compared to the M2 and M3 plants, respectively (Figure 7B).

The relationship of sodium and potassium in the root (Na/K_{root}) in M1 did not fit any of the regression models tested; it showed an average of 1.36 for all EC_a levels. The highest and lowest Na/K^+_{root} ratios in M1 were 2.22 and 1.26 at EC_a levels of 1.8 and 4.4, respectively (Figure 7C). The Na/K^+_{root} ratio in M2 fit a quadratic model but it was not significant based on the regression analysis; it showed an average of 1.04 for all EC_a levels. In M3, the highest Na/K^+_{root} ratios were observed at EC_a levels of 0.5 and 4.4 dS m^{-1}, corresponding to 1.88 and 1.95, respectively. The largest reduction was 0.84 at the 2.5 dS m^{-1} level. The best results for the Na/K^+_{root} was observed in the M1 plants, with increases in the Na/K^+_{root} ratio of 139% and 137% compared to the M2 and M3 plants, respectively.

The interaction of the EC_a and AMF was significant for the root colonization rate ($p < 0.001$), number of spores in the soil ($p < 0.001$), and easily extractable glomalin content ($p < 0.001$) (Table 7).

Table 7. Analysis of variance for root colonization rate (TCR) (A) and soil spore density (B) of landrace corn plants as a function of EC_a (dS m^{-1}) and the AMF.

		Test F	
FV	**GL**	**% TCR**	**Number of Spores**
AMF	2	447.963 ***	298.393 ***
EC_a (d Sm^{-1})	3	4.582 *	85.332 ***
AMF × EC_a	6	13.412 ***	42.446 ***

FV—source of variation; GL—degrees of freedom; AMF—arbuscular mycorrhizal fungus; (EC_a)—electrical conductivity of irrigation water; *** significant at a probability level of 0.001 ($p < 0.001$); * significant at a probability level of 0.05 ($p < 0.5$).

The colonization rate (%TCR) in the M3 plants followed a quadratic regression model (Figure 8A). Colonization decreased with increasing EC_a levels in the waste. The lowest percentage occurred at the 3.2 dS m^{-1} level, corresponding to 63.5%. In M2, the percentage increased linearly as a function of the EC_a level. The highest value, 46%, was observed at the 4.4 dS m^{-1} level (Figure 8A). The best results were observed in the M3 plants, with increases in the colonization rate of 83% and 53% at levels of 1.8 and 3.1 dS m^{-1}, respectively, compared to the M2 plants under the same EC_a condition (Figure 8A).

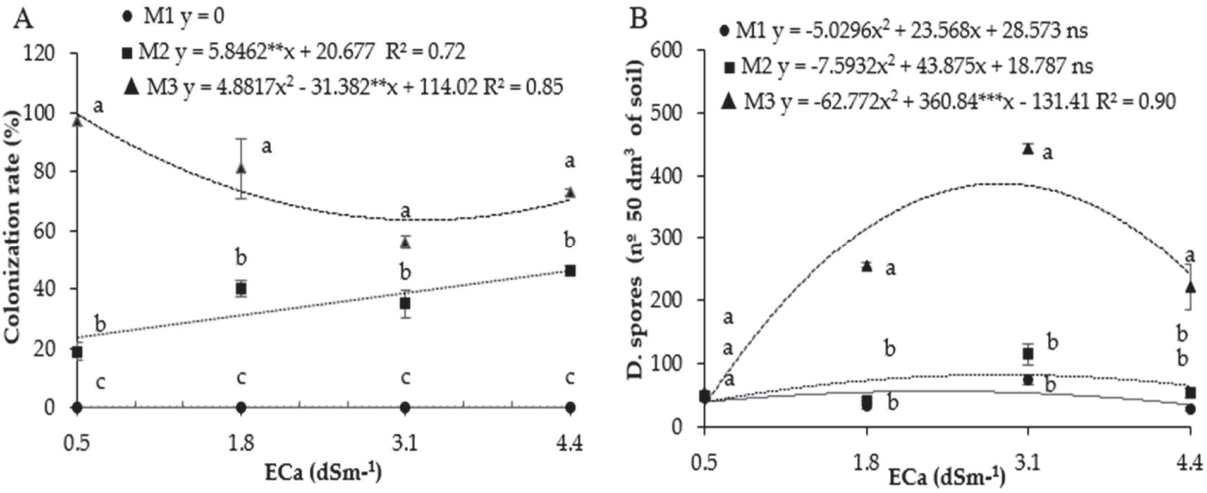

Figure 8. Root colonization rate (**A**) and soil spore density (**B**) of landrace corn plants as a function of EC_a (dS m^{-1}) and the AMF. ● M1—control plants without fungal inoculum; ■ M2—plants with *G. albida* fungal inoculum; ▲ M3—plants with *G. albida* fungal inoculum plus soil microbiota. D, $n = 3$. Similar lowercase letters in columns (AMF) indicate no statistical difference according to Tukey's test ($p < 0.05$), *** $p < 0.001$; ** $p < 0.01$ indicate significance for regression and ns—not significant.

The spore density was higher in the M3 plants compared to the M2 and M1 plants at all EC_a levels (Figure 8B). The highest spore density in M3 occurred at the 2.9 dS m^{-1} level, corresponding to 650 spores per 50 dm^3 of soil. At the 4.4 dS m^{-1} level, there was a 29% reduction in the number of spores compared to the 3.1 dS m^{-1} level. Treatments M1 and M2 did not differ from each other (Figure 8B).

4. Discussion

4.1. Physiological Response of Maize Irrigated with Saline Waste and Inoculated with the AMF G. albida

Irrigation with saline waste reduced the gas exchange and photochemical efficiency in all the maize plants, regardless of the mycorrhizal treatment, limiting the gs, AN, and E, while increasing the A/gs and leaf temperature.

Irrigation with saline water affected the photosynthetic tissues, reduced photosynthesis, and consequently, plant productivity [19]. This reduction occurred due to variations in the osmotic potential caused by excess salts, leading to a decrease in the water content within plant cells, directly affecting physiological processes [53].

As indicated by the results, the reduction in gs, AN, and E in maize is due to stomatal closure, one of the plant's first responses to osmotic stress induced by an increase in soil EC_a [54]. This response is a physiological strategy that plants use to reduce transpiration and limit water loss. However, stomatal closure also reduces CO_2 influx, since assimilation depends on substomatal air spaces for carboxylation sites [55].

The increase in leaf temperature in all the maize plants was due to stomatal closure and reduced E, which is also a pathway that aids in the dissipation of leaf heat. These results correspond to the findings of [56], who observed reductions in E, gs, and AN, as well as an increase in Tl in maize plants as a result of increasing irrigation water EC_a.

Damage to the photosystems is reinforced by the decrease in ETR, which showed a significant interaction with the EC_a levels and mycorrhizal conditions in the soil. The M1 and M2 plants' ETR increase with the EC_a level up to 2.3 dS m^{-1}, demonstrating a high amount of energy, whereas the M3 condition showed a linear decrease as a function of saline waste EC_a, indicating a greater capacity for ETR adaptation to salinity levels. Ref. [57] states that the effects of salinity can reduce the electron transport rate (ETR), probably due to a higher consumption rate of ATP and NADPH, leading to reduced CO_2 assimilation [58].

Damage to the photosystems was also confirmed by the reduction in quantum efficiency (Y) and the maximum quantum efficiency of PSII (Fv/Fm) at higher EC_a levels. The reductions in these parameters indicate a restriction in the photochemical capacity of maize plants [59,60]. Similarly, the Fv/Fm ratio indicated disturbances to the photosynthetic system. Its decrease indicated a decline in PSII photochemical efficiency [61].

The increase in Fo' and YNPQ in the maize plants also supported the hypothesis of damage to the photosynthetic apparatus. The accumulation of energy in chlorophyll, indicated by Fo', explains the increase in YNPQ, suggesting that energy dissipation occurred in the form of heat through the regulatory photoprotective mechanism, the xanthophyll cycle [62]. This result suggests a high photoprotective capacity in maize plants, especially at higher salinity levels, with a more intense response in plants exposed to *G. albida* alone (M2).

Indeed, our findings indicate that irrigation with saline waste affects the physiology of Creole maize plants. However, the level of damage to photosynthesis was considered low compared to other reports in the literature. In one study [63], at a similar EC_a level (4.5 dS m^{-1}), the gs, E, and A/gs values were lower than those found in this study, with respective increases of 150%, 25%, and 400% in Creole maize. These results are likely due to the characteristics of the Creole variety itself, which, by its nature, has greater

adaptive capacity to conditions in its cultivation areas [64]. Additionally, it was noted that interaction with *G. albida* produced a better performance in terms of energy dissipation as heat, a characteristic already present in Creole maize and intensified by *G. albida.*

4.2. Na/K Balance in the Growth and Development of Creole Corn Irrigated with Saline Waste and Inoculated with the AMF Gigaspora albida

Saline waste contains high concentrations of Na^+ and Cl^- ions in its composition. Irrigation with this residue affects plant development [65] and disrupts ionic homeostasis in photosynthetic tissues, causing damage to plant physiological processes [66]. Our findings indicate that the interaction between *G. albida* and soil microbiota helped mitigate the effects of high salinity in different parts of the plants, alleviating salt stress through a reduction in ionic stress.

Corn plants irrigated with saline waste exhibited an increased sodium content due to the higher electrical conductivity (EC_a). However, the association with the AMF *G. albida* (M2) and *G. albida* combined with soil microbiota (M3) reduced the Na^+ content while maintaining K^+ influx in leaf tissues, promoting ionic balance and reducing the Na^+/K^+ ratio in the leaves, particularly at intermediate EC_a levels. This suggests a mitigating effect that reduced ionic stress in photosynthetic tissues.

In the control plants (M1), the sodium accumulation in the leaf tissues and other plant parts was the highest compared to the other treatments. This clearly indicates that plants without association with *G. albida* were less selective in sodium uptake. Even though they maintained a high potassium influx, the excessive sodium accumulation increased the foliar Na^+/K^+ ratio, negatively impacting plant growth.

A study [28] demonstrated that *G. albida* improved the tolerance of eucalyptus seedlings by enhancing the K^+/Na^+ ratio and reducing sodium accumulation. These results reinforce our findings, suggesting that *G. albida* may contribute to reducing sodium levels in corn leaves under high EC_a conditions.

The sodium accumulation in the stalk increased linearly with the EC_a level in all the corn plants. However, the Na^+ concentration was modulated by the mycorrhizal treatments. Plants in the M3 group accumulated less sodium than those in the M1 and M2 groups, indicating a higher degree of selectivity for this ion in the stalk due to the interaction between *G. albida* and soil microbiota. On the other hand, the K^+ concentration varied among the mycorrhizal treatments. In M1, the K^+ levels significantly increased up to 2.7 dS m^{-1} but did not remain high at elevated EC_a levels (4.4 dS m^{-1}), suggesting possible competition with Na^+ ions, which may have limited K^+ uptake [66].

For the M2 plants, the K^+ accumulation was linear, whereas in M3, it occurred at the highest salinity level (4.4 dS m^{-1}). This supports the idea that *G. albida* may have induced an adaptive response in corn plants by enhancing K^+ absorption and maintaining a lower Na^+/K^+ ratio, particularly at higher salinity levels. This suggests an effort to maintain cellular osmotic potential and sustain stomatal turgor pressure, thereby improving the photosynthetic processes [67,68].

The Na^+ concentration in the roots of the M1 and M2 plants increased linearly with EC_a. However, in M3, the highest concentration was only observed at the highest EC_a level (4.4 dS m^{-1}), which increased the root Na^+/K^+ ratio. The allocation of Na^+ to root cells may act as a defense mechanism to reduce ionic toxicity in photosynthetic tissues while increasing potassium influx, lowering root osmotic potential, and improving water uptake [6]. This enhances the plant's tolerance to high salinity effects [16].

The results in the M3 plants may reflect the benefits conferred by the AMF–soil microbiota interactions. Salinity conditions can induce higher expression of genes encoding membrane transporter proteins, which directly contribute to Na^+ extrusion into the soil solution and K^+ influx into the xylem, thereby maintaining a favorable Na^+/K^+ ratio [19,69].

For corn, the literature indicates that the expression of genes such as *ZmAKT2*, *ZmSOS1*, and *ZmSKOR* in the roots contributes to K^+ and Na^+ homeostasis [70]. Additionally, under high salt stress conditions, another significant contribution of AMFs is the expression of aquaporins, proteins that regulate water flow across membranes in both leaves and roots, thereby improving plant water availability [71].

The lower Na^+/K^+ ratio in the aerial parts and higher ratio in the roots of the M3 plants may have provided favorable water and nutrient conditions, enhancing growth [19].

Our findings suggest that *G. albida* in combination with soil microbiota improved plant growth and development in the M3 plants. When comparing biomass production in M1 with that of M3, the results indicate that the increased dry shoot mass (MSPA), plant height (AP), number of leaves (NF), and stem diameter (DC) observed in this treatment resulted from improved ionic homeostasis induced by the symbiotic relationship between the corn plants, *G. albida*, and soil microbiota interactions. However, despite the high Na^+/K^+ ratio in the leaves and stems of M1 plants, these plants showed the second-best performance in terms of growth and biomass accumulation, demonstrating the strong adaptive capacity of Creole corn.

The benefits of *G. albida* have been widely reported in the literature. To improve the quality of *Dipteryx alata* seedlings, Ref. [26] investigated the benefits of *G. albida* in seedling development and found that its symbiotic interaction enhanced the relative water content (TRA) in plants. It was reported that, under severe salinity conditions (10, 15, and 20 dS m^{-1}), *G. albida* increased eucalyptus seedling tolerance by maintaining the RWC above 60% at the highest level (20 dS m^{-1}), with even higher percentages at lower salinity levels [28].

The increased MSPA, AP, NF, and DC in the M3 corn plants likely resulted from improved water and nutrient conditions induced by the symbiotic relationship between *G. albida* and the soil microbiota, particularly under intermediate salinity conditions (2.5 dS m^{-1}) where the most significant gains were observed. In M2, under the effect of EC_a, the MSPA, root dry mass (MSRA), AP, NF, and DC were the least significant among treatments, even though the foliar Na^+/K^+ ratio was reduced. This suggests that inoculation with *G. albida* alone (without the complete soil microbiota) was insufficient to mitigate the negative effects of high salinity.

Under high EC_a levels, the root growth in the corn plants was modulated by the mycorrhizal treatments. The difference in the MSRA between M3 and M1 (control) at 2.0 dS m^{-1} was associated with the beneficial effects of *G. albida* and native soil microbiota interactions. According to the literature, mycorrhizal plants under intermediate salinity conditions may develop a more extensive root system to improve soil exploration, water uptake, and nutrient absorption [72].

The increased root development in M1 at 4.4 dS m^{-1} may indicate an adjustment mechanism in the allocation of photoassimilates, clearly represented in the root-to-shoot ratio (R/PA). This suggests that the M1 plants directed more energy toward root development, explaining the reduction in shoot dry mass (MSRA). The lower root investment in M3 may result from a more linear adjustment and greater adaptation to Na^+ accumulation in root cells. Sodium accumulation may have induced better osmotic adjustment and an improved root water status, explaining the increased SDM even at the highest EC_a level (4.4 dS m^{-1}).

4.3. Gigaspora albida's Response to the Reverse Osmosis Brine

Soil salinity affects not only plants but can also interfere with hyphal growth and development, the colonization capacity, and the spore germination of AMFs [73]. In this study, the colonization percentage of *G. albida* in the M2 maize plants increased as a function

of the EC_a of the saline brine. On the other hand, the plants in the M3 group showed a gradual adjustment, with a tendency toward higher colonization at higher saline levels. In saline environments, several factors can influence colonization, affecting spore germination, reducing fungal growth, and impairing the propagation of hyphae and arbuscules [74,75].

A recent study [76] showed that the interaction between AMFs and soil bacteria modulated maize growth and increased AMF colonization by 80% under high salinity conditions. Ref. [77] using strains of the AMF *Claroideoglomus claroideum* (Cc), observed an increase in the colonization of lettuce (*Lactuca sativa*) plants, resulting in higher yields and improved nutritional conditions for the crop.

In this study, plant colonization in the M2 group was lower compared to that of M3. This reduction was due to the presence of a single AMF, *G. albida*. However, high salinity was not a limiting factor for colonization. In M3, colonization decreased with increasing EC_a but showed a tendency to rise again. Nonetheless, compared to the M2 plants, colonization in the M3 plants was higher, which may be attributed to the interaction of *G. albida* with native AMF species in the soil and other organisms that possibly enhanced the mycorrhizal effect in maize plants, helping to alleviate the salt stress.

The tolerance of *G. albida* to high salinity levels (10, 15, and 20 dS m^{-1}) in eucalyptus clones was also confirmed in [28], where greater root colonization and spore density with *G. albida* were observed.

Spore density was affected by the salinity of the brine at the highest level. However, at an intermediate level (2.9 dS m^{-1}), there was a greater AMF response in terms of spore production. This behavior was similar across all three mycorrhizal conditions, indicating that this salinity level stimulated the highest sporulation potential of AMF in this study. Comparing the mycorrhizal treatments, the significant increase in spore density in M3 compared to M2 was due to the combination of spores of *G. albida* with the spores of native AMFs in the soil. Although there was no statistical difference between M1 and M2 at 2.9 dS m^{-1}, the number of spores in M2 increased by 53%, indicating that *G. albida* was also sporulating. These results suggest that intermediate salinity levels may induce higher spore production in *G. albida*, which may also positively affect native AMFs in the soil.

The results of Ref. [78] support our findings; they observed an increase in AMF spore numbers in a rotational maize and bean crop irrigated with saline water. Ref. [79] found that the increase in spore numbers under high salinity conditions was due to the adaptive capacity of AMF communities. There are few literature reports on the effects of high salinity on arbuscular mycorrhizal fungal spore induction. In this study, the evaluation period was short (50 days), and the results are still preliminary, requiring further long-term field studies to better understand the effects of high salinity on spore production and to determine the salinity threshold beyond which germination may be adversely affected.

5. Conclusions

Irrigation with saline wastewater produced using reverse osmosis affects the physiology of *criollo* maize. The symbiotic relationship in both mycorrhizal treatments, M2 and M3, mitigated the effects of excess energy in PSII by promoting heat dissipation.

The interaction between *G. albida* and the soil microbiota mitigated the ionic stress in the aerial part of *criollo* maize by favoring a lower Na^+/K^+ ratio and higher MSPA, MSRA, AP, and DC between the levels of 1.8 and 3.1 dS m^{-1}.

Criollo maize irrigated with saline wastewater adapted by investing in root growth to tolerate the high salinity.

The interaction of *G. albida* with criollo maize was not sufficient to mitigate the negative effects of high salinity, resulting in the lowest growth performance.

Irrigation with wastewater reduced the colonization percentage of *G. albida* in the roots. An EC of 2.9 dS m^{-1} increased the spore density in the soil.

Author Contributions: M.V.d.M.A.: Conceptualization, Methodology, Validation, Formal Analysis, Investigation, Data Curation, Writing—Original Draft, Visualization, Writing—Review and Editing. N.d.S.D.: Writing—Original Draft, Visualization, Writing—Review and Editing, Supervision, Project administration. C.C.d.A.: Validation, Writing—Original Draft, Writing—Review and Editing, Visualization, Supervision. E.C.M.S.: Writing—Original Draft, Writing—Review and Editing, Visualization, Supervision. P.H.d.A.G.: Methodology, Investigation. M.F.C.F.: Methodology, Investigation. M.H.d.A.S.: Methodology, Investigation. N.d.S.R.: Methodology, Investigation. M.A.C.L.: Methodology, Investigation. M.E.d.C.S.: Methodology, Investigation. L.Â.M.: Methodology. K.T.O.P.: Writing—Original Draft, Writing—Review and Editing. R.C.L.M., Writing—Original Draft, Writing—Review and Editing. M.C.d.M.: Methodology, J.F.d.M.: Writing—Original Draft, Writing—Review and Editing. All authors have read and agreed to the published version of the manuscript.

Funding: This research received no external funding.

Institutional Review Board Statement: Not applicable.

Data Availability Statement: The data generated and analyzed during the current study are available from the corresponding author upon request.

Acknowledgments: The authors thank the Federal Rural University of Semi-Arid, in partnership with the State University of Rio Grande do Norte and the Coordination for the Improvement of Higher Education Personnel (CAPES), for providing a scholarship.

Conflicts of Interest: The authors declare that they have no known competing financial interests or personal relationships that could have appeared to influence the work reported in this paper.

References

1. Gheyi, H.R.; Paz, V.P.S.; Medeiros, S.S.; Galvão, C.O. *Recursos Hídricos em Regiões Semiáridas: Estudos e Aplicações*; Instituto Nacional do Semiárido: Campina Grande, Brazil; Universidade Federal do Recôncavo da Bahia: Cruz das Almas, Brazil, 2011.
2. da Silva Dias, N.; dos Santos Fernandes, C.; de Sousa Neto, O.N.; da Silva, C.R.; da Silva Ferreira, J.F.; da Silva Sá, F.V.; de Oliveira Batista, C.N. Potential Agricultural Use of Reject Brine from Desalination Plants in Family Farming Areas. In *Saline and Alkaline Soils in Latin America: Natural Resources: Management and Productive Alternatives*; Springer: Cham, Switzerland, 2021; pp. 101–118.
3. Dias, N.S.; Blanco, F.F.; Souza, E.R.; Ferreira, J.F.S.; Neto, O.N.S.; Queiroz, Í.S.R. Efeitos dos sais na planta e tolerância das culturas à salinidade. In *Manejo da Salinidade na Agricultura: Estudos Básicos e Aplicados*; Gheyi, H.R., Dias, N.S., Lacerda, C.F., Gomes Filho, E., Eds.; INCTSal: Fortaleza, Brazil, 2016; pp. 151–162.
4. Venancio, J.B.; Da Silva Dias, N.; De Medeiros, J.F.; De Moraes, P.L.D.; Nascimento, C.W.A.; Sousa Neto, O.N.; Silva Sá, F.V. Yield and 24 morphophysiology of onion grown under salinity and fertilization with silicon. *Sci. Hortic.* **2022**, *301*, 111095. [CrossRef]
5. Qun, W.; Shao, H.; Xu, Z.; Liu, J.; Zhang, D.; Huang, Y. Salinity tolerance mechanism of osmotin and osmotin-like proteins: A promising candidate for enhancing plant salt tolerance. *Curr. Genom.* **2017**, *18*, 553–556.
6. Wang, H.; An, T.; Huang, D.; Liu, R.; Xu, B.; Zhang, S.; Deng, X.; Siddique, K.H.M.; Chen, Y. Arbuscular mycorrhizal symbioses alleviating salt stress in maize is associated with a decline in root-to-leaf gradient of Na+/K+ ratio. *BMC Plant Biol.* **2021**, *21*, 457. [CrossRef]
7. Sá, F.D.S.; Gheyi, H.R.; De Lima, G.S.; Ferreira Neto, M.; De Paiva, E.P.; Silva, L.D.A.; Moreira, R.C.L. Cultivation of West Indian cherry irrigated with saline water under phosphorus and nitrogen proportions. *Semin. Ciênc. Agrár.* **2020**, *41*, 395–406. [CrossRef]
8. Sá, F.V.D.S.; Silva, I.E.D.; Ferreira Neto, M.; Lima, Y.B.D.; Paiva, E.P.D.; Gheyi, H.R. Phosphorus doses alter the ionic homeostasis of cowpea irrigated with saline water. *Rev. Bras. Eng. Agríc. E Ambient.* **2021**, *25*, 372–379. [CrossRef]
9. Okan, O. Effect of Salinity on Physiological Processes in Plants. In *Microorganisms in Saline Environments: Strategies and Functions, Soil Biology*; Giri, B., Varma, A., Eds.; Springer: Berlin/Heidelberg, Germany, 2019; Volume 56, pp. 237–262.
10. Goharrizi, K.J.; Amirmahani, F.; Salehi, F. Assessment of changes in physiological and biochemical traits in four pistachio rootstocks under drought, salinity and drought + salinity stresses. *Physiol. Plant.* **2020**, *168*, 973–989. [CrossRef]
11. Brito, M.E.B.; Fernandes, P.D.; Gheyi, H.R.; Melo, A.S.; Filho, W.S.S.; Santos, R.T.S. Sensibilidade à salinidade de híbridos trifoliados e outros porta-enxertos de citros. *Rev. Caatinga* **2014**, *27*, 17–27.

12. Santos, M.R.D.; Brito, C.F.B. *Irrigation with Saline Water, Conscious Agricultural Option*; Universidade Estadual de Goiás: Anápolis, Brazil, 2016.
13. Gul, Z.; Tang, Z.H.; Arif, M.; Ye, Z. An insight into abiotic stress and influx tolerance mechanisms in plants to cope in saline environments. *Biology* **2022**, *11*, 597. [CrossRef]
14. Sarker, U.; Oba, S. The response of salinity stress-induced A. tricolor to growth, anatomy, physiology, non-enzymatic and enzymatic antioxidants. *Front. Plant Sci.* **2020**, *11*, 559876. [CrossRef]
15. Fageria, N.K. *Solos Tropicais e Aspectos Fisiológicos das Culturas*; EMBRAPA-DPU: Brasília, Brazil, 1989; p. 425.
16. Dar, M.H.; Razvi, S.M.; Singh, N.; Mushtaq, A.; Dar, S.; Hussain, S. Arbuscular mycorrhizal fungi for salinity stress: Anti-stress role and mechanisms. *Pedosphere* **2023**, *33*, 212–224. [CrossRef]
17. Wakeel, A. Potassium-sodium interactions in soil and plant under saline-sodic conditions. *J. Plant Nutr. Soil Sci.* **2013**, *176*, 344–354.
18. Folli-Pereira, M.D.S.; Meira-Haddad, L.S.A.; Bazzolli, D.M.S.; Kasuya, M.C.M. Arbuscular mycorrhiza and plant tolerance to stress. *Rev. Bras. Ciênc. Solo* **2012**, *36*, 1663–1679.
19. Evelin, H.; Devi, T.S.; Gupta, S.; Kapoor, R. Mitigation of salinity stress in plants by arbuscular mycorrhizal symbiosis: Current understanding and new challenges. *Front. Plant Sci.* **2019**, *10*, 470.
20. Ndiate, N.I.; Zaman, Q.U.; Francis, I.N.; Dada, O.A.; Rehman, A.; Asif, M.; Haider, F.U. Soil amendment with arbuscular mycorrhizal fungi and biochar improves salinity tolerance, growth, and lipid metabolism of common wheat (*Triticum aestivum* L.). *Sustainability* **2022**, *14*, 3210. [CrossRef]
21. Lúcio, W.S.; Lacerda, C.F.; Filho, P.F.M.; Hernandez, F.F.F.; Neves, A.L.R.; Gomes-Filho, E. Growth and physiological responses of melon plants inoculated with mycorrhizal fungi under salt stress. *Semin. Ciênc. Agrár.* **2013**, *34*, 1587–1602.
22. Souza, M.C.G.D.; Morais, M.B.D.; Andrade, M.D.S.; Vasconcelos, M.A.D.; Sampaio, S.S.; Albuquerque, C.C.D. Mycorrhization and saline stress response in Hyptis suaveolens. *Ciênc. Rural* **2020**, *50*, 1–10.
23. Giri, B.; Kapoor, R.; Mukerji, K.G. Improved tolerance of Acacia nilotica to salt stress by arbuscular mycorrhiza, Glomus fasciculatum may be partly related to elevated K/Na ratios in root and shoot tissues. *Microb. Ecol.* **2007**, *54*, 753–760.
24. Colla, G.; Rouphael, Y.; Cardarelli, M.T.; Tullio, M.; Rivera, C.M.; Rea, E. Alleviation of salt stress by arbuscular mycorrhizal in zucchini plants grown at low and high phosphorus concentration. *Biol. Fertil. Soils* **2008**, *44*, 501–509.
25. Evelin, H.; Kapoor, R.; Giri, B. Arbuscular mycorrhizal fungi in alleviation of salt stress: A review. *Ann. Bot.* **2009**, *104*, 1263–1280.
26. Souza, T.; Souza, T. Glomeromycota classification. In *Handbook of Arbuscular Mycorrhizal Fungi*; Springer: Berlin/Heidelberg, Germany, 2015; pp. 87–128.
27. Souza, G.G.; Santos, S.C.; Santos, C.C.; Dias, A.S.; Silverio, J.M.; Trovato, V.W.; Flauzino, D.S. Fungos micorrízicos arbusculares promovem o crescimento de Dipteryx alata Vogel. *Rev. Bras. Biol.* **2023**, *83*, 275172.
28. Klinsukon, C.; Lumyong, S.; Kuyper, T.W.; Boonlue, S. Colonization by arbuscular mycorrhizal fungi improves salinity tolerance of eucalyptus (*Eucalyptus camaldulensis*) seedlings. *Sci. Rep.* **2021**, *11*, 4362. [CrossRef] [PubMed]
29. Fall, A.F.; Nakabonge, G.; Ssekandi, J.; Founoune-Mboup, H.; Apori, S.O.; Ndiaye, A.; Badji, A.; Ngom, K. Roles of Arbuscular Mycorrhizal Fungi on Soil Fertility: Contribution in the Improvement of Physical, Chemical, and Biological Properties of the Soil. *Front. Fungal Biol.* **2022**, *3*, 723892.
30. Boorboori, M.; Lackóová, L. Arbuscular mycorrhizal fungi and salinity stress mitigation in plants. *Front. Plant Sci.* **2025**, *15*, 1504970.
31. Zhou, Y.; Liu, D.; Li, F.; Yuanhua, D.; Jin, Z.; Liao, Y.; Li, X.; Peng, S.; Delgado-Baqueirizo, M.; Li, X. Superiority of native soil core microbiomes in supporting plant growth. *Nat. Commun.* **2024**, *15*, 6599.
32. Nanjudappa, A.; Bagyaraj, D.J.; Saxena, K.A.; Kumar, M.; Chakdar, H. Interaction between arbuscular mycorrhizal fungi and Bacillus spp. in soil enhancing growth of crop plants. *Fungal Biol. Biotechnol.* **2019**, *6*, 23.
33. Artursson, V.; Finlay, R.D.; Jansson, J.K. Interactions between arbuscular mycorrhizal fungi and bacteria and their potential for stimulating plant growth. *Environ. Microbiol.* **2005**, *8*, 1.
34. Hashem, A.; Abd_Allah, E.F.; Alqarawi, A.A.; Al-Huqail, A.A.; Wirth, S.; Egamberdieva, D. The Interaction between Arbuscular Mycorrhizal Fungi and Endophytic Bacteria Enhances Plant Growth of Acacia gerrardii under Salt Stress. *Front. Microbiol.* **2016**, *7*, 1089.
35. Conti, G.; Urcelay, C.; Gundel, P.E.; Piñeiro, G. The potential of arbuscular mycorrhizal fungi to improve soil organic carbon in agricultural ecosystems: A meta-analytical approach. *Ecol. Func.* **2025**, 1–15. [CrossRef]
36. Silva, F.C.D. *Manual de Análises Químicas de Solos, Plantas e Fertilizantes*, 2nd ed.; Embrapa Informação Tecnológica: Brasília, Brazil, 2009; p. 627.
37. Freitas, M.S.M.; Martins, M.A.; Vieira, I.J.C. Produção e qualidade de óleos essenciais de *Mentha arvensis* em resposta à inoculação de fungos micorrízicos arbusculares. *Pesqui. Agropecu. Bras.* **2004**, *39*, 887–894.
38. Hoagland, D.R.; Arnon, D.I. *The Water-Culture Method for Growing Plants Without Soil*; California Agricultural Experiment Station: Berkeley, CA, USA, 1950; p. 347.

39. Von Pinho, R.G.; Borges, I.D.; Pereira, J.L.D.A.R.; Dos Reis, M.C. Marcha de absorção de macronutrientes e acúmulo de matéria seca em milho. *Rev. Bras. Milho E Sorgo* **2009**, *8*, 157–173.
40. Campos, D.T.S.; Andrade, J.A.C.; Cassiolato, A.M.R. Crescimento e micorrízação de genótipos de milho em casa de vegetação. *Bragantia* **2021**, *69*, 555–562. [CrossRef]
41. Sá, F.D.S.; Gheyi, H.R.; De Lima, G.S.; De Paiva, E.P.; Silva, L.D.A.; Moreira, R.C.L.; Fernandes, P.D.; Dias, A.S. Ecophysiology of West Indian cherry irrigated with saline water under phosphorus and nitrogen doses. *Biosci. J.* **2019**, *35*, 211–221. [CrossRef]
42. Oxborough, K.; Baker, N.R. Resolving chlorophyll a fluorescence images of photosynthetic efficiency into photochemical and non-photochemical components–calculation of qP and Fv-/Fm-; without measuring Fo. *Photosynth. Res.* **1997**, *54*, 135–142. [CrossRef]
43. Kramer, D.M.; Johnson, G.; Kiirats, O.; Edwards, G.E. New fluorescence parameters for the determination of QA redox state and excitation energy fluxes. *Photosynth. Res.* **2004**, *79*, 209–218. [CrossRef] [PubMed]
44. Huerta, A.S. Comparación de métodos de laboratorio y de campo para el área del cafeto. *Cenicafé* **1932**, *13*, 33–42.
45. Gomide, M.B.; Lemos, O.V.; Tourino, D.; Carvalho, M.M.; Carvalho, J.G.; Duarte, C.S. Comparação entre métodos de determinação de área foliar em cafeeiros Mundo Novo e Catuaí. *Ciênc. Prát.* **1977**, *1*, 118–123.
46. Benincasa, M.M.P. *Análise de Crescimento de Plantas*; FUNEP: Jaboticabal, Brazil, 1988.
47. Phillips, J.M.; Hayman, D.S. Improved procedures for clearingf roots and staining parasitic and vesicular-arbuscular mycorrhizal fungi for rapid assessment of infection. *Trans. Br. Mycol. Soc.* **1970**, *55*, 158–161. [CrossRef]
48. Giovanetti, M.; Mosse, B. An evaluation of techniques for measuring vesicular arbuscular mycorrhizal infection in roots. *New Phytol.* **1908**, *84*, 489–500. [CrossRef]
49. Gerdemann, J.W.; Nicolson, T.H. Spores of mycorrhizal Endogone species extracted from soil by wet sieving and decanting. *Trans. Br. Mycol. Soc.* **1963**, *46*, 235–244. [CrossRef]
50. Jenkins, W.R. A rapid centrifugal flotation technique for separating nematodes from soil. *Plant Dis. Report.* **1964**, *48*, 338.
51. Malibari, A.A.; Fassi, F.A.; Ramadan, E.M. Incidence and infectivity of vesicular-arbuscular mycorrhizas in some saudi soils. *Plant Soil* **1988**, *122*, 105–111.
52. Ferreira, D.F. Sisvar: A Computer Analysis System To Fixed Effects Split Plot Type Designs. *Rev. Bras. Biom.* **2019**, *37*, 529–535.
53. Negrão, S.; Schmöckel, S.M.; Tester, M. Evaluating physiological responses of plants to salinity stress. *Ann. Bot.* **2017**, *119*, 1–11. [CrossRef]
54. Mastrogiannidou, E.; Chatzissavvidis, C.; Antonopoulou, C.; Tsabardoukas, V.; Giannakoula, A.; Therios, I. Response of pomegranate cv. wonderful plants to salinity. *J. Soil Sci. Plant Nutr.* **2016**, *16*, 621–636.
55. Zahra, N.; Hinai, M.S.A.; Hafeez, M.B.; Rehman, A.; Wahid, A.; Siddique, K.H.M.; Farooq, M. Regulation of photosynthesis under salt stress and associated tolerance mechanisms. *Plant Physiol. Biochem.* **2022**, *178*, 55–69. [PubMed]
56. Rodrigues, V.D.S.; Sousa, G.G.D.; Soares, S.D.C.; Leite, K.N.; Ceita, E.D.; Sousa, J.T.M.D. Gas exchanges and mineral content of corn crops irrigated with saline water. *Rev. Ceres* **2021**, *68*, 453–459.
57. Tatagiba, S.D.; Moraes, G.A.B.K.; Nascimento, K.J.T.; Peloso, A.F. Limitações fotossintéticas em folhas de plantas de tomateiro submetidas a crescentes concentrações salinas. *Rev. Eng. Na Agric.* **2014**, *22*, 138–149. [CrossRef]
58. Penella, C.; Landi, M.; Guidi, L.; Nebauer, S.G.; Pellegrini, E.; San Bautista, A.; Calatayud, A. Salt-tolerant rootstock increases yield of pepper under salinity through maintenance of photosynthetic performance and sinks strength. *J. Plant Physiol.* **2016**, *193*, 1–11. [CrossRef]
59. Klughammer, C.; Schreiber, U. Complementary PSII quantum yield calculated from simple fluorescence parameters measured by PAM fluorometry and saturation pulse method. *PAM Appl. Notes* **2008**, *1*, 27–35.
60. Silva, S.S.D.; Lima, G.S.D.; Lima, V.L.A.D.; Soares, L.A.D.A.; Gheyi, H.R.; Fernandes, P.D. Quantum yield, photosynthetic pigments and biomass of mini watermelon under irrigation strategies and potassium. *Rev. Caatinga* **2021**, *34*, 659–669.
61. Glynn, P.; Fraser, C.; Gillian, A. Foliar salt tolerance of Acer genotypes using chlorophyll fluorescence. *J. Arboric.* **2003**, *29*, 61–65.
62. Sacramento, B.L.D.; Azevedo Neto, A.D.D.; Alves, A.T.; Moura, S.C.; Ribas, R.F. Photosynthetic parameters as physiological indicators of tolerance to cadmium stress in sunflower genotypes. *Rev. Caatinga* **2018**, *31*, 907–916.
63. Sousa, H.C.; Sousa, G.G.D.; Lessa, C.I.; Lima, A.F.D.; Ribeiro, R.M.; Rodrigues, F.H.D.C. Growth and gas exchange of corn under salt stress and nitrogen doses. *Rev. Bras. Eng. Agríc. E Ambient.* **2021**, *25*, 174–181.
64. Zeven, A.C. Landraces: Uma revisão de definições e classificações. *Euphytica* **1998**, *104*, 127–139.
65. Khalid, M.F.; Huda, S.; Yong, M.; Li, L.; Li, L.; Chen, Z.H.; Ahmed, T. Alleviation of drought and salt stress in vegetables: Crop 885 responses and mitigation strategies. *Plant Growth Regul.* **2023**, *99*, 177–194.
66. Rabie, G.H.; Almadini, A.M. Role of bioinoculants in development of salt-tolerance of Vicia faba plants under salinity stress. *887 Afr. J. Biotechnol.* **2005**, *4*, 210–222.
67. White, P.J. Ion uptake mechanisms of individual cells and roots: Short-distance transport. In *Marschner's Mineral Nutrition of Higher Plants*; Marschner, P., Holanda, P., Eds.; Elsevier: Amsterdã, The Netherlands, 2012; pp. 7–47.

68. Ketehouli, T.; Idrice Carther, K.F.; Noman, M.; Wang, F.-W.; Li, X.-W.; Li, H.-Y. Adaptation of Plants to Salt Stress: Characterization of Na+ and K+ Transporters and Role of CBL Gene Family in Regulating Salt Stress Response. *Agronomy* **2019**, *9*, 687. [CrossRef]
69. Chen, J.; Zhang, H.; Zhang, X.; Tang, M. Arbuscular mycorrhizal symbiosis alleviates salt stress in black locust through improved photosynthesis, water status, and K+/Na+ homeostasis. *Front. Plant Sci.* **2017**, *8*, 1739.
70. Estrada, B.; Aroca, R.; Barea, J.M.; Ruiz-Lozano, J.M. Native arbuscular mycorrhizal fungi isolated from a saline habitat improved maize antioxidant systems and plant tolerance to salinity. *Plant Sci.* **2013**, *201*, 42–51.
71. Ouziad, F.; Wilde, P.; Schmelzer, E.; Hildebrandt, U.; Bothe, H. Analysis of expression of aquaporins and Na+/H+ transporters in tomato colonized by arbuscular mycorrhizal fungi and affected by salt stress. *Environ. Exp. Bot.* **2006**, *57*, 177–186.
72. Pellegrino, E.; Öpik, M.; Bonari, E.; Ercoli, L. Responses of wheat to arbuscular mycorrhizal fungi: A meta-analysis of field studies from 1975 to 2013. *Soil Biol. Biochem.* **2015**, *84*, 210–217.
73. Porcel, R.; Aroca, R.; Ruiz-Lozano, J.M. Salinity stress alleviation using arbuscular mycorrhizal fungi. A review. *Agron. Sustain. Dev.* **2012**, *32*, 181–200.
74. Juniper, S.; Abbott, L.K. Soil salinity delays germination and limits growth of hyphae from propagules of arbuscular mycorrhizal fungi. *Mycorrhiza* **2006**, *16*, 371–379.
75. Hirrel, M.C. The effect of sodium and chloride salts on the germination of Gigaspora margarita. *Mycologia* **1981**, *73*, 610–617.
76. Chen, Q.; Deng, X.; Elzenga, J.T.M.; Van Elsas, J.D. Effect of soil bacteriomes on mycorrhizal colonization by *captura*—Interactive effects on maize (*Zea mays* L.) growth under salt stress. *Biol. Fertil. Soils* **2022**, *58*, 515–525.
77. Santander, C.; Sanhueza, M.; Olave, J.; Borie, F.; Valentine, A.; Cornejo, P. Arbuscular mycorrhizal colonization promotes the tolerance to salt stress in lettuce plants through an efficient modification of ionic balance. *J. Soil Sci. Plant Nutr.* **2019**, *19*, 321–331.
78. Bezerra, M.E.J.; Lacerda, C.F.; Sousa, G.G.; Gomes, V.F.F.; Mendes Filho, P.F. Biomass, microbial activity and AMF in crop rotation system of maize/cowpea using saline water. *Eng. Agrícola Rev. Ciênc. Agron.* **2010**, *41*, 562–570.
79. Bencherif, K.; Boutekrabt, A.; Fontaine, J.; Laruelle, F.; Dalpe, Y.; Sahraoui, A.L.H. Impact of soil salinity on arbuscular mycorrhizal fungi biodiversity and microflora biomass associated with Tamarix articulata Vahll rhizosphere in arid and semi-arid Algerian areas. *Sci. Total Environ.* **2015**, *533*, 488–494.

agriculture

MDPI

Article

The Identification of Drought Tolerance Candidate Genes in *Oryza sativa* L. ssp. *Japonica* Seedlings through Genome-Wide Association Study and Linkage Mapping

Tao Liu [1], Shuangshuang Li [1], Haoqiang Du [1], Jingnan Cui [1], Shanbin Xu [1], Jingguo Wang [2], Hualong Liu [2], Detang Zou [2], Wenhe Lu [1,*] and Hongliang Zheng [1,2,*]

[1] College of Agriculture, Northeast Agricultural University, Harbin 150030, China; neaustudent@126.com (T.L.); shuangshuangli@neau.edu.cn (S.L.); 17390928573@163.com (H.D.); b20030102@neau.edu.cn (J.C.); 18713599521@126.com (S.X.)

[2] Key Laboratory of Germplasm Enhancement, Physiology and Ecology of Food Crops in Cold Region, Ministry of Education, Northeast Agricultural University, Harbin 150030, China; 55190292@163.com (J.W.); liuhualongneau@163.com (H.L.); zoudtneau@126.com (D.Z.)

* Correspondence: luwenhe60@163.com (W.L.); hongliangzheng@neau.edu.cn (H.Z.)

Abstract: Drought stress poses a significant threat to rice production, necessitating the identification of genes associated with drought tolerance. This study employed a combination of genome-wide association study (GWAS) and linkage mapping to pinpoint seedling drought tolerance genes in *Japonica* rice. Using the leaf rolling scale (LRS) as the phenotypic index, we assessed rice drought tolerance under polyethylene glycol-induced drought during the seedling stage. A lead SNP C8_28933410 by GWAS was identified, which was located within *qLRS-8-1* identified by linkage mapping on chromosome 8. Combing the LD block analyses and QTL interval, a 138.6 kb overlap interval was considered as the candidate region. Haplotype analysis, qRT-PCR, sequence analysis, and mutant phenotype verification led to the speculation that *LOC_Os08g05520* is a candidate gene associated with drought tolerance. Our findings provide a valuable reference for breeders aiming to enhance rice drought tolerance.

Keywords: *Japonica* rice; GWAS; linkage mapping; drought tolerance; candidate genes

1. Introduction

Rice is one of the main staple food crops globally, sustaining over four billion people. With increasing food demand due to industrialization and population growth, rice production faces significant opportunities and challenges. Approximately half of the world's rice production is affected to some extent by arid conditions [1]. Therefore, there is an urgent need for the development of drought-tolerant rice varieties in breeding programs. Breeders commonly employ leaf rolling as a negative selection criterion, where a plant with more rolled leaves under drought conditions is considered drought sensitive, serving as an indicator of drought severity. Leaf rolling quantitative trait loci (QTL) have been studied across different genetic backgrounds of rice. *qLRS1.1*, identified through meta-analysis, was found to reside in the same genomic region related to the leaf rolling score (LRS) [2–4]. Furthermore, *qLRI1-1*, *qLRI9-1*, and *qLRI10-1* were identified as the leaf rolling indices on chromosomes 1, 9, and 10, which explained 18.8%, 6.7%, and 8.3% of the phenotypic variance, respectively [5]. Meta-QTLs found that *qLRI9-1* was co-located with *DRO1* (deeper rooting 1) in the same region, which was a quantitative trait locus controlling root growth angle and negatively regulated by auxin in rice [6]. To date, 35 rolled-leaf mutants in rice have been identified, with several representative rolled-leaf genes successfully cloned, for example, *OsAGO7* (*ZIP/Ago7*) [7], *OsCOW1/NAL7* (narrow leaf 7) [8], *SLL1* (shallot-like 1) [9], *ADL1* (adaxialized leaf 1) [10], *LC2* (leaf inclination 2) [11], *NRL1* (narrow and rolled

leaf 1) [12,13], *ACL1* (abaxially curled leaf 1) [14], *ROC5* (rice outermost cell-specific gene 5) [15], *CFL1* (curly flag leaf 1) [16], *RL14* (rolling-leaf 14) [17], *SRL1* (semi-rolled leaf 1) [18], *OsZHD1* (a zinc finger homeodomain 1) [19], *OsMYB103L* (R2R3-MYB transcription factor) [20], *SLL2* (shallot-like 2) [21], *REL1* (rolled and erect leaf 1) [22], and *SRL2* (semi-rolled leaf 2) [23]. While most cloned rolled-leaf genes are associated with rice vesicular cells, only a few are related to the paraxial or distal polarity of rice leaf development.

The combination of genome-wide association study and linkage mapping provides a novel approach for the dissection of complex traits in crops. Generally, the joint analysis of these two methods enhances the reliability and accuracy of trait mapping. This has been demonstrated in various crops, revealing traits such as plant height and ear position [24], male inflorescence size [25], husk traits [26], *Fusarium verticillioides* seed rot resistance [27], thermotolerance of seed-set [28], and flower time-related traits [29] in maize. Coincident regions have also been identified for panicle traits in wheat [30]. Similarly, *qAT11* has been identified as a primary alkali tolerance QTL in rice [31]. These studies underscore the feasibility of identifying QTLs or genes associated with seedling drought through the integration of GWAS and linkage mapping.

In this study, we employed a joint analysis method to determine the genetic basis of drought tolerance in rice seedlings. Our findings highlight *LOC_Os08g05520* as a new candidate gene crucial for drought tolerance in rice breeding.

2. Materials and Methods

2.1. Plant Materials

The natural population consisted of 295 *Japonica* rice varieties originating from the three northeastern provinces of China, Russia, Japan, North Korea, and the Republic of Korea This natural population was also used in previous studies [31,32]. The RIL (Recombinant Inbred Lines) consists of 195 individuals constructed by KY131 (drought sensitive) and XBJZ (drought tolerant).

2.2. Drought Tolerance Evaluation at the Seedling Stage

The rice kernels were dried in a 40 °C oven for 7 days to break dormancy [33]. The seed surface was disinfected with 2.5% sodium hypochlorite for 30 min, rinsed with sterile water three times, and then immersed in distilled water for 2 days at 30 °C in a dark environment. Sixty seeds with the same bud length were divided into two parts and cultured in chernozem soil, with 10 seeds per treatment for three replicates. The seeds were grown in a light incubator at 27 °C during the day and 22 °C at night with a relative humidity of 70%. At the two leaves and one core stage, Yoshida nutrient solution (pH = 5.5, 460.854 mg/L) was added to the control every 7 days. Simultaneously, Yoshida plus 20% PEG-6000 nutrient solution (pH = 5.5, 460.854 mg/L) was used for treatment for 10 days. After 10 days of drought stress, LRS was evaluated in three replicates based on the standard evaluation system [34]. Leaf begins to fold (V-shaped) means LRS equals 1; deep leaf fold (deep V) means LRS equals 3; the blade is U-shaped means LRS equals 5; blade edges fastened together (O type) means LRS equals 7; and tightly crimped blade means LRS equals 9. GWAS and linkage analyses were performed using the mean values of three replicates of the LRS.

2.3. GWAS for Leaf Rolling

A total of 788,369 SNPs with minor allele frequency (MAF) $\geq$ 5% and missing rate $\leq$ 20% were selected for GWAS [32]. Considering the group structure and kinship, TASSEL 5.0 [35] was used for association analysis of the LRS using a mixed linear model (MLM). The number of valid and independent SNPs was counted using GEC software (http://pmglab.top/gec/#/download, accessed on 1 May 2021), considering $p < 5.46 \times 10^{-6}$ as the threshold to determine the significance of SNP marker association with LRS. If at least two significant SNPs were located in the same LD (linkage disequilibrium) interval, these SNPs were defined as the same QTL, and the SNP with the smallest p value was

regarded as the lead SNP. Manhattan maps and Q-Q plots were created using the CMplot package in R 3.3.2.

2.4. QTL Mapping for LRS

The linkage group was constructed using 527 bin markers and the 10 K Array genotype technique at the MOLBREEDING Biotech Company. The total length of the genetic map was 1875.6 cM, and the mean distance between the markers was 3.58 cM (Figure S1). QTL mapping was performed using the inclusive composite interval mapping (ICIM) method and QTL IciMapping Version 4.2 (https://isbreeding.caas.cn/rj/qtllcmapping/, accessed on 1 May 2021). The threshold for QTL identification (LOD score) was set to 3.0, and the step was set to 1 cM.

2.5. Haplotype Analysis and Quantitative Real Time PCR

In this study, the co-localisation intervals between GWAS and linkage mapping were regarded as important QTLs. In GWAS, if a significant site is a false positive, the site can be visually judged by LD block analysis. LDBlockShow was a fast and convenient tool for visualization LD and haplotype blocks based on variant call format files. To rule out false positive sites, the lead SNPs $\pm$ 2 Mb as a block were analysed by LDBlockShow [36]. SNPs with non-synonymous mutations (including the promoter region 1500 bp before ATG and exons of candidate genes) were downloaded from the Rice SNP-Seek Database (https://snp-seek.irri.org/_snp.zul, accessed on 1 May 2021). Haplotype analysis was performed on 295 *japonica* rice varieties using Origin Pro 2019b software, and the database which was utilized was "GWAS for Leaf Rolling in 2.3". The expression of candidate genes in the leaves was evaluated using qRT-PCR. After 24 h of drought stress with 20% PEG-6000, fresh leaves of KY131 and XBJZ were sampled under 20% PEG-6000 and control conditions. Total RNA was extracted using the TranZol Up RNA Kit (Trans Gen Biotech, Beijing, China). cDNA was synthesised from the total RNA using the HiFiScript cDNA Synthesis Kit (Cwbio, Beijing, China). qRT-PCR analysis was performed using a Roche LightCycler96 (Roche, Basel, Switzerland). All primer sequences are listed in Table S1. Relative gene expression quantity was calculated using the $2^{-\Delta\Delta Ct}$ method [37].

2.6. Prediction of Candidate Genes and Sequence Alignment

Based on the results of haplotype and gene expression analyses, *LOC_Os08g05520* was predicted to be a candidate gene. Thereafter, the candidate gene was cloned by PCR, and at the same time, sequencing was completed in KY131 and XBJZ. SnapGene software (https://www.snapgene.com/, accessed on 1 May 2021) was used for sequence alignment.

2.7. Acquisition of LOC_Os08g05520 Mutants

The mutant seeds of the T1 generation with a ZH11 genetic background were obtained from BIOGLE GENETECH (http://www.biogle.cn/, accessed on 1 May 2021), which was created using CRISPR/Cas9 in August 2020. During the next two seasons, the T1 seeds were planted in the field for seed propagation and separation. Finally, two homozygous T3 generation lines (named CR1 and CR2) were selected in October 2022, which had sufficient seeds for drought tolerance identification.

In osmotic stress, ZH11 wild, CR1, and CR2 were planted in two rows in one pool under two conditions (20% PEG-6000 treatment and control) for 10 days at the two leaves and one core stage. LRS was investigated with three repeats. In addition to osmotic stress, we analysed the differences in LRS between the mutants and wild type using the water deprivation method. The control was cultured under normal conditions. For the drought treatment, the plants were deprived of water for 20 days at the three-leaf stage. LRS and plant height were investigated with three repeats after 20 days' cultivation. The mutant and wild plants were then transplanted into pots for recovery culturing under the same cultivation conditions as those used in field production. At the maturity stage, plant heights, tillering numbers, effective panicle numbers, grain numbers per spike, thousand-grain

weights, and yields per plant were measured in triplicate in the treatment and control groups. Significance analysis ($p < 0.05$) and mapping were performed using the Origin software package (OriginLab origin 2019b).

3. Results

3.1. Phenotypic Variation

The mean values, standard deviations, and ranges for the natural population and 195 RILs are listed in Table S2. LRS varied significantly among the 295 accessions, ranging from 1.0 to 9.0, with a mean value of 5.0. The mean LRS for the 195 RILs was 4.7, with a range from 1.0 to 9.0. The frequency distribution of leaf rolling among the 295 accessions and the RIL population is shown in Figure 1a,b. The parents' performance under normal conditions and drought stress is illustrated in Figure 1c,d. The LRS of the parents under drought treatment was graded as 3.0 and 7.0, respectively. The distribution of phenotypic values basically conforms to normal distribution both in the natural and linkage population. All these prove that leaf rolling character belongs to quantitative character inheritance.

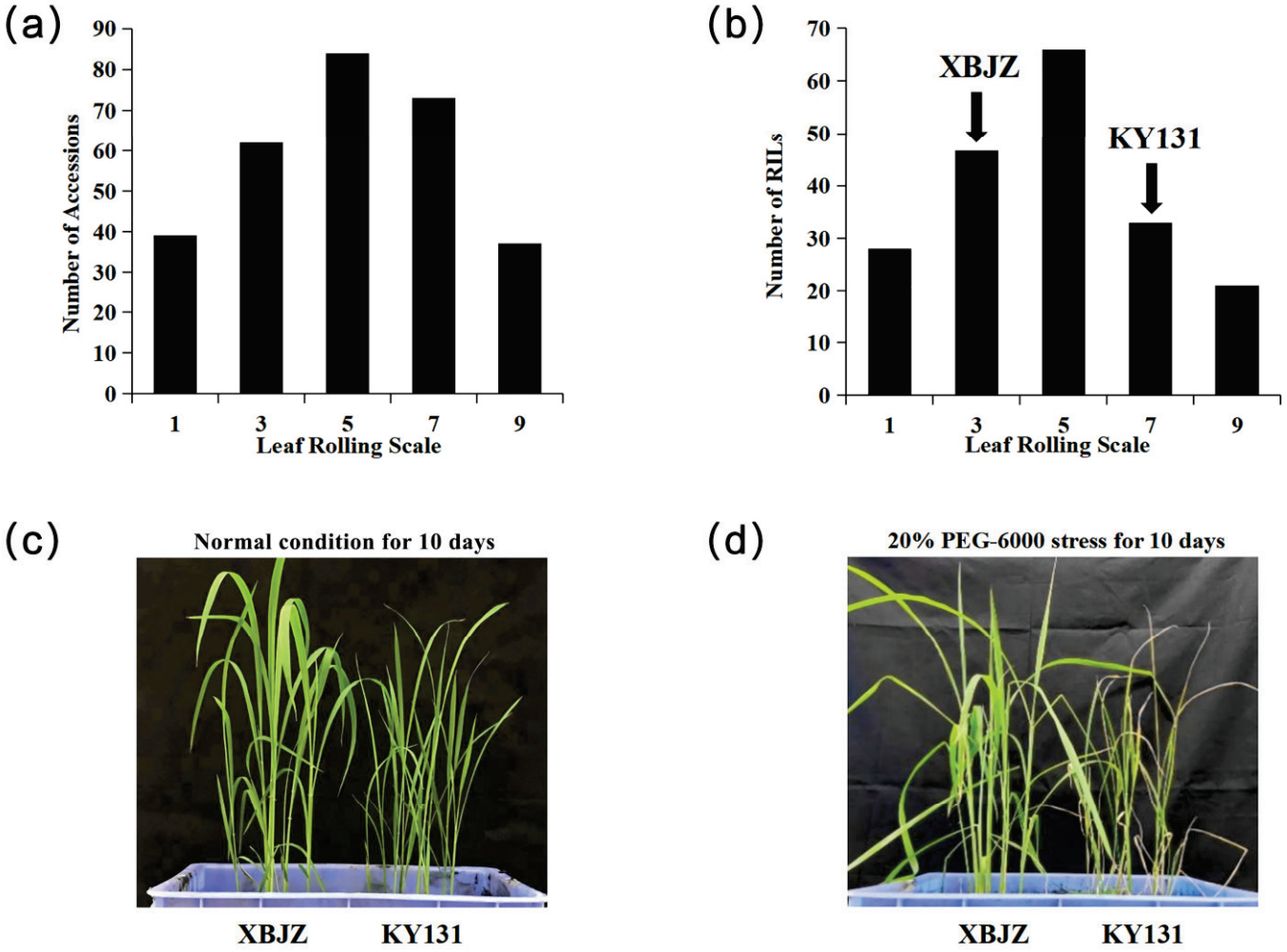

Figure 1. LRS variation of 295 accessions, RILs, parental performance under normal and drought conditions. (**a**) LRS distribution in natural populations. (**b**) LRS distribution in RILs. (**c**) performance of two parents under normal condition for 10 days at the two leaves and one core stage. (**d**) performance of two parents under 20% PEG-6000 stress for 10 days at the two leaves and one core stage.

3.2. GWAS for LRS in Natural Population

The GWAS results are showed in Manhattan and Q-Q plots in Figure 2a,b, respectively. Eight SNPs were significantly associated with leaf rolling (Table 1). These SNPs were

located on chromosomes 1, 4, 7, and 8, with R^2 values ranging from 10.11% to 14.16%. While sporadically distributed on chromosomes 1, 4, and 7, they exhibited a significant association with leaf rolling. Notably, on chromosome 8, four SNPs were distributed in clusters that were significantly associated with leaf rolling, indicating linkage disequilibrium among these SNPs. The bottom left corner of the Q-Q plots showed that the model was reasonable, and the top right corner showed that the correlation sites were found.

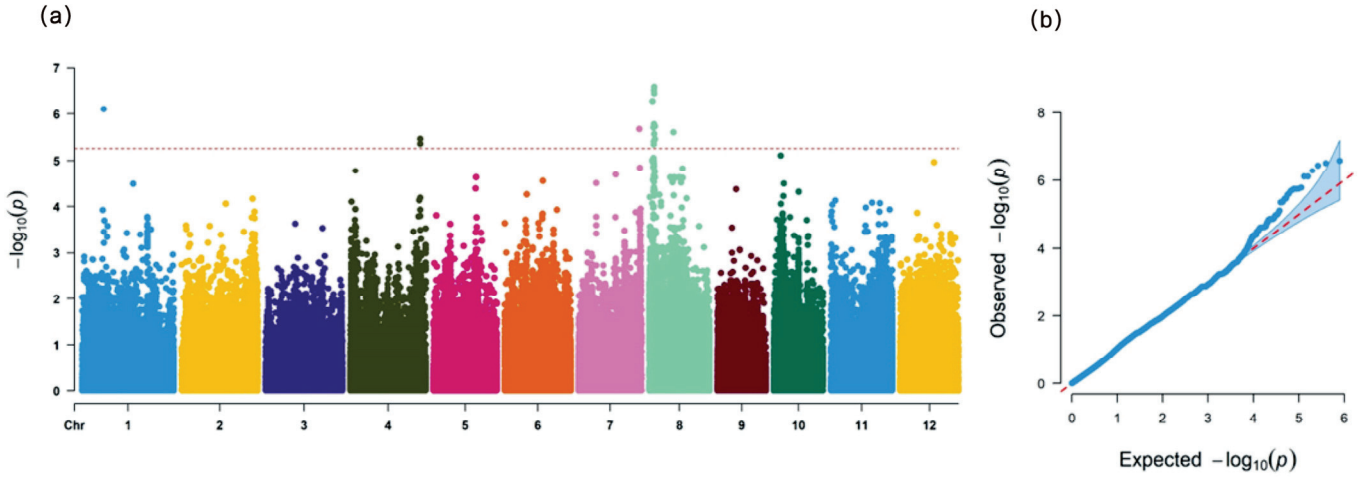

Figure 2. Manhattan plots and quantile-quantile (Q-Q) plots of GWAS for the leaf rolling scale. (**a**) Manhattan plots for leaf rolling scale. (**b**) Quantile-quantile (Q-Q) plots for leaf rolling scale.

Table 1. Lead SNPs for LRS identified by GWAS.

Trait	Lead SNP	Chr.	Position	*p* Value	*R*2 (%)	QTL in Previous Study
LRS	Chr1_10152936	1	10152936	7.86×10^{-7}	12.2	
	Chr4_32975130	4	32975130	3.42×10^{-6}	10.86	*qRL-4-1* [38]
	Chr7_15152008	7	15152008	2.11×10^{-6}	10.11	*qRL-7* [39], *qRl7a* [40]
	Chr8_1427905	8	1427905	5.22×10^{-7}	14.16	
	Chr8_1941918	8	1941918	1.95×10^{-6}	11.37	
	Chr8_2154790	8	2154790	1.66×10^{-6}	12.8	*qRL-8-1* [39]
	Chr8_2933410	8	2933410	1.84×10^{-6}	11.42	
	Chr8_11324046	8	11324046	2.45×10^{-6}	11.16	

*R*2 (%): Phenotypic variance explained.

3.3. Linkage Mapping for LRS in RIL Population

Two QTLs associated with LRS were localised on chromosomes 4 and 8 (Table 2; Figure S1), with LOD values of 5.32 and 3.94, respectively. *qLRS-4-1* was located between markers C4_32680431 and C4_33516075, elucidating 14.69% of the phenotypic variation. In addition, *qLRS-8-1* was located between markers C8_2397444 and C8_3005090, accounting for 9.94% of the phenotypic variation.

Table 2. QTLs for leaf rolling identified by linkage mapping.

QTLs	Left Marker	Right Marker	Chr.	LOD	*R*2 (%)	Additive Effect	Known QTLs	Known Genes
qLRS-4-1	C4_32680431	C4_33516075	4	5.32	14.69	−0.78	*qRL-4-1* [38]	*OsJAZ1* [41]
qLRS-8-1	C8_2397444	C8_3005090	8	3.94	9.94	−0.64	*qRL-8-1* [39]	*OsMYB103L* [20]

*R*2 (%): Phenotypic variance explained.

3.4. Haplotype Analysis of Candidate Genes

By comparing the results of GWAS and linkage analysis, the lead SNPs Chr4_32975130 and Chr8_2933410 were located in the *qLRS-4-1* and *qLRS-8-1* intervals, respectively (Figure 3a,b). LDBlockShow analysis revealed 57 candidate genes between C4_32792207 and C4_33164790 (Table S3) and 22 candidate genes between C8_2866488 and C8_3016330 (Table S4). 57 candidate genes include 41 expressed proteins, eight retrotransposon proteins, one putative protein, and seven known functional genes. Twenty-two candidate genes include 21 expression proteins and one retrotransposon protein. Based on the overlapping region of the linkage mapping, the range was further narrowed from 149.8 kb to 138.6 kb. Haplotype analysis of these genes was performed, revealing significant differences in the haplotypes of four genes (*LOC_Os04g55150*, *LOC_Os04g55190*, *LOC_Os08g05520*, and *LOC_Os08g05610*) compared to those of LRS (Figure 4e–h). Among the four candidate genes, there were totals of 231, 234, 227, and 261 varieties with haplotypes, respectively. Among these genes, except for three non-synonymous mutations in *LOC_Os04g55150* in the untranslated regions, all other non-synonymous mutations were in exons (Figure 4a–d).

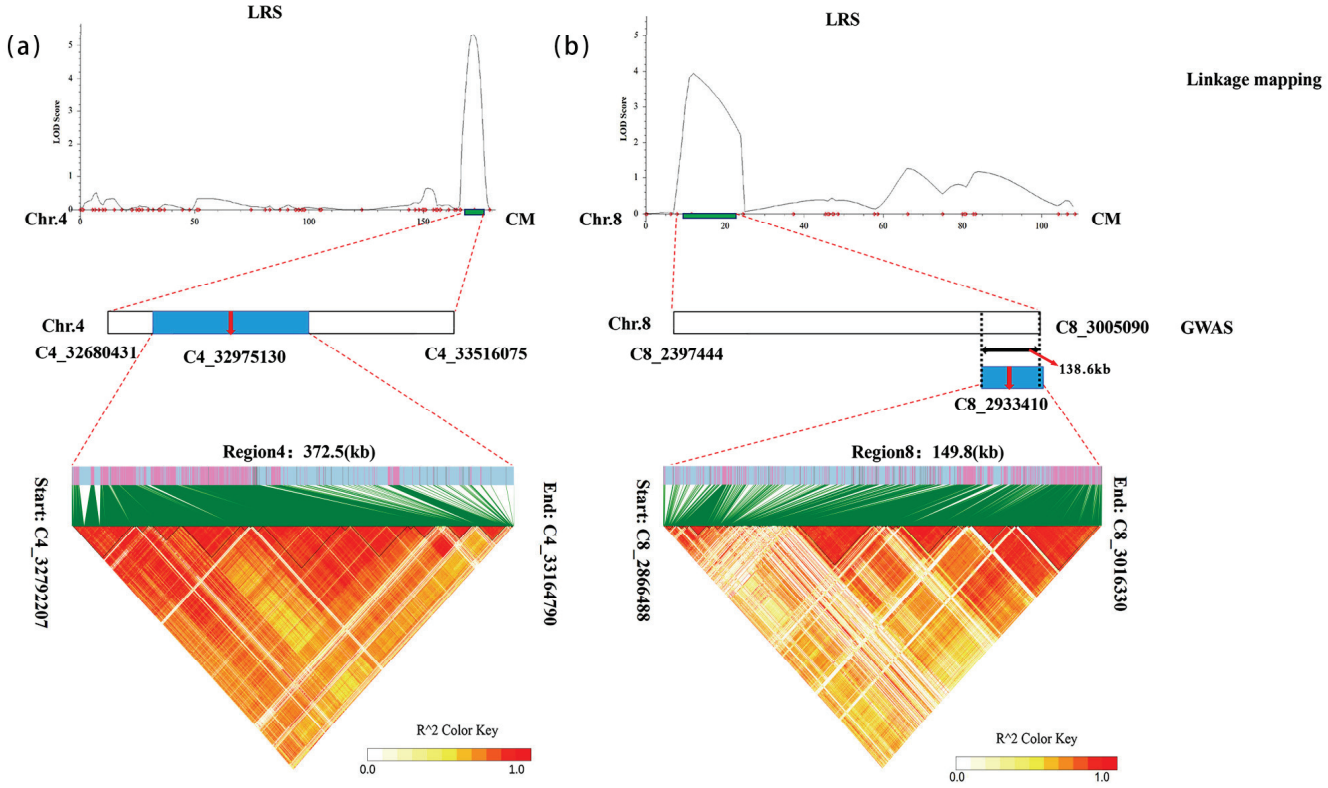

Figure 3. Co-localisation results for the LRS interval obtained through linkage mapping and GWAS. (**a**) Drought tolerance QTLs were mapped to the interval between markers C4_32680431 and C4_33516075 using linkage mapping. LDBlockShow narrowed down the candidate region to 372.5 kb. (**b**) Drought tolerance QTLs were mapped to the interval between markers C8_2397444 and C8_3005090 using linkage mapping. LDBlockShow further narrowed the candidate region to 149.8 kb. By intercepting the co-localisation interval, the candidate region was further narrowed to 138.6 kb between markers C8_2866488 and C8_3005090.

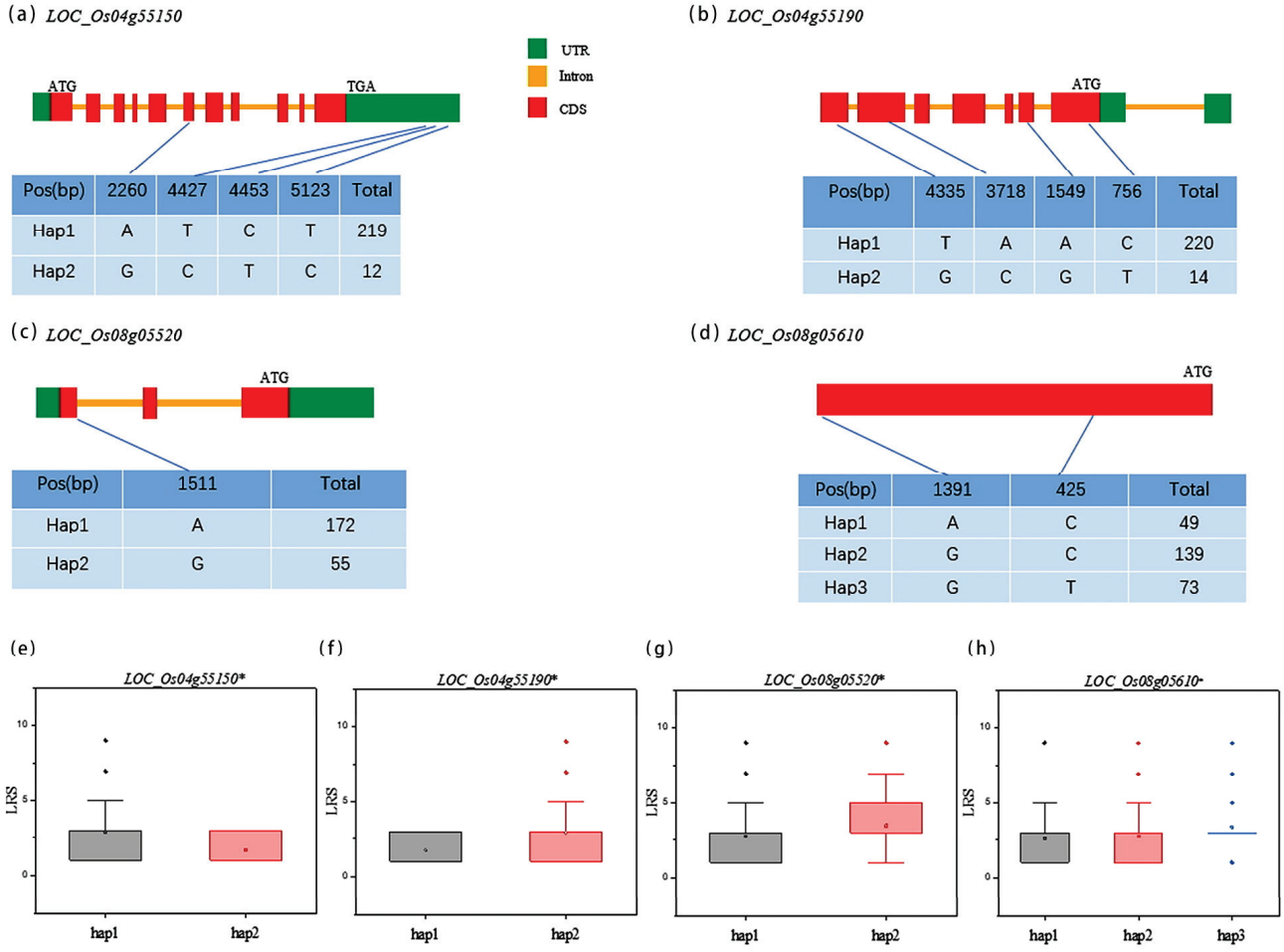

Figure 4. Structure and haplotype analysis of four candidate genes. (**a**–**d**) represent the gene structure and the variety number of haplotype combinations of *LOC_Os04g55150*, *LOC_Os04g55190*, *LOC_Os08g05520*, and *LOC_Os08g05610*. (**e**–**h**) represent the haplotype analysis of *LOC_Os04g55150*, *LOC_Os04g55190*, *LOC_Os08g05520*, and *LOC_Os08g05610*. * $p < 0.05$, based on ANOVA.

3.5. Gene Expression and Sequence Analysis of Candidate Genes

The expression of the four genes in the leaves was evaluated using qRT-PCR, and the results from the average of three replicates are shown in Figure 5. Under control conditions, no differences were observed in the expression levels of the four genes between the parents. However, under drought treatment, the expression levels of two genes showed significant differences between the parents (Figure 5a,c). There were no differences between *LOC_Os04g55190* and *LOC_Os08g05610* (Figure 5b,d). Taking the fact that KY131 is drought-sensitive and the variety XBJZ is drought-tolerant into consideration, *LOC_Os04g55150* and *LOC_Os08g05520* can be regarded as the candidate genes. Specifically, the expression of *LOC_Os08g05520* in XBJZ was significantly upregulated under drought stress compared to that in KY131 (Figure 5c).

LOC_Os04g55150 and *LOC_Os08g05520* were sequenced in KY131 and XBJZ, respectively, revealing no differences between the parental sequences of *LOC_Os04g55150* (Figure S2). Nevertheless, compared with the sequence of KY131, *LOC_Os08g05520* in XBJZ exhibited a 1 bp (A→C) mutation in the promoter region and a 2 bp deletion (A and T) in the first exon. Considering differences in parental drought resistance, we hypothesised that *LOC_Os08g05520* was a candidate gene for drought resistance in rice. *LOC_Os08g05520* encodes a MYB-like DNA binding domain containing protein that has been previously reported to affect stem degradation in rice [20].

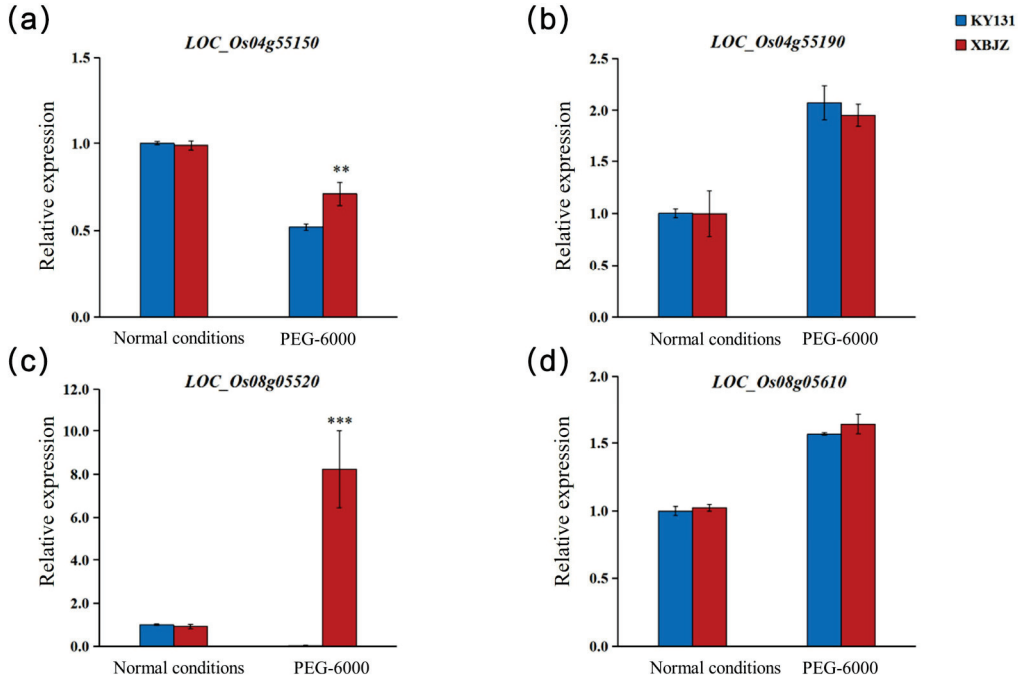

Figure 5. Expression differences of the four candidate genes under normal conditions and 20% PEG stress after 24 h cultivation. (**a**) *LOC_Os04g55150* expressed under normal conditions and 20% PEG-6000 stress. (**b**) *LOC_Os04g55190* expressed under normal conditions and 20% PEG-6000 stress. (**c**) *LOC_Os08g05520* expressed under normal conditions and 20% PEG-6000 stress. (**d**) *LOC_Os08g05610* expressed under normal conditions and 20% PEG-6000 stress. ** $p < 0.01$, *** $p < 0.001$, Students' *t* test.

3.6. Drought Tolerant Function Verification by Mutant

To further confirm the function of *LOC_Os08g05520* under drought conditions, we generated two homozygous mutant lines (designated as CR1 and CR2). Compared to the wild-type sequences, CR1 exhibited an 8 bp knockout at the target site, while CR2 featured an A base insertion (Figure 6a). Under control conditions, no discernible differences were observed in the growth of mutant and wild-type rice seedlings (Figure 6b). However, under drought treatment conditions, the mutant plants CR1 and CR2 demonstrated enhanced drought tolerance, as evidenced by an average LRS of 1.8 and 2.0, respectively, in contrast to an average LRS of 7.1 in the wild type (Figure 6c,d). This finding underscores the significant contribution of *LOC_Os08g05520* knockout to the improvement of drought tolerance in rice.

The performances of the wild type, CR1, and CR2 in the three-leaf stage after 20 d of water deprivation are shown in Figure 7. Under normal conditions, no significant differences in plant height or LRS were observed among the wild type, CR1, and CR2, indicating that the mutants and wild type had a consistent phenotype. The average LRS of the wild type was 2.6 under normal conditions, whereas it was 6.6 after 20 d of water deprivation. Under normal conditions, the average plant height of the wild type was 37.4 cm, but it was 28.6 cm after 20 d of water deprivation. After water deprivation, the LRS of the wild type differed significantly from those of CR1 and CR2 ($p < 0.001$), as shown in Figure 8a. No difference in LRS was observed between CR1 and CR2, which had a mean LRS of 2.2 that was higher than the mean LRS under normal conditions. After 20 d of water deprivation, the difference in plant height between the wild type and CR1 was significant ($p < 0.05$), the difference between wild type and CR2 was highly significant ($p < 0.01$), and no significant difference was observed between CR1 and CR2 (Figure 8b). Thus, the growth of the wild type was strongly affected by water deprivation, which caused the LRS of the leaves to increase and the plant height to decrease. The mutants (CR1 and CR2) were less affected by water deprivation, and their LRS and plant heights were similar to those of the control group.

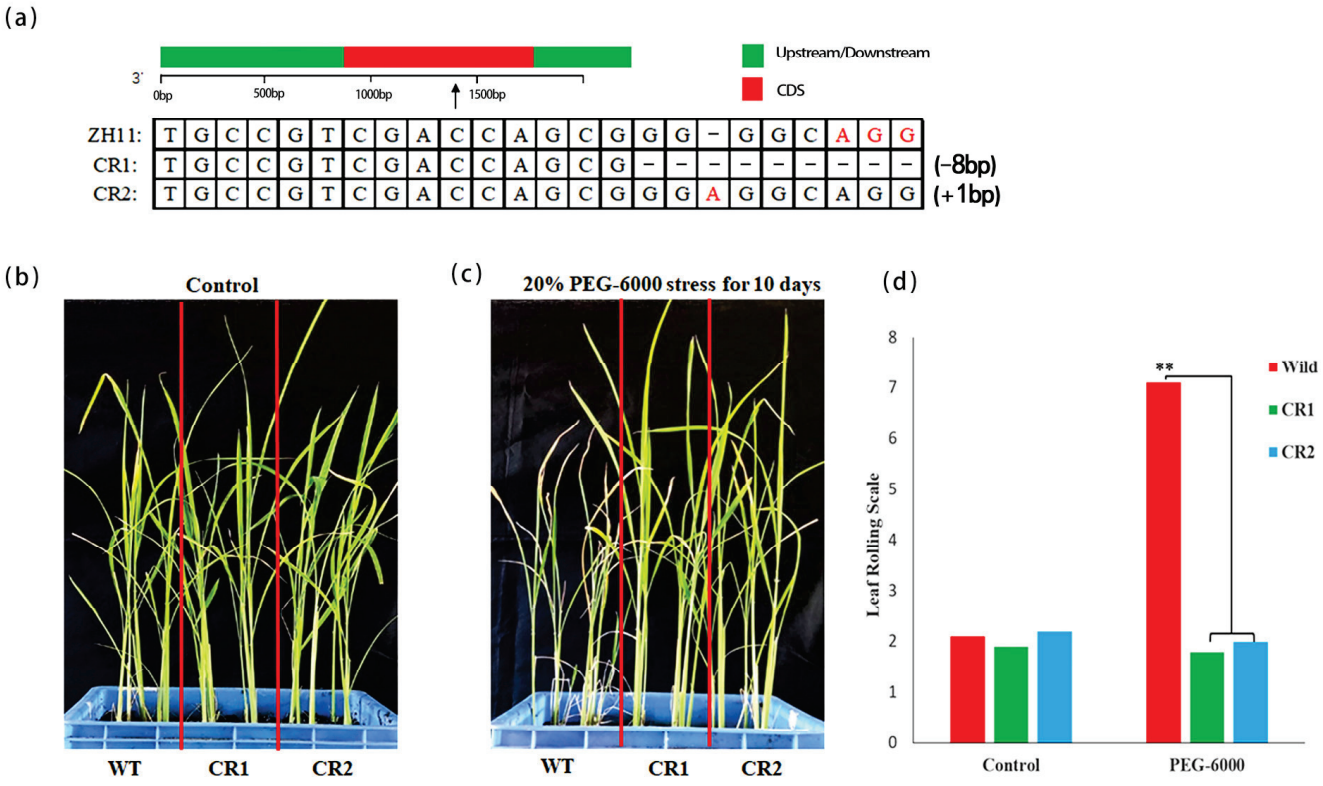

Figure 6. Sequence comparison of wild type and mutants, and phenotypic differences between 20% PEG-6000 and normal conditions. (**a**) DNA sequence comparison between ZH11, CR1, and CR2. (**b**) ZH11 wild, CR1, and CR2 planted in two rows in one pool under control conditions for 10 days. (**c**) ZH11 wild, CR1, and CR2 planted in two rows in one pool under 20% PEG-6000 treatment for 10 days. (**d**) Significant differences in LRS of wild type, CR1, and CR2 (** $p < 0.01$, Students' t test).

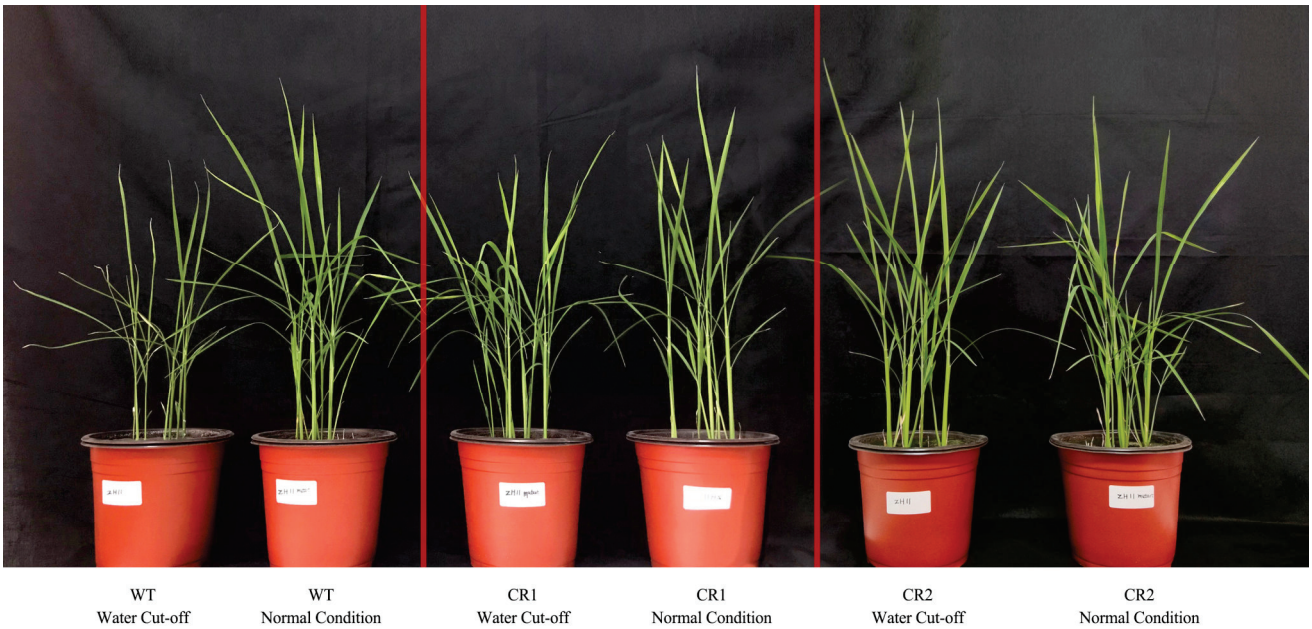

Figure 7. LRS difference between wild type, CR1, and CR2 after 20 days of water cut-off at the three-leaf stage and under normal conditions.

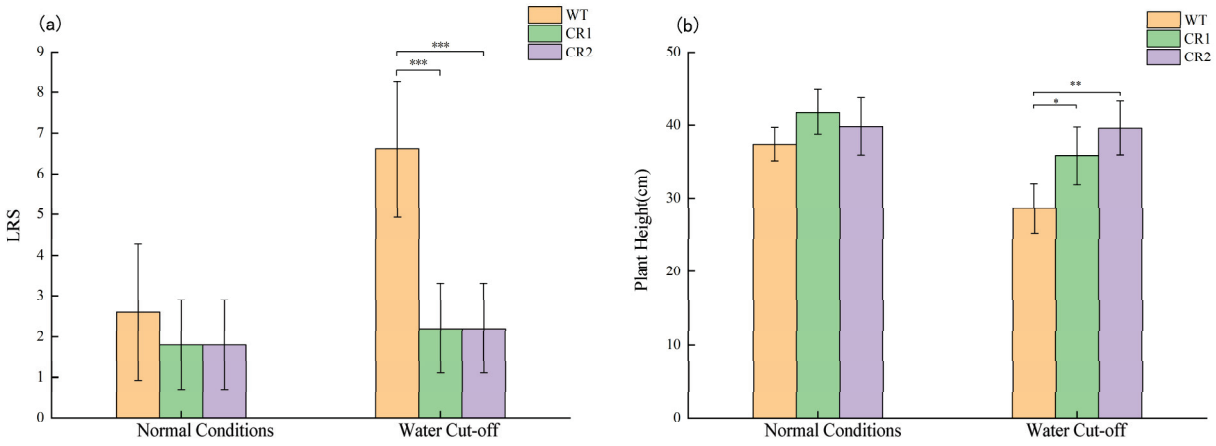

Figure 8. Comparison of plant height, LRS of wild type and mutants under 20 days' water cut-off, and normal conditions at three-leaf stage. (**a**) LRS. (**b**) Plant height. *, **, and *** represent the significance of ANOVA at $p < 0.05$, $p < 0.01$, and $p < 0.001$, respectively.

3.7. Comparison of Yield and Yield Components

To verify whether water deprivation and recovery had an effect on the final rice yields of the mutants, we continued to track the plant heights, yields, and yield-component traits of CR1, CR2, and the wild type after recovery and under normal conditions. Under normal conditions, no significant differences in plant height, tillering number, effective panicle number, grain number per spike, thousand-grain weight, or yield per plant were observed among the wild type, CR1, and CR2. According to the average phenotype and variation amplitude, mutants CR1 and CR2 exhibited high consistencies with the wild type. In the water deprivation recovery group, the differences between the wild type and CR1 and between the wild type and CR2 were significant or extremely significant ($p < 0.05$, $p < 0.01$, and $p < 0.001$), whereas the difference between CR1 and CR2 was not significant. Thus, the water deprivation treatment had larger effects on plant height, tillering number, effective panicle number, grain number per spike, thousand-grain weight, and yield per plant in the wild type, but had little effect on the growth and development of CR1 and CR2 (Figure 9a–f).

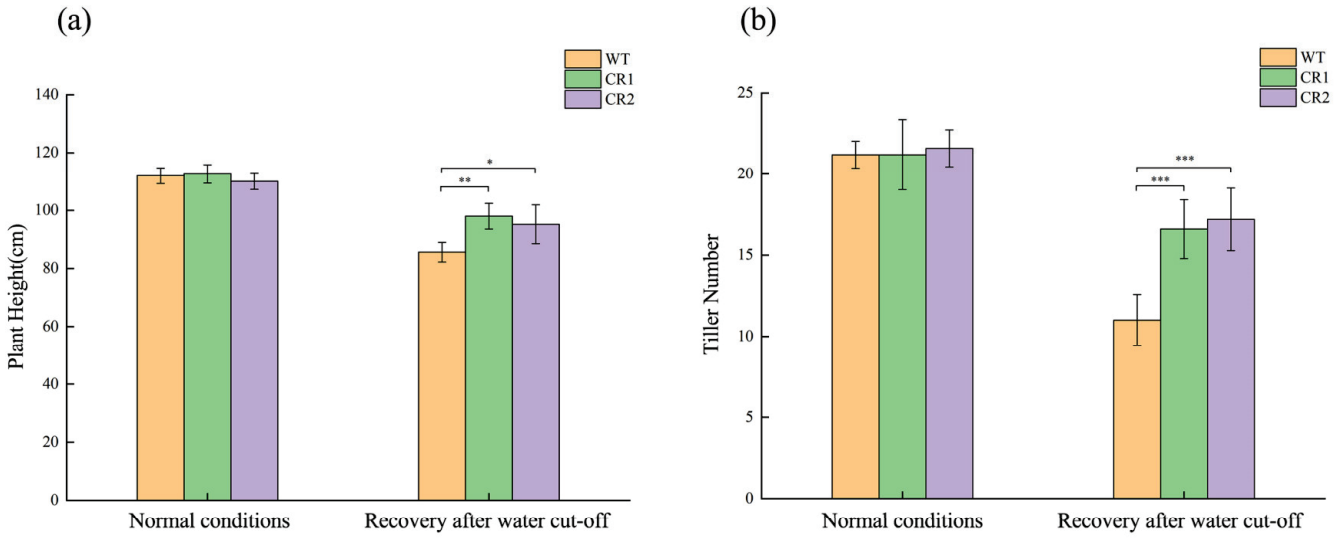

Figure 9. *Cont.*

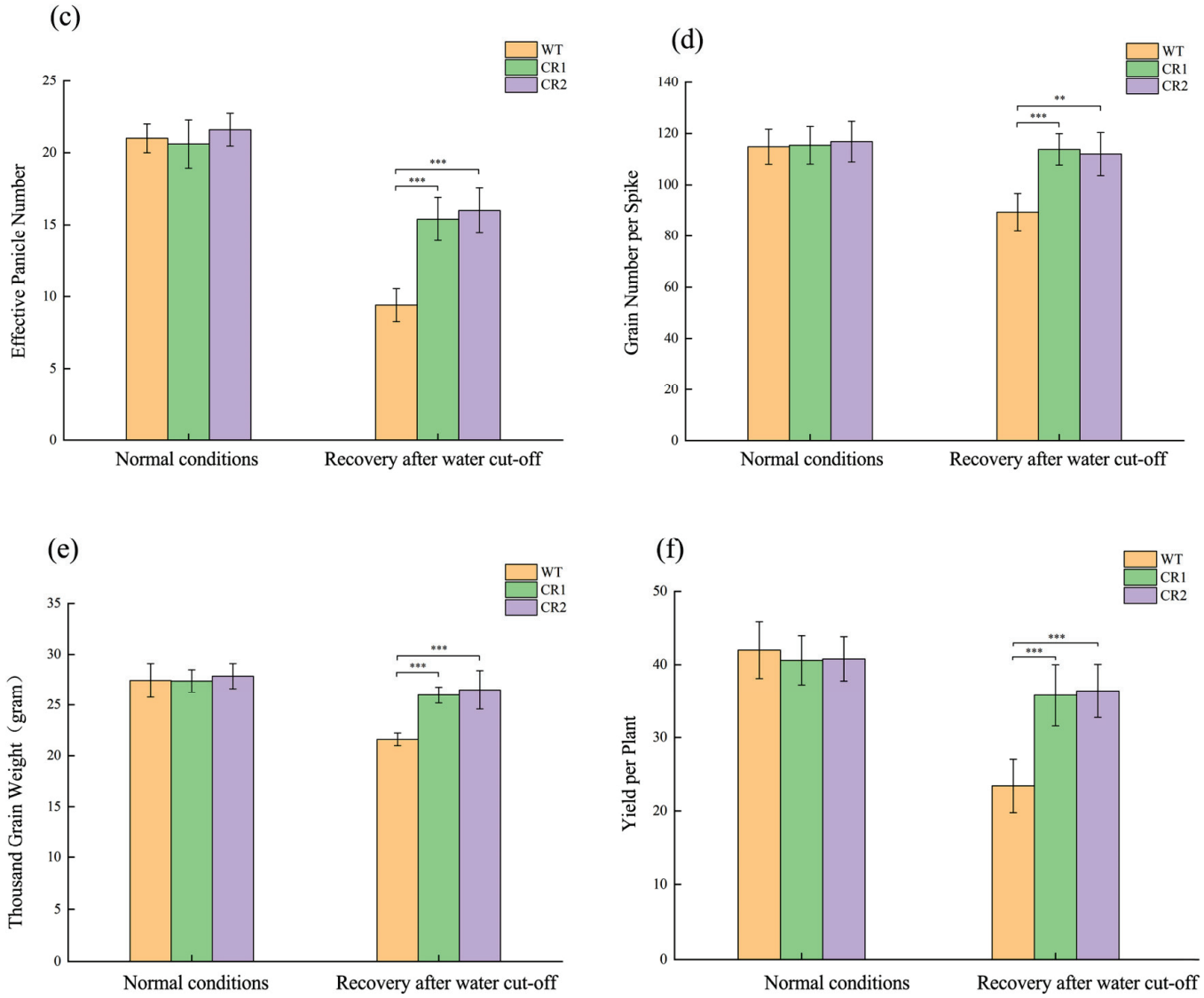

Figure 9. Comparison of plant height, yield, and yield component traits of wild type and mutants under 20 d water cut-off recovery and normal conditions at the maturity stage. (**a**) Plant height. (**b**) Tiller number. (**c**) Effective panicle number. (**d**) Grain number per spike. (**e**) Thousand grain weight. (**f**) Yield per plant. *, **, and *** represent the significance of ANOVA at $p < 0.05$, $p < 0.01$, and $p < 0.001$, respectively.

4. Discussion

The rice seedling stage is sensitive to drought stress, inhibiting vegetative growth and yield. Targeting highly drought-tolerant cultivars with drought-related genes is the most promising method for improving modern crop breeding [42]. This study selected LRS, which has been used for drought tolerance screening [43]. LRS values exhibited a continuous approximately normal distribution. It presents a typical genetic pattern of quantitative traits and is controlled by multiple genes. The identification of these QTLs is beneficial for drought tolerance in the marker-assisted breeding selection of rice.

Parent-based QTL mapping and GWAS are effective and accurate tools for the detection of QTLs for complex traits in crops [44]. The combination of the two methods can effectively improve the breadth and accuracy of QTL detection. The combination of linkage mapping and GWAS has achieved great success in gene mining for complex quantitative traits in rice. For example, a linkage mapping and GWAS joint strategy have been used to identify QTLs associated with grain shape and weight, which revealed the co-detection

of the QTLs *qGLE-12-1* and *qGLE-12-2* (Chromosome 12), *qGTE-3-1* (Chromosome 3), and *qGWL-5-1* and *qLWRL-5-1* (Chromosome 5), associated with grain length, width, and length-width ratio [45]. Similar research strategies have been applied to salinity tolerance at the seedling stage, resulting in the identification of a 195-kb region on chromosome 12 which was selected as the candidate interval based on the overlapping regions in the GWAS and the linkage mapping [46]. These studies demonstrate that the integration of linkage mapping and GWAS provides an excellent method for identifying QTL and molecular markers for rapid breeding deployment. In this study, a lead SNP C8_28933410 by GWAS was identified, which was located within *qLRS-8-1* identified by linkage mapping on chromosome 8. Combing the LD block analyses and QTL interval, a 138.6 kb overlap interval was considered as the candidate region.

In this study, eight lead SNPs and two QTLs were identified for leaf rolling scale. In previous studies, some loci were located within the same interval or overlapped with known QTLs. For example, *OsJAZ1*, which negatively regulates drought resistance in the seedling and reproductive stages of rice by negatively regulating ABA and jasmonic acid signaling [41], was within the *qLRS-4-1* identified by linkage mapping. *qLRS-4-1* was also located in the same interval as *qRL-4-1* [38], identified between RM5473 and RM348. Chr4_32975130 was also detected by GWAS in *qRL-4-1* cells, further confirming this candidate region. Similarly, *qLRS-8-1* was located at a smaller location interval than *qRL-8-1* [39], between RM1235 and RM331. Another important finding was that the five lead SNPs on chromosome 8 were distributed in *qRL-8-1*. *OsMYB103L* [20] controlled leaf curling and mechanical strength in rice within *qLRS-8-1* was identified by linkage mapping. In our study, GWAS identified two new drought-tolerant QTLs, Chr1_10152936 and Chr7_15152008.

Here, we found that *LOC_Os08g05520* is a novel functional gene associated with drought tolerance in rice. *LOC_Os08g05520* encodes an R2R3-MYB transcription factor, influencing leaf rolling and mechanical strength in rice, namely *OsMYB103L*. *OsMYB103L* interacts with *SLR1* (slender rice 1), an inhibitory factor in GA signaling, and is involved in the GA-mediated regulation of the cellulose synthesis pathway. In addition, *OsMYB103L* directly binds to and regulates the expression of the *CESA4*, *CESA7*, *CESA9*, and *BC1* promoters. GA mediates cellulose synthesis and secondary wall formation via the *SLR1-MYB103L-CESAs* pathway [47]. Researchers have found that the expression levels of several cellulose synthase genes (*CESAs*) significantly increased, similar to the cellulose content in *OsMYB103L* overexpressing lines. The knockdown of *OsMYB103L* by RNA interference leads to the opposite phenotype [20,47,48]. Therefore, we speculate that *OsMYB103L* may regulate the cellulose content and expression levels of several *CESAs* to affect drought tolerance in rice.

5. Conclusions

In conclusion, our study successfully identified *LOC_Os08g05520* as a pivotal candidate gene associated with drought tolerance in *japonica* rice seedlings. The findings present a valuable resource for breeders aiming to improve their drought tolerance in rice varieties. Looking ahead, further research could develop into elucidating the specific mechanisms by which *LOC_Os08g05520* confers drought tolerance, providing deeper insights into the molecular pathways involved. Additionally, exploring other candidate genes and pathways may offer a more comprehensive understanding of the complex genetic basis of drought tolerance in rice.

Supplementary Materials: The following supporting information can be downloaded at: https://www.mdpi.com/article/10.3390/agriculture14040603/s1, Figure S1: The genetic and linkage group of RIL population. Figure S2: Sequence comparison of LOC_Os08g05520 between parents. Table S1: Primers for qRT-PCR in this study. Table S2: Descriptive statistics for leaf rolling scale in the parents, 195 recombinant inbred lines (RILs), and 295 rice accessions. Table S3: Summary of functional annotation results for genes in the candidate region on chromosome 4. Table S4: Summary of functional annotation results for genes in the candidate region on chromosome 8.

Author Contributions: Conceptualization, J.C., S.X. and D.Z.; Data curation, S.L. and J.W.; Formal analysis, T.L., S.L., S.X. and H.L.; Funding acquisition, W.L. and H.Z.; Investigation, S.L., H.D. and S.X.; Methodology, T.L., H.D., S.X. and H.L.; Project administration, W.L. and H.Z.; Resources, J.W.; Software, T.L., H.D. and J.C.; Supervision, H.L., D.Z., W.L. and H.Z.; Validation, T.L., J.C. and D.Z.; Visualization, J.W., W.L., and H.Z.; Writing—original draft, T.L.; Writing—review and editing, T.L., S.L. and H.Z. All authors have read and agreed to the published version of the manuscript.

Funding: This research received no external funding.

Institutional Review Board Statement: Not applicable.

Data Availability Statement: Data are contained within the article.

Acknowledgments: We appreciate and thank the anonymous reviewers for their helpful comments that led to an overall improvement in the manuscript. We also thank the Journal Editor Board for their help and patience throughout the review process.

Conflicts of Interest: The authors declare no conflicts of interest.

References

1. Bouman, B.A.M.; Peng, S.; Castañeda, A.R.; Visperas, R.M. Yield and water use of irrigated tropical aerobic rice systems. *Agric. Water Manag.* **2005**, *74*, 87–105. [CrossRef]
2. Trijatmiko, K.R.; Supriyanta Prasetiyono, J.; Thomson, M.J.; Vera Cruz, C.M.; Moeljopawiro, S.; Pereira, A. Meta-analysis of quantitative trait loci for grain yield and component traits under reproductive stage drought stress in an upland rice population. *Mol. Breed.* **2014**, *34*, 283–295. [CrossRef] [PubMed]
3. Courtois, B.; McLaren, G.; Sinha, P.K.; Prasad, K.; Yadav, R.; Shen, L. Mapping QTLs associated with drought avoidance in upland rice. *Mol. Breed.* **2000**, *6*, 55–66. [CrossRef]
4. Price, A.H.; Townend, J.; Jones, M.P.; Audebert, A.; Courtois, B. Mapping QTLs associated with drought avoidance in upland rice grown in the Philippines and West Africa. *Plant Mol. Biol.* **2002**, *48*, 683–695. [CrossRef] [PubMed]
5. Han, B.; Wang, J.; Li, Y.; Ma, X.; Jo, S.; Cui, D.; Wang, Y.; Park, D.; Song, Y.; Cao, G.; et al. Identification of quantitative trait loci associated with drought tolerance traits in rice (*Oryza sativa* L.) under PEG and field drought stress. *Euphytica* **2018**, *214*, 74. [CrossRef]
6. Uga, Y.; Sugimoto, K.; Ogawa, S.; Rane, J.; Ishitani, M.; Hara, N.; Kitomi, Y.; Inukai, Y.; Ono, K.; Kanno, N.; et al. Control of root system architecture by *DEEPER ROOTING 1* increases rice yield under drought conditions. *Nat. Genet.* **2013**, *45*, 1097–1102. [CrossRef] [PubMed]
7. Shi, Z.; Wang, J.; Wan, X.; Shen, G.; Wang, X.; Zhang, J. Over expression of rice OsAGO7 gene induces upward curling of the leaf blade that enhanced erect leaf habit. *Planta* **2007**, *226*, 99–108. [CrossRef] [PubMed]
8. Fujino, K.; Matsuda, Y.; Ozawa, K.; Nishimura, T.; Koshiba, T.; Fraaije, M.W.; Sekiguchi, H. NARROW LEAF 7 controls leaf shape mediated by auxin in rice. *Mol. Genet. Genom.* **2008**, *279*, 499–507. [CrossRef] [PubMed]
9. Zhang, G.H.; Xu, Q.; Zhu, X.D.; Qian, Q.; Xue, H.W. SHALLOT-LIKE1 is a KANADI transcription factor that modulates rice leaf rolling by regulating leaf abaxial cell development. *Plant Cell* **2009**, *21*, 719–735. [CrossRef]
10. Hibara, K.; Obara, M.; Hayashida, E.; Abe, M.; Ishimaru, T.; Satoh, H.; Itoh, J.-I.; Nagato, Y. The ADAXIALIZED LEAF1 gene functions in leaf and embryonic pattern formation in rice. *Dev. Biol.* **2009**, *334*, 345–354. [CrossRef]
11. Zhao, S.Q.; Hu, J.; Guo, L.B.; Qian, Q.; Xue, H.W. Rice leaf inclination2, a VIN3-like protein, regulates leaf angle through modulating cell division of the collar. *Cell Res.* **2010**, *20*, 935–947. [CrossRef] [PubMed]
12. Wu, C.; Fu, Y.; Hu, G.; Si, H.; Cheng, S.; Liu, W. Isolation and characterization of a rice mutant with narrow and rolled leaves. *Planta* **2010**, *232*, 313–324. [CrossRef] [PubMed]
13. Hu, J.; Zhu, L.; Zeng, D.; Gao, Z.; Guo, L.; Fang, Y.; Zhang, G.; Dong, G.; Yan, M.; Liu, J.; et al. Identification and characterization of NARROW AND ROLLED LEAF 1, a novel gene regulating leaf morphology and plant architecture in rice. *Plant Mol. Biol.* **2010**, *73*, 283–292. [CrossRef] [PubMed]
14. Li, L.; Shi, Z.Y.; Li, L.; Shen, G.Z.; Wang, X.Q.; An, L.S.; Zhang, J.L. Overexpression of ACL1 (abaxially curled leaf 1) increased bulliform cells and induced abaxial curling of leaf blades in rice. *Mol. Plant* **2010**, *3*, 807–817. [CrossRef] [PubMed]
15. Zou, L.P.; Sun, X.H.; Zhang, Z.G.; Liu, P.; Wu, J.X.; Tian, C.J.; Qiu, J.L.; Lu, T.G. Leaf rolling controlled by the homeodomain leucine zipper Class IV gene Roc5 in rice. *Plant Physiol.* **2011**, *156*, 1589–1602. [CrossRef] [PubMed]
16. Wu, R.; Li, S.; He, S.; Wassmann, F.; Yu, C.; Qin, G.; Schreiber, L.; Qu, L.J.; Gu, H. CFL1, a WW domain protein, regulates cuticle development by modulating the function of HDG1, a Class IV homeodomain transcription factor, in rice and Arabidopsis. *Plant Cell* **2011**, *23*, 3392–3411. [CrossRef] [PubMed]
17. Fang, L.; Zhao, F.; Cong, Y.; Sang, X.; Du, Q.; Wang, D.; Li, Y.; Ling, Y.; Yang, Z.; He, G. Rolling-leaf14 is a 2OG-Fe (II) oxygenase family protein that modulates rice leaf rolling by affecting secondary cell wall formation in leaves. *Plant Biotechnol. J.* **2012**, *10*, 524–532. [CrossRef] [PubMed]

18. Xiang, J.J.; Zhang, G.H.; Qian, Q.; Xue, H.W. SEMI-ROLLED LEAF1 encodes a putative glycosylphosphatidylinositol-anchored protein and modulates rice leaf rolling by regulating the formation of bulliform cells. *Plant Physiol.* **2012**, *159*, 1488–1500. [CrossRef]
19. Xu, Y.; Wang, Y.; Long, Q.; Huang, J.; Wang, Y.; Zhou, K.; Zheng, M.; Sun, J.; Chen, H.; Chen, S.; et al. Overexpression of OsZHD1, a zinc finger homeodomain class homeobox transcription factor, induces abaxially curled and drooping leaf in rice. *Planta* **2014**, *239*, 803–816. [CrossRef] [PubMed]
20. Yang, C.; Li, D.; Liu, X.; Ji, C.; Hao, L.; Zhao, X.; Li, X.; Chen, C.; Cheng, Z.; Zhu, L. OsMYB103L, an R2R3-MYB transcription factor, influences leaf rolling and mechanical strength in rice (*Oryza sativa* L.). *BMC Plant Biol.* **2014**, *14*, 158. [CrossRef] [PubMed]
21. Zhang, J.J.; Wu, S.Y.; Jiang, L.; Wang, J.L.; Zhang, X.; Guo, X.P.; Wu, C.Y.; Wan, J.M. A detailed analysis of the leaf rolling mutant sll2 reveals complex nature in regulation of bulliform cell development in rice (*Oryza sativa* L.). *Plant Biol.* **2015**, *17*, 437–448. [CrossRef] [PubMed]
22. Chen, Q.; Xie, Q.; Gao, J.; Wang, W.; Sun, B.; Liu, B.; Zhu, H.; Peng, H.; Zhao, H.; Liu, C.; et al. Characterization of Rolled and Erect Leaf 1 in regulating leave morphology in rice. *J. Exp. Bot.* **2015**, *66*, 6047–6058. [CrossRef] [PubMed]
23. Liu, X.; Li, M.; Liu, K.; Tang, D.; Sun, M.; Li, Y.; Shen, Y.; Du, G.; Cheng, Z. Semi-Rolled Leaf2 modulates rice leaf rolling by regulating abaxial side cell differentiation. *J. Exp. Bot.* **2016**, *67*, 2139–2150. [CrossRef] [PubMed]
24. Li, X.; Zhou, Z.; Ding, J.; Wu, Y.; Zhou, B.; Wang, R.; Ma, J.; Wang, S.; Zhang, X.; Xia, Z.; et al. Combined linkage and association mapping reveals QTL and candidate genes for plant and ear height in maize. *Front. Plant Sci.* **2016**, *7*, 833. [CrossRef] [PubMed]
25. Wu, X.; Li, Y.; Shi, Y.; Song, Y.; Zhang, D.; Li, C.; Buckler, E.S.; Li, Y.; Zhang, Z.; Wang, T. Joint-linkage mapping and GWAS reveal extensive genetic loci that regulate male inflorescence size in maize. *Plant Biotechnol. J.* **2016**, *14*, 1551–1562. [CrossRef] [PubMed]
26. Cui, Z.; Xia, A.; Zhang, A.; Luo, J.; Yang, X.; Zhang, L.; Ruan, Y.; He, Y. Linkage mapping combined with association analysis reveals QTL and candidate genes for three husk traits in maize. *Theor. Appl. Genet.* **2018**, *131*, 2131–2144. [CrossRef] [PubMed]
27. Ju, M.; Zhou, Z.; Mu, C.; Zhang, X.; Gao, J.; Liang, Y.; Chen, J.; Wu, Y.; Li, X.; Wang, S.; et al. Dissecting the genetic architecture of Fusarium verticillioides seed rot resistance in maize by combining QTL mapping and genome-wide association analysis. *Sci. Rep.* **2017**, *7*, 46446. [CrossRef] [PubMed]
28. Gao, J.; Wang, S.; Zhou, Z.; Wang, S.; Dong, C.; Mu, C.; Song, Y.; Ma, P.; Li, C.; Wang, Z.; et al. Linkage mapping and genome-wide association reveal candidate genes conferring thermotolerance of seed-set in maize. *J. Exp. Bot.* **2019**, *70*, 4849–4864. [CrossRef] [PubMed]
29. Shi, J.; Wang, Y.; Wang, C.; Wang, L.; Zeng, W.; Han, G.; Qiu, C.; Wang, T.; Tao, Z.; Wang, K.; et al. Linkage mapping combined with GWAS revealed the genetic structural relationship and candidate genes of maize flowering time-related traits. *BMC Plant Biol.* **2022**, *22*, 328. [CrossRef]
30. Liu, K.; Sun, X.; Ning, T.; Duan, X.; Wang, Q.; Liu, T.; An, Y.; Guan, X.; Tian, J.; Chen, J. Genetic dissection of wheat panicle traits using linkage analysis and a genome-wide association study. *Theor. Appl. Genet.* **2018**, *131*, 1073–1090. [CrossRef] [PubMed]
31. Li, X.; Zheng, H.; Wu, W.; Liu, H.; Wang, J.; Jia, Y.; Li, J.; Yang, L.; Lei, L.; Zou, D.; et al. QTL mapping and candidate gene analysis for alkali tolerance in *japonica* rice at the bud stage based on linkage mapping and genome-wide association study. *Rice* **2020**, *13*, 48. [CrossRef]
32. Li, N.; Zheng, H.; Cui, J.; Wang, J.; Liu, H.; Sun, J.; Liu, T.; Zhao, H.; Lai, Y.; Zou, D. Genome-wide association study and candidate gene analysis of alkalinity tolerance in *japonica* rice germplasm at the seedling stage. *Rice* **2019**, *12*, 24. [CrossRef] [PubMed]
33. Shiratsuchi, H.; Ohdaira, Y.; Yamaguchi, H.; Fukuda, A. Breaking the dormancy of rice seeds with various dormancy levels using steam and high temperature treatments in a steam nursery cabinet. *Plant Prod. Sci.* **2017**, *20*, 183–192. [CrossRef]
34. International Rice Research Institute. *Standard Evaluation System for Rice*; IRRI: Manila, Philippines, 1996.
35. Bradbury, P.J.; Zhang, Z.; Kroon, D.E.; Casstevens, T.M.; Ramdoss, Y.; Buckler, E.S. TASSEL: Software for association mapping of complex traits in diverse samples. *Bioinformatics* **2007**, *23*, 2633–2635. [CrossRef] [PubMed]
36. Dong, S.S.; He, W.M.; Ji, J.J.; Zhang, C.; Guo, Y.; Yang, T.L. LDBlockShow: A fast and convenient tool for visualizing linkage disequilibrium and haplotype blocks based on variant call format files. *Brief Bioinform.* **2021**, *22*, bbaa227. [CrossRef] [PubMed]
37. Livak, K.J.; Schmittgen, T.D. Analysis of relative gene expression data using real-time quantitative PCR and the $2^{-\Delta\Delta CT}$ method. *Methods* **2001**, *25*, 402–408. [CrossRef] [PubMed]
38. Gao, Y.; Lu, C.; Wang, M.; Wang, P.; Yan, X.; Xie, K.; Wan, J. QTL mapping for rolled leaf gene in rice. *Jiangsu J. Agric. Sci.* **2007**, *23*, 5–10.
39. Yuan, G.; Cheng, B.; Hong, D. Construction of SSR linkage map and analysis of QTLs for rolled leaf in *japonica* rice. *Rice Sci.* **2010**, *17*, 8–34.
40. Zhang, Q.; Zheng, T.; Hoang, L.; Wang, C.; Nafisah; Joseph, C.; Zhang, W.; Xu, J.; Li, Z. Joint mapping and allele mining of the rolled leaf trait in rice (*Oryza sativa* L.). *PLoS ONE* **2016**, *11*, e0158246. [CrossRef]
41. Fu, J.; Wu, H.; Ma, S.; Xiang, D.; Liu, R.; Xiong, L. OsJAZ1 attenuates drought resistance by regulating JA and ABA signaling in rice. *Front. Plant Sci.* **2017**, *8*, 2108. [CrossRef]
42. Oladosu, Y.; Rafii, M.Y.; Samuel, C.; Fatai, A.; Magaji, U.; Kareem, I.; Kamarudin, Z.S.; Muhammad, I.; Kolapo, K.K. Drought resistance in rice from conventional to molecular breeding: A review. *Int. J. Mol. Sci.* **2019**, *20*, 3519. [CrossRef] [PubMed]
43. Swapna, S.; Shylaraj, K.S. Screening for osmotic stress responses in rice varieties under drought condition. *Rice Sci.* **2017**, *24*, 253–263. [CrossRef]

44. Raj, S.R.G.; Nadarajah, K. QTL and Candidate Genes: Techniques and Advancement in Abiotic Stress Resistance Breeding of Major Cereals. *Int. J. Mol. Sci.* **2023**, *24*, 6. [CrossRef] [PubMed]
45. Kang, J.-W.; Kabange, N.R.; Phyo, Z.; Park, S.-Y.; Lee, S.-M.; Lee, J.-Y.; Shin, D.; Cho, J.H.; Park, D.-S.; Ko, J.-M.; et al. Combined Linkage Mapping and Genome-Wide Association Study Identified QTLs Associated with Grain Shape and Weight in Rice (*Oryza sativa* L.). *Agronomy* **2020**, *10*, 1532. [CrossRef]
46. Xu, S.; Cui, J.; Cao, H.; Liang, S.; Ma, T.; Liu, H.; Wang, J.; Yang, L.; Xin, W.; Jia, Y.; et al. Identification of candidate genes for salinity tolerance in Japonica rice at the seedling stage based on genome-wide association study and linkage mapping. *Front. Plant Sci.* **2023**, *14*, 1184416. [CrossRef] [PubMed]
47. Ye, Y.; Liu, B.; Zhao, M.; Wu, K.; Cheng, W.; Chen, X.; Liu, Q.; Liu, Z.; Fu, X.; Wu, Y. CEF1/OsMYB103L is involved in GA-mediated regulation of secondary wall biosynthesis in rice. *Plant Mol. Biol.* **2015**, *89*, 385–401. [CrossRef] [PubMed]
48. Hirano, K.; Kondo, M.; Aya, K.; Miyao, A.; Sato, Y.; Antonio, B.A.; Namiki, N.; Nagamura, Y.; Matsuoka, M. Identification of transcription factors involved in rice secondary cell wall formation. *Plant Cell Physiol.* **2013**, *54*, 1791–1802. [CrossRef] [PubMed]

agriculture

MDPI

Article

Effects of Silicon Alone and Combined with Organic Matter and *Trichoderma harzianum* on Sorghum Yield, Ions Accumulation and Soil Properties under Saline Irrigation

José Orlando Nunes da Silva [1,*], Luiz Guilherme Medeiros Pessoa [1,*], Emanuelle Maria da Silva [1], Leonardo Raimundo da Silva [2], Maria Betânia Galvão dos Santos Freire [3], Eduardo Soares de Souza [1], Sérgio Luiz Ferreira-Silva [1], José Geraldo Eugênio de França [1], Thieres George Freire da Silva [1] and Eurico Lustosa do Nascimento Alencar [4]

[1] Graduate Program in Crop Production, Federal Rural University of Pernambuco, Serra Talhada 56909-535, PE, Brazil; silva.emanuelle16@gmail.com (E.M.d.S.); eduardo.ssouza@ufrpe.br (E.S.d.S.); sergio.luiz@ufrpe.br (S.L.F.-S.); geraldo.eugenio@ufrpe.br (J.G.E.d.F.); thieres.silva@ufrpe.br (T.G.F.d.S.)
[2] Academic Unit of Serra Talhada, Federal Rural University of Pernambuco, Serra Talhada 56909-535, PE, Brazil; leonardosilvalr1@gmail.com
[3] Graduate Program in Soil Science, Federal Rural University of Pernambuco, Recife 52171-900, PE, Brazil; maria.freire@ufrpe.br
[4] Irrigated Agriculture Station of Parnamirim, Federal Rural University of Pernambuco, Parnamirim 56163-000, PE, Brazil; eurico.alencar@ufrpe.br
* Correspondence: joseorlando.agro@gmail.com (J.O.N.d.S.); luiz.pessoa@ufrpe.br (L.G.M.P.)

Abstract: The action of silicon as a salt stress mitigator has been investigated in isolation, and its combined efficacy with other salt stress mitigators needs to be addressed. This work verified whether silicon, in combination with organic matter and *Trichoderma harzianum*, enhances the production of forage sorghum under saline irrigation and its effects on soil properties. The field experiment was conducted in Parnamirim (PE), a semiarid region of Brazil. Forage sorghum (*Sorghum sudanense* (Piper) Stapf) was irrigated with saline water (3.12 dS m^{-1}) and subjected to the application of non-silicon, silicon alone, and silicon combined with *Trichoderma* and organic matter over three consecutive cuts (every three months after germination). Silicon applied in combination significantly increased the content of nutrient ions K^+, P, Ca^{2+}, and Mg^{2+} in sorghum leaves, stems, and panicles and increased P content in the soil by 170, 288, and 92% for the first, second, and third cuts, respectively. When silicon was applied in combination, sorghum's dry and fresh matter (total yield for the three cuts) increased to 62.53 and 182.43 t ha^{-1}, respectively. In summary, applying silicon (Si) combined with *Trichoderma* and organic matter promotes higher nutrient ion contents in soil and sorghum plants and a higher forage sorghum yield.

Keywords: biosaline agriculture; salt stress attenuators; salt tolerance; sorghum yield

1. Introduction

Food production is directly linked to climate, and this means that crop yields, water use, and soil quality are affected by climate change [1]. Increased concentrations of atmospheric greenhouse gases are likely indicators that climate change significantly impacts soil salinization [2], by increasing air temperature and thereby increasing soil water and groundwater evaporation. Consequently, the capillary movement of groundwater and soil water will rise in dry seasons, accelerating the soil salinization process in arid regions of the world [3]. Thus, salt-affected areas have increased, mainly due to increased evapotranspiration, lower precipitation, increased use of poor-quality water, poor irrigation management, and inappropriate soil management practices [4]. Given this scenario, one of the main challenges of current world agriculture is ensuring food security under extreme abiotic stress, such as saline stress.

In much of the Brazilian semiarid region, producers already suffer from problems related to the availability of good quality water for use in irrigated agriculture [5]. This has caused an increase in groundwater use for irrigation purposes, which generally have high saline contents, with high concentrations of sodium and chlorine in their composition [6,7]. The excessive use and mismanagement of these waters, combined with poor soil management and lack of drainage [8], has limited food and fodder production and contributed enormously to soil degradation and desertification of the region [9].

Salinity affects plant production and plant metabolism at all stages of growth [10] through nutritional imbalances [11], reduction in osmotic potential [12], and ionic and oxidative toxicity [13], causing morphological [14], physiological, and biochemical damage [15]. Despite the Brazilian semiarid region's current scenario concerning the increasing use of saline water for crop irrigation, cultivation strategies that favor mitigating saline stress on plants still need to be explored. In this context, it is essential and urgent to carry out studies investigating ways to minimize salt stress and promote crop production that meet the region's demand.

To address this issue, using crops with agricultural potential and a tolerance to high salinity is a promising alternative to ensure plant production in the Brazilian semiarid region and around the globe [16]. In this sense, forage sorghum (*Sorghum bicolor* (L.) Moench) is an essential source of animal feed that has increased its importance in many semiarid regions of the globe due to its high yield and ability to use water effectively, even under water and salt stress conditions [10,17].

Although sorghum is recommended for cultivation in saline environments [18], its salt tolerance can be improved by using salt stress attenuators. Thus, it is crucial to investigate the effectiveness of salt stress attenuators in mitigating the effects of salt on different crops and increasing the range of possibilities for success in the yield of salt-tolerant plants.

Silicon (Si) has been widely studied as a saline stress attenuator [19–21]. The effectiveness of Si in attenuating salt stress in plants can occur through several mechanisms. Zhu and Gong [22] report that Si has a relieving effect on salt stress in plants by reducing the ionic toxicity of Na^+ and Cl^-; decreasing oxidative damage by increasing the activity of antioxidant enzymes; regulating the biosynthesis of compatible solutes; affecting lignin biosynthesis; and by regulating levels of plant hormones and polyamines. Although several studies report the beneficial effects of Si on crops growing in saline environments, few studies evaluate the effectiveness of Si combined with other salinity attenuators.

Organic treatments correspond to a wide variety of products made by organic compounds that can be added to the soil to increase soil fertility and favor plant growth, improving agricultural sustainability, habitats, biogeochemical cycles, and soil biological activity [23]. These correspond to organic fertilizers, applied to the soil as beneficial microorganisms (*Rhizobium*, arbuscular mycorrhizal fungi, *Trichoderma*, *Azospirillum*, etc.) and organic soil conditioners (manure, biochar, etc.), which tend to improve the physical properties of the soil, accelerate the leaching of salts and Na^+, increase the percentage of aggregate stability, and reduce the percentage of exchangeable sodium (ESP) and electrical conductivity (EC) [24].

Trichoderma is an important fungus commonly found in soils, which can spread rapidly, colonizing and surviving in the rhizosphere for extended periods [25]. *Trichoderma* promotes root growth and has a high capacity to mobilize and absorb nutrients from the soil, increasing the efficiency of nutrient utilization by plants and promoting crop growth and production [26], thus providing greater tolerance to various environmental stresses [27]. Additionally, *Trichoderma* alleviates the effects of salinity on plants by increasing the activity of antioxidative defense systems [28]. On the other hand, using manure as a source of organic matter in soils is a common practice in the Brazilian semiarid region. In this sense, using *Trichoderma* can potentiate the mineralization of the organic matter applied as manure and increase the solubilization of nutrients for the plants, since salinity reduces the absorption of nutrients and their efficiency in crops [29].

Although the benefits of Si as an attenuator of salt stress in plants are well documented in the literature [18,20,30,31], in the Brazilian semiarid region, its use for this purpose is still incipient, and investigations are needed to assess its effectiveness in mitigating salt stress. Furthermore, its association with organic treatments still needs to be reported in the literature. Thus, we hypothesize that the combined application of Si with organic treatments can increase the performance of sorghum under saline stress. The objective of this study was to evaluate the effectiveness of the application of Si alone and combined with organic matter and *Trichoderma harzianum* on the yield of forage sorghum under saline irrigation, as well as to verify changes in the soil chemical properties in response to the application of saline attenuators.

2. Materials and Methods

2.1. Study Area

The study was carried out at the Parnamirim Irrigated Agriculture Station—Federal Rural University of Pernambuco (UFRPE), in Parnamirim (PE), located in a semiarid region of Brazil (latitude 8°5′08″ S, longitude 39°34′27″ W and an altitude of 390 m) (Figure 1). According to the Köppen classification, the climate in the region is semiarid, of the BSwh type. The average annual rainfall in the study area is 431.8 mm [32]. However, the rainy season in the region is short and occurs from December to March.

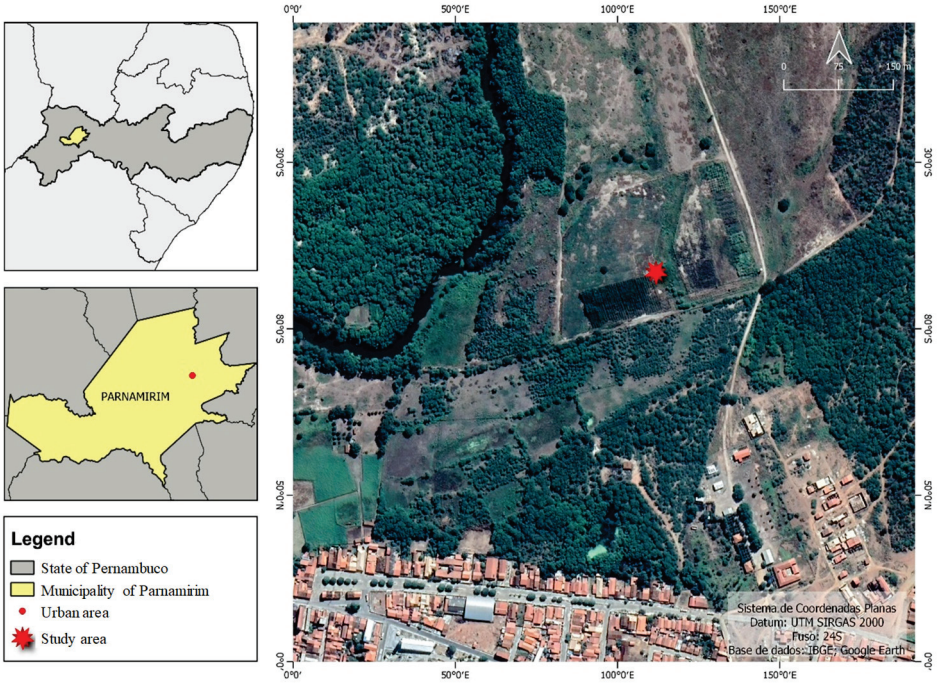

Figure 1. Location of the experimental field in Parnamirim (PE), a semiarid region of Brazil.

The region's principal economic activity is the production of goats and sheep. It requires a forage supply in large quantities. As the rainy season in the region is short, many producers resort to groundwater use in the driest months to guarantee forage production. However, these waters do not have a good quality for irrigation use due to the high saline content, which compromises forage production.

The experiment was conducted in the field, in saline Fluvisol soil [33]. The chemical and physical properties of the soil used in the experiment at depths of 0–10, 10–20, 20–40, and 40–60 cm are shown in Table 1.

Table 1. Chemical and textural characterization of soil in the experimental area.

Soil Property	Soil Layer (cm)			
	0–10	**10–20**	**20–40**	**40–60**
	Chemical property			
pH	6.05	6.09	6.16	6.32
OM (g kg^{-1})	25.08	19.35	18.00	11.75
P (mg dm^{-3})	28.40	19.73	14.83	9.75
K^+ ($cmol_c$ dm^{-3})	0.51	0.34	0.24	0.14
Na^+ ($cmol_c$ dm^{-3})	0.30	0.37	0.52	0.82
Ca^{2+} (cmolc dm^{-3})	9.06	8.54	8.79	9.98
Mg^{2+} ($cmol_c$ dm^{-3})	5.29	5.40	5.21	5.53
H + Al ($cmol_c$ dm^{-3})	0.96	0.89	0.76	0.60
SB ($cmol_c$ dm^{-3})	15.14	14.65	14.93	16.48
CEC ($cmol_c$ dm^{-3})	16.10	15.54	15.69	17.08
ESP (%)	1.86	2.38	3.31	4.80
	Saturation extract			
EC (dS m^{-1})	3.56	6.21	7.22	5.77
Ca^{2+} ($mmol_c$ L^{-1})	31.88	58.88	60.45	43.85
Mg^{2+} ($mmol_c$ L^{-1})	12.03	22.78	25.15	18.00
K^+ ($mmol_c$ L^{-1})	9.63	5.78	5.08	2.13
Na^+ ($mmol_c$ L^{-1})	5.58	9.40	12.18	13.15
SAR ($mmol_c$ L^{-1})	1.20	1.50	1.83	2.23
	Soil texture			
Sand (%)	14.20	10.30	11.30	10.92
Silt (%)	72.12	75.62	71.62	75.48
Clay (%)	13.68	14.08	17.08	13.60

EC—electrical conductivity of saturation extract; pH—hydrogen potential; OM—organic matter; SB—sum of base; CEC—cation exchange capacity; ESP—exchangeable sodium percentage; SAR—sodium adsorption ratio.

2.2. Experimental Design

The experiment was conducted in a randomized block design, with five treatments and four replications. The saline stress attenuators used were silicon (Si) applied alone and silicon in combination with organic matter (goat manure) (OM) and *Trichoderma harzianum* (T), tested using the forage sorghum crop (*Sorghum sudanense* (Piper) Stapf), cultivar IPA Sudan 4202. The treatments were: sorghum without application of salinity attenuator (control); sorghum + Si; sorghum + Si + OM; sorghum + Si + T; and sorghum + Si + T + OM. The dimensions of the experimental units were 20.0 m × 16.5 m for the total area, 4 m × 4 m for the plots, and 2 m × 2 m for the useful plots (where plants and soil samples were collected). The adopted spacing was 0.50 m between rows and ten plants per linear meter.

For the study, three sorghum cuts (the first cut plus two regrowths) were carried out between June 2021 and April 2022, totaling ten months, among which it was possible to evaluate the sorghum growth responses to the application of salinity attenuators during the region's dry and rainy seasons (Figure 2). There was no rain between the sowing and the first cut (1st cycle), while in the 2nd and 3rd cuts, the accumulated precipitation values were equal to 176.5 and 252 mm, respectively.

Irrigation was carried out using a drip irrigation system with an efficiency of 96%, the flow of each dripper set at 1.06 L h^{-1}, emitters spaced at 40 cm, and an application interval of 48 h, based on the total replacement of crop evapotranspiration (ETc) [34]. The reference evapotranspiration (ETo) was determined by the model proposed by Penman–Monteith and adapted by FAO-56 [34]. Meteorological data were collected at an automatic INMET station (National Institute of Meteorology) [Salgueiro, Pernambuco, Brazil], located 50 km from the experimental area. Rainfall data were collected in the experiment area using a manual rain gauge.

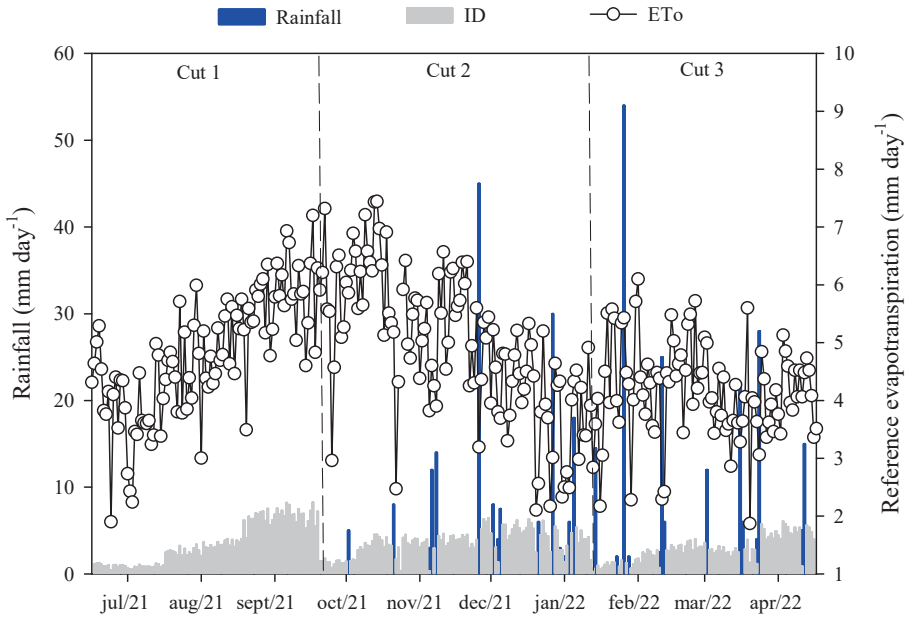

Figure 2. Meteorological conditions in the municipality of Parnamirim (PE) during the experimental period. ID—irrigation depth (mm day^{-1}); ETo—reference evapotranspiration (mm day^{-1}).

The water for irrigation came from an artesian well (Table 2), classified as C_4S_1, with a very high risk of promoting soil salinization and a low risk of soil sodification, according to [35].

Table 2. Chemical properties of irrigation water during the experimental period.

pH	EC	Ca^{2+}	Mg^{2+}	K^+	Na^+	Cl^-	HCO_3^-	SO_4^{2-}	B	Cu	Fe	Mn	Zn	SAR
	dS m^{-1}	---------- mmol$_c$ L^{-1} ----------								--------- mg L^{-1} ---------				mmol$_c$ L$^{-0.5}$
7.23	3.12	9.29	9.23	0.12	11.73	26.38	5.70	0.76	0.11	0.02	0.02	0.03	0.20	3.85

pH—hydrogen potential; EC—electrical conductivity; SAR—sodium adsorption ratio.

Potassium silicate, the silicon source used in this work, is a fertilizer containing at least 10% K^+ in K_2O and 10% silicon. It was applied twice via the soil (the first application was performed one week after sowing and the second after an interval of 15 days) and two foliar applications (the first within 15 days after the applications via soil and the second 15 days after the first foliar application), in all cycles. The spray concentrations were 5 mL L^{-1} and 10 mL L^{-1} for soil and foliar applications, respectively, as recommended by the manufacturer. In both conditions, 39.06 mL m^{-1} linear was applied.

T. harzianum was obtained from the commercial product Trichodermil SC I306. In the first cut, two applications were carried out via soil, the first at sowing and the second with an interval of 30 days after the first application. In the 2nd and 3rd cuts, an application was made at the beginning of each regrowth. In all applications, the syrup concentration was 12.5 mL L^{-1}, as recommended by the manufacturer. The applications were carried out using a costal manual pump in the planting line, with a volume of 39.06 mL of mixture per linear meter.

At the time of sowing, the soil was fertilized with goat manure (source of organic matter) (Table 3) in the proportion of 50 Mg ha^{-1}, in the treatments that included the application of organic matter. According to [36], this dose provides the best performance for the sorghum crop. The manure was previously tanned and incorporated into the surface layer of the soil.

Table 3. Characterization of goat manure used as an organic matter source in the experiment.

D	C	N	P	K^+	Na^+	Ca^{2+}	Mg^{2+}	pH	EC
g cm^{-3}	---------- g kg^{-1} ----------								dS m^{-1}
0.8158	119.70	17.90	8.70	4.50	1.10	27.70	10.20	7.87	1.87

D—density of manure; C—total organic carbon; N—total nitrogen; pH—hydrogen potential; EC—electrical conductivity.

2.3. Soil Sampling

Soil samples were collected at the end of each sorghum cut, in the "useful plots", at depths of 0–10, 10–20, 20–40, and 40–60 cm. All samples were air-dried and sieved through a 2 mm mesh. Then, the samples were submitted for the analysis of elements in the exchange complex and the soil saturation extract (soil soluble complex).

2.4. Soil Analysis

2.4.1. Soluble Complex

The saturated paste was prepared according to the methodology described by [37]. For this, distilled water was added to 500 g of soil until complete saturation was reached [37]. After 12 h of rest, the soil solution was extracted by suction. In the soil solution, the electrical conductivity (EC) was measured at 25 °C, using a conductivity meter, as well as the concentrations of Ca^{2+}, Mg^{2+}, Na^+, and K^+ (cations) and Cl^- (anions). Ca^{2+} and Mg^{2+} were determined by atomic absorption spectrometry, and Na^+ and K^+ were determined by flame emission photometry [37]. Cl^- was determined by titration with $AgNO_3$ solution, using K_2CrO_4 as an indicator [37].

2.4.2. Exchangeable Complex

Soil pH was measured directly in the 1:2.5 soil/water mixture suspension using a potentiometer. The exchangeable cations (Ca^{2+}, Mg^{2+}, Na^+, and K^+) were determined after washing soil samples with 96° alcohol. Exchangeable cations were extracted with 1 mol L^{-1} ammonium acetate solution. After that, Ca^{2+} and Mg^{2+} were determined by atomic absorption spectrometry, and Na^+ and K^+ were determined by flame emission photometry [37]. The exchangeable sodium percentage (ESP) was calculated by the ratio of exchangeable Na^+ to the cation exchange capacity (CEC), according to [37] (Equation (1)).

$$ESP\ (\%) = (Na^+/CEC) \times 100 \quad (1)$$

Soil-available phosphorus was extracted with 0.5 mol L^{-1} $NaHCO_3$ solution at pH 8.5, and determined by colorimetry with ammonium molybdate, using a spectrophotometer at 882 nm [38].

2.5. Content of Sodium, Potassium, Calcium, Magnesium, Chloride, and Phosphorus in the Plant

The sorghum plants were fractionated into leaves, stems, and panicles, and the dry mass of the sorghum plant fractions was ground in a Wiley-type mill to determine the elements Ca^{2+}, Mg^{2+}, Na^+, K^+, and P.

To determine Na^+, K^+, and Cl^- concentrations, we added 25 mL of ultra-pure water to 100 mg of dry matter in a closed container and boiled for 1 h at 100 °C [39]. The obtained extract was filtered, and the Na^+ and K^+ contents were determined by flame emission photometry. To determine Cl^-, 10 mL of the extract was collected and titrated with silver nitrate (28 mM $AgNO_3$), using potassium chromate (5% K_2CrO_4) as an indicator.

To determine P, Ca^{2+}, and Mg^{2+} concentrations, we added 25 mL of 1 mol L^{-1} HCl solution to 500 mg of dry plant mass and heated it at 80 °C for 15 min [40]. After that, Ca^{2+} and Mg^{2+} were determined by atomic absorption spectrometry, and P was determined by molybdenum blue spectrophotometry at a wavelength of 660 nm [40].

With the values of these elements' concentrations per fraction of the plants and the dry mass production of each fraction, the contents of the elements in each fraction of the

aerial part were calculated. For that, we multiplied the ion concentration by the dry mass of each plant compartment [41].

2.6. Sorghum Productivity and Water Use Efficiency (WUE)

The fresh and dry yields of forage sorghum were obtained at the end of the three sorghum cuts, with representative plants of the "useful plot". The plants were harvested and weighed at the end of each sorghum cut to obtain average fresh mass values. Then, the plants were placed in a forced circulation oven at 65 °C for 72 h until they reached constant weight, to determine the dry mass of forage sorghum. The productivity values of fresh and dry mass were multiplied by the plant stand (number of plants ha^{-1}) to obtain the productivity of shoots (dry and fresh mass in Mg of plants ha^{-1}). In this study, we had a homogeneous stand of 200,000 plants ha^{-1} for all treatments. The total productivity of fresh and dry mass was obtained by adding the values found for the productivity of the three sorghum cuts.

From the ratio between the DMY and the sum of the ET_C for the cycle, the water use efficiency (WUE) was calculated in g L^{-1}.

2.7. Statistical Analysis

Data were subjected to an analysis of variance and normality testing, as well as a comparison of the means using the Scott–Knott test at a 5% probability level, with the statistical program Rstudio (version 4.2.2) (R Core Team, 2022). Graphs were created using SigmaPlot (version 14.0) (Systat Software Inc., San Jose, CA, USA).

3. Results

3.1. Soil Chemical Properties

3.1.1. Salinity Parameters

Applying Si, *Trichoderma*, and organic matter mitigated the increase in soil salinity due to the use of saline irrigation over time, which could be observed in the second and third cuts. In the first cut, there was a significant difference ($p \leq 0.05$) in EC values only in the 10–20 cm layer, where the treatment with the application of Si + T obtained the lowest value. In the second cut, the application of isolated or combined Si in all soil layers efficiently attenuated the increase in EC, with isolated Si promoting the lowest values. In the third cut, the treatments promoted differentiation in EC values in the 10–20 cm and 40–60 cm layers, where the application of Si alone and Si + T had the best attenuation in the increase in EC, respectively (Figure 3A).

There was a change in pH in the soil layers 20–40 and 40–60 cm (cut 1), 0–10 and 40–60 cm (cut 2), and 10–20 and 20–40 cm (cut 3). Applying Si alone or combined promoted increases in soil pH values (Figure 3B). Regarding ESP, the effect of Si alone or combined did not enable significant differences ($p \leq 0.05$) concerning the control treatment in the first sorghum cut in all layers (Figure 3C). In the second and third cuts, there was a tendency for Si alone or combined to attenuate the increase in ESP concerning the control treatment. The control treatment was the least efficient in attenuating the rise in ESP, with values varying from 43% (10–20 cm) to 28% (40–60 cm) in the second cut and from 46% (10–20 cm) to 25% (40–60 cm) in the third cut.

3.1.2. Soluble Complex

The application of combined Si promoted increases in the levels of nutrient ions (K^+, Ca^{2+}, and Mg^{2+}) in the soil solution while reducing the levels of toxic ions (Na^+ and Cl^-) (Table 4). For K^+, in the first cut, the highest concentrations were observed with the application of Si + T + OM, ranging from 1.53 (0–10 cm) to 0.36 $mmol_c$ L^{-1} (40–60 cm). In the second cut, the highest concentration of K^+ was observed with the application of Si + T. In the third cut, applying Si + T promoted a higher concentration of K+ on the surface (0–10 cm). There was no difference in the concentration of K^+ in the subsoil layers (10–20, 20–40, and 40–60 cm) concerning the control treatment (Table 4).

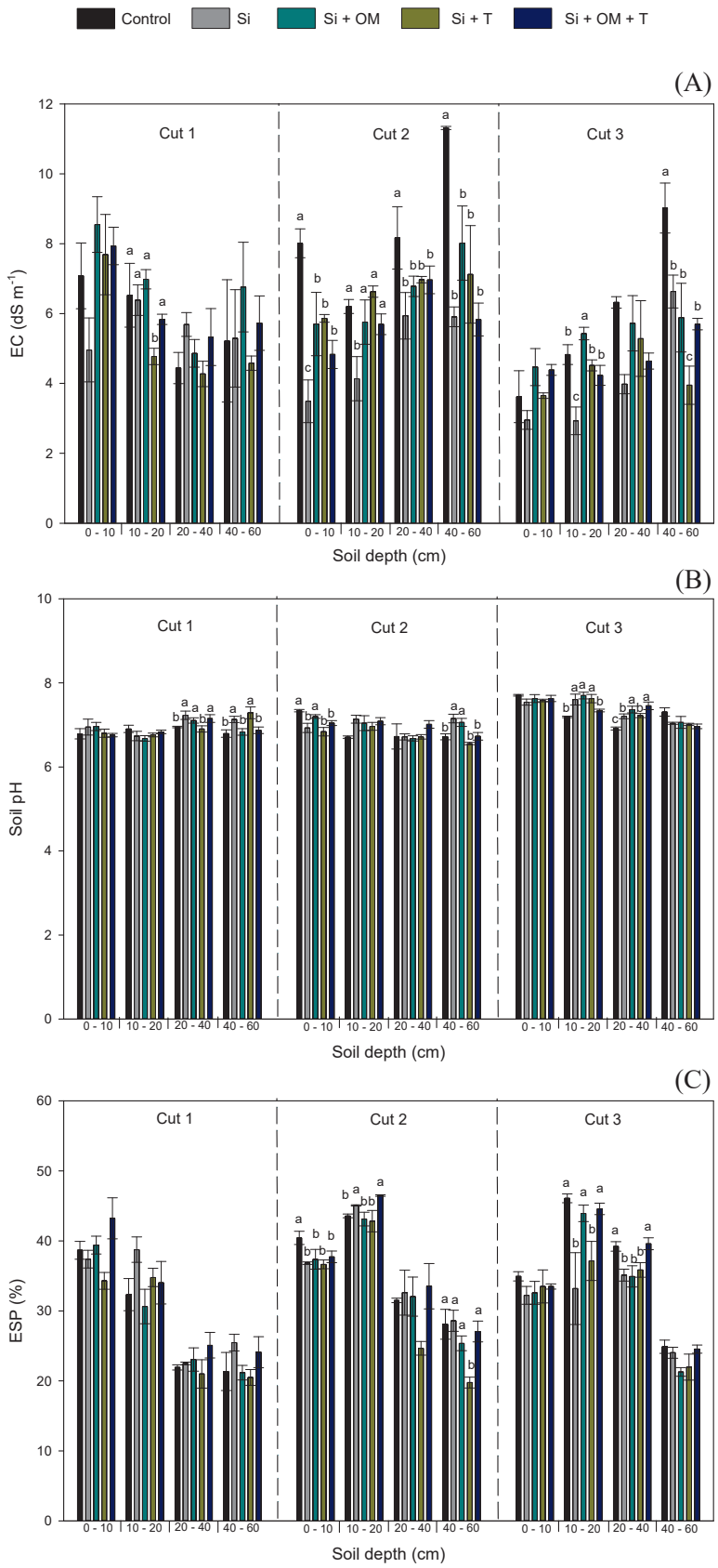

Figure 3. Mean values of the saline variables: electrical conductivity—EC (**A**), soil pH (**B**), and exchangeable sodium percent—ESP (**C**) at depths of 0–10, 10–20, 20–40, and 40–60 cm for each cut, depending on the tested saline attenuator. Different letters indicate significant differences at $p \leq 0.05$. Si = silicon; Si + OM = silicon + organic matter; Si + T = silicon + *Trichoderma harzianum*; Si + OM + T = silicon + organic matter + *Trichoderma harzianum*.

Table 4. Soluble ions concentrations for each studied soil layer in response to the tested saline attenuator along the three sorghum cuts. Different letters in the line indicate significant differences at $p \leq 0.05$.

Soil Layer (cm)	Cut 1					Cut 2					Cut 3				
	C	Si	Si + OM	Si + T	Si + T + OM	C	Si	Si + OM	Si + T	Si + T + OM	C	Si	Si + OM	Si + T	Si + T + OM
								K^+ ($mmol_c\ L^{-1}$)							
0–10	0.79 c	0.51 d	1.50 a	0.97 b	1.53 a	0.67 b	0.67 b	0.76 b	0.92 a	0.94 a	0.36 c	0.44 c	0.40 c	0.56 a	0.49 b
10–20	0.71 b	0.64 b	0.80 b	0.65 b	1.13 a	0.31 b	0.22 b	0.34 b	0.47 a	0.31 b	0.38 a	0.24 b	0.31 a	0.32 a	0.31 a
20–40	0.42 b	0.45 b	0.39 b	0.49 b	0.60 a	0.35 a	0.24 b	0.29 b	0.36 a	0.25 b	0.34	0.29	0.36	0.30	0.23
40–60	0.39	0.47	0.52	0.36	0.36	0.30 b	0.28 b	0.34 b	0.64 a	0.33 b	0.40 a	0.43 a	0.33 b	0.30 b	0.29 b
								Na^+ ($mmol_c\ L^{-1}$)							
0–10	124.37 a	84.69 b	144.26 a	90.22 b	119.69 a	133.57 a	72.07 c	107.30 b	90.58 c	83.41 c	60.27 c	48.98 d	74.95 b	86.12 a	76.61 b
10–20	77.42 b	111.44 a	95.03 b	87.48 b	90.82 b	122.82 a	98.4 b	116.85 a	94.76 b	114.46 a	103.56 a	68.97 b	80.24 b	71.91 b	113.73 a
20–40	43.62	50.41	56.41	42.21	67.62	81.03 a	80.43 a	62.52 b	70.28 a	55.95 b	93.08 a	74.95 b	102.57 a	63.46 b	88.76 a
40–60	46.34 c	75.67 b	57.83 c	52.01 c	99.85 a	121.33 a	63.12 b	72.07 b	61.32 b	63.71 b	51.22 b	82.59 a	52.51 b	43.57 b	57.58 b
								Cl^- ($mmol_c\ L^{-1}$)							
0–10	64.58 a	29.58 b	88.75 a	44.58 b	73.75 a	72.08 a	20.00 b	41.25 b	44.58 b	31.67 b	13.33 c	13.75 c	27.92 a	22.08 b	32.08 a
10–20	68.75 a	56.25 b	59.58 b	44.58 c	45.42 c	53.75 a	26.25 b	45.42 a	52.08 a	52.92 a	34.58	20.63	25.63	39.58	27.50
20–40	41.25	42.50	30.42	36.25	42.08	79.38 a	37.92 c	57.92 b	59.58 b	58.75 b	50.42 a	27.08 b	56.25 a	40.42 b	29.17 b
40–60	42.08	42.92	37.92	31.25	43.75	98.33 a	47.08 b	52.08 b	58.75 b	46.25 b	84.17 a	44.17 b	50.42 b	27.08 c	44.58 b
								Ca^{2+} ($mmol_c\ L^{-1}$)							
0–10	23.36 b	18.61 b	39.50 a	26.31 b	43.30 a	29.20 a	13.19 b	33.12 a	25.09 a	25.44 a	10.54 b	10.43 b	16.93 a	14.94 a	18.77 a
10–20	35.19 b	29.75 b	46.04 a	23.14 b	30.81 b	24.50 b	14.06 c	32.72 a	29.80 a	23.98 b	17.38 a	11.11 b	20.63 a	19.18 a	20.21 a
20–40	31.42	30.75	33.69	30.43	35.71	38.26 a	23.79 b	38.18 a	42.91 a	40.45 a	26.81 a	16.56 c	31.28 a	32.68 a	22.85 b
40–60	34.28	38.26	42.30	32.26	39.28	60.73 a	30.96 b	37.45 b	63.01 a	42.03 b	38.00 a	28.54 a	43.56 a	19.64 b	32.24 a
								Mg^{2+} ($mmol_c\ L^{-1}$)							
0–10	12.07 b	9.46 b	31.87 a	22.99 a	24.11 a	15.58	7.08	12.56	14.15	10.48	5.10 c	4.11 c	9.05 a	7.46 b	9.55 a
10–20	19.34	16.95	20.27	16.48	17.06	13.77 b	6.91 b	11.08 b	21.23 a	13.60 b	9.76	4.28	5.65	5.92	5.65
20–40	17.61	20.41	16.90	15.22	18.68	28.80 a	14.32 b	22.55 a	16.95 b	16.84 b	13.28 a	8.28 b	16.95 a	7.41 b	12.29 a
40–60	33.60 a	28.36 a	10.94 b	15.99 b	20.38 b	23.26	18.82	15.63	16.62	20.52	31.43 a	14.43 b	24.91 a	9.66 b	16.79 b

Si = silicon; Si + OM = silicon + organic matter; Si + T = silicon + *Trichoderma harzianum*; Si + OM + T = silicon + organic matter + *Trichoderma harzianum*.

There was a higher concentration of Ca^{2+} in the soil solution on the surface (0–10 and 10–20 cm) with the application of Si + OM and Si + T + OM in the first cut (Table 4). In the second cut, the application of Si + OM and Si + T promoted a significant increase ($p \leq 0.05$) in Ca^{2+} levels in the 10–20 cm layer, while in the third cut, the application of Si + OM, Si + T, and Si + T + OM promoted increases in Ca^{2+} content in the 0–10 cm layer.

Applications of Si + OM, Si + T, and Si + T + OM also promoted increased Mg^{2+} in the soil solution on the surface (0–10 cm) in the first cut (Table 4). In the second cut, there was an increase in Mg^{2+} content in the 10–20 cm layer with the application of Si + T, while in the third cut, there was an increase in the surface (0-10 cm) with the application of Si + OM, Si + T, and Si + T + OM. There was no difference in the other layers compared to the control treatment ($p \leq 0.05$).

Concerning Na^{+} concentrations, the application of Si + T most attenuated its concentration during the first cut compared to the other treatments (Table 4). In the second cut, isolated Si and its combinations effectively attenuated the increase in Na^{+} concentration in the soil solution in all layers evaluated. In the third cut, Si + OM and Si + T attenuated the rise in Na^{+} in the soil solution (Table 4).

The concentration of Cl^{-} in the soil solution was lower in the first cut for the Si and Si + T treatments in the 0–10 cm layer, while in the 10–20 cm layer, all forms of Si application proved effective for reducing Cl^{-} levels. In the second cut, isolated and combined Si presented the lowest concentrations of Cl- in soil solution in the layers of 0–10, 20–40, and 40–60 cm. In the third cut, there was an attenuation of Cl^{-} levels in the subsurface, with the application of Si, Si + T, and Si + T + OM in the 20–40 cm layer and the 40–60 cm layer, the application of Si + T was the combination that obtained the lowest concentration of Cl^{-} (Table 4).

3.1.3. Sorptive Complex

Regarding the soil assortative complex, the application of Si, alone and combined, also promoted a greater concentration of nutrient ions (K^{+}, Ca^{2+}, Mg^{2+}, and P) and reductions in the concentration of exchangeable Na^{+} (Table 5). Applying Si + OM and Si + T + OM provided a higher concentration of K^{+} in the 10–20 cm layer during the first cut. In the second cut, all forms of Si application showed a higher concentration of K^{+} on the surface (0–10 cm). In the third cut, only the application of Si was superior in surface area (0–10 cm) (Table 5).

The Ca^{2+} concentration was higher with the application of Si + OM in the 0–10 cm layer and with Si + OM, Si + T, and Si + T + OM in the 20–40 cm layer during the first cut of sorghum. In the second cut, only the application of Si + T + OM in the 0–10 cm layer showed a higher concentration of Ca^{2+}. In the third cut, the highest concentrations of Ca^{2+} were also observed on the surface (0–10 cm) with the application of Si + OM and Si + T + OM (Table 5).

Concerning Mg^{2+} in the first and second cuts, its highest concentration was observed on the surface (0–10 cm) with Si + OM and Si + T + OM. In the third cut, this increase was observed in the subsurface (20–40 cm) with the application of Si + OM and Si + T + OM (Table 5). A lower concentration of Na^{+} was observed from the second cut of sorghum on the surface (0–10 cm) with any form of application of Si, isolated or combined. In the subsurface (40–60 cm), only the application of Si + T attenuated the Na^{+} concentration. The Na^{+} concentration was attenuated in the 10–20 and 20–40 cm layers during the third cut by applying Si, Si + OM, and Si + T (Table 5).

Available P presented the highest concentration on the surface in treatments with the application of organic matter (Si + OM and Si + T + OM) during the first cut. In the second cut, similarly to the first, the treatments where organic matter was applied showed the highest concentrations of P on the surface (0–10 cm), and it was also possible to observe differences in the 40–60 cm layer with the application of Si, Si + T and Si + T + OM, which presented higher concentrations compared to the control treatment. In the third cut, treatments applying organic matter also stand out concerning the others (Table 5).

Table 5. Ions concentrations in the exchange complex for each studied soil layer, in response to the tested saline attenuator along the three sorghum cuts. Different letters in the line indicate significant differences at $p \leq 0.05$.

Soil Layer (cm)	Cut 1					Cut 2					Cut 3				
	C	**Si**	**Si + OM**	**Si + T**	**Si + T + OM**	**C**	**Si**	**Si + OM**	**Si + T**	**Si + T + OM**	**C**	**Si**	**Si + OM**	**Si + T**	**Si + T + OM**
							K^+ ($cmol_c\ kg^{-1}$)								
0–10	1.14	1.54	1.35	1.11	1.38	0.79 c	1.23 a	1.01 b	1.25 a	1.03 b	0.58 b	0.96 a	0.65 b	0.74 b	0.63 b
10–20	0.59 c	0.60 c	0.85 b	0.69 c	1.07 a	0.45 b	0.35 b	0.54 b	0.77 a	0.69 a	0.42	0.29	0.41	0.43	0.45
20–40	0.35 a	0.26 b	0.28 b	0.24 b	0.33 a	0.31	0.26	0.26	0.37	0.35	0.22	0.24	0.21	0.21	0.21
40–60	0.21	0.22	0.19	0.21	0.26	0.33 a	0.23 b	0.26 b	0.37 a	0.23 b	0.21	0.22	0.14	0.21	0.24
							Na^+ ($cmol_c\ kg^{-1}$)								
0–10	6.23	6.02	6.34	5.52	6.96	6.51 a	5.93 b	6.02 b	5.90 b	6.07 b	5.63	5.19	5.25	5.39	5.39
10–20	5.02	6.02	4.76	5.41	5.29	6.86	7.00	6.70	6.66	7.22	7.16 a	5.16 b	6.83 a	5.77 b	6.93 a
20–40	3.44	3.53	3.62	3.29	3.94	4.94	5.12	5.03	3.87	5.26	6.15 a	5.51 b	5.48 b	5.63 b	6.21 a
40–60	3.65	4.35	3.62	3.50	4.12	4.80 a	4.88 a	4.33 a	3.38 b	4.62 a	4.25	4.10	3.64	3.75	4.19
							Ca^{2+} ($cmol_c\ kg^{-1}$)								
0–10	14.79 b	15.31 b	18.67 a	14.19 b	16.12 b	18.12 b	16.52 b	18.23 b	19.45 b	22.79 a	18.21 b	17.88 b	18.72 a	16.78 c	19.30 a
10–20	15.28	15.41	15.84	15.13	16.05	17.41	16.74	16.18	16.75	17.09	16.38	16.04	16.59	16.56	16.08
20–40	16.75 b	16.47 b	18.67 a	18.00 a	19.20 a	18.07	18.61	18.29	18.31	19.47	16.38	16.81	16.49	16.49	17.16
40–60	20.52 a	19.70 a	17.08 b	17.96 b	19.68 a	19.32	18.34	20.12	20.04	19.45	18.02	17.25	17.21	17.52	17.44
							Mg^{2+} ($cmol_c\ kg^{-1}$)								
0–10	9.85 b	9.02 c	11.04 a	9.90 b	10.93 a	9.06 b	8.29 c	8.73 b	8.73 b	10.49 a	13.34 a	12.49 b	12.92 b	12.57 b	13.32 a
10–20	10.20	10.34	10.95	10.31	10.86	8.73 a	8.84 a	8.91 a	8.27 b	9.17 a	12.90 a	13.21 a	12.95 a	11.70 b	13.19 a
20–40	12.00 a	9.87 b	11.96 a	9.17 b	9.39 b	9.15	9.30	9.61	9.46	9.90	11.85 b	12.16 b	13.30 a	11.78 b	12.81 a
40–60	13.25 a	13.03 a	11.56 b	12.42 a	11.28 b	11.81	11.02	10.53	9.81	11.04	13.98	14.64	12.75	12.55	13.69
							P ($mg\ kg^{-1}$)								
0–10	45.72 b	56.19 b	123.17 a	43.10 b	113.66 a	38.14 c	44.79 c	97.20 b	40.63 c	148.32 a	42.16 b	32.29 b	81.07 a	38.60 b	70.40 a
10–20	35.52 c	42.11 c	52.67 b	38.41 c	69.87 a	23.87	34.42	37.21	39.06	47.86	26.94 c	35.57 b	41.96 a	28.16 c	44.73 a
20–40	24.43	25.81	26.77	27.74	24.84	24.63	23.03	25.21	28.08	31.62	30.97 a	23.09 b	34.92 a	23.87 b	20.92 b
40–60	23.34	30.13	24.87	21.58	28.85	17.10 c	26.42 b	21.18 c	32.56 a	26.42 b	30.18	21.06	21.62	27.53	26.77

Si = silicon; Si + OM = silicon + organic matter; Si + T = silicon + Trichoderma harzianum; Si + OM + T = silicon + organic matter + Trichoderma harzianum.

3.2. Ions Content at Plant Tissue

The total Na^+ content in the aerial part of the plant differed only in the second cut, where the application of Si + T presented a higher content (Table 6). We observed that the Na^+ content in the leaf was lower in all treatments with the application of isolated or combined Si, compared to the control treatment, and that sorghum tends to concentrate more Na^+ in the stalk, having the Si + T treatment present the highest content (Table 6).

About K^+, the application of Si alone or combined promoted a more significant accumulation of this element in the aerial part of sorghum in the first and third cuts than the control treatment. In the leaves, the application of S + T + OM favored a more significant accumulation of K^+. In the stalks, in the third cut, the control treatment showed a lower accumulation of K^+ than the others. There was also a difference in the content of this ion in the panicle, with treatments with the application of organic matter (Si + OM and Si + T + OM) showing the highest values.

In the third sorghum cut, the application of Si + OM, Si + T, and Si + T + OM favored a more significant accumulation of Cl^- in the aerial part of the plant, so that most of the Cl^- was more significantly present in the plant stalks. In the leaves, the concentration of Cl^- was significantly higher in the control treatment and with the application of Si + T + OM. In contrast, in the stalks, the control treatment and Si alone showed lower contents of this element (Table 6).

Applying Si + OM, Si + T, and Si + T + OM also favored a more significant accumulation of P in the aerial part of sorghum in the three cuts. Si + T + OM promoted the highest P contents, with 92.27, 118.93, and 113.55 mg of P in the first, second, and third cuts, respectively. The accumulation of Ca^{2+} and Mg^{2+} in the sorghum leaf, stalk, and panicle was enhanced with the application of Si alone and combined with T and OM; however, combined Si (Si + OM, Si + T, and Si + T + OM) promoted more significant accumulation of these elements in different parts of the plant as well the aerial part of sorghum, in the three cuts (Table 6).

Table 6. Ions content in each part of the plant and all plant shoots, in response to the tested saline attenuator for the three sorghum cuts. Different letters in the column indicate significant differences at $p \leq 0.05$.

Treatment	Na^+ (g)			K^+ (g)			Cl^- (g)			P (mg)			Ca^{2+} (g)			Mg^{2+} (g)		
	Cut 1	Cut 2	Cut 3	Cut 1	Cut 2	Cut 3	Cut 1	Cut 2	Cut 3	Cut 1	Cut 2	Cut 3	Cut 1	Cut 2	Cut 3	Cut 1	Cut 2	Cut 3
									Leaves									
Control	0.05	0.15 a	0.06	0.78 b	0.67	0.36	0.41	0.32	0.31 a	33.84	43.73 a	27.09 c	0.20 b	0.22	0.16 b	0.13 b	0.10 c	0.09
Si	0.07	0.06 b	0.04	0.90 b	0.48	0.30	0.44	0.24	0.24 b	44.47	32.49 b	30.44 b	0.26 a	0.24	0.21 a	0.18 a	0.12 c	0.10
Si + OM	0.06	0.08 b	0.05	0.85 b	0.57	0.41	0.38	0.30	0.22 b	41.27	48.72 a	23.93 c	0.21 b	0.24	0.22 a	0.17 a	0.11 c	0.10
Si + T	0.06	0.10 b	0.07	0.84 b	0.64	0.38	0.36	0.37	0.23 b	46.79	43.16 a	25.05 c	0.27 a	0.26	0.23 a	0.18 a	0.13 b	0.11
Si + OM + T	0.06	0.10 b	0.05	1.06 a	0.63	0.39	0.52	0.34	0.30 a	47.92	45.66 a	34.01 a	0.28 a	0.29	0.25 a	0.20 a	0.15 a	0.13
									Stems									
Control	0.16 b	0.22 b	0.07	2.65 b	2.11	0.86 b	2.07 a	1.14	0.82 b	23.75	41.42	24.33 b	0.21 a	0.22 b	0.21 b	0.22 a	0.23 a	0.21
Si	0.11 b	0.19 b	0.14	2.72 b	2.19	1.68 a	1.47 b	1.32	1.06 b	16.94	35.99	53.85 a	0.15 b	0.18 b	0.20 b	0.15 b	0.17 b	0.23
Si + OM	0.21 b	0.30 b	0.17	3.75 a	2.93	1.82 a	2.07 a	1.19	1.32 a	31.03	56.92	41.75 b	0.22 a	0.20 b	0.28 a	0.25 a	0.20 b	0.26
Si + T	0.32 a	0.80 a	0.15	4.16 a	2.35	1.92 a	2.21 a	1.73	1.27 a	19.99	56.99	64.87 a	0.21 a	0.30 a	0.26 a	0.20 a	0.25 a	0.27
Si + OM + T	0.17 b	0.39 b	0.12	3.22 b	2.82	1.79 a	2.14 a	1.46	1.30 a	24.33	60.54	67.31 a	0.23 a	0.29 a	0.27 a	0.23 a	0.29 a	0.28
									Panicles									
Control	0.02	0.02	0.01	0.15 b	0.14	0.05 c	0.05	0.02	0.03	6.52 c	14.36	5.31	0.01 c	0.02 c	0.03 c	0.03 c	0.02 b	0.02 c
Si	0.03	0.03	0.01	0.19 b	0.13	0.04 c	0.10	0.04	0.03	12.01 b	11.26	3.16	0.02 b	0.04 b	0.06 b	0.05 b	0.04 b	0.04 b
Si + OM	0.05	0.02	0.02	0.42 a	0.14	0.10 a	0.11	0.04	0.06	18.60 a	13.05	9.85	0.04 a	0.06 a	0.09 a	0.09 a	0.06 a	0.07 a
Si + T	0.05	0.03	0.01	0.27 b	0.13	0.04 c	0.11	0.02	0.04	20.38 a	15.21	532	0.03 b	0.06 a	0.06 b	0.06 a	0.06 a	0.06 a
Si + OM + T	0.06	0.02	0.01	0.35 a	0.14	0.07 b	0.10	0.03	0.07	20.02 a	12.72	12.24	0.03 a	0.06 a	0.07 b	0.07 a	0.06 a	0.07 a
									Plant shoot									
Control	0.23	0.38 b	0.14	3.58 b	2.93	1.28 b	2.54	1.49	1.16 b	64.11 b	99.50 b	56.73 c	0.42 c	0.46 b	0.40 b	0.37 c	0.35 b	0.31 b
Si	0.21	0.28 b	0.18	3.82 b	2.79	2.03 a	2.02	1.60	1.33 b	73.41 b	79.74 b	87.45 b	0.44 c	0.47 b	0.46 b	0.38 c	0.33 b	0.38 b
Si + OM	0.32	0.40 b	0.24	5.02 a	3.64	2.33 a	2.57	1.53	1.61 a	90.91 a	118.69 a	75.53 c	0.48 b	0.49 b	0.59 a	0.51 a	0.38 b	0.43 a
Si + T	0.43	0.93 a	0.23	5.26 a	3.12	2.35 a	2.67	2.12	1.54 a	87.16 a	115.36 a	95.25 b	0.51 a	0.62 a	0.56 a	0.44 b	0.44 a	0.43 a
Si + OM + T	0.30	0.51 b	0.19	4.63 a	3.60	2.25 a	2.76	1.83	1.66 a	92.27 a	118.93 a	113.55 a	0.55 a	0.64 a	0.59 a	0.50 a	0.49 a	0.47 a

Si = silicon; Si + OM = silicon + organic matter; Si + T = silicon + *Trichoderma harzianum*; Si + OM + T = silicon + organic matter + *Trichoderma harzianum*.

3.3. Sorghum Yield and Water Use Efficiency

In all sorghum cuts, applying Si combined with T and/or OM, significantly increased the fresh and dry mass of the shoot in the three sorghum cuts (Table 7). The highest accumulated yields (total of the three cuts) were also achieved with the application of combined Si, where Si + OM, Si + T, and Si + T + OM obtained, respectively, yields of 62.03, 62.53, and 59.05 t ha^{-1} of dry matter, and 182.43, 179.45, and 169.62 t ha^{-1} of fresh mass (Table 7). It corresponds to gains in dry mass for the Si + OM, Si + T, and Si + T + OM treatments, of 38, 39, and 31% compared to the control treatment (without application of Si) and 26, 27, and 20% compared to the treatment where Si was applied alone. Regarding fresh mass, also for the Si + OM, Si + T, and Si + T + OM treatments, the accumulated gains concerning the control treatment (without application of Si) and Si alone were similar—25, 23, and 11%.

Table 7. Mean values of sorghum dry matter yield (DMY) and sorghum fresh matter yield (FMY) for each cut and the total of the three cuts, depending on the tested saline attenuator. Different letters in the column indicate significant differences at $p \leq 0.05$.

Saline Attenuator	DMY (t ha^{-1})				FMY (t ha^{-1})			
	Cut 1	Cut 2	Cut 3	Total Yield	Cut 1	Cut 2	Cut 3	Total Yield
Control	16.99 b	17.59 b	10.21 c	44.80 b	52.33 b	52.28 c	41.76 b	146.37 b
Si	18.09 b	19.34 b	11.71 c	49.14 b	55.42 b	49.25 c	41.58 b	146.24 b
Si + OM	22.09 a	21.06 b	18.88 a	62.03 a	62.58 a	58.78 b	61.07 a	182.43 a
Si + T	19.96 b	27.36 a	15.21 b	62.53 a	58.61 b	67.14 a	53.70 a	179.45 a
Si + OM + T	23.69 a	20.56 b	14.80 b	59.05 a	66.20 a	51.22 c	52.20 a	169.62 a

Si = silicon; Si + OM = silicon + organic matter; Si + T = silicon + *Trichoderma harzianum*; Si + OM + T = silicon + organic matter + *Trichoderma harzianum*.

Applying Si + OM, Si + T, and Si + T + OM increased the water use efficiency (WUE) of sorghum plants, compared to the control and Si alone, in the three sorghum cuts. Regarding the accumulated values, Si + OM, Si + T, and Si + T + OM obtained a water use efficiency of 15.3, 15.05, and 14.65 g of dry mass per liter of water, respectively, compared to 10.98 and 12.02 g L^{-1} of dry mass from the control treatments and with application of Si alone, respectively (Table 8). It meant an increased water use efficiency for Si + OM, Si + T, and Si + T + OM of 40, 37, and 33%, compared to the control treatment and 27, 25, and 22% compared to Si alone.

Table 8. Mean values of water use efficiency (WUE) by sorghum for each cut and the total of the three cuts, depending on the tested saline attenuator. Different letters in the column indicate significant differences at $p \leq 0.05$.

Saline Attenuator	WUE (g DM L^{-1} H_2O)			
	Cut 1	Cut 2	Cut 3	Total WUE
Control	4.89 b	3.55 b	2.55 c	10.98 b
Si	5.20 b	3.90 b	2.92 c	12.02 b
Si + OM	6.35 a	4.25 b	4.71 a	15.30 a
Si + T	5.74 b	5.52 a	3.79 b	15.05 a
Si + OM + T	6.81 a	4.14 b	3.69 b	14.65 a

Si = silicon; Si + OM = silicon + organic matter; Si + T = silicon + *Trichoderma harzianum*; Si + OM + T = silicon + organic matter + *Trichoderma harzianum*.

4. Discussion

Increasing soil salinity through irrigation with saline water is a common challenge in semiarid regions around the globe. Biosaline agriculture, in conjunction with saline stress attenuators, proved to be efficient in improving the productivity of crops and enabling agricultural production under salty stress conditions. In our study, silicon combined with

Trichoderma harzianum and organic matter was more effective in mitigating the effects of saline irrigation on forage sorghum and mainly favoring its growth and yield.

4.1. Salinity Parameters

The decrease in EC over time can be explained by the precipitation observed during the experiment period, which was 176.5 and 252 mm during the second and third sorghum cuts, respectively, totaling 428.5 mm. Soil salinity is seasonal and follows climate change, so salinity is higher in dry periods and tends to decrease in rainy periods, as water promotes the dilution of the salts present, which are leached out of the soil profile, thus promoting its washing.

In addition to this natural decrease caused by rain, it was observed that treatments with Si and other salt stress attenuators also reduced EC compared to the control treatment, emphasizing the application of isolated Si and Si + T. Ref. [42] stated that silicon interacts with soil moisture and can regulate EC. As all salt stress attenuators were applied with silicon, alone or combined, our results are in agreement with previous studies such as [43,44], which had also observed that the application of silicon reduced the EC of the soil and favored plant growth. A similar result was found by [45], who, studying different sources of Si in a saline soil cultivated with corn, also found a decrease in EC with the application of potassium silicate.

In saline and sodic soils, silicon interacts with Na^+ present in the soil and forms sodium silicate (Na_2SiO_3), which increases the mobility and absorption of Ca^{2+}, Mg^{2+}, and K^+ and reduces the transport of Na^+ and Cl^- to the roots of plants, favoring their leaching [30]. Furthermore, Ref. [42] stated that Si's ability to bind to other minerals and its adsorption on clay particles makes it difficult for more Na or Cl ions to bind to essential mineral nutrients or to the surface of soil particles, which can reduce the availability of these salts and their absorption by plant roots in the soil, and consequently promote their leaching.

The predominance of Cl^- and Na^+ in the soil solution mainly influenced the increase in EC in the control treatment, reflecting the low quality of the water used in this experiment, which contains a high concentration of these ions in its composition (Table 2). According to [6,9], the predominance of Na^+ and Cl^- in the soil solution in irrigated areas is expected due to the low groundwater quality in the region. The predominance of ions in the soil solution was in the following order: $Na^+ > Cl^- > Ca^{2+} > Mg^{2+} > K^+$. The high concentration of these elements in the soil solution contributes to increasing the ionic strength of the soil solution and, consequently, its electrical conductivity [46].

Soil pH showed high variability between treatments in all soil layers. It ranged from 6.68 to 7.75, values above the ideal range for sorghum cultivation, which is 5.5 to 6.5 [47], but which are in line with expectations for salt-affected soils in semiarid regions [48]. This increase may be due to the imbalance in ionic composition resulting from excess Na^+ and the presence of bicarbonates (5.70 $mmol_c\ L^{-1}$), which are also present in the water used for irrigation (Table 2) [49,50].

In general, applying Si alone or in combination promoted an increase in pH in some soil layers. Previous studies have demonstrated positive correlations between silicon and soil pH [51,52], as well as increases in soil pH in response to the application of silicon sources in the soil [31,53]. It occurs because OH^- ions are released during the dissolution of silicate fertilizers [54], contributing to an increase in soil pH. Ref. [55] further stated that the mineral Si has an alkaline nature, and its surface can easily transport exchangeable cations in large quantities and exchangeable H^+ in small quantities, resulting in solid hydrolysis of exchangeable cations in the soil, which produces a high proportion of NaOH in the soil solution and increases soil pH.

Compared to the initial soil sample (Table 1), ESP increased between 200 and 400% in the soil layers across the three sorghum cuts. The soil was classified as saline-sodic [37], with an EC > 4 dS m^{-1} and a PST > 15%. Increased sodicity promotes physical deterioration of the soil, mainly affecting water infiltration into the soil and root penetration [56,57]. The

soil used in this study is especially susceptible to salinization and sodification due to its finer texture (Table 1) [58,59]. However, despite the increase, the application of Si alone or combined allowed this increase in ESP to be smaller than the control treatment, mainly related to the decrease in Na^+ in the soil sorptive complex and the increase in K^+, Ca^{2+}, and Mg^{2+}.

4.2. Soluble and Sorptive Complex

Compared to the initial soil characterization (Table 1), there was a reduction in soluble K^+, Ca^{2+}, and Mg^{2+}, while soluble Na^+ increased by approximately 10 times in the soil layers along the sorghum cuts. This increase in Na^+ levels is explained by its high concentration in the irrigation water used in this work. Thus, the components of the soluble fraction of the soil are quickly altered in areas using irrigation with saline water [60]. Furthermore, it is normal for nutrient ions to decrease over time due to the absorption of these nutrients by plants, especially K^+, which sorghum absorbed in more significant quantities in this experiment.

Si applied alone was ineffective in increasing nutrient concentrations in the soil, since, in its composition, the only nutrient provided in addition to Si is K^+. Still, it reduced the concentrations of Na^+ and Cl^- in the soil, with the treatment which proved to be more effective in mitigating soil salinity when applied in combination with *Trichoderma*. Although there was a reduction in the levels of Ca^{2+}, Mg^{2+}, and K^+ compared to the initial characterization of the soil, in general, the applied silicon combined with organic matter and *Trichoderma* (Si + OM, Si + T, and Si + T + OM) presented higher concentration values of K^+, Ca^{2+}, and Mg^{2+} in the solution as well the soil sorption complex, compared to the control.

Adding organic matter can mitigate the effect of salts and improve plant growth, as it is a source of nutrients, increasing their availability, while also increasing water retention, improving soil structure, and increasing the bioactivity of microorganisms [61,62]. The action of *Trichoderma* may be associated with the fungus' ability to increase the availability of nutrients in the soil through the secretion of organic acids into the root environment, as well as acting as a decomposer and mineralizer of OM, releasing the nutrients present in it more quickly [63–66].

In the soil exchange complex, the abundance of cations was in the following order: $Ca^{2+} > Mg^{2+} > Na^+ > K^+$. Ref. [9] observed the same sequence of cation abundance in cultivated soils in semiarid Brazil. Some cations are adsorbed more strongly to soil colloids, with this binding force being more significant the greater the charge on the ion and the smaller its hydrated radius [67]. Ca^{2+} and Mg^{2+} (present in high levels in irrigation water), because they have a greater charge (+2) and a smaller hydrated radius than Na and K (+1), are more easily retained in the soil exchange complex. Regarding Na^+ and K^+, although K^+ has a smaller ionic radius, the high concentration of soluble Na^+ in the soil solution causes it to become more adsorbed [68].

Concerning available P, treatments applying organic matter (S + OM and Si + T + OM) contributed most to its increase. Ref. [69] stated that the organic P present in OM can contribute to the long-term supply of P to crops through mineralization processes, so that organic P constitutes, on average, 25% of the total P in agricultural soils. It has also been demonstrated that the long-term application of organic fertilizer can improve soil P availability, reducing P sorption by competition or altered pH, accelerating the dissolution of soil metal oxides by organic acids, and promoting microbial P mineralization [70–72]. Additionally, Ref. [73] found that organic amendments can improve crop yield and phosphate fertilizer use efficiency by altering soil P fractions and increasing phosphatase activity. Similarly, Ref. [74] showed that combining organic and chemical fertilizers increased vegetable production and decreased total P leaching losses by >20%. In addition to increasing P availability and soil organic carbon (C), applying organic matter improves soil aggregation and environmental conditions for the soil microbial community, consequently improving SOM mineralization and nutrient cycling [75,76].

4.3. Ions Content at Plant Tissue Level

In sorghum plants, a higher content of K^+ without Na^+ was observed with the application of Si alone or in combination. In other crops, the isolated efficiency of Si, OM, and T in improving the absorption of K^+ at the expense of Na^+ has been proven, such as in spinach [77], fava beans [78], wheat [79], and in sorghum itself [18,80,81]. It may have occurred due to Si's ability to increase the absorption of K^+ at the expense of Na^+, thus balancing the Na^+/K^+ ratio [19,20,82]. Furthermore, Si forms a silica barrier in the roots that reduces the passage of Na^+ to the shoot [20,83]. This is supported by the results of this study, since Na^+ was the cation absorbed the least by sorghum, despite its higher concentration in the soil solution. The accumulation of ions in the sorghum shoot followed the following order: $K^+ > Cl^- > Ca^{2+} > Mg^{2+} > Na^+ > P$.

Despite the low absorption of Na^+ by plants, this behavior was not observed for the Cl^- content, which was high, second only to K^+. Other authors observed the opposite effect, such that the application of Si reduced the absorption of Cl^- in different cultures. Si decreased Cl^- absorption in rice, while Cl^- concentration in roots was not changed [84]. Similar results were found in okra [85] and grapevine [86].

The greater absorption of Cl^- with the application of attenuators (Si + OM, Si + T, and Si + T + OM) did not negatively affect sorghum production, since these were the same treatments that obtained the highest fresh and dry mass production. The high K^+ content in the plant may justify not affecting production, as potassium is an activator of many cytoplasmic enzymes necessary for photosynthesis and respiration [87]. Therefore, a deficiency in K^+ suppresses photosynthesis and even reduces plant growth, while an increase in its absorption can alleviate the harmful effects of salinity [88]. Furthermore, K^+ plays a vital role in maintaining and creating turgor pressure and adjusting plant water balance [87].

Applying Si + OM, Si + T, and Si + T + OM increased the K^+, Ca^{2+}, Mg^{2+}, and P content in the aerial part of sorghum plants. It can be explained by the ability of OM to improve soil fertility. As already reported, applying organic matter enhances soil aggregation, improving environmental conditions for the soil microbial community and consequently improving SOM mineralization and nutrient cycling [75,76]. Trichoderma, in addition to exuding organic acids, can solubilize nutrients, especially phosphates, assists in the mineralization of organic matter, improves soil fertility, and improves the efficiency of nutrient use by plants, consequently contributing to their growth [25,63,89]. Trichoderma spp. is also related to the production of phytohormones, such as auxins, that help plant growth [90]. Such substances favor cell elongation in higher plants and increase the surface of the root system, enabling greater access to soil nutrients [91,92].

4.4. Sorghum Yield and Water Use Efficiency

Isolated Si increased sorghum dry matter productivity by around 10%, and this gain may be mainly associated with the reduction in the EC of the saturation extract in this treatment. However, the EC of all treatments did not exceed the threshold salinity for forage sorghum (10 dS m^{-1}) [93]. However, Si's ability to reduce Na^+ and Cl^- concentrations in the soil changes the ionic composition of the EC and reduces the toxicity caused by these ions [30,42]. The gain in productivity with combined Si (Si + OM, Si + T, and Si + T + OM) is associated with improvements in chemical attributes, soil fertility, and plant nutrition promoted by saline stress attenuators [19,94–96]. This study evidenced this by a reduction in toxic ions (Na^+ and Cl^-) in the soil and an increase in nutrient ions (K^+, Ca^{2+}, Mg^{2+}, and P) in the soil and plant tissue using combined Si.

Trichoderma are recognized as synthesizers of phytohormones, such as auxin, and hormone-like compounds called harzianolide, substances that, together with auxin, act to expand the cell wall and increase biomass production by plants [97,98]. OM acts as a source of nutrients, soil conditioner, and food for the soil microbiota, and these characteristics improve fertility, soil aggregation, and nutrient cycling, thus promoting better nutrition and more significant biomass accumulation by sorghum [99,100]. The productivity obtained

in this study is compatible with that found even when forage sorghum is irrigated with good-quality water [101–103].

Regarding WUE, in the bibliography, we found positive results on the efficiency of Si [104,105], OM [106,107], and T [108,109] in improving WUE. It is known that T increases root growth [110,111], and as a result, a greater area of soil is explored by the roots, resulting in better absorption and efficiency in the use of water by sorghum. Ref. [112] reported that *Trichoderma* increased sorghum root biomass by 50% under salinity. T also acts on stomatal regulation, thus reducing water loss and improving WUE [108]. Meanwhile, OM promotes greater water retention in the soil (irrigation + rain), increasing available water and its absorption by sorghum [113]. Si mainly contributes by adjusting nutritional imbalances, the photosynthetic system, and antioxidant mechanisms, factors associated with WUE [104].

5. Conclusions

Due to the soil in this study being, in particular, more susceptible to salinization and sodification due to its finer texture, the chemical quality of the soil deteriorated over time (>EC, ESP, Na^+ and Cl^-), making this type of soil unsuitable for irrigation with saline water. However, the applications of salt stress attenuators used in this study caused this increase in salinity parameters to be reduced in comparison with the control treatment. This way, the risk of degradation and loss of the soil's productive capacity using mitigating agents is lower. The association of silicon with organic matter and *Trichoderma harzianum* increases the concentration of soluble K^+ in the soil and the content of this element in plants. In this sense, plants' tolerance to salinity is increased, since K^+ participates in several critical metabolic processes in plants, alleviating the harmful effects of salinity. In general, the tested combinations improve plant nutrition by increasing the absorption of K^+, P, Ca^{2+}, and Mg^{2+} and, consequently, increasing the tolerance of forage sorghum to saline stress. In general, plants subjected to combined Si were better nourished and exposed to greater soil water retention and lower concentrations of toxic ions (Na^+ and Cl^-). Thus, productive capacity and WUE were improved. Therefore, agricultural practices with combined Si management (Si + T, Si + OM, and Si + T + OM) are essential for semiarid regions, as they favor the development of forage sorghum and allow the use of saline waters common to these regions.

Author Contributions: Conceptualization, J.O.N.d.S., L.G.M.P. and E.M.d.S.; methodology, J.O.N.d.S., L.G.M.P. and M.B.G.d.S.F.; field work and laboratory analyses, J.O.N.d.S. and L.R.d.S.; data curation, E.S.d.S. and S.L.F.-S.; writing—original draft, J.O.N.d.S., L.G.M.P. and E.M.d.S.; writing—review and editing, T.G.F.d.S. and J.G.E.d.F.; supervision, E.L.d.N.A.; funding acquisition, L.G.M.P. All authors have read and agreed to the published version of the manuscript.

Funding: Conselho Nacional de Desenvolvimento Científico e Tecnológico (CNPQ) obtained through the Call CNPq/MCTI/FNDCT n° 18/2021 (UNIVERSAL), Track A—Emerging Groups (Project Number: 409937/2021-5).

Institutional Review Board Statement: Not applicable.

Data Availability Statement: The data presented in this study are available on request from the corresponding author.

Conflicts of Interest: The authors declare no conflict of interest.

References

1. Corwin, D.L. Climate change impacts on soil salinity in agricultural areas. *Eur. J. Soil Sci.* **2021**, *72*, 842–862. [CrossRef]
2. Haj-Amor, Z.; Bouri, S. Use of HYDRUS-1D–GIS tool for evaluating effects of climate changes on soil salinization and irrigation management. *Arch. Agron. Soil Sci.* **2020**, *66*, 193–207. [CrossRef]
3. Mukhopadhyay, R.; Sarkar, B.; Jat, H.S.; Sharma, P.C.; Bolan, N.S. Soil salinity under climate change: Challenges for sustainable agriculture and food security. *J. Environ. Manag.* **2021**, *280*, 111736. [CrossRef] [PubMed]
4. Shao, H.; Chu, L.; Lu, H.; Qi, W.; Chen, X.; Liu, J.; Kuang, S.; Tang, B.; Wong, V. Towards sustainable agriculture for the salt-affected soil. *L. Degrad. Dev.* **2019**, *30*, 574–579. [CrossRef]

5. Lima, A.O.; Lima-Filho, F.P.; Dias, N.S.; Chipana-Rivera, R.; Ferreira Neto, M.; Souza, A.M.; Rego, P.R.A.; Fernandes, C.S. Variation of the water table and salinity in alluvial aquifers of underground dams in the semi-arid region of Rio Grande do Norte, Brazil. *Biosci. J.* **2019**, *35*, 477–484. [CrossRef]
6. Fernandes, J.G.; Freire, M.B.G.S.; Cunha, J.C.; Galvíncio, J.D.; Correia, M.M.; Santos, P.R. Qualidade físico-química das águas utilizadas no Perímetro Irrigado Cachoeira II, Serra Talhada, Pernambuco. *Rev. Bras. Ciênc. Agrár.–Braz. J. Agric. Sci.* **2009**, *4*, 27–34. [CrossRef]
7. Lessa, C.I.N.; Lacerda, C.F.; Cajazeiras, C.C.D.A.; Neves, A.L.R.; Lopes, F.B.; Silva, A.O.; Souza, H.C.; Gheyi, H.R.; Nogueira, R.S.; Lima, S.C.R.V.; et al. Potential of Brackish Groundwater for Different Biosaline Agriculture Systems in the Brazilian Semi-Arid Region. *Agriculture* **2023**, *13*, 550. [CrossRef]
8. Pessoa, L.G.M.; Freire, M.B.G.D.S.; Wilcox, B.P.; Green, C.H.M.; Araújo, R.J.T.; Filho, J.C.D.A. Spectral reflectance characteristics of soils in northeastern Brazil as influenced by salinity levels. *Environ. Monit. Assess.* **2016**, *188*, 616. [CrossRef]
9. Pessoa, L.G.M.; Freire, M.B.G.S.; Green, C.H.M.; Miranda, M.F.A.; Filho, J.C.A.; Pessoa, W.R.L.S. Assessment of soil salinity status under different land-use conditions in the semiarid region of Northeastern Brazil. *Ecol. Indic.* **2022**, *141*, 109139. [CrossRef]
10. Ali, A.Y.A.; Ibrahim, M.E.H.; Zhou, G.; Zhu, G.; Elsiddig, A.M.I.; Suliman, M.S.E.; Elradi, S.B.M.; Salah, E.G.I. Interactive impacts of soil salinity and jasmonic acid and humic acid on growth parameters, forage yield and photosynthesis parameters of sorghum plants. *S. Afr. J. Bot.* **2022**, *146*, 293–303. [CrossRef]
11. Saadat, S.; Homaee, M. Modeling sorghum response to irrigation water salinity at early growth stage. *Agric. Water Manag.* **2015**, *152*, 119–124. [CrossRef]
12. Parihar, P.; Singh, S.; Singh, R.; Singh, V.P.; Prasad, S.M. Effect of salinity stress on plants and its tolerance strategies: A review. *Environ. Sci. Pollut. Res.* **2015**, *22*, 4056–4075. [CrossRef] [PubMed]
13. Xie, Z.; Song, R.; Shao, H.; Song, F.; Xu, H.; Lu, Y. Silicon improves maize photosynthesis in saline-alkaline soils. *Sci. World J.* **2015**, *2015*, 245072. [CrossRef] [PubMed]
14. Ji, X.; Tang, J.; Zhang, J. Effects of Salt Stress on the Morphology, Growth and Physiological Parameters of *Juglansmicrocarpa* L. Seedlings. *Plants* **2022**, *11*, 2381. [CrossRef]
15. Dehnavi, A.R.; Zahedi, M.; Ludwiczak, A.; Perez, S.C.; Piernik, A. Effect of Salinity on Seed Germination and Seedling Development of Sorghum (*Sorghum bicolor* (L.) Moench) Genotypes. *Agronomy* **2020**, *10*, 859. [CrossRef]
16. Pessoa, L.G.M.; Silva, L.F.D.S.; Freire, M.B.G.D.S.; Ferreira-Silva, S.L.; Green, C.H.M.; Melo, H.F.; Fernandes, J.G.; Freire, F.J. Effectiveness of soil conditioners to enhance salt extraction ability of *Salicornia ramosissima* in saline-sodic soil for different soil moisture contents. *Int. J. Phytoremediat.* **2022**, *24*, 447–455. [CrossRef]
17. Silva, M.M.A.; Pessoa, L.G.M.; Simplício, J.B.; Souza, W.L.D.S.; Freire, M.B.G.D.S.; Souza, E.S.; Santos, E.S.; Miranda, M.F.A.; Junior, C.C.P. Soil conditioners as candidates to mitigate salt/water stress effects on sorghum growth and soil properties. *Aust. J. Crop Sci.* **2021**, *15*, 98–106. [CrossRef]
18. Hurtado, A.C.; Chiconato, D.A.; Prado, R.M.; Junior, G.D.S.S.; Gratao, P.L.; Felisberto, G.; Viciedo, D.O.; Santos, D.M.M. Different methods of silicon application attenuate salt stress in sorghum and sunflower by modifying the antioxidative defense mechanism. *Ecotoxicol. Environ. Saf.* **2020**, *203*, 110964. [CrossRef]
19. Yin, L.; Wang, S.; Tanaka, K.; Fujihara, S.; Itai, A.; Den, X.; Zhang, S. Silicon-mediated changes in polyamines participate in silicon-induced salt tolerance in *Sorghum bicolor* L. *Plant Cell Environ.* **2016**, *39*, 245–258. [CrossRef]
20. Dhiman, P.; Rajora, N.; Bhardwaj, S.; Sudhakaran, S.S.; Kumar, A.; Raturi, G.; Chakraborty, K.; Guspta, O.P.; Devana, B.N.; Tripathi, D.K.; et al. Fascinating role of silicon to combat salinity stress in plants: An updated overview. *Plant Physiol. Biochem.* **2021**, *162*, 110–123. [CrossRef]
21. Abdolzadeh, A.; Zarooshan, M.; Sadeghipour, H.R.; Mehrabanjoubani, P. Effect of silicon and nano silicon application on wheat (C3) and sorghum (C4) under salinity stress. *J. Plant Prod. Res.* **2022**, *29*, 173–190. [CrossRef]
22. Zhu, Y.; Gong, H. Beneficial effects of silicon on salt and drought tolerance in plants. *Agron. Sustain. Dev.* **2014**, *34*, 455–472. [CrossRef]
23. Kumari, R.; Bhatnagar, S.; Mehla, N.; Vashistha, A. Potential of organic amendments (AM fungi, PGPR, vermicompost and seaweeds) in combating salt stress: A Review. *Plant Stress* **2022**, *6*, 100111. [CrossRef]
24. Miranda, M.F.A.; Freire, M.B.G.S.; Almeida, B.G.; Freire, F.J.; Pessoa, L.G.M.; Freire, A.G. Phytodesalination and chemical and organic conditioners to recover the chemical properties of saline-sodic soil. *Soil Sci. Soc. Am. J.* **2021**, *85*, 132–145. [CrossRef]
25. Fu, J.; Xiao, Y.; Wang, Y.; Liu, Z.; Yang, K. Saline–alkaline stress in growing maize seedlings is alleviated by *Trichoderma asperellum* through regulation of the soil environment. *Sci. Rep.* **2021**, *11*, 11152. [CrossRef] [PubMed]
26. Saravanakumar, K.; Arasu, V.S.; Kathiresan, K. Effect of Trichoderma on soil phosphate solubilization and growth improvement of *Avicennia marina*. *Aquat. Bot.* **2013**, *104*, 101–105. [CrossRef]
27. Hashem, A.; Abd_Allah, E.F.; Alqarawi, A.A.; Huqail, A.A.A.; Egamberdieva, D. Alleviation of abiotic salt stress in *Ochradenus baccatus* (Del.) by *Trichoderma hamatum* (Bonord.) Bainier. *J. Plant Interact.* **2014**, *9*, 857–868. [CrossRef]
28. Zhang, F.; Wang, Y.; Liu, C.; Chen, F.; Ge, H.; Tian, F.; Yang, T.; Zhang, Y. Trichoderma harzianum mitigates salt stress in cucumber via multiple responses. *Ecotoxicol. Environ. Saf.* **2019**, *170*, 436–445. [CrossRef]
29. Cruz, J.L.; Coelho, E.F.; Coelho Filho, M.A.; Santos, A.A. Salinity reduces nutrients absorption and efficiency of their utilization in cassava plants. *Ciência Rural* **2018**, *48*, 1–12. [CrossRef]

30. Hoffmann, J.; Berni, R.; Hausman, J.F.; Guerriero, G. A review on the beneficial role of silicon against salinity in non-accumulator crops: Tomato as a model. *Biomolecules* **2020**, *10*, 1284. [CrossRef]
31. Greger, M.; Landberg, T.; Vaculík, M. Silicon influences soil availability and accumulation of mineral nutrients in various plant species. *Plants* **2018**, *7*, 41. [CrossRef] [PubMed]
32. Rodrigues, A.C.F.; Rodrigues, E.S.C.; Silva, W.G.; Galvão, S.R.S. Classificação da precipitação pluviométrica anual para o município de Parnamirim—PE utilizando Índice de Anomalia de Chuva (IAC). *Rev. Semiárido Visu* **2019**, *7*, 275–284. [CrossRef]
33. Embrapa. *Sistema Brasileiro de Classificação de Solos*; Centro Nac.: Rio de Janeiro, Brazil, 2013.
34. Allen, R.G.; Pereira, L.S.; Raes, D.; Smith, M. Crop evapotranspiration: Guidelines for computing crop requirements. *Irrig. Drain. Pap.* **1998**, *56*, 300. [CrossRef]
35. Richards, L.A. Diagnosis and improvement of saline and alkali soils. *Soil Sci. Soc. Am. J.* **1954**, *18*, 348. [CrossRef]
36. Freitas, G.A.; Sousa, C.R.; Capone, A.; Afférri, F.S.; Silva, R.R. Adubação orgânica no sulco de plantio e sua influência no desenvolvimento do sorgo. *J. Biotechnol. Biodivers.* **2012**, *3*, 61–67. [CrossRef]
37. USSL. *Diagnosis and Improvement of Saline and Alkali Soils*; US Government Printing Office: Washington, DC, USA, 1954. [CrossRef]
38. Olsen, S.R.; Cole, C.; Watanabe, F.; Dean, L. *Estimation of Available Phosphorous in Soils by Extraction with Sodium Bicarbonate*; US Department: Washington, DC, USA, 1954.
39. Silva, M.M.A.; Santos, H.R.B.; Silva, E.N.; Neto, J.B.; Hermínio, P.J.; Ramalho, T.L.; Nunes, V.G.; Simões, A.N.; Souza, E.S.; Ferreira-Silva, S.L. Higher control of Na+ and Cl− transport to the shoot along with K^+/Na^+ selectivity is determinant for differential salt resistance in grapevine rootstocks. *J. Plant Growth Regul.* **2023**, *42*, 5713–5726. [CrossRef]
40. Embrapa. *Manual de Análises Químicas de Solos. Plantas e Fertilizantes*; Embrapa Informação Tecnológica: Rio de Janeiro, Brasil, 2009.
41. Queiroz, G.C.M.; Medeiros, J.F.; Silva, R.R.; Morais, F.M.S.; Sousa, L.V.; Souza, M.V.P.; Santos, E.N.; Ferreira, F.N.; Silva, J.M.C.; Clemente, M.I.B.; et al. Growth, solute accumulation, and ion distribution in sweet sorghum under salt and drought stresses in a Brazilian Potiguar semiarid área. *Agriculture* **2023**, *13*, 803. [CrossRef]
42. Khan, I.; Awan, S.A.; Rizwan, M.; Ali, S.; Hassan, M.J.; Brestic, M.; Zhang, X.; Huang, L. Effects of silicon on heavy metal uptake at the soil-plant interphase: A review. *Ecotoxicol. Environ. Saf.* **2021**, *222*, 112510. [CrossRef]
43. Wang, B.; Chu, C.; Wei, H.; Zhang, L.; Ahmad, Z.; Wu, S.; Xie, B. Ameliorative effects of silicon fertilizer on soil bacterial community and pakchoi (*Brassica chinensis* L.) grown on soil contaminated with multiple heavy metals. *Environ. Pollut.* **2020**, *267*, 115411. [CrossRef]
44. Véras, M.L.M.; Alves, L.S.; Silva, T.I.; Silva, I.N.; Costa, A.S.D.N.; Melo, E.N.; Cordovil, H.P.L.; Dantas, A.P.J.; Souza, N.A.; Dias, T.J. Silicon as mitigator of salt stress in mango tree seedlings. *Aust. J. Crop Sci.* **2021**, *15*, 1146–1150. [CrossRef]
45. Rizwan, A.; Zia-ur-Rehman, M.; Rizwan, M.; Usman, M.; Anayatullah, S.; Alharby, H.F.; Bamagoos, A.A.; Alharbi, B.M.; Ali, S. Effects of silicon nanoparticles and conventional Si amendments on growth and nutrient accumulation by maize (*Zea mays* L.) grown in saline-sodic soil. *Environ. Res.* **2023**, *227*, 115740. [CrossRef] [PubMed]
46. Black, A.S.; Campbell, A.S. Ionic strength of soil solution and its effect on charge properties of some New Zealand soils. *J. Soil Sci.* **1982**, *33*, 249–262. [CrossRef]
47. Ramírez-Jaramillo, G.; Lozano-Contreras, M.G.; Ramírez-Silva, J.H. Agroclimatic conditions for growing *Sorghum bicolor* L. Moench, under irrigation conditions in Mexico. *OALib* **2020**, *7*, 100813. [CrossRef]
48. Negacz, K.; Malek, Ž.; Vos, A.; Vellinga, P. Saline soils worldwide: Identifying the most promising areas for saline agriculture. *J. Arid Environ.* **2022**, *203*, 104775. [CrossRef]
49. Whalen, J.K.; Chang, C.; Clayton, G.W.; Carefoot, J.P. Cattle manure amendments can increase the pH of acid soils. *Soil Sci. Soc. Am. J.* **2000**, *64*, 962–966. [CrossRef]
50. Zhang, Y.; Yang, J.; Yao, R.; Wang, X.; Xie, W. Short-term effects of biochar and gypsum on soil hydraulic properties and sodicity in a saline-alkali soil. *Pedosphere* **2020**, *30*, 694–702. [CrossRef]
51. Miles, N.; Manson, A.D.; Rhodes, R.; van Antwerpen, R.; Weigel, A. Extractable Silicon in Soils of the South African Sugar Industry and Relationships with Crop Uptake. *Commun. Soil Sci. Plant Anal.* **2014**, *45*, 2949–2958. [CrossRef]
52. Yanai, J.; Taniguchi, H.; Nakao, A. Evaluation of available silicon content and its determining factors of agricultural soils in Japan. *Soil Sci. Plant Nutr.* **2016**, *62*, 511–518. [CrossRef]
53. Camargo, M.S.; Pereira, H.S.; Korndörfer, G.H.; Queiroz, A.A.; Reis, C.B. Soil reaction and absorption of silicon by rice. *Sci. Agric.* **2007**, *64*, 176–180. [CrossRef]
54. Haynes, R.J. What effect does liming have on silicon availability in agricultural soils? *Geoderma* **2019**, *337*, 375–383. [CrossRef]
55. Ma, C.; Ci, K.; Zhu, J.; Sun, Z.; Liu, Z.; Li, X.; Zhu, Y.; Tang, C.; Wang, P.; Liu, Z. Impacts of exogenous mineral silicon on cadmium migration and transformation in the soil-rice system and on soil health. *Sci. Total Environ.* **2021**, *759*, 143501. [CrossRef] [PubMed]
56. Freire, M.B.G.S.; Ruiz, H.A.; Ribeiro, M.R.; Ferreira, P.A.; Alvarez, V.H.; Freire, F.J. Estimativa do risco de sodificação de solos de Pernambuco pelo uso de águas salinas. *Rev. Bras. Eng. Agríc. Ambient.* **2003**, *7*, 227–232. [CrossRef]
57. Minhas, P.S.; Qadir, M.; Yadav, R.K. Groundwater irrigation induced soil sodification and response options. *Agric. Water Manag.* **2019**, *215*, 74–85. [CrossRef]
58. Pessoa, L.G.M.; Freire, M.B.G.S.; Filho, J.C.A.; Santos, P.R.; Miranda, M.F.A.; Freire, F.J. Characterization and classification of halomorphic soils in the semiarid region of northeastern Brazil. *J. Agric. Sci.* **2019**, *11*, 405. [CrossRef]

59. Silva, M.O.; Freire, M.B.G.S.; Mendes, A.M.S.; Freire, F.J.; Duda, G.P.; Sousa, C.E.S. Risco de salinização em quatro solos do Rio Grande do Norte sob irrigação com águas salinas. *Rev. Bras. Ciênc. Agrár.–Braz. J. Agric. Sci.* **2007**, *2*, 8–14. [CrossRef]
60. Yu, P.; Liu, S.; Yang, H.; Fan, G.; Zhou, D. Short-term land use conversions influence the profile distribution of soil salinity and sodicity in northeastern China. *Ecol. Indic.* **2018**, *88*, 79–87. [CrossRef]
61. Feng, X.; Zhang, L. Vermiculite and humic acid improve the quality of green waste compost as a growth medium for *Centaurea cyanus* L. *Environ. Technol. Innov.* **2021**, *24*, 101945. [CrossRef]
62. Liu, X.; Zhang, L. The effectiveness of composted green waste amended with vermiculite and humic acid powders as an alternative cultivation substrate for cornflower cultivation. *Commun. Soil Sci. Plant Anal.* **2021**, *52*, 2945–2957. [CrossRef]
63. Ikram, M.; Ali, N.; Jan, G.; Iqbal, A.; Hamayun, M.; Jan, F.G.; Hussain, A.; Lee, I.J. *Trichoderma reesei* improved the nutrition status of wheat crop under salt stress. *J. Plant Interact.* **2019**, *14*, 590–602. [CrossRef]
64. Kusumawati, R.; Pangestu, H.E.; Basmal, J. Effect of *Trichoderma* addition on sargassum organic fertilizer. *IOP Conf. Ser. Earth Environ. Sci.* **2021**, *715*, 012059. [CrossRef]
65. Pratiwi, V.; Oktarina, H.; Sriwati, R. The potential of *Trichoderma* spp. and *Pseudomonas auregenosa* as patchouli waste decomposer. *IOP Conf. Ser. Earth Environ. Sci.* **2021**, *667*, 012019. [CrossRef]
66. Pelagio-Flores, R.; Esparza-Reynoso, S.; Garnica-Vergara, A.; López-Bucio, J.; Herrera-Estrella, A. *Trichoderma*-induced acidification is an early trigger for changes in arabidopsis root growth and determines fungal phytostimulation. *Front. Plant Sci.* **2017**, *8*, 822. [CrossRef] [PubMed]
67. Batista, M.A.; Inoue, T.T.; Esper Neto, M.; Muniz, A.S. Princípios de fertilidade do solo, adubação e nutrição mineral. In *Hortaliças-Fruto*; EDUEM: Maringá, Brazil, 2018; pp. 113–162. [CrossRef]
68. Carneiro, C.E.A.; Fioretto, R.A.; Fonseca, I.C.B.; Carneiro, G.E.S. Calcário, potássio, fosfato e silício na produtividade do solo. *Acta Sci. Agron.* **2006**, *28*, 465–470. [CrossRef]
69. Stutter, M.I.; Shand, C.A.; George, T.S.; Blackwell, M.S.; Dixon, L.; Bol, R.; MacKay, R.L.; Richardson, A.E.; Condron, L.M.; Haygarth, P.M. Land use and soil factors affecting accumulation of phosphorus species in temperate soils. *Geoderma* **2015**, *258*, 29–39. [CrossRef]
70. Hunt, J.F.; Ohno, T.; He, Z.; Honeycutt, C.W.; Dail, D.B. Inhibition of phosphorus sorption to goethite, gibbsite, and kaolin by fresh and decomposed organic matter. *Biol. Fertil. Soils* **2007**, *44*, 277–288. [CrossRef]
71. Yan, X.; Wang, D.; Zhang, H.; Zhang, G.; Wei, Z. Organic amendments affect phosphorus sorption characteristics in a paddy soil. *Agric. Ecosyst. Environ.* **2013**, *175*, 47–53. [CrossRef]
72. Bi, Q.-F.; Li, K.J.; Zheng, B.X.; Liu, X.P.; Li, H.Z.; Jin, B.J.; Ding, K.; Yang, X.; Lin, X.Y.; Zhu, Y.G. Partial replacement of inorganic phosphorus (P) by organic manure reshapes phosphate mobilizing bacterial community and promotes P bioavailability in a paddy soil. *Sci. Total Environ.* **2020**, *703*, 134977. [CrossRef]
73. Qaswar, M.; Chai, R.; Ahmed, W.; Jing, H.; Han, T.; Liu, K.; Zhang, H. Partial substitution of chemical fertilizers with organic amendments increased rice yield by changing phosphorus fractions and improving phosphatase activities in fluvo-aquic soil. *J. Soils Sediments* **2020**, *20*, 1285–1296. [CrossRef]
74. Zhang, Y.; Gao, W.; Luan, H.; Tang, J.; Li, R.; Li, M.; Zhang, H.; Huang, S. Long-term organic substitution management affects soil phosphorus speciation and reduces leaching in greenhouse vegetable production. *J. Clean. Prod.* **2021**, *327*, 129464. [CrossRef]
75. Lin, Y.; Ye, G.; Kuzyakov, Y.; Liu, D.; Fan, J.; Ding, W. Long-term manure application increases soil organic matter and aggregation, and alters microbial community structure and keystone taxa. *Soil Biol. Biochem.* **2019**, *134*, 187–196. [CrossRef]
76. Ding, L.-J.; Su, J.-Q.; Sun, G.-X.; Wu, J.-S.; Wei, W.-X. Increased microbial functional diversity under long-term organic and integrated fertilization in a paddy soil. *Appl. Microbiol. Biotechnol.* **2018**, *102*, 1969–1982. [CrossRef] [PubMed]
77. Kong, F.; Ling, X.; Iqbal, B.; Zhou, Z.; Meng, Y. Integrated usage of *Trichoderma harzianum* and biochar to ameliorate salt stress on spinach plants. *Arch. Agron. Soil Sci.* **2021**, *69*, 18–31. [CrossRef]
78. El-Baki, G.A.; Mostafa, D. The potentiality of *Trichoderma harzianum* in alleviation the adverse effects of salinity in faba bean plants. *Acta Biol. Hung.* **2014**, *65*, 451–468. [CrossRef] [PubMed]
79. Tuna, A.L.; Kaya, C.; Higgs, D.; Murillo-Amador, B.; Aydemir, S.; Girgin, A.R. Silicon improves salinity tolerance in wheat plants. *Environ. Exp. Bot.* **2008**, *62*, 10–16. [CrossRef]
80. Chen, D.; Cao, B.; Wang, S.; Liu, P.; Deng, X.; Yin, L.; Zhang, S. Silicon moderated the K deficiency by improving the plant-water status in sorghum. *Sci. Rep.* **2016**, *6*, 22882. [CrossRef] [PubMed]
81. Hurtado, A.C.; Chiconato, D.A.; Prado, R.M.; Sousa Junior, G.S.; Felisberto, G. Silicon attenuates sodium toxicity by improving nutritional efficiency in sorghum and sunflower plants. *Plant Physiol. Biochem.* **2019**, *142*, 224–233. [CrossRef]
82. Hurtado, A.C.; Chiconato, D.A.; Prado, R.M.; Sousa Junior, G.S.; Viciedo, D.O.; Díaz, Y.P.; Calzada, K.P.; Gratão, P.L. Silicon alleviates sodium toxicity in sorghum and sunflower plants by enhancing ionic homeostasis in roots and shoots and increasing dry matter accumulation. *Silicon* **2021**, *13*, 475–486. [CrossRef]
83. Yin, L.; Wang, S.; Li, J.; Tanaka, K.; Oka, M. Application of silicon improves salt tolerance through ameliorating osmotic and ionic stresses in the seedling of Sorghum bicolor. *Acta Physiol. Plant.* **2013**, *35*, 3099–3107. [CrossRef]
84. Shi, Y.; Wang, Y.; Flowers, T.J.; Gong, H. Silicon decreases chloride transport in rice (*Oryza sativa* L.) in saline conditions. *J. Plant Physiol.* **2013**, *170*, 847–853. [CrossRef]

85. Abbas, T.; Balal, R.M.; Shahid, M.A.; Pervez, M.A.; Ayyub, C.M.; Aqueel, M.A.; Javaid, M.M. Silicon-induced alleviation of NaCl toxicity in okra (*Abelmoschus esculentus*) is associated with enhanced photosynthesis, osmoprotectants and antioxidant metabolism. *Acta Physiol. Plant.* **2015**, *37*, 6. [CrossRef]
86. Soylemezoglu, G.; Demir, K.; Inal, A.; Gunes, A. Effect of silicon on antioxidant and stomatal response of two grapevine (*Vitis vinifera* L.) rootstocks grown in boron toxic, saline and boron toxic-saline soil. *Sci. Hortic.* **2009**, *123*, 240–246. [CrossRef]
87. Karimi, G.; Pourakbar, L.; Moghaddam, S.S.; Danesh, Y.R.; Djordjevi'c, J.P. Effectiveness of fungal bacterial biofertilizers on agrobiochemical attributes of quinoa (*Chenopodium quinoa* willd.) under salinity stress. *Int. J. Environ. Sci. Technol.* **2022**, *19*, 11989–12002. [CrossRef]
88. Shabala, S.; Cuin, T.A. Potassium transport and plant salt tolerance. *Physiol. Plant* **2008**, *133*, 651–669. [CrossRef] [PubMed]
89. Wang, L.; Sun, X.; Li, S.; Zhang, T.; Zhang, W.; Zhai, P. Application of organic amendments to a coastal saline soil in north China: Effects on soil physical and chemical properties and tree growth. *PLoS ONE* **2014**, *9*, e89185. [CrossRef] [PubMed]
90. Carvalho, D.D.C.; Mello, S.C.M.; Lobo Júnior, M.; Silva, M.C. Controle de *Fusarium oxysporum* f.sp. phaseoli in vitro e em sementes, e promoção do crescimento inicial do feijoeiro comum por *Trichoderma harzianum*. *Trop. Plant Pathol.* **2011**, *36*, 28–34. [CrossRef]
91. Bortolin, G.S.; Wiethan, M.M.S.; Vey, R.T.; Oliveira, J.C.P.; Köpp, M.M.; Silva, A.C.F. *Trichoderma* na promoção do desenvolvimento de plantas de *Paspalum regnellii* Mez. *Rev. Ciênc. Agrár.* **2019**, *42*, 131–140. [CrossRef]
92. Kakabouki, I.; Tataridas, A.; Mavroeidis, A.; Kousta, A.; Karydogianni, S.; Zisi, C.; Kouneli, V.; Konstantinou, A.; Folina, A.; Konstantas, A.; et al. Effect of colonization of *Trichoderma harzianum* on growth development and CBD content of hemp (*Cannabis sativa* L.). *Microorganisms* **2021**, *9*, 518. [CrossRef]
93. Instituto Agronômico de Pernambuco (IPA). Sorgo Sudão: Sudão 4202—Cultivar Tolerante a Salinidade e Com Aptidão Para Feno. 2007. Available online: http://www.infoteca.cnptia.embrapa.br/infoteca/handle/doc/487334 (accessed on 15 October 2023).
94. Aishwarya, S.; Viswanath, H.S.; Singh, A.; Singh, R. Biosolubilization of different nutrients by *Trichoderma* spp. and their mechanisms involved: A review. *Int. J. Adv. Agric. Sci. Technol.* **2020**, *7*, 34–39.
95. Naveed, M.; Sajid, H.; Mustafa, A.; Niamat, B.; Ahmad, Z.; Yaseen, M.; Kamram, M.; Rafique, M.; Ahmar, S.; Chen, J.T. Alleviation of salinity-induced oxidative stress, improvement in growth, physiology and mineral nutrition of canola (*Brassica napus* L.) through calcium-fortified composted animal manure. *Sustainability* **2020**, *12*, 846. [CrossRef]
96. Sousa, R.A.; Lacerda, C.F.; Neves, A.L.R.; Costa, R.N.T.; Hernandez, F.F.F.; Sousa, C.H.C. Crescimento do sorgo em função da irrigação com água salobra e aplicação de compostos orgânicos. *Rev. Bras. Agric. Irrig.* **2018**, *12*, 2315–2326. [CrossRef]
97. Cai, F.; Yu, G.; Wang, P.; Wei, Z.; Fu, L.; Shen, Q.; Chen, W. Harzianolide, a novel plant growth regulator and systemic resistance elicitor from *Trichoderma harzianum*. *Plant Physiol. Biochem.* **2013**, *73*, 106–113. [CrossRef] [PubMed]
98. Rajesh, R.W.; Rahul, M.S.; Ambalal, N.S. *Trichoderma*: A significant fungus for agriculture and environment. *Afr. J. Agric. Res.* **2016**, *11*, 1952–1965. [CrossRef]
99. Klepper, K.; Ahmad, R.; Blair, G. Impact of feedlot manure and nitrogen additions on forage yields, nutrient balance and soil nitrate, phosphate and salinity. *Commun. Soil Sci. Plant Anal.* **2020**, *51*, 2658–2669. [CrossRef]
100. Yang, R.; Sun, Z.; Liu, X.; Long, X.; Gao, L.; Shen, Y. Biomass composite with exogenous organic acid addition supports the growth of sweet sorghum (*Sorghum bicolor* 'Dochna') by reducing salinity and increasing nutrient levels in coastal saline–alkaline soil. *Front. Plant Sci.* **2023**, *14*, 1163195. [CrossRef]
101. Cunha, E.E.; Lima, J.M.P. Caracterização de genótipos e estimativa de parâmetros genéticos de características produtivas de sorgo forrageiro. *Rev. Bras. Zootec.* **2010**, *39*, 701–706. [CrossRef]
102. Oliveira, L.B.; Pires, A.J.V.; Viana, A.E.S.; Matsumoto, S.N.; Carvalho, G.G.P.; Ribeiro, L.S.O. Produtividade, composição química e características agronômicas de diferentes forrageiras. *Rev. Bras. Zootec.* **2010**, *39*, 2604–2610. [CrossRef]
103. Rodrigues, C.R.; Comassetto, D.S.; Dornelles, R.R.; Rosa, F.Q.; Oaigen, R.P.; Castagnara, D.D.; Valle, T.A.; Azevedo, E.B. Produção, composição bromatológica e fenológica de forrageiras estivais na Região Sul do Brasil. *Agrarian* **2020**, *13*, 82–92. [CrossRef]
104. Alayafi, A.H.; Al-Solaimani, S.G.M.; El-Wahed, M.H.A.; Alghabari, F.M.; El Sabagh, A. Silicon supplementation enhances productivity, water use efficiency and salinity tolerance in maize. *Front. Plant Sci.* **2022**, *13*, 953451. [CrossRef]
105. Khan, W.; Aziz, T.; Hussain, I.; Ramzani, P.M.A.; Reichenauer, T.G. Silicon: A beneficial nutrient for maize crop to enhance photochemical efficiency of photosystem II under salt stress. *Arch. Agron. Soil Sci.* **2017**, *63*, 599–611. [CrossRef]
106. Wang, X.; Nie, J.; Wang, P.; Zhao, J.; Yang, Y.; Wang, S.; Zang, H. Does the replacement of chemical fertilizer nitrogen by manure benefit water use efficiency of winter wheat—*Summer* maize systems? *Agric. Water Manag.* **2021**, *243*, 106428. [CrossRef]
107. Wang, X.; Yan, J.; Zhang, X.; Zhang, S.; Chen, Y. Organic manure input improves soil water and nutrients use for sustainable maize (*Zea mays*. L) productivity on the Loess Plateau. *PLoS ONE* **2020**, *15*, e0238042. [CrossRef] [PubMed]
108. Oljira, A.M.; Hussain, T.; Waghmode, T.R.; Zhao, H.; Sun, H.; Liu, X.; Liu, B. *Trichoderma* enhances net photosynthesis, water use efficiency, and growth of wheat (*Triticum aestivum* L.) under salt stress. *Microorganisms* **2020**, *8*, 1565. [CrossRef] [PubMed]
109. Pereira, T.S.; Paula, A.M.; Ferrari, L.H.; Silva, J.; Pinheiro, J.B.; Cajamarca, S.M.N.; Busato, J.G. *Trichoderma*-inriched vermicompost extracts reduces nematode biotic stress in tomato and bell pepper crops. *Agronomy* **2021**, *11*, 1655. [CrossRef]
110. Scudeletti, D.; Crusciol, C.A.C.; Bossolani, J.W.; Moretti, L.G.; Momesso, L.; Tubana, B.S.; Hungria, M. *Trichoderma asperellum* inoculation as a tool for attenuating drought stress in sugarcane. *Front. Plant Sci.* **2021**, *12*, 645542. [CrossRef]

111. Sousa, T.P.; Chaibub, A.A.; Silva, G.B.; Filippi, M.C.C. *Trichoderma asperellum* modulates defense genes and potentiates gas exchanges in upland rice plants. *Physiol. Mol. Plant Pathol.* **2020**, *112*, 101561. [CrossRef]
112. Cabral-Miramontes, J.P.; Olmedo-Monfil, V.; Lara-Banda, M.; Zúñiga-Romo, E.R.; Aréchiga-Carvajal, E.T. Promotion of plant growth in arid zones by selected *Trichoderma* spp. strains with adaptation plasticity to alkaline pH. *Biology* **2022**, *11*, 1206. [CrossRef]
113. Ahmed, B.A.O.; Inoue, M.; Moritani, S. Effect of saline water irrigation and manure application on the available water content, soil salinity, and growth of wheat. *Agric. Water Manag.* **2010**, *97*, 165–170. [CrossRef]

agriculture

MDPI

Article

Integrating Agro-Morpho-Physiological Traits and SSR Markers for Detecting the Salt Tolerance of Advanced Spring Wheat Lines under Field Conditions

Muhammad Bilawal Junaid, Salah El-Hendawy *, Ibrahim Al-Ashkar, Nasser Al-Suhaibani and Majed Alotaibi

Department of Plant Production, College of Food and Agriculture Sciences, King Saud University, Riyadh 11451, Saudi Arabia; 438106409@student.ksu.edu.sa (M.B.J.); ialashkar@ksu.edu.sa (I.A.-A.); nsuhaib@ksu.edu.sa (N.A.-S.); malotaibia@ksu.edu.sa (M.A.)

* Correspondence: mosalah@ksu.edu.sa

Abstract: To successfully enhance the salt tolerance of genotypes, it is crucial to conduct field-based trials, establish effective screening criteria and analysis tools, evaluate salt tolerance at various growth stages, and integrate phenotypic assessment-based traits with molecular markers. This study aimed to assess the salt tolerance of 16 F8 recombinant inbred lines (RILs) and eight genotypes by analyzing 13 agro-morpho-physiological traits using various analysis tools and SSR markers under both control and high salinity levels (15 dS m^{-1}) in real field conditions. Analysis of variance (ANOVA), comparison of mean values, calculation of reduction percentage, and multivariate analysis were used to compare the assessed traits among genotypes and identify which traits are the most effective ones in describing the salt tolerance of these genotypes. A heatmap cluster analysis (HMCA) was also employed to categorize the salt tolerance of genotypes into different clusters based on the stress tolerance index (STI) for all traits. The ANOVA results revealed significant statistical differences ($p \leq 0.05$) between the genotypes and salinity levels for all assessed traits in each season and their combined data. Moreover, the 150 mM NaCl treatment led to decreases in the assessed traits by 10.2% to 36.9% when compared to the control treatments. Furthermore, the mean values of assessed traits for certain genotypes were approximately one to three times greater than those of other genotypes. Principal component analysis has identified plant dry weight, green leaf area, leaf area index, and grain yield per hectare as effective screening criteria for explaining the substantial variation observed among the genotypes. The HMCA successfully grouped genotypes into three distinct clusters and distinguished the salt-tolerant genotypes from the salt-sensitive and intermediate ones. The 24 genotypes/RILs were classified into three main groups according to the allelic data of 40 SSRs associated with salt-tolerant genes. A weak yet significant correlation was observed between the similarity coefficients of agro-morpho-physiological traits and SSR markers, as determined by the Mantel test (r = 0.13, $p < 0.03$, and alpha = 0.05). In conclusion, this study has successfully identified several traits, particularly those associated with SSR markers, that greatly contribute to our understanding of the phenotypic and genotypic basis influencing the salt tolerance of wheat genotypes in real field conditions. Consequently, assessing these traits for a large number of wheat plant materials in a rapid and cost-effective manner will be greatly importance in breeding programs aimed at improving salt stress tolerance in this vital food crop. This will be the main focus of our forthcoming research.

Keywords: chlorophyll content; mantel test; multivariate analysis; relative water content; saline water; stress tolerance index; yield components

1. Introduction

Currently, numerous environmental stresses present a substantial threat to global food security. On the other hand, global food production needs to be increased by about

70% to ensure food security for the projected population of 9.7 billion people by 2050 [1]. Although the annual increase of 1.0–1.6% in the production of most major food crops, such as wheat, rice, and maize, the impact of environmental stresses on grain yield (GY) surpasses this growth rate. This situation will intensify the pressure on global food security in the coming years [2]. Salinity is widely recognized as one of the most prominent of these environmental stresses that greatly reduces GY for most food crops in many parts of the world. Under moderate salinity stress (40–80 mM NaCl), the average GY of most major food crops may be globally reduced by over 50% [3–5]. Statistically, salinity stress currently affects about 20% of cultivated areas. Furthermore, it is projected to reach 50% or more by 2050, as approximately 1.5 million hectares of cultivated land are salinized annually due to both natural and human factors. In addition, salinity stress significantly restricts the productivity of approximately 33% of irrigated lands, which are responsible for producing around one-third of the world's food supply [4,6]. Moreover, there is a loss of over USD 13 billion annually due to irrigation-induced salinity alone [7]. All these facts about salinity may explain why there is a close association between food crises and salinity issues in the agricultural sector, particularly in arid and semiarid countries.

Bread wheat (*Triticum aestivum* L.) is a moderately salt-tolerant crop with a salinity threshold of about 7.0 dS m^{-1} (70 mM NaCl). However, higher salinity concentrations such as 15.0 dS m^{-1} (150 mM NaCl) can cause a significant decrease in its potential yield of up to 60%, especially when grown in open-field conditions [8]. Therefore, the introduction of salt-tolerant genotypes that can produce satisfactory GY even in environments with high salt concentrations is recognized as the most beneficial approach for sustaining wheat production under salinity conditions [3,6,8]. Therefore, the primary goal of plant breeders is to exploit genetic variations in salt tolerance within wheat germplasm in order to identify potential donors with salt tolerance and incorporate them into breeding programs. The ultimate end of this goal is to create new wheat genotypes that exhibit greater tolerance to salt stress compared to others. Despite the simplicity of this goal, there has been little progress in developing high-yielding wheat genotypes that are tolerant to salinity. According to the literature, this lack of progress can be attributed to several reasons. Firstly, several screening experiments only assess the salt tolerance of genotypes during germination and the early vegetative phase without considering that the salt tolerance of genotypes can vary throughout different growth stages [9,10]. Thus, experiments that evaluate the performance of genotypes under salt stress conditions during both the vegetative and reproductive stages are urgently needed. Secondly, the majority of experiments evaluating the salinity tolerance of genotypes and understanding the mechanism of salt tolerance are conducted in controlled conditions, such as a greenhouse and growth chamber, using sand or hydroponics as growth media. However, these conditions do not accurately reflect the complexity of field conditions and thus do not provide a reliable proof of concept for plant performance in open-field conditions [4,11]. Thirdly, there is a lack of appropriate evaluation methods and screening criteria that can accurately assess the salt tolerance of genotypes under open-field conditions. Under real field conditions, the wheat plants are exposed to high variability in physical and chemical properties of soil, temporal and spatial variability in salt and water contents in the root zone at different growth stages, and fluctuations in air temperature and humidity [4,8,10]. Fourthly, although the mechanisms associated with salt stress responses in plants are complex and polygenic traits, there are few screening studies that evaluate the salt tolerance of genotypes based on multiple traits. It is known that the different components of salinity stress, including osmotic, ionic, and essential ion imbalance components, simultaneously cause many morphological, physiological, and metabolic changes [4,12,13]. Fifthly, the evaluation of salt tolerance is primarily focused on the GY criterion, even though direct selection for GY is often inefficient due to its low heritability. Therefore, evaluating the salt tolerance of genotypes based on secondary traits that are highly correlated with GY and have a high heritability can make the assessment of the salt tolerance of genotypes more accurate and efficient [14,15].

In general, the different components of salinity stress interact together and result in a notable reduction in several agro-morpho-physiological traits, including plant dry weight (PDW), leaf area (LA), total chlorophyll content (Chlt), and leaf water content (LRWC), as well as different yield components such as thousand-grain weight (TGW), spike length (SL), grain number per spike (GNPS), spike number per plant (SNPP), and harvest index (HI). It is worth noting that these traits show a reduction even at low salinity levels [3,8,16]. For instance, Munns et al. [3] reported that a low salinity level may not reduce wheat GY despite reducing PDW and LA. However, GY only decreases once a certain salinity threshold is reached. Similarly, Radi et al. [17] and Uzair et al. [18] showed that salt stress caused a significant reduction in wheat PDW, with a more pronounced effect on salt-sensitive genotypes compared to salt-tolerant ones. Importantly, PDW and LA exhibit high heritability coupled with a high expected genetic gain from selection and are strongly associations with GY under salinity conditions [15,19,20]. Therefore, PDW and LA traits can serve as effective screening criteria for distinguishing salt-tolerant genotypes from salt-sensitive ones in real field conditions.

As toxic ions build up in the leaf blade, the negative effect of salt stress on photosynthetic pigments can be detected before irreversible morphological damage becomes apparent [21]. Furthermore, Munns et al. [3] found that the wheat lines with high levels of Na^+ lose chlorophyll at a faster rate compared to those with low Na^+ levels. In addition, Omrani et al. [20] conducted a study using seven generations of wheat grown under normal and saline conditions in the field, and they reported a high broad-sense heritability for Chlt and SPAD values in saline conditions. Moreover, a strong positive correlation between Chlt and overall plant salinity tolerance was found in several field crops, including wheat, barley, rapeseed, and chickpea [22,23]. Considering this, the maintenance of photosynthetic pigments in saline conditions can be seen as a key physiological criterion for differentiating between salt-tolerant and salt-sensitive genotypes.

A high concentration of salt in the root zone can impair the plant's ability to absorb water, similar to the effects of drought stress. This subsequently results in an imbalance in the plants' water status, specifically their LRWC, which reflects the balance between water uptake and transpiration. A reduction in LRWC can affect and alter various physiological and metabolic processes [24]. Therefore, the ability of genotypes to maintain optimal water content levels in tissues is an important mechanism for counteracting the effects of salinity stress. Previous studies have also shown a moderate broad-sense heritability for RWC under salt stress conditions [24]. Accordingly, LRWC can be considered an important physiological criterion for evaluating the salt tolerance of genotypes.

Because wheat GY is significantly influenced by the environment and exhibits low heritability, especially under environmental stresses, plant breeders rely on yield-related traits, including TGW, SL, GNPS, and SNPP, as indirect screening criteria to evaluate genotypes and improve their yield under both normal and stress conditions [25,26]. In addition, HI, which represents the ratio of GY to biological yield (BY) and indicates the allocation of photosynthetic products between source and sink organs, is also an important indirect screening criterion. Therefore, the secondary traits with high heritability can be considered essential agronomic criteria for evaluating the salt stress tolerance of genotypes [14,27,28].

Although several agro-morpho-physiological traits have been identified as effective screening criteria, these traits are often affected by environmental conditions and are also dependent on the developmental growth stages. Furthermore, this becomes even more problematic in salt tolerance assessment because any change in the environment can alter the salt tolerance between genotypes [29]. Therefore, when agro-morpho-physiological traits are used alone, they show some restrictions in assessing genetic diversity in salt tolerance. Moreover, assessing the salt tolerance of genotypes based on conventional phenotypic variance is expensive and time-consuming. Fortunately, molecular markers have helped identify the genes responsible for the complex agro-morpho-physiological traits that confer salt tolerance in several field crops. This has resulted in a more efficient and cost-effective evaluation process [14,15,30]. Therefore, in order to enhance the precision of salt

tolerance evaluation in genotypes, it is crucial to integrate phenotypic assessment based on agro-morpho-physiological traits with molecular markers to identify the candidate genes involved in the variation of these traits. Molecular markers offer a vast number of markers that can be used to compare individual genotypes across different environmental conditions. Furthermore, they are not limited by crop growth stages, enabling the combination of different tolerance traits into a single efficient genotype. Additionally, they provide objective data that can be analyzed. Among the various molecular markers available for genetic characterization, simple sequence repeat (SSR) or microsatellite markers are extensively used for cultivar identification, germplasm characterization, genetic diversity, and molecular mapping due to their numerous advantages, including cost-effectiveness, the presence of multi-alleles, high levels of polymorphism, high-throughput capabilities, abundance, co-dominant, locus-specificity, informative, lack of bias, and repeatability [15,31–33]. Therefore, SSR markers can play a vital role with phenotypic traits in evaluating the salt tolerance of wheat genotypes and identifying the most salt-tolerant ones. Fortunately, there are several successful SSR primers, including Gwm 312, Xgwm312, and Xwmc170, that have been used to assess the salt tolerance of wheat genotypes. These primers are effective in identifying the Nax1 gene, which serves as an indicator of Na^+ exclusion [34–36]. Thus, SSR analysis of DNA polymorphism can be instrumental in identifying the key genes associated with salt tolerance.

The main objectives of this study were to (1) assess the salt tolerance of 16 F8 recombinant inbred lines (RILs) and eight genotypes grown in real field conditions, using different agro-morpho-physiological traits, (2) identify which traits can serve as effective screening criteria for distinguishing salt tolerance among genotypes, employing multivariate and cluster analysis, and (3) validate these screening criteria by examining the genetic basis using SSR markers, specifically by examining the association between the matrices of the traits and SSR data using Mantel test.

2. Materials and Methods

2.1. Plant Materials

The genetic plant materials used in this study consisted of 24 diverse bread wheat genotypes (*Triticum aestivum* L.). These genotypes comprised 8 varieties and 16 F8 recombinant inbred lines (RILs). The eight varieties included three parents (Sakha-93, Sakha-61, and Sids-1) and other five cultivars (Kharchia 65, Shandawel-1, Misr-1, Gemiza-9, and Kawz). Based on our previous evaluations in the pot experiment and actual saline field conditions, the three parents, Sakha-93, Sakha-61, and Sids-1, were considered to be salt-tolerant, salt-sensitive, and moderately salt-tolerant genotypes, respectively [8,12,37]. Kharchia 65 was also considered a salt-tolerant genotype and is used as a standard cultivar for evaluating wheat's salt tolerance [12,37–39]. Based on the study of Mansour et al. [40] under actual saline field growing conditions, Shandawel-1, Misr-1, and Gemiza-9 were considered to be salt-sensitive, moderately salt-sensitive, and moderately salt-tolerant genotypes, respectively. Among sixteen RILs developed at the Faculty of Agriculture, Suez Canal University, Ismailia, Egypt, and the College of Food and Agriculture Sciences, King Saud University, Riyadh, Saudi Arabia, five were derived from a cross between Sakha 93 and Sids 1 and eleven were derived from a cross between Sakha 93 and Sakha 61.

2.2. Experimental Site and Growth Conditions

All genetic plant materials were evaluated under open-field conditions at the Research Station (24°25′ N, 46°34′ E, 400 m a.s.l.) of the Department of Plant Production, College of Food and Agriculture Sciences, King Saud University, Riyadh, Saudi Arabia (Figure 1), during the winter seasons of 2019/2020 (S1) and 2020/2021 (S2). According to data from the meteorological station located near the research station (approximately 500 m away from the field experiment) and during the wheat's growing stages (December to April), the minimum temperature ranged from 7 °C to 19.5 °C in S1 and 8.3 °C to 20 °C in S2. The maximum temperature ranged from 21.3 °C to 34.1 °C in S1 and from 22.3 °C to

35.5 °C in S2. Precipitation ranged from 0.0 mm to 6.25 mm in S1 and 0.32 mm to 3.66 mm in S2. Analysis of soil samples taken from the experimental farm at a depth of 0–30 cm showed that the soil texture is sandy loam (i.e., 14.9% clay, 28.4% silt, and 56.7% sand) and characterized by the following physicochemical properties: organic matter, 0.46%; Walkley–Black C, 0.34%; bulk density, 1.48 g cm^{-3}; electrical conductivity (EC), 1.12 dS m^{-1}; pH, 7.85; $CaCO_3$, 29.22%; available N, 3.98 g kg^{-1}; available K, 1.67 mg kg^{-1}; available P, 0.07 mg kg^{-1}; water holding capacity, 18.56%; and permanent wilting point, 7.21%.

Figure 1. Plot layouts of genotypes grown under control and salinity treatments in real field conditions.

2.3. Experimental Design, Agronomic Practices, and Treatments

The field experiment was conducted as a split-plot design with three replications. Salinity levels, including the control (≈0.35 dS m^{-1}) and a high salinity concentration of 15.0 dS m^{-1}, were referred to as the main plot, while twenty-four bread wheat RILs/genotypes were assigned at random to the subplots. Therefore, the field experiment included 144 experimental units (2 salinity levels × 24 RILs/genotypes × 3 replications). Each experimental unit had five rows of planting, with a length of 1.5 m, row spacing of 20 cm, and a space of 50 cm between experimental units. The replications and salinity levels were separated by buffer zones of 1 and 3 m, respectively.

In both growing seasons, the different genotypes were sown at a seeding rate of 15 g m^{-2} during the optimum period, which was the fourth week of November. All genotypes were fertilized with a recommended dose of nitrogen–phosphorus–potassium (NPK) fertilizer at a rate of 150, 100, and 90 kg ha^{-1}, respectively. The NPK fertilizers were applied in the form of ammonium nitrate (33.5% N), calcium superphosphate (18.5% P_2O_5), and potassium chloride (50% K_2O), respectively. Before sowing, the entire amount of P, half the dose of K, and one-third of the nitrogen (N) were applied. The second one-third of N was applied at the late tillering growth stage, while the second half dose of K and the last dose of N were applied at the late booting growth stage. The other recommended agronomic practices, such as removing weeds and protecting plants from pests and diseases, were carried out in a timely manner to raise a healthy crop.

All genotypes in both the control and salinity treatments were irrigated with fresh water for up to 21 days after sowing in order to achieve a high germination percentage and good seedling establishment. Subsequently, the genotypes in the high salinity treatment were irrigated with artificial saline water containing 8.8 g NaCl L^{-1} (150 mM NaCl), while in the control treatment, they continued to be irrigated with fresh water until the last irrigation. To control the amount of water delivered to each subplot, a low-pressure surface irrigation system was used. This system consisted of a 76 mm diameter main line, which delivered either saline or fresh water from a five cubic-meter water tank to the subplots. The main line was branched off to the sub-main hoses and equipped with a manual control valve at each subplot (Figure 1). The amount of irrigation water for each irrigation event and the irrigation frequency were determined based on the plant phenology and daily climatic data of the experimental site. Based on these data, the total amount of irrigation water applied for each treatment was 4800 m^3 ha^{-1}. To monitor the build-up of salinity concentration in the root zone of plants during the growing season, soil samples were collected from different places of the salinity treatment at a depth of 0–80 cm, and their electrical conductivity was measured. This monitoring approach ensured that the desired salinity level was consistently maintained throughout the duration of the experiment. Based on the EC analysis conducted on soil samples, the EC of these samples did not exceed 16.3 dS m^{-1}.

2.4. Phenotypic Characterization

Agro-Morpho-Physiological Characteristics

Phenotypic observations were recorded on 13 agro-morpho-physiological parameters at different growth stages. Observations of plant dry weight (PDW), green leaf area (GLA), and leaf area index (LAI) were recorded at 75 (booting stage) and 90 (anthesis stage) days after sowing on ten randomly selected plants from each experimental unit. The green leaf blades of 10 plants were separated and run through a leaf area meter (LI 3100; LI-COR Inc., Lincoln, NE, USA) to measure the GLA. Subsequently, the different parts of the ten plants (stems, leaves, and spikes) were oven-dried at 75 °C until their weight became constant to determine the PDW. The values of LAI were obtained by dividing the values of GLA per plant by the ground area per plant.

Observations of leaf relative water content (LRWC) and total chlorophyll content (Chlt) were recorded at anthesis stage on ten randomly selected fully expanded leaves from each experimental unit, with five leaves for each measurement. An area of approximately 0.20 cm^2 was excised from each of five leaves. These were immediately weighed, soaked in distilled water in the dark at 25 °C for 24 h, and then dried at 75 °C until their weight became constant. This allowed for the recording of the fresh weight (FW), turgid weight (TW), and dry weight (DW). The percentage of LRWC was then calculated using the following formula:

$$\text{LRWC} = (\text{FW} - \text{DW})/(\text{TW} - \text{DW}) \times 100 \quad (1)$$

Approximately 0.4 g of leaf tissue was cut from the other five leaves, washed with distilled water, and soaked in 80% (v/v) acetone at room temperature in darkness until the tissue was completely bleached. The extracted sap was then centrifuged for 5 min at 400 rpm and adjusted to a total volume of 15 mL with 80% acetone. The absorbance of the extract was measured spectrophotometrically at 645 nm (A645) and 663 nm (A663) using a UV/VIS spectrophotometer (UV-2550, Shimadzu, Tokyo, Japan). Finally, the concentrations of Chlt were calculated according to Arnon [41] and Lichtenthaler [42] using the following formula:

$$\text{Chlt (mg g}^{-1}\text{ FW}^{-1}) = [(20.21 \times \text{A645}) + (8.02 \times \text{A663})] \times \text{V}/(1000 \times \text{W}) \quad (2)$$

where V and W are the volume of the extract solution (15 mL) and the weight of the fresh weight of leaf tissue (0.4 g).

Observations of the number of grains per spike (GNPS), thousand-grain weight (TGW), biological yield (BY), grain yield (GY), and harvest index (HI) were recorded at the maturity stage, which was in the fourth week of April in both growing seasons. Observations of NGPS and TGW were recorded from fifty randomly selected spikes from each experimental unit, and observations of BY and GY (in ton ha^{-1}) were recorded from a 0.75 m^2 area of each experimental unit. The area was harvested by hand, air-dried for one week, and weighed to record the BY. The plants were then threshed, and the grains were collected, cleaned, adjusted to 14% moisture content, and weighed to record the GY. The values of HI were obtained by dividing the values of GY by BY.

2.5. Genotypic Characterization

DNA Isolation and SSR Marker Analysis

Genomic DNA was isolated from twenty-day-old seedlings using the Wizard Genomic DNA Purification Kit (PROMEGA Corporation Biotechnology, Madison, WI, USA). After isolation, the samples were treated with RNase and then immediately transferred to a −20 °C freezer. The concentration of the final isolated DNA was determined at 260 nm using a UV–visible spectrophotometer, while its quality was checked by running the isolated DNA on a 0.8% agarose gel. Subsequently, the quantified DNA stock was standardized to a final concentration of 25 ng μL^{-1}.

Sixty different SSR primers (markers) covering most of the chromosomes of the hexaploid wheat genomes were used to characterize the genetic diversity of 24 wheat germplasms in this study (Table S1). These markers were chosen because they have been reported in several previous studies as being associated with salt tolerance in wheat [15,34,43–46]. Sequences of these SSR markers can be found on the Grain Genes website (http://wheat.pw.usda.gov/ggpages/maps.shtml; accessed on 11 January 2022) and presented in Table 1. The polymerase chain reaction (PCR) was carried out in a 20 µL mixture with the following composition: 1.5 µL of DNA sample, 8 µL of nuclease-free water, 10 µL of Green Master Mix (Promega Corporation, Madison, WI, USA), and 0.5 µL of both forward and reverse primers. The temperature cycles of PCR profiles were programmed with an initial denaturation for 4 min at 94 °C, followed by 40 cycles of denaturation for 1 min at 94 °C, 1 min at the primer-specific annealing temperature (as mentioned in Table 1 for each SSR primer), 2 min at 72 °C for extension, and 10 min at 72 °C for a final extension before cooling to 4 °C. The PCR amplification products were analyzed via capillary electrophoresis using the QI Axcel Advanced System Device (Qiagen, Hilden, Germany). The SSR markers amplified bands of each amplified loci were scored visually for their presence or absence with each primer. The scores were obtained in the form of binary matrix with '1' and '0' indicating the presence and absence of bands in each genotype, respectively.

Table 1. Mean square values for the effects of the year, salinity, genotype, and their possible interactions by ANOVA on different agro-morpho-physiological traits of 24 wheat genotypes evaluated under two salinity levels for each year and the combined analysis of two years.

Source of Variance	df	PDW-1	GLA-1	LAI-1	PDW-2	GLA-2	LAI-2	LRWC	Chlt	GNPS	TGW	BY	GY	HI
								First Year						
Salinity (S)	1	86.5 ***	78,446.4 **	92.66 ***	288.5 ***	49,905.7 **	59.7 ***	1870.9 *	38.1 ***	1005.9 **	2111.0 **	963.4 **	147.8 ***	371.9 **
Genotype (G)	23	1.3 ***	358.0 ***	0.27 ***	3.3 ***	320.0 ***	0.25 ***	108.7 ***	1.64 ***	130.1 ***	61.6 ***	9.07 ***	1.09 ***	24.1 ***
G × S	23	0.55 ***	226.3 ***	0.17 **	2.08 ***	220.0 ***	0.16 ***	20.6 *	0.45 ***	24.7 *	15.31 ^{ns}	8.98 ***	0.61 ***	37.6 ***
								Second year						
Salinity (S)	1	73.3 **	41,957.6 **	37.5 **	282.3 ***	31,273.9 **	32.9 **	3701.1 **	36.6 **	746.7 **	768.03 *	942.8 ***	144.1 ***	387.3 **
Genotype (G)	23	0.99 ***	372.5 ***	0.414 ***	3.11 ***	369.0 ***	0.37 ***	39.6 ***	1.89 ***	90.63 ***	81.8 ***	9.79 ***	1.09 ***	23.13 ***
G × S	23	0.52 ***	374.1 ***	1.16 ***	1.85 ***	230.9 ***	0.59 ***	37.46 ***	0.60 ***	28.69 ***	13.57 **	8.94 ***	0.61 ***	30.18 ***
								Combined two years						
Year (Y)	1	0.54 *	25,267.5 **	6.85 ***	0.037 ^{ns}	18,842.1 **	4.72 ***	587.0 ***	3.37 ***	1268.4 *	6610.2 *	5.62 *	0.113 ^{ns}	9.86 ^{ns}
Salinity (S)	1	159.51 ***	117,572 **	124.07 *	570.85 *	80,095.9 **	90.59 **	5417.4 **	74.8 ***	1743.1 *	2712.6 *	1905.9 *	291.9 ***	759.1 ***
S ×Y	1	0.272 ^{ns}	2831.1 ***	6.13 ***	0.017 ^{ns}	1083.5 ^{ns}	1.99 ***	154.56 **	0.007 ^{ns}	9.64 ^{ns}	166.26 ***	0.057 ^{ns}	0.012 ^{ns}	0.078 ^{ns}
Genotype (G)	23	2.20 ***	590.9 ***	0.408 ***	6.359 ***	572.6 ***	0.369 **	105.15 ***	3.11 ***	189.9 ***	130.16 ***	18.38 ***	2.162 ***	45.13 ***
G × Y	23	0.05 ^{ns}	139.6 **	0.275 ***	0.075 ^{ns}	116.4 ***	0.255 **	43.16 ***	0.42 ***	30.79 ***	13.28 ^{ns}	0.465 ^{ns}	0.021 ^{ns}	2.00 ^{ns}
G × S	23	1.02 ***	380.6 ***	0.779 ***	3.88 ***	282.9 ***	0.414 **	43.39 ***	0.88 ***	32.56 ***	16.37 *	17.34 ***	1.19 ***	64.01 ***
G × S × Y	23	0.058 ^{ns}	219.8 ***	0.556 ***	0.046 ^{ns}	168.1 ***	0.328 **	14.69 *	0.17 **	20.83 **	12.51 ^{ns}	0.582 ^{ns}	0.020 ^{ns}	3.728 ^{ns}

Abbreviations of PDW, GLA, LAI, LRWC, Chlt, GNPS, TGW, BY, GY, and HI are plant dry weight (g plant^{-1}), green leaf area (cm^2 plant^{-1}), leaf area index, leaf relative water content (%), total chlorophyll content (mg g^{-1} FW), grain number per spike, thousand-grain weight (g), biological yield (ton ha^{-1}), grain yield (ton ha^{-1}), and harvest index (%), respectively. Values 1 and 2 represent measurements at 70 and 90 days after sowing, respectively. Those sharing the same letter for year, salinity, genotype, and their possible interactions in the same column do not differ significantly at the 0.05 level according to Tukey's test. ^{ns}, *, **, and *** indicate non-significant and significant at $p \leq 0.05$, 0.01, and 0.001, respectively.

2.6. Statistical Analysis

The analysis of the phenotypic data involved several techniques. Initially, before analyzing the data of agro-morpho-physiological traits, the normal distribution and variance homogeneity of all traits were tested using the Shapiro–Wilk and Bartlett's chi-squared tests, respectively, from the tapply function of the base package in the statistical software R. Thereafter, an analysis of variance (ANOVA) was conducted, using SAS software (Version 9.2; Cary, NC, USA), to test for significant differences in morpho-physiological traits between salinity treatments and genotypes. The differences among the mean values of genotypes for each morpho-physiological trait under control or salinity conditions were compared using Tukey's HSD post hoc test at a 5% probability level. The level of correlation between different parameters across years, replications, and genotypes under control or salinity conditions was estimated using Pearson's correlation matrix. To reduce the dimensionality and complexity of data, detect interrelationships among multiple traits, and identify the parameters that contribute most to the variation in tested wheat genotypes, principal component analysis (PCA) was performed on the genotype-by-parameter matrix of means. A biplot was then made using the XLSTAT package. Furthermore, a heatmap cluster analysis based on the stress tolerance index (STI) for traits was performed to express the inter-relationships between traits and genotypes and to group genotypes according to their level of salt tolerance. The STI was calculated for each trait using the following formula suggested by [47]:

$$\text{STI} = (V_C \times V_S)/(V_C)^2 \quad (3)$$

where V_C and V_S are the values of the trait of each genotype under control and salinity conditions, respectively.

For the genotypic data analysis, the SSR data were scored visually to determine the presence or absence of each primer. The SSR bands were then scored as qualitative characters, representing "present" as 1 and "absent" as 0, resulting in the creation of a binary matrix. Based on the Jaccard dissimilarity coefficient, a dissimilarity matrix was generated to assess the pairwise genetic dissimilarity between genotypes. Within the same statistical package, the agglomerative hierarchical clustering (AHC) analysis was conducted using the unweighted pair group average method (UPGMA). The Mantel test was performed to assess the similarity between the Euclidean distance matrices based on morpho-physiological traits and the genetic distance matrices based on the SSR data [48].

Finally, a stepwise multiple linear regression (SMLR) analysis was performed to identify the most influential SSR markers associated with each morpho-physiological trait under both control and salinity conditions, as well as the STI for each trait. The molecular marker observations and morpho-physiological traits were considered as independent and dependent variables, respectively. The critical significance level of the coefficients of determination (R^2) was tested at a 5% probability level.

3. Results

3.1. Analysis of Variance

The results of the ANOVA showed statistically significant differences ($p \leq 0.001$) among the salinity levels (S), genotypes (G), and their interaction (G × S) for all agro-morpho-physiological traits in each year and in the combined analysis of two years (Table 1). Statistically significant differences ($p \leq 0.05$, 0.01, and 0.001) were also observed among the years (Y) for all traits, except for PDW at 90 days after sowing (DAS), GY, and HI. The interaction effect between S × Y and G × Y was highly significant for GLA and LAI at 70 DAS, LAI at 90 DAS, and LRWC. The G × Y interaction had a significant effect on GLA at 90 DAS, Chlt, and GNPS, whereas the S × Y interaction had no significant effect; the opposite was true for TGW (Table 1). The three-way interaction (G × S × Y) had a significant effect on GLA and LAI at 70 and 90 DAS, LRWC, Chlt, and GNPS (Table 1).

3.2. Genotypic Performance in Different Morpho-Physiological Traits under Control and Salinity Conditions

Generally, a high salinity level (150 mM NaCl) significantly decreased all agro-morpho-physiological traits compared to the control treatment. When averaged across the two years, the 150 mM NaCl treatment resulted in decreases of 25.9% in PDW, 28.5% in GLA, and 36.9% in LAI measured at 70 DAS. Additionally, it led to decreases of 34.0% in PDW, 28.6% in GLA, and 38.3% in LAI measured at 90 DAS. It also resulted in reductions of 11.1% in LRWC, 33.0% in Chlt, 10.6% in GNPS, 13.4% in TGW, 27.8% in BY, 34.9% in GY, and 10.2% in HI compared to the control treatment (Tables 2 and 3). Based on the aforementioned percentage reduction, LRWC, GNPS, TGW, and HI were the traits least affected by salinity stress. Conversely, the other traits were severely affected, with salinity stress causing reductions of more than 25% in the mean values of these traits. In addition, significant differences were observed among genotypes for most agro-morpho-physiological traits under both control and salinity conditions. The maximum values for these traits were approximately one to two times higher under control conditions and one to three times higher under salinity conditions compared to the minimum values (Tables 2 and 3). At 70 DAS, PDW, GLA, and LAI ranged from 4.4 to 7.1 g plant^{-1}, 129.5 to 155.6 cm^2 plant^{-1}, and 2.75 to 4.09 under control conditions, while, under salinity conditions, they ranged from 3.4 to 5.2 g plant^{-1}, 83.2 to 115.6 cm^2 plant^{-1}, and 1.71 to 2.79, respectively. At 90 DAS, PDW, GLA, and LAI ranged from 6.4 to 11.0 g plant^{-1}, 106.2 to 128.2 cm^2 plant^{-1}, and 2.31 to 3.35 under control conditions, while, under salinity conditions, they ranged from 4.3 to 6.4 g plant^{-1}, 63.9 to 98.2 cm^2 plant^{-1}, and 1.31 to 2.24, respectively (Table 2). Both physiological traits (LRWC and Chlt) ranged from 72.3 to 88.6% and 2.20 to 4.60 mg g^{-1} FW under control conditions and from 59.0 to 76.7% and 1.00 to 3.84 mg g^{-1} FW under salinity conditions, respectively (Table 3). The different yield components (GNPS, TGW, BY, GY, and HI) ranged from 37.4 to 54.8, 38.3 to 56.4 g, 14.6 to 21.8 ton ha^{-1}, 4.7 to 6.8 ton ha^{-1}, and 25.4 to 39.4% under control conditions, and from 33.7 to 48.3, 32.7 to 48.5 g, 9.4 to 15.5 ton ha^{-1}, 2.7 to 4.8 ton ha^{-1}, and 22.9 to 35.9% under salinity conditions, respectively (Table 3).

Table 2. Mean values of plant dry weight (PDW), green leaf area (GLA), and leaf area index (LAI) measured at 70 and 90 days after sowing of 24 wheat genotypes under control (C) and salinity (S) conditions over two years.

Genotypes	70 Days						90 Days					
	PDW		GLA		LAI		PDW		GLA		LAI	
	C	S	C	S	C	S	C	S	C	S	C	S
Sakha-93	6.23 cd	5.20 a	130.79 ef	111.78 ab	3.48 f–i	2.44 b–e	8.63 de	6.40 a	111.79 fgh	94.69 ab	2.97 e–i	2.07 ab
Sids-1	5.58 f–i	4.81 abc	134.94 c–f	94.4 ef	3.61 d–i	2.07 g–j	7.57 hi	5.59 cde	113.03 d–h	78.09 f–i	3.02 d–h	1.71 d–h
Sakha-61	5.91 def	3.59 kl	143.59 bc	83.23 g	3.74 b–g	1.71 k	8.53 def	4.76 ghi	112.07 e–h	63.87 k	2.93 e–i	1.31 i
Kharchia-65	5.29 ijk	4.83 abc	130.76 ef	106.49 abcd	3.56 d–i	2.38 b–g	6.97 jkl	5.89 a–d	112.10 e–h	89.30 a–e	3.05 b–g	2.0 a–d
Kawz	5.59 f–i	4.08 f–j	153.74 a	102.82 bcd	3.08 jkl	2.79 a	8.88 cd	5.72 b–e	121.39 a–d	86.18 b–f	2.5 jk	2.25 a
Gemiza-9	5.59 f–i	4.31 e–h	148.60 ab	103.85 bcd	3.11 jk	2.61 abc	7.77 gh	6.05 abc	124.10 abc	91.07 a–d	2.76 hij	2.05 ab
MISR-1	5.83 d–g	4.08 f–j	138.87 cde	105.91 bcd	2.75 mn	2.65 ab	7.13 ijk	5.27 efg	116.49 b–g	90.47 a–d	2.31 kl	1.98 a–e
Shandaweel-1	5.74 e–h	3.71 jkl	140.64 bcd	92.29 fg	2.83 klm	2.30 d–h	7.68 ghi	4.71 ghi	119.89 a–f	80.32 e–i	2.47 k	1.81 b–g
RIL-1	7.14 a	4.36 def	139.99 b–e	105.47 bcd	3.51 e–i	2.25 d–	10.97 a	5.67 bcde	112.19 e–h	87.54 b–e	2.81 ghi	1.86 b–g
RIL-2	5.42 g–j	4.78 a–d	154.42 a	115.61 a	4.01 ab	2.47 bcd	8.70 de	6.33 a	126.47 a	98.17 a	3.29 abc	2.10 ab
RIL-3	6.02 c–e	4.95 ab	137.94 c–f	110.7 ab	3.57 d–i	2.36 b–g	9.60 b	5.87 a–d	109.04 gh	90.76 a–d	2.82 ghi	1.94 b–f
RIL-4	5.53 f–i	4.38 def	154.94 a	110.93 ab	4.09 a	2.34 c–g	6.7 klm	5.55 cde	127.06 a	91.79 abc	3.35 a	1.94 a–f
RIL-5	6.11 cde	4.69 b–e	143.35 bc	111.64 ab	3.78 a–f	2.39 b–f	7.54 hij	5.73 b–e	115.14 c–h	94.66 ab	3.03 c–g	2.03 abc
RIL-6	4.42 n–q	3.41 l	155.64 a	110.70 ab	4.01 ab	2.46 b–e	6.81 klm	5.21 e–h	128.21 a	91.41 a–d	3.30 ab	2.03 abc
RIL-7	6.06 cde	4.83 abc	148.38 ab	100.03 c–f	3.73 b–h	2.17 d–i	10.50 a	6.25 ab	125.23 ab	83.27 c–h	3.15 a–e	1.81 b–g
RIL-8	5.34 h–k	4.14 f–i	148.25 ab	108.10 abc	3.94 abc	2.24 d–i	7.73 gh	5.2 e–h	123.77 abc	86.62 b–f	3.28 a–d	1.80 b–g
RIL-9	5.56 f–i	3.9 h–k	143.26 bc	91.66 fg	3.84 a–d	1.98 ijk	8.23 efg	4.92 fgh	115.91 c–g	72.25 ijk	3.11 a–f	1.56 ghi
RIL-10	5.86 def	4.35 d–g	148.61 ab	83.20 g	3.81 a–e	1.82 jk	9.38 bc	4.73 ghi	120.98 a–e	64.77 jk	3.10 a–f	1.42 hi
RIL-11	5.58 f–i	3.57 kl	129.47 f	94.28 ef	3.34 ij	2.01 h–k	8.91 cd	4.66 hi	106.18 hi	73.40 ij	2.73 ij	1.56 ghi
RIL-12	6.43 bc	4.05 f–j	134.73 c–f	110.98 ab	3.56 d–i	2.39 b–f	9.53 b	5.73 b–e	108.29 gh	85.28 c–g	2.86 f–i	1.84 b–g
RIL-13	5.73 e–h	4.27 e–h	131.87 def	98.22 def	3.44 ghi	2.12 f–j	8.03 fgh	5.36 def	108.28 gh	76.67 ghi	2.83 ghi	1.66 fgh
RIL-14	5.43 g–j	3.77 i–l	142.70 bc	98.02 def	3.63 d–i	2.18 d–i	7.46 hij	5.46 def	115.45 c–g	75.81 hi	2.93 e–i	1.68 e–h
RIL-15	6.72 ab	4.45 c–f	141.57 bc	103.91 bcd	3.64 c–i	2.15 e–i	8.87 cd	5.62 cde	113.57 d–h	82.67 d–h	2.93 e–i	1.72 c–h
RIL-16	5.05 –m	3.93 g–k	131.35 ef	84.35 g	3.43 hi	1.72 k	6.43 lmn	4.29 i	109.05 gh	66.15 jk	2.85 f–i	1.35 i

Those sharing the same letter in the same column do not differ significantly at the 0.05 level according to Tukey's test.

Table 3. Mean values of leaf relative water content (LRWC), total chlorophyll content (Chlt), grain number per spike (GNPS), thousand-grain weight (TGW), biological yield (BY), grain yield (GY), and harvest index (HI) of 24 wheat genotypes under control (C) and salinity (S) conditions over two years.

Genotypes	LRWC		Chlt		GNPS		TGW		BY		GY		HI	
	C	S	C	S	C	S	C	S	C	S	C	S	C	S
Sakha-93	78.9 b–g	73.82 abc	3.35 def	2.89 b	46.95 e–k	45.0 b–e	43.21 i–m	41.94 bc	17.76 ghi	13.58 c–g	5.58 fgh	4.03 cd	31.61 e–l	29.64 c–g
Sids-1	76.05 g–j	69.83 efg	3.34 def	1.50 k	43.61 l–p	39.95 h–k	44.25 f–l	40.12 b–e	21.75 a	13.37 d–h	5.53 ghi	3.71 def	25.5 v–y	27.74 f–i
Sakha-61	78.44 c–h	67.12 ghi	2.28 m–q	1.0 l	44.32 k–o	39.5 i–l	46.91 c–h	38.82 c–f	14.64 m–p	12.40 ghi	5.77 efg	3.07 h	39.62 a	24.77 kl
Kharchia-65	78.4 d–h	73.3 bcd	4.6 a	3.84 a	40.03 q–u	37.54 k–n	45.56 d–j	42.26 b	18.24 fgh	14.25 a–e	5.39 h–k	4.34 bc	29.59 j–r	30.56 b–e
Kawz	81.83 bc	70.37 d–g	3.08 fg	2.58 c	54.82 a	45.83 a–d	38.34 p–t	32.7 i	18.76 efg	12.36 ghi	6.41 b	3.69 ef	34.42 bcd	29.88 b–f
Gemiza-9	82.23 b	76.72 a	2.49 k–n	2.18 de	49.62 cde	44.15 c–f	45.05 e–k	34.57 hi	19.98 cde	13.82 b–f	5.89 ef	4.23 bc	29.57 j–r	30.71 bcd
MISR-1	80.42 b–e	75.75 ab	2.77 h–k	2.13 def	51.67 abc	47.94 ab	47.54 b–f	41.13 bcd	18.1 f–i	14.84 abc	6.04 de	4.24 bc	33.46 c–f	28.62 d–h
Shandaweel-1	75.22 h–l	68.5 e–h	3.05 fgh	1.69 jk	54.34 ab	45.36 a–d	41.79 k–o	36.94 e–h	20.42 bcd	12.61 fghi	6.43 b	3.48 fg	31.73 e–k	27.63 f–j
RIL-1	73.09 j–o	68.11 fgh	2.37 l–o	1.84 f–j	49.18 c–f	40.9 g–j	44.15 g–l	39.66 b–f	20.36 bcd	12.29 hi	6.24 bcd	3.49 fg	30.75 g–n	28.42 d–h
RIL-2	75.46 h–k	71.84 cde	2.73 ijk	2.0 e–i	47.14 e–k	45.54 a–d	46.73 c–h	41.17 bcd	20.96 abc	14.81 abc	6.33 bcd	4.79 a	30.28 g–p	32.38 b
RIL-3	78.03 d–h	70.81 cdef	3.25 ef	1.74 ijk	46.2 f–l	38.58 j–m	47.17 b–g	41.55 bc	19.21 def	13.39 d–h	5.62 fgh	3.76 def	29.43 k–r	28.14 d–i
RIL-4	77.84 d–h	68.99 e–h	3.31 def	1.98 e–j	43.64 l–p	39.64 i–l	46.44 c–i	42.01 bc	20 bcde	14.48 a–d	5.8 efg	3.81 de	29.09 l–t	26.34 h–k
RIL-5	77.6 d–h	70.97 c–f	3.59 bcd	2.32 cd	44.23 k–o	42.94 d–h	44.95 e–k	41.49 bc	18.86 efg	14.39 a–d	5.49 g–j	4.28 bc	29.31 k–s	29.78 b–f
RIL-6	75.85 g–j	70.87 c–f	2.57 j–m	2.07 d–h	51.23 bcd	48.34 a	42.45 j–n	37.97 d–g	18.86 efg	15.03 ab	6.09 cde	4.21 bc	32.29 d–i	28.0 e–i
RIL-7	76.99 f–i	68.99 e–h	3.47 cde	2.31 cd	45.62 h–m	44.02 c–g	47.59 b–f	42.79 b	19.62 de	14.65 abc	6.78 a	3.74 def	34.7 bcd	25.57 ijk
RIL-8	75.96 g–j	69.45 efg	2.26 n–q	2.03 d–i	48.68 c–h	46.34 abc	44.15 g–l	37.52 e–h	17.25 hij	13.76 c–f	6.39 bc	4.43 b	37.05 ab	32.19 bc
RIL-9	72.31 k–p	59.03 j	2.87 g–j	1.79 h–k	47.73 e–j	36.45 l–o	48.45 bcd	39.74 b–f	19.86 cde	9.36 k	5.71 fg	3.34 gh	28.81 m–u	35.9 a
RIL-10	76.17 g–j	63.91 i	2.2 n–r	1.82 g–j	45.98 f–m	39.92 h–k	48.91 bc	39.86 b–f	21.25 ab	12.33 ghi	6.54 ab	3.33 gh	30.89 f–m	27.02 g–k
RIL-11	88.57 a	69.05 e–h	2.64 i–l	1.89 e–j	48.9 c–g	42.95 d—h	49.71 bc	39.68 b–f	16.5 jk	10.94 j	5.22 i–l	2.74 i	31.66 e–l	25.04 jkl
RIL-12	79.02 b–g	68.97 e–h	3.58 bcd	2.06 d–h	37.37 u–	34.95 no	50.49 b	41.83 bc	16.43 jkl	15.5 a	5.17 jkl	3.55 efg	31.62 e–l	22.92 l
RIL-13	80.32 b–f	70.45 c–g	2.85 g–j	1.93 e–j	48.5 c–i	41.65 f–j	47.63 b–e	39.69 b–f	18.02 f–i	13.12 e–h	4.74 mn	3.6 efg	26.45 t–x	27.47 f–j
RIL-14	78.3 d–h	65.81 hi	3.66 bc	2.06 d–h	46.25 f–l	33.67 o	43.69 h–l	36.73 fgh	16.89 ij	13.67 c–f	5.01 lm	3.33 gh	29.71 i–q	24.44 kl
RIL-15	77.01 e–i	65.94 hi	4.38 a	2.11 d–g	37.48 u–x	35.48 mno	56.43 a	48.51 a	15.24 lmn	14.15 b–e	4.96 lm	3.74 def	32.62 d–g	26.75 h–k
RIL-16	80.43 bcd	67.68 fgh	3.45 cde	1.88 f–j	43.19 l–q	41.92 e–i	39.65 n–s	35.25 ghi	15.2 lmn	11.57 ij	5.17 kl	3.04 hi	33.99 cde	26.37 h–k

Those sharing the same letter in the same column do not differ significantly at the 0.05 level according to Tukey's test.

The relative changes in each agro-morpho-physiological trait for every genotype are presented in Table 4. These changes indicate the percentage reduction of each trait under high salinity levels compared to the control treatment. The different color shades in Table 4 represent the range of reduction percentages. The color gradient, ranging from dark blue to dark orange, reflects the gradient in reduction percentages of the trait from the minimum to the maximum. Generally, there was a wide range in the reduction percentages for all agro-morpho-physiological traits, except for LRWC, GNPS, and TGW, which exhibited a narrow range. The reduction percentages ranged from 8.7% to 39.2%, 14.5% to 44.0%, and 3.7% to 54.3% for PDW, GLA, and LAI at 70 DAS; 15.5% to 49.5%, 15.3% to 46.5%, and 10.0% to 55.2% for PDW, GLA, and LAI at 90 DAS; and 4.8% to 22.0%, 9.9% to 56.1%, 2.9% to 23.3%, 5.6% to 52.8%, 19.5% to 49.1%, and −24.8% to 37.2% for LRWC, Chlt, GNPS, TGW, BY, GY, and HI, respectively (Table 4). Additionally, the salt-tolerant genotypes Sakha 93 and Kharachia-65 exhibited the lowest reduction percentages for most agro-morpho-physiological traits, while the salt-sensitive genotypes Sakha 61 and Shandaweel-1 displayed the highest reduction percentages. Among the RILs, three out of eleven (RIL9, RIL10, and RIL11) from the crossing between Sakha 93 and Sakha 61 and all RILs (RIL12–RIL16) from the crossing between Sakha 93 and Sids1 had the highest reduction percentages for most agro-morpho-physiological traits. Conversely, the remaining RILs from the crossing between Sakha 93 and Sakha 61 (RIL1–RIL8) showed the opposite trend (Table 4). Kawz and Misr-1 exhibited the lowest reduction percentage in LAI at 70 and 90 DAS (3.7–14.5%). In contrast, the reduction percentage for this trait surpassed 30% in the majority of RILs and genotypes. The minimum reduction percentage in PDW and GLA at 70 and 90 DAS was observed in Sakha 93 and Kharachia-65. Although RIL12 and RIL15 had the lowest reduction percentage in BY (5.6% and 4.1%), they had an adequate reduction percentage in GY (31.4% and 24.5%) and HI (27.3% and 18.6%). Seven genotypes (Sids-1, Kharachia-65, Gemiza-9, RIL2, RIL5, RIL9, and RIL13) exhibited an increase in HI under salinity conditions compared to the control (Table 3). Consequently, the reduction percentages of HI in these genotypes were negative (Table 4).

Table 4. Reduction percentage of different agro-morpho-physiological traits under high salinity level relative to the control treatment for each genotype.

Genotypes	PDW-1	GLA-1	LAI-1	PDW-2	GLA-2	LAI-2	LRWC	Chlt	GNPS	TGW	BY	GY	HI
Sakha-93	16.6	14.5	29.7	25.9	15.3	30.3	6.4	13.9	4.1	2.9	23.5	27.9	5.7
Sids-1	13.8	30.0	42.5	26.1	30.9	43.3	8.2	55.0	8.4	9.3	38.5	32.9	−9.1
Sakha-61	39.2	42.0	54.3	44.2	43.0	55.2	14.4	56.1	10.9	17.2	15.3	46.8	37.2
Kharchia-65	8.7	18.6	33.2	15.5	20.3	34.3	6.5	16.5	6.2	7.2	21.9	19.5	−3.1
Kawz	26.9	33.1	9.6	35.6	29.0	10.0	14.0	16.3	16.4	14.7	34.1	42.4	12.6
Gemiza-9	22.9	30.1	16.0	22.1	26.6	25.8	6.7	12.3	11.0	23.3	30.9	28.2	−3.7
MISR-1	30.0	23.7	3.7	26.1	22.3	14.5	5.8	22.9	7.2	13.5	18.0	29.7	14.3
Shandaweel-1	35.4	34.4	18.7	38.7	33.0	26.5	8.9	44.8	16.5	11.6	38.2	45.9	12.5
RIL-1	38.9	24.7	36.0	48.3	22.0	33.8	6.8	22.3	16.8	10.2	39.7	44.1	7.4
RIL-2	11.9	25.1	38.5	27.3	22.4	36.4	4.8	26.5	3.4	11.9	29.3	24.3	−6.9
RIL-3	17.8	19.7	34.0	38.9	16.8	31.4	9.3	46.5	16.5	11.9	30.3	33.0	3.9
RIL-4	20.9	28.4	42.8	17.1	27.8	42.1	11.4	40.3	9.2	9.5	27.6	34.4	9.3
RIL-5	23.4	22.1	36.7	24.0	17.8	33.2	8.5	35.3	2.9	7.7	23.7	22.0	−2.1
RIL-6	22.9	28.9	38.7	23.5	28.7	38.5	6.6	19.2	5.7	10.6	20.3	30.8	13.2
RIL-7	20.3	32.6	41.7	40.5	33.5	42.5	10.4	33.5	3.5	10.1	25.3	44.8	26.1
RIL-8	22.4	27.1	43.1	32.7	30.0	45.3	8.6	9.9	4.8	15.0	20.2	30.7	13.2
RIL-9	29.9	36.0	48.6	40.3	37.7	49.9	18.4	37.4	23.6	18.0	52.8	41.5	−24.8
RIL-10	25.7	44.0	52.4	49.5	46.5	54.4	16.1	17.2	13.2	18.5	42.0	49.1	12.3
RIL-11	36.1	27.2	39.9	47.7	30.9	42.7	22.0	28.3	12.2	20.2	33.7	47.5	20.9
RIL-12	37.0	17.6	32.8	39.9	21.3	35.7	12.7	42.5	6.5	17.2	5.6	31.4	27.3
RIL-13	25.4	25.5	38.4	33.3	29.2	41.4	12.3	32.1	14.1	16.7	27.2	24.0	−4.3
RIL-14	30.6	31.3	39.9	26.8	34.3	42.6	15.9	43.9	27.2	15.9	19.1	33.5	17.8
RIL-15	33.8	26.6	41.0	36.7	27.2	41.2	14.4	51.8	5.3	14.0	7.1	24.5	18.6
RIL-16	22.2	35.8	49.9	33.3	39.3	52.7	15.9	45.5	2.9	11.1	23.9	41.1	22.6

Abbreviations of PDW, GLA, LAI, LRWC, Chlt, GNPS, TGW, BY, GY, and HI are plant dry weight (g plant^{-1}), green leaf area (cm^2 plant^{-1}), leaf area index, leaf relative water content (%), total chlorophyll content (mg g^{-1} FW), grain number per spike, thousand-grain weight (g), biological yield (ton ha^{-1}), grain yield (ton ha^{-1}), and harvest index (%), respectively. Values 1 and 2 represent measurements at 70 and 90 days after sowing, respectively. The color gradient, ranging from dark blue to dark orange, reflects the reduction percentages of the trait, gradually transitioning from the minimum to the maximum.

3.3. Correlation Matrix between Different Agro-Morpho-Physiological Traits under Control and Salinity Conditions

In general, the different agro-morpho-physiological traits showed stronger correlations with each other under salinity conditions compared to control conditions (Table 5). Under control conditions, the PDW, GLA, and LAI at 70 DAS exhibited a strong positive correlation with themselves at 90 DAS; that is, correlation coefficients (r) ranged from 0.72 to 0.96. Meanwhile, under salinity conditions, the three traits displayed a moderate to strong positive correlation with each other at both 70 and 90 DAS (r ranged from 0.41 to 0.96; Table 5). The LRWC showed a moderate negative correlation with LAI at 70 and 90 DAS under control conditions (r = −0.44). Meanwhile, under salinity conditions, this trait had a moderate to strong positive correlation with PDW, GLA, LAI at 70 and 90 DAS, Chlt, GNPS, BY, and GY (r ranged from 0.43 to 0.61; Table 5). Under control conditions, Chlt exhibited only significant correlations with GNPS (−0.62) and GY (0.50). However, under salinity conditions, Chlt had a moderate to strong positive correlation with all traits ((r ranged from 0.43 to 0.61), except TGW and HI (Table 5). Under salinity conditions, GY was substantially and positively correlated with all traits except TGW. However, under control conditions, GY was only positively correlated with GLA at 70 and 90 DAS, Chlt, GNPS, and BY. There was a negative correlation between BY and HI under both control and salinity conditions; however, this correlation was only significant under control conditions (Table 5).

Table 5. Pearson's correlation matrix of different agro-morpho-physiological traits under control (upper right) and salinity (lower left) conditions over two years (n = 104).

	1	2	3	4	5	6	7	8	9	10	11	12	13
PDW-1 (1)		−0.25	−0.16	0.72 ***	−0.38	−0.27	−0.15	0.12	−0.28	0.45 *	−0.04	−0.05	−0.01
GLA-1 (2)	0.44 *		0.39	0.001	0.90 ***	0.39	−0.34	−0.35	0.31	−0.13	0.38	0.64 **	0.22
LAI-1 (3)	0.25	0.79 ***		0.03	0.29	0.96 ***	−0.44 *	−0.01	−0.44 *	0.22	0.07	0.01	−0.03
PDW-2 (4)	0.75 ***	0.75 ***	0.65 **		−0.16	−0.08	−0.12	−0.18	−0.03	0.34	0.13	0.29	0.12
GLA-2 (5)	0.49 *	0.95 ***	0.86 ***	0.77 ***		0.41 *	−0.33	−0.28	0.36	−0.22	0.49 *	0.72 ***	0.15
LAI-2 (6)	0.41 *	0.85 ***	0.96 ***	0.75 ***	0.93 ***		−0.44 *	0.02	−0.39	0.14	0.17	0.08	−0.08
LRWC (7)	0.44 *	0.56 **	0.68 ***	0.51 **	0.67 ***	0.66 **		0.03	0.08	0.01	−0.43 *	−0.36	0.10
Chlt (8)	0.43 *	0.47 *	0.51 **	0.50 **	0.50 **	0.58 **	0.43 *		−0.62 **	0.17	−0.24	0.50 **	−0.26
GNPS (9)	−0.05	0.21	0.42 *	0.04	0.37	0.42 *	0.55 **	0.07		−0.55 **	0.36	0.53 **	0.10
TGW (10)	0.48 *	0.32	−0.08	0.34	0.22	0.001	−0.08	0.15	−0.35		−0.19	−0.30	−0.09
BY (11)	0.34	0.69 ***	0.55 **	0.60 **	0.66 **	0.56 **	0.60 **	0.32	0.16	0.35		0.56 **	−0.56 **
GY (12)	0.49 *	0.76 ***	0.69 ***	0.65 **	0.83 ***	0.75 ***	0.61 **	0.48 *	0.43 *	0.17	0.68 ***		0.37
HI (13)	0.25	0.24	0.30	0.20	0.34	0.36	0.05	0.27	0.30	−0.13	−0.24	0.54 **	

Abbreviations of PDW, GLA, LAI, LRWC, Chlt, GNPS, TGW, BY, GY, and HI are plant dry weight (g plant^{-1}), green leaf area (cm^2 plant^{-1}), leaf area index, leaf relative water content (%), total chlorophyll content (mg g^{-1} FW), grain number per spike, thousand-grain weight (g), biological yield (ton ha^{-1}), grain yield (ton ha^{-1}), and harvest index (%), respectively. Values 1 and 2 represent measurements at 70 and 90 days after sowing, respectively. *, **, and *** indicate significant at $p \leq 0.05$, 0.01, and 0.001, respectively.

3.4. Principal Component Analysis for Agro-Morpho-Physiological Traits under Control and Salinity Conditions

The potential relationships between different agro-morpho-physiological traits and genotypes under control and salinity conditions were assessed using a biplot of a principal component analysis (PCA). The first four and three principal components (PCs) had eigenvalues greater than one and explained 80.24% and 78.97% of the total variation among traits and genotypes under control and salinity conditions, respectively (Figure 2). However, the first two components explained the highest percentages of variance: 51.86% and 68.82% of the total variability under control and salinity conditions, respectively. Therefore, the PCA-biplot was created using the first two PCs (Figure 3). Under control conditions, PC1 explained 30.60% of the total variability and was mostly associated with GLA at 70 and 90 DAS and GY. PC2 explained 21.26% of the total variability and was strongly associated with LAI at 70 and 90 DAS, GNPS, and TGW (Figure 2). Under salinity conditions, PC1 explained 53.47% of the total variability and was mainly influenced by GLA and LAI at 70 and 90 DAS, PDW at 90 DAS, and GY. PC2 explained 15.35% of the total variability and was mainly associated with TGW and GNPS (Figure 2). PC3 and PC4 accounted for 16.14% and 12.24% of the total variation in the data under control conditions and 10.15% and 5.77%

under salinity conditions, respectively. PC3 was strongly related to PDW at 70 and 90 DAS under control conditions and BY and HI under salinity conditions, while PC4 showed a strong association with BY and HI under control conditions and Chlt under salinity conditions (Figure 2). PC5 explained only 6.22% and 5.30% of the total variation under control and salinity conditions, respectively, and was strongly influenced by physiological parameters (LRWC and Chlt) under control conditions and by PDW at 70 DAS and LRWC under salinity conditions (Figure 2).

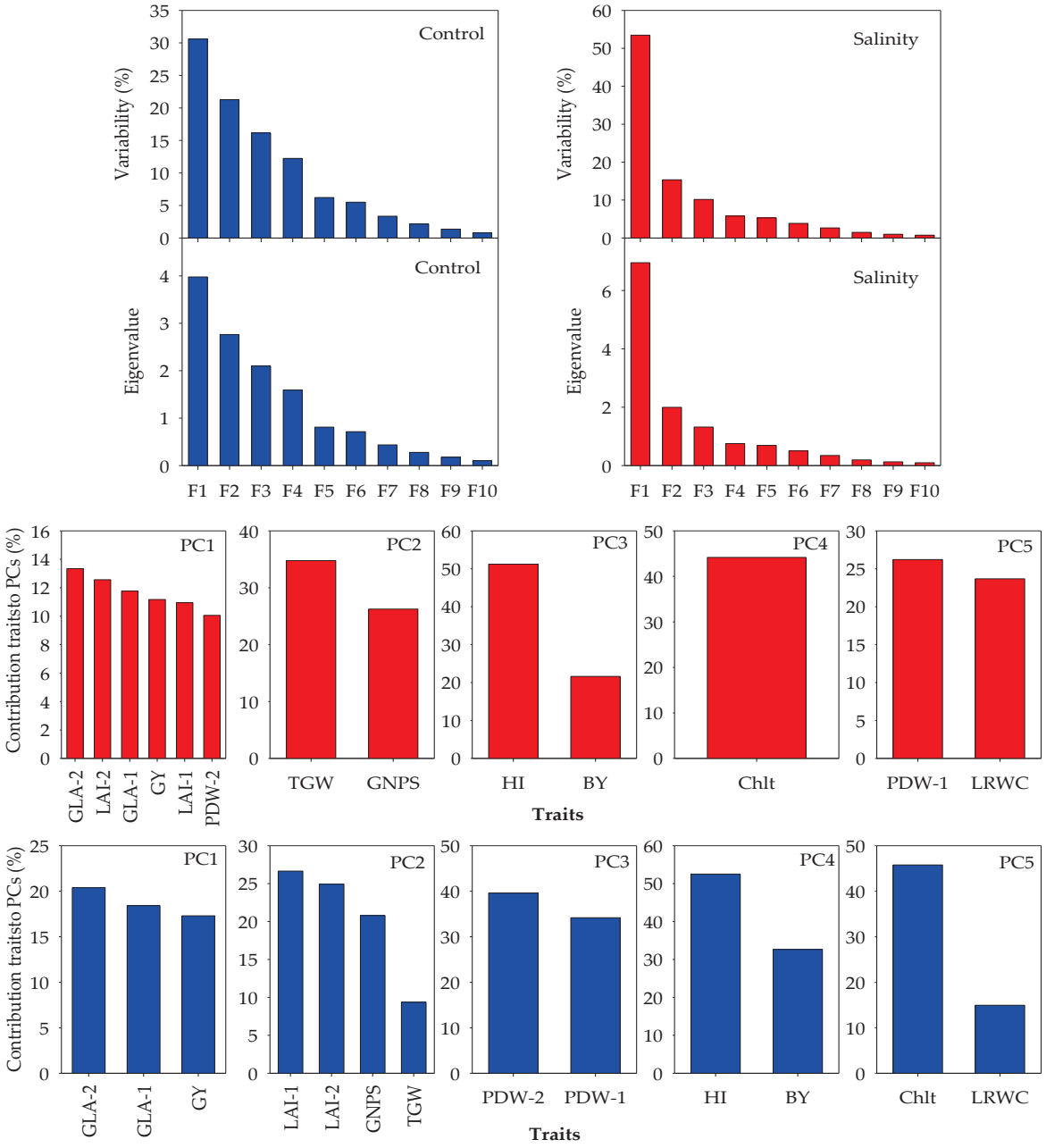

Figure 2. Eigenvalue and variability percentage of the first ten principal components (PCs) and contribution of the traits to first five PCs under control and salinity conditions. Abbreviations of PDW, GLA, LAI, LRWC, Chlt, GNPS, TGW, BY, GY, and HI are plant dry weight (g plant^{-1}), green leaf area (cm^2 plant^{-1}), leaf area index, leaf relative water content (%), total chlorophyll content (mg g^{-1} FW), grain number per spike, thousand-grain weight (g), biological yield (ton ha^{-1}), grain yield (ton ha^{-1}), and harvest index (%), respectively. Values 1 and 2 represent measurements at 70 and 90 days after sowing, respectively.

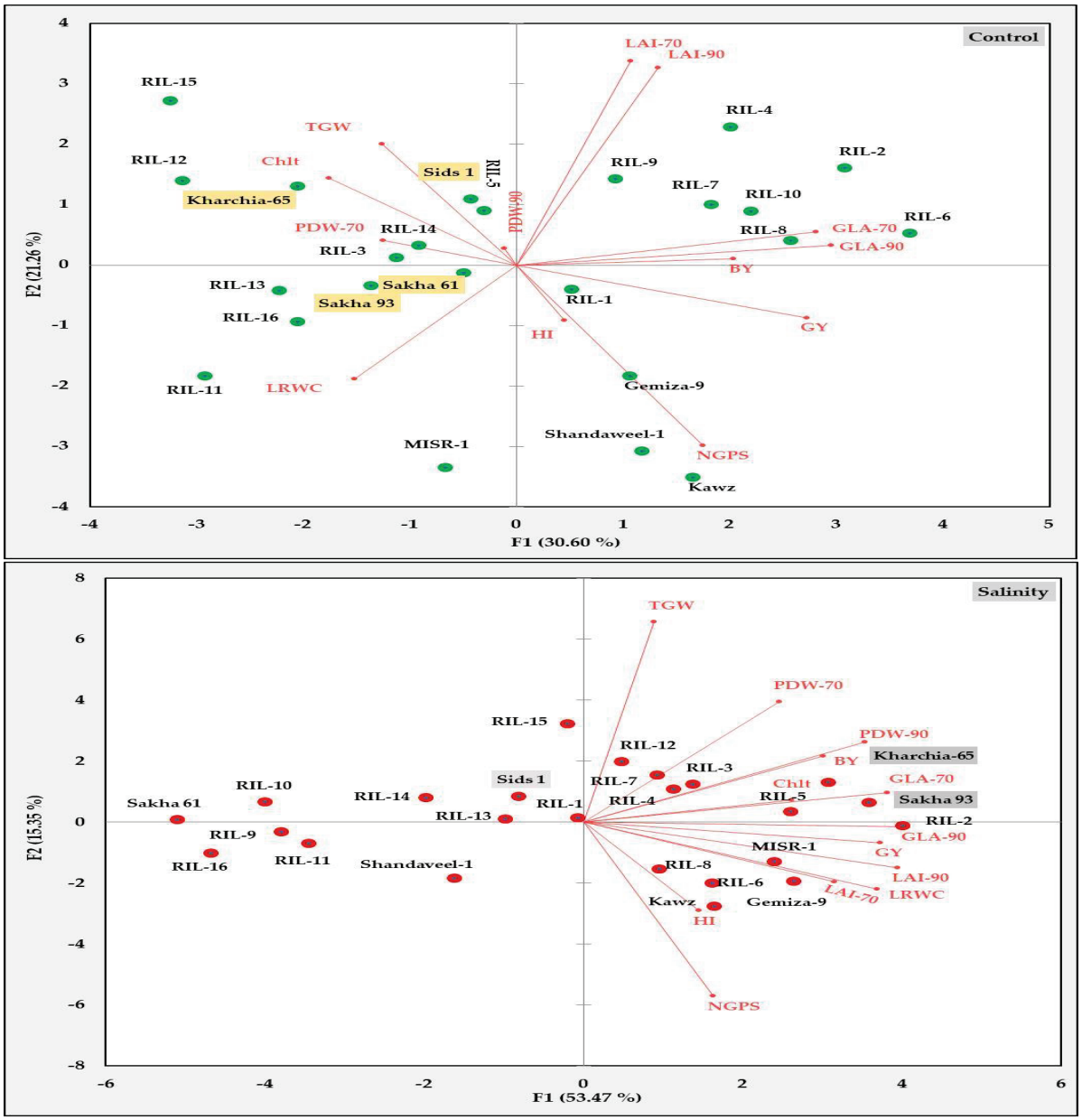

Figure 3. Principal component analysis biplot for genotypes and traits under control and salinity conditions. Abbreviations of PDW, GLA, LAI, LRWC, Chlt, GNPS, TGW, BY, GY, and HI are plant dry weight (g plant^{-1}), green leaf area (cm^2 plant^{-1}), leaf area index, leaf relative water content (%), total chlorophyll content (mg g^{-1} FW), grain number per spike, thousand-grain weight (g), biological yield (ton ha^{-1}), grain yield (ton ha^{-1}), and harvest index (%), respectively. Values 1 and 2 represent measurements at 70 and 90 days after sowing, respectively.

According to the PCA biplot (Figure 3), the thirteen agro-morpho-physiological traits discriminated the different genotypes into four main groups under control conditions and three main groups under salinity conditions. Under control conditions, RILs 2, 4, 6, 7, 8, 9, and 10 were found to be located in the positive region of PC1 and PC2. They showed a strong association with GLA and LAI at 70 and 90 DAS and a moderate association with BY. The genotypes located in the negative region of PC1 and PC2 were the salt-tolerant genotype Sakha 93, the salt-sensitive genotype Sakha 61, Misr-1, and RILs 11, 16, and 19. These genotypes were closely correlated with LRWC. The third group included the salt-tolerant genotype Kharachia-65, the moderately salt-tolerant genotype Sids 1, and RILs 3, 5, 12, 14, and 15. These genotypes were highly correlated with TGW and Chlt,

moderately correlated with PDW at 70 DAS, and weakly correlated with PDW at 90 DAS. Gemeza 9, Shendaweel-1, Kawz, and RIL1 were located in the positive region of PC1 and the negative region of PC2 and were closely correlated with GY and GNPS and weakly correlated with HI (Figure 3).

Under salinity conditions, the two salt-tolerant genotypes Sakha 93 and Kharachia-65 were grouped together with RILs 2, 6, and 8 and situated along the positive region of PC1 and PC2. These genotypes showed a strong correlation with PDW at 70 and 90 DAS, GLA at 70 DAS, Chlt, and BY (Figure 3). Gemeza 9, Kawz, Misr 1, and RILs 2, 6, and 8 were located in the positive region of PC1 and the negative region of PC2. They were closely correlated with the remaining traits. Salt-sensitive genotype Sakha 61, Sids 1, Shendaweel-1, and RILs 1, 9, 10, 11, 13, 14, 15, and 16 leaned towards the negative region of PC1 and positive or negative region of PC2. These genotypes did not show any relationship with morpho-physiological traits (Figure 3).

3.5. Clustering of Genotypes and Traits Based on Stress Tolerance Index

The two-way clustering was performed using the salt tolerance index (STI) for each agro-morpho-physiological trait. This was carried out to group genotypes into different sub-clusters based on their similarities and to assess the contribution of each trait in response to salt stress. Based on this analysis, the genotypes and traits were grouped into three column clusters and three row clusters, respectively (Figure 4). Clusters 1, 2, and 3 comprised 4, 8, and 12 genotypes, respectively, as well as two, three, and eight traits. The salt-sensitive genotype Sakha 61 and three RILs (9, 10, and 11) were grouped together in Cluster 1 (Figure 4). They exhibited a low STI (0.49–0.89) for all agro-morpho-physiological traits (Figure 5). The opposite was true of the genotypes in Cluster 2, which included two salt-tolerant genotypes, Kharachia-65 and Sakha 93, a moderately salt-tolerant genotype, Sids-1, and five RILs (2, 3, 4, 5, and 13) (Figure 4). These genotypes exhibited a high STI value (0.63–1.01) for all traits (Figure 5). The remaining genotypes (Gemeza 9, Shendaweel-1, Kawz, and Misr 1) and RILs were grouped together in Cluster 3 (Figure 4) and exhibited higher STI values than Cluster 1 and lower STI values than Cluster 2 for all traits (0.57–0.92), with a few exceptions (Figure 5). Therefore, the genotypes and RILs in Clusters 1, 2, and 3 can be considered salt-sensitive (S), salt-tolerant (T), and intermediate (I) genotype groups, respectively.

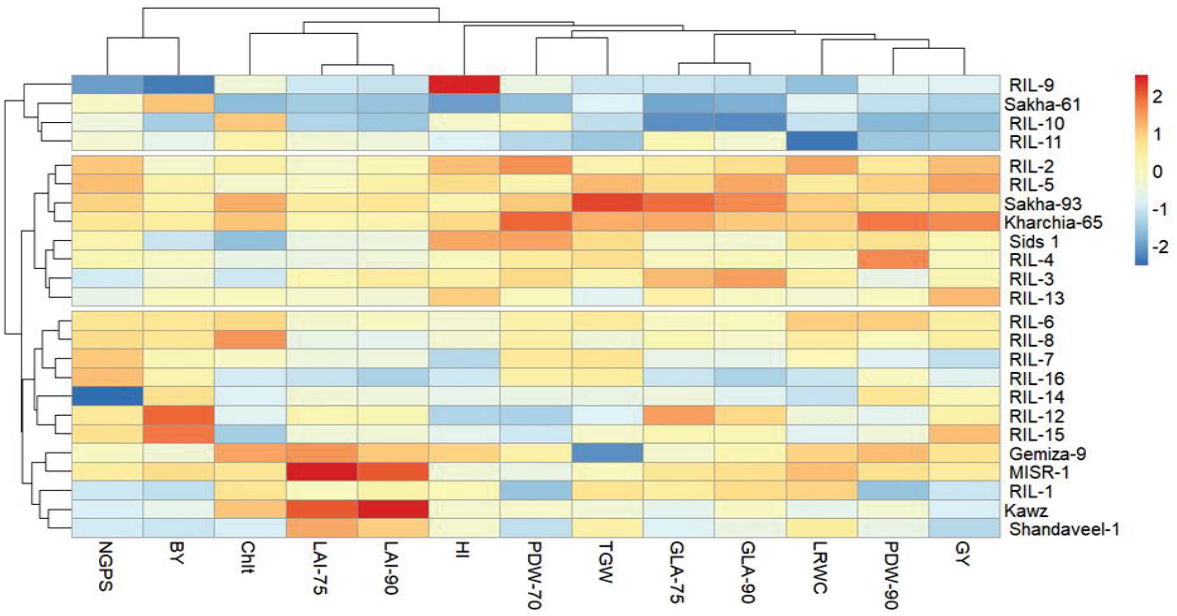

Figure 4. Heatmap cluster analysis displaying the associations among 24 wheat genotypes based on salt tolerance index (STI) of different traits. The different colors and densities were adjusted based on

associations between genotypes and STI for each trait. The darker red indicates higher values, while the darker blue indicates lower values. Abbreviations of PDW, GLA, LAI, LRWC, Chlt, GNPS, TGW, BY, GY, and HI are plant dry weight (g plant^{-1}), green leaf area (cm^2 plant^{-1}), leaf area index, leaf relative water content (%), total chlorophyll content (mg g^{-1} FW), grain number per spike, thousand-grain weight (g), biological yield (ton ha^{-1}), grain yield (ton ha^{-1}), and harvest index (%), respectively. Values 1 and 2 represent measurements at 70 and 90 days after sowing, respectively.

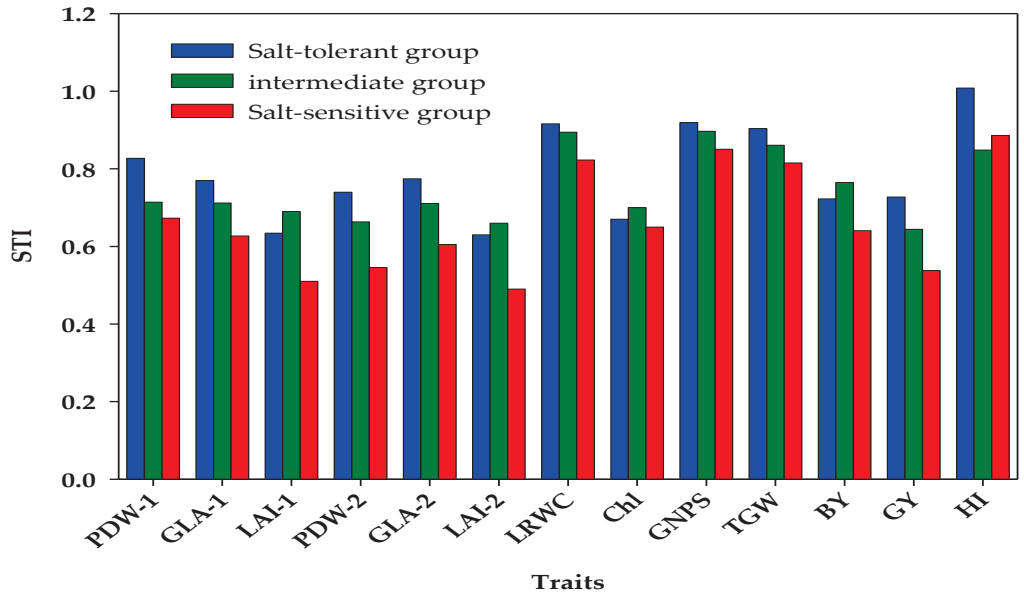

Figure 5. Salt tolerance index (STI) of measured traits for salt-tolerant (T), intermediate (I), and salt-sensitive (S) genotypes groups. Abbreviations of PDW, GLA, LAI, LRWC, Chlt, GNPS, TGW, BY, GY, and HI are plant dry weight (g plant^{-1}), green leaf area (cm^2 plant^{-1}), leaf area index, leaf relative water content (%), total chlorophyll content (mg g-1 FW), grain number per spike, thousand-grain weight (g), biological yield (ton ha^{-1}), grain yield (ton ha^{-1}), and harvest index (%), respectively. Values 1 and 2 represent measurements at 70 and 90 days after sowing, respectively.

The GNPS and BY traits were grouped into Cluster 1, and the STI for the former trait was higher in the T group, followed by the I and S groups, while the STI for the latter trait was higher in the I group, followed by the T and S groups (Figures 4 and 5). The STI values for the traits of Cluster 2 (LAI at 70 and 90 DAS and Chlt) were highest in the I group, followed by the T group. The S group had the lowest STI values for these traits. For the traits in Cluster 3, the T group consistently had higher STI values, followed by the I and S groups (Figures 4 and 5). Additionally, the lowest STI values were observed for the Chlt, LAI at 70 DAS, GLA, and PDW at 70 and 90 DAS, and GY. The STI values for these traits in the S group decreased by 18.8%, 22.1%, 18.6%, 21.9%, 26.2%, 18.6%, and 26.1%, respectively, compared to those in the T group (Figure 5).

The results in Table 6 show that, under control conditions, both the I and S groups achieved higher mean values for most morpho-physiological traits compared to the T group. However, under salinity conditions, the opposite was observed. Under control conditions, both the I and S groups attained higher mean values for all traits compared to the T group, except for LAI at 70 and 90 DAS for the I group and Chlt and BY for both groups. The T group exhibited higher values for these traits compared to the I and S groups. Meanwhile, under salinity conditions, both the I and S groups displayed a reduction in the mean values of various agro-morpho-physiological traits by 1.7–13.6% and 2.8–28.5%, respectively, compared to the T group (Table 6). Furthermore, the S group was significantly more affected by salinity stress than the T and I groups. The mean values of different agro-morpho-physiological traits under salinity conditions decreased by 8.4–37.1%, 10.6–36.0%,

and 15.0–50.7% in the T, I, and S groups, respectively, when compared to the control conditions (Table 6).

Table 6. Mean values of different traits for salt-tolerant (T), intermediate (I), and salt-sensitive (S) genotypes groups under control (C) and salinity (S) conditions.

	T-Group			I-Group			S-Group		
	C	**S**	**%Change**	**C**	**S**	**%Change**	**C**	**S**	**%Change**
PDW-1	5.74	4.74	17.5	5.78	4.09	29.1	5.73	3.85	32.7
PDW-2	7.97	5.84	26.7	8.31	5.43	34.7	8.76	4.77	45.6
GLA-1	139.88	107.47	23.2	143.70	102.20	28.9	141.23	88.09	37.6
GLA-2	115.36	89.26	22.6	118.13	83.90	29.0	113.79	68.57	39.7
LAI-1	3.69	2.32	37.1	3.43	2.32	32.3	3.68	1.88	49.1
LAI-2	3.04	1.93	36.7	2.84	1.85	35.1	2.97	1.46	50.7
LRWC	77.83	71.25	8.4	78.03	69.76	10.6	78.87	64.78	17.9
Chlt	3.38	2.28	32.6	3.09	2.08	32.8	2.49	1.63	34.8
NGPS	45.04	41.36	8.2	47.45	42.41	10.6	46.73	39.71	15.0
TGW	45.74	41.28	9.8	45.11	38.80	14.0	48.49	39.52	18.5
BY	19.35	13.92	28.0	18.09	13.69	24.4	18.06	11.26	37.7
GY	5.56	4.04	27.3	5.88	3.76	36.0	5.81	3.12	46.3
HI	28.80	28.98	-0.6	32.57	27.57	15.4	32.66	28.18	13.7

Abbreviations of PDW, GLA, LAI, LRWC, Chlt, GNPS, TGW, BY, GY, and HI are plant dry weight (g plant^{-1}), green leaf area (cm^2 plant^{-1}), leaf area index, leaf relative water content (%), total chlorophyll content (mg g^{-1} FW), grain number per spike, thousand-grain weight (g), biological yield (ton ha^{-1}), grain yield (ton ha^{-1}), and harvest index (%), respectively. Values 1 and 2 represent measurements at 70 and 90 days after sowing, respectively.

3.6. Clustering of Genotypes Based on SSR Markers and Their Association with Those Derived from Agro-Morpho-Physiological Traits Using Mantel Test

The 24 genotypes/RILs were divided into three distinct clusters based on the allelic data of 40 SSRs linked to salt-tolerant genes (Figure 6). In general, the SSR data separated the salt-sensitive check genotype Sakha 61 from the two salt-tolerant check genotypes Sakha 93 and Kharachia-65. Cluster 1 included two, two, and one genotype(s)/RIL(s) from the S, T, and I groups, respectively. Cluster 2 included two, three, and four genotypes/RILs from the S, T, and I groups, respectively. Cluster 3 did not include any genotypes/RILs from the S group, while it included three and seven genotypes/RILs from the T and I groups, respectively (Figure 4).

The clustering pattern of 24 genotypes/RILs based on their STI of all agro-morpho-physiological traits (phenotypic distance) was associated with those derived from 40 SSRs linked to salt-tolerant genes (genetic distance) using the Mantel test. The Mantel test showed a significant positive correlation (r = 0.13, $p < 0.03$, and alpha = 0.05) between agro-morpho-physiological traits and SSR data, which indicates that the molecular and phenotypic classifications are somewhat correlated. These positive correlations were necessary, as agro-morpho-physiological traits are typically used as an efficient way of routinely accessing several genotypes in a breeding program without the use of molecular markers.

3.7. Association of SSR Markers with Morpho-Physiological Traits and Their Salt Tolerance Index

The stepwise linear regression was used to identify the most influential SSR markers associated with different agro-morpho-physiological traits under both control and salinity conditions, as well as with an STI. In general, the different markers showed significant association with all agro-morpho-physiological traits under both control (R^2 ranged from 0.24 to 0.88) and salinity (R^2 ranged from 0.38 to 0.78) conditions. They also demonstrated association with the STIs of all traits (R^2 ranged from 0.25 to 0.85), except for PDW at 70 and 90 DAS under control conditions, TGW under salinity conditions, and the STI for BY (Table 7). Two markers, Wmc154 and Wmc367, were significantly associated with PDW at 70 DAS under salinity conditions (R^2 = 0.51) and with the STI of this trait (R^2 = 0.50). Five

markers (Gwm55, Wmc154, Wmc405, Barc110, and Cfd18) and three markers (Wmc154, Barc182, and Wmc419) exhibited highly significant associations with PDW at 90 DAS under salinity conditions (R^2 = 0.76) and with the STI of this trait (R^2 = 0.69), respectively. The marker Gmw350 showed a significant association with GLA at 70 and 90 DAS under control conditions, whereas the marker WMC154 displayed a significant association with the STI for both traits. Under salinity conditions, markers Gmw350 and Wmc154 exhibited a highly significant association with GLA at 70 DAS (R^2 = 0.59), while Barc44 and Cfd9 markers had a highly significant association with GLA at 90 DAS (R^2 = 0.68). The combination of two markers and three markers accounted for 51.0% and 66.0% of the total variations in LAI at 70 DAS among genotypes. Similarly, the combination of five markers and three markers accounted for 88.0% and 77.0% of the total variation in LAI at 90 DAS among genotypes under both control and salinity conditions, respectively. However, when it came to the STI of LAI at 70 and 90 DAS, the combinations of two markers and three markers justified 60.0% and 81.0% of the total variation, respectively (Table 7).

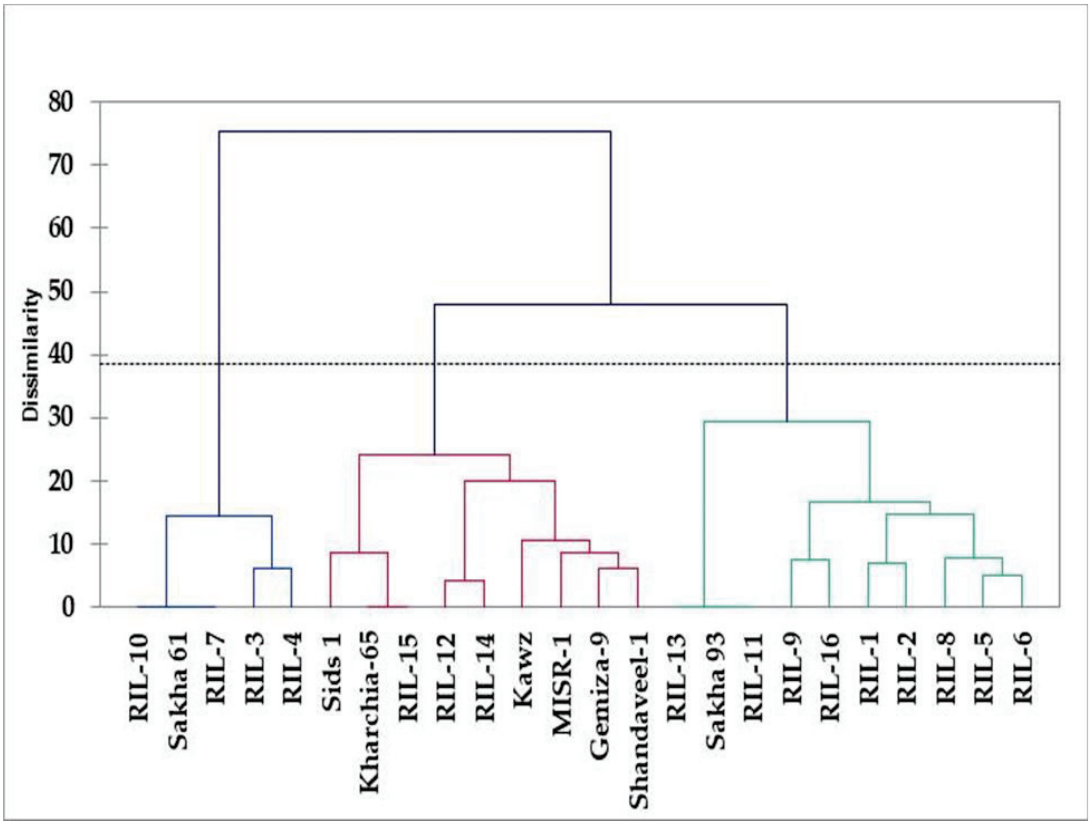

Figure 6. Genotypic clustering of 24 tested genotypes based on 40 simple sequence repeat (SSR) markers linked to salt-tolerant genes using unweighted clustering trees.

Regarding the two physiological traits (LRWC and Chlt), the markers showed a significantly stronger association with both traits under salinity conditions (R^2 = 0.54 and 0.74) and with the STI for both traits (R^2 = 0.85 and 0.47) compared to control conditions (R^2 = 0.24 and 0.37). One and two markers accounted for more variation in LRWC and Chlt among genotypes under control conditions. Two and three markers accounted for more variation in LRWC and Chlt among genotypes under salinity conditions. Three and four markers accounted for more variation in STI for LRWC and Chlt among genotypes, respectively.

Table 7. Associating the most influential SSR markers with different agro-morpho-physiological traits under control and salinity conditions as well as with a stress tolerance index (STI).

Control				Salinity				STI			
Trait	**Markers**	**R^2 Par.**	**R^2 Cum**	**Trait**	**Markers**	**R^2 Par.**	**R^2 Cum**	**Trait**	**Markers**	**R^2 Par.**	**R^2 Cum**
GLA-1	Gwm350	0.32 **	0.32	PDW-1	Wmc154	0.31 ***	0.51	PDW-1	Wmc154	0.34 ***	0.50
GLA-2	Gwm350	0.31 **	0.31		Wmc367	0.20 *			Wmc367	0.16 *	
LAI-1	Wmc661	0.37 ***	0.51	PDW-2	Gwm55	0.26 ***	0.76	PDW-2	Wmc154	0.45 ***	0.69
	Gwm55	0.14 **			Wmc154	0.19 **			Barc 182	0.11 ***	
LAI-2	Gwm210	0.29 ***	0.88		Wmc405	0.12 *			Wmc419	0.13 ***	
	Barc34	0.25 ***			Barc110	0.12 **		GLA-1	Wmc154	0.31 ***	0.31
	Wmc18	0.22 ***			Cfd18	0.07 *		GLA-2	Wmc154	0.25 **	0.25
	Gwm296	0.09 **		GLA-1	Gwm350	0.33 **	0.59	LAI-1	Cfd18	0.46 ***	0.60
	Cfd49	0.03 ***			Wmc154	0.26 **			Gwm410	0.14 **	
LRWC	Wmc11	0.24 *	0.24	GLA-2	Barc44	0.39 ***	0.65	LAI-2	Cfd18	0.41 ***	0.81
Chlt	Barc110	0.29 ***	0.37		Cfd9	0.26 **			Gwm249	0.13 ***	
	Cfd18	0.08 *		LAI-1	Cfd1	0.29 ***	0.66		Wmc405	0.14 *	
GNPS	Barc34	0.29 **	0.45		Cfd9	0.27 ***			Wmc245	0.13 ***	
	Barc167	0.16 *			Wmc405	0.10 ***		LRWC	Barc109	0.61 ***	0.85
TGW	Barc34	0.21 ***	0.62	LAI-2	Barc44	0.39 **	0.77		Wmc154	0.14 ***	
	Gwm410	0.20 **			Cfd9	0.28 ***			Wmc177	0.10 ***	
	Gwm335	0.12 *			Wmc405	0.10 ***		Chlt	Barc167	0.29 **	0.47
	Wmc367	0.09 **		LRWC	Barc44	0.36 ***	0.54		Cfd9	0.18 **	
BY	Cfd9	0.21 **	0.42		Wmc11	0.18 *		NGPS	Barc112	0.26 ***	0.61
	Wmc177	0.11 **		Chlt	Wmc245	0.24 *	0.74		Gwm539	0.16 ***	
	Gwm55	0.10 **			Cfd9	0.15 ***			Barc110	0.20 ***	
GY	Barc167	0.49 ***	0.49		Cfd9	0.35 ***		TGW	Gwm210	0.54 ***	0.82
HI	Cfd9	0.18 *	0.41	GNPS	Gwm335	0.38 ***	0.38		Wmc503	0.09 ***	
	Wmc503	0.23 *		BY	Wmc154	0.16 *	0.58		Wmc405	0.12 ***	
					Cfd66	0.18 *			Gwm174	0.08 **	
					Wmc154	0.13 **		GY	Wmc154	0.30 ***	0.69
					Gwm314	0.11 *			Cfd66	0.22 *	
				GY	Barc44	0.37 ***	0.66		Wmc367	0.09 **	
					Cfd9	0.15 *			Barc110	0.08 *	
					Barc34	0.14 *		HI	Gwm174	0.36 ***	0.68
				HI	Gwm55	0.31 ***	0.78		Cfd18	0.17 **	
					Wmc154	0.16 ***			Cfd49	0.14 **	
					Barc58	0.22 ***					
					Gwm296	0.09 *					

Abbreviations of PDW, GLA, LAI, LRWC, Chlt, GNPS, TGW, BY, GY, and HI are plant dry weight (g plant^{-1}), green leaf area (cm^2 plant^{-1}), leaf area index, leaf relative water content (%), total chlorophyll content (mg g^{-1} FW), grain number per spike, thousand-grain weight (g), biological yield (ton ha^{-1}), grain yield (ton ha^{-1}), and harvest index (%), respectively. Values 1 and 2 represent measurements at 70 and 90 days after sowing, respectively. *, **, and *** indicate significant at $p \leq 0.05$, 0.01, and 0.001, respectively.

Regarding the yield and yield component traits, the markers demonstrated a stronger association with STI for GNPS (R^2 = 0.61) compared to GNPS under control (R^2 = 0.45) and salinity (R^2 = 0.38) conditions. Specifically, two markers accounted for a greater amount

of variation in GNPS under control conditions, one marker under salinity conditions, and three markers for STI in this trait (Table 7). Additionally, the markers exhibited a stronger correlation with GY and HI under salinity conditions (R^2 = 0.66 and 0.78) and with STI for both traits (R^2 = 0.69 and 0.68) compared to GY and HI under control conditions (R^2 = 0.49 and 0.41). Only one marker explained more variation in GY, while two markers explained more variation in HI among genotypes under control conditions. However, under salinity conditions and for STI in both traits, more than two markers explained the variation in GY and HI among genotypes (Table 7). There were no markers that showed a significant association with TGW under salinity conditions and STI for BY. However, TGW under control conditions and the STI for this trait were significantly associated with four markers. These four markers accounted for 62.0% and 82.0% of the total variation among genotypes, respectively. Regarding the BY, three and four markers accounted for 42.0% and 58.0% of the total variation for this trait among genotypes under control and salinity conditions, respectively (Table 7).

4. Discussion

Salinity stress is one of the most well-known abiotic stressors that significantly decreases wheat production in many arid and semiarid countries. Therefore, it is crucial to provide farmers with salt-tolerant genotypes. This approach is not only the most beneficial but also the most economical way to sustain wheat production in saline conditions. However, the tolerance of genotypes to salinity stress is influenced by a multitude of intricate and interconnected mechanisms and polygenic traits. As a result, genotypes display a wide range of responses to salinity stress at different levels, including morphological, physiological, biochemical, and molecular. Furthermore, the acquisition of salt tolerance in genotypes necessitates a significant amount of genetic variability across multiple traits. Furthermore, it is of utmost importance to evaluate the salt tolerance of different genotypes in real field conditions, where plants are exposed to a range of environmental factors. Therefore, it is essential to gain a comprehensive understanding of how various traits respond to salinity stress in different genotypes at different stages of growth under real field conditions. This knowledge is crucial for the success of breeding programs aiming to develop salt-tolerant varieties [4,9,10,49]. In this study, we investigated the impact of salt stress on multiple morphological, physiological, and agronomic traits in different wheat genotypes cultivated under actual field conditions. The ANOVA results revealed significant statistical differences between the genotypes and salinity levels for all traits examined, both within each year and when the data from both years were combined (see Table 1). Additionally, certain genotypes exhibited average trait values that were approximately one to three times higher than those of the other genotypes, irrespective of whether they were exposed to control or salinity conditions (Tables 2 and 3). Additionally, there was a wide range among genotypes in the percentage reduction of the tested traits under high salinity levels compared to the control treatment (Table 4). All of these findings indicate that there is genetic variation among the tested genotypes in terms of salt tolerance. Additionally, the assessed traits have proven to be effective screening criteria for distinguishing between salt-tolerant and salt-sensitive genotypes. The results presented in Table 4 further support these findings, as they demonstrate that the genotypes Sakha 93 and Kharachia-65, as well as the majority of the RILs from the cross between Sakha 93 and Sakha 61, exhibited the lowest reduction percentages for the majority of the agro-morpho-physiological traits. This confirms the salinity stress tolerance of these RILs/genotypes. Conversely, the genotypes Sakha 61 and Shandaweel-1, which are salt-sensitive, displayed the opposite trend.

Under salinity stress conditions, various agro-morpho-physiological traits are negatively affected due to the combined stresses of osmotic and ionic toxicity, as well as a deficiency in essential nutrients. These three factors contribute to a decrease in cell division and elongation, cell membrane stability, leaf turgidity, leaf water content, biomass accumulation, photosynthetic capacity, metabolic functions, chlorophyll pigments, light interception, protein synthesis, and source–sink activity. Additionally, salinity stress induces

the production of high levels of reactive oxygen species. As a result, these detrimental effects of salinity stress lead to a significant reduction in plant growth indicators such as PDW, LA, and LAI, as well as physiological indicators like LRWC and Chl content, and agronomic indicators including GY, BY, HI, TGW, and GNPS [20,23,25,26,28,40]. Therefore, these various indicators are essential attributes that play a significant role in evaluating genotypes for their capacity to endure salinity conditions. In this study, LWRC, GNPS, and TGW demonstrated the least susceptibility to salinity stress. However, other traits exhibited reductions exceeding 25% in their average values due to salinity stress (Tables 2 and 3). These findings indicate that genotypes have a substantial impact on the diversity observed in LWRC, GNPS, and TGW, thereby making these characteristics unique to each genotype. Nevertheless, it is important to consider these traits in conjunction with other agro-morpho-physiological traits when evaluating salt tolerance based on effective screening criteria. Similarly, previous reports have indicated that PDW, LA, Chlt, GNPS, and GY are essential screening criteria for assessing the salinity tolerance of wheat genotypes [3,16,40]. These findings can be attributed to the significant decrease in these characteristics, even when exposed to low and medium salinity stresses. Moreover, traits like PDW, LA, and Chlt can act as reliable indicators of the plant's overall response to salt stress throughout different growth stages. It is crucial to acknowledge that the final crop production (GY) is greatly influenced by the strong correlation between GY and the growth and physiological traits that take place at different growth stages [15,49]. The results of this study indicated a noteworthy and positive correlation between GY and the growth traits (PDW, LA, and LAI) assessed at 70 and 90 DAS. Additionally, physiological traits (LRWC and Chlt) exhibited a significant association with GY under salinity conditions (Table 5). Therefore, these traits have been recognized as essential for evaluating wheat genotypes in terms of their salt tolerance. As a result, it can be inferred that the identification of traits closely associated with salt stress tolerance can serve as a benchmark for effectively differentiating between salt-tolerant and salt-sensitive genotypes.

The main goal of PCA, a type of multivariate analysis, is to illustrate the relationships among traits themselves and the correlations between traits and genotypes. As a result, it enables the assessment of salt tolerance in genotypes by considering all the examined traits. Additionally, it assists in identifying the most influential trait that contributes the most to the overall variance and effectively distinguishes between salt-tolerant and sensitive genotypes [9,50,51]. The PCA results in this study successfully identified the screening criteria that effectively evaluate the salt tolerance of wheat genotypes under real field conditions. This study revealed that the PDW at 90 DAS, GLA, and LAI at 70 and 90 DAS, GY, TGW, and GNPS played a significant role in describing the greatest variation observed among different genotypes in saline conditions (Figure 2). Furthermore, the thirteen morpho-agro-physiological traits were able to successfully differentiate the various genotypes into three distinct groups when exposed to salinity conditions. Additionally, they effectively separated the salt-tolerant genotypes (Sakha 93 and Kharachia-65) from the salt-sensitive ones (Sakha 61 and Shendaweel-1), with the most salt-tolerant genotypes positioned on the right side and the most sensitive ones on the left side under salinity conditions. However, when grown under normal control conditions, the salt-tolerant and salt-sensitive genotypes were grouped together and placed on the left side (Figure 3). These results indicate that PCA has the potential to distinguish between genotypes based on their salt tolerance in real field conditions by utilizing multiple traits. Likewise, PCA has been widely and successfully used by several studies to accurately evaluate the salt tolerance of genotypes using multiple parameters [4,9,52–54].

Generally, when plants are exposed to high levels of salt, their growth tends to decrease. This decrease in growth is attributed to a reduction in the activity of the plant's cellular metabolic pathways, leading to a decrease in the synthesis of important compounds. Additionally, the plant's energy and metabolic resources are redirected towards activating mechanisms that help the plant's ability to tolerate salinity stress rather than being allocated towards the growth of various plant organs and the production of plant biomass. As a

result, the plant's ability to accumulate biomass, also known as PDW, is negatively affected as a consequence. Moreover, the simultaneous existence of osmotic and ionic stresses caused by salinity can cause substantial changes in leaf structure. This leads to cell death, necrosis, and senescence of leaves, ultimately leading to a noticeable reduction in both GLA and LAI [4,6,40,55]. The ultimate GY is significantly impacted by different plant traits, particularly those related to biomass distribution and the capture and transformation of sunlight. Furthermore, these traits are primarily established during critical growth stages throughout the crop's life cycle. As a result, GY serves as a comprehensive indicator of the plant's overall lifespan and highlights the magnitude and importance of the negative impacts caused by salinity stresses experienced by the plants [56,57]. The explanations mentioned above offer support for the important role of PDW, GLA, LAI, and GY in explaining the considerable variation observed among different genotypes. The results of Figures 1 and 2 validate these findings and demonstrate that PC1, which accounted for 53.47% of the total variability and was able to isolate the salt-tolerant genotypes, exhibited a strong correlation with these four traits. Additionally, there is a strong acute angle between their vectors under salinity conditions.

To categorize the genotypes according to their salt tolerance and identify those that simultaneously exhibit high trait values and potential for salt tolerance, we utilized hierarchical cluster analysis-based STI for all traits. In this study, the heatmap clustering pattern based on STI of all traits successfully grouped genotypes into three distinct clusters and distinguished the salt-tolerant genotypes (T) from the salt-sensitive (S) and intermediate (I) ones (Figure 4). Additionally, the three clusters of genotypes exhibited significant variations in STI for all traits. The T group displayed the highest values of STI for almost all traits, followed by the I group. However, the S group had the lowest values for all traits except HI (Figure 5). These findings indicate that using hierarchical cluster analysis in combination with STI of multiple traits is an effective method for assessing the salt tolerance of wheat genotypes in real field conditions. In this study, this approach effectively differentiated between salt-tolerant and salt-sensitive genotypes, irrespective of growth stages and salinity levels. Several previous studies have confirmed the effectiveness of this approach in categorizing genotypes based on their tolerance to various abiotic stresses, including salinity and drought. However, it is worth noting that the majority of research evaluating the salt tolerance of genotypes through this approach was conducted in controlled environments such as greenhouses and growth chambers [15,52,58,59].

While the aforementioned approach successfully distinguishes the salt tolerance of genotypes, it is important to note that most agro-morpho-physiological traits are typically influenced by environmental conditions. Therefore, any changes in the environment can potentially influence salt tolerance among genotypes. Additionally, assessing the salt tolerance of genotypes based on multiple agro-morpho-physiological traits can be costly and time-consuming. As a result, when solely relying on phenotypic traits, there are limitations in accurately assessing the genetic diversity in salt tolerance. Therefore, there is an urgent need for a complementary approach to accurately evaluate the genetic diversity in salt tolerance of genotypes in a rapid and cost-effective manner. One prominent approach in molecular breeding involves selecting genotypes using molecular markers that are linked to quantitative trait loci (QTLs) responsible for key agro-morpho-physiological traits under salinity stress. This approach is particularly useful in cases where candidate genes are unavailable. Among these markers, SSR markers serve as a potential tool for assessing the degree of genetic variation in salt tolerance in several crops [15,31–33,46]. This approach offers numerous advantages that have already been mentioned in the Introduction section. In this study, cluster analysis based on SSR data successfully grouped the salt-tolerant genotypes and salt-sensitive genotypes into separate main clusters (Figure 6). Furthermore, the clustering pattern of the tested genotypes, based on the hierarchical cluster analysis approach in combination with STI of multiple traits, was found to be associated with the clusters derived from the cluster analysis based on SSR data. This association was demonstrated through a positive and significant correlation observed in Mantel's test

(r = 0.13, $p < 0.03$, and alpha = 0.05). However, this association was weak, indicating a lack of agreement between the phenotypic and molecular aspects. Despite the weak association, there were significant correlations between phenotypic traits and molecular characteristics. Therefore, this association is crucial as agro-morpho-physiological traits are an effective approach for regularly evaluating several genotypes in a breeding program, even in the absence of molecular markers. Previous studies have also reported a weak correlation between the clustering of genotypes, determined by phenotypic traits, and their clustering based on SSR marker data [60,61]. However, other studies have found a strong correlation between the clustering of genotypes based on agro-morpho-physiological traits and their clustering based on SSR marker data [15,46,62,63]. There are multiple reasons that may explain the weak correlation between phenotypic and molecular data in this study. Firstly, the measurements of different agro-morpho-physiological traits were conducted under complex and environmentally influenced field conditions. This complexity may have introduced variability and affected the accuracy of the data. Secondly, agro-morpho-physiological traits are influenced by polygenes, which allow plants to adapt to diverse environmental conditions through phenotypic plasticity. On the other hand, microsatellite variability is primarily neutral, which makes it a reliable tool for providing an unbiased representation of diversity and accurately distinguishing stress tolerance among closely related genotypes. Lastly, the limited number of markers and genotypes used in this study may have contributed to the weak correlation observed. With a larger sample size and more markers, a stronger correlation might have been detected.

Given the importance of markers associated with various agro-morpho-physiological traits and their role in salt tolerance, we have identified 18 and 19 markers that are linked to different traits under salinity conditions (with R^2 values ranging from 0.38 to 0.78) and STI (with R^2 values ranging from 0.25 to 0.85), respectively (Table 7). These findings further suggest that the thirteen agro-morpho-physiological traits measured in this study can be used as valuable indicators for evaluating the genetic diversity of salt tolerance in wheat. Moreover, they offer valuable insights into the mechanisms that contribute to salt tolerance in different wheat genotypes under real field conditions. Among the effective SSR markers used in this study, the marker known as cfd 9 from the D genome [64] was amplified under salinity conditions and showed a significant association with various traits, including GLA-2, LAI-1, LAI-2, Chlt, and GY. The D genome primarily regulates salt tolerance in hexaploid wheat, which validates the phenotypic assessment of genotypes [65]. El-Hendawy et al. [46] conducted a study that revealed a strong correlation between Wmc 154 and water absorption in the presence of 60 and 120 mM NaCl. The current study validates the observed correlation, as the amplification of wmc 154 was solely observed with PDW-1, PDW-2, GLA-1, GLA-2, LRWC, and GY under salinity conditions and with STI. In contrast, no correlation with wmc 154 was observed under control conditions. It is not surprising that multiple markers exhibit correlations with more than two variables, considering their polygenic background. In our study, we found that certain SSR markers, which are associated with desirable traits, were only observed in wheat crops under salinity stress conditions. These markers hold significant potential for future breeding programs focused on improving salinity tolerance in wheat crops grown in field conditions.

5. Conclusions

This study has yielded important findings on the agro-morpho-physiological traits that can be used as screening criteria, along with their correlation with SSR markers, to evaluate the salt tolerance of wheat genotypes in real field conditions. Our results indicate that PDW, GLA, and LAI measured at different growth stages and GY are effective traits for evaluating the salt tolerance of wheat genotypes grown in field conditions. Clustering genotypes based on STI for all traits or based on SSR data successfully grouped the tested genotypes into three distinct categories and distinguished the salt-tolerant genotypes from the sensitive ones. Therefore, a significant association between agro-morpho-physiological traits and SSR markers data was detected. However, this association was found weak on the

Mantel test. The traits identified in this study can be recommended as valuable screening criteria for evaluating the salt tolerance of different wheat plant materials grown in field conditions. However, there is an urgent need for a rapid, cost-effective, and large-scale phenotypic identification tool to detect these traits in a large number of wheat materials under field conditions. This will be the focus of our future study.

Supplementary Materials: The following supporting information can be downloaded at https://www.mdpi.com/article/10.3390/agriculture13112135/s1. Table S1: List of SSR markers, their sequence, and annealing temperature that were used in this study across 24 wheat genotypes.

Author Contributions: Conceptualization, S.E.-H., M.B.J., M.A., N.A.-S. and I.A.-A.; methodology, S.E.-H., M.B.J. and I.A.-A.; software, S.E.-H., M.B.J., N.A.-S., I.A.-A. and M.A.; validation, S.E.-H. and M.B.J.; formal analysis, S.E.-H., M.B.J., N.A.-S., I.A.-A. and M.A.; investigation, S.E.-H. and M.B.J.; resources, S.E.-H., M.B.J. and I.A.-A.; data curation, S.E.-H., I.A.-A., M.A., N.A.-S. and M.B.J.; writing—original draft preparation, S.E.-H.; writing—review and editing, S.E.-H.; visualization, S.E.-H.; supervision, S.E.-H.; project administration, S.E.-H.; funding acquisition, S.E.-H. All authors have read and agreed to the published version of the manuscript.

Funding: This research was funded by the Deputyship for Research and Innovation, "Ministry of Education", in Saudi Arabia, research number (IFKSUOR3-579-1).

Institutional Review Board Statement: Not applicable.

Data Availability Statement: All data are presented within the article.

Conflicts of Interest: The authors declare no conflict of interest.

References

1. United Nations. *World Population Prospects 2022: Data Sources*; United Nations: New York, NY, USA, 2022.
2. Ray, D.K.; Mueller, N.D.; West, P.C.; Foley, J.A. Yield trends are insufficient to double global crop production by 2050. *PLoS ONE* **2013**, *8*, e66428. [CrossRef]
3. Munns, R.; James, R.A.; Läuchli, A. Approaches to increasing the salt tolerance of wheat and other cereals. *J. Exp. Bot.* **2006**, *57*, 1025–1043. [CrossRef]
4. El-Hendawy, S.E.; Hassan, W.M.; Al-Suhaibani, N.A.; Refay, Y.; Abdella, K.A. Comparative performance of multivariable agro-physiological parameters for detecting salt tolerance of wheat cultivars under simulated saline field growing conditions. *Front. Plant Sci.* **2017**, *8*, 435. [CrossRef] [PubMed]
5. Majeed, A.; Muhammad, Z.; Islam, S.; Ahmad, H. Salinity imposed stress on principal cereal crops and employing seed priming as a sustainable management approach. *Acta Ecol. Sin.* **2019**, *39*, 280–283. [CrossRef]
6. Munns, R.; Tester, M. Mechanisms of salinity tolerance. *Annu. Rev. Plant Biol.* **2008**, *59*, 651–681. [CrossRef] [PubMed]
7. Munns, R.; Gilliham, M. Salinity tolerance of crops–what is the cost? *New Phytol.* **2015**, *208*, 668–673. [CrossRef] [PubMed]
8. El-Hendawy, S.; Ruan, Y.; Hu, Y.; Schmidhalter, U. A comparison of screening criteria for salt tolerance in wheat under field and controlled environmental conditions. *J. Agron. Crop Sci.* **2009**, *195*, 356–367. [CrossRef]
9. Mubushar, M.; El-Hendawy, S.; Tahir, M.U.; Alotaibi, M.; Mohammed, N.; Refay, Y.; Tola, E. Assessing the suitability of multivariate analysis for stress tolerance indices, biomass, and grain yield for detecting salt tolerance in advanced spring wheat lines irrigated with saline water under field conditions. *Agronomy* **2022**, *12*, 3084. [CrossRef]
10. Matković Stojšin, M.; Petrović, S.; Banjac, B.; Zečević, V.; Roljević Nikolić, S.; Majstorović, H.; Đorđević, R.; Knežević, D. Assessment of genotype stress tolerance as an effective way to sustain wheat production under salinity stress conditions. *Sustainability* **2022**, *14*, 6973. [CrossRef]
11. Tao, R.; Ding, J.; Li, C.; Zhu, X.; Guo, W.; Zhu, M. Evaluating and screening of agro-physiological indices for salinity stress tolerance in wheat at the seedling stage. *Front. Plant Sci.* **2021**, *12*, 646175. [CrossRef]
12. El-Hendawy, S.E.; Hu, Y.; Yakout, G.M.; Awad, A.M.; Hafiz, S.E.; Schmidhalter, U. Evaluating salt tolerance of wheat genotypes using multiple parameters. *Eur. J. Agron.* **2005**, *22*, 243–253. [CrossRef]
13. Sultana, R.; Wang, X.; Azeem, M.; Hussain, T.; Mahmood, A.; Fiaz, S.; Qasim, M. Coumarin-mediated growth regulations, antioxidant enzyme activities, and photosynthetic efficiency of Sorghum bicolor under saline conditions. *Front. Plant Sci.* **2022**, *13*, 799404. [CrossRef] [PubMed]
14. Abbasi, G.H.; Akhtar, J.; Anwar-ul-Haq, M.; Malik, W.; Ali, S.; Chen, Z.-H.; Zhang, G. Morpho-physiological and micrographic characterization of maize hybrids under NaCl and Cd stress. *Plant Growth Regul.* **2015**, *75*, 115–122. [CrossRef]
15. Al-Ashkar, I.; Alderfasi, A.; Ben Romdhane, W.; Seleiman, M.F.; El-Said, R.A.; Al-Doss, A. Morphological and genetic diversity within salt tolerance detection in eighteen wheat genotypes. *Plants* **2020**, *9*, 287. [CrossRef] [PubMed]
16. Genc, Y.; Taylor, J.; Lyons, G.; Li, Y.; Cheong, J.; Appelbee, M.; Oldach, K.; Sutton, T. Bread wheat with high salinity and sodicity tolerance. *Front. Plant Sci.* **2019**, *10*, 1280. [CrossRef] [PubMed]

17. Radi, A.A.; Farghaly, F.A.; Hamada, A.M. Physiological and biochemical responses of salt-tolerant and salt-sensitive wheat and bean cultivars to salinity. *J. Biol. Earth Sci.* **2013**, *3*, 72–88.
18. Uzair, M.; Ali, M.; Fiaz, S.; Attia, K.; Khan, N.; Al-Doss, A.A.; Khan, M.R.; Ali, Z. The characterization of wheat genotypes for salinity tolerance using morpho-physiological indices under hydroponic conditions. *Saudi J. Biol. Sci.* **2022**, *29*, 103299. [CrossRef]
19. Al-Naggar, A.; Sabry, S.; Atta, M.; El-Aleem, O. Effects of salinity on performance, heritability, selection gain and correlations in wheat (*Triticum aestivum* L.) doubled haploids. *Sci. Agric.* **2015**, *10*, 70–83.
20. Omrani, S.; Arzani, A.; Esmaeilzadeh Moghaddam, M.; Mahlooji, M.J.P.o. Genetic analysis of salinity tolerance in wheat (*Triticum aestivum* L.). *PLoS ONE* **2022**, *17*, e0265520.
21. Zarco-Tejada, P.J.; Pushnik, J.; Dobrowski, S.; Ustin, S. Steady-state chlorophyll a fluorescence detection from canopy derivative reflectance and double-peak red-edge effects. *Remote Sens. Environ.* **2003**, *84*, 283–294. [CrossRef]
22. Mohamed, I.A.; Shalby, N.; El-Badri, M.A.A.; Saleem, M.H.; Khan, M.N.; Nawaz, M.A.; Qin, M.; Agami, R.A.; Kuai, J.; Wang, B. Stomata and xylem vessels traits improved by melatonin application contribute to enhancing salt tolerance and fatty acid composition of *Brassica napus* L. plants. *Agronomy* **2020**, *10*, 1186. [CrossRef]
23. Touchan, H.; Basal, O. Evaluating the tolerance of chickpea (Cicer arietinum L.) genotypes to salinity stress based on a complex of morpho-physiological and yielding traits. *J. Water Land Dev.* **2022**, 119–129. [CrossRef]
24. Aloui, M.; Mahjoub, A.; Cheikh, N.B.; Ludidi, N.; Abdelly, C.; Badri, M. Genetic Variation in Responses to Salt Stress in Tunisian Populations of Medicago ciliaris. *Agronomy* **2022**, *12*, 1781. [CrossRef]
25. Bustos-Korts, D.; Boer, M.P.; Malosetti, M.; Chapman, S.; Chenu, K.; Zheng, B.; Van Eeuwijk, F.A. Combining crop growth modeling and statistical genetic modeling to evaluate phenotyping strategies. *Front. Plant Sci.* **2019**, *10*, 1491. [CrossRef]
26. Ma, C.; Liu, L.; Liu, T.; Jia, Y.; Jiang, Q.; Bai, H.; Ma, S.; Li, S.; Wang, Z. QTL mapping for important agronomic traits using a wheat55K SNP array-based genetic map in tetraploid wheat. *Plants* **2023**, *12*, 847. [CrossRef] [PubMed]
27. Reynolds, M.; Foulkes, M.J.; Slafer, G.A.; Berry, P.; Parry, M.A.; Snape, J.W.; Angus, W.J. Raising yield potential in wheat. *J. Exp. Bot.* **2009**, *60*, 1899–1918. [CrossRef]
28. El-Hendawy, S.; Al-Suhaibani, N.; Al-Ashkar, I.; Alotaibi, M.; Tahir, M.U.; Solieman, T.; Hassan, W.M. Combining genetic analysis and multivariate modeling to evaluate spectral reflectance indices as indirect selection tools in wheat breeding under water deficit stress conditions. *Remote Sens.* **2020**, *12*, 1480. [CrossRef]
29. Moraes, G.A.F.d.; Menezes, N.L.d.; Pasqualli, L.L. Comportamento de sementes de feijão sob diferentes potenciais osmóticos. *Ciência Rural* **2005**, *35*, 776–780. [CrossRef]
30. Abulela, H.A.; El Shafee, E.; Farag, H.M.; Yacoub, I.H.; Elarabi, N.I. Evaluation of the morpho-physiological traits and the genetic diversity of some Egyptian bread wheat cultivars under salt stress conditions. *Cereal Res. Commun.* **2022**, *50*, 733–753. [CrossRef]
31. Singh, A.K.; Chaurasia, S.; Kumar, S.; Singh, R.; Kumari, J.; Yadav, M.C.; Singh, N.; Gaba, S.; Jacob, S.R. Identification, analysis and development of salt responsive candidate gene based SSR markers in wheat. *BMC Plant Biol.* **2018**, *18*, 249. [CrossRef]
32. Devi, R.; Ram, S.; Rana, V.; Malik, V.K.; Pande, V.; Singh, G.P. QTL mapping for salt tolerance associated traits in wheat (*Triticum aestivum* L.). *Euphytica* **2019**, *215*, 210. [CrossRef]
33. Irshad, A.; Ahmed, R.I.; Ur Rehman, S.; Sun, G.; Ahmad, F.; Sher, M.A.; Aslam, M.Z.; Hassan, M.M.; Qari, S.H.; Aziz, M.K. Characterization of salt tolerant wheat genotypes by using morpho-physiological, biochemical, and molecular analysis. *Front. Plant Sci.* **2022**, *13*, 956298. [CrossRef] [PubMed]
34. Lindsay, M.P.; Lagudah, E.S.; Hare, R.A.; Munns, R. A locus for sodium exclusion (Nax1), a trait for salt tolerance, mapped in durum wheat. *Funct. Plant Biol.* **2004**, *31*, 1105–1114. [CrossRef] [PubMed]
35. Byrt, C.S. Genes for Sodium Exclusion in Wheat. Doctoral Dissertation, University of Adelaide, Adelaide, Australia, 2008.
36. Rustamova, S.M.; Suleymanova, Z.J.; Isgandarova, T.Y.; Zulfugarova, S.T.; Mammadov, A.C.; Huseynova, I.M. Identification of stress responsive genes by using molecular markers to develop tolerance in wheat. In *Wheat Production in Changing Environments: Responses, Adaptation and Tolerance*; Springer: Singapore, 2019; pp. 421–442.
37. El-Hendawy, S.E.; Hu, Y.; Schmidhalter, U. Growth, ion content, gas exchange, and water relations of wheat genotypes differing in salt tolerances. *Aust. J. Agric. Res.* **2005**, *56*, 123–134. [CrossRef]
38. Sharma, P.; Varma, S.; Datta, K.; Kumar, B. Salinity effects on some morpho-physiological water relations and mineral composition characteristics of two cultivars of wheat with varying salt resistance. *Ann. Biol.* **1994**, *10*, 39.
39. Ashraf, M. Exploitation of genetic variation for improvement of salt tolerance in spring wheat. *Prosp. Saline Agric.* **2002**, *37*, 113–121.
40. Mansour, E.; Moustafa, E.S.; Desoky, E.-S.M.; Ali, M.M.; Yasin, M.A.; Attia, A.; Alsuhaibani, N.; Tahir, M.U.; El-Hendawy, S. Multidimensional evaluation for detecting salt tolerance of bread wheat genotypes under actual saline field growing conditions. *Plants* **2020**, *9*, 1324. [CrossRef]
41. Arnon, D.I. Copper enzymes in isolated chloroplasts. *Polyphenoloxidase in Beta vulgaris. Plant Physiol.* **1949**, *24*, 1–15.
42. Lichtenthaler, H.K. Chlorophylls and carotenoids: Pigments of photosynthetic biomembranes. *Methods Enzymol.* **1987**, *148*, 350–382.
43. Byrt, C.S.; Platten, J.D.; Spielmeyer, W.; James, R.A.; Lagudah, E.S.; Dennis, E.S.; Tester, M.; Munns, R. HKT1; 5-like cation transporters linked to Na+ exclusion loci in wheat, Nax2 and Kna1. *Plant Physiol.* **2007**, *143*, 1918–1928. [CrossRef]
44. Shahzad, A. Biochemical Markers for Screening Wheat for Salt Tolerance. Doctoral Dissertation, University of Agriculture Faisalabad, Faisalabad, Pakistan, 2007.

45. Huang, S.; Spielmeyer, W.; Lagudah, E.S.; Munns, R. Comparative mapping of HKT genes in wheat, barley, and rice, key determinants of Na+ transport, and salt tolerance. *J. Exp. Bot.* **2008**, *59*, 927–937. [CrossRef]
46. El-Hendawy, S.; Elshafei, A.; Al-Suhaibani, N.; Alotabi, M.; Hassan, W.; Dewir, Y.H.; Abdella, K. Assessment of the salt tolerance of wheat genotypes during the germination stage based on germination ability parameters and associated SSR markers. *J. Plant Interact.* **2019**, *14*, 151–163. [CrossRef]
47. Fernandez, G.C. Effective selection criteria for assessing plant stress tolerance. In Proceedings of the International Symposium on Adaptation of Vegetables and Other Food Crops in Temperature and Water Stress, Shanhua, Taiwan, 13–16 August 1992; pp. 257–270.
48. Mantel, N. Ranking procedures for arbitrarily restricted observation. *Biometrics* **1967**, *23*, 65–78. [CrossRef]
49. EL Sabagh, A.; Islam, M.S.; Skalicky, M.; Ali Raza, M.; Singh, K.; Anwar Hossain, M.; Hossain, A.; Mahboob, W.; Iqbal, M.A.; Ratnasekera, D. Salinity stress in wheat (*Triticum aestivum* L.) in the changing climate: Adaptation and management strategies. *Front. Agron.* **2021**, *3*, 661932. [CrossRef]
50. Pour-Aboughadareh, A.; Sanjani, S.; Nikkhah-Chamanabad, H.; Mehrvar, M.R.; Asadi, A.; Amini, A. Identification of salt-tolerant barley genotypes using multiple-traits index and yield performance at the early growth and maturity stages. *Bull. Natl. Res. Cent.* **2021**, *45*, 117. [CrossRef]
51. Jadidi, O.; Etminan, A.; Azizi-Nezhad, R.; Ebrahimi, A.; Pour-Aboughadareh, A. Physiological and molecular responses of barley genotypes to salinity stress. *Genes* **2022**, *13*, 2040. [CrossRef]
52. Al-Ashkar, I.; Alderfasi, A.; El-Hendawy, S.; Al-Suhaibani, N.; El-Kafafi, S.; Seleiman, M.F. Detecting salt tolerance in doubled haploid wheat lines. *Agronomy* **2019**, *9*, 211. [CrossRef]
53. Sivakumar, J.; Prashanth, J.E.P.; Rajesh, N.; Reddy, S.M.; Pinjari, O.B. Principal component analysis approach for comprehensive screening of salt stress-tolerant tomato germplasm at the seedling stage. *J. Biosci.* **2020**, *45*, 141. [CrossRef]
54. Javed, M.M.; Al-Doss, A.A.; Tahir, M.U.; Khan, M.A.; El-Hendawy, S. Assessing the Suitability of Selection Approaches and Genetic Diversity Analysis for Early Detection of Salt Tolerance of Barley Genotypes. *Agronomy* **2022**, *12*, 3217. [CrossRef]
55. Arif, Y.; Singh, P.; Siddiqui, H.; Bajguz, A.; Hayat, S. Biochemistry. Salinity induced physiological and biochemical changes in plants: An omic approach towards salt stress tolerance. *Plant Physiol.* **2020**, *156*, 64–77.
56. Richards, R. Selectable traits to increase crop photosynthesis and yield of grain crops. *J. Exp. Bot.* **2000**, *51*, 447–458. [CrossRef]
57. Pennacchi, J.P.; Carmo-Silva, E.; Andralojc, P.J.; Feuerhelm, D.; Powers, S.J.; Parry, M.A. Dissecting wheat grain yield drivers in a mapping population in the UK. *Agronomy* **2018**, *8*, 94. [CrossRef]
58. Alam, M.S.; Tester, M.; Fiene, G.; Mousa, M.A.A. Early growth stage characterization and the biochemical responses for salinity stress in tomato. *Plants* **2021**, *10*, 712. [CrossRef]
59. Masuda, M.S.; Azad, M.A.K.; Hasanuzzaman, M.; Arifuzzaman, M. Evaluation of salt tolerance in maize (*Zea mays* L.) at seedling stage through morphological characters and salt tolerance index. *Plant Physiol. Rep.* **2021**, *26*, 419–427. [CrossRef]
60. De Leon, T.B.; Linscombe, S.; Gregorio, G.; Subudhi, P.K. Genetic variation in Southern USA rice genotypes for seedling salinity tolerance. *Front. Plant Sci.* **2015**, *6*, 374. [CrossRef] [PubMed]
61. Ali, M.N.; Yeasmin, L.; Gantait, S.; Goswami, R.; Chakraborty, S. Screening of rice landraces for salinity tolerance at seedling stage through morphological and molecular markers. *Physiol. Mol. Biol. Plants* **2014**, *20*, 411–423. [CrossRef]
62. Ahmad Alkuddsi, Y.; Patil, S.; Manjula, S.; Nadaf, H.; Patil, B. Relationship between SSR-based molecular marker and cotton F 1 inter specific hybrids performance for seed cotton yield and fiber properties. *Genom. Appl. Biol.* **2013**, *4*, 22–34.
63. Tahjib-Ul-Arif, M.; Sayed, M.A.; Islam, M.M.; Siddiqui, M.N.; Begum, S.; Hossain, M.A. Screening of rice landraces (*Oryza sativa* L.) for seedling stage salinity tolerance using morpho-physiological and molecular markers. *Acta Physiol. Plant.* **2018**, *40*, 70. [CrossRef]
64. Shahzad, A.; Ahmad, M.; Iqbal, M.; Ahmed, I.; Ali, G. Evaluation of wheat landrace genotypes for salinity tolerance at vegetative stage by using morphological and molecular markers. *Genet. Mole. Res.* **2012**, *11*, 679–692. [CrossRef]
65. Dvořák, J.; Gorham, J. Methodology of gene transfer by homoeologous recombination into Triticum turgidum: Transfer of K+/Na+ discrimination from Triticum aestivum. *Genome* **1992**, *35*, 639–646. [CrossRef]

agriculture

MDPI

Article

Effect of Electrical Conductivity Levels and Hydrogen Peroxide Priming on Nutrient Solution Uptake by Chives in a Hydroponic System

Patrícia Ferreira da Silva [1,*], Bárbara Davis Brito dos Santos [2], José Dantas Neto [2], Alberto Soares de Melo [3], Rigoberto Moreira de Matos [2], Semako Ibrahim Bonou [2], Tonny José Araújo da Silva [1], Edna Maria Bonfim-Silva [1], Ana Paula Candido Gabriel Berilli [4] and Thiago Franco Duarte [1]

[1] Departamento de Engenharia Agrícola, Instituto de Ciências Agrárias e Tecnológicas—ICAT, Universidade Federal de Rondonópolis, Av. dos Estudantes, 5055, Cidade Universitária, Bloco C, Rondonópolis 78736-900, MG, Brazil; tonnyjasilva@gmail.com (T.J.A.d.S.); edna.bonfim@ufr.edu.br (E.M.B.-S.); thiago.duarte@ufr.edu.br (T.F.D.)

[2] Unidade Acadêmica de Engenharia, Universidade Federal de Campina Grande, Rua Aprígio Veloso—Bodocongó, CM Block, Campina Grande 58109-970, PB, Brazil; bdavis.2340@gmail.com (B.D.B.d.S.); zedantas1955@gmail.com or jose.dantas@ufcg.edu.br (J.D.N.); rigobertomoreira@gmail.com (R.M.d.M.); bonouibrahim@gmail.com (S.I.B.)

[3] Coordenação do Programa de Pós-Graduação em Ciências Agrárias, Centro de Ciências Biológicas e da Saúde, Universidade Estadual da Paraíba, Rua Baraúnas, 351—Universitário, Campina Grande 58429-500, PB, Brazil; alberto.melo@servidor.uepb.edu.br

[4] Instituto Federal do Espírito Santo—Campus de Alegre Zona Rural, Alegre 29520-000, ES, Brazil; ana.berilli@ifes.edu.br

* Correspondence: patrycyafs@yahoo.com.br or patricia.silva@ufr.edu.br

Abstract: The use of water of high electrical conductivity has become common in hydroponic systems, especially in regions with water scarcity. However, the use of inferior-quality water can affect crop yields. In this scenario, some studies have tested the use of chemical conditioning agents such as hydrogen peroxide to minimize the negative effects of stress on plants. From this perspective, this study aimed to evaluate the action of priming with hydrogen peroxide as a salt stress attenuator on the nutrient solution uptake and productivity of chives in a hydroponic system. The study was conducted in a protected environment with a randomized block design with a split-plot arrangement. The treatments consisted of a main plot consisting of the electrical conductivity of the nutrient solution (1.0, 2.0, 3.0, 4.0, and 5.0 dSm^{-1}) and a subplot with five hydrogen peroxide concentrations (0.0, 0.15, 0.30, 0.45, and 0.60 mM). The increase in the electrical conductivity of the nutrient solution reduced bulb length, the solution volume applied, water uptake, total fresh mass, and the solution use efficiency by plants. Throughout the cultivation cycle in the hydroponic system, the consumption of nutrient solution was 459 mm lost by evapotranspiration. Acclimation with 0.60 mM hydrogen peroxide associated with 1 dSm^{-1} of electrical conductivity of the nutrient solution favors bulb diameter in chives. The increase in electrical conductivity compromises the productive yield of chives.

Keywords: *Allium schoenoprasum*; abiotic stress; soilless cultivation; use efficiency of the nutrient solution

1. Introduction

Chive (*Allium schoenoprasum*) is a plant species of the family Alliaceae grown in tropical and temperate regions [1]. This vegetable has a high nutrient value and is rich in minerals, bioactive compounds, and substances with antioxidant and antihypertensive properties [2].

Chive cultivation is usually performed by family farmers in regions known as 'green belts,' which play significant economic and social roles and contribute to improving the

income and quality of life of its producers [3]. In the last few years, hydroponic chive cultivation has been intensified in green belts in an effort to reduce water consumption and allow cultivation with water sources of high electrical conductivity [4–6].

Chives achieve maximum yields in plantations using water with electrical conductivities up to 0.7 dSm^{-1}, above which the yield is linearly reduced, and cultivation is compromised (both above and belowground) due to the high salt concentrations in regions where water shortage prevails [4,5]. Santos et al. [6] stated that, under hydroponic conditions, this electrical conductivity value could be increased, favoring cultivation with water of higher salinities. Salt stress limits the yield of vegetable crops by causing stomatal closure and thus reducing the transpiration rate, the internal CO_2 concentration, and the photosynthetic rates [7].

Recent studies have shown that using nutrient solutions with high electrical conductivity significantly reduces the percentage of total, shoot, and root dry matter; bulb diameter; bulb length; and the contents of chlorophyll 'a', 'b', and carotenoids, reflecting decisively on the nutritional performance, concentration of minerals, photochemical content, and secondary metabolites of chives [5,6,8–10]. Under hydroponic conditions with electrical conductivities ranging from 0.7 to 9 dSm^{-1}, there is an expressive reduction in all growth, physiological, biochemical, and production aspects in chive plants [4–6].

The accumulation of mineral salts in nutrient solutions provided to plants in hydroponic systems can cause oxidative stress and toxicity, triggering morphological, structural, enzymatic, and metabolic changes, and, in extreme cases, causing plant death. From this perspective, studying plant responses to water uptake under different electrical conductivities becomes essential [11].

In this scenario, aiming to mitigate the effects of stress caused to plants by the high electrical conductivity of nutrient solutions in hydroponic systems, seed acclimation (priming) with hydrogen peroxide (H_2O_2) has proved to be an efficient approach [6]. According to Qureshi et al. [12], the exogenous application of H_2O_2 triggers a cell signaling system in the plant metabolism of several species, stimulating the production of antioxidant enzymes, which, in turn, increase plants' capacity to minimize the harmful effects caused by such stresses. Furthermore, Carvalho et al. [13] stated that, when applied to rice seeds, hydrogen peroxide mitigates the effects of salt stress by stimulating the accumulation of proteins and soluble carbohydrates, increasing water uptake.

Seed priming associated with alternative technologies for the utilization of saline and brackish water in plantations, e.g., hydroponics, which is notorious for the energy reorganization and absence of matric potential, clears the path, increasing plant production using low-quality water, which is often the only irrigation source in regions that withstand water shortage [14]. In addition, hydroponics has allowed producers to increase the plant tolerance threshold, constituting an alternative to reduce the effects of stress on crops.

The hypothesis to be elucidated is that priming with hydrogen peroxide in chive seedlings can attenuate salt stress due to the high electrical conductivities of the nutrient solutions in a hydroponic environment. The tolerance of chives to different electrical conductivities is influenced by salt concentrations in the nutrient solution, the time of exposure to salt, and phenological stages [4–6]. However, studies are scarce under hydroponic conditions, and there are fewer studies considering the effects of stress resulting from solutions with different water conductivities and the application of seed priming with H_2O_2 associated with hydroponic cultivation, aiming to quantify the crop's water consumption.

From this perspective, this study aimed to evaluate the action of hydrogen peroxide priming as a salt stress attenuator on the nutrient solution uptake and the productivity of chives in hydroponic systems.

2. Materials and Methods

2.1. Location of the Experiment and Construction of the Hydroponic System

The study was conducted in a protected environment at the Agricultural Engineering Academic Unit of the Federal University of Campina Grande (UFCG), located in Campina Grande, PB, at the geographic coordinates 7°13′11″ S and 35°53′31″ W, and at an elevation of 550 m a.s.l. The experiment started on 25 May 2019 and ended on 28 August 2019.

During the experiment, some meteorological parameters inside the plant nursery were monitored using a digital thermohygrometer that recorded the maximum, mean, and minimum daily temperatures (°C) and the relative air humidity (%) throughout the cultivation cycle. For the cultivation cycle in the protected environment, the mean temperature and humidity values were 24 °C and 72%, respectively, and the maximum values were 30.5 °C and 81%, respectively, which are ideal temperature and moisture ranges for chive cultivation under protected conditions [6].

2.2. Establishment of the Hydroponic System

Five hydroponic benches were set up inside the plant nursery using 50 mm PVC tubes similar to nutrient film technique (NFT). The between-row spacing was 0.60 m, and the height of the tubes was 0.76 m, with a 2% slope so that the solution provided to each treatment could run across the profile through gravity. At the end of each profile, a structure was set up to direct the nutrient solution to the return piping into the reservoir, also through gravity, thus forming a closed circulation hydroponic system meant to save water and nutrients (Figure 1).

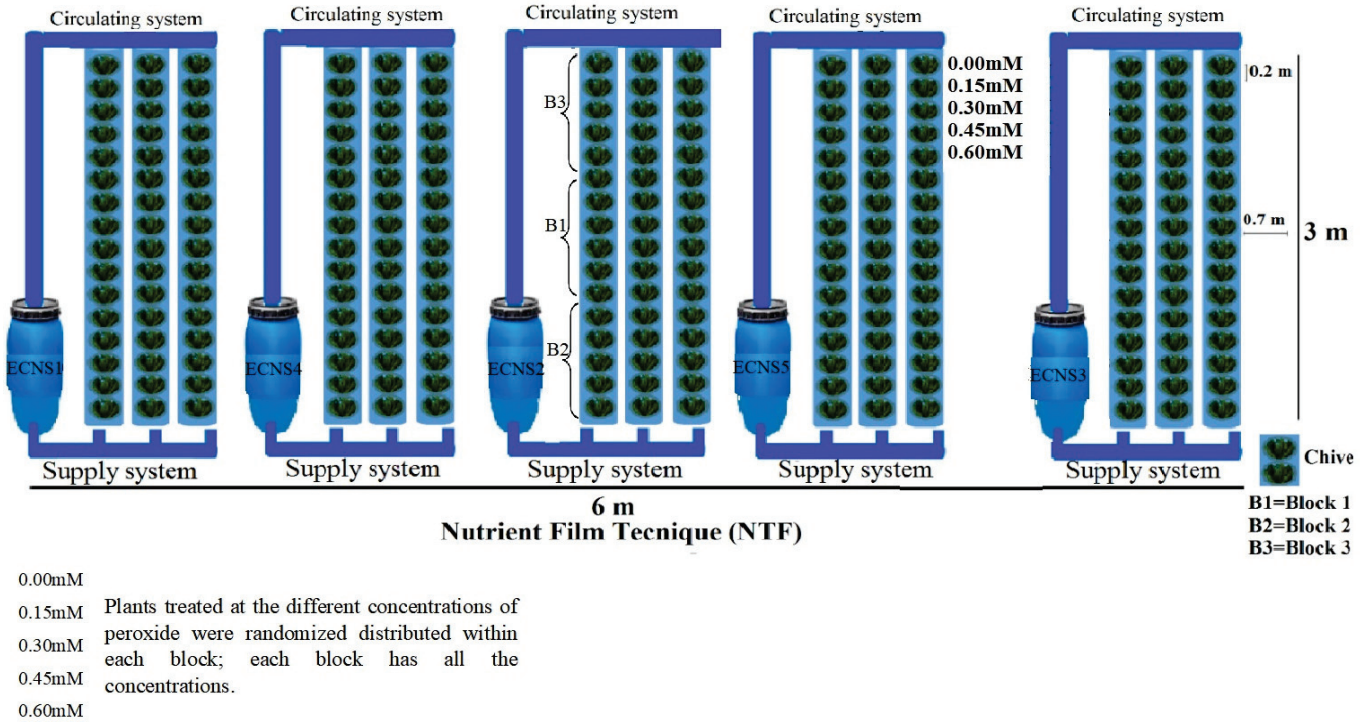

Figure 1. Experimental design of the NTF System, with the hydroponic growing benches.

The holes through which the plants were inserted were perforated using a driller coupled to a circular saw using a between-plant spacing of 0.20 m, with each profile having 3 m in length and receiving 15 plants. In the hydroponic system, the circulation of the solution in the profiles was scheduled to occur three times a day at 240 min intervals, following the recommendation of Silva Junior [5] for chives. Each profile had 15 chive plants at each different electrical conductivity (Solutions), totaling 48 plants at each profile and 225 plants in the experiment (Figure 1).

2.3. Treatments and Experimental Design

A randomized block design organized in a split-plot arrangement was adopted in the experiment so that the main plot was composed of five electrical conductivity levels of the nutrient solution (ECNS1 = 1.0, ECNS2 = 2.0, ECNS3 = 3.0, ECNS4 = 4.0, and ECNS5 = 5.0 dSm^{-1} at 25 °C). The subplot was composed of five hydrogen peroxide concentrations (0.0, 0.15, 0.30, 0.45, and 0.60 mM) used as stimulators of salt stress mitigation in chive seeds.

Plants treated at the different concentrations of peroxide were randomly distributed within each block, with three blocks in total, and with each block containing all concentrations. Each useful plot consisted of three plants spaced by 0.20 m within each hydroponic profile, distributed on five benches. In each experimental unit, two plants formed the edges, i.e., the first and the last plant. Each replicate consisted of three hydroponic profiles connected to a 100 L reservoir to store the nutrient solution, which was pumped by an electric pump.

The preparation of the nutrient solution followed the recommendations of Furlani et al. [15] for leafy vegetables. The formulation used to prepare the nutrient solution was the compound Hidrogood Fert® (Holambra, Brazil), which contains the following macronutrients: Nitrogen (N), Phosphorus (P), Potassium (K), Magnesium (Mg), Sulfur (S), and micronutrients: Boron (B), Copper (Cu), Molybdenum (Mo), Manganese (Mn), and Zinc (Zn). The concentration of each nutrient was as follows in all treatments: 75 g N; 67.5 g P; 210 g K; 27.75 g Mg; 32.25 g S; 0.45 g B; 0.075 g Cu; 0.52 g Mo; 0.37 g Mn; 0.15 g Zn. Calcium Iron Nitrate was added to the solution, also from Hidrogood Fert®. The recommendations indicated by Furlani et al. [15] for the preparation of the hydroponic solution for chives consisted of adding, for each 1000 L of water, 750 g of the Hidrogood Fert Compound, 550 g Calcium Nitrate, and 25 g Fe EDDHA. The water used to prepare the hydroponic solution was stored in a cistern belonging to the Federal University of Campina Grande—UFCG.

Sodium chloride was subsequently added to the solution to reach the desired electrical conductivity level, according to Richard's Equation (1) [16]. The nutrient solution was prepared using water stored in a cistern near the experimental area.

$$C = 640 * ECns \quad (1)$$

where C—Salt concentration (sodium chloride) to be added to the nutrient solution, mgL^{-1}; ECns—Electrical conductivity to be achieved, dSm^{-1}.

In order to promote the mitigation (acclimation/priming) of the effect of different electrical conductivities of the nutrient solution, chive seeds were added in dark containers and soaked in different hydrogen peroxide concentrations for 24 h [17]. After the stress tolerance induction, sowing was performed in germination trays filled with a commercial substrate by sowing five seeds per cell, which were irrigated twice a day and kept in a plant nursery.

The chive cultivar 'Todo Ano Evergreen—Nebuka' was used in the study due to its adaptation to semi-arid conditions [6]. Fifteen days after sowing, the seedlings were transplanted into the hydroponic system. Then, the seeds were inserted in 180 mL plastic cups perforated at the sides and at the bottom and filled with a coconut fiber substrate, after which they were inserted into the holes of the hydroponic pipeline.

Throughout the cultivation cycle, the electrical conductivity and the pH were measured with conductivity and pH meters. The pH remained at 6.0 throughout the cultivation cycle.

The evapotranspiration inside the protected environment was determined by using a Class-A mini tank set up at the center of the plant nursery at 0.20 m from the ground, and the evaporation readings were performed daily using a ruler. The reference evapotranspiration (ET_0) was determined according to Equation (2), as previously described [18].

The alternative tank coefficient (Kp) of 1.0, recommended by Prados [19], was used in the experiment as the ideal parameter for mini tanks inside protected environments.

$$ET_0 = K_p * E_v \quad (2)$$

where ET_0—reference evapotranspiration, in mm day^{-1}; K_p—tank coefficient, non-dimensional; E_v—mini tank evaporation, in mm day^{-1}.

The volume of the nutrient solution to be applied in each profile was determined based on the reference evapotranspiration of the plant nursery added by 50%. Over time, as the uptake decreased, more solution was added to maintain the reservoir at 60% of its total capacity and thus prevent the lack of solution for the daily circulation schedule.

2.4. Variables Analyzed

Bulb length (BL) was evaluated 90 days after sowing using a ruler, whereas bulb diameter (BD) was measured at the base of the plant using a digital caliper (mm).

The contents of chlorophyll 'a', 'b,' and carotenoids were determined using five 0.6-cm^2 fresh leaf disks from the middle part of the plant, which were placed in Eppendorf tubes containing 1.5 mL of 80% acetone. The samples were then stored in a refrigerator for 48 h at 8 °C.

The extraction process was performed in triplicates. After this period, 0.5 mL aliquots were removed, and the absorbance of the solution was determined by spectrophotometry at 647, 663, and 470 nm. The total contents of chlorophyll a, b, and carotenoids were determined using the equations established by Lichtenthaler [20], and the results were expressed as μg g^{-1} of fresh matter (MF):

Chlorophyll 'a' = 12.25 (A663) − 2.79 (A647);

Chlorophyll 'b' = 21.50 (A647) − 5.10 (A663);

Total carotenoids = [1000 (A470) − 1.82 Chl 'a' − 85.02 Chl 'b']/198.

The total plant fresh matter (kg $plant^{-1}$), which represents the yield of chives, was measured using a precision balance.

The use efficiency of the nutrient solution was quantified based on the methodology of [20] using Equation (3).

$$EUS = \frac{MFT}{CSC} \quad (3)$$

EUS—use efficiency of the nutrient solution, kg $plant^{-1}$ mm^{-1};

MFT—total fresh matter, kg;

CSC—consumption of the nutrient solution, mm.

The consumption of the nutrient solution per cycle was quantified by summing the volumes added throughout the cultivation cycle.

2.5. Statistical Analysis

The data obtained were checked for normality using the Shapiro–Wilk test and their homoscedasticity was determined by the Bartlett test at 5% of probability (Table 1).

After the basic assumptions of the ANOVA were met (Table 1), the analysis of variance was performed through the F-test. When significance was verified, regression was used to analyze the data.

The data that showed significant effects of the treatments were adjusted through linear and quadric polynomial regression (isolated factors and interaction between factors) and using the response surface model (for the interaction between factors). Tukey's test was applied when the regression model did not fit. The results of the interaction between factors are presented in the response surface format ($z = a + bx + cx^2 + dy + ey^2$) only for the equations with determination coefficients (R^2) higher than 0.60. For lower R^2 values, in the response surface model, the interactions were represented by linear and quadratic polynomial regression.

The statistical analyses employed the software programs Sisvar 5.6 [21] and Statistica 7 version 7.0 [22].

Table 1. Shapiro–Wilk normality test and Bartlett's test of homogeneous variances for the parameters of chives cultivated in a hydroponic system.

	Normality			Homoscedasticity		
Variable	**Test**	***p*-Value**	**Regular**	**Test**	***p*-Value**	**Homogeneous Variances**
VC (mm)	Shapiro–Wilk	0.21 *	Yes	Bartlett	0.9953 *	Yes
TFM (g)	Shapiro–Wilk	0.98 *	Yes	Bartlett	0.8287 *	Yes
TFM (kg)	Shapiro–Wilk	0.98 *	Yes	Bartlett	0.8287 *	Yes
ENS (kg plant^{-1} mm$^{-1)}$	Shapiro–Wilk	0.22 *	Yes	Bartlett	0.4211 *	Yes
BL (mm)	Shapiro–Wilk	0.15 *	Yes	Bartlett	0.2340 *	Yes
BD (mm)	Shapiro–Wilk	0.15 *	Yes	Bartlett	0.3080 *	Yes
CLOA (μg g^{-1} of (MF))	Shapiro–Wilk	0.10 *	Yes	Bartlett	0.8501 *	Yes
CLOB (μg g^{-1} of (MF))	Shapiro–Wilk	0.10 *	Yes	Bartlett	0.7058 *	Yes
CARO (μg g^{1} of (MF))	Shapiro–Wilk	0.10 *	Yes	Bartlett	0.8075 *	Yes

Volume of nutrient solution applied (VC); total shoot fresh matter marketed (MFT) and water-use efficiency of the nutrient solution (ENS); chlorophyll a (CLOA), chlorophyll b (CLOB), and carotenoids (CARO) * significant at the 5% probability level.

3. Results

3.1. Growth, Yield, and Solution Use Efficiency of Chives as a Function of Electrical Conductivity and Hydrogen Peroxide

The summary of the analysis of variance for the sources of variation referring to the electrical conductivity of the nutrient solution (ECNS), hydrogen peroxide concentrations (H_2O_2) (CP), and the interaction between them (ECNS × CP) on bulb length (BL, mm), bulb diameter (BD, mm), chlorophyll (CLOA, CLOB, and Carotenoids (CARO), μg g^{1} of MF), the volume of the nutrient solution applied (VC, mm), total shoot fresh matter marketed (MFT, kg), and water-use efficiency (ENS, kg plant^{-1} mm^{-1}) of chives 90 days after sowing are found in Table 2.

Table 2. Summary of the analysis of variance for bulb length, bulb diameter, chlorophyll 'a'(CLOA), 'b'(CLOB), carotenoids (CARO), volume of nutrient solution applied (VC, mm), total shoot fresh matter marketed (MFT, kg), and water-use efficiency of the nutrient solution (ENS, kg plant^{-1} mm^{-1}) in hydroponic chives 90 days after sowing.

Sources of Variation	**GL**	**F Statistics**							
		BL	**BD**	**CLOA**	**CLOB**	**CARO**	**VC**	**MFT**	**ENS**
Block	2	8.2 ^{ns}	3.9 ^{ns}	0.1 ^{ns}	0.6 ^{ns}	0.4 ^{ns}	1.4 ^{ns}	0.4 ^{ns}	0.5 ^{ns}
ECNS	4	34.9 **	8.1 **	1.2 ^{ns}	0.8 ^{ns}	1.8 ^{ns}	29.7 **	9.1 *	9.2 *
CP	4	2.5 ^{ns}	0.2 ^{ns}	0.4 ^{ns}	0.7 ^{ns}	0.05 ^{ns}	20.3 ^{ns}	1.0 ^{ns}	0.8 ^{ns}
ECNS x CP	16	1.5 ^{ns}	2.5 *	1.1 ^{ns}	0.8 ^{ns}	1.4 ^{ns}	3.3 ^{ns}	1.5 ^{ns}	1.6 ^{ns}
Residual 1	8	-	-	-	-	-	-	-	-
Residual 2	40	-	-	-	-	-	-	-	-
		mm		**μg g^{-1} of (MF)**			**mm**	**kg**	**(kg Plant^{-1} mm^{-1})**
General mean	-	10.2	6.1	848.5	349.4	166.0	3.0	0.03	0.01
CV1%	-	5.6	9.5	20.8	35.2	32.1	6.4	20.4	19.6
CV2%	-	8.3	8.5	14.7	28.7	24.8	8.0	18.4	18.1

** significant at 1%; * significant at 5%; ^{ns} non-significant.

The different electrical conductivities of the nutrient solution significantly influenced bulb length, bulb diameter, the nutrient solution volume applied, total fresh matter, and the water-use efficiency of the nutrient solution at the significance levels of 1% and 5% (Table 2). Furthermore, the different hydrogen peroxide concentrations applied to the seeds for acclimation (priming), aiming to mitigate the effect of different electrical conductivities of the nutrient solution, did not influence any of the variables studied. However, there was a significant interaction between the electrical conductivity and the hydrogen peroxide concentrations at 5% of probability on bulb diameter 90 days after sowing para for the chive cultivar 'Todo Ano Evergreen—Nebuka' (Table 2).

The variables of chlorophyll 'a', chlorophyll 'b', and carotenoids were not influenced by the electrical conductivity of the nutrient solution or the hydrogen peroxide concentrations applied for seed priming (Table 2). The mean contents of CLOA, CLOB, and CARO were 848.5, 349.4, and 166.0 μg g^{-1} of MF, respectively, well below those reported by Silva et al. [8] for *Allium schoenoprasum* (23,820, 9840, and 6330 μg g^{-1}). When studying the isolated effect of hydrogen peroxide concentrations applied as priming on chive seeds when the plants were grown under hydroponic conditions, there was no significant difference between the different concentrations at the 5% probability level in bulb length, bulb diameter, chlorophyll "a", "b", carotenoids, volume of solution applied, total fruit mass, and nutrient solution use efficiency (Table 3).

Table 3. Mean values for BL, BD, CLOA, CLOB, CARO, VC, MFT, and ENS as a function of different hydrogen peroxide concentrations applied as priming to chive seedlings.

Concentrations (H_2O_2)	BL	BD	CLOA	CLOB	CARO	VC	MFT	ENS
	mm		μg g^{-1} of (MF)			mm	kg	(kg Plant^{-1} mm^{-1})
0.00 mM	10.16 a	6.04 a	858.02 a	373.17 a	169.49 a	3.08 a	0.038 a	0.013 a
0.15 mM	10.58 a	6.17 a	894.94 a	341.21 a	164.58 a	3.08 a	0.040 a	0.013 a
0.30 mM	10.54 a	6.13 a	853.72 a	338.71 a	163.52 a	3.08 a	0.040 a	0.013 a
0.45 mM	9.74 a	6.11 a	761.24 a	323.36 a	167.65 a	3.08 a	0.038 a	0.012 a
0.60 mM	10.06 a	6.23 a	874.83 a	370.85 a	164.97 a	3.08 a	0.040 a	0.013 a

Means followed by the same lowercase letter in the column do not differ from each other by the Tukey's at 5% probability level.

The seed germination percentage of chives treated with hydrogen peroxide remained in accordance with the recommendation of the seed manufacturer, i.e., higher than 80%. It is noteworthy that, in the treatments with hydrogen peroxide application, there was faster germination and high uniformity, thus reaffirming the data of Santos et al. [23], who obtained 81% germination percentage for chives using the same cultivar and treatments used as in this study.

The mathematical model that best fit the bulb length parameter was the quadratic one, and the maximum yield for this variable was obtained at 4.64 dSm^{-1} of ECNS, corresponding to a BL of 10.9 mm (Figure 2a).

There was an interaction between ECNS × CP on bulb diameter, and the highest BD values (mm) were obtained at the lowest salinity of the nutrient solution (1 dSm^{-1}) associated with the highest hydrogen peroxide concentration applied during seed priming (0.60 mM) (Figure 2b). Furthermore, as the electrical conductivity of the nutrient solution increased, the stress-mitigating effect of hydrogen peroxide and bulb diameter decreased.

Mean values of the nutrient solution applied (a), total shoot mass marketed (b), and use efficiency of the nutrient solution (c) for chives 90 days after sowing in a hydroponic system for the isolated factor of the electrical conductivity of the nutrient solution are found in Figure 3.

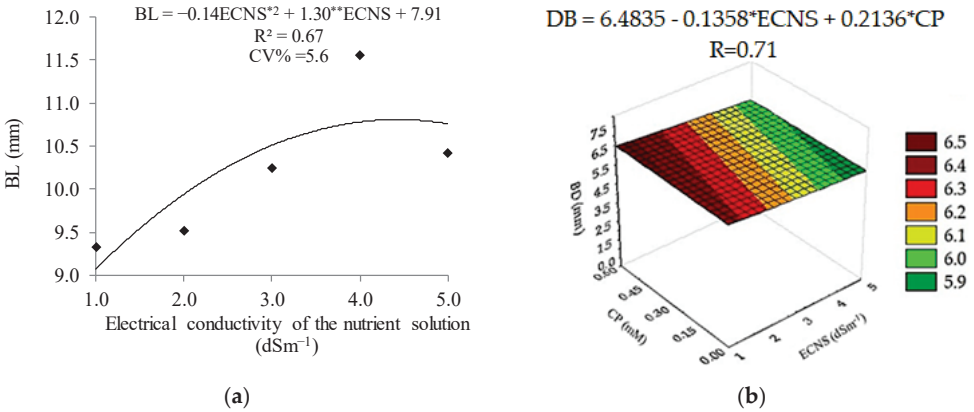

Figure 2. Bulb length (**a**) and bulb diameter (**b**) of chives subjected to different electrical conductivities of the nutrient solution and priming with hydrogen peroxide 90 days after sowing in hydroponic cultivation. ** significant at 1%; * significant at 5%.

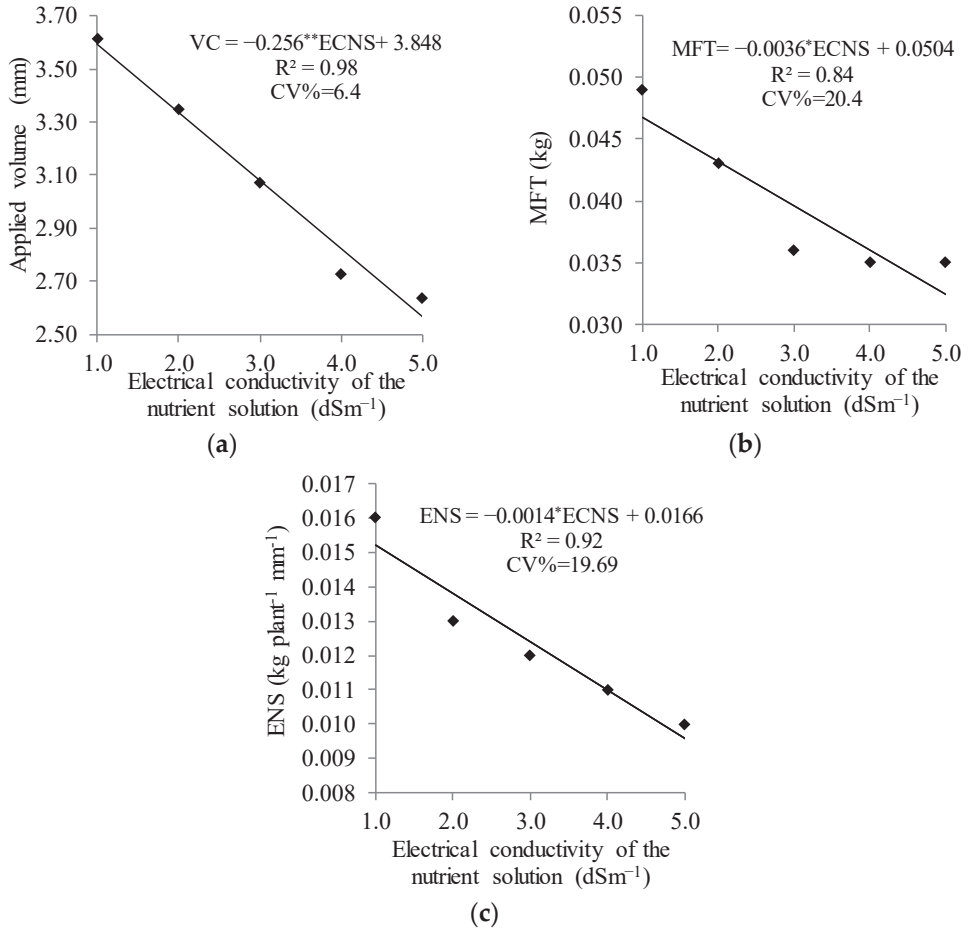

Figure 3. Volume of the nutrient solution applied (**a**), total shoot mass marketed (**b**), and use efficiency of the nutrient solution (**c**) in a hydroponic system for the salinity levels of the nutrient solutions. ** significant at 1%; * significant at 5%.

When analyzing the volume of nutrient solution applied to chives 90 days after sowing in the hydroponic system, it was observed that as the electrical conductivity of the nutrient solution increased, the nutrient solution volume absorbed by plants decreased (Figure 3a), with the linear model best fitting the maximum volume obtained at the ECNS of 1 dSm^{-1} and the lowest at ECNS 5 dSm^{-1}, corresponding, respectively, to 3.592 and 2.568 m, with a decrease per unit increase of the electrical conductivity of the nutrient

solution corresponding to 0.256 mm at each application cycle in the hydroponic system (Figure 3a). When comparing the ECNS of 1 dSm^{-1} with that of ECNS of 5 dSm^{-1}, a percentage reduction of 28.6% was observed in the volume of nutrient solution applied.

The mathematical model that best fit the total dry mass of chives as a function of the electrical conductivity of the nutrient solution was the linear model, i.e., as the electrical conductivity increased, the MFT decreased (Figure 3b), with every 1 dSm^{-1} increase in the electrical conductivity reducing the total fresh mass of chives by 3.6 g. This scenario indicates a 30.7% reduction when comparing the ECNS1 to the ECNS5.

The use efficiency of the nutrient solution in hydroponics under different electrical conductivity levels of chives highlighted a linear adjustment with a progressive reduction as the electrical conductivity of the nutrient solution increased, with the maximum use efficiency of the nutrient solution being obtained at 1 dSm^{-1}, corresponding to a EUS of 0.0152 kg per plant mm^{-1} of the solution provided to the system and a percent difference of 36.84%, between ECNS1 and ECNS5, i.e., the ECNS of 1 dSm^{-1} provides a use efficiency of 14.6 g mm^{-1} of nutrient solution applied (Figure 3c).

3.2. Water Consumption of Chives as a Function of Different Water Conductivities of the Nutrient Solution

Furthermore, when analyzing the mean uptake per plant and per cycle of chive plants as a function of the electrical conductivity of the nutrient solution (Table 4), there was a reduction in water consumption (in mm) per plant when the salinity of the nutrient solution increased, with the maximum uptake obtained at the electrical conductivity (ECNS) of 1 dSm^{-1}, i.e., the lower the ECNS, the more water is consumed by plants to perform the essential activities of their metabolism and, consequently, the higher their yield [7].

Table 4. Water consumption of chives cultivated in a hydroponic system, per plant and per cycle, as a function of different water conductivities of the nutrient solution.

Treatments	Mean Consumption (mm Plant)	Mean Consumption (mm Cycle)
ECNS1	6.38	459.0
ECNS2	5.92	426.5
ECNS3	5.43	391.0
ECNS4	4.83	347.6
ECNS5	4.66	335.4

4. Discussion

4.1. Growth, Yield, and Solution Use Efficiency of Chives as a Function of Electrical Conductivity and Hydrogen Peroxide

Depending on the electrical conductivity of water, stress causes damage to agriculture in all parts of the world, reducing plant growth and productivity. In this scenario, research seeking alternatives to mitigate the effects of salts on plants is essential, but it is a challenge to mitigate the implications of high electrical conductivity on plants under hydroponic cultivation. Therefore, the strategy of using priming with hydrogen peroxide in chive seeds to attenuate salt stress in hydroponic environments becomes an interesting alternative. The results indicate that the application of hydrogen peroxide (0.0, 0.15, 0.30, 0.45, and 0.60 Mm) did not attenuate salt stress due to the high levels of electrical conductivity (1, 2, 3, 4, and 5 dSm^{-1}) provided in the nutrient solution to chives in a hydroponic environment.

However, when 0.60 Mm of hydrogen peroxide was applied as priming, there were greater gains in bulb diameter in ECNS1. Furthermore, with the increase in electrical conductivity, the diameter was reduced, as well as the mitigating effect of H_2O_2. Therefore, it is possible that the concentrations of hydrogen peroxide applied to the seeds may have been insufficient to trigger the metabolism of chive plants in the cell signaling system, which stimulates the production of antioxidant enzymes that contribute to increasing the plant's ability to resist the harmful effects of salts.

Although no significant effects of the action of H_2O_2 on chive seeds have been verified as attenuating agents, these are initial studies that encourage further research with other hydrogen peroxide concentrations to obtain possible concentrations that may serve as attenuating agents. The hydrogen peroxide concentrations capable of acclimating seeds to abiotic stresses vary from 0.05 µM to 200 mM. This variation is related to the form of application, the time that the seed was exposed to hydrogen peroxide, and the morphological and physiological characteristics of each species [10,12,24].

Priming in chive seeds contributes to increasing seed performance by metabolically advancing seed germination, resulting in uniform seedling emergence, even though no statistical difference was found between the different concentrations regarding the growth, consumption, and production variables of chive plants grown in hydroponic systems. There were probably no significant differences between the hydrogen peroxide concentrations used as they were not enough to promote the accumulation of reactive oxygen species (ROS), which are substances produced in the mitochondria that coordinate the metabolism with the function of eliminating unnecessary cells, acting decisively in the plant's defense mechanism under salt stress conditions [6,12,25,26].

When hydrogen peroxide activates the molecules that contribute to accumulating ROS, the result is the mitigation of salt stress, contributing to osmotic adjustment and favoring development in terms of growth, photosynthesis, and plant reproductive organs, helping increase the tolerance of plants to stress, i.e., hydrogen peroxide acts as an attenuator [6,10,26].

When exposed to salt stress due to high electrical conductivities of the nutrient solution even under hydroponic cultivation, chive plants showed reduced bulb diameter, water use efficiency, and nutrient solution consumption as the ECNS was increased by 1 dSm^{-1}, with a mean percent reduction of 30.76%. Our results reveal that a high electrical conductivity of the nutrient solution causes toxicity in hydroponic chives and failure in the plant's osmotic adjustment, even after priming. A relevant factor is that chlorophyll synthesis was not altered when plants underwent salt stress, indicating that the osmotic adjustment of chives occurs mainly as a function of increased chlorophyll synthesis.

High salt concentrations in the nutrient solution could negatively influence the essential metabolic processes for plant development, including nutrient uptake [27]. In this scenario, the nutrient uptake, transport, and assimilation processes of the nutrient solution do not occur adequately due to the antagonistic and competitive effects of salt excess and the pH increase in the nutrient medium, resulting in nutrient imbalances and reduced plant growth and development [28,29]. It should be noted that hydroponic cultivation tends to reduce the impacts of high electrical conductivities by adding nutrients into the medium, reducing such impacts by the absence of matric potential [8].

The lower carotenoid content in relation to the chlorophyll values is related to the inverse relationship between these variables, with higher chlorophyll contents possibly justifying the lower carotenoid values in chives. These variations in the contents of chlorophyll and total carotenoids can be influenced by the climatic conditions to which the plants were subjected [7,8].

It is evident that the synthesis of chlorophyll and carotenoids is essential to quantify the final quality of green vegetables since their chlorophyll forms are sensitive to heat, oxygen, light, enzymes, the action of metals, and oxidation, with the latter being the leading cause of carotenoid degradation, depending on oxygen availability, the type of carotenoids, and their physical state. As a result, this degradation is continuously stimulated by light, heat, metals, oxidative enzymes, and peroxides and is inhibited by antioxidants [8].

The electrical conductivity of the nutrient solution negatively influenced the bulb length of chives, although below the threshold found by [4] under direct cultivation. This result is justified by the fact that hydroponic cultivation contributes to reducing the effects of salts on plants compared to direct cultivation due to the absence of matric potential and the saturation state of plants, increasing the free energy of water and facilitating its uptake by plants [5].

The reductions in bulb diameter as a function of the electrical conductivity of the nutrient solution could be related to stomatal closure and reductions in gas exchange due to the stress condition, thus reducing the uptake of the nutrient solution and limiting plant growth [30].

The electrical conductivity of the nutrient solution [31] above the plant tolerance threshold is reflected in the reduction in crop growth and development even under hydroponic conditions, which may have contributed to the reduced bulb diameter of chives. Recent studies using hydrogen peroxide to mitigate the effect of salt stress corroborate that this attenuator can influence physiological responses to stress, such as stomatal opening and closing [6,11]. The beneficial effects of hydrogen peroxide on stress effects could be associated with its role as a signaling molecule, regulating several metabolic pathways [12,32]. It has been reported that the increase in the electrical conductivity of the nutrient solution decreases water and nutrient uptake; as a result, a lower water volume needs to be applied in the circulation system at higher electrical conductivity levels of the nutrient solution. These results are similar to those obtained by Cruz et al. [33] when studying the stress index, water potential, and leaf succulence of cauliflower cultivated in a hydroponic system of high electrical conductivity.

Our results reveal linear reductions in the nutrient solution application rate observed in all electrical conductivity regimes. The total consumption of the nutrient solution was not changed between treatments, or only partially since water uptake by plants was cumulatively reduced, corroborating the research findings on the effect of NaCl or macronutrient-imposed salinity on the crop yield and water use efficiency of hydroponic basil [34].

The fresh mass reduction in plants cultivated in hydroponic systems with high electrical conductivity of the nutrient solution is a classic plant response observed by different authors in several vegetable crops [6,8,27,34,35]. This result is attributed to a reduction in the water potential of the external solution generated due to the osmotic effect of the salt present in the nutrient solution, hindering water and nutrient uptake by plant roots, which reduces leaf turgor and the MFT [36].

The ENS reduction is justified by the negative effect caused by salts present in the nutrient solution on the total fresh matter of chives plants. It should be noted that the use efficiency of the nutrient solution is important when working with nutrient solutions with high electrical conductivity since salt stress can cause higher uptake reductions compared to plant production.

Under water or salt stress, the water use efficiency can vary due to the reduction in stomatal conductance, which affects the photosynthetic rate more intensely than leaf transpiration rate [7]. When this process becomes severe, cell dehydration in the mesophyll inhibits photosynthesis, thus affecting the mesophyll metabolism, water use efficiency, and crop yield.

There was a reduction in the use efficiency of the nutrient solution of more than 20% when the plants were subjected to different electrical conductivities of the nutrient solution. This result may be more apparent when the species is susceptible to salt stress. Our results are similar to those obtained by Faliagka et al. [34] and Evanidi et al. [37] when studying basil subjected to different electrical conductivities of the nutrient solution, observing a 25% reduction in the use efficiency of the nutrient solution.

4.2. Water Consumption of Chives as a Function of Different Water Conductivities of the Nutrient Solution

The maximum consumption of nutrient solution (<460 mm cycle) was obtained at an electrical conductivity of 1 dSm^{-1}. From this value on, there was a reduction in consumption. This value is considered acceptable for hydroponic chive cultivation since the water consumption of this crop under field conditions is superior to 550 mm per cycle [3]. Quantifying water consumption during the cultivation cycle in hydroponic systems can contribute to improving and planning water resources in any region by estimating the

water volume to be used before the crop is established in the hydroponic system [38]. This parameter is an efficient guideline for designing hydroponic systems, aiming to collect and store water for this purpose in green belts.

The water uptake reductions recorded for hydroponic chive cultivation when the seeds were subjected to acclimation with hydrogen peroxide and different electrical conductivities of the nutrient solution are within the acceptable range, as reported by Paulus [39] in their study with hydroponic lettuce, obtaining acceptable NFT reductions from 3.9 to 10.0% per unit increase in the electrical conductivity of the nutrient solution in two cultivation cycles.

When studying cumulative water consumption in hydroponic coriander using brackish water, [9] observed reductions of 5.26 and 5.85% per unit increment in the ECw for the periods of 1–20 and 1–24 DAT, respectively. Our results reveal similar conclusions with different species, indicating that the higher the electrical conductivity of the nutrient solution in hydroponic systems, the lower the total nutrient uptake by plants due to the reduction in the osmotic potential of the nutrient solution, delaying the transport of water from roots to fruits and leaves, with negative effects on expansion, growth, and production [40].

The use efficiency of the nutrient solution of 14.6 g for each mm of nutrient solution lost by evapotranspiration is considered acceptable. This result corroborates the data of Mendez-Cifuentes et al. [41] in a study on different open and closed hydroponic systems, who observed that in order to produce 1 kg of vegetables in an open cultivation system, approximately 53 L of water is required to achieve a yield of 95%, with 86% water consumption. On the other hand, in the closed system, the nutrient solution volume required is only 22 L.

Even under hydroponic conditions in which water and nutrients are supplied in a form that is readily assimilable by the plants, the different electrical conductivities of the nutrient solution tend to reduce water and nutrient uptake and productivity [8,26,40]. This result may be less evident when the species is less susceptible to salt stress and when subjected to acclimation with hydrogen peroxide [6,8].

5. Conclusions

The increase in electrical conductivity of the nutrient solution reduces bulb length, volume applied, water consumption in the solution, total marketable fresh mass, and the use efficiency of the nutrient solution by plants. Acclimation with hydrogen peroxide alone did not influence the yield of chives in a hydroponic system. The contents of chlorophyll a, b, and carotenoids are not influenced by the electrical conductivity of the nutrient solution or the hydrogen peroxide concentrations used for the acclimation. The highest consumption of nutrient solution by chive plants throughout the cultivation cycle was 459 mm, lost by evapotranspiration. The acclimation of chive seeds (0.60 mM) associated with 1 dSm^{-1} solution is the best combination for bulb diameter. Each increase of 1 dSm^{-1} in the electrical conductivity of the nutrient solution reduces the total fresh mass of chive plants by 1.4 g. The electrical conductivity of the nutrient solution to obtain the maximum yield of chives in hydroponic cultivation is 1 dSm^{-1}.

Author Contributions: Conceptualization, P.F.d.S. and B.D.B.d.S.; methodology, J.D.N. and R.M.d.M.; software, A.P.C.G.B.; validation, P.F.d.S., A.S.d.M., T.J.A.d.S., E.M.B.-S. and T.F.D.; formal analysis, B.D.B.d.S., A.S.d.M., S.I.B., R.M.d.M. and J.D.N.; investigation, B.D.B.d.S.; resources, P.F.d.S.; data curation, R.M.d.M. and S.I.B.; writing—original draft preparation, E.M.B.-S., A.S.d.M. and T.J.A.d.S.; writing—review and editing, P.F.d.S., T.J.A.d.S., A.S.d.M. and T.F.D.; visualization, A.P.C.G.B., P.F.d.S. and J.D.N.; supervision, P.F.d.S.; project administration, B.D.B.d.S.; funding acquisition, B.D.B.d.S. All authors have read and agreed to the published version of the manuscript.

Funding: This research was funded by Coordination for the Improvement of Higher Education Personnel-CAPES, grant number 88882.314940/2019-1.

Institutional Review Board Statement: Not applicable.

Data Availability Statement: All the data reported here are available from the authors upon request.

Conflicts of Interest: The authors declare no conflict of interest.

References

1. Thakulla, D.; Dunn, B.; Hu, B.; Goad, C.; Maness, N. Nutrient solution temperature affects growth and Brix parameters of seventeen *Lettuce* cultivars grown in an NFT hydroponic system. *Horticulturae* **2021**, *7*, 321. [CrossRef]
2. Singh, P.; Mahajan, V.; Shabeer, T.P.A.; Banerjee, K.; Jadhav, M.R.; Kumar, P.; Gopal, J. Comparative evaluation of different Allium accessions for allicin and other allyl thiosulphinates. *Ind. Crops Prod.* **2020**, *147*, 112215. [CrossRef]
3. Carvalho, J.; Marcuzzo, L.L. Efeito da altura da poda na produtividade de cebolinha-verde. *Rev. Agron. Bras.* **2021**, *5*, 1–4. [CrossRef]
4. Silva, P.F.; Cavalcante, V.S.; Santos, J.C.C.; Costa, E.S.; Barbosa, J.T.V. Análise quantitativa da cebolinha irrigada com água salina. *Comun. Sci.* **2014**, *5*, 241–251.
5. Silva Júnior, F.J.; Santos Júnior, J.A.; Dias, N.S.; Gheyi, H.R.; Rivera, R.C.; Silva, G.F.; Fernande, C.S. Green onion production under strategies of replacement and frequencies of circulation of brackish nutritive solutions. *Biosci. J.* **2019**, *35*, 796–805. [CrossRef]
6. Santos, B.D.B.; Silva, P.F.; Matos, R.M.; Neto, J.D.; Lima, V.L.A.; Bonou, S.I.; Melo, A.S.; Melo, Y.L. Induction of salt stress tolerance in chives by priming with H_2O_2 in hydroponic cultivation. *Chil. J. Agric. Res.* **2021**, *81*, 317–325. [CrossRef]
7. Taiz, L.; Zeiger, E.; Moller, I.M.; Murphy, A. *Fisiologia e Desenvolvimento Vegetal*; Artmed: Porto Alegre, Brazil, 2017.
8. Silva, P.G.A.; Borges, C.D.; Miguel, A.C.A.; Jacomino, A.P.; Mendonça, C.R.B. Características físico-químicas de cebolinhas comum e europeia. *Braz. J. Food Technol.* **2015**, *18*, 293–298. [CrossRef]
9. Silva, C.B.; Silva, J.C.; Santos, D.P.; Santos, M.A.L. Função produção da cultura da cebolinha verde (*Allium fistulosum* L.): Níveis de água salina e adubo orgânico no Agreste Alagoano. *Rev. Ambient.* **2018**, *10*, 12–22. [CrossRef]
10. Dantas, M.V.; de Lima, G.S.; Gheyi, H.R.; de Silva, L.A.; Silva, P.C.C.; dos Soares, L.A.A.; Lopes, I.A.P.; Roque, I.A. Peróxido de hidrogênio e solução nutritiva salina no cultivo hidropônico de abobrinha italiana. *Semin. Ciências Agrárias* **2022**, *43*, 1167–1186. [CrossRef]
11. Nigam, B.; Dubey, R.S.; Rathore, D. Protective role of exogenously supplied salicylic acid and PGPB (*Stenotrophomonas* sp.) on spinach and soybean cultivars grown under salt stress. *Sci. Hortic.* **2022**, *293*, e110654. [CrossRef]
12. Qureshi, M.K.; Gawroński, P.; Munir, S.; Jindal, S.; Kerchev, P. Hydrogen peroxide-induced stress acclimation in plants. *Cell. Mol. Life Sci.* **2022**, *79*, 2–16. [CrossRef]
13. Carvalho, F.E.L.; Lobo, A.K.M.; Bonifacio, A.; Martins, M.O.; Lima Neto, M.C.; Silveira, J.A.G. Aclimatação ao estresse salino em plantas de arroz induzida pelo pré-tratamento com H_2O_2. *Rev. Bras. De Eng. Agrícola E Ambient.* **2011**, *15*, 416–423. [CrossRef]
14. Zhou, H.; Chen, J.; Wang, F.; Li, X.; Génard, M.; Kang, S. Hydroponic crops are an alternative for semi-arid regions, as they increase water savings, since a controlled environment ensures that irrigation systems are more accurate, so that water is used rationally, with rapid plant development and high productivity. *Agric. Water Manag.* **2020**, *241*, e106331.
15. Furlani, P.R.; Silveira, L.C.P.; Bolonhezi, D.; Faquin, V. *Cultivo Hidropônico de Plantas*; IAC: Campinas, Brazil, 1999; p. 52.
16. Richards, L.A. *Diagnosis and Improvement of Saline and Alkali Soils*; US Department of Agriculture: Washington, DC, USA, 1954; p. 160.
17. Bakhshandeh, E.; Gholamhossieni, M. Quantification of soybean seed germination response to seed deterioration under PEG-induced water stress using hydrotime concept. *Acta Physiol. Plant.* **2018**, *40*, 126. [CrossRef]
18. Mantovani, E.C.; Bernardo, S.; Palaretti, L.F. *Irrigação: Princípios e Métodos*, 3rd ed.; Editora UFV: Viçosa, Brazil, 2012; 355p.
19. Prados, N.C. Contribución al Estudio de los Cultivos Enarenados en Almeria: Necessidades Hídricas y Extración Del Nutrientes Del Cultivo de Tomate de Crescimento Indeterminado en Abrigo de Polietileno. Ph.D. Thesis, Universidad de Almería, Almeria, Espana, 1986; 195p.
20. Lichtenthaler, H.K. Chlorophylls and carotenoids: Pigments of photosynthetic biomembranes. *Methods Enzymol.* **1987**, *148*, 350–382. [CrossRef]
21. Ferreira, D.F. SISVAR: A computer analysis system to fixed effects split plot type designs. *Rev. Bras. De Biom.* **2019**, *37*, 529–535. [CrossRef]
22. STATSOFT. *Inc. STATISTICA (Data Analysis Software System)*, Version 7; STATSOFT. Inc.: Tulsa, OK, USA, 2004.
23. Santos, B.D.B.; Bonou, S.I.; Matos, R.M.; Silva, P.F.; Cabral, J.H.A.; Oliveira, R.C.; Dantas Neto, J.; Lima, V.L.A. Tratamento pré-germinativo de sementes de cebolinha com peróxido de hidrogênio. *Rev. Ibero Am. De Ciências Ambient.* **2019**, *10*, 307–313. [CrossRef]
24. Anand, A.; Thakur, A.K.M.; Koul, A. Hydrogen peroxide signaling integrates with phytohormones during the germination of magnetoprimed tomato seeds. *Sci. Rep.* **2019**, *9*, 8814. [CrossRef]
25. Gammoudi, N.; Karmous, I.; Zerria, K. Efficiency of pepper seed invigoration through hydrogen peroxide priming to improve in vitro salt and drought stress tolerance. *Hortic. Environ. Biotechnol.* **2020**, *61*, 703–714. [CrossRef]
26. Silva, A.A.R.; do Nascimento Sousa, P.F.; de Lima, G.S. Hydrogen Peroxide Reduces the Effect of Salt Stress on Growth and Postharvest Quality of Hydroponic Mini Watermelon. *Water Air Soil Pollut.* **2022**, *233*, 198. [CrossRef]
27. Sahin, U.; Ors, S.; Ekinci, M.; Turan, M. Effects of individual and combined effects of salinity and drought on physiological, nutritional and biochemical properties of cabbage (*Brassica oleracea* var. capitata). *Sci. Hortic.* **2018**, *240*, 196–204. [CrossRef]
28. Silva, M.G.; Oliveira, I.S.; Soares, T.M.; Gheyi, H.R.; Santana, G.O.; Pinho, J.S. Growth, production and water consumption of coriander in hydroponic system using brackish waters. *Rev. Bras. De Eng. Agrícola E Ambient.* **2018**, *22*, 547–552. [CrossRef]

29. Silva, M.G.; Soares, T.M.; Gheyi, H.R.; Costa, I.P.; Vasconcelos, R.S. Growth, production and water consumption of coriander grown under different recirculation intervals and nutrient solution depths in hydroponic channels. *Emir. J. Food Agric.* **2020**, *32*, 281–294. [CrossRef]
30. Lima, L.A.; de Oliveira, F.A.; Alves, R.E.C.; Linhares, P.S.F.; De Medeiros, A.M.A.; Bezerra, F.M.S. Tolerância da berinjela à salinidade da água de irrigação. *Rev. Agroambiente* **2015**, *9*, 27–34. [CrossRef]
31. Tayebi-Meigooni, A.; Awang, Y.; Biggs, A.R.; Ghasemzadeh, A. Salt-induced changes in growth and damage avoidance mechanisms of hydroponically grown Chinese kale (*Brassica alboglabra* L.). *Springer Nat.* **2019**, *6*, 99–105.
32. Baxter, A.; Mittler, R.; Suzuki, N. EROS as key players in plant stress signalling. *J. Exp. Bot.* **2014**, *65*, 1229–1240. [CrossRef]
33. Cruz, A.F.S.; Silva, G.F.; Silva, E.F.F.; Soares, H.R.; Santos, J.S.G.; Lira, R.M. Stress index, water potentials and leaf succulence in cauliflower cultivated hydroponically with brackish water. *Rev. Bras. De Eng. Agrícola E Ambient.* **2018**, *22*, 622–627. [CrossRef]
34. Faliagka, S.; Elvanidi, A.; Spanoudaki, S.; Kunze, A.; Max, J.F.J.; Katsoulas, N. Effect of NaCl or Macronutrient-Imposed Salinity on Basil Crop Yield and Water Use Efficiency. *Horticulturae* **2021**, *7*, 296. [CrossRef]
35. Nguyen, V.Q.; Van, H.T.; Le, S.H.; Nguyen, T.H.; Nguyen, H.T.; Lan, N.T. Production of hydroponic solution from human urine using adsorption–desorption method with coconut shell-derived activated carbon. *Environ. Technol. Innov.* **2021**, *23*, e101708. [CrossRef]
36. Mouroutoglou, C.; Kotsiras, A.; Ntatsi, G.; Savvas, D. Impact of the Hydroponic Cropping System on Growth, Yield, and Nutrition of a Greek Sweet Onion (*Allium cepa* L.) Landrace. *Horticulturae* **2021**, *7*, 432. [CrossRef]
37. Elvanidi, A.; Reascos, C.M.B.; Gourzoulidou, E.; Kunze, A.; Max, J.F.J.; Katsoulas, N. Implementation of the circular economy concept in greenhouse hydroponics for ultimate use of water and nutrients. *Horticulturae* **2020**, *6*, 83. [CrossRef]
38. Alves, L.S.; Silva, M.G.; Gheyi, H.R.; Paz, V.P.S.; Soares, T.M.; Rafael, R.S.M. Uso de águas salobras no cultivo da chicória em condições hidropônicas. *Irriga* **2019**, *24*, 758–769. [CrossRef]
39. Paulus, D.; Paulus, E.; Nava, G.A.; Moura, C.A. Crescimento, consumo hídrico e composição mineral de alface cultivada em hidroponia com águas salinas. *Rev. Ceres* **2012**, *59*, 110–117. [CrossRef]
40. Chrysargyris, A.; Petropoulos, S.A.; Prvulovic, D.; Tzortzakis, N. Performance of hydroponically cultivated geranium and common verbena under salinity and high electrical conductivity levels. *Agronomy* **2021**, *11*, 1237. [CrossRef]
41. Mendez-Cifuentes, A.; Valdez-Aguilar, L.A.; Cadena-Zapata, M.; González-Fuentes, J.A.; HernandezMaruri, J.A.; Alvarado-Camarillo, D. Water and fertilizer use efficiency in subirrigated containerized tomato. *Water* **2020**, *12*, 1313. [CrossRef]

agriculture

MDPI

Article

Beneficial Microorganisms Affect Soil Microbiological Activity and Corn Yield under Deficit Irrigation

Josinaldo Lopes Araujo [1,*], Jackson de Mesquita Alves [2], Railene Hérica Carlos Rocha [1], José Zilton Lopes Santos [3], Rodolfo dos Santos Barbosa [1], Francisco Marcelo Nascimento da Costa [1], Geovani Soares de Lima [1], Leandro Nunes de Freitas [1], Adriana Silva Lima [1], Antonio Elizeneudo Peixoto Nogueira [1], André Alisson Rodrigues da Silva [1], Leônidas Canuto dos Santos [4], Francisco Bezerra Neto [5] and Francisco Vaniés da Silva Sá [6]

[1] Department of Agricultural Sciences, Federal University of Campina Grande, Pombal 58840-000, PB, Brazil; railene.herica@professor.ufcg.edu.br (R.H.C.R.); rodolfobar2011bar.rb@gmail.com (R.d.S.B.); francisconasciment33@gmail.com (F.M.N.d.C.); geovanisoareslima@gmail.com (G.S.d.L.); leandronunes_agr@ufcg.edu.br (L.N.d.F.); adriana.silva@professor.ufcg.edu.br (A.S.L.); elyzyneudo@gmail.com (A.E.P.N.); andrealisson_cgpb@hotmail.com (A.A.R.d.S.)

[2] Department of Soil Science, Federal University of Viçosa, Viçosa 36570-900, MG, Brazil; mesquitajackson2018@gmail.com

[3] Faculty of Agricultural Science, University of Amazonas, Manaus 69067-005, AM, Brazil; ziltonlopes@ufam.edu.br

[4] Department of Soil Science, Federal University of Lavras, Lavras 37200-900, MG, Brazil; leonidas.santos2@estudante.ufla.br

[5] Agricultural Sciences Center, Federal Rural University of Semi-Arid, Mossoró 59625-900, RN, Brazil; bezerra@ufersa.edu.br

[6] Agricultural Sciences Center, State University of Paraíba, Catolé do Rocha 58884-000, PB, Brazil; vanies@ufersa.edu.br

* Correspondence: josinaldo.lopes@professor.ufcg.edu.br

Abstract: Water scarcity is one of the main factors that decrease the growth and productivity of corn, since it negatively affects gas exchange and the general metabolism of the crop. The use of beneficial microorganisms (BM) has been considered a potential attenuator of water stress. This study aimed to evaluate the effect of BM and water deficit on growth, gas exchange, grain yield, and soil microbial activity. A field experiment was carried out, in which the treatments were composed of a 2 × 4 factorial scheme, corresponding to two irrigation levels (100% of ETc and 50% of ETc) and to four treatments (T) referring to the soil inoculation with BM (C: control; T1: *Bacillus amyloliquefaciens* + *Azospirillum brasiliense*; T2: *B. subtilis*; and T3: *A. brasiliense*). The evaluations were carried out in the flowering phase (plant growth, gas exchange, and foliar nitrogen content) and at the end of the plant cycle (grains yield, mineral nitrogen, and microbiological activity). The 50% reduction in irrigation depth severely restricted corn growth and gas exchange and decreased the grain yield by 38%. The water deficit increased the protein content in the grains and the concentration of mineral nitrogen in the soil when the plants were inoculated with BM. Under water stress, inoculation with BM increased corn productivity by 35% and increased soil microbial activity. The inoculation of plants with BM, either in combination (*Bacillus amyloliquefaciens* + *A. brasiliense*) or alone (*B. subtilis*), attenuated the adverse effects of water deficit in maize.

Keywords: plant growth-promoting bacteria; water stress; *Zea mays*; photosynthesis; water stress attenuators

1. Introduction

The water deficit affects not only the arid and semi-arid regions of the world but also areas located in countries with a humid tropical climate, such as Brazil [1]. In these areas, prolonged water scarcity periods can reduce the productivity of important crops, such as

corn [2]. Water stress negatively affects plants' physiological and biochemical processes that restrict growth, development, and productivity [3,4]. Drought causes a decrease in cell turgor, which is essential for proper cellular metabolisms, such as photosynthesis, enzyme activity, and nutrient uptake [4,5].

Corn (*Zea mays* L.) is one of the most important crops in the world due to its multiplicity of uses, especially as raw material for the food industry. However, in areas where water scarcity is more pronounced, as in many developing countries and the semi-arid region of Brazil, the use of corn in human food as a main diet component is expressive [6]. Thus, in these areas, water deficit is one factor that threatens food security. Therefore, it is necessary to find strategies to mitigate the adverse effects of water deficit in essential crops such as corn.

Previous research has demonstrated that beneficial microorganisms (BM) (also called plant growth-promoting bacteria) have the potential to attenuate environmental stresses in plants, such as water deficit [7–10]. BM in the soil can induce plants to produce osmoregulant substances such as organic acids, amino acids, and soluble sugars and, thus, act synergistically, contributing to drought tolerance [11,12]. These microorganisms can produce auxins such as indole acetic acid, increasing the length of plant roots and, thus, leading to the greater uptake of water and nutrients from the soil [8]. In this sense, it has been observed that the inoculation of corn with *Bacillus amyloliquefaciens* increased the nutrient uptake and promoted growth mechanisms in plants, increasing the concentration of amino acids such as tryptophan, isoleucine, alanine, valine, and tyrosine and sugars such as fructose and glucose [11]. Likewise, Lima and collaborators [13] observed that the inoculation of corn with *B. subtilis* increased the leaf water content and stomatal regulation without impairing the photosynthetic rates. In addition to the effects on plants, BM can affect the biological activity of the soil, favor specific populations of microorganisms that act in key soil processes such as mineralization and the nitrification of soil nitrogen, and thus reduce the losses of this nutrient through leaching and volatilization processes [14,15].

The use of BM in agriculture is advantageous, because it is an environmentally friendly technology, since it can increase crop productivity and soil fertility without exerting any toxic effect on the environment [16,17]. The mechanisms of action of BM on plants such as nitrogen fixation, phosphate solubilization, the synthesis of phytohormones (especially IAA), and osmoregulant substances (such as amino sugars), especially in a controlled environment, have been demonstrated in some studies [9,15,18]. However, it is necessary to expand these studies, especially under field conditions, for a better understanding of the effects of BM on the physiological aspects of plants and on soil microbiological activity, which could represent modes of action of BM as attenuating water deficit in plants. In this sense, we hypothesized that BM improves the gas exchange of corn under a water deficit, promotes an increase in soil biological activity, and thus attenuates the adverse effects of irrigation deficit, increasing growth and productivity.

This study aimed to evaluate the effect of beneficial bacteria on gas exchange, growth, production, and the protein content in corn grains and soil microbiological activity under a water deficit.

2. Materials and Methods

2.1. Experimental Site Description

This research was carried out from July to November 2021 in field conditions at the experimental farm belonging to the Center for Agro-Food Science and Technology—CCTA of UFCG, located in the Sertão Paraibano mesoregion in the municipality of São Domingos—Paraíba. According to the Köppen classification adapted for Brazil, the climate is tropical semi-arid (Bsh), with an average annual temperature above 26.7 °C and an average yearly rainfall of 872 mm [19]. Climatological data for the experimental period (Figure 1) were collected using the AGRITEMPO agrometeorological monitoring system [20]. During the experimental period, no rainfall was recorded in the area.

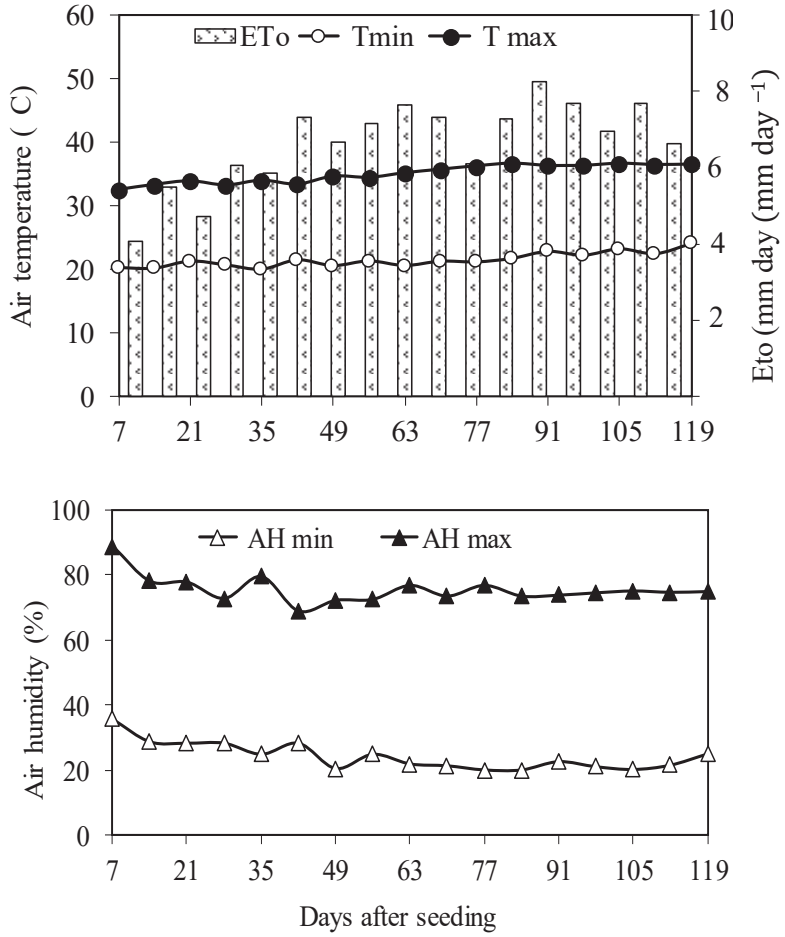

Figure 1. Reference evapotranspiration (ETo), maximum (Tmax) and minimum (Tmin) temperatures, and maximum (AHmax) and minimum (AHmin) air relative humidity during the field experiment period.

Before installing the experiment, a composite sample of soil from the area was obtained from 15 collection points, randomly obtained in the layer from 0 to 20 cm. The soil of the experimental site, classified as Planosol [21], was analyzed for its chemical and physical attributes (Table 1) at the Laboratory of Soils and Plant Nutrition of CCTA/UFCG, according to the methodology described by Emprapa [22].

Table 1. Physical and chemical attributes of the soil samples used in the experiment.

Chemicals Attributes	Value	Physical Attributes	Value
pH ($CaCl_2$)	6.20	total sand (g kg^{-1})	444
P (mg kg^{-1})	291	silt (g kg^{-1})	353
K^+ ($cmol_c$ dm^{-3})	1.19	clay (g kg^{-1})	203
Na^+ ($cmol_c$ dm^{-3})	0.54	BD (g cm^{-3})	1.36
Ca^{2+} ($cmol_c$ dm^{-3})	5.80	PD (g cm^{-3})	2.59
Mg^{2+} ($cmol_c$ dm^{-3})	3.40	TP (m^3 m^{-3})	0.47
H + Al ($cmol_c$ dm^{-3})	2.30	FC (%)	12.87
SOM (g kg^{-1})	6.40	PWP (%)	5.29
V (%)	83.0	AW (%)	7.58

SOM: soil organic matter, V: saturation of bases, BD: bulk density, PD: soil particle density, TP: total porosity, permanent wilting point (PWP), and AWC: available water content.

2.2. Treatments and Experimental Design

A field experiment was carried out, in which the treatments were composed of a 2 × 4 factorial scheme, corresponding to two irrigation levels (100% of ETc and 50% of ETc) and to four treatments (T) referring to the application of BM (C: control; T1: *Bacillus amyloliquefaciens* BV 03 + *Azospirillum brasiliense*; T2: *B. subtilis* BV-09; and T3: *A. brasiliense*). A randomized block design was used (Appendix A) with five replications, making a total of 40 subplots in the experiment as a whole.

2.3. Soil Tillage and Experiment Installation Details

Soil tillage consisted of carrying out two harrowing, the first being heavy and the second light, before sowing, aiming to break down and level the soil; after which, the planting furrows would be opened. The plants were grown at a spacing of 0.2 m × 1.0 m, corresponding to an estimated stand of 5 plants per linear meter. The spacing between plots was 1.0 m, while the blocks were separated by 2.0 m. The plots consisted of five cultivation lines measuring 4.0 m × 4.0 m. The portion of plot for data collection consisted of the three central lines measuring 2.0 m in length, resulting in an estimated total of 30 plants (Appendix A).

Sowing was carried out on 7 September 2021 using seeds of the hybrid corn cultivar K9555VIP3, which was chosen because it has a short cycle (about 110 days), high productivity, and resistance to the fall armyworm. The planting was carried out manually one day after planting fertilization (7 September 2021), sowing one seed per hole with spacings of 0.2 m.

The fertilization was carried out according to the Fertilization Recommendation Manual for the State of Pernambuco [23] based on the interpretation of the soil analysis of the experimental area. In the planting, 30 kg of N, 60 kg of P_2O_5, 45 kg of K_2O, and 24 kg of S in the form of magnesium sulfate were applied. Supplementary fertilization with nitrogen and potassium was applied at the rate of 50 kg of N per ha in the V4 stage (plants with four expanded leaves) and 50 kg of N, 45 kg of K_2O, 1 kg of B, and 2 kg of Zn in the V6 stage (plants with six expanded leaves). The nutrient sources used were urea (45% of N), potassium chloride (58% of K_2O), simple superphosphate (18% of P_2O_5), magnesium sulfate (9% of Mg and 12% of S), boric acid (17% B), and zinc sulfate (20% Zn). The N and K supplementary fertilizations were carried out via fertigation using the irrigation system.

2.4. Treatments Composition Composition and Application of Treatments

The inoculation with BM was carried out exclusively via fertigation using suspensions of microorganisms in a proportion of 4 L ha^{-1}. The T1 treatment (*Bacillus amyloliquefaciens* + *A. brasiliense*) consisted of 1.0 L ha^{-1} of the commercial product containing 3.0×10^9 CFU/mL of *B. amyloliquefaciens* and 3.0 L ha^{-1} of the commercial product containing 1.0×10^9 CFU/mL of *A. Brasiliense*. Treatment T2 corresponded to the commercial product containing 1.0×10^8 CFU/mL of *Bacillus subtilis* BV-09, and treatment T3 corresponded to the commercial product containing 1.0×10^9 CFU/mL of *A. Brasiliense* applied at a dose of 4 L ha^{-1}. Treatments were performed seven days after seedling emergence. The doses of each product (or combination) were diluted in water at a rate of 4 L per 2500 L of water and were applied using a manual sprayer on the root zone of the plants. The same procedure was adopted in the control treatment but used only water without any product.

2.5. Irrigation Management

The plants were drip irrigated, with drippers spaced 0.20 m. After the emergence and standardization of the number of plants per plot, the plants were irrigated following the different water regimes. The total irrigation volume required (*TIR*) of each irrigation level was obtained by the following Equation (1) [24]:

$$TIR = \frac{(FC - PWP) \times Z \times BD \times f}{10 \times Ea} \quad (1)$$

where *TIR* corresponded to the initial total water depth to be applied in mm, *FC* was the soil moisture corresponding to the field capacity in %, *PWP* was the soil moisture corresponding to the wilting point in %, *Z* was the effective corn root system depth (30 cm), *BD* was the soil bulk density in g cm^{-3}, *f* was the water availability factor for maize (0.5), and *Ea* was the application efficiency (0.90). During the experiment, meteorological data were obtained from the automatic meteorological station in the municipality of São Gonçalo, Paraíba, as it is the closest to the experiment site, through the website [25].

The control of the volume of water corresponding to each water regime was performed daily at a standardized time according to the ratio of the flow rate of the drippers by the time to reach the proportions of crop evapotranspiration (ETc). As the time interval for each volume of the respective water regime was reached, successive disconnections of the drip strips corresponding to each irrigation level were performed. The irrigation depth corresponding to 100% of ETc was calculated according to Jesen's equation [26] using the following expression: ETc = $Kc \times ETo$. ETc is the crop evapotranspiration in mm day^{-1}, *ETo* is the reference evaporation in mm day^{-1}, and *Kc* is the crop coefficient. The *Kc* values adopted for corn (initial stage: 0.13, vegetative stage: 0.55, flowering: 1.00, reproductive stage: 1.20, and final stage: 0.90) as a function of its phenological phases were based on [27]. The daily supply of irrigation depths was carried out through the irrigation time considering the characteristics of the cultivation system and the irrigation system according to Equation (2):

$$Ti = \frac{Eto \times Kc \times A}{Ea \times n \times q} \quad (2)$$

where *Ti* is the irrigation time in hours, *ETo* is the reference evaporation in mm day^{-1}, *A* is the area occupied by a plant in m^2, *n* is the number of drippers per plant, *q* is the dripper flow in L h^{-1}, and *Ea* is the application efficiency (0.90). Water application uniformity tests were determined according to the Christiansen Uniformity Coefficient (CUC) evaluation methodology proposed by Christiansen [28].

2.6. Phytosanitary Control

Weed control was done mechanically and manually using simple tools such as hand hoes. Regarding insects, there was no need to apply any product for pest control due to the low incidence in the area.

2.7. Assessment of Growth, Gas Exchange, and Leaf Nitrogen Content

In the female inflorescence stage gas exchange, the culm diameter, plant height, and leaf area index (LAI) were determined. On this occasion, photosynthesis (A) (μmol CO_2 m^{-2} s^{-1}), stomatal conductance (gs) (mol m^{-2} s^{-1}), the transpiration rate (E) (mmol H_2O m^{-2} s^{-1}), and intercellular CO_2 concentration (Ci) (mol CO_2 m^{-2} s^{-1}), with an infrared gas analyzer (IRGA) (LCpro Analytical Development, Kings Lynn, UK) with a constant light source of 2000 μmol of photons and ambient CO_2 concentration, were evaluated. Readings were taken from 7:00 a.m. to 9:00 a.m. using the diagnostic sheet (leaf opposite to the cob) [29]. The LAI was estimated using a photosynthetically active radiation meter (AccuPAR model LP-80). Readings were taken from 8:00 a.m. to 11:00 a.m. In each plot, five readings were performed below the leaves close to the ground, corresponding to the four cardinal points of the plot. The diagnostic leaves of five plants of each useful plot were collected on the same day to determine the total nitrogen (N) content. The leaves were dried in a forced circulation oven at 60–65 °C and then ground in a Willey-type knife mill. Then, sulfuric digestion was performed, followed by distillation and titration [29].

2.8. Mineral Nitrogen Contents and Soil Microbiological Activity

In each useful plot, four soil subsamples were collected close to the planting line under the influence of the corn rhizosphere in the layer from 0 to 20 cm. After homogenization, 20 g of the composite samples were immediately placed in plastic flasks containing 100 mL of a 1.0 mol L^{-1} KCl (potassium chloride) solution, then placed in a refrigerator [30].

After defrosting, shaking at 180 rpm, and filtering, 20 mL of the extract were placed in distillation tubes to determine the NH_4^+ (ammonium) and NO_3^- (nitrate) contents by the Kjeldahl nitrogen micro still method [30]. Initially, 0.2 g of calcined MgO was added to each distillation tube. After distillation, the ammonium fractions were obtained by titration with HCl (hydrochloric acid) 0.07143 mol L^{-1} after being collected in indicators with boric acid. Nitric nitrogen was determined using the same extract (same tube) used for ammonium distillation and then adding 0.2 g of Devarda's alloy and sending it to a new distillation. Then, it was titrated with the same acid used for ammonium. Mineral nitrogen was calculated by adding $NH_4^+ + NO_3^-$.

The remaining soil composite samples from each plot were frozen to further evaluate the soil respiration rate, microbial biomass carbon, and metabolic quotient. Soil microbial respiration was measured by capturing the C-CO_2 produced in the soil by NaOH (sodium hydroxide) in a hermetically sealed environment [31]. Biomass carbon was evaluated using the irradiation/extraction method, which has, as its basic principle, the elimination of microorganisms by electromagnetic radiation from a microwave oven [32–34]. Each soil sample was subdivided into irradiated and nonirradiated samples. After irradiation, the samples were transferred to a 125 mL Erlenmeyer flask and identified according to the procedure. Then, 80 mL of K_2SO_4 (potassium sulfate) extracting solution was added. The samples were shaken for 30 min in a horizontal shaker at 150 rpm and then kept at rest for 30 min. Subsequently, the samples were filtered in recipients with filter paper. The carbon present in the extracts was determined by pipetting 10 mL of the filtered extract into a 125 mL Erlenmeyer flask, where 2 mL of 0.066 mol L^{-1} $K_2Cr_2O_7$ (potassium dichromate) solution was added. Then, 10 mL of H_2SO_4 (sulfuric acid) was added. After the samples were lowered to room temperature, 50 mL of distilled water was added to each Erlenmeyer flask, and the titration was performed by adding three drops of ferroin as an indicator and ammoniacal ferrous sulfate 0.03 mol L^{-1} ammoniacal ferrous sulfate.

2.9. Grain Yield and Protein Content

The ears were harvested manually five to eight days after the grains reached physiological maturity, with a moisture level below 15% (wet basis). The harvest was carried out using the useful plot, collecting 10 ears to assess the characteristics of the ears, the thousand-grain weight, and the grain yield. Based on the grain yield in the 16 m^2 plots, by extrapolation to 10,000 m^2, the yields in kg ha^{-1} were calculated. The yield data were corrected to 13% moisture (wet basis). The moisture content of the grains was evaluated using the oven method at 105 °C for 24 h [35]. The protein contents in the grains were determined by the Kjeldahl micro still method [30] with sulfuric extraction and subsequent distillation. For this, the total nitrogen (N) contents were initially determined in 0.5 g of ground grains and later converted into crude protein by a multiplication factor of 6.25 [36]. The protein yield was obtained by multiplying the protein content by the grain yield and adjusting the units.

2.10. Statistical Analysis

Data referring to the measured variables were submitted to an analysis of variance (ANOVA) and Tukey's test at the 0.05 probability level using SISVAR® statistical software version 5.6 [37]. A multivariate analysis of the results was performed using the principal components analysis (PCA), synthesizing the amount of relevant information contained in the original data set in a smaller number of dimensions [38]. From the reduction of the dimensions, the original data of the variables of each component were submitted to a multivariate analysis of variance (MANOVA) using Hotelling [39] at the 0.05 probability level for the irrigation levels (I) and the related treatments' beneficial microorganisms (BM), as well as for the I × BM interaction. Only variables with a correlation coefficient greater than or equal to 0.6 were kept in each principal component (PC) [40]. For the multivariate statistical analysis, software Statistica v. 7.0 was used [41].

3. Results

3.1. Plant Growth and Leaf Nitrogen Content

According to the analysis of variance (Table 2), the irrigation levels influenced the plant height (PH), leaf area index (LAI), stem diameter (CD), and leaf nitrogen content (leaf N), while the treatments related to inoculation with plant growth-promoting bacteria (BM) influenced only the index and the variables LAI and leaf N (Table 2). There were interactions between irrigation levels and BM treatments only for the LAI and PH. The ETc irrigation level of 50% decreased the PH, LAI, CD, and leaf N values by approximately 20%, 32%, 6%, and 22%, respectively (Figure 2). Under water deficit (50% of ETc), treatment C (without inoculation) provided a higher PH value compared to treatment T3 (*Azospirillum brasiliense*). Still, both did not differ between treatments T1 (*Bacillus amyloliquefaciens* + *A. brasiliense*) and T2 (*B. subtilis*). Under full irrigation (100% of ETc), the treatments with BM did not change the plant height. The T1 treatment provided a higher LAI value than the control treatment. However, these treatments did not differ from the others. Treatment T2 increased the leaf N content when compared to the control and treatment T1 but not when compared to treatment T3.

Table 2. Summary of the analysis of variance for the leaf area index (LAI), plant height (PH), stem diameter (CD), and nitrogen content in leaves (N leaf).

Source of Variance	DF	PH	LAI	CD	Leaf N
		Mean Square			
Irrigation levels (I)	1	45,611.032 **	1.917 **	27.400 **	290.005 **
Blocks (replications)	4	490.803	0.112	22.98	20.256
Microorganisms (BM)	3	82.916 ^{ns}	0.129 *	0.448 ^{ns}	13.0878 **
I × BM	3	605.121 **	0.074 *	1.493 ^{ns}	1.898 ^{ns}
Error	28	131.743	0.034	1.066	2.488
CV (%)	-	6.89	9.37	3.94	7.20

CV: coefficient of variation. ** $p < 0.01$ and * $p < 0.05$ by F test. ^{ns} Stands for nonsignificant data at the 0.05 probability level. DF: degrees of freedom.

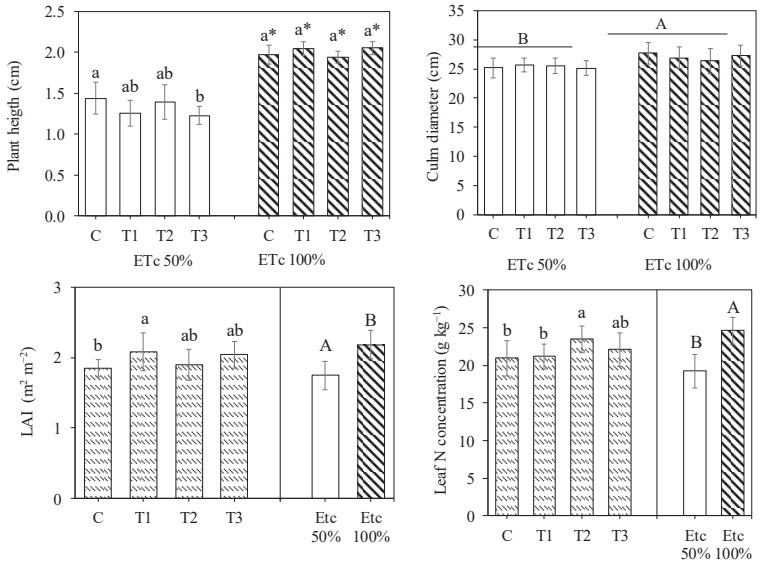

Figure 2. Leaf area index, plant height, culm diameter, and nitrogen content in leaves as a function of applying plant growth-promoting bacteria (BM) (C: control, T1: *Bacillus amyloliquefaciens* + *Azospirillum brasiliense*, T2: *B. subtilis*, and T3: *A. brasiliense*). Data are means ± S.E. Lowercase letters compare the treatments referring to BM application, and uppercase compare the irrigation levels. * Indicates significant differences between irrigation levels (50% ETc and 100% ETc) by Tukey's test at the 0.05 probability level.

3.2. Gas Exchange

The irrigation levels influenced the photosynthetic rate (A), stomatal conductance (Gs), transpiration rate (E), and intercellular concentration of CO_2 (Ci) (Table 3). The treatments related to BM only influenced the values of Ci and E. There was an interaction between the irrigation levels and the treatments with BM only for the transpiration rate, which was also affected by the treatments with BM. On average, a water deficit reduced the photosynthetic rate, stomatal conductance, and transpiration rate by 22%, 41%, and 16%, respectively (Figure 3). Treatment T3 provided the lowest value of Ci without differing from treatment T2. Treatments C and T1 provided similar values of Ci. On average, water restriction increased the Ci by 13% compared to full irrigation. At the 50% ETc irrigation level, the T3 treatment provided a 35% increase in the E value compared to the control treatment without differing from the T1 and T2 treatments. Under full irrigation, treatment T2 stood out, increasing the evapotranspiration rate by 32% compared to the control. However, this treatment was similar to treatments T1 and T3.

Table 3. Summary of the analysis of variance for the CO_2 assimilation rate (A), internal CO_2 concentration (Ci), stomatal conductance (gs), and transpiration rate (E).

Source of Variance	DF	A	Ci	Gs	E
		Mean Square			
Irrigation levels (I)	1	1192.326 **	603.049 *	0.509 **	16.593 **
Blocks (replications)	4	405.009	56.204	0.165	25.570
Microorganisms (BM)	3	71.679 ^{ns}	567.319 **	0.039 ^{ns}	6.732 **
I × BM	3	63.089 ^{ns}	191.019 ^{ns}	0.029 ^{ns}	0.778 **
Error	28	61.239	85.196	0.021	0.814
CV (%)	-	17.57	15.11	32.90	12.38

CV: coefficient of variation. ** Significant ($p < 0.01$) and * Significant ($p < 0.05$) by F test. ^{ns} Stands for nonsignificant data at the 5% probability level. DF: degrees of freedom.

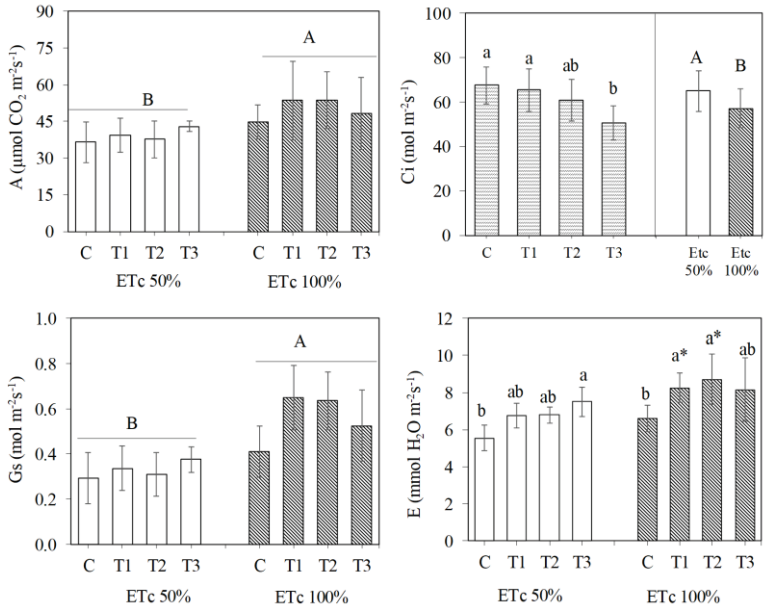

Figure 3. CO_2 assimilation rate (A), internal CO_2 concentration (Ci), stomatal conductance (gs), and transpiration rate (E) as a function of the application of plant growth-promoting bacteria (BM) (C: control, T1: *Bacillus amyloliquefaciens* + *Azospirillum brasiliense*, T2: *B. subtilis*, and T3: *A. brasiliense*) and the irrigation levels. Data are means ± S.E. Lowercase letters compare the treatments referring to BM application, and uppercase compares the irrigation level. * Indicates a significant difference between the irrigation levels by Tukey's test at the 0.05 probability level.

3.3. Grain Yield and Protein Yield

According to the analysis of variance, the irrigation levels influenced the cob length and weight, thousand-grain weight (TGW), grain yield (GY), protein concentration in the grain (PC), and grain protein yield (GPY) (Table 4). The treatments related to BM influenced the cob length, GY, and GPY. There was an I × BM interaction for TGW, GY, and GPY. At both irrigation levels, the treatments related to BM did not influence the ear length (Figure 4). On average, a water deficit decreased the ear length by 28%. The ear weight was higher in the T3 treatment, which differed only from the T2 treatment, and water deficit reduced the ear weight by 35%. Under irrigation restriction, TGW was superior in the T2 treatment but differed only from treatment T1, while, under full irrigation, the BM treatments did not change the results of this variable. The full irrigation level provided higher values and TGW in treatments T1 and T2. On average, water restriction decreased the grain yield by 38%. However, at this level of irrigation, the T1 treatment provided an increase of 34% compared to the control, which represented 74% of the average productivity of the treatments without water restriction. At both irrigation levels, the treatments related to BM did not affect the protein concentration in the grains. However, the water restriction increased the value of this variable by 12%. The protein yield followed the same trend as the grain yield; that is, under an irrigation deficit, the highest value was provided by treatment T1, while, under full irrigation, the treatments related to BM did not affect the value of this variable.

Table 4. Summary of the analysis of variance for the cob length, cob weight, thousand-grain weight (TGW), grain productivity (GY), grain protein concentration (PC), and grain protein production (GPY).

		Mean Square		
Source of Variance	**DF**	**Cob Length**	**Cob Weight**	**TGW**
Irrigation levels (I)	1	317.109 **	88,258.659 **	5808.908 **
Blocks (replications)	4	16.567	1506.904	2367.481
Microorganisms (BM)	3	2.565 ^{ns}	2141.909 **	234.574 ^{ns}
I × B	3	7.064 ^{ns}	696.635 ^{ns}	862.145 *
Error	28	4.262	376.260	232.861
CV (%)	-	11.86	8.72	5.01
Source of variance	DF	GY	PC	GPY
Irrigation levels (I)	1	121,010,430.8 **	9.844 **	558,005.970 **
Blocks (replications)	4	1,748,237.0	0.069	14,160.126
BM	3	2,916,790.2 **	0.580 ^{ns}	21,538.689 **
I × BM	3	1,160,782.8 *	0.593 ^{ns}	18,627.769 *
Error	28	318,616.4	0.406	4391.232
CV (%)	-	7.75	7.13	10.31

CV: coefficient of variation. ** $p < 0.01$ and * $p < 0.05$ by F test. ^{ns} Stands for nonsignificant data at the 0.05 probability level. DF: degrees of freedom.

3.4. Mineral Nitrogen Contents and Soil Microbiological Activity

According to the analysis of variance, the irrigation levels (I), treatments related to BM, and the interaction I × BM affected the levels of ammonium (NH_4^+), nitrate (NO_3^-), and mineral nitrogen ($NH_4^+ + NO_3^-$) in the ground (Table 5). The irrigation levels and I × BM interaction influenced the soil respiration (Sresp), microbial biomass carbon concentration (C-mic), and respiratory quotient (qCO_2). The irrigation deficit provided the highest levels of NH_4^+, NO_3^-, and mineral nitrogen ($NH_4^+ + NO_3^-$) in the soil, with increments of 81%, 106%, and 93%, respectively, compared to full irrigation (Figure 5). In water restriction conditions, the T1 treatment was superior to the other treatments and provided an increase of 47% compared to the control. On the other hand, the NO_3^- levels were higher in treatments T2 and T3, which, together with the T1 treatment, were higher than the control.

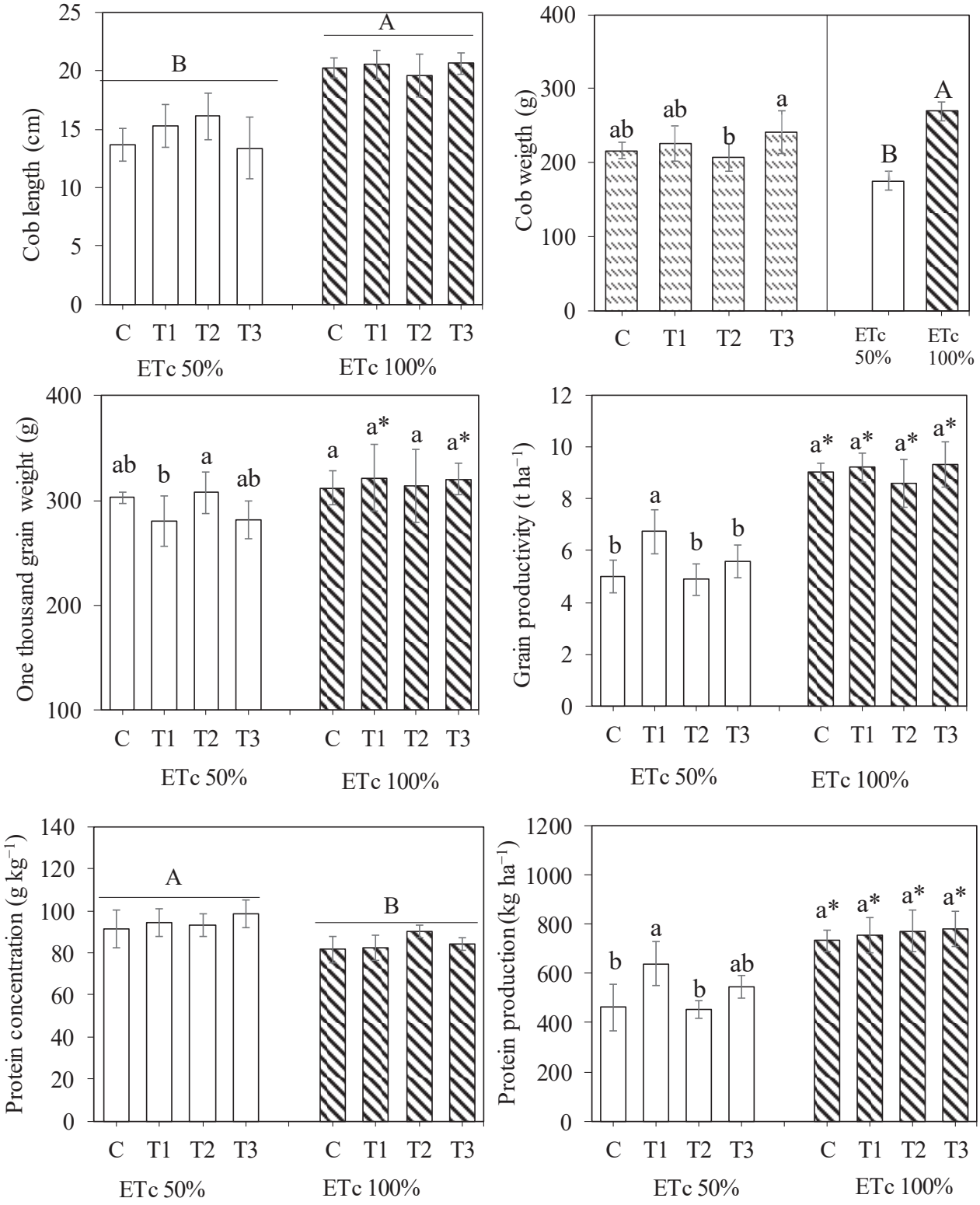

Figure 4. Yield characteristics and proteins in corn grains as a function of applying plant growth-promoting bacteria (BM) (C: control, T1: *Bacillus amyloliquefaciens* + *Azospirillum brasiliense*, T2: *B. subtilis*, and T3: *A. brasiliense*) and the irrigation levels. Data are means ± S.E. Lowercase letters compare the treatments referring to PGPB application, and uppercase compares the irrigation level. * Indicates a significant difference between the irrigation levels by Tukey's test at the 0.05 probability level.

Table 5. Summary of the analysis of variance for the soil nitrogen concentrations of ammonium (NH_4^+), nitrate (NO_3^-), and mineral nitrogen (NH_4^+ + NO_3^-); soil respiration (Sresp); biomass carbon (C-mic); and metabolic quotient (qCO_2).

Source of Variance	DF	Mean Square NH_4^+	NO_3^-	Mineral N
Irrigation levels (I)	1	5790.039 **	11,945.664 **	29,787.444 **
Blocks (replications)	4	268.351563	262.609375	443.141
Microorganisms (BM)	3	522.539 *	2132.265 **	2556.707 **
I × BM	3	685.872 **	1225.638 **	1493.382 **
Error	28	134.914063	153.234	133.017
CV (%)	-	26.16	27.21	13.45
Source of variance	DF	Sresp	C-mic	qCO_2
Irrigation levels (I)	1	78.167 *	363,778.833 **	0.077 **
Blocks (replications)	4	4.322	8329.880	0.001
BM	3	30.192 ^{ns}	6113.058	0.009 **
I × BM	3	230.833 **	16,440.665 *	0.012 **
Error	28	13.722	3724.769	0.001
CV (%)	-	20.28	24.86	23.38

CV: coefficient of variation. ** $p < 0.01$ and * $p < 0.05$ by F test. ^{ns} Stands for nonsignificant data at the 0.05% probability level. DF: degrees of freedom.

In the same way, the mineral nitrogen contents were higher in the treatments constituted by the inoculation of BM. Under full irrigation, the treatments related to BM did not change the concentrations of nitrate, ammonium, and mineral nitrogen. Under irrigation deficit, the highest soil respiration rates (Sresp) were obtained in treatments T1 and T2, which were superior to the control and T3 treatment (Figure 5). Under full irrigation conditions, the effect was inverse; the control and T3 treatments were superior to the T1 and T2 treatments. There was no difference between irrigation levels in the T1 treatment. The concentration of C-mic under irrigation deficit was lower in the control treatment but differed only from the T2 treatment. Under full irrigation, BM treatments did not change the C-mic values. On average, there was a 44% reduction in C-mic under full irrigation. The qCO_2 values did not differ between the BM treatments under full irrigation, while, under irrigation deficit, the lowest values were provided by treatments T1 and T2. However, the T1 treatment did not differ from the control treatment. In all BM treatments, the qCO_2 values were higher at the full irrigation level.

3.5. Principal Component Analysis

The multidimensional space of the original variables was reduced to two principal components (PC1 and PC2) with eigenvalues greater than $\lambda > 1.0$, according to Kaiser (1960). The eigenvalues and percentages that explained the variation for each component represented 87.21% of the total variation (Table 6). PC1 explained 76.12% of the total variance, formed by most of the variables analyzed. PC2 represented 11.09% of the remaining variance. The two-dimensional projections of the effects of the treatments and variables in the first and second main components (PC1 and PC2) are shown in Figure 6. According to the groupings of the variables presented, in PC 1, it was observed that most of the variables evaluated in the plants were positively correlated with the irrigation level of 100% of ETc, regardless of the BM treatments. In turn, the variables assessed in the soil were associated with the level of irrigation at 50% of ETc, with an emphasis on treatments T2 and T3.

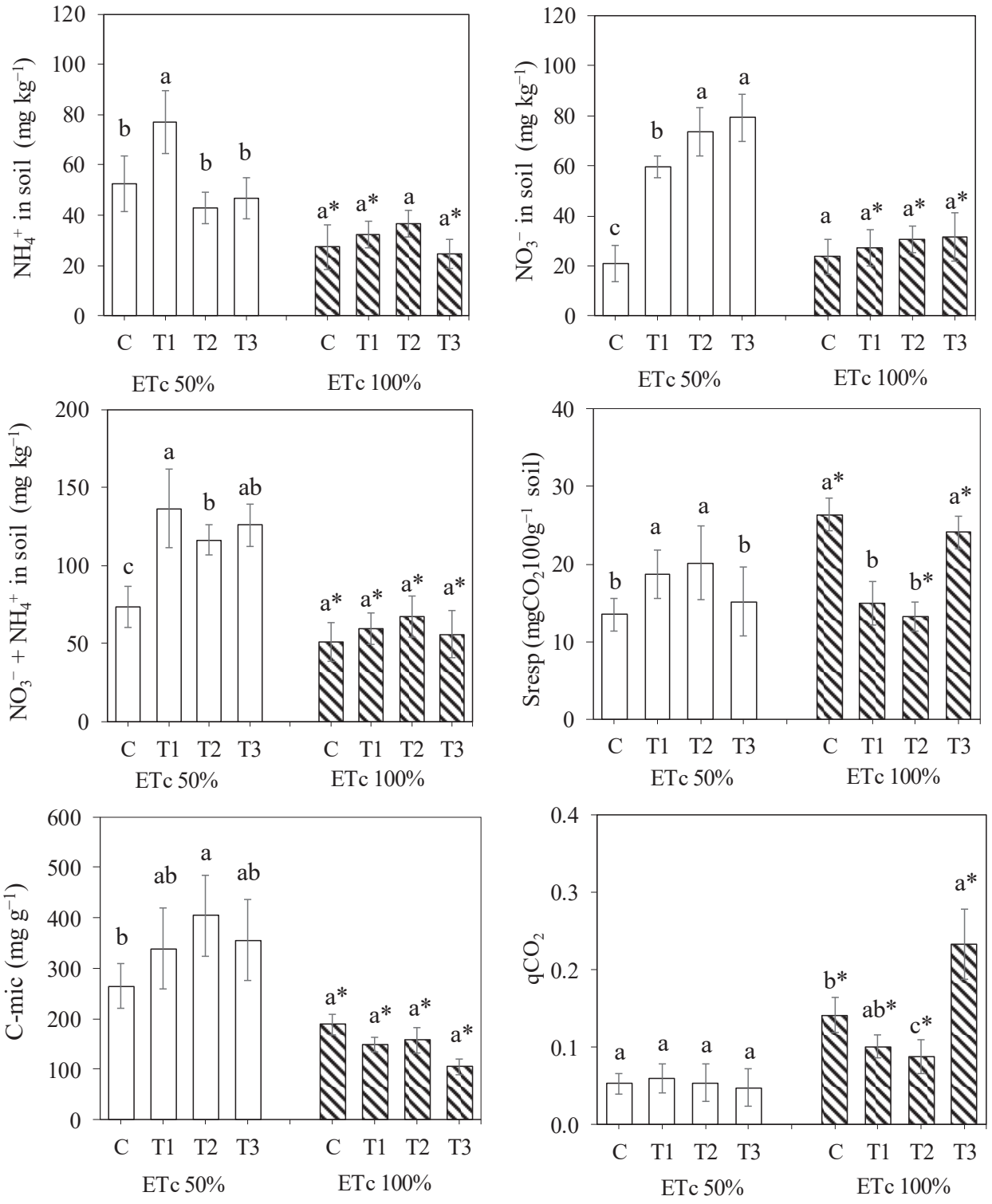

Figure 5. Nitrogen concentrations of ammonium (NH_4^+), nitrate (NO_3^-), and mineral nitrogen ($NH_4^+ + NO_3^-$); soil respiration; microbial biomass carbon (C-mic); and metabolic quotient (qCO_2) as a function of the application of plant growth-promoting bacteria (PGPB) (C: control, T1: *Bacillus amyloliquefaciens* + *Azospirillum brasiliense*, T2: *B. subtilis*, and T3: *A. brasiliense*) and the irrigation levels. Data are means ± S.E. Lowercase letters compare the treatments referring to the PGPB application. * Indicates a significant difference between the irrigation levels by Tukey's test at the 0.05 probability level.

Table 6. Eigenvalues, percentages of the total variance explained, in the multivariate analysis of variance (MANOVA), and correlations (r) between the original variables and the principal components.

Parameter	Principal Components	
	PC1	PC2
Eigenvalues (λ)	11.42	1.66
Percentage total variance (S^2%)	76.12	11.09
Hotelling test (T^2) for irrigation levels (L)	0.01	0.01
Hotelling test (T^2) for beneficial microorganisms (BM)	0.01	0.01
Hotelling test (T^2) for interaction (L × BM)	0.01	0.01
Variables	Correlation coefficient	
Grain yield (GY)	0.96	0.08
Internal CO_2 concentration (Ci)	−0.84	0.26
Transpiration rate (E)	0.65	−0.75
stomatal conductance (GS)	0.92	−0.29
CO_2 assimilation rate (A)	0.95	−0.28
Leaf área index (LAI)	0.93	−0.14
Plant heigth (PH)	0.94	0.27
Culm diameter (CD)	0.96	0.12
Grain protein concentration (GPC)	−0.82	−0.46
Grain protein production (GPY)	0.91	−0.09
Nitrogen content in leaves (Nleaf)	0.90	−0.08
Nitrogen concentration as ammonium (NH_4^+)	−0.78	−0.06
Nitrogen concentration as nitrate (NO_3^-)	−0.67	−0.68
Microbial biomass carbon (C-mic)	−0.94	−0.23
Metabolic quotient (qCO_2)	0.86	−0.02

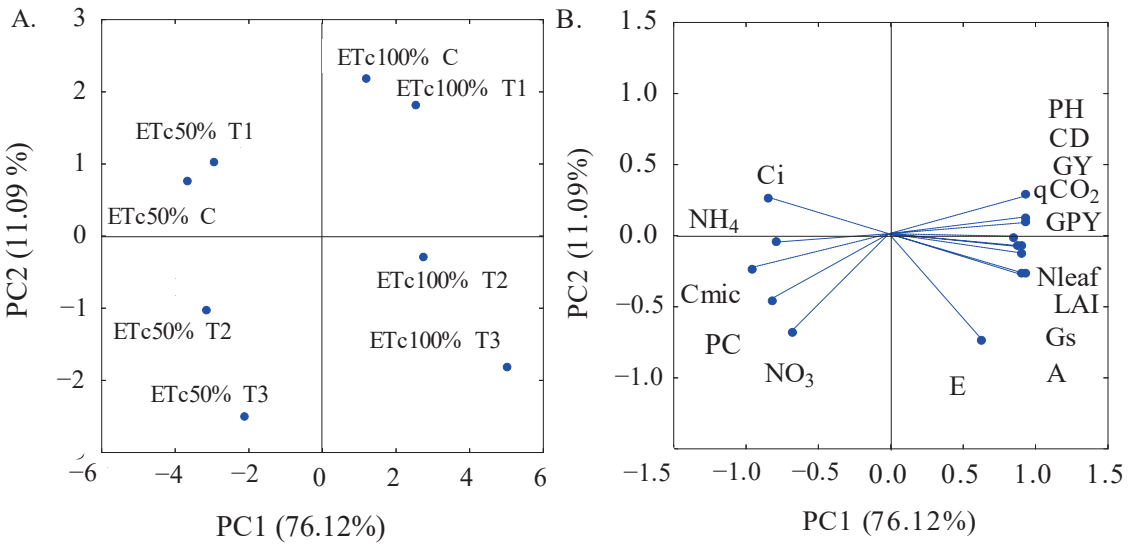

Figure 6. Two-dimensional projection of the scores of the main components for the factors irrigation levels and plant growth-promoting bacteria (**A**) and of the variables analyzed (**B**) in the two main components (PC1 and PC2). C: control, T1: *Bacillus amyloliquefaciens* + *Azospirillum brasiliense*, T2: *B. subtilis*, and T3: *A. brasiliense*).

4. Discussion

In the present study, the possibility of BM attenuating the adverse effects of water deficit in corn was evaluated through the plant variables (growth, gas exchange, productivity, and protein content) and soil (mineral nitrogen and microbiological activity). The water deficit imposed by the 50% ETc water depth reduced corn's growth and leaf area, as well as the nitrogen content in the leaves. Drought stress causes a decrease in cell turgor, which is

essential for proper cellular metabolism, such as photosynthesis, enzymatic activity [3,4], and nutrient absorption [5]. In addition, under water deficit, nitrogen contact with the roots, through diffusion and mainly by mass flow, can be reduced [42], decreasing the uptake of this nutrient by the plant [5]. On the other hand, regardless of the irrigation level, the inoculation of plants with *Bacillus subtilis* promoted an increase of 13% in the leaf area index and 12% in the N content of the leaves compared to the treatment without the inoculation. *B. subtilis* also increased the leaf area in sweet peppers [43] and leaf N content in sugarcane [44]. Aquino [45] observed that five strains of *B. subtilis* increased the foliar N content in corn crops compared to uninoculated plants. This indicates that *B. subtilis* fixed atmospheric N and improved corn nitrogen nutrition [13]. However, the effect of treatments containing BM on maize growth was not well defined, as observed in other studies [7,13].

The gas exchange measurement showed that corn plants closed their stomata (decreased stomatal conductance) under water deficit to reduce water loss. This result was accompanied by a decrease in the photosynthetic rate, an increase in the internal concentration of CO_2, and a decrease in the transpiration rate. In water restriction conditions, corn inoculation with *Azospirillum brasiliense* increased the transpiration rate by 35% compared to the treatment without inoculation. Physiological changes with the use of BM have also been reported in previous works [7,46]. BM application in the soil can lead to stimulating the production of osmoregulatory substances by the plant and, thus, act synergistically, contributing to drought tolerance [11,12]. These organisms can produce auxins such as indole acetic acid, increasing the length of plant roots, thus leading to a greater absorption of water and nutrients from the soil [8]. In this sense, it has been observed [12] that the inoculation of corn with *B. amyloliquefaciens* increased the nutrient absorption and promoted growth mechanisms in plants, such as an increased concentration of amino acids such as tryptophan, isoleucine, alanine, valine, and tyrosine and sugars such as fructose and glucose.

The negative effects of water restriction on maize growth and gas exchange were also reflected in a lower grain yield (38% reduction). Water scarcity negatively affects corn development at all phenological stages, promoting an increase in flowering days, maturation days, and anthesis interval and a decrease in leaf area, negatively affecting flowering and grain filling and seriously compromising corn production [6]. At the irrigation level of 50% of ETc, the inoculation of plants with *B. amyloliquefaciens* and with *A. brasiliense* provided a productivity increase of 35% in relation to stressed plants without the inoculation. In previous works, it was observed that the inoculation of *B. amyloliquefaciens* and *B. subtilis*, associated or not with other BM, was efficient in attenuating water stress in several cultures, promoting an increase in growth and production [9,15,18]. Water restriction increased the protein content (12% increase) in the grains. Other studies have also reported this effect [16,45]. Probably, the increase in protein concentration was due to the decrease in the thousand-grain weight (8% on average in the BM treatments) compared to the level of complete irrigation combined with a decrease in the rate of carbon assimilation and, consequently, the starch synthesis, increasing the proportion of proteins in the grains [46]. Despite the increase in the protein content in the grains, the water deficit reduced the protein yield by 31% due to the severe decrease in grain yield. Although the water deficit caused this antagonistic effect between the protein content and the yield, this is a relevant aspect to be addressed in future research, because there is a possibility that there is a balancing point between the increase in the protein content in the grains caused by water stress and adequate corn grain yield through irrigation depth management during the phenological phases of the crop [47,48].

The concentration of mineral nitrogen (N), as ammonium (NH_4^+) or NO_3^-, increased due to the water deficit. In previous works, higher concentrations of mineral N were also observed in soil under water deficits [5,8,49]. Water restriction possibly decreased the rate of N absorption and accumulation by corn, providing higher levels of mineral N in the soil and decreasing the levels of this nutrient in the leaves. The inoculation of plants with *B.*

amyloliquefaciens + *A. brasiliense* consistently increased the NH_4^+ content and respiration rate under water restriction but not under full irrigation. The role of BM in increasing mineral N in the soil needs to be better understood. Previous research demonstrated that *B. subtilis* decreased N volatilization in the form of NH_3 after mineralization [15]. In addition, an inoculation with *B. amyloliquefaciens* + *A. brasiliense* could provide an increase in the diversity of microorganisms involved in the mineralization of organic matter [50] or even stimulate the decomposition of organic matter and N mineralization [51] or stimulate root growth and increase the soil organic matter content [52]. The increase in productivity in the T1 treatment is possibly due to the synergistic effect between *B. amyloliquefaciens* and *A. brasiliense.* In another work, with a corn crop, the authors observed that the solubilization of phosphorus bound to calcium and iron, and the mineralization of sodium phytate was greater when they were inoculated together in comparison to the separate inoculations, enhancing the release of organic acids. In the present work, the increase in microbial biomass carbon under the water deficit, mainly in the T2 treatment (*B. subtilis*), was due to the higher microbiological activity. However, at this level of irrigation, the metabolic quotient was not altered. In this sense, Gebauer and collaborators [17] observed that a water deficit favored certain groups of microorganisms that promoted plant growth in soil cultivated with wheat and barley, which was interpreted as an adaptive strategy of plants to water stress.

The multivariate principal component analysis (PCA) demonstrated, more emphatically, a clear separation of the average variables in the plants (except the internal CO_2 and protein content) from the variables measured in the soil. Thus, according to PC1, the variables measured in the plants were closely related to the level of full irrigation (100% ETc). In comparison, most of the variables measured in the soil benefited from the irrigation deficit (50% ETc). The PCA also showed that the inoculation of corn with BM favored soil biological activity and promoted an increase in the grain yield, especially under the water deficit.

5. Conclusions

Our results suggest that combined *Bacillus amyloliquefaciens* co-inoculated with *Azospirillum brasiliense* contributed to attenuating the adverse effects of water deficit in maize. Under the water deficit, *Bacillus subtilis* and *A. brasiliense* inoculated separately did not prevent water stress in corn but increased the mineral nitrogen content in the soil. In the present study, a 50% reduction in irrigation depth severely restricted corn growth, gas exchange, and decreased the grain yield by 38%. On the other hand, the water deficit increased the protein content in the grains and the concentration of mineral nitrogen in the soil, especially when the plants were inoculated with plant growth-promoting bacteria (BM). In water stress conditions, the inoculation with BM increased corn productivity by 35% and increased soil microbial activity. The findings of this research reinforced the results of previous research and represented a breakthrough in understanding the role of the interactions between plants and microorganisms in adapting to environmental adversities such as water stress.

Author Contributions: Conceptualization, J.L.A. and R.H.C.R.; methodology, J.L.A., J.d.M.A., J.Z.L.S., R.d.S.B., F.M.N.d.C., G.S.d.L., L.N.d.F., A.S.L. and A.E.P.N.; software, A.A.R.d.S. and J.L.A.; validation, F.B.N., J.L.A. and J.Z.L.S.; formal analysis, G.S.d.L. and A.A.R.d.S.; investigation, J.L.A.; resources, J.L.A. and G.S.d.L.; data curation, J.L.A., R.H.C.R. and J.d.M.A.; writing—original draft preparation, J.L.A., F.B.N. and L.C.d.S.; writing—review and editing, J.L.A., F.V.d.S.S. and J.Z.L.S.; visualization, J.Z.L.S.; supervision, J.L.A.; project administration, J.L.A.; and funding acquisition, J.L.A. All authors have read and agreed to the published version of the manuscript.

Funding: This research received no external funding.

Institutional Review Board Statement: Not applicable.

Data Availability Statement: The data used to support the findings of this study are included within the article.

Acknowledgments: Acknowledgments are due to the companies Vitamais® Agropecuária LTDA and Ecofertil® Fertilizantes Orgânicos, for supplying the corn seeds, fertilizers, and irrigation materials.

Conflicts of Interest: The authors declare no conflict of interest.

Appendix A

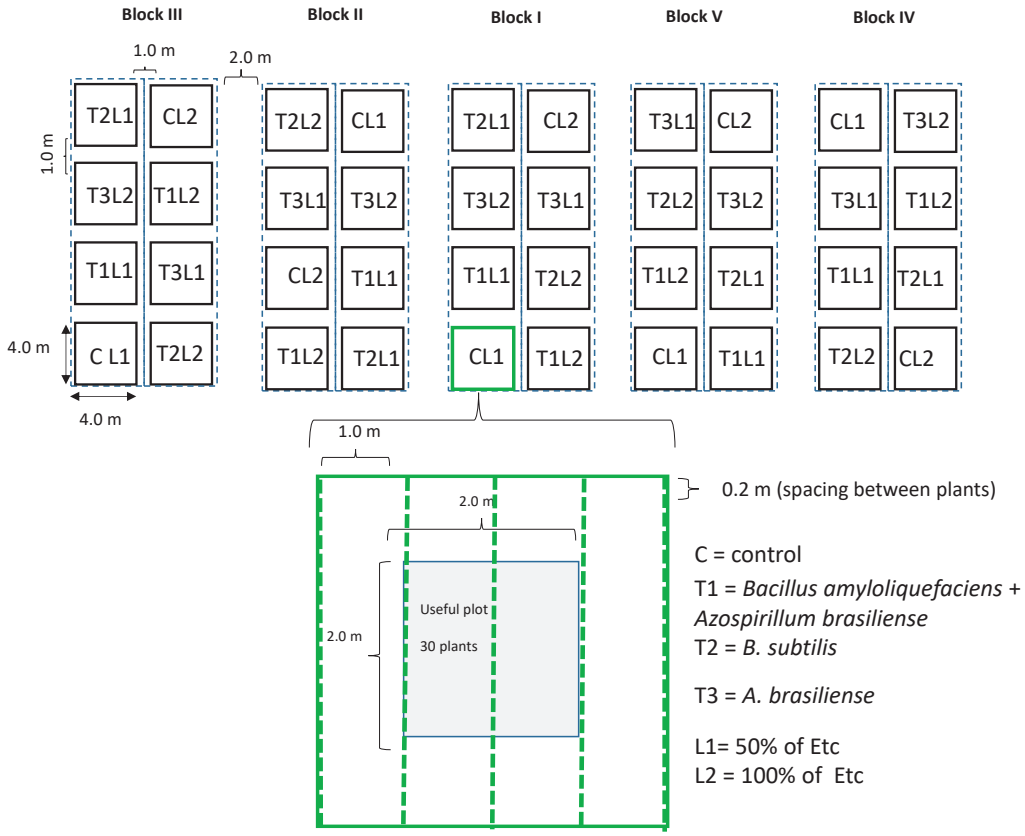

Figure A1. Experimental design used in the research showing the distribution of blocks, combination of irrigation depths with treatments with beneficial microorganisms, delimitation of experimental plots, and useful plot, as well as spacing between blocks, plots, planting rows, and plants.

Figure A2. Overview of the experimental area showing the installation of the drip irrigation system.

Figure A3. Overview of the experimental area showing maize plants in the early stages of growth.

References

1. Morengo, M.L.; Mateus, N.P.A.; Silva, R.C.; Bender, F. Extreme drought in the Brazilian Pantanal in 2019–2020:characterization, causes, and impacts. *Front. Water* **2021**, *3*, e639204. [CrossRef]
2. Getirana, A.; Libonati, R.; Cataldi, M. Brazil in water crisis: It need a drougth plan. *Nature* **2021**, *600*, 218–220. Available online: https://www.nature.com/articles/d41586-021-03625-w (accessed on 25 November 2022). [CrossRef] [PubMed]
3. Colmenero-Flores, J.M.; Arbona, V.; Morillon, R.; Gómez-Cadenas, A. Salinity and water deficit. In *The Genus Citrus*; Woodhead Publishing: Cambridge, UK, 2020; pp. 291–309. [CrossRef]
4. Seleiman, M.F.; Al-Suhaibani, N.; Ali, N.; Akmal, M.; Alotaibi, M.; Refay, Y.; Dindaroglu, T.; Abdul-Wajid, H.H.; Leoniardo, M. Drought stress impacts plants and different approaches to alleviate its diverse effects. *Plants* **2021**, *10*, 259. [CrossRef]
5. Kundel, D.; Lori, M.; Fliessbach, A.; van Kleunen, M.; Meyer, S.; Mader, P. Drought effects on nitrogen provisioning in different agricultural systems: Insights gained and lessons learned from a field experiment. *Nitrogen* **2021**, *2*, 1–17. [CrossRef]
6. Sah, R.P.; Chakraborty, M.; Prasad, K.; Pandidt, M.; Tudu, V.K.; Chakravarty, M.K.; Narayan, S.C.; Rana, M.; Moharana, D. Impact of water deficit stress in maize: Phenology and yield components. *Sci. Rep.* **2020**, *10*, e2944. [CrossRef]
7. Tiepo, A.N.; Hertel, M.F.; Rocha, S.S.; Calzavara, K.; Oliveira, A.L.M.; Pimenta, J.A.; Oliveita, H.C.; Bianchini, E.; Stolf-Moreira, R. Enhanced drought tolerance in seedlings of Neotropical tree species inoculated with plant growth-promoting bacteria. *Pl. Physiol. Biochem.* **2018**, *130*, 277–288. [CrossRef]
8. Lu, H.; Qi, X.; Rahman, S.; Qiao, D.; Li, P.; Han, Y.; Zhao, Z. Rice Physiological response with *Bacillus subtilis* and saccharomyces cerevisiae inoculation into soil under reclaimed water–fresh water combined irrigation. *Water* **2021**, *13*, 773. [CrossRef]
9. Ribeiro, V.P.; Gomes, E.A.; Sousa, S.M.; Lana, U.G.P.; Coelho, A.M.; Marriel, I.E.; Paiva, C.A.O. Co-inoculation with tropical strains of *Azospirillum* and *Bacillus* is more efficient than single inoculation for improving plant growth and nutrient uptake in maize. *Arch. Microbiol.* **2022**, *204*, e143. [CrossRef]
10. Zhang, Y.; Tian, Z.; Xi, Y.; Wang, X.; Chen, S.; He, M.; Chen, Y.; Guo, Y. Improvement of salt tolerance of *Arabidopsisthaliana* seedlings inoculated with endophytic *Bacillus cereus* KP120. *J. Plant Inter.* **2022**, *17*, 884–893. [CrossRef]
11. Vinci, G.; Cozzolino, V.; Mazzei, P.; Monda, H.; Savy, D.; Drosos, M.; Piccolo, A. Effects of *Bacillus amyloliquefaciens* and different phosphorus sources on maize plants as revealed by NMR and GC-MS based metabolomics. *Plant Soil* **2018**, *429*, 437–450. [CrossRef]
12. Matos, C.C.; Costa, M.D.; Silva, I.R.; Silva, A.A. Competitive capacity and rhizosphere mineralization of organic matter during soil-herb microbiota interactions. *Planta Daninha* **2019**, *37*, e019182676. [CrossRef]
13. Lima, B.C.; Moro, A.L.; Santos, A.C.P.; Bonifácio, A.; Araujo, A.S.F.; Araujo, F.F. *Bacillus subtilis* ameliorates water stress tolerance in maize and common bean. *J. Plant Interac.* **2019**, *14*, 432–439. [CrossRef]
14. Zhou, S.; Zhang, X.; Liao, X.; Wu, Y.; Mi, J.; Wang, Y. Effect of different proportions of three microbial agents on ammonia mitigation during the composting of layer manure. *Molecules* **2019**, *24*, 2513. [CrossRef] [PubMed]
15. Sun, B.; Baia, Z.; Bao, L.; Xue, L.; Zhang, S.; Weid, Y.; Zhang, Z.; Zhuang, G.; Zhuang, X. *Bacillus subtilis* biofertilizer mitigating agricultural ammonia emission and shifting soil nitrogen cycling microbiomes. *Environ. Int.* **2020**, *144*, e105989. [CrossRef]
16. Ahmadian, K.; Jalilian, J.; Pirzad, A. Nano-fertilizers improved drought tolerance in wheat under deficit irrigation. *Agric. Water Manag.* **2021**, *244*, e106544. [CrossRef]
17. Gebauer, L.; Breitkreuz, C.; Heintz-Buschart, A.; Reitz, T.; Buscot, F.; Tarkka, M.; Bouffaud, M.-L. Water deficit history selects plant-beneficial soil bacteria differently under conventional and organic farming. *Front. Microbiol.* **2022**, *13*, e824437. [CrossRef]
18. Sheteiwy, M.S.; Elgawad, H.M.; Xiong, Y.-C.; Macovei, A.; Brestic, M.; Skalicky, M.; Shaghaleh, H.; Hamound, Y.A.; El-Sawah, A.M. Inoculation with *Bacillus amyloliquefaciens* and mycorrhiza confers tolerance to drought stress and improves seed yield and quality of soybean plants. *Physiol. Plant.* **2021**, *172*, 2153–2169. [CrossRef]

19. Coelho, M.A.; Soncin, N.B. *Geography of Brazil*; Moderna: São Paulo, Brazil, 1982; 368p.
20. AGRITEMPO. Agrometeorological Monitoring System: Meteorological Stations for the State of Paraiba. Available online: https://www.agritempo.gov.br/agritempo/jsp/Estacao/index.jsp?siglaUF=PB (accessed on 15 October 2021).
21. EMBRAPA—Empresa Brasileira de Pesquisa Agropecuária. *Brazilian Soil Taxonomy System*, 3rd ed.; EMBRAPA: Brasília, Brazil, 2013; 353p.
22. EMBRAPA—Empresa Brasileira de Pesquisa Agropecuária; Centro Nacional de Pesquisa em solo. *Manual of Soil Analysis Methods*, 2nd ed.; EMBRAPA: Rio de Janeiro, Brazil, 2011; 225p.
23. Cavalcante, F.J.A. *Fertilization Recommendations for the State of Pernambuco (Brazil)*, 2nd ed.; Instituto Agronômico de Pernambuco—IPA: Recife, Brazil, 2008; 212p.
24. Mantovani, E.C.; Bernardo, S.; Palaretti, L.F. *Irrigação: Princípios e Métodos*; UFV: Viçosa, Brazil, 2009; 355p.
25. SISDAGRO. Instituto Nacional de Meteorologia—Inmet. In *Decision Support System for Agriculture*; SISDAGRO: Brasília, Brazil, 2021. Available online: http://sisdagro.inmet.gov.br/sisdagro/app/index (accessed on 23 July 2021).
26. Jesen, M.E. Water consumption by agriculture plants. In *Water Deficit Growth*; Kozlowski, T.T., Ed.; Academic Press: New York, NY, USA, 1968; pp. 1–19.
27. Allen, R.G.; Pereira, L.S.; Raes, D.; Smith, M. Crop evapotranspiration-Guidelines for computing crop water requirements-FAO Irrigation and drainage paper 56. *Fao Rome* **1998**, *300*, D05109.
28. Christiansen, J.E. *Irrigation by Sprinkling*; University of California: Agricultural Experiment Station: Berkeley, CA, USA, 1943; 124p.
29. Malavolta, E.; Vitti, G.C.; Oliveira, S.A. *Assessment of the Nutritional Status of Plants: Principles and Applications*; Associação Brasileira da Potassa e do Fosfato: Piracicaba, Brazil, 1997; 319p.
30. Tedesco, M.J.; Gianello, C.; Bissani, C.A.; Bohnen, H.; Volkweiss, S.J. *Analysis of Soil, Plants and Other Materials*, 2nd ed.; (UFRGS. Boletim Técnico, 5); Universidade Federal do Rio Grande do Sul, Departamento de Solos: Porto Alegre, Brazil, 1995; 118p.
31. Alef, K.; Nannipieri, P. (Eds.) *Methods in Applied Soil Microbiology and Biochemistry*; Academic Press: Cambridge, MA, USA, 1995; 576p.
32. Ferreira, A.S.; Camargo, F.A.O.; Vidor, C. Use of microwaves in the evaluation of soil microbial biomass. *Rev. Bras. Ci. Sol.* **1999**, *23*, 991–996. [CrossRef]
33. Islam, K.R.; Weil, R.R. Microwave irradiation of soil for routine measurement of microbial biomass carbon. *Biol. Fert Soils* **1998**, *27*, 408–416. [CrossRef]
34. Brookes, P.C.; Powlson, D.S.; Jenkinson, D.S. Measurement of microbial biomass phosphorus in soil. *Soil Biol. Biochem.* **1982**, *14*, 319–329. [CrossRef]
35. BRASIL. Ministry of Agriculture, Livestock and Supply. *Rules for Seed Analysis—Ministry of Agriculture, Livestock and Supply*; Secretaria de Defesa Agropecuária—Brasília: Mapa/ACS: Brasília, Brazil, 2009; p. 399.
36. Mariotti, F.; Tomé, D.; Miranda, P.P. Converting nitrogen into protein—Beyond 6.25 and Jones' factors. *Crit. Rev. Food Sci. Nutr.* **2008**, *48*, 177–184. [CrossRef]
37. Ferreira, D.F. Sisvar: A computer statistical analysis system. *Ci. Agrotec.* **2011**, *35*, 1039–1042. [CrossRef]
38. Govaerts, B.; Sayre, K.D.; Lichter, K.; Dendooven, L.; Deckers, J. Influence of permanent raised bed planting and residue management on physical and chemical soil quality in rain fed maize/wheat systems. *Plant Soil* **2007**, *291*, 39–54. [CrossRef]
39. Hotelling, H.; Eisenhart, C.; Hastay, M.W.; Wallis, W.A. Multivariate quality control. In *Techniques of Statistical Analysis*; John Wiley & Sons: New York, NY, USA, 1947; 73p.
40. Hair, F.J.; Black, W.C.; Babin, B.J.; Anderson, R.E.; Tatham, R.L. *Análise Multivariada de Dados*, 6th ed.; Tradução Adonai Schlup Sant'Anna; Bookman: Porto Alegre, Brazil, 2009; 688p.
41. Statsoft, Inc. *Software Statistica 7.0. Data analysis software system*, Version 7; E.A.U.: Tulsa, OK, USA, 2004. Available online: https://statsoft-academic.com.br/(accessed on 20 January 2023).
42. McMurtrie, R.E.; Nasholm, T. Quantifying the contribution of mass flow to nitrogen acquisition by an individual plant root. *New Phytol.* **2018**, *218*, 119–130. [CrossRef] [PubMed]
43. Liliana Lara-Capistrán, L.; Zulueta-Rodríguez, R.; Bernardo Murillo-Amador, B.; Romero-Bastidas, M.; Rivas-García, T.; Hernández-Montiel, L.G. Agronomic response of sweet pepper (*Capsicum annuum* L.) to application of *Bacillus subtilis* and vermicompost in greenhouse. *Terra Latinoamericana.* **2021**, *38*, 693–704. [CrossRef]
44. Fonseca, M.d.C.d.; Bossolani, J.W.; de Oliveira, S.L.; Moretti, L.G.; Portugal, J.R.; Scudeletti, D.; de Oliveira, E.F.; Crusciol, C.A.C. Bacillus subtilis inoculation improves nutrient uptake and physiological activity in sugarcane under drought stress. *Microorganisms* **2022**, *10*, 809. [CrossRef]
45. Aquino, J.P.A.; Macedo-Junior, F.B.; Antunes, J.E.L.; Figueiredo, M.B.V.; Alcântara Neto, F.; Araujo, A.S.F. Endophytic bacteria promoting plant growth in maize and sorghum. *Pesq. Agropec. Trop.* **2019**, *49*, 1–9. [CrossRef]
46. Calzavara, A.K.; Paiva, P.H.G.; Gabriel, L.C.; Oliveira, A.L.M.; Milani, K.; Oliveira, H.C.; Bianchini, E.; Pimeta, J.A.; Oliveira, M.C.N.; Dias-Pereira, J.; et al. Associative bacteria influence maize (*Zea mays* L.) growth, physiology and root anatomy under different nitrogen levels. *Plant Biol.* **2018**, *20*, 870–878. [CrossRef]
47. Pang, B.; Zhang, K.; Kisekka, I.; Bean, S.; Zhang, M.; Wang, D. Evaluating effects of deficit irrigation strategies on grain sorghum attributes and biofuel production. *J. Cer. Sci.* **2018**, *79*, 13–20. [CrossRef]

48. Correia, P.M.P.; Silva, A.B.; Vaz, M.; Carmo-Silva, E.; Silva, J.M. Efficient Regulation of CO_2 Assimilation Enables Greater Resilience to High Temperature and Drought in Maize. *Front. Plant Sci.* **2021**, *12*, e675546. [CrossRef] [PubMed]
49. MacDonald, B.C.T.; Schwenke, G.D.; McPherson, A.; Mercer, C.; Baird, J.; Nachimuthu, G. Soil water deficit effects on soil inorganic nitrogen in alternate furrow flood irrigated Australian cotton production systems. *Soil Res.* **2022**, *60*, 137–146. [CrossRef]
50. Huang, Y.; Zheng, L.; Huang, Y.; Jia, Z.; Song, S.; Li, Z. Effects of different application methods of *Bacillus subtilis* agent on soil microbial diversity and growth of muskmelon. *Chin. J. Biotech.* **2020**, *36*, 2644–2656. [CrossRef]
51. Dar, Z.M.; Masood, A.; Mughal, A.H.; Asif, M. Review on drought tolerance in plants induced by plant growth promoting rhizobacteria. *Int. J. Curr. Microbiol. Appl. Sci.* **2018**, *7*, 2802–2804. [CrossRef]
52. Plett, D.; Ranathunge, K.; Melino, V.J.; Kuya, N.; Uga, Y.; Kronzucker, H.J. The intersection of nitrogen nutrition and water use in plants: New paths toward improved crop productivity. *J. Exp. Bot.* **2020**, *71*, 4452–4468. [CrossRef]

agriculture

MDPI

Article

Discontinuous Hydration Cycles with Elicitors Improve Germination, Growth, Osmoprotectant, and Salt Stress Tolerance in *Zea mays* L.

Kleane Targino Oliveira Pereira [1], Salvador Barros Torres [1], Emanoela Pereira de Paiva [1], Tatianne Raianne Costa Alves [1], Maria Lilia de Souza Neta [1], Jefferson Bittencourt Venâncio [1], Lauter Silva Souto [2], Clarisse Pereira Benedito [1], Tayd Dayvison Custódio Peixoto [1], Miguel Ferreira Neto [1], Nildo da Silva Dias [1] and Francisco Vanies da Silva Sá [1,*]

[1] Department of Agronomic and Forest Science, Federal Rural University of the Semi-Arid—UFERSA, Mossoró 59625-900, Brazil
[2] Center for Agro-Food Science and Technology, Federal University of Campina Grande, Pombal 58840-000, Brazil
* Correspondence: vanies_agronomia@hotmail.com; Tel.: +55-(83)9-9861-9267

Abstract: Saline stress impairs germination and initial plant growth. However, discontinuous hydration cycles induce osmotic tolerance in seeds and can improve the response of maize seeds to saline stress. The objective of this study was to evaluate the action of discontinuous hydration cycles with different salt stress tolerance elicitors on germination, growth, and osmotic adjustment of maize cultivars. Maize seeds of BR 206 and BRS 5037 Cruzeta cultivars were subjected to the following treatments: 0.0 mmol of NaCl (control), 250 mmol of NaCl (salt stress), salt stress + three discontinuous hydration cycles (DHCs) of seeds in water, salt stress + DHCs with gibberellic acid, salt stress + DHCs with hydrogen peroxide, salt stress + DHCs with salicylic acid, and salt stress + DHCs with ascorbic acid. Salt stress reduced the germination, growth, and biomass accumulation in maize seedlings—the BR 206 cultivar outperformed BRS 5037 Cruzeta. Discontinuous hydration cycles with water failed to improve the salt stress tolerance of maize seeds. However, discontinuous hydration cycles with gibberellic acid, hydrogen peroxide, and salicylic acid promoted salt stress tolerance in maize due to increased synthesis of osmoprotectants. Our results revealed salicylic acid is appropriate for discontinuous hydration cycles in maize seeds.

Keywords: *Zea mays* L.; salicylic acid; gibberellic acid; H_2O_2; salinity

1. Introduction

Zea mays L. is one of the world's most commercially relevant annual crops. Between 2000–2020, Brazil maintained its position as the third largest producer of maize, behind the United States and China. In 2020, production was 100 million tons [1]. The expected 2020/21 season production is 112.3 million tons [2]. Some factors may influence this species' yield, especially in semi-arid regions. Water deficit, associated with rainfall irregularities and dry climate, followed by salinity, are the main threats to plant growth and agricultural yield [3,4].

Semi-arid regions commonly have saline and sodic soils, which affect crops' germination process and growth as they restrict water absorption and contain toxic Na^+ and Cl^- ions [5,6]. High concentrations of these ions in the tissues hinder the mobilization of nutrient reserves, preventing germination and embryo growth. To acclimate to salt stress, plants adjust ionically by compartmentalizing organic ions in vacuoles or excluding ions in the roots [7,8].

Osmotic adjustment occurs through the accumulation of organic solutes, such as L-proline, soluble amino-N, soluble sugars, and other osmoprotective agents, in the cytosol

to reduce the cellular osmotic potential [6,9]. Ionic toxicity and osmotic stress are direct effects that can cause oxidative stress and several secondary stresses. Oxidative stress causes changes in plant metabolism, leading to excessive production of reactive oxygen species (ROS) that cause damage to cytoplasmic membranes and even cell death [6,10].

Plants produce osmoprotective agents to balance metabolic changes and reduce the effects caused by salts; among them, sugars and amino acids are produced in more significant quantities and accumulated in plant cells. *Proline* is an osmoprotectant that acts on antioxidant activity through the accumulation in chloroplasts of plant cells in response to the effects of environmental stresses, including salt stress. Thus, this amino acid performs several functions, such as stabilizing cellular structures and signaling the production of enzymes to eliminate ROS, reducing the deleterious effects of abiotic stresses [11,12].

Recent studies have shown that using hydropriming, organic acids, and hydrogen peroxide in pre-germination treatment in seeds attenuates the effects of salt stress [13–15]. Discontinuous hydration cycles (DHCs), known as water memory, constitute a pre-germination technique adopted to mitigate abiotic stresses [16–18]. DHCs are mainly studied in forest species to minimize water stress, but recently some studies have been conducted with agricultural species, such as Sorghum [*Sorghum bicolor* (L.) Moench.] [19] and fruit crops such as *Annona squamosa* L. [20]. These studies demonstrate that DHCs improve the tolerance of seeds and seedlings to dehydration.

The discontinuous hydration process occurs naturally in arid and semi-arid regions. In these regions, when water becomes available (rainy season), the seeds begin the imbibition process, which is quickly interrupted when the water becomes unavailable (dry spells). Seeds start losing water to the environment slowly, without causing damage to internal tissues. This process can occur in cycles until hydration is sufficient to initiate the metabolic activities of the seeds and consequently continue the germination process [16–18]. Thus, the species acclimate to climatic adversities and respond efficiently to abiotic stresses that occur in the field.

We hypothesize that discontinuous hydration cycles with stress tolerance elicitors can mitigate salt stress in maize seeds. We also hypothesized that discontinuous hydration cycles in drought-tolerant maize seeds could induce salt stress tolerance. Maize tolerance to salinity is influenced by the concentration of salts, time of exposure to stress, phenological stages, and genotype [13,21]. Therefore, the mechanisms of tolerance and changes in metabolism, seed germination, and seedling growth are expressed differently depending on genotype and environment [22]. Thus, this study aimed to evaluate the action of discontinuous hydration cycles with different salt stress tolerance elicitors on germination, growth, and osmotic adjustment of maize cultivars.

2. Materials and Methods

2.1. Location and Acquisition of Seeds

The experiment was conducted between June and December 2019 in the Seed Analysis Laboratory and Plant Physiology Laboratory of the Federal Rural University of the Semi-Arid Region (UFERSA), in the municipality of Mossoró/RN, Brazil (5°11′ S and 37°20′ W, and 18 m altitude).

Maize seeds, of cultivars BR 206 and BRS 5037 Cruzeta, were obtained from the private company GranSafra Sementes and EMPARN (Empresa de Pesquisa Agropecuária do Rio Grande do Norte), respectively. After receipt, they were stored in a controlled environment (16–18 °C and 40% relative humidity) throughout the experimental phase. We chose these maize cultivars for their characteristics favorable to grain production, biomass, and drought tolerance. These cultivars are indicated for production in the Brazilian semi-arid region, and in addition to being drought-stress tolerant, they can be salt-stress tolerant. Cultivar BR 206 is a drought-tolerant double hybrid, with an aptitude for grain yield, with an average yield of 8800 kg ha^{-1}. The BRS 5037 Cruzeta cultivar is drought tolerant and has an aptitude for biomass and grain production, with an average grain yield of 4290 kg ha^{-1}.

2.2. Imbibition Curve and Experimental Design

Initially, the moisture content of the seeds was quantified using the oven method at 105 ± 3 °C for 24 h [23], using two replicates of 4.5 ± 0.5 g. The moisture content was calculated based on the wet mass and expressed as a percentage.

The imbibition curve was obtained with two replicates of 50 seeds. These were weighed on a digital analytical scale (0.001 g) before imbibition and after each predetermined time interval until the emergence of the primary root. Imbibition was performed via immersion in water, with the seeds arranged in a beaker with 100 mL of distilled water and kept in germination chambers at 25 °C. Initially, seed weighing was performed every hour for eight hours of imbibition. Then, weighing was performed every two hours until thirty-four hours of imbibition. Finally, seed weighings were performed every four hours until fifty-two hours of hydration, when primary root protrusion was observed in 50% of the seeds of each replicate (Figure 1).

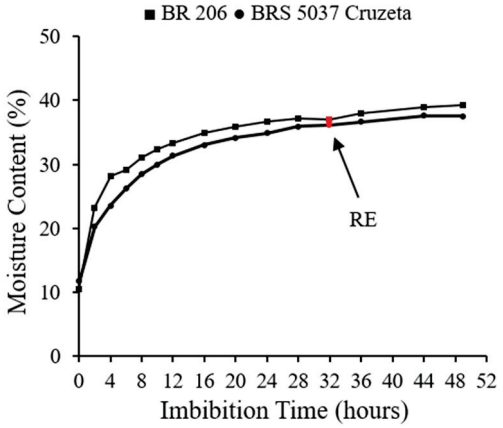

Figure 1. Imbibition curve of maize (*Zea mays* L.) seeds, cultivars BRS 5037 Cruzeta and BR 206, by immersion in water. RE = root emergence.

The experiment was conducted in a completely randomized design, following a 2 × 7 factorial arrangement, with four replicates of 50 seeds. We used two maize cultivars (BR 206 and BRS 5037 Cruzeta) plus seven saline stress combinations with three discontinuous hydration cycles (DHCs) of seeds with stress elicitors. The seven combinations were: 1—0.0 mmol of NaCl (control); 2—250 mmol of NaCl (salt stress); 3—salt stress + DHCs in water; 4—salt stress + DHCs with gibberellic acid (50 μM GA_3) [24]; 5—salt stress + DHCs with hydrogen peroxide (5 mmol (H_2O_2); 6—salt stress + DHCs with salicylic acid (50 μM SA); and 7—salt stress + DHCs with ascorbic acid (50 μM ASC) [24].

Maize seeds underwent three hydration–dehydration cycles. In the hydration process, the 200 seeds, comprising the four replications of 50 seeds, were soaked in 180 mL of the elicitor agent for two hours in a germination chamber at 25 °C in the dark. Subsequently, the seeds underwent twelve hours of dehydration at room temperature (28–30 °C) [16–18]. The DHCs were defined according to the data obtained in the imbibition curve (Figure 1), and the dehydration time was based on preliminary tests. At the end of the DHCs, the seeds had a moisture content of around 25%.

2.3. Germination and Seedling Length

After the DHCs, the seeds were sown in a paper roll moistened with distilled water (0.0 mM NaCl–control) and saline water in the other treatments at 250 mM NaCl, obtained by the dissolution of sodium chloride (NaCl), corresponding to 14.61 g L^{-1}. We obtained the mM NaCl treatment in preliminary tests. The paper rolls were incubated in a germinator at 25 °C. Germination evaluations, first germination count, and germination percentage were performed four and seven days after sowing, according to Brazilian rules for seed analysis [23].

The lengths of the shoots and roots of normal seedlings were measured at the end of the germination test. Shoot length—SL (measured from the collar to the seedling apex) and primary root length—RL (measured from the collar's base to the root's tip) were measured with a ruler graduated in centimeters.

2.4. Dry Mass of Seedlings and Salinity Tolerance index

After the growth measurements, 15 seedlings were placed in kraft paper bags and dried in a forced air circulation oven at 65 °C until they reached a constant weight. Subsequently, they were weighed on a precision scale to obtain shoot (SDM), root (RDM), and total dry mass (TDM), and data were expressed in g plant^{-1}. In the calculations of the indices, the total dry mass production of the cultivars was used as the main parameter to determine their tolerance to salt stress.

Total DM data were used to calculate the percentages partitioned between the vegetative organs and the salinity tolerance index by comparing the data of the salt stress treatments with those of the control (EC = 4.13 μSm^{-1} at 25 °C), using Equation (1).

$$STI(\%) = \frac{DM\ of\ salt\ stress\ treatment}{DM\ of\ control\ treatment} \times 100, \quad (1)$$

STI: salinity tolerance index;
DM: dry mass.

2.5. Osmotic Homeostasis

Total soluble sugars (TSS), amino acids (AA), and proline (PRO) were obtained from the fresh mass of 10 seedlings. At the time of extraction, the fresh mass was macerated in liquid nitrogen with a crucible and pestle. The plant material sample from each replication was analyzed in triplicate. Then, 0.2 g was weighed, and the material was placed in Eppendorf-type screw cap tubes. Then, 1 mL of 80% ethyl alcohol was added, and the samples were kept in a water bath at 60 °C for 20 min. The material was kept in a centrifuge cooled at 4 °C for 10 min at 10 RPM (procedure performed three times), and the supernatant was collected to quantify the sugars. The total soluble sugars were determined by measuring the absorbance at 620 nm using the anthrone method [25], with glucose as the standard substance, and the results were expressed in mg GLU g^{-1} of fresh mass. The supernatant obtained in the extraction process was used to quantify the amino acid (AA) contents in determining total free amino acids. For this, the acid ninhydrin method was applied, with the absorbance measurement at 570 nm [26], using glycine as the standard substance, and the results were expressed in μM GLY g^{-1} of fresh mass. Proline determination followed the methodology described by [27]. Proline concentrations were determined based on a standard curve obtained from L-proline and by measuring the absorbance at 520 nm. The results were expressed in μM PRO g^{-1} of fresh mass.

2.6. Statistical Analysis

The data were subjected to analysis of variance (F test); the Scott–Knott test compared the means of discontinuous hydration cycles at a 5% probability level, and Student's *t*-test compared the means of the cultivars at a 5% probability level. Statistical analyses were performed with the computer program SISVAR [28].

3. Results

3.1. Germination and Seedling Length

The interaction between maize cultivars and pre-germination treatments was significant for the first germination count (p = 0.0000), germination (p = 0.0021), shoot length (p = 0.0215), and root length (p = 0.0007) (Table 1).

Table 1. F-test and means test (SE, n = 4) for first germination count (FGC), germination (G), shoot length (SL), and root length (RL) for *Zea mays* L. seeds subjected to salt stress tolerance elicitors in three discontinuous hydration cycles (DHCs).

F-Test (*p*-Value)					
Variation Sources		**FGC**	**G**	**SL**	**RL**
DHCs		0.0000	0.0000	0.0000	0.0000
Cultivars (C)		0.0000	0.0000	0.0145	0.0000
DHCs × C		0.000	0.0021	0.0215	0.0007
Means-test					
Cultivars	**DHCs**	**FGC (%)**	**G (%)**	**SL(cm)**	**RL (cm)**
BR 206	1 (control)	100 ± 0.0 aA	100 ± 0.0 aA	7.8 ± 0.38 aA	16.5 ± 0.12aA
	2	47 ± 4.2 dA	95 ± 1.0 aA	1.8 ± 0.08 bA	3.8 ± 0.09 cA
	3	77 ± 4.5 cA	97 ± 1.3 aA	2.1 ± 0.15 bA	4.7 ± 0.31 bA
	4	85 ± 3.3 bA	97 ± 1.0 aA	1.9 ± 0.10 bA	5.2 ± 0.33 bA
	5	81 ± 1.9 bA	96 ± 0.8 aA	2.1 ± 0.08 bA	5.0 ± 0.11 bA
	6	76 ± 1.5 cA	98 ± 0.0 aA	2.2 ± 0.01 bA	4.9 ± 0.33 bA
	7	70 ± 5.5 cA	98 ± 0.8 aA	1.9 ± 0.13 bA	5.0 ± 0.14 bA
BRS 5037 Cruzeta	1 (control)	98 ± 1.3 aA	99 ± 0.5 aA	7.9 ± 0.13aA	14.0 ± 0.51 aB
	2	21 ± 3.1 dB	85 ± 1.7 cB	1.1 ± 0.13 cB	3.5 ± 0.30 cA
	3	45 ± 1.3 bB	92 ± 1.0 bB	1.7 ± 0.15 bA	4.5 ± 0.33 bA
	4	45 ± 3.3 bB	92 ± 1.7 bB	1.3 ± 0.08 cB	4.9 ± 0.24 bA
	5	45 ± 2.9 bB	92 ± 1.7 bB	1.8 ± 0.07 bA	3.7 ± 0.47 cB
	6	32 ± 1.4 cB	86 ± 2.2 cB	2.2 ± 0.10 bA	4.8 ± 0.22 bA
	7	38 ± 3.8 bB	92 ± 1.0 bB	2.1 ± 0.14 bA	3.8 ± 0.19 cB

1—0.0 mmol of NaCl (control); 2—250 mmol of NaCl (salt stress); 3—salt stress + DHCs in water; 4—salt stress + DHCs with gibberellic acid (50 μM GA_3); 5—salt stress + DHCs with hydrogen peroxide (5 mmol (H_2O_2); 6—salt stress + DHCs with salicylic acid (50 μM SA); and 7—salt stress + DHCs with ascorbic acid (50 μM ASC). Means followed by the same lowercase letter in the column do not differ by the Scott–Knott test at a 5% probability level, and means followed by the same uppercase letter in the column do not differ from each other by the Student's *t*-test at 5% probability level.

Salt stress reduced the first germination count (FGC) of the BR 206 and BRS 5037 Cruzeta cultivars by 53 and 77 percentage points, compared to the control treatment. For the BR 206 cultivar, three discontinuous hydration cycles (DHCs) improved FGC compared to salt stress. Still, DHCs with GA_3 and H_2O_2 led to results closer to those found in control, with 38 and 34 percentage points more in FGC than salt stress, respectively (Table 1). For the BRS 5037 Cruzeta cultivar, DHCs favored FGC, compared to salt stress. Still, DHCs with elicitors were similar to DHCs with water, except for salicylic acid, which was inferior to DHCs with water (Table 1). The best response to DHCs with elicitors occurred for the BR 206 cultivar, compared to the BRS 5037 Cruzeta cultivar (Table 1).

Salt stress did not affect the germination of the BR 206 cultivar (Table 1). However, salt stress reduced the germination of the BRS 5037 Cruzeta cultivar by 14 percentage points. The DHCs improved germination by an average of seven percentage points compared to salt stress, except for DHCs with salicylic acid, which was similar to salt stress. The best germination levels under salt stress conditions were obtained by the BR 206 cultivar, compared to the BRS 5037 Cruzeta cultivar, in all treatments with salt stress (Table 1).

Seedlings subjected to salt stress had reduced shoot length (SL). For the BR 206 cultivar, treatments with DHCs were not sufficient to overcome the stress caused by salt excess. For the BRS 5037 Cruzeta cultivar, DHCs with elicitors promoted higher SL (mean of 77.3%) than that found for the treatment with salt stress, except for DHCs with gibberellic acid. Only salt stress and DHCs with gibberellic acid promoted different results among cultivars (Table 1).

Root length (RL) was reduced under the salt stress condition. Compared to salt stress, treatments with DHCs favored an average increase of 30.5% in RL for the BR 206 cultivar. For the BRS 5037 Cruzeta cultivar, there was a reduction in RL under salt stress, but the

DHCs favored increments of 28.5% in the root for DHCs with water, 40% for DHCs with H_2O_2, and 37.1% for DHCs with salicylic acid (Table 1).

The results presented for SL using DHCs with attenuators for the BR 206 cultivar showed no significant difference caused by salt stress. Still, this cultivar invested significantly in RL under salt stress with attenuators (Figure 2). For the BRS 5037 Cruzeta cultivar, the DHCs with water and DHCs with salicylic acid favored both SL and RL. The DHCs with hydrogen peroxide (H_2O_2) and DHCs with ascorbic acid also favored the highest SL for this cultivar. The results indicate that these treatments mitigated salt stress. Even under salt stress, the two cultivars formed seedlings with coleoptile and root development (Figure 2). However, in this study, the formation of coleoptile was reduced in all salt stress treatments compared to the control.

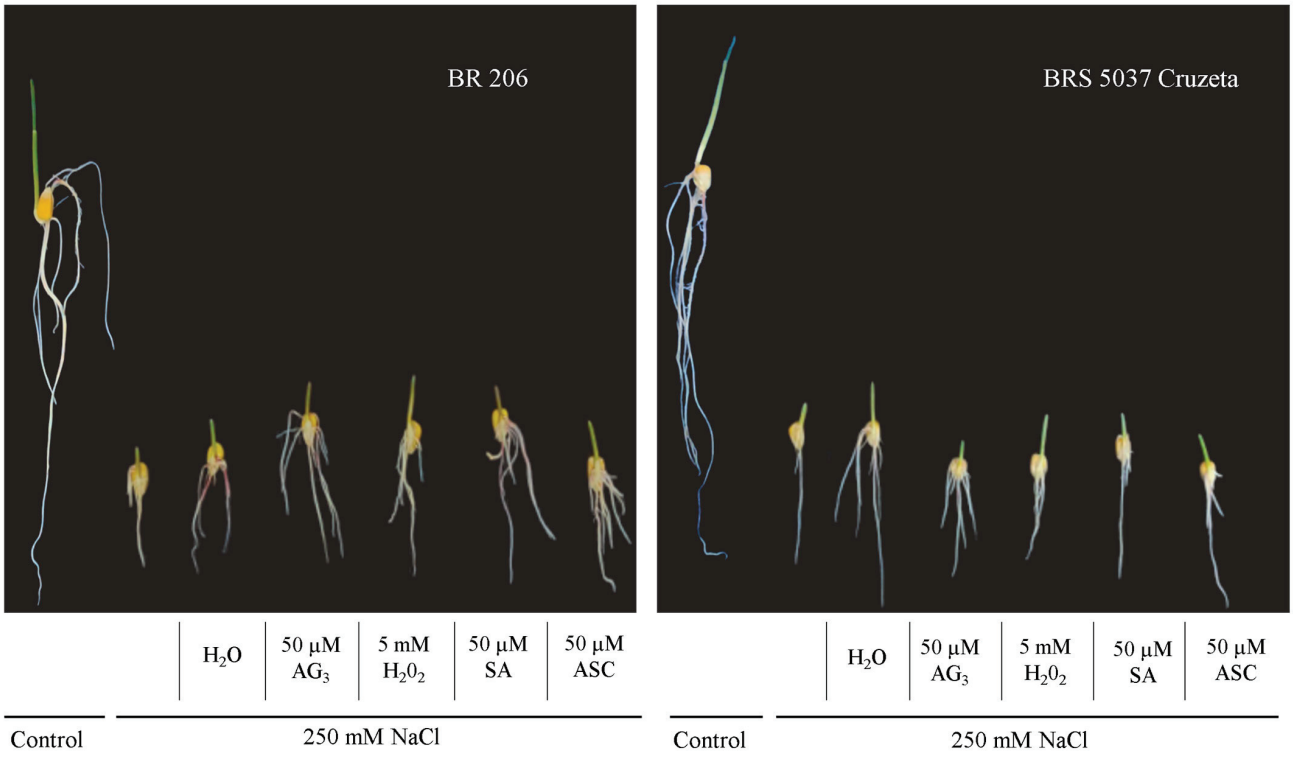

Figure 2. *Zea mays* L. seeds subjected to salt stress tolerance elicitors in three discontinuous hydration cycles (DHCs).

3.2. Dry Mass of Seedlings and Salinity Tolerance Index

The interaction between cultivars and pre-germination treatments was significant for shoot dry mass (p = 0.0000), root dry mass (p = 0.0000), total dry mass (p = 0.0000), and salinity tolerance index (p = 0.0000) (Table 2).

Shoot dry mass (SDM) was reduced in the salt stress, but, for the BR 206 cultivar, the DHCs with water favored a 70.6% increase in SDM compared to salt stress. For the BRS 5037 Cruzeta cultivar, the DHCs with water, DHCs with salicylic acid, and DHCs with ascorbic acid, the SDM increased by 74.5, 83.6, and 87.27%, respectively, compared to salt stress. SDM was higher for the BR 206 cultivar than the BRS 5037 Cruzeta cultivar, regardless of salinity (Table 2).

The BR 206 cultivar had a 68.6% reduction in root dry mass (RDM) under saline stress compared to the control. However, having applied DHCs with gibberellic acid, DHCs with H_2O_2, DHCs with salicylic acid, and DHCs with ascorbic acid, the BR 206 cultivar produced 117.6, 104.4, 99.4, and 86.2% more RDM than in the treatment with salt stress, respectively. For the BR 3057 Cruzeta cultivar, salt stress caused a 60.6% reduction in RDM compared to the control, and the treatments with DHCs did not increase this variable. The BR 206 cultivar obtained higher RDM than the BRS 5037 Cruzeta cultivar (Table 2).

The total dry mass (TDM) of the BR 206 cultivar was reduced by 67.1% under salt stress compared to the control. All treatments with DHCs increased TDM in the BR 206 cultivar; however, DHCs with gibberellic acid, DHCs with H_2O_2, and DHCs with salicylic acid showed better performance, with values on average 67.5% higher than those of salt stress (Table 2). Compared to the control, the BR 3057 Cruzeta underwent a reduction of 64.4% in TDM under salt stress. In this cultivar, the TDM accumulations in DHCs with water, DHCs with H_2O_2, and DHCs with salicylic acid were 45.5, 39.9, and 60.7% higher than those obtained under salt stress, respectively. The BR 206 cultivar produced more TDM than the BR 3057 Cruzeta cultivar, regardless of salinity (Table 2).

Regarding the salinity tolerance index (STI), the cultivars BR 206 and BR 3057 Cruzeta were sensitive (STI < 40%) to salt stress. For the BR 206 cultivar, all treatments with DHCs improved STI, and plants changed from sensitive to moderately sensitive to salinity (40% < STI < 60%) (Table 2). For the BRS 3057 Cruzeta cultivar, all treatments with DHCs, except for DHCs with gibberellic acid, improved STI, and plants changed from sensitive to moderately sensitive to salinity (40% < STI < 60%) (Table 2).

Table 2. F-test and means-test (SE, n = 4) for shoot dry mass (SDM), root dry mass (RDM), total dry mass (TDM), and salinity tolerance index (STI) for *Zea mays* L. seeds subjected to salt stress tolerance elicitors in three discontinuous hydration cycles (DHCs).

F-Test (*p*-Value)					
Variation Sources		**SDM**	**RDM**	**TDM**	**STI**
DHCs		0.0000	0.0000	0.0000	0.0000
Cultivars (C)		0.0000	0.0000	0.0000	0.0000
DHCs × C		0.0000	0.0000	0.0000	0.0000
Means-test					
Cultivars	DHCs	SDM mg plant^{-1}	RDM mg plant^{-1}	TDM mg plant^{-1}	STI %
BR 206	1 (control)	35.8 ± 0.5 aA	50.6 ± 1.9 aA	86.5 ± 1.8 aA	100.0 ± 0.0 aA
	2	12.6 ± 1.0 dA	15.9 ± 0.5 dA	28.5 ± 1.3 dA	32.9 ± 1.5 dA
	3	21.5 ± 0.5 bA	21.5 ± 1.1 cA	43.1 ± 0.7 cA	49.8 ± 0.8 cA
	4	13.6 ± 0.4 dA	34.6 ± 1.6 bA	48.2 ± 1.8 bA	55.8 ± 2.1 bA
	5	15.8 ± 0.8 cA	32.5 ± 0.8 bA	48.3 ± 1.3 bA	55.9 ± 1.5 bA
	6	15.0 ± 1.2 cA	31.7 ± 2.0 bA	46.7 ± 1.3 bA	54.0 ± 1.5 bA
	7	13.9 ± 1.1 dA	29.6 ± 1.2 bA	43.5 ± 1.9 cA	50.3 ± 2.2 cA
BRS 5037 Cruzeta	1 (control)	25.8 ± 0.6 aB	25.9 ± 0.7 aB	51.7 ± 1.1 aB	100.0 ± 0.0 aA
	2	5.5 ± 0.6 cB	10.2 ± 0.4 bB	15.8 ± 0.9 cB	30.5 ± 1.7 eA
	3	9.7 ± 0.4 bB	13.3 ± 0.8 bB	23.0 ± 1.0 bB	44.5 ± 1.8 cB
	4	6.5 ± 0.2 cB	12.5 ± 0.5 bB	19.1 ± 0.7 cB	36.8 ± 1.4 dB
	5	10.1 ± 0.4 bB	12.0 ± 0.9 bB	22.1 ± 1.2 bB	42.7 ± 2.3 cB
	6	11.6 ± 0.3 bB	13.8 ± 0.7 bB	25.4 ± 0.8 bB	49.0 ± 1.6 bB
	7	10.3 ± 0.1 bB	11.6 ± 1.1 bB	21.9 ± 1.1 bB	42.4 ± 2.1 cB

1—0.0 mmol of NaCl (control); 2—250 mmol of NaCl (salt stress); 3—salt stress + DHCs in water; 4—salt stress + DHCs with gibberellic acid (50 μM GA_3); 5—salt stress + DHCs with hydrogen peroxide (5 mmol (H_2O_2); 6—salt stress + DHCs with salicylic acid (50 μM SA); and 7—salt stress + DHCs with ascorbic acid (50 μM ASC). Means followed by the same lowercase letter in the column do not differ by the Scott–Knott test at a 5% probability level, and means followed by the same uppercase letter in the column do not differ from each other by the Student's *t*-test at 5% probability level.

3.3. Osmotic Homeostasis

The interaction between maize cultivars and pre-germination treatments was significant for the total soluble sugars (p = 0.0000), amino acids (p = 0.0001), and proline (p = 0.0000) (Table 3).

The maize BR 206 cultivar under control, salt stress, and DHCs with salicylic acid treatments obtain the highest total soluble sugars (TSS) levels. However, for the other treatments, the TSS content was lower than that found in control. All treatments with salt stress for the BRS 5037 Cruzeta cultivar led to higher TSS content than the control

(Table 3). In this cultivar, DHCs with salicylic acid favored the highest production of TSS, with 49.6 mg g^{-1} of FM. The BR 206 cultivar produced more TSS than the BRS 5037 Cruzeta cultivar; however, under DHCs with salicylic acid, the contents of these sugars were similar.

Table 3. F-test and means-test (SE, n = 4) for total soluble sugars (TSS), amino acids (AA), and proline (PRO) for *Zea mays* L. seeds subjected to salt stress tolerance elicitors in three discontinuous hydration cycles (DHCs).

F-Test (*p*-Value)				
Variation Sources		**TSS**	**AA**	**PRO**
DHCs		0.0000	0.0000	0.0000
Cultivars (C)		0.0000	0.0000	0.0000
DHCs × C		0.0000	0.0001	0.0000
Means-test				
Cultivars	**DHCs**	**TSS mg GLU g^{-1} FM**	**AA μmol GLY g^{-1} FM**	**PRO μmol PRO g^{-1} FM**
BR 206	1 (control)	50. 1 ± 2.0 aA	47.5 ± 2.3 dA	0.7 ± 0.2 eA
	2	51.2 ± 0.5 aA	68.9 ± 4.4 bA	59.7 ± 0.8 aA
	3	47.1 ± 0.4 bA	65.1 ± 5.1 cA	48.5 ± 1.7 cA
	4	45.1 ± 1.5 bA	79.9 ± 1.5 aA	48.3 ± 1.9 cA
	5	44.2 ± 2.1 bA	57.7 ± 1.1 cA	41.7 ± 2.4 dA
	6	49.5 ± 1.4 aA	78.3 ± 1.9 aA	58.2 ± 1.5 aA
	7	47.5 ± 3.0 bA	61.3 ± 2.9 cA	53.2 ± 2.7 bA
BRS 5037 Cruzeta	1 (control)	25.8 ± 0.9 cB	22.6 ± 1.1 dB	0.3 ± 0.01 cA
	2	39.9 ± 0.6 bB	46.9 ± 1.8 cB	34.8 ± 4.0 bB
	3	35.7 ± 1.2 bB	55.7 ± 1.5 bB	30.5 ± 0.4 bB
	4	39.0 ± 0.7 bB	68.8 ± 1.5 aB	45.4 ± 0.9 aA
	5	39.7 ± 1.1 bB	56.5 ± 5.0 bB	29.8 ± 1.8 bB
	6	49.6 ± 1.1 aA	62.5 ± 5.1 aB	33.6 ± 0.5 bB
	7	37.0 ± 1.0 bB	67.8 ± 2.5 aA	32.5 ± 0.7 bB

1—0.0 mmol of NaCl (control); 2—250 mmol of NaCl (salt stress); 3—salt stress + DHCs in water; 4—salt stress + DHCs with gibberellic acid (50 μM GA_3); 5—salt stress + DHCs with hydrogen peroxide (5 mmol (H_2O_2); 6—salt stress + DHCs with salicylic acid (50 μM SA); and 7—salt stress + DHCs with ascorbic acid (50 μM ASC). Means followed by the same lowercase letter in the column do not differ by the Scott–Knott test at a 5% probability level, and means followed by the same uppercase letter in the column do not differ from each other by the Student's *t*-test at 5% probability level.

Salt stress increased the synthesis of amino acids (AA) by 44.9 and 107.5% in the cultivars BR 206 and BRS 5034 Cruzeta compared to the control, respectively (Table 3). For the BR 206 cultivar, DHCs with gibberellic acid and DHCs with salicylic acid increased the synthesis of AA by 15.9 and 13.7% when compared to salt stress, respectively. For the BRS 5037 Cruzeta cultivar, DHCs with gibberellic acid, DHCs with salicylic acid, and DHCs with ascorbic acid increased the synthesis of AA by 44.6, 33.2, and 44.5% compared to salt stress, respectively (Table 3).

Salt stress increased proline accumulation for the cultivars BR 206 and BRS 5037 Cruzeta by 58.98 and 34.46 μM g^{-1} of FM compared to the control, respectively. For the BR 206 cultivar, the highest proline contents occurred under salt stress and DHCs with salicylic acid. The highest proline accumulation for the BRS 5037 Cruzeta cultivar occurred under DHCs with gibberellic acid. Under salt stress conditions, the BR 206 cultivar produced more proline than the BRS 5037 Cruzeta cultivar, but under DHCs with gibberellic acid, the proline contents were similar between the cultivars (Table 3).

4. Discussion

Salt stress causes damage to irrigated agriculture around the world. Research that can improve plant responses to saline stress is essential, but it is challenging to attenuate salinity under severe salinity stress conditions. We found a strategy to do this. We improved maize seedlings' response under severe salt stress (250 mM NaCl) using water memory

and salt stress tolerance elicitors. We found that three discontinuous hydration cycles and different salt stress elicitors mitigated the effect of salt stress and contributed to the improvement of germination, growth, and accumulated dry mass of the maize cultivars. Despite drought tolerance, when exposed to severe saline stress (250 mM NaCl), maize cultivars were sensitive and reduced shoot dry mass by 64–79%, and root dry mass by 61–69% (Figure 3). The use of discontinuous hydration cycles (DHCs) of maize seeds with gibberellic acid (50 µM GA_3), hydrogen peroxide (5 mmol (H_2O_2), and salicylic acid (50 µM SA) promoted losses to shoot dry mass in cultivar BR 206 of 56-62%, and to root dry mass of 32–37% compared to the control. For BRS 5037 Cruzeta, for the DHCs with salicylic acid (50 µM SA), the losses of shoot dry mass were 55%, and 47% of root dry mass compared to the control (Figure 3). Using DHCs in maize seeds under severe stress improved the degree of salinity tolerance of the seedlings, changing them from sensitive to moderately sensitive to salt stress.

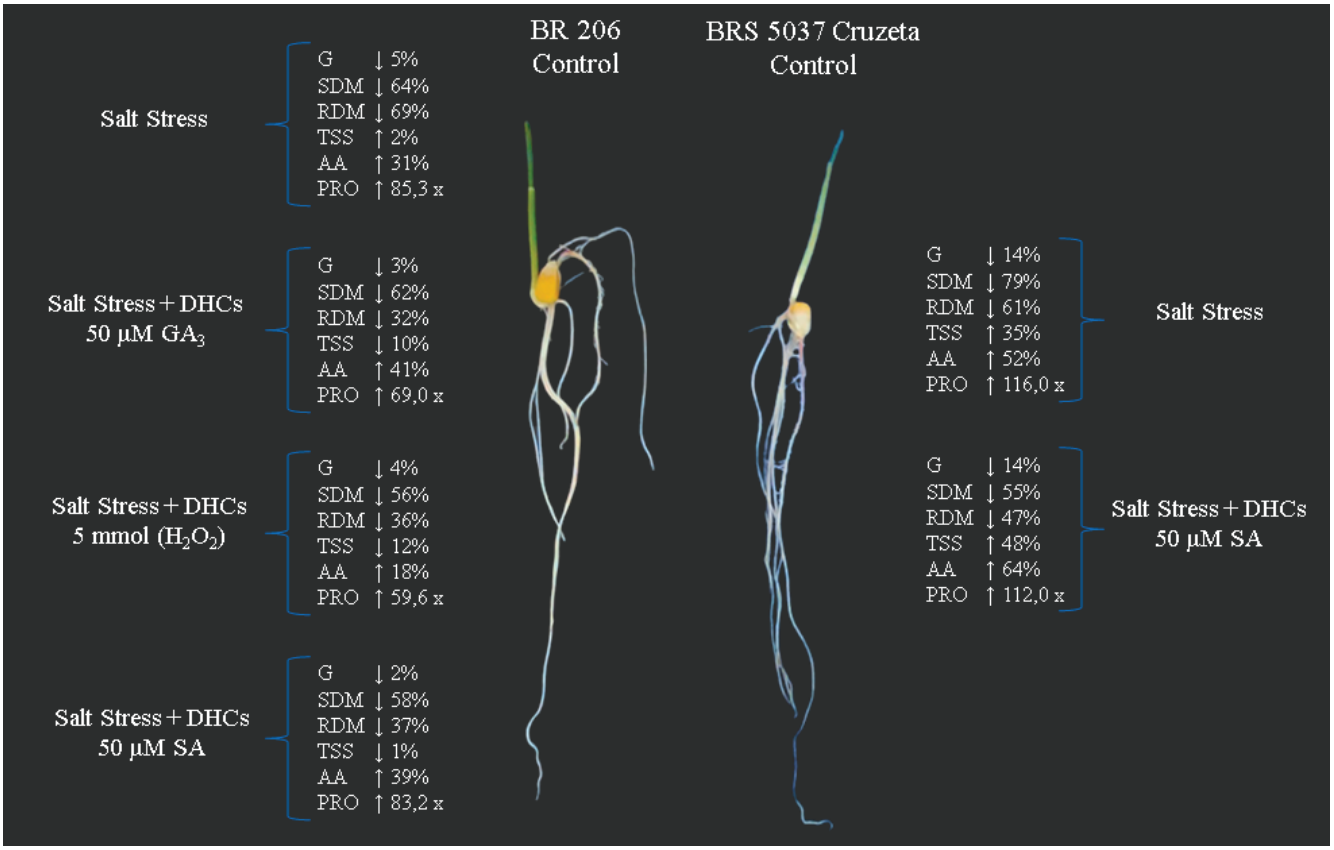

Figure 3. Responses of BR 206 and BRS 5037 Cruzeta maize cultivars subjected to salt stress tolerance elicitors in three discontinuous hydration cycles (DHCs) compared to control.

Morphophysiological parameters in both maize cultivars were reduced by salt stress. The results for the BR 206 cultivar were higher than those found for BRS 5037 Cruzeta, except for RL and STI, which were similar. Regarding the FGC of the BR 206 cultivar, DHCs with gibberellic acid stood out, with 85% of seeds germinated. Still, it did not differ statistically from the use of H_2O_2, which led to 81% of seeds germinating. We have found that this result was observed because gibberellins (GA_3) act as stress signaling agents. The responses adopted by plants are for better water absorption, germination, and growth of seedlings, even under unfavorable conditions, such as salt stress [29–31]. Like GA_3, H_2O_2 acts as an oxidative stress signaling agent and, when applied at low concentrations, interacts with hormones that control the germination process [32,33], which explains the higher number of seedlings and uniform germination in FGC in these treatments.

Generally, salt stress conditions reduce the germination percentage of maize seeds [13,29], but this result may vary according to the cultivar. For the BR 206 cultivar, there was no difference in germination among treatments. Even under induced salt stress (250 mM NaCl), all treatments resulted in germination greater than 95%. For the BRS 5037 Cruzeta cultivar, salt stress resulted in a loss of 14 percentage points compared to the control treatment, which proves the variation in germination potential among cultivars. The small changes in the final germination count suggest the need for other parameters to determine the degree of tolerance of maize cultivars. In this context, parameters related to growth and biomass accumulation contribute to explaining maize germination results under salt stress conditions, as they are more sensitive to the effects of salinity [13,34–36].

Maize seedlings respond to salt stress by reducing shoot growth [15,24]. The maize growth decrease occurs due to an osmotic imbalance caused by excess salts. Excess salts decrease water absorption, mobilization of seed nutrient reserves, and elongation of radicle cells, and affect DNA division and synthesis [13,34]. Osmotic stress reduces photosynthetic capacity through stomatal closure and reduction in leaf expansion, consequently decreasing shoot growth [37]. The initial growth is decreased by salt stress; however, as a survival strategy, maize plants invest in root growth before the endosperm reserves are exhausted, corroborating the findings of [24]. Our results reveal that DHCs with tolerance elicitors promote greater shoot length than saline stress, with more significant results in BRS 5037 Cruzeta cultivar, except for DHCs with gibberellic acid. The root length response after DHCs was higher for both cultivars than saline stress, except for DHCs with H_2O_2 in BRS 5037 Cruzeta.

Our results reveal that 250 mM NaCl causes toxicity in maize cultivars, causing deficiency in the osmotic adjustment of the plants, even after treatment with DHCs with tolerance elicitors. According to Roy et al. [37], one of the first plant tolerance mechanisms is an osmotic adjustment, regulated by long-distance signals that reduce the length and are triggered before Na^+ accumulation, which we verified for maize cultivars. The second strategy occurs via ionic exclusion by decreasing the transport of Na^+ and Cl^- in the roots and consequently reducing the accumulation of ions in the leaves. Tolerance to high salt concentrations in leaves is due to the compartmentalization of ions in plant cell vacuoles.

The DHCs with tolerance elicitors contributed to the maize seedlings' tolerance of the salt concentrations, mainly via the investment in the root length from the increase in adventitious roots, primarily in the cultivar BR 206. The increase in the fasciculated root system is significant because seedlings can remove water and nutrients from the environment before the reserves present in the endosperm are exhausted [24]. This response is expressive in the dry mass of seedlings of maize cultivars.

The DHCs with attenuators increased the biomass accumulation of seedlings of maize cultivars subjected to salt stress. The attenuators minimized the effects of salt stress on maize biomass accumulation, but the cultivars showed divergent responses to the attenuators. The DHCs with water favored the increase in SDM in the BR 206 cultivar, but the results of RDM and TDM were lower than those obtained with the other attenuators. On the other hand, the DHCs with gibberellic acid did not increase SDM, RDM, and TDM for the BRS 5037 Cruzeta cultivar. The highest biomass accumulations occurred with DHCs with gibberellic acid, hydrogen peroxide, and salicylic acid for the BR 206 cultivar, and DHCs with water, DHCs with hydrogen peroxide, DHCs with salicylic acid, and DHCs with ascorbic acid for the BRS 5037 cultivar.

Recent studies with discontinuous hydration cycles in water have induced the tolerance of forest species to water stress at the morphophysiological level [17,38–40]. Discontinuous hydration cycles allow the seeds to improve the expression of vigor in an adverse environment, so their hydration and dehydration favor stress acclimation. The authors report that, during this process, metabolic, energetic, and respiratory activities are initiated by the mobilization of reserves, along with β-oxidation of fatty acids, nitrogen mobilization, and the improvement of membrane permeability. These improvements favor embryonic growth and root emergence in plants under water stress, which is new to salt stress.

Discontinuous hydration cycles improved the tolerance of the cultivars BR 206 and BRS 5037 Cruzeta to osmotic restriction induced by excess salts. Maize seeds showed high sensitivity to salt stresses of 250 mM NaCl, with biomass losses close to 70% compared to the control. However, in the DHCs with attenuators, the seedlings changed from sensitive to moderately sensitive to salinity, with biomass losses lower than 60% for BRS 5037 Cruzeta and lower than 50% for BR 206. The increase in dry mass occurred after DHCs with salt stress tolerance elicitors, which corroborates the research results on using DHCs with water to mitigate stress [17–19]. The response demonstrates that the dehydration process cannot erase this hydration memory, which is already a cause of stress, and the seeds have greater tolerance to the new stress [41]. The dehydration process naturally damages the lipid membranes. The diacylglycerol present in plant cells (plastid and endoplasmic reticulum) is a precursor in synthesizing glycerolipids that disorganizedly cause electrolyte leakage [40] that can affect seedling development. Seeds invest their metabolic energy in membrane repair rather than growth to reduce this damage.

Salt stress naturally increased the synthesis of amino acids compared to the control; however, the DHCs with gibberellic acid and DHCs with salicylic acid further increased the synthesis of amino acids, mainly proline, in both cultivars. The BR 206 cultivar obtained higher amino acid and proline levels than the BRS 5037 Cruzeta cultivar. This greater capacity for the synthesis of osmolytes of the BR 206 cultivar is related to its higher tolerance. Osmotic adjustment in plant cells ensures the maintenance of water entry and cell turgor, limiting the damage caused at the beginning of stress [42,43].

An important fact is that the synthesis of sugars was not altered between control and salt stress in both cultivars, indicating that the osmotic adjustment of maize occurs mainly via the increase in amino acid synthesis. However, under DHCs with water, H_2O_2, and ascorbic acid, there was a decrease in sugar synthesis to the detriment of increased amino acid synthesis. Only under DHCs with gibberellic acid and salicylic acid did the increase in the synthesis of amino acids not coincide with a decrease in the synthesis or degradation of sugars, which are more efficient in inducing osmotic adjustment in maize.

DHCs with tolerance elicitors potentiated the responses adopted by maize cultivars under saline stress. Germination and growth of BRS 5037 Cruzeta maize decreased more under saline stress than BR 206 maize. Therefore, this cultivar is more sensitive to saline stress. Cultivar BR 206 responded better to salt stress tolerance elicitors, such as gibberellic acid, salicylic acid, and hydrogen peroxide. However, cultivar BRS 5037 Cruzeta responded only to treatment with salicylic acid because it is more salinity-sensitive than BR 206 maize (Figure 3). Salicylic acid is a salt stress tolerance elicitor indicated for salinity-sensitive maize cultivars. Khan et al. [44] indicate that salicylic acid is a phenolic compound that favors the growth and development of plants through regulation and production. In cultivar BR 206, elicitors promoted osmotic adjustment, verifying significant increases in AA and PRO in DHCs with GA3, H_2O_2, and SA compared to control and saline stress without elicitors. However, in cultivar BRS 5037 Cruzeta, DHCs-SA significantly increased TSS, AA, and PRO compared to control and salt stress without elicitors. The DHCs with salicylic acid allowed the shoot and root length results and the accumulation of amino acids to be similar between the two cultivars. However, the TSS accumulation in the salinity-sensitive cultivar treated with DHCs-SA was significant for acclimatization to salt stress. Our results confirm that salicylic acid favors plant growth and development [44]. The salicylic acid promotes an increase in proline production, increasing osmotic adjustment, allowing for more water absorption and triggering antioxidant enzyme activity [30,45]. This result may be more apparent when the species is susceptible to saline stress, as observed for BRS 5037 Cruzeta cultivar.

5. Conclusions

Salt stress (250 mM NaCl) reduced maize germination, growth, and dry mass accumulation, and the BR 206 cultivar was more salinity-tolerant than the BRS 5037 Cruzeta cultivar. Discontinuous hydration cycles with water failed to increase the salt stress tolerance of

maize seeds. However, discontinuous hydration cycles with gibberellic acid, hydrogen peroxide, and salicylic acid promoted salt stress tolerance in maize. Discontinuous hydration cycles with saline stress tolerance elicitors improve germination, growth, and dry mass accumulation of maize under saline stress, mainly by inducing the synthesis of the osmoprotectant, such as proline, amino acids, and sugars. The osmotic adjustment in the salinity-tolerant cultivar—BR 206—occurred via the increase in amino acids and proline, and in the salinity-sensitive cultivar—BRS 5037 Cruzeta—via the increase in sugars, amino acids, and proline. The salinity-tolerant cultivar—BR 206—responded to three stress elicitors: gibberellic acid, hydrogen peroxide, and salicylic acid. However, the salinity-sensitive cultivar—BRS 5037 Cruzeta—responded only to salicylic acid. Salicylic acid is the most suitable elicitor for discontinuous hydration cycles in maize seeds aiming to increase salt stress tolerance.

Author Contributions: K.T.O.P., S.B.T., E.P.d.P. and F.V.d.S.S. contributed to the study conception and design. Conduction of the experiment, data collection, and analysis were performed by K.T.O.P., T.R.C.A. and M.L.d.S.N. K.T.O.P. and F.V.d.S.S. wrote the first draft of the manuscript. S.B.T., E.P.d.P., M.L.d.S.N., J.B.V., L.S.S., C.P.B., T.D.C.P., M.F.N., N.d.S.D. and F.V.d.S.S. contributed to the manuscript revision, read, and approved the final version. All authors have read and agreed to the published version of the manuscript.

Funding: This research was funded by Coordenação de Aperfeiçoamento de Pessoal de Nível Superior, grant number 001.

Data Availability Statement: All data are presented in the paper.

Conflicts of Interest: The authors declare no conflict of interest.

References

1. Food and Agriculture Organization of the United Nations Statistics (FAOSTAT). Estimative. 2020. Available online: http://www.fao.org/faostat/en/#data (accessed on 10 March 2022).
2. Food and Agriculture Organization of the United Nations (FAO). Global Information and Early Warmning System 2021 (GIEWS). *Country Briefs.* Available online: https://www.fao.org/giews/countrybrief/country.jsp?code=BRA (accessed on 10 March 2022).
3. Companhia Nacional de Abastecimento (CONAB). Acompanhamento da Safra 2021/22, Brasileira de Grãos. Brasília, DF, Sexto Levantamento. Available online: https://www.conab.gov.br/info-agro/safras/graos/boletim-da-safra-de-graos (accessed on 15 March 2022).
4. Saxena, R.; Kumar, M.; Tomar, R.S. Plant responses and resilience towards drought and salinity stress. *Plant Arch.* **2019**, *19*, 50–58. Available online: http://www.plantarchives.org/SPL%20ISSUE%20SUPP%202,2019/50-58.pdf (accessed on 25 May 2022).
5. Ferreira, P.A.; Silva, J.B.L.; Ruiz, H.A. Aspectos físicos e químicos de solos em regiões áridas e semiáridas. In *Manejo da Salinidade na Agricultura: Estudo Básico e Aplicado*, 2nd ed.; Gheyi, H.R., Dias, N.S., Lacerda, C.F., Gomes Filho, E., Eds.; INCTSal: Fortaleza, Brasil, 2016; Volume 1, pp. 17–34.
6. Liang, W.; Ma, X.; Wan, P.; Liu, L. Plant salt-tolerance mechanism: A review. *Biochem. Biophys. Res. Commun.* **2018**, *495*, 286–291. [CrossRef] [PubMed]
7. Ludwiczak, A.; Osiak, M.; Cárdenas-Pérez, S.; Lubínska-Mielínska, S.; Piernik, A. Osmotic stress or ionic composition: Which affects the early growth of crop species more? *Agronomy* **2021**, *11*, 435. [CrossRef]
8. Silva, H.A.; Oliveira, D.F.A.; Avelino, A.P.; Macêdo, C.E.C.; Barros-Galvão, T.; Voigt, E.L. Salt stress differentially regulates mobilisation of carbon and nitrogen reserves during seedling establishment of *Pityrocarpa moniliformis*. *Plant Biol.* **2019**, *21*, 1110–1118. [CrossRef] [PubMed]
9. Andrade, W.L.; Melo, A.S.; Melo, Y.L.; Sá, F.V.S.; Rocha, M.M.; Oliveira, A.P.S.; Fernandes Júnior, P.I. Bradyrhizobium inoculation plus foliar application of salicylic acid mitigates water deficit effects on cowpea. *J. Plant Growth Regul.* **2021**, *40*, 656–667. [CrossRef]
10. Sidhu, G.P.S.; Singh, H.P.; Batish, D.R.; Kohli, R.K. Tolerance and hyperaccumulation of cadmium by a wild, unpalatable herb *Coronopus didymus* (L.) Sm. (*Brassicaceae*). *Ecotoxicol. Environ. Saf.* **2017**, *135*, 209–215. [CrossRef]
11. Ghaffari, H.; Tadayon, M.R.; Nadeem, M.; Cheema, M.; Razmjoo, J. Proline-mediated changes in antioxidant enzymatic activities and the physiology of sugar beet under drought stress. *Acta Physiol. Plant.* **2019**, *41*, 23. [CrossRef]
12. Meena, M.; Divyanshu, K.; Kumar, S.; Swapnil, P.; Zehra, A.; Shukla, V.; Yadav, M.; Upadhyay, R.S. Regulation of L-proline biosynthesis, signal transduction, transport, accumulation and its vital role in plants during variable environmental conditions. *Heliyon* **2019**, *5*, e02952. [CrossRef]

13. Akter, L.; Fakir, O.A.; Alam, M.K.; Islam, M.U.; Chakraborti, P.; Alam, M.J.; Rashid, M.H.; Begum, M.; Kader, M.A. Amelioration of salinity stress in maize seed germination and seedling growth attributes through seed priming. *Open J. Soil Sci.* **2018**, *8*, 137–146. [CrossRef]
14. Costa, A.A.; Paiva, E.P.; Torres, S.B.; Souza Neta, M.L.; Pereira, K.T.O.; Leite, M.S.; Sá, F.V.S. Seed priming improves *Salvia hispanica* L. seed performance under salt stress. *Acta Sci. Agron.* **2021**, *43*, e52006. [CrossRef]
15. Singh, P.K.; Shahi, S.K.; Singh, A.P. Effects of salt stress on physico-chemical changes in maize (*Zea mays* L.) plants in response to salicylic acid. *Indian J. Plant Sci.* **2015**, *4*, 69–77. Available online: https://www.cibtech.org/J-Plant-Sciences/PUBLICATIONS/2015/VOL-4-NO-1/13-JPS-DEC-016-2014-PRAMOD-EFFECTS-SALICYLIC.pdf (accessed on 15 March 2022).
16. Lima, A.; Meiado, M. Discontinuous hydration alters seed germination under stress of two populations of cactus that occur in different ecosystems in Northeast Brazil. *Seed Sci. Res.* **2017**, *27*, 292–302. [CrossRef]
17. Lima, A.T.; Cunha, P.H.J.; Dantas, B.F.; Meiado, M.V. Does discontinuous hydration of *Senna spectabilis* (DC.) H.S. Irwin & Barneby var. excelsa (Schrad.) H.S. Irwin & Barneby (*Fabaceae*) seeds confer tolerance to water stress during seed germination? *J. Seed Sci.* **2018**, *40*, 36–43. [CrossRef]
18. Nicolau, P.B.; Silva, F.E.; Felix, F.C.; Torres, S.B.; Pacheco, M.V.; Pereira, M.D. Discontinuous hydration on the germination of *Mimosa caesalpiniifolia* and *Pityrocarpa moniliformis* seeds under water stress. *Rev. Caatinga* **2020**, *33*, 555–561. [CrossRef]
19. Sarmento, E.C.S.; Oliveira, F.S.; Cabral, F.A.S.; Oliveira, D.F.; Dutra, A.D. Physiological potential of sorghum seeds under discontinuous hydration and water deficiency conditions. *Rev. Ciência Agronômica* **2020**, *51*, e20207200. [CrossRef]
20. Santos Júnior, J.L.; Freitas, R.S.; Silva, E.C. Discontinuous hydration improves germination and drought tolerance in *Annona squamosa* seedlings. *Res. Soc. Dev.* **2021**, *10*, e56710313706. [CrossRef]
21. Farooq, M.; Hussain, M.; Wakeel, A.; Siddique, K.H.M. Salt stress in maize: Effects, resistance mechanisms, and management. A review. *Agron. Sustain. Dev.* **2015**, *35*, 461–481. [CrossRef]
22. Shi, R.; Tong, L.; Du, T.; Shukla, M.K. Response and modeling of hybrid maize seed vigor to water deficit at different growth stages. *Water* **2020**, *12*, 3289. [CrossRef]
23. Ministério da Agricultura, Pecuária e Abastecimento (MAPA). *Regras Para Análise de Sementes*; MAPA/SDA: Brasília, Brazil, 2009.
24. Pereira, K.T.O.; Sá, F.V.S.; Torres, S.B.; Paiva, E.P.; Alves, T.R.C.; Oliveira, R.R. Exogenous application of organic acids in maize seedlings under salt stress. *Braz. J. Biol.* **2021**, *84*, e250727. [CrossRef]
25. Yemm, E.W.; Willis, A.J. The estimation of carbohydrates in plant extracts by anthrone. *Biochem. J.* **1954**, *57*, 508–514. [CrossRef]
26. Yemm, E.W.; Armar, E.C.; Ricketts, R.E. The determination of amino acid with ninhydrin. *Analyst* **1955**, *80*, 209–213. [CrossRef]
27. Bates, L.S.; Waldren, R.P.; Teare, I.D. Rapid determination of free proline for water-stress studies. *Plant Soil* **1973**, *39*, 205–207. [CrossRef]
28. Ferreira, D.F. Sisvar: A computer analysis system to fixed effects split plot type designs. *Rev. Bras. Biom.* **2019**, *37*, 529–535. [CrossRef]
29. Asad, F.; Dilawar, N.; Rahman, N.; Wisal; Shakeel, M.; Ghazal, M. Effect of indole-3- acetic acid and gibberellic acid (GA_3) on seeds germination, growth performance and biochemical constituents of *Zea mays* L. growing under the salt stress. *Pure Appl. Biol.* **2022**, *11*, 639–650. [CrossRef]
30. Khan, A.; Bilal, S.; Khan, A.L.; Imran, M.; Shahzad, R.; Harrasi, A.A.; Rawahi, A.; Al-Azhri, M.; Mohanta, T.K.; Lee, I.-J. Silicon and gibberellins: Synergistic function in harnessing ABA signaling and heat stress tolerance in date palm (*Phoenix dactylifera* L.). *Plants* **2020**, *9*, 620. [CrossRef]
31. Sá, F.V.S.; Brito, M.E.B.; Silva, L.A.; Moreira, R.C.L.; Paiva, E.P.; Souto, L.S. Exogenous application of phytohormones mitigates the effect of salt stress on *Carica papaya* plants. *Rev. Bras. Eng. Agríc. Ambient.* **2020**, *24*, 170–175. [CrossRef]
32. Rodrigues, M.H.B.S.; Silva, J.N.; Alves, E.U.; Bruno, R.L.A. Hydrogen peroxide as a mitigation of salt stress on the germination of *Myracroduon urundeuva* (Allemão) Engl. Seeds. *Sci. For.* **2021**, *49*, e3557. [CrossRef]
33. Sies, H. Hydrogen peroxide as a central redox signaling molecule in physiological oxidative stress: Oxidative eustress. *Redox Biol.* **2017**, *11*, 613–619. [CrossRef]
34. Braz, R.S.; Lacerda, C.F.; Assis Júnior, R.N.; Ferreira, J.F.S.; Oliveira, A.C.; Ribeiro, A.A. Growth and physiology of maize under water salinity and nitrogen fertilization in two soils. *Rev. Bras. Eng. Agríc. Ambient.* **2019**, *23*, 907–913. [CrossRef]
35. Catão, H.C.R.M.; Caixeta, F.; Lopes, A.M.; Nery-Silva, F.A.; Sá-Júnior, A. Antioxidant activity and physiological performance of popcorn seed after saline stress and analysis of seedling images. *Ciência Agrotecnol.* **2020**, *44*, e005020. [CrossRef]
36. Soothar, M.K.; Hamani, A.K.M.; Sootaha, R.M.K.; Sun, J.; Yang, G.; Bhatti, S.M.; Traore, A. Assessment of acidic biochar on the growth, physiology and nutrients uptake of maize (*Zea Mays* L.) seedlings under salinity stress. *Sustainability* **2021**, *13*, 3150. [CrossRef]
37. Roy, S.J.; Negrão, S.; Tester, M. Plantas de cultivo resistentes ao sal. *Curr. Opin. Biotechnol.* **2014**, *26*, 115–124. [CrossRef] [PubMed]
38. Bai, B.; Sikron, N.; Gendler, T.; Kazachkova, Y.; Barak, S.; Grafi, G.; Khozin-Goldberg, I.; Fait, A. Ecotypic variability in the metabolic response of seeds to diurnal hydration-dehydration cycles and its relationship to seed vigor. *Plant Cell Physiol.* **2012**, *53*, 38–52. [CrossRef] [PubMed]
39. Gonçalves, B.G.; Ribeiro, L.M.; Dias, D.S.; Mazzottini-dos-Santos, H.C.; Martins, C.P.S.; Lopes, P.S.N.; Mercadante-Simões, M.O. Embryo responses to extreme water events provide insights into the behavior of *Butia capitata* (*Arecaceae*) seed banks during hydration cycles. *Environ. Exp. Bot.* **2020**, *169*, 103904. [CrossRef]

40. Hu, X.-L.; Yu, X.-M.; Chen, H.-Y.; Li, W.-Q. Turnover of glycerolipid metabolite pool and seed viability. *Int. J. Mol. Sci.* **2018**, *19*, 1417. [CrossRef]
41. Chen, K.; Arora, R. Priming memory invokes seed stress-tolerance. *Environ. Exp. Bot.* **2013**, *94*, 33–45. [CrossRef]
42. Bowne, J.; Bacic, A.; Tester, M.; Roessner, U. Abiotic stress and metabolomics. *Annu. Plant Rev. Biol. Plant Metab.* **2011**, *43*, 61–85. [CrossRef]
43. Wan, Q.; Hongbo, S.; Zhaolong, X.; Jia, L.; Dayong, Z.; Yihong, H. Salinity tolerance mechanism of osmotin and osmotin-like proteins: A promising candidate for enhancing plant salt tolerance. *Curr. Genom.* **2017**, *18*, 553–556. [CrossRef]
44. Khan, M.I.R.; Fatma, M.; Per, T.S.; Anjum, N.A.; Khan, N.A. Salicylic acid-induced abiotic stress tolerance and underlying mechanisms in plants. *Front. Plant Sci.* **2015**, *6*, 462. [CrossRef]
45. Sharma, L.; Priya, M.; Kaushal, N.; Bhandhari, K.; Chaudhary, S.; Dhankher, O.P.; Prasad, P.V.; Siddique, K.H.; Nayyar, H. Plant growth-regulating molecules as thermoprotectants: Functional relevance and prospects for improving heat tolerance in food crop. *J. Exp. Bot.* **2020**, *71*, 569–594. [CrossRef]

agriculture

MDPI

Article

Growth, Solute Accumulation, and Ion Distribution in Sweet Sorghum under Salt and Drought Stresses in a Brazilian Potiguar Semiarid Area

Gabriela Carvalho Maia de Queiroz [1,*], José Francismar de Medeiros [1,*], Rodrigo Rafael da Silva [1], Francimar Maik da Silva Morais [1], Leonardo Vieira de Sousa [1], Maria Vanessa Pires de Souza [2], Elidayane da Nóbrega Santos [1], Fagner Nogueira Ferreira [1], Juliana Maria Costa da Silva [1], Maria Isabela Batista Clemente [1], Jéssica Christie de Castro Granjeiro [1], Matheus Nathan de Araújo Sales [1], Darcio Cesar Constante [1], Reginaldo Gomes Nobre [1] and Francisco Vanies da Silva Sá [1]

[1] Agricultural Sciences Center, Federal Rural University of Semi-Arid, Mossoró 59625-900, RN, Brazil
[2] Agricultural Engineering Department, Federal University of Ceará, Fortaleza 60455-760, CE, Brazil
* Correspondence: gabriela.queiroz@alunos.ufersa.edu.br (G.C.M.d.Q.); jfmedeir@ufersa.edu.br (J.F.d.M.)

Abstract: Agriculture in semiarid regions commonly face problems because of salt and availability of irrigation water. Considering this, studies on cultures resistant to salt and water stresses involving sweet sorghum are required. Therefore, the aim was to evaluate the growth and other mechanisms of tolerance to salinity and water deficit in BRS 506 sweet sorghum. The experimental design was conducted in Upanema-RN, Brazil, in randomized blocks, where the isolated and interactive effect of 3 salinity levels, expressed as the electrical conductivity of irrigation water (1.5, 3.8, and 6.0 dS m^{-1}), and 3 irrigation depths (55, 83, and 110% of crop evapotranspiration) were evaluated. During the cycle, sorghum adapted to the salinity and deficit irrigation depth, since stem height reduced only −5.5% with increasing salinity and −11.95% with decreasing irrigation depth, and aerial dry mass was affected by interaction only at the end of the cycle. Proline, total amino acids, and total soluble sugars were not differenced by stresses. Additionally, around 68.71% of total Na^+ was at roots at the end of the cycle. In summary, sorghum BRS 506 was more tolerant to salt than water stress and used Na^+ compartmentalization in root cells as the main tolerance mechanism.

Keywords: salinity; sorghum; stress response; tolerance; water deficit; tolerance

1. Introduction

In a world of 7.7 billion people, water security is already at risk, and it is expected to aggravate in 2050, especially in developing countries such as Africa and Asia, where clean water is already a major issue [1]. When it comes to agricultural purposes, this lack of both quantity and quality water availability directly affects crop production, since irrigation uses around 25% of groundwaters, serving 38% of the world's irrigated land [2]. Besides this, water scarcity, climate change, and inadequate agricultural management practices have posed a risk to arable land, where 1.5 million ha of production are lost each year due to soil salinity [3]. Therefore, it is interesting to explore crops that are tolerant to salinity and water scarcity, so that there is a balance between social, economic, and environmental aspects of agricultural production.

Among such crops is sorghum, which can be used for different purposes depending on the type (graniferous, biomass, sugar, or broom). In particular, sweet sorghum accumulates a juice rich in sugars in the stalk, so that it can be used in the formation of byproducts such as bioethanol, brown sugar, and molasses, while the rest of the plant can be used for fodder. As it offers greater profitability, the most exploited b-product in saccharin cultivars is bioethanol, whose productivity can be compared to the bioconversion of 12–13 tons of

corn kernels [4]. Considering adjustments due to fermentation efficiency, a biomass yield between 50 and 120 t ha^{-1} can generate about 10,000 L ha^{-1} of bioethanol [4].

Such information is especially necessary for semiarid regions, since the salinity of the soil and irrigation water, as well as the reduced water availability, are common factors in these environments, and therefore, there is a limitation in agricultural development. To promote this development and, consequently, provide an additional source of income in these regions, sweet sorghum stands out in relation to other grasses, such as corn, given that it presents moderate tolerance to salinity, without loss of production when irrigated with 4.5 dS m^{-1} EC water [5], and sped up development under water stress conditions [6]. Therefore, knowing how sweet sorghum metabolism responds to salinity and water scarcity is essential to inform rural producers about what should be prioritized in irrigation water: quality or quantity.

Sweet sorghum growth parameters affected by salt and drought stresses include reduction in leaf area, shoot and root lengths, leaf fresh and dry weights, and total dry mass [7,8]. The presence of salts in soil solution, as well as the unavailability of water, alters its water potential, impairing water absorption and consequently reducing growth. Additionally, both stresses induce ion toxicity in cells followed by an osmotic imbalance, disturbing plant growth and development [9]. However, since sweet sorghum is salt [7] and drought tolerant [4], it means that it adopts physiological, biochemical, and molecular strategies to cope with these stresses [10].

One of the biochemical mechanisms is solute accumulation, as proline, soluble sugars, and amino acids. Proline prevents membrane damage and cell apoptosis by eliminating reactive oxygen species (ROS), OH^- radicals, and signaling redox reactions [11,12]. Soluble sugars have the potential to tampon cell redox potential, protect its structure [13], and maintain photosynthetic activity, ensuring water absorption [14]. On the other hand, amino acids form proteins, are a pool of nitrogen in source and sink tissues, and represent an important precursor of secondary metabolites, promoting crop improvement [15].

Changes in the distribution of toxic ions such as Na^+ and Cl^- are also common in many tolerant crops to deal with abiotic stresses. Ion redistribution acts as a tool for osmotic balance, a process that demands the synthesis of more ATP in order to prevent excessive cation, anion accumulation, and preventing cell membrane damage [16]. Indeed, salt-tolerant plants accumulate excessive Na^+ and Cl^- ions in root tissues to ensure plant growth. This mechanism aims to avoid the translocation of these ions to leaves, where they could damage photosynthetic apparatus and put the survival of the plant at risk [17].

It is common to find in the literature how plant metabolism responds to saline or water stresses isolated, either by changes in growth, electrolyte leakage and relative water content in the leaves, solute accumulation, and/or ionic distribution [7,10,18,19]. However, studies addressing the influence of both stresses are still scarce, and since both can occur simultaneously in nature, it is essential to understand not only the isolated effect but also the interactive effect of both stresses on plant development. In this sense, the innovative approach of this study helps to understand which variables are and which are not affected by the interactive effect of salt and drought stresses. This information provides a better understanding of BRS 506 sweet sorghum tolerance mechanisms and can help other studies involving sweet sorghum cultivars.

Our research seeks to study the sorghum cultivar BRS 506 because, despite already being established in the Brazilian market, it is still not much discussed in the literature. Additionally, it is noteworthy to highlight that no sorghum cultivars were developed specifically for the Brazilian northeast semiarid. In this sense, our research aims to give visibility to this region and help breeding programs to develop cultivars adapted to it, and therefore, addressing its economic development. The study of sorghum responses to abiotic stresses provides a better understanding of the mechanisms adopted by sorghum to resist these stresses. In addition, using lower-quality water for irrigation of this crop appears as an alternative to reduce costs with minimal productivity losses. In this context, the present

study aimed to evaluate how the saccharin sorghum cultivar BRS 506 responds to deficit irrigation depths and high salinity levels.

2. Materials and Methods

2.1. Location and Characterization of the Experimental Area

The research occurred in an open field, in an experimental area of the Cumaru site, at the municipality of Upanema, Rio Grande do Norte, Brazil (5°33′30″ S; 77°11′56″ W). The climate classification in the region is BSh, hot and dry [20], with an annual rainfall of 633 mm over the last 30 years, concentrated in the months of February to May and an average annual temperature of 26 °C [21,22].

During the execution of the experiment, a meteorological station installed at the site monitored daily data referring to temperature, global radiation, wind speed, and air humidity. There was no occurrence of rainfall in the studied period. The data are shown in Figure 1.

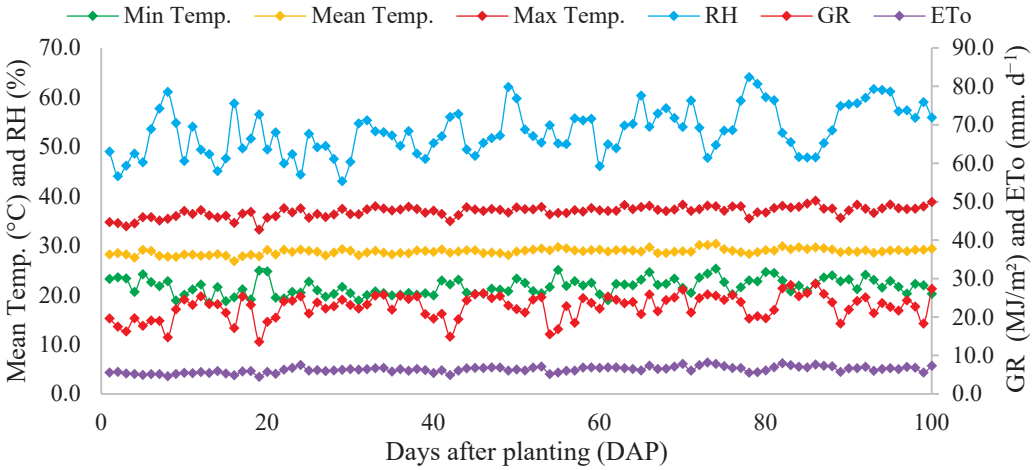

Figure 1. Minimum (Min.), mean, and maximum (Max.) temperatures (Temp.), relative humidity (RH), Global radiation (GR), and reference evapotranspiration (ET_o) registered in the area during the experiment.

The experiment took place on a Cambisol, whose preparation consisted of plowing and harrowing 15 days before planting. Before sowing, we performed foundation fertilization with 17.76 kg ha^{-1} of nitrogen and 65.34 kg ha^{-1} of phosphorus. The physical and chemical characterization of 0–30 and 30–60 cm layers are shown in Table 1.

Table 1. Physical and chemical characterization of the 0–20 cm layer of the soil in the studied area before the experiment was conducted.

Layer	Soil Physics					
	Coarse Sand	Fine Sand	Silt	Clay	Soil Density	
cm	g g^{-1}				g cm^{-3}	
0–30	0.544	0.223	0.044	0.190	1.64	
30–60	0.480	0.218	0.052	0.250	1.62	
	Soil chemistry					
	ECex	pH	Ca^{2+}	Mg^{2+}	Na^{+}	K^{+}	P
	dS m^{-1}		cmol$_c$ dm^{-3}				mg dm^{-3}
0–30	0.90	7.50	4.80	1.50	0.35	0.46	15
30–60	0.80	7.20	5.10	1.60	0.39	0.45	8

Note: Ecex: Electrical conductivity of extract.

For soil salinity we used saturation paste, where we determined the electrical conductivity and percentage of exchangeable sodium. Electrical conductivity was obtained with the aid of a conductivity meter, whereas for PST, we determined Na^+, K^+, Ca^{2+}, and Mg^{2+}, where Na^+ and K^+ were extracted with Melich-1 and Ca^{2+} and Mg^{2+} with KCl [23].

In the week before planting, we used volumetric rings of approximately 50 cm^3 to collect undisturbed samples in layers 20, 40, and 60 cm to check soil moisture and guarantee the treatments applied. We covered the samples with aluminum foil to preserve the soil structure and took them to the laboratory to be cleaned. With this material, the samples were weighed to determine the soil density (Ds) and subjected to tensions of 1, 3, 6, and 10 kPa in a tension table and 30, 60, 100, 300, and 1500 kPa in a Richards chamber for determination of volumetric humidity. Data were presented as 0–30 and 30–60 cm layers.

At the beginning of the third week of the experiment, tensiometers were installed at depths of 20 cm to represent 0–30 cm layer, and at 40 cm, representing 30–60 cm layer, to verify the water retention in the soil. We recorded the height of the water column on the tensiometers and measured the tension with a tensimeter, twice a week, always before starting irrigation. Based on the observed volumetric humidity, we obtained water retention curves in these layers. The curves, as well as the determined parameters of the Van Genuchten equation can be seen in Figure 2.

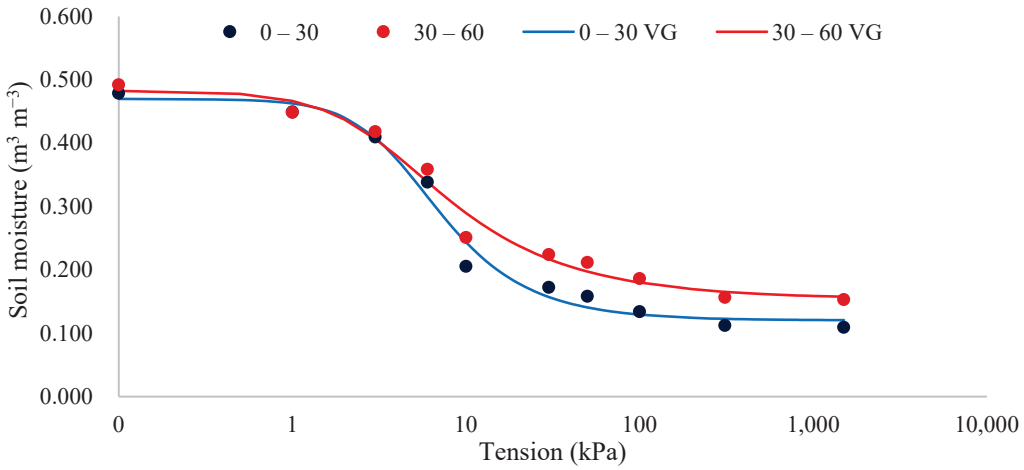

Figure 2. Retention curves at 0–30 and 30–60 cm layers observed in the experimental area.

2.2. Plant Material, Experimental Design, and Treatments

The crop studied was sweet sorghum (*Sorghum bicolor* L. Moench), cultivar BRS 506, whose seeds were donated by the Instituto Agronômico do Pernambuco (IPA). Sorghum was planted in early August 2021, at the beginning of the dry period. We choose cultivar BRS 506 because it has the potential for the economic development of semiarid regions, since sorghum has moderate tolerance to salinity stress [5] and develops well under water scarcity [24]. In addition, it has a dual purpose: while the plant material can be used for fodder, the juice in the stalks can generate byproducts such as bioethanol, honey, or brown sugar.

The experimental design was in randomized blocks, comprising 4 blocks in a 3 × 3 double factorial scheme, with 3 salinity levels and 3 irrigation depths, corresponding to 9 treatments (Figure 3). The area consisted of 36 experimental plots, where each plot comprised 2 double rows of sorghum, 7.0 m long, spaced 1.35 × 0.25 × 0.10 m.

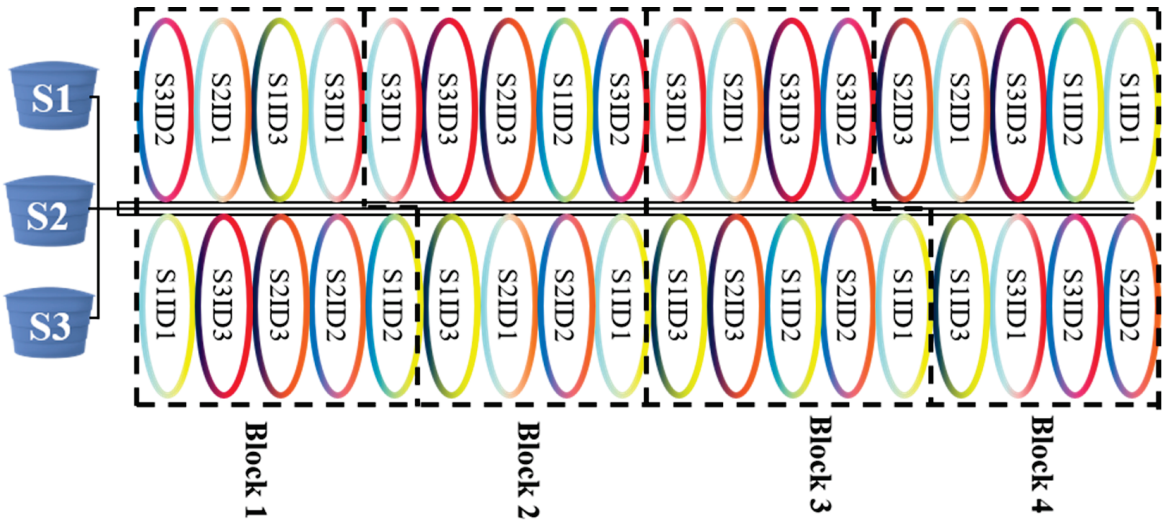

Figure 3. Sketches of the experimental area.

The adopted irrigation was done by dripping, and the water used in the experiment came from a tubular well near, of conductivity 1.5 dS m^{-1}. To establish salinities, conductivities 1.5; 3.8, and 6.0 dS m^{-1}, based on crop tolerance [5]. The salinity levels were got by mixing NaCl, $CaCl.2H_2O$, and $MgSO_4.7H_2O$ salts, until the final molar ratio of loads of 7:2:1 for Na^+, Ca^{2+}, and Mg^{2+}, in order to represent the average composition of the waters of the northeastern in the semiarid region [25].

The irrigation depths were delimited according to crop evapotranspiration (Figure 4). Figure 4 shows the historical series in Mossoró in the last 30 years, where it can be seen that the ETo registered in area was similar to the historical average. ETc was calculated using the Penman–Monteith–FAO equation [26] based on data obtained from the meteorological station installed in the area.

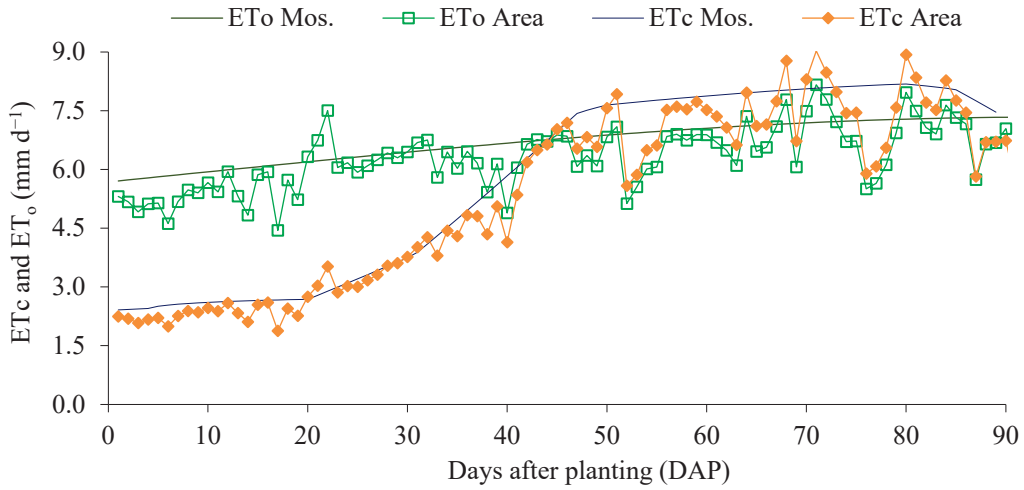

Figure 4. ETc e ETo registered at Mossoró (Mos) and observed in the experiment area (Area) during the experiment.

The flow rates were ascertained according to the spacing between the drippers after flow tests. For the ID1 depth (55% of ETc), the drippers were spaced at 0.30 m, while for ID2 (83% of ETc) and ID3 (110% ETc), 0.20 m, with the difference that for ID3 2 drip tapes were used. To guarantee the applied depths, weekly flow tests were carried out based on water pressure, using a manometer. On average, the outflows of the emitters were

1.5 l h^{-1}, with an emission uniformity coefficient of 95%, based on evaluations carried out at the beginning and middle of the crop cycle.

2.3. Growth Parameters

To measure the sorghum leaf area, we quantified: number of leaves (*NL*), width (W_D), and length (L_D) of the diagnosis leaf at 39 and 60 days after planting (DAP). Leaves were counted manually, considering only the photosynthetically active ones, while WD and LD were measured with a measuring tape, considering only 1 decimal place. The number of leaves and the width and length of the diagnosis leaf were used to calculate the leaf area, according to Equation (1) [27]:

$$LA = NL \times L_D \times W_D \times 0.747 \quad (1)$$

Total height (TH), shoot height (SH), and stem diameter (SD) were measured at 39, 60, and 81 DAP. For TH, we measured from the base of the stem to the apex of the panicle, while SH was measured from the base of the stem to the base of the last leaf, in which a 2 m ruler was used for both. The stem diameter was measured with a digital caliper at approximately 20 cm from the ground, considering 2 decimal places. Data for each plot comprised of the average of data from 5 plants.

Throughout the cycle, 2 plants per plot were collected in the 3 sorghum growth stages: 39 (beginning), 60 (flowering), and 81 (ending) DAP. In the laboratory, the roots were washed and brushed to remove excess soil, and the stem was cut into pieces to facilitate drying in the oven. Then, the samples were taken to the forced circulation oven at 65 °C for 72–96 h, until they reached constant mass. After drying, the root, stem, and leaves were weighed to get the dry mass (DM), used to quantify the content of ions. For growth, the sum of the dry mass of the leaves and stem was considered, and therefore, the aerial dry mass (ADM).

2.4. Electrolyte Leakage and Relative Water Content

For electrolyte leakage (*EL*) analysis, each plot was represented by 10 leaf disks of 0.79 cm^2, cut from the diagnosis leaves of 5 plants at 39, and 60 DAP. The disks were initially immersed in deionized water, from which the initial electrical conductivity (EC_i) was measured, and placed in a water bath for 2 h at 85 °C, where the final electrical conductivity (EC_f) was measured. *EL* was calculated by the ratio of conductivities measured, as elucidated in Equation (2) [11]:

$$EL(\%) = \frac{EC_f}{EC_i} \times 100 \quad (2)$$

The relative water content (*RWC*) was measured in the same 5 diagnosis leaves per plot used in the analysis of electrolyte leakage, from which 15 leaf disks of 0.79 cm^2 were cut, and later weighed on a precision scale to get the fresh mass of the disks (FM_D). The disks were immersed in deionized water for 24 h to get the saturated mass of the disks (SM_D) and weighed again. Subsequently, excess water from the disks was removed with a paper towel, so that they were placed in paper envelopes, identified, and dried in an oven at 65 °C for 24 h to get the dry mass of the disks (DM_D). The RWC calculation was performed according to Equation (3) [28]:

$$RWC(\%) = \frac{FM_D - DM_D}{SM_D - DM_D} \times 100 \quad (3)$$

2.5. Proline, Total Amino Acids, and Total Soluble Sugars

At 81 DAP, 3 diagnosis leaves per plot were collected for proline (PRO), total amino acids (TAA), and total soluble sugars (TSS). At the time of collection, the leaves were stored in plastic bags, identified, placed in a cooler with ice, and immediately taken to the

laboratory, where they were placed in an ultra-freezer at −80 °C until analysis. Analyses were performed using an extract obtained from 400 mg of leaf tissue, which was macerated in liquid nitrogen and dissolved in 6 mL of alcohol, then centrifuged. The analysis of proline used an aliquot of 750 µL [29], total amino acids, 200 µL [30], and total soluble sugars, 20 µL [31].

2.6. Concentration and Content of Na^+, K^+, and Cl^-

With the material dried in an oven at 65 °C obtained in the determination of the dry mass (Topic 2.3), the samples were ground in a Willey SL-31 knife mill and sieved in the 1.00 mm mesh to quantify the Na^+, K^+, and Cl^- concentrations. The extract used in the Na^+ and K^+ analyses comprised 0.5 g of material taken to the muffle at 500 °C for 3 h and later diluted at 25 mL of HNO_3, with readings by flame photometry [32]. For Cl^-, 0.5 g of material was diluted in 50 mL of $Ca(NO_3)_2$, then taken to a shaking table for 15 min and titrated with $AgNO_3$, using 5% K_2CrO_4 as solution indicator [33]. Cl^- concentration was done according to Equation (4):

$$Cl = \frac{V_{Cl} - V_{AgNO_3}}{100} \times 1000 \quad (4)$$

With the values of the concentrations, it was possible to calculate the content and distribution of ions by organ. The content refers to the product between the ion concentration and the dry mass of each organ, in other words, the total of Na^+, K^+, and Cl^- in the roots, shoot, or leaves. The distribution was obtained by the ration between the ion content in the organ (e.g., total Na^+ in the root, shoot, or leaf) and in the whole plant (e.g., Na^+ content in roots relative to the total Na^+ in plant).

2.7. Statistical Analysis

Data were submitted to analysis of variance (ANOVA) with the statistical significance of the F test. Tukey's test at 5% significance was used to compare means when there were isolated effects and when the interaction was significant. The software used for the ANOVA was RStudio, with R version 4.2.2.1 [34], through the ExpDes.pt package, while Statistica [35] was used to perform Pearson correlation matrixes.

For the variables where interaction was significant, we tested eight equation models, using the ExpAnalysis3D package, considering the effects of salinity (Salt) and irrigation depth (ID) at the linear, quadratic level, up to the simple interaction. The equations were chosen by the Akaike Information Criteria (AIC), in which those with the lowest AIC were selected. Equations that presented regression deviation with a significance level below 0.05 were not considered.

3. Results

3.1. Growth Parameters

Salt and ID affected growth parameters mainly at the beginning of the cycle, where both the isolated effect of Salt and ID were significant for LA, SH, and TH (Table 2). During the entire cycle, water stress was more severe than saline stress for plant development, but there was no statistical difference between 1.5 and 3.8 dS m^{-1} ECs, while the reduction of applied irrigation depth reduced progressively SH and TH at 39 and 60 DAP. However, sorghum showed minimal losses in growth parameters at 55% of ETc, compared to 110% ETc, like SH, where the loss was −11.95% at 81 DAP.

The Salt × ID interactive effect was observed only for ADM at 81 DAP. There was no significant difference between the salinities under L1 and L2 irrigation depths, nor between the irrigation depths under S1 salinity (Table 3). On average, at the end of the cycle, the aerial dry mass varied between 160 and 210 g, approximately.

Table 2. F Test values for leaf area (LA), stem diameter (SD), shoot height (SH), total height (TH), and aerial dry mass (ADM) measured at 39, 60, and 81 DAP.

		39 DAP					60 DAP					81 DAP			
SV	**DF**	**LA**	**SD**	**SH**	**TH**	**ADM**	**LA**	**SD**	**SH**	**TH**	**ADM**	**SD**	**SH**	**TH**	**ADM**
Block	3	1.69	3.10 *	1.61	1.61	3.00	0.57	0.89	1.39	1.38	0.23	1.27	0.24	0.67	2.83
Salt	2	3.41 *	3.66 *	15.16 **	15.16 **	2.47	5.00 *	0.32	6.71 **	3.15	0.85	0.23	3.46 *	0.33	1.54
ID	2	10.74 **	3.12	52.86 **	52.86 **	4.24 *	0.41	0.09	37.15 **	34.21 **	0.08	0.69	20.62 **	3.29	0.91
Salt × ID	4	0.44	0.05	0.73	0.73	1.99	0.09	0.54	0.71	0.68	1.44	1.09	0.48	1.22	4.31 **
C. V. (%)		14.2	6.1	10.1	5.2	17.0	19.4	5.9	6.6	5.8	14.3	7.2	5.0	17.2	10.0
							Mean values								
		cm^2	mm	cm		g	cm^2	mm	cm		g	mm	cm		g
1.5 dS m^{-1}		2309.2 a	17.87 ab	68.0 a	132.1 a	51.09 a	2392.0 b	17.81 a	224.7 a	249.3 a	133.08 a	16.69 a	211.6 a	243.0 a	530.55
3.8 dS m^{-1}		2180.2 ab	18.07 a	63.2 a	127.4 a	45.63 a	2512.3 ab	18.04 a	219.7 a	246.5 a	143.53 a	16.47 a	207.1 ab	256.9 a	569.43
6.0 dS m^{-1}		1984.6 b	16.96 b	54.2 b	118.0 b	44.25 a	3014.1 a	18.15 a	204.2 b	235.6 a	139.28 a	16.37 a	200.6 b	248.0 a	556.23
55% ETc		1852.9 b	17.00 a	48.1 c	111.5 c	42.52 b	2719.6 a	18.09 a	190.0 c	218.4 c	140.34 a	16.67 a	194.6 b	237.4 a	545.14
83% ETc		2190.7 a	17.99 a	63.2 b	127.4 b	46.47 ab	2663.9 a	17.91 a	218.5 b	247.3 b	137.22 a	16.18 a	203.7 b	235.3 a	569.44
110% ETc		2430.5 a	17.91 a	74.1 a	138.9 a	51.98 a	2534.8 a	18.00 a	240.1 a	265.7 a	138.34 a	16.67 a	221.0 a	275.2 a	541.63

* 5% significance; ** 1% significance. Different letters in each column indicate significant differences at 0.05 level according Tukey Test.

Table 3. Breakdown of aerial dry mass at 81 DAP (ADM_81).

ADM_81				
	g			
	55% ETc	83% ETc	110% ETc	Mean
1.5 dS m^{-1}	176.74 aA	183.93 aA	169.88 bA	530.55
3.8 dS m^{-1}	175.38 aB	184.14 aAB	209.91 aA	569.43
6.0 dS m^{-1}	193.02 aAB	201.37 aA	161.84 bB	556.23
Mean	545.14	569.44	541.63	
No tested equations were significant				

Lowercase letters compare column means and uppercase letters compare row means.

3.2. Electrolyte Leakage and Relative Water Content

At 39 DAP, both electrolyte leakage and relative water content were influenced by the Salt × ID interaction (Table 4). At 60 DAP, only salinity affected EL and RWC. At flowering, the 6.0 dS m^{-1} EC resulted in an EL 13.29% higher than that observed under 1.5 dS m^{-1} EC, and 9.29% than observed at 3.8 dS m^{-1}. EC of 6.0 dS m^{-1} reduced RWC by −3.08% when compared to 1.5 dS m^{-1} and by −0.36% compared to 3.8 dS m^{-1}. Despite being statistically significant, the percentage difference between the studied ECs was small, both for EL and RWC, what reinforces the idea of tolerance.

Table 4. F Test values for electrolyte leakage (EL) and Relative Water Content (RWC) at 39 and 60 DAP.

		39 DAP		**60 DAP**	
SV	**DF**	**EL**	**RWC**	**EL**	**RWC**
Block	3	0.79	2.95	14.21 **	0.75
Salt	2	0.48	1.89	3.91 *	4.09 *
ID	2	5.41 *	0.85	2.67	0.31
Salt × ID	4	4.60 **	3.72 *	1.66	1.32
C. V. (%)		19.7	3.2	11.4	2.9
			Mean values		
		%		%	
1.5 dS m^{-1}		11.45 a	89.87 a	22.12 b	95.87 a
3.8 dS m^{-1}		10.68 a	90.54 a	22.93 ab	93.26 ab
6.0 dS m^{-1}		11.44 a	92.09 a	25.06 a	92.92 b
55% ETc		12.36	90.21 a	24.41 a	94.19 a
83% ETc		9.52	90.61 a	23.72 a	94.35 a
110% ETc		11.70	91.68 a	21.98 a	93.51 a

* 5% significance; ** 1% significance. Different letters in each column indicate significant differences at 0.05 level according Tukey Test.

Considering the beginning of the cycle, the highest EL was observed in the treatment of higher water stress combined with less salt stress (S1ID1 = 15.26%) and under higher salt stress and absence of water stress (S3ID3 = 14.13%) (Table 5). The response surface is represented in Figure 5. As for the RWC, it was maximum in the treatment of maximum stress (S3ID1 = 94.75%); however, the RWC in S3ID1 was only 8.57% higher than that observed in the treatment of lesser RWC (S2ID1 = 87.27%) (Table 5). For EL_39, the linear effect of Salt was significant, showing a continuous increase in EL with salinity, and a quadratic effect for ID, with lower EL at 83% of ETc.

Table 5. Breakdown of electrolyte leakage and relative water content variables whose interaction was significant.

	EL_39					RWC_39			
	55% ETc	**83% ETc**	**110% ETc**	**Mean**		**55% ETc**	**83% ETc**	**110% ETc**	**Mean**
1.5 dS m^{-1}	15.26 aA	9.26 aB	9.84 bB	11.45	1.5 dS m^{-1}	88.62 bA	90.18 aA	90.81 aA	89.87
3.8 dS m^{-1}	11.60 abA	9.33 aA	11.13 abA	10.68	3.8 dS m^{-1}	87.27 bB	92.43 aA	91.94 aAB	90.54
6.0 dS m^{-1}	10.21 bB	9.98 aB	14.13 aA	11.44	6.0 dS m^{-1}	94.75 aA	89.22 aB	92.30 aAB	92.09
Mean	12.36	9.52	11.70		Mean	90.21	90.61	91.68	
$EL\_39 = 44.72^{***} - 3.12\,EC^{***} - 6.99.10^{-1}\,ID^{***} + 3.30.10^{-3}\,ID^{2\,**} + 3.78.10^{-2}\,ECID^{***}$ ($R^2 = 0.95$)					No tested equations were significant				

EL_39: Electrolyte leakage at 39 DAP; RWC_39: Relative water content at 39 DAP. * 5% significance; ** 1% significance; *** 0.1% significance. Lowercase letters compare column means and uppercase letters compare row means.

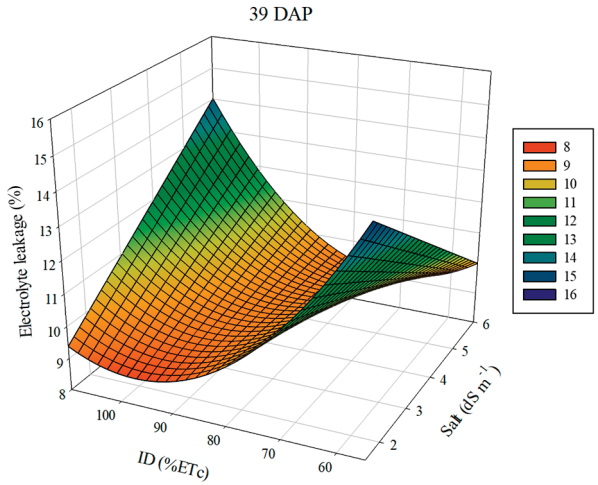

Figure 5. Response surfaces for electrolyte leakage at 39 DAP.

3.3. Proline, Total Amino Acids, and Total Soluble Sugars

According to the F test, even at 81 DAP—ending of the crop cycle—the studied salinities or irrigation depths did not result in a significant difference in the accumulation of organic solutes (Table 6).

Table 6. F Test values for proline, total amino acids, and total soluble sugars at 81 DAP.

SV	DF	Proline	Total Amino Acids	Total Soluble Sugars
Block	3	2.87 ns	1.10 ns	0.93 ns
Salt	2	0.72 ns	0.08 ns	1.56 ns
ID	2	0.07 ns	0.36 ns	2.73 ns
Salt × ID	4	1.21 ns	0.26 ns	0.87 ns
C. V. (%)		2.6	11.5	18.1
			General mean	
			µmol g FM^{-1}	µg g FM^{-1}
		3.96	12.21	17.97

ns: Non-significant.

3.4. Concentration and Content of Na^+, K^+, and Cl^- at Plant Tissue

At 39 DAP Salt influenced the concentration of K^+ in the roots and Na^+ in the shoot, with no effect on leaves (Table 7). During flowering time (60 DAP), increasing EC promoted higher Na^+ concentration in roots and leaves, whereas decreasing ID increased Na^+ concentration in leaves. At 81 DAP, the isolated effect of Salt was observed on K^+ in roots and leaves, with no isolated effect of ID for the ions in the organs studied. In all variables, the isolated effects of Salt or ID were disregarded when the interaction was significant.

Table 7. F test values for Na^+, K^+ and Cl^- concentration in roots, shoot and leaves at 39, 60, and 81 DAP.

		39 DAP			60 DAP			81 DAP		
SV	**DF**	**Na^+**	**K^+**	**Cl^-**	**Na^+**	**K^+**	**Cl^-**	**Na^+**	**K^+**	**Cl^-**
					Roots					
			mg g^{-1}			mg g^{-1}			mg g^{-1}	
Block	3	0.72	0.43	0.05	1.66	0.34	0.68	0.33	0.69	2.17
Salt	2	129.43 **	10.77 **	17.75 **	223.17 **	1.30	97.08 **	184.44 **	16.47 **	42.73 **
ID	2	1.30	1.90	16.24 **	0.68	6.80 **	1.65	4.78 *	1.69	3.46 *
Salt × ID	4	12.62 **	2.76	3.53 *	0.64	11.67 **	16.83 **	3.49 *	2.63	3.34 *
C. V. (%)		16.4	14.9	11.9	17.7	12.0	11.7	13.5	16.9	13.5
1.5 dS m^{-1}		1.64	13.19 a	13.56	1.00 c	10.00 a	10.42	2.55	10.71 a	15.92
3.8 dS m^{-1}		4.93	10.30 b	16.58	6.89 b	9.48 a	17.44	7.73	7.17 c	22.50
6.0 dS m^{-1}		5.92	13.41 a	18.11	9.90 a	10.24 a	21.08	8.89	8.87 b	26.92
55% ETc		4.06 a	13.00 a	18.64	5.94 a	10.00	16.75 a	6.98	9.49 a	23.00
83% ETc		4.42 a	12.35 a	14.67	5.68 a	10.75	15.50 a	6.30	8.90 a	22.33
110% ETc		4.00 a	11.54 a	14.94	6.18 a	8.97	16.69 a	5.90	8.36 a	20.00
					Shoot					
SV	DF		mg g^{-1}			mg g^{-1}			mg g^{-1}	
Block	3	1.54	6.05	0.23	0.15	2.59	3.20*	0.32	0.72	1.47
Salt	2	42.52 **	1.45	0.43	78.00 **	2.83	0.75	97.64 **	13.05 **	1.60
ID	2	0.07	3.16	0.23	17.56 **	6.77 **	3.07	18.03 **	10.15 **	2.41
Salt × ID	4	1.45	2.41	0.65	5.85 **	4.90 **	1.74	13.63 **	4.47 **	3.32 *
C. V. (%)		15.5	7.3	8.8	17.0	11.4	10.3	20.6	10.6	10.5
1.5 dS m^{-1}		0.55 c	56.98 a	46.83 a	0.27	18.74	24.00 a	0.15	14.61	18.08 a
3.8 dS m^{-1}		0.84 b	54.20 a	47.17 a	0.69	20.89	25.17 a	0.42	12.26	17.33 a
6.0 dS m^{-1}		1.01 a	55.32 a	48.33 a	0.65	19.55	24.17 a	0.60	15.20	18.72 a
55% ETc		0.80 a	55.38 a	46.83 a	0.51	17.85	23.00 a	0.44	12.51	18.17 a
83% ETc		0.80 a	53.50 a	48.00 a	0.44	20.26	24.92 a	0.46	14.38	18.83 a
110% ETc		0.79 a	57.62 a	47.50 a	0.65	21.08	25.42 a	0.28	15.19	17.14 a
					Leaves					
SV	DF		mg g^{-1}			mg g^{-1}			mg g^{-1}	
Block	3	0.52	3.22 *	3.96 *	1.95	0.56	6.42 **	1.50	2.70	7.37 **
Salt	2	0.90	0.41	1.57	5.53 *	0.30	0.86	0.00	6.78 **	2.66
ID	2	1.40	0.32	0.17	6.79 **	3.03	2.42	2.01	0.90	1.44
Salt × ID	4	1.39	1.14	1.84	1.85	1.47	4.02 *	0.37	0.84	2.93 *
C. V. (%)		17.2	6.8	9.1	18.2	9.7	6.5	19.4	9.0	8.6
1.5 dS m^{-1}		0.41 a	27.74 a	16.83 a	0.14 b	13.62 a	14.58 a	0.12 a	11.65 ab	15.33 a
3.8 dS m^{-1}		0.39 a	27.08 a	16.00 a	0.17 ab	14.04 a	15.08 a	0.12 a	10.86 b	14.75 a
6.0 dS m^{-1}		0.43 a	27.27 a	15.83 a	0.17 a	13.82 a	14.94 a	0.12 a	12.45 a	16.00 a
55% ETc		0.43 a	27.70 a	16.08 a	0.18 a	14.42 a	15.28 a	0.12 a	11.37 a	15.58 a
83% ETc		0.38 a	27.13 a	16.17 a	0.14 b	13.96 a	14.92 a	0.13 a	11.94 a	15.67 a
110% ETc		0.41 a	27.26 a	16.42 a	0.15 ab	13.09 a	14.42 a	0.11 a	11.65 a	14.83 a

* 5% significance; ** 1% significance. Different letters in each column indicate significant differences at 0.05 level according Tukey Test.

The lowest K^+ concentration in the root at 39 DAP was observed under an EC of 3.8 dS m^{-1} (10.30 mg g^{-1}), equivalent to a content of 78.21 mg (Table 8), 4.16% of the total K^+ in the plant. In the shoot, the effect of salinity on the Na^+ concentration was gradual, in which under EC of 1.5 dS m^{-1} the content was 15.15 mg, (41.85% of the total sorghum), 3.8 dS m^{-1} was 18.74 mg (28.67%), and under 6.0 dS m^{-1} was 23.54 mg (34.86%). In leaves, the isolated effect of salinity did not occur for Na^+, K^+ or Cl^-. Regarding the effect of irrigation depth for Na^+ in leaf, the irrigation depth at 55% of ETc resulted in a concentration of 0.18 mg g^{-1}, about 28.57% higher than that observed at 83% of ETc (0.14 mg g^{-1}).

Table 8. F test values for content of Na^+ (CNa^+), content of K^+ (CK^+), and content of Cl^- (CCl^-) in roots, shoot, and leaves at 39, 60, and 81 DAP.

		39	DAP		60	DAP		81	DAP
Trat	**CNa^+**	**CK^+**	**CCl^-**	**CNa^+**	**CK^+**	**CCl^-**	**CNa^+**	**CK^+**	**CCl^-**
					Roots				
		mg			mg			mg	
S1ID1	17.2 ± 1.9	77.0 ± 6.1	110.7 ± 8.4	12.2 ± 1.1	161.6 ± 11.9	174.6 ± 18.5	45.8 ± 6.1	223.6 ± 33.3	233.4 ± 33.7
S1ID2	10.4 ± 1.7	113.2 ± 11.1	93.9 ± 4.9	16.8 ± 1.7	210.0 ± 15.1	169.1 ± 20.3	76.9 ± 5.8	273.6 ± 17.3	327.6 ± 25.7
S1ID3	7.2 ± 0.7	116.1 ± 13.3	96.2 ± 11.5	24.3 ± 2.3	162.4 ± 22.6	214.6 ± 28.2	60.0 ± 7.8	260.4 ± 22.7	284.5 ± 15.6
S2ID1	23.4 ± 1.4	61.2 ± 3.9	105.1 ± 4.8	121.3 ± 11.0	153.1 ± 16.6	316.7 ± 24.7	153.6 ± 6.0	149.0 ± 16.1	429.1 ± 27.8
S2ID2	36.1 ± 3.8	82.3 ± 4.7	112.9 ± 14.9	102.3 ± 13.6	146.2 ± 5.9	212.2 ± 18.9	155.8 ± 13.3	171.6 ± 18.9	362.7 ± 13.6
S2ID3	60.7 ± 2.5	91.1 ± 5.8	171.2 ± 10.2	129.4 ± 16.2	186.9 ± 14.9	368.1 ± 37.7	159.8 ± 22.7	114.1 ± 14.7	360.1 ± 33.8
S3ID1	27.1 ± 2.9	80.9 ± 7.9	100.4 ± 10.0	174.0 ± 5.8	201.6 ± 16.5	377.3 ± 15.5	212.1 ± 18.9	190.0 ± 14.9	532.7 ± 43.8
S3ID2	38.1 ± 3.7	62.5 ± 6.0	91.0 ± 3.0	152.8 ± 7.0	185.2 ± 10.1	377.1 ± 21.5	165.9 ± 11.2	172.2 ± 22.2	416.0 ± 24.5
S3ID3	42.0 ± 4.7	100.4 ± 7.8	138.3 ± 15.1	136.3 ± 12.3	100.8 ± 10.1	243.8 ± 25.6	141.8 ± 12.5	154.4 ± 17.7	320.5 ± 15.7
					Shoot				
		mg			mg			mg	
S1ID1	12.6 ± 1.8	1175.5 ± 38.5	1045.7 ± 45.4	21.3 ± 1.9	1578.0 ±123.3	2103.7 ± 48.9	19.2 ± 1.6	1668.9 ± 151.2	1582.9 ± 21.7
S1ID2	18.5 ± 2.2	1713.6 ± 158.5	1445.7 ± 164.1	25.2 ± 2.2	1664.3 ± 245.3	2267.2 ± 206.4	19.3 ± 1.9	2097.7 ± 252.6	1843.1 ± 173.3
S1ID3	14.4 ± 2.3	1835.3 ± 199.3	1397.3 ± 169.1	29.8 ± 3.7	2110.4 ± 242.1	2458.4 ± 256.3	22.5 ± 2.2	2291.6 ± 160.7	1751.8 ± 307.8
S2ID1	15.3 ± 1.1	1064.2 ± 139.2	876.7 ± 115.7	70.6 ± 3.5	1809.8 ± 144.5	2358.4 ± 198.2	63.1 ± 8.0	1410.7 ± 151.6	1875.9 ± 160.5
S2ID2	16.5 ± 1.6	1126.6 ± 145.6	1087.2 ± 123.2	64.3 ± 7.8	2599.5 ± 289.4	2893.0 ± 166.4	60.7 ± 5.1	1975.0 ± 121.4	1936.5 ± 213.2
S2ID3	24.5 ± 2.4	1704.8 ± 264.7	1402.9 ± 205.8	79.4 ± 9.2	2130.8 ± 127.0	2553.9 ± 67.2	61.0 ± 8.6	2098.4 ± 90.1	1614.5 ± 174.2
S3ID1	22.7 ± 1.1	1287.5 ± 122.1	1075.3 ± 122.3	64.9 ± 7.8	2073.6 ± 163.9	2584.6 ± 278.5	109.1 ± 11.5	2291.7 ± 86.5	2103.5 ± 148.1
S3ID2	21.3 ± 1.3	1235.7 ± 108.4	1102.7 ± 105.4	41.7 ± 1.9	1789.6 ± 115.0	2145.8 ± 82.2	128.2 ± 15.3	2318.8 ± 145.9	1761.7 ± 131.6
S3ID3	26.6 ± 3.7	1345.8 ± 93.3	1235.5 ± 157.7	96.2 ± 8.1	2200.9 ± 301.0	2733.6 ± 252.0	35.5 ± 4.5	1878.7 ± 204.2	1927.4 ± 222.5
					Leaves				
		mg			mg			mg	
S1ID1	9.2 ± 0.6	589.0 ± 51.4	357.5 ± 24.9	6.7 ± 0.7	534.7 ± 25.2	586.9 ± 54.2	4.9 ± 0.5	439.8 ± 34.8	586.0 ± 33.8
S1ID2	9.6 ± 1.7	650.3 ± 33.6	374.5 ± 37.5	4.6 ± 1.6	519.0 ± 61.4	544.7 ± 47.0	4.9 ± 0.4	481.8 ± 46.9	623.4 ± 52.3
S1ID3	9.9 ± 1.3	720.2 ± 103.2	454.2 ± 53.9	4.3 ± 0.6	483.0 ± 25.2	515.0 ± 43.8	3.9 ± 0.2	442.7 ± 33.7	582.5 ± 18.2
S2ID1	7.9 ± 1.0	515.8 ± 54.7	279.1 ± 20.4	6.1 ± 0.7	506.0 ± 52.8	522.6 ± 46.9	4.0 ± 0.4	378.0 ± 7.7	544.1 ± 34.0
S2ID2	8.2 ± 0.6	574.9 ± 36.2	350.4 ± 33.0	7.1 ± 0.6	676.3 ± 81.0	740.9 ± 84.0	5.8 ± 0.4	493.6 ± 33.0	669.0 ± 33.5
S2ID3	9.4 ± 0.6	675.6 ± 72.8	418.5 ± 40.0	6.3 ± 0.7	490.2 ± 19.5	533.0 ± 25.4	4.2 ± 0.4	433.4 ± 17.4	552.6 ± 56.4
S3ID1	10.1 ± 0.8	662.0 ± 83.1	383.0 ± 45.4	8.4 ± 0.4	636.0 ± 73.3	666.7 ± 61.8	4.7 ± 0.5	499.3 ± 18.7	679.9 ± 63.5
S3ID2	6.8 ± 0.7	495.2 ± 51.4	295.7 ± 12.1	4.5 ± 0.8	425.0 ± 36.1	444.0 ± 19.0	5.2 ± 0.6	530.7 ± 34.7	679.3 ± 48.5
S3ID3	9.5 ± 0.9	544.2 ± 43.8	299.7 ± 30.6	6.3 ± 0.8	451.1 ± 25.4	519.7 ± 24.2	4.9 ± 0.7	550.0 ± 26.5	677.3 ± 27.8

At 60 DAP there was a sharp increase in Na^+ concentration in the root according to salinity. Under 1.5 dS m^{-1} EC, the Na^+ content in root was 17.8 mg, increasing to 117.7 mg at 3.8 dS m^{-1} and 154.4 mg under 6.0 dS m^{-1}, representing 36.05, 59.80, and 68.09% in the root in relation to the whole plant, respectively. In leaves, the Salt effect was also significant, but only between ECs 1.5 and 6.0 dS m^{-1}, whose distribution was 11.33 and 2.75%, respectively. As for the irrigation depths, the isolated effect was observed for the Na^+ concentration in leaves, between 55 and 83% of ETc, representing a content of 7.0 and 5.4 mg, respectively.

At the end of the cycle, at 81 DAP, Salt affected the K^+ concentration in roots and leaves, while ID effects were disregarded since they were significant when the interaction was significant. In roots, the highest K^+ concentration occurred under 1.5 dS m^{-1} EC (10.70 mg g^{-1}), representing a content of 252.23 mg (Table 8), while in leaves, maximum concentration was observed at 6.0 dS m^{-1} (12.45 mg g^{-1}), equivalent to a content of 526.7 mg.

Analyzing the interaction effect at the beginning of the cycle, it was significant for Na^+ and Cl^- concentration in roots (Table 7). The lowest Na^+ concentration in roots was in the least stressful treatment S1ID3 (0.80 mg g^{-1}) (Table 9), corresponding to a content of 7.2 mg. It is worth mentioning that in the treatments under lower salinity (1.5 dS m^{-1}), the distribution of Na^+ in roots regarding the whole plant was 31.65% on average, being 44.23% in S1ID1, and decreasing as the irrigation depth increased, being 27.42% in S1ID2 and 23.31% in S1ID3.

For Cl^- in roots at 39 DAP (Figure 6), the regression analysis showed the linear and quadratic effect of ID, as well as the simple interaction (Table 9). The highest Cl^- concentration was observed in S3ID1 (19.33 mg g^{-1}), corresponding to a content of 100.4 mg (Table 8). However, the highest Cl^- contents were observed in S2ID3 (171.2 mg) and S3ID3 (138.3 mg) (Table 8), this was due to the increase in irrigation depth significantly increasing dry mass, and therefore, the larger irrigation depths presented greater content.

Table 9. Breakdown of ion concentration variables at 39 DAP whose interaction was significant.

	Na_R39					Cl_R39			
	55% ETc	83% Etc	110% Etc	Mean		55% Etc	83% Etc	110% Etc	Mean
1.5 dS m^{-1}	2.83 bA	1.28 cB	0.80 bB	1.64	1.5 dS m^{-1}	18.33 aA	11.67 bB	10.67 bB	13.56
3.8 dS m^{-1}	4.08 aB	4.81 bAB	5.88 aA	4.93	3.8 dS m^{-1}	18.25 aA	15.00 abA	16.50 aA	16.58
6.0 dS m^{-1}	5.27 aB	7.16 aA	5.33 aB	5.92	6.0 dS m^{-1}	19.33 aA	17.33 aA	17.67 aA	18.11
Mean	4.06	4.42	4.00		Mean	18.64	14.67	14.94	
No tested equations were significant					Cl_R39 = 42.81 *** − $9.98.10^{-1}$ EC − $6.15.10^{-1}$ ID *** + $2.77.10^{-3}$ ID^2 ** + $2.43.10^{-2}$ ECID ** (R^2 = 0.93)				

Na_R39: Na^+ concentration in roots at 39 DAP; Cl_R39: Cl^- concentration in roots at 39 DAP. * 5% significance; ** 1% significance; *** 0.1% significance. Lowercase letters compare column means and uppercase letters compare row means.

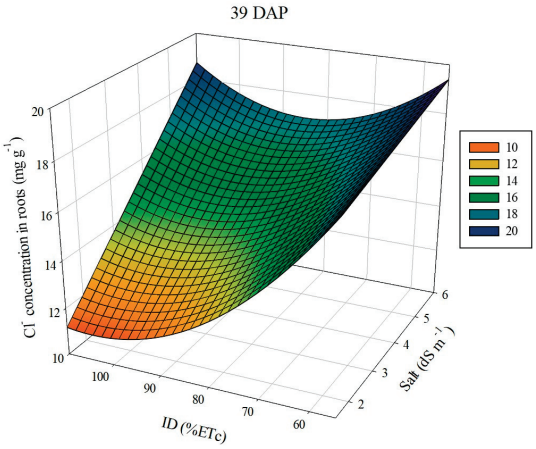

Figure 6. Response surface for Cl^- concentration in roots at 39 DAP.

At 60 DAP, the interaction affected K^+ and Cl^- in roots, Na^+ and K^+ in the shoot, and Cl^- in leaves (Table 7). In roots, the K^+ concentrations were maximum in S3ID1 and S3ID2 (11.75 and 11.91 mg g^{-1}) (Table 10), corresponding to contents of 201.6 and 185.2 mg, respectively, slightly above 7% of the K^+ was allocated in roots in these treatments. Likewise, the Cl^- concentration was maximum in roots in S3ID1 and S3ID2, corresponding to a content of 377.3 and 377.1 mg, just over 10% in the root concerning the whole plant.

In shoot at 60 DAP, the Na^+ concentrations were minimum in the 1.5 dS m^{-1} EC, regardless of the depth, representing an average Na^+ content of 25.4 mg, while for the other salinities the ID at 110% of ETc (content = 68.5 mg g^{-1}, on average) resulted in a higher concentration of Na^+ than IDs at 55 and 83% ETc (Table 8). For the K^+ concentration, the effect of ID was significant for 1.5 and 3.8 dS m^{-1} ECs, while the effect of Salt was only observed at 83% ETc (content = 2017.8 mg, on average). It is worth mentioning that K^+ was distributed more in the shoot than in other organs, where between 69.10 and 79.48% of the total K^+ in sorghum was in this organ. In leaves, the Cl^- concentration was maximum in the greater stress treatment: S3ID1 (16.33 mg g^{-1}), while the lowest concentrations (14.00 mg g^{-1}) were observed at S3ID2 and S1ID3. There was no effect of ID at 1.5 and 3.8 dS m^{-1} salinities, and there was no effect of Salt at 110% of ETc.

At the end of the cycle, the interaction was significant for Na^+ and Cl^- concentrations in roots, Na^+, K^+, and Cl^- concentrations in shoot, and Cl^- in leaves (Table 7). The increase in salinity resulted in a gradual increase in the content of Na^+ in roots at ID of 83% of ETc, where the content was 76.9, 155.8, and 165.9 mg for S1ID2, S2ID2, and S3ID2, respectively (Table 8). In addition, the effect of the irrigation depth was significant for the Na^+ concentration in roots at 3.8 and 6.0 dS m^{-1} salinities, but not for 1.5 dS m^{-1}, where the content was 60.9 mg on average. The Cl^- concentration in roots was maximum in the treatment of greater stress, S3ID1 (31.00 mg g^{-1}) (Table 11), in which under an ID at 55% of ETc, the effect of Salt was gradual, corresponding to a content of 45.8, 153.6, and 212.1 mg for S1ID1, S2ID1, and S3ID1, respectively (Table 8).

Table 10. Breakdown of ion concentration variables at 60 DAP whose interaction was significant.

	K_R60					**Cl_R60**			
	mg g^{-1}					mg g^{-1}			
	55% ETc	83% ETc	110% ETc	Mean		55% ETc	83% ETc	110% ETc	Mean
1.5 dS m^{-1}	9.73 abAB	11.31 aA	8.97 abB	10.00	1.5 dS m^{-1}	10.50 cA	9.00 cA	11.75 cA	10.42
3.8 dS m^{-1}	8.52 bB	9.02 bAB	10.88 aA	9.48	3.8 dS m^{-1}	17.75 bB	13.25 bC	21.33 aA	17.44
6.0 dS m^{-1}	11.75 aA	11.91 aA	7.05 bB	10.24	6.0 dS m^{-1}	22.00 aA	24.25 aA	17.00 bB	21.08
Mean	10.00	10.75	8.97		Mean	16.75	15.50	16.69	
No tested equations were significant					No tested equations were significant				
	Na_S60					**K_S60**			
	mg g^{-1}					mg g^{-1}			
	55% ETc	83% ETc	110% ETc	Mean		55% ETc	83% ETc	110% ETc	Mean
1.5 dS m^{-1}	0.22 bA	0.27 bA	0.32 bA	0.27	1.5 dS m^{-1}	15.94 aB	17.50 bB	22.78 aA	18.74
3.8 dS m^{-1}	0.72 aAB	0.59 aB	0.75 aA	0.69	3.8 dS m^{-1}	18.43 aB	23.90 aA	20.35 aAB	20.89
6.0 dS m^{-1}	0.60 aB	0.45 aB	0.89 aA	0.65	6.0 dS m^{-1}	19.16 aA	19.38 bA	20.12 aA	19.55
Mean	0.51	0.44	0.65		Mean	17.85	20.26	21.08	
No tested equations were significant					No tested equations were significant				
	Cl_L60								
	mg g^{-1}								
	55% ETc	83% ETc	110% ETc	Mean					
1.5 dS m^{-1}	15.00 abA	14.75 abA	14.00 aA	14.58					
3.8 dS m^{-1}	14.50 bA	16.00 aA	14.75 aA	15.08					
6.0 dS m^{-1}	16.33 aA	14.00 bB	14.50 aB	14.94					
Mean	15.28	14.92	14.42						
No tested equations were significant									

K_R60: K^+ concentration in roots at 60 DAP; Cl_R60: Cl^- concentration in roots at 60 DAP; Na_S60: Na^+ concentration in the shoot at 60 DAP; K_S60: K^+ concentration in shoot at 60 DAP; Cl_L60: Cl^- concentration in leaves at 60 DAP. Lowercase letters compare column means and uppercase letters compare row means.

Table 11. Breakdown of ion concentration variables at 81 DAP whose interaction was significant.

	Na_R81					**Cl_R81**			
	mg g^{-1}					mg g^{-1}			
	55% ETc	83% ETc	110% ETc	Mean		55% ETc	83% ETc	110% ETc	Mean
1.5 dS m^{-1}	2.32 bA	2.71 cA	2.63 bA	2.55	1.5 dS m^{-1}	14.00 cA	17.75 bA	16.00 bA	15.92
3.8 dS m^{-1}	8.67 aA	7.04 bB	7.48 aAB	7.73	3.8 dS m^{-1}	24.00 bA	22.50 abA	21.00 abA	22.50
6.0 dS m^{-1}	9.94 aA	9.15 aA	7.60 aB	8.89	6.0 dS m^{-1}	31.00 aA	26.75 aAB	23.00 aB	26.92
Mean	6.98	6.30	5.90		Mean	23.00	22.23	20.00	
Na_R81 = 4.84 ** + 5.27 EC *** − $3.96.10^{-1}$ EC^2 *** + $2.07.10^{-2}$ ID − $1.07.10^{-2}$ ECID ** (R^2 = 0.99)					Cl_R81 = 4.54 + 5.80 EC *** + $9.77.10^{-2}$ ID * − $4.0.10^{-2}$ ECID ** (R^2 = 0.97)				
	Na_S81					**K_S81**			
	mg g^{-1}					mg g^{-1}			
	55% ETc	83% ETc	110% ETc	Mean		55% ETc	83% ETc	110% ETc	Mean
1.5 dS m^{-1}	0.14 cA	0.13 cA	0.17 bA	0.15	1.5 dS m^{-1}	12.21 bB	14.50 aB	17.14 aA	14.61
3.8 dS m^{-1}	0.45 bA	0.44 bA	0.36 aA	0.42	3.8 dS m^{-1}	10.12 bB	14.12 aA	12.55 bAB	12.26
6.0 dS m^{-1}	0.72 aA	0.80 aA	0.30 abB	0.60	6.0 dS m^{-1}	15.22 aA	14.52 aA	15.87 aA	15.20
Mean	0.44	0.46	0.28		Mean	12.51	14.38	15.19	
No tested equations were significant					K_C81 = 9.72 *** − 2.36 EC ** + $5.22.10^{-1}$ EC^2 *** + $1.14.10^{-1}$ ID *** − $1.73.10^{-2}$ ECID ** (R^2 = 0.84)				
	Cl_S81					**Cl_L81**			
	mg g^{-1}					mg g^{-1}			
	55% ETc	83% ETc	110% ETc	Mean		55% ETc	83% ETc	110% ETc	Mean
1.5 dS m^{-1}	16.00 bB	19.75 aA	18.50 aAB	18.08	1.5 dS m^{-1}	14.50 aA	15.50 aA	16.00 aA	15.33
3.8 dS m^{-1}	19.00 abA	17.75 aAB	15.25 aB	17.33	3.8 dS m^{-1}	16.00 aA	15.25 aAB	13.00 bB	14.75
6.0 dS m^{-1}	19.50 aA	19.00 aA	17.67 aA	18.72	6.0 dS m^{-1}	16.25 aA	16.25 aA	15.50 aA	16.00
Mean	18.17	18.83	17.14		Mean	15.58	15.67	14.83	
Cl_C81 = 5.94 + $1.28.10^{-2}$ EC + $2.11.10^{-1}$ EC^2 + $3.07.10^{-1}$ ID * − $1.57.10^{-3}$ ID^2* − $1.76.10^{-2}$ ECID * (R^2 = 0.62)					Cl_F81 = 17.86 ** − 1.21 EC * + $1.81.10^{-1}$ EC^2 − $1.35.10^{-2}$ ID (R^2 = 0.36)				

Na_R81: Na^+ concentration in roots at 81 DAP; Cl_R81: Cl^- concentration in roots at 81 DAP; Na_S81: Na^+ concentration in shoot at 81 DAP; K_S81: K^+ concentration in shoot at 81 DAP; Cl_S81: Cl^- concentration in shoot at 81 DAP; Cl_L81: Cl^- concentration in leaves at 81 DAP. * 5% significance; ** 1% significance; *** 0.1% significance. Lowercase letters compare column means and uppercase letters compare row means.

In the shoot, the interaction influenced the content of all ions studied (Table 7), response surfaces are shown in Figure 7. The salinity considerably increased the Na^+ concentrations in the treatments under 55 and 83% of ETc IDs, in which the 6.0 dS m^{-1} EC increased the Na^+ concentration in 414.29% for ID1 and 515.39% for ID2 compared to 1.5 dS m^{-1} EC (Table 11). The irrigation depth was only significant at 6,0 dS m^{-1} EC, in which the lowest Na^+ concentration occurred at S3ID3 (0.30 mg g^{-1}). As for K^+, the levels ranged from 10.12 to 17.14 mg g^{-1} (Table 11) (content = 72.4 and 76.3 mg), while for the Cl^- concentrations, they were between 15.25 and 19.75 mg g^{-1} (Table 11) (content = 1614.5 and 1843.1 mg). It is worth mentioning that K^+ and Cl^- were more distributed in the shoot, between 71.32 and 79.30% for K^+, and 61.55 and 65.99% for Cl^-. In leaves, the Cl^- concentration was influenced by the salinity only in the treatments under 110% of ETc ID, being the 3.8 dS m^{-1} the EC that showed lowest content (13.00 mg g^{-1}, content = 552.6 mg), whereas the effect of ID was significant only at treatments under 3.8 dS m^{-1} EC (Table 11).

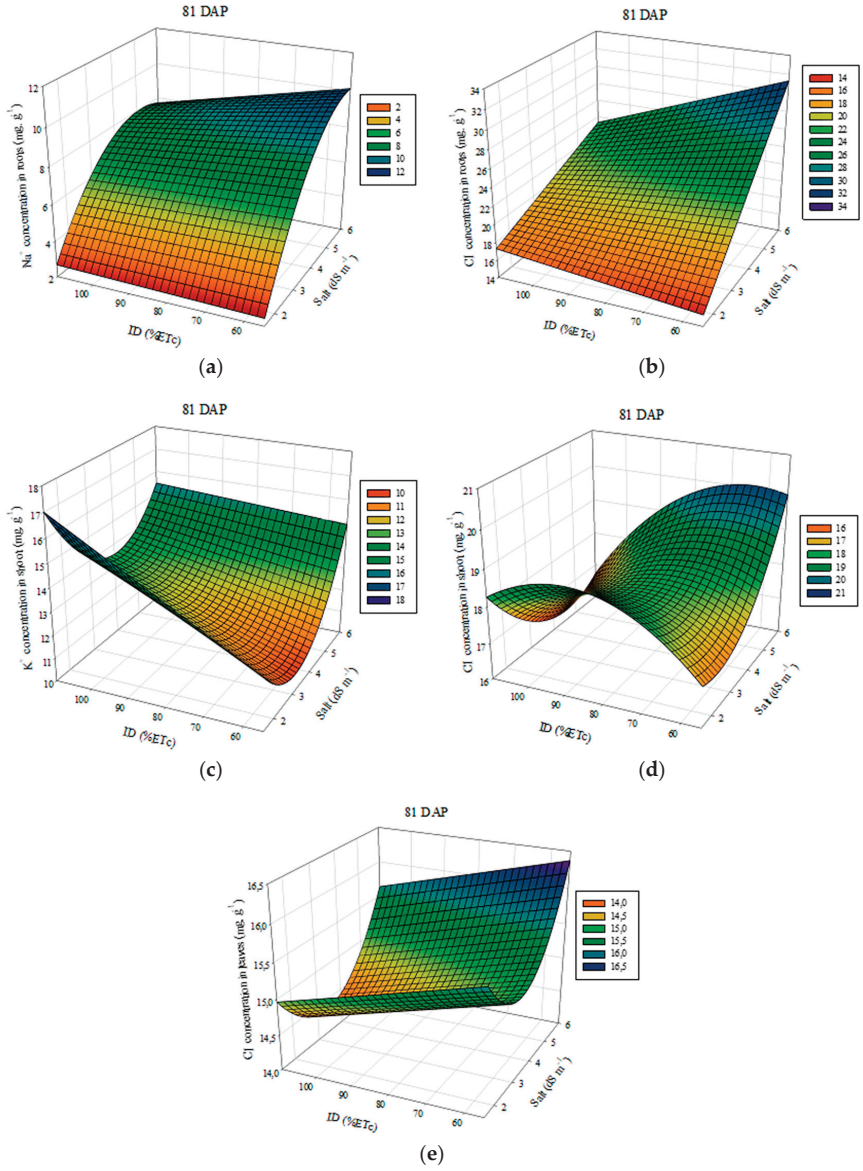

Figure 7. Response surfaces for: Na^+ concentration in roots (**a**); Cl^- concentration in roots (**b**); K^+ concentration in shoot (**c**); Cl^- concentration in shoot (**d**); and Cl^- concentration in leaves (**e**) at 81 DAP.

3.5. Pearson Correlation Matrix

At 39 DAP, regarding variables related to growth, SH and TH were strongly influenced by leaf area (r = 0.76; r = 0.76) and also showed strong correlation with each other (r = 1.00) (Table 12). As for the variables related to ion content, Na^+ in roots was strongly correlated with Cl^- in roots (r = 0.64), and with Na^+ in the shoot (r = 0.72), while Cl^- in roots, besides Na^+ in roots, correlated negatively with total (r = −0.68) and shoot (r = −0.68) heights. Among plant parts, the ions correlated with each other from very weak to weak.

Table 12. Pearson correlation matrix for variables measured at 39 DAP.

	EL39	RWC39	ADM_39	Na_R39	K_R39	Cl_R39	Na_S39	K_S39	Cl_S39	Na_L39	K_L39	Cl_L39	LA39	SD39	SH39	TH39
EL39	1.00															
RWC39	−0.07	1.00														
ADM_39	−0.31	0.09	1.00													
Na_R39	0.07	0.14	−0.30	1.00												
K_R39	0.07	0.18	−0.12	−0.21	1.00											
Cl_R39	0.37	−0.00	−0.38	0.64	0.04	1.00										
Na_S39	0.02	0.19	−0.37	0.72	−0.03	0.50	1.00									
K_S39	−0.08	0.11	0.04	−0.31	0.05	−0.22	−0.16	1.00								
Cl_S39	−0.19	0.23	−0.10	0.09	0.06	0.12	0.26	0.29	1.00							
Na_L39	0.37	−0.04	−0.16	0.01	0.15	0.32	0.33	0.03	0.14	1.00						
K_L39	0.09	−0.00	0.24	−0.22	0.21	−0.09	−0.18	0.28	0.18	0.08	1.00					
Cl_L39	−0.26	−0.13	0.19	−0.21	0.04	−0.13	−0.09	−0.12	0.19	0.15	0.00	1.00				
LA39	0.17	0.11	0.29	−0.16	−0.16	−0.49	−0.38	0.13	0.03	−0.26	0.21	−0.10	1.00			
SD39	−0.09	0.15	0.23	−0.17	−0.14	−0.26	−0.33	0.00	−0.03	−0.32	0.06	−0.06	0.52	1.00		
SH39	−0.13	0.13	0.56	−0.36	−0.14	−0.68	−0.39	0.14	−0.07	−0.23	0.12	0.04	0.76	0.52	1.00	
TH39	−0.13	0.13	0.56	−0.36	−0.14	−0.68	−0.39	0.14	−0.07	−0.23	0.12	0.04	0.76	0.52	1.00	1.00

EL39: Electrolyte leakage; RWC39: Relative water content; ADM_39: Aerial dry mass; Na_R39: Na^+ concentration in roots; K_R39: K^+ concentration in roots; Cl_R39: Cl^- concentration in roots; Na_S39: Na^+ concentration in shoot; K_S39: K^+ concentration in shoot; Cl_S39: Cl^- concentration in shoot; Na_L39: Na^+ concentration in leaves; K_L39: K^+ concentration in leaves; Cl_L39: Cl^- concentration in leaves; LA39: Leaf area; SD39: Stem diameter; SH39: Shoot height; TH39: Total height. All variables at 39 DAP.

Compared to 39 DAP, at flowering (60 DAP), the variables linked to growth were much less correlated, except for total height and shoot height (r = 0.99) (Table 13). However, Na^+ concentration in roots remained strongly correlated with Cl^- in roots (r = 0.83) and Na^+ in shoot (r = 0.74). There was also a correlation between K^+ and Cl^- in shoot (r = 0.63). As with flowering, for the growth variables at the end of the cycle, only SH and TH showed a strong correlation (r = 0.84) (Table 14). Root Na^+ continued to be linked to root Cl^- (r = 0.82) and shoot Na^+ (r = 0.83), root Cl^- also correlated strongly with shoot Na^+ (r = 0.74).

Table 13. Pearson correlation matrix for variables measured at 60 DAP.

	EL60	RWC60	ADM_60	Na_R60	K_R60	Cl_R60	Na_S60	K_S60	Cl_S60	Na_L60	K_L60	Cl_L60	LA60	SD60	SH60	TH60
EL60	1.00															
RWC60	−0.16	1.00														
ADM_60	0.03	−0.09	1.00													
Na_R60	0.17	−0.32	0.16	1.00												
K_R60	−0.14	0.18	−0.03	0.06	1.00											
Cl_R60	0.13	−0.18	0.03	0.83	0.36	1.00										
Na_S60	0.08	−0.46	0.21	0.74	−0.34	0.52	1.00									
K_S60	0.12	−0.12	0.18	0.13	−0.18	0.05	0.26	1.00								
Cl_S60	−0.09	0.05	−0.18	0.08	−0.24	−0.10	0.17	0.63	1.00							
Na_L60	0.15	−0.16	0.16	0.40	0.02	0.34	0.35	−0.06	−0.04	1.00						
K_L60	−0.07	0.15	0.25	0.06	0.37	0.10	−0.04	0.10	0.19	0.24	1.00					
Cl_L60	0.26	−0.12	0.42	0.10	0.07	0.06	0.07	0.16	0.11	0.09	0.45	1.00				
LA60	0.27	−0.15	0.07	0.42	0.11	0.42	0.29	−0.06	−0.18	0.24	0.25	0.15	1.00			
SD60	0.05	−0.17	−0.05	0.01	−0.04	0.03	−0.07	0.06	0.08	−0.01	0.29	0.05	0.35	1.00		
SH60	−0.18	−0.00	−0.02	−0.29	−0.26	−0.33	−0.03	0.43	0.40	−0.34	−0.38	−0.18	−0.38	0.09	1.00	
TH60	−0.15	−0.03	−0.03	−0.25	−0.22	−0.28	−0.03	0.42	0.39	−0.34	−0.37	−0.15	−0.29	0.14	0.99	1.00

Note: EL60: Electrolyte leakage; RWC60: Relative water content; ADM_60: Aerial dry mass; Na_R60: Na^+ concentration in roots; K_R60: K^+ concentration in roots; Cl_R60: Cl^- concentration in roots; Na_S60: Na^+ concentration in shoot; K_S60: K^+ concentration in shoot; Cl_S60: Cl^- concentration in shoot; Na_L60: Na^+ concentration in leaves; K_L60: K^+ concentration in leaves; Cl_L60: Cl^- concentration in leaves; LA60: Leaf area; SD60: Stem diameter; SH60: Shoot height; TH60: Total height. All variables at 60 DAP.

Table 14. Pearson correlation matrix for variables measured at 81 DAP.

	Pro	TAA	TSS	ADM_81	Na_R81	K_R81	Cl_R81	Na_S81	K_S81	Cl_S81	Na_L81	K_L81	Cl_L81	SD81	SH81	TH81
Pro	1.00															
TAA	0.25	1.00														
TSS	−0.02	−0.12	1.00													
ADM_81	−0.13	0.41	−0.14	1.00												
Na_R81	0.15	−0.07	0.27	0.13	1.00											
K_R81	0.14	0.23	−0.11	−0.19	−0.48	1.00										
Cl_R81	0.13	0.08	0.23	0.10	0.82	−0.17	1.00									
Na_S81	0.06	−0.01	0.16	0.31	0.83	−0.25	0.74	1.00								
K_S81	0.25	−0.06	−0.30	−0.10	−0.12	0.24	−0.01	0.01	1.00							
Cl_S81	−0.00	−0.35	0.16	−0.17	0.12	0.22	0.22	0.20	0.33	1.00						
Na_L81	−0.12	−0.23	0.13	−0.42	0.08	−0.06	0.23	0.11	−0.11	−0.01	1.00					
K_L81	0.10	−0.22	0.26	−0.04	0.10	−0.07	0.01	0.21	0.40	0.38	0.06	1.00				
Cl_L81	−0.06	−0.25	0.02	−0.43	0.14	0.29	0.33	0.21	0.18	0.47	0.31	0.06	1.00			
SD81	−0.15	0.17	0.03	0.03	−0.10	−0.03	−0.14	−0.05	−0.13	−0.25	0.04	−0.06	0.07	1.00		
SH81	0.13	0.12	−0.49	−0.13	−0.31	−0.02	−0.39	−0.45	0.37	−0.21	−0.30	−0.14	−0.12	0.04	1.00	
TH81	−0.04	0.05	−0.55	−0.15	−0.32	0.05	−0.32	−0.40	0.47	−0.07	−0.14	−0.12	−0.04	0.18	0.84	1.00

Note: Pro: Proline; TA: Total amino acids; TSS: Total soluble sugars; ADM_81: Aerial dry mass; Na_R81: Na^+ concentration in roots; K_R81: K^+ concentration in roots; Cl_R81: Cl^- concentration in roots; Na_S81: Na^+ concentration in shoot; K_S81: K^+ concentration in shoot; Cl_S81: Cl^- concentration in shoot; Na_L81: Na^+ concentration in leaves; K_L81: K^+ concentration in leaves; Cl_L81: Cl^- concentration in leaves; LA81: Leaf area; SD81: Stem diameter; SH81: Shoot height; TH81: Total height. All variables at 81 DAP.

3.6. Soil Parameters

3.6.1. Soil Salinity

Salt was significant in ECex and exchangeable sodium percentage (ESP) in the soil for both the 0–20 and 20–40 cm layers. The irrigation depth was significant only in the 20–40 cm layer for ECex and ESP of the soil (Table 15). Soil ECex reduced when water with a salinity of 6.0 dS.m^{-1} was applied to the two layers studied, this can be explained because the plant absorbs a higher concentration of Na^+ in the roots, reducing the concentration of soluble salts in the soil as can be seen in Table 15.

Table 15. Electrical conductivity (EC) and Exchangeable sodium percentage (ESP) of soil solution in the 0–30 and 30–60 cm layers.

		0–20 cm		20–40 cm	
SV	**DF**	**EC**	**ESP**	**EC**	**ESP**
Block	3	1.75	0.22	0.52	0.57
Salt	2	7.93 **	71.26 **	20.94 **	46.21 **
ID	2	0.90	1.63	12.57 **	0.07
Salt × ID	4	0.52	0.39	1.81	0.40
C. V. (%)		51.4	24.4	34.5	36.7
1.5 dS m^{-1}		1.58	2.85	1.72	1.99
3.8 dS m^{-1}		3.84	9.76	4.77	8.46
6.0 dS m^{-1}		2.71	12.50	4.20	13.38
55% ETc		2.98	9.24	4.71	7.78
83% ETc		2.87	7.93	3.76	7.85
110% ETc		2.27	7.94	2.22	8.20

* 5% significance; ** 1% significance.

Under different irrigation depths, ECex reduced with the greater availability of water being leached into deeper soil layers. In this sense, the use of water with a higher salt content, using 10% more of the water requirement of the crop, in addition to providing a development condition for the crop with salts more dissolved in the root zone, allows soil salts to be leached, avoiding the soil degradation process.

Salinity was significant for ESP in both layers when different salinities of irrigation water were used, with an increase in ESP as water electrical increased. Considering that soil becomes sodic for ESP greater than 15%, even using a salinity of 6.0 dS m^{-1}, no sodification process was observed in the studied layers, remaining below the conditions for sodification process.

3.6.2. Soil Water Retention

Under tensions of 0, 1, and 3 kPa, the moisture content was practically the same in both layers. Under 6, 10, 30, and 60 kPa, higher moisture was observed in the surface layer, whereas with increasing tensions to 100, 300, and 1500 kPa, the 0–30 cm layer showed higher soil water content. Regardless of the depth used, the increase in salinity promoted higher moisture content in the 0–30 and 30–60 cm soil layers (Table 16). The highest moisture content was observed when EC 6.0 dS m^{-1} water was used. However, this higher moisture content does not mean that water is available for the plant. This is because of the reduction of the osmotic potential of the soil solution caused by salts, the plant needs to direct a lot of energy to absorb water.

Table 16. Moisture observed at 0–30 and 30–60 cm layers according to the treatments applied.

Treatment	Period from Sowing (Days)						Period from Sowing (Days)					
	15–21	**22–35**	**36–49**	**50–63**	**64–77**	**78–91**	**15–21**	**22–35**	**36–49**	**50–63**	**64–77**	**78–91**
	Moisture at 0–30 cm Layer (m^3 m^{-3})						**Moisture at 30–60 cm Layer (m^3 m^{-3})**					
S1ID1	0.125	0.121	0.121	0.121	0.122	0.121	0.178	0.161	0.160	0.159	0.160	0.160
S1ID2	0.138	0.121	0.121	0.121	0.122	0.121	0.189	0.162	0.160	0.160	0.160	0.160
S1ID3	0.136	0.130	0.127	0.133	0.133	0.129	0.200	0.165	0.177	0.192	0.186	0.182
S2ID1	0.128	0.123	0.123	0.124	0.124	0.122	0.178	0.161	0.160	0.159	0.159	0.159
S2ID2	0.137	0.126	0.125	0.129	0.137	0.125	0.191	0.166	0.169	0.177	0.188	0.170
S2ID3	0.137	0.132	0.125	0.131	0.136	0.128	0.197	0.188	0.171	0.191	0.196	0.185
S3ID1	0.133	0.130	0.128	0.129	0.126	0.124	0.184	0.161	0.177	0.170	0.178	0.171
S3ID2	0.132	0.127	0.128	0.131	0.125	0.127	0.181	0.163	0.173	0.177	0.173	0.167
S3ID3	0.135	0.134	0.125	0.132	0.134	0.131	0.199	0.197	0.188	0.197	0.192	0.187

4. Discussion

Sorghum resisted to salinity, water scarcity, and their interaction. The main mechanism observed was the compartmentalization of Na^+ ions in the root cells, preventing them from being transported to the leaves, which could cause damage to the photosynthetic apparatus. We also noted that the Salt × ID interaction was significant for most variables associated with ion concentration, especially at the end of the cycle. The combined effects of these stresses are poorly discussed in the literature, but they can occur naturally, which makes it interesting to understand how this interaction affects plant metabolism.

4.1. Concentration and Content of Na^+, K^+, and Cl^-

At the beginning of the cycle, under salinity of 1.5 dS m^{-1}, the irrigation depth reduction caused an increase in Na^+ concentration in roots, reaching 2.83 mg g^{-1} in S1ID1, equivalent to a content of 17.2 mg in which approximately 44.23% of the Na^+ was allocated in roots. This suggests that there is a limit to the concentration of Na^+ in the soil solution that induces the compartmentalization of Na^+ in root cells. In S1ID3, Na^+ was translocated to the shoot (45.30%), probably because, due to S1ID3 being the lowest stress condition, the concentration of this ion did not generate a physiological response of compartmentalization in roots. This compartmentalization of Na^+ can also be evidenced because the increase in salinity resulted in higher levels of Na^+ in roots, reaching a maximum of 7.16 mg. g^{-1} in S3ID2 (content = 39.1 mg).

The K^+/Na^+ ratio is an excellent parameter for identifying sorghum genotypes that are tolerant or sensitive to salinity [36]. Furthermore, in the roots, it was higher in treatments under 1.5 dS m^{-1} EC, showing a greater allocation of Na^+ to the other organs as salinity increases. The chemical similarity of the K^+ and Na^+ ions can cause an exchange of K^+ for Na^+ in biochemical reactions and a consequent change in the structure of proteins [37], impairing plant development.

Regarding Cl^- in roots, higher irrigation depths also increased the amount of Cl^- in the soil solution because more Cl^- ions are dissolved in the irrigation water, which is

reinforced because two of the three salts used in the irrigation water are a source of Cl^-, contributing to a more expressive content of this anion.

At 60 DAP, only salinity interfered with the Na^+ concentration in roots, with an average of 1.00 mg g^{-1} for irrigation at 1.5 dS m^{-1}, corresponding to a content of 17.8 mg, and therefore, 36.05% allocated in roots. This is possibly related to the absorption of Na^+, considering that compared to 39 DAP the Na^+ content under 1.5 dS m^{-1} in the entire plant was lower. Apparently, at lower salinity it is possible for the sorghum the non-absorption of Na^+ ions as a tolerance mechanism; at other salinities, the higher concentration of solutes in the soil solution may prevent this selectivity from occurring.

The K^+ content at flowering was influenced by the interaction of stresses in roots and shoot, whereas in leaves there was no isolated or interactive effect. In roots, Cl^- was also affected by the interactive effect of stresses, and in the shoot, the interaction was significant for Na^+. These responses show an excess of Na^+ and Cl^- in the root zone, in order to interfere with the absorption of K^+ and generate nutrient imbalance, reduction of enzymatic activity, ionic stress and formation of ROS [38]. It is also worth mentioning Cl^-, which has high mobility [39], and probably interfered with its content in the leaves, since the reduction in irrigation depth was significant for the increase in Cl^- content at a salinity of 6.0 dS m^{-1}.

At 81 DAP, Na^+ remained concentrated in roots, representing between 55.59 and 77.61% of the total Na^+ in sorghum, although it was expected that there would be an exclusion of these ions by Na^+/H^+ antiporters [10]. However, the salt content in roots can be a positive aspect for the survival of the plant, since it helps to maintain an osmotic gradient favorable to water absorption [18].

There was no significant difference in the Na^+ content in leaves, even at the end of the cycle, when the plant had been under poor irrigation for a long time, the sorghum continued to prioritize the non-translocation of Na^+ ions to the leaves, which could damage the photosynthetic apparatus [36]. In leaves, the high cytosolic balance of the K^+/Na^+ ratio, varying between 86.68 and 115.63, leads to greater plant growth and tolerance to saline stress [40].

4.2. Growth Parameters

At the beginning of the cycle (39 DAP), the highest concentration of salts in the 6.0 dS m^{-1} EC water can lead to changes in the water potential of sorghum metabolism and reduction of the osmotic potential of the soil solution [10,41], reducing LA, SD, SH and TH. It is noteworthy that the increase in EC from 1.5 dS m^{-1} to 3.8 dS m^{-1} did not statistically reduce any of the variables associated with growth, showing tolerance. In addition, germination is a sensitive period for plant development, and salinity at this stage may be even more critical for sorghum development.

The ID effect at 39 DAP is also linked to changes in soil and plant water potential because, under water scarcity, sorghum closes stomata to reduce water loss. This stomatal closure, however, despite reducing losses via transpiration, also reduces photosynthesis and consequently the production of biomass [18]. It is interesting to point out that SD was not affected by ID in any of the seasons studied, possibly because—since BRS 506 sorghum is a saccharin cultivar—there is a preference to keep SD for broth storage. However, there was a reduction in SH according to ID at all times, which may be linked to lower lignin production under water stress [42]. In this sense, considering that the lignin production decreased according to ID, the shoot height reduced, but the sorghum sought to maintain the stem diameter.

At 60 DAP, it was possible to observe that fewer variables associated with growth were affected by the isolated effects of Salt and ID, so the sorghum developed stress response mechanisms to tolerate them. It is interesting to emphasize this, since the flowering period is a period more sensitive to water scarcity for sorghum [43].

At 81 DAP, only SH was affected by the isolated effects of Salt and ID, reinforcing the idea of tolerance. Under abiotic stresses, tolerant cultivars seek to keep the photosynthetic

system stable and increase the efficiency of CO_2 fixation, minimizing the damage caused by these through apoplastic barriers [10]. The Salt × ID interaction was significant only at the end of the cycle, for ADM_81, in which the salinity effect was not significant in the 55 and 83% of ETc irrigation depths, showing that more brackish waters can be used even in smaller irrigation depths.

4.3. Electrolyte Leakage and Relative Water Content

Electrolyte leakage refers to the integrity of the plasma membrane, the disruption of which results in increased permeability, and therefore, increased leakage. This permeability results from changes in the composition and structure of the membrane, caused by the action of ions from salts when the plant is subjected to salinity, probably being the first sign of response to saline stress [44]. However, greater extravasation of electrolytes does not mean that the plant is sensitive to salinity. Hniličková et al [45], studying *P. oleracea* under saline stress, found EL between 86.7% and 92.4%; however, these values were attributed to the high content of K^+ in the cytoplasm, given that K^+ is abundant in plant cells and whose efflux is mainly responsible for the extravasation of electrolytes [46].

The relative water content is associated with the turgor of plant cells, being an excellent indicator of the water status of the plant. Here, the combined effect of stresses was observed only at 39 DAP, which leads to the idea that the beginning of the cycle is more sensitive to applied stresses. During cycle, at 60 DAP, only salinity changed the RWC, while the isolated or interactive effect of water depth was not significant, which is possibly linked to the sorghum roots. When comparing sorghum with less drought-tolerant crops such as maize, the sorghum root system is deeper, with possibly greater hydraulic conductivity and water transport from the root to the other organs [47].

4.4. Proline, Total Amino Acids, and Total Soluble Sugars

Proline production can occur both under the isolated effects of salinity or deficient irrigation depth, but Wang et al. (2022), studying germination of sweet sorghum cultivars, found that the combination of these stresses resulted in greater gene expression of P5CS, P5CR, and OAT linked to proline production. In sorghum, proline production occurs under moderate stress [48], but according to the results obtained in this study, the applied stresses were not sufficient to differentiate the production of this solute, which may indicate tolerance of the BRS 506 cultivar. There are still controversies about the production of proline by sorghum, since a sensitive cultivar can accumulate the same amount of proline as a tolerant one [17].

The accumulation of amino acids is linked to a better development of the culture because they are constituents of proteins and an important precursor of secondary metabolites [15], and as for proline, the accumulation was not significant for this study. Sugar production is also a common strategy used by sorghum as osmoregulation, as it maintains the plant's water potential and water absorption capacity [10], but it was not observed here either. Although the accumulation of organic solutes as a means of tolerance is common, in the studied sorghum, their production was not observed, indicating that the application of treatments did not result in significant stress for the leaves. However, other studies with the cultivar BRS 506 involved with the expression of genes linked to the production of proline, amino acids, and sugars are recommended, to explain what was observed here.

4.5. Pearson Correlation Matrix

Pearson's correlation showed greater interdependence between the variables linked to growth at the beginning of the cycle. Whatever the effects of saline and/or water stress on one of the sorghum organs, the others are affected. This indicates the crop's sensitivity to abiotic stresses at the time of plant establishment, both in terms of drought sensitivity [43] and salinity. At the other times, only TH and SH showed correlation, for obvious reasons, given that the shoot height is inherent to the total height.

As for ions, the relationship between Na^+ in the root and shoot, as well as Na^+ with Cl^- in roots, was the only strong correlation observed in the three studied periods. The fact that both Na^+ and Cl^- are correlated in the root is linked to the moment of water absorption, given that they are the constituent ions of NaCl, one of the salts applied in irrigation water. It is worth mentioning that throughout the cycle, there was a trend towards a greater distribution of Na^+ in the root and of Cl^- in the stem, that is, the correlation of both in the root is not linked to a greater distribution in the root than in the other organs.

As for the relationship between Cl^- and total and shoot height at 39 DAP, sorghum is a fast-growing plant, especially in the vegetative stage, so the energy from photosynthesis is used intensively in cell elongation and division, growth promoters. At flowering, sorghum intensifies transpiration, which promotes the translocation of Cl^- from free spaces, so more nutrients are absorbed [49]. During flowering, K^+ and Cl^- in the shoot may be related to the fact that the shoot is the organ with the highest biomass, and therefore, the probability of ions accumulating in the shoot is greater. Here, Na^+ was not translocated to the shoot because it is being stored in the roots, whereas Cl^-, although similar to Na^+ and can confer toxicity to the plant, is a highly mobile anion [39], being easily carried from roots to shoot. For the same reason, at the end of the cycle, the relationship between Cl^- in the root and Na^+ in the leaf suggests a preference in the distribution of these ions in different parts of the plant because of their toxicity, requiring further studies to verify this hypothesis.

5. Conclusions

Our research showed that the main tolerance mechanism adopted by the BRS 506 sorghum was the distribution of Na^+ ions to the root cells so the sorghum adapted to salt and water stress. In fact, when aiming at deficit irrigation in order to reduce water costs, the sorghum showed that even under a depth of 55% of the ETc, waters with EC of up to 6.0 dS m^{-1} can be adopted without loss in the aerial dry mass. However, when irrigation waters are EC of 3.8 dS m^{-1}, irrigation at 110% ETc is preferable, and under EC of 6.0 dS m^{-1}, 83% of ETc.

According to our study, BRS 506 sorghum can be irrigated with lower-quality water and in smaller quantities. This information is especially beneficial to small rural producers in semiarid regions who live in areas with water scarcity and salinity problems. As future prospects, we seek to highlight BRS 506 sorghum as a crop to be explored in the Brazilian semiarid region. In addition, crop development programs can also benefit from this research, given that we observed ionic redistribution as sufficient to tolerate stress, without altering the production of osmoregulatory substances such as proline, soluble sugars, and total amino acids.

Author Contributions: Conceptualization, G.C.M.d.Q., J.F.d.M. and R.R.d.S.; methodology, G.C.M.d.Q., J.F.d.M., R.R.d.S., F.M.d.S.M., L.V.d.S., M.V.P.d.S., E.d.N.S., F.N.F., J.M.C.d.S., M.I.B.C., J.C.d.C.G., M.N.d.A.S. and D.C.C.; validation, J.F.d.M. and F.V.d.S.S.; formal analysis, G.C.M.d.Q., J.F.d.M. and R.R.d.S.; investigation, G.C.M.d.Q., J.F.d.M., R.R.d.S., F.M.d.S.M., L.V.d.S., M.V.P.d.S., E.d.N.S., F.N.F., J.M.C.d.S., M.I.B.C., J.C.d.C.G., M.N.d.A.S. and D.C.C.; resources, J.F.d.M.; data curation, G.C.M.d.Q. and J.F.d.M.; writing—original draft preparation, G.C.M.d.Q. and F.V.d.S.S.; writing—review and editing, G.C.M.d.Q., J.F.d.M. and R.G.N.; supervision, J.F.d.M.; project administration, J.F.d.M.; funding acquisition, J.F.d.M. All authors have read and agreed to the published version of the manuscript.

Funding: This research was funded by Conselho Nacional de Desenvolvimento Científico e Tecnológico—CNPq (310.020/2018-2) and Fundação de Amparo e Promoção da Ciência, Tecnologia e Inovação do RN—FAPERN (10910019.000263/2021-43).

Institutional Review Board Statement: Not applicable.

Data Availability Statement: The data used to support the findings of this study are included within the article.

Acknowledgments: Acknowledgments are due to the Conselho Nacional de Desenvolvimento Científico e Tecnológico (CNPq), Fundação de Amparo e Promoção da Ciência, Tecnologia e Inovação do RN (FAPERN), Coordenação de Aperfeiçoamento de Pessoal de Nível Superior (CAPES) and Universidade Federal Rural do Semi-Árido (UFERSA) for the financial support provided for this research.

Conflicts of Interest: The authors declare no conflict of interest.

References

1. Boretti, A.; Rosa, L. Reassessing the projections of the World Water Development Report. *Npj Clean. Water* **2019**, *2*, 15. [CrossRef]
2. UNESCO World Water Assessment. *The United Nations World Water Development Report 2022—Groundwater: Making the Invisible Visible*, 1st ed.; UNESCO: Paris, France, 2022; 225p.
3. FAO. *The State of the World's Land and Water Resources for Food and Agriculture 2021—Systems at Breaking Point*, 1st ed.; FAO: Rome, Italy, 2022; 393p.
4. Dar, R.A.; Dar, E.A.; Kaur, A.; Phutela, U.G. Sweet sorghum-a promising alternative feedstock for biofuel production. *Renew. Sustain. Energy Rev.* **2018**, *82*, 4070–4090. [CrossRef]
5. Ayer, R.S.; Westcot, D.W. Salinity Problems. In *Water Quality for Agriculture*, 1st ed.; FAO: Rome, Italy, 1985; pp. 13–58.
6. Motsi, H.; Molapo, M.; Phiri, E.E. A review of the adaptive capacity of sweet sorghum to improve food security and poverty alleviation in sub-Saharan Africa. *S. Afr. J. Bot.* **2022**, *150*, 323–329. [CrossRef]
7. Nxele, N.; Klein, A.; Ndimba, B.K. Drought and salinity stress alters ROS accumulation, water retention, and osmolyte content in sorghum plants. *S. Afr. J. Bot.* **2017**, *108*, 261–266. [CrossRef]
8. Silva, M.L.S.; Sousa, H.G.; Silva, M.L.S.; Lacerda, C.F.; Gomes-Filho, E. Growth and photosynthetic parameters of saccharine sorghum plants subjected to salinity. *Acta Sci. Agron.* **2019**, *41*, 42607. [CrossRef]
9. Gupta, A.; Bano, A.; Rai, S.; Mishra, R.; Singh, M.; Sharma, S.; Pathak, N. Mechanistic insights of plant-microbe interaction towards drought and salinity stress in plants for enhancing the agriculture productivity. *Plant Stress* **2022**, *4*, 100073. [CrossRef]
10. Yang, Z.; Li, J.L.; Liu, L.N.; Xie, Q.; Sui, N. Photosynthetic Regulation Under Salt Stress and Salt-Tolerance Mechanism of Sweet Sorghum. *Front. Plant Sci.* **2020**, *10*, 1722. [CrossRef]
11. Martins, A.C.; Larré, C.F.; Bortolini, F.; Borella, J.; Eichholz, R.; Delias, D.; Amarante, L. Tolerância ao déficit hídrico: Adaptação diferencial entre espécies forrageiras. *Iheringia Série Botânica* **2018**, *73*, 228–239. [CrossRef]
12. Wang, Z.; Wei, Y.; Zhao, Y.; Wang, Y.; Zou, F.; Huang, S.; Yang, X.; Xu, Z.; Hu, H. Physiological and transcriptional evaluation of sweet sorghum seedlings in response to single and combined drought and salinity stress. *S. Afr. J. Bot.* **2022**, *146*, 459–471. [CrossRef]
13. Ma, Y.; Dias, M.C.; Freitas, H. Drought and Salinity Stress Responses and Microbe-Induced Tolerance in Plants. *Front. Plant Sci.* **2020**, *11*, 1750. [CrossRef]
14. Ogbaga, C.C.; Stepien, P.; Dyson, B.C.; Rattray, N.J.W.; Ellis, D.I.; Goodacre, R.; Johnson, G.N. Biochemical Analyses of Sorghum Varieties Reveal Differential Responses to Drought. *PLoS ONE* **2016**, *11*, 0154423. [CrossRef] [PubMed]
15. Dinkeloo, K.; Boyd, S.; Pilot, G. Update on amino acid transporter functions and on possible amino acid sensing mechanisms in plants. *Semin. Cell Dev. Biol.* **2018**, *74*, 105–113. [CrossRef] [PubMed]
16. Punia, H.; Tokas, J.; Mor, V.S.; Bhuker, A.; Malik, A.; Singh, N.; Satpal; Alsahli, A.A.; Hefft, D.I. Deciphering reserve mobilization, antioxidant potential, and expression analysis of starch synthesis in sorghum seedlings under salt stress. *Plants* **2021**, *10*, 2463. [CrossRef] [PubMed]
17. Ukwatta, J.; Pabuayon, I.C.M.; Park, J.; Chen, J.; Chai, X.; Zhang, H.; Zhu, J.; Xin, Z.; Shi, H. Comparative physiological and transcriptomic analysis reveals salinity tolerance mechanisms in *Sorghum bicolor* (L.) Moench. *Planta* **2021**, *254*, 98. [CrossRef] [PubMed]
18. Almodares, A.; Hadi, M.R.; Kholdebarin, B.; Samedani, B.; Kharazian, Z. The response of sweet sorghum cultivars to salt stress and accumulation of Na+, Cl− and K+ ions in relation to salinity. *J. Environ. Biol.* **2014**, *35*, 733–739. [PubMed]
19. Marta, A.; Mancini, M.; Orlando, F.; Natali, F.; Capecchi, L.; Orlandini, S. Sweet sorghum for bioethanol production: Crop responses to different water stress levels. *Biomass Bioenergy* **2014**, *64*, 211–219. [CrossRef]
20. Dubreuil, V.; Fante, K.P.; Planchon, O.; Neto, J.L.S. Os tipos de climas anuais no Brasil: Uma aplicação da classificação de Köppen de 1961 a 2015. *Confins* **2018**. [CrossRef]
21. EMPARN. Relatório Pluviométrico. 2022. Available online: https://meteorologia.emparn.rn.gov.br/relatorios/relatorios-pluviometricos (accessed on 27 February 2023).
22. Mendes, K.R.; Portela, J.C.; Gondim, J.E.F.; Ribeiro, M.A.; Medeiros, J.F.; Queiroz, G.C.M. Physical, chemical and structural attributes of soil in agroecosystems in the Brazilian Semiarid region. *Rev. Ciência Agronômica* **2022**, *53*, e20207630.
23. Teixeira, P.C.; Donagemma, G.K.; Fontana, A.; Teixeira, W.G. *Manual de Métodos de Análise de Solo*, 3rd ed.; EMBRAPA: Brasília, Brazil, 2017; 574p.
24. Neves, A.L.A.; Santos, R.D.; Pereira, L.G.R.; Oliveira, G.F.; Scherer, C.B.; Verneque, R.S.; McAllister, T. Agronomic characteristics, silage quality, intake and digestibility of five new Brazilian sorghum cultivars. *J. Agric. Sci.* **2015**, *153*, 371–380. [CrossRef]

25. Medeiros, J.F. Qualidade da Água de Irrigação e Evolução da Salinidade nas Propriedades Assistidas Pelo "GAT" Nos Estados do RN. Ph.D. Thesis, Universidade Federal da Paraíba, Paraíba, Brazil, 1992.
26. Allen, R.G.; Pereira, L.S.; Raes, D. *Crop Evapotranspiration (Guidelines for Computing Crop Water Requirements)*, 1st ed.; FAO: Rome, Italy, 2004.
27. Stickler, F.C.; Wearden, S.; Pauli, A.W. Leaf Area determination in Grain Sorghum. *Agron. J.* **1961**, *53*, 187–188. [CrossRef]
28. Weatherley, P.E. Studies in the water relations of the cotton plant. *New. Phytol.* **1950**, *49*, 81–97. [CrossRef]
29. Bates, L.S.; Waldren, R.P.; Teare, I.D. Rapid determination of free proline for water-stress studies. *Plant. Soil.* **1973**, *39*, 205–207. [CrossRef]
30. Yemm, E.W.; Cocking, E.C.; Ricketts, R.E. The determination of amino-acids with ninhydrin. *Analyst* **1955**, *80*, 209–214. [CrossRef]
31. Yemm, E.W.; Willis, A.J. The estimation of carbohydrates in plant extracts by anthrone. *Biochem. J.* **1954**, *57*, 508. [CrossRef] [PubMed]
32. EMBRAPA. *Manual de Análises Químicas de Solos, plantas e Fertilizante*, 1st ed.; EMBRAPA: Brasília, Brasil, 2009; 370p.
33. Silva, E.B.; Nogueira, F.D.; Guimarães, P.T.G. *BT 31—Análise de Cloreto em Tecido Vegetal*, 1st ed.; Editora UFLA: Lavras, Brasil, 2021.
34. Posit | The Open-Source Data Science Company. Available online: https://posit.co/ (accessed on 27 February 2023).
35. Statistica. Available online: https://www.statistica.com/en/ (accessed on 27 February 2023).
36. Mansour, M.M.F.; Emam, M.M.; Salama, K.H.A.; Morsy, A.A. Sorghum under saline conditions: Responses, tolerance mechanisms, and management strategies. *Planta* **2021**, *254*, 24. [CrossRef] [PubMed]
37. Sayyad-Amin, P.; Borzouei, A.; Jahansooz, M.R.; Parsaeiyan, M. Root biochemical responses of grain and sweet-forage sorghum cultivars under saline conditions at vegetative and reproductive phases. *Rev. Bras. De Bot.* **2016**, *39*, 115–122. [CrossRef]
38. Hussain, S.; Hussain, S.; Ali, B.; Ren, X.; Chen, X.; Li, Q.; Saqib, M.; Ahmad, N. Recent progress in understanding salinity tolerance in plants: Story of Na+/K+ balance and beyond. *Plant. Physiol. Biochem.* **2021**, *160*, 239–256. [CrossRef]
39. Gull, M.; Kausar, A. Screening The Variability in Salt Tolerance of Sorghum Bicolor L. By Nutrients Uptake and Growth Analysis of Four Genotypes. *Pharmacophore* **2019**, *10*, 43–50.
40. Wang, M.; Zheng, Q.; Shen, Q.; Guo, S.; River, Y.; Key, J. The Critical Role of Potassium in Plant Stress Response. *Int. J. Mol. Sci.* **2013**, *14*, 7370–7390. [CrossRef]
41. Kausar, A.; Gull, M. Influence of salinity stress on the uptake of magnesium, phosphorus, and yield of salt susceptible and tolerant sorghum cultivars (*Sorghum bicolor* L.). *J. Appl. Biol. Biotechnol.* **2019**, *7*, 53–58. [CrossRef]
42. Perrier, L.; Rouan, L.; Jaffuel, S.; Clément-Vidal, A.; Roques, S.; Soutiras, A.; Baptiste, C.; Bastianelli, D.; Fabre, D.; Dubois, C.; et al. Plasticity of Sorghum Stem Biomass Accumulation in Response to Water Deficit: A Multiscale Analysis from Internode Tissue to Plant Level. *Front. Plant Sci.* **2017**, *8*, 1516. [CrossRef]
43. Abreha, K.B.; Enyew, M.; Carlsson, A.S.; Vetukuri, R.R.; Feyissa, T.; Motlhaodi, T.; Ng'uni, D.; Geleta, M. Sorghum in dryland: Morphological, physiological, and molecular responses of sorghum under drought stress. *Planta* **2021**, *255*, 20. [CrossRef] [PubMed]
44. Mansour, M.M.F.; Salama, K.H.A. Cellular basis of salinity tolerance in plants. *Environ. Exp. Bot.* **2004**, *52*, 113–122. [CrossRef]
45. Hniličková, H.; Hnilička, F.; Orsák, M.; Hejnák, V. Effect of salt stress on growth, electrolyte leakage, Na+ and K+ content in selected plant species. *Plant Soil Environ.* **2019**, *65*, 90–96. [CrossRef]
46. Demidchik, V.; Straltsova, D.; Medvedev, S.S.; Pozhvanov, G.A.; Sokolik, A.; Yurin, V. Stress-induced electrolyte leakage: The role of K+-permeable channels and involvement in programmed cell death and metabolic adjustment. *J. Exp. Bot.* **2014**, *65*, 1259–1270. [CrossRef] [PubMed]
47. Hasan, S.A.; Rabei, S.H.; Nada, R.M.; Abogadallah, G.M. Water use efficiency in the drought-stressed sorghum and maize in relation to expression of aquaporin genes. *Biol. Plant* **2017**, *61*, 127–137. [CrossRef]
48. Weimberg, R.; Lerner, H.R.; Poljakoff-Mayber, A. Changes in growth and water-soluble solute concentrations in Sorghum bicolor stressed with sodium and potassium salts. *Physiol. Plant* **1984**, *62*, 472–480. [CrossRef]
49. Uribe, R.A.; Silvério, P.C.; Costa, G.H.; Nogueira, L.C.; Leite, L.A. Chloride levels in biomass sorghum due to fertilization sources. *Biomass Bioenergy* **2020**, *143*, 105845. [CrossRef]

agriculture

MDPI

Article

Irrigation Depth and Potassium Doses Affect Fruit Yield and Quality of Figs (*Ficus carica* L.)

Elias Ariel Moura [1,*], Vander Mendonça [1], Vladimir Batista Figueirêdo [1], Luana Mendes Oliveira [1], Marlenildo Ferreira Melo [1], Toni Halan Silva Irineu [1], Alex Danilo Monte Andrade [1], Edvan Alves Chagas [2], Pollyana Cardoso Chagas [3], Enoch Souza Ferreira [1], Luciana Freitas Medeiros Mendonça [4] and Francisco Romário Andrade Figueiredo [1]

[1] Departamento de Fitotecnia, Universidade Federal Rural do Semi-Árido, Mossoró 59625-900, RN, Brazil
[2] Departamento de Produção Vegetal, Empresa Brasileira de Pesquisa Agropecuária, Boa Vista 69301-970, RR, Brazil
[3] Departamento de Produção Vegetal, Universidade Federal de Roraima, Boa Vista 69310-000, RR, Brazil
[4] Departamento de Fitotecnia, Universidade Federal de Campina Grande, Pombal 58840-000, PB, Brazil
* Correspondence: eliasariel90@gmail.com

Abstract: The need to diversify agricultural production has fostered the cultivation of several crops under environmental conditions atypical to their origin, justifying the extreme importance of studies on the agricultural management of crops in semiarid regions. In this context, this study aimed to evaluate the effects of irrigation depth and potassium doses on fig quality under semiarid conditions. The experiment was conducted in a 4 × 4 split-split-plot design, in randomized block design, with three replicates. The plots corresponded to four irrigation levels (50%, 75%, 100%, and 125% ETc), the subplots consisted of four potassium doses (0, 60, 120, and 240 g K_2O $plant^{-1}$), and the sub-subplot corresponded to the crop years (2018/19 and 2019/20). Results showed that water deficit reduced fig productivity, and the irrigation levels equal to or greater than 100% ETc performed cumulatively throughout the growing cycles. Therefore, irrigation depths from 85.19% to 95.16% ETc are recommended for greater water-use efficiency and fruit quality. Furthermore, potassium fertilization mitigated water stress in fig plants, allowing for reduced irrigation levels, especially in the second year, without compromising fruit traits.

Keywords: crop evapotranspiration; mineral fertilization; organoleptic qualities; semiarid conditions; water deficit

1. Introduction

The cultivation of figs (*Ficus carica* L.) in semiarid conditions is highly favorable. The high temperature and low relative humidity in the semiarid region reduce the incidence of fungal diseases, in addition to improving the organoleptic characteristics of the fruits [1]. However, the region suffers from water scarcity, and difficult-to-manage water resources face increased water demand [2]. Water deficit is one of the main factors that limit plant growth by reducing cell turgor and extension [3]. In addition, the growth rate and crop yield are negatively affected due to impaired photosynthesis and enzymatic activity and the excessive production of reactive oxygen species (ROS) [4,5].

In 'Abboudi' and 'Gizy' fig cultivars, irrigation below 100% ETc caused a water deficit that significantly reduced the plant morphometric and physiological traits [6]. In 'Roxo-de-Valinhos' cultivars, irrigation at 100% ETc increased production and improved the morphological characteristics of fruits during the rainy period [7]. In this sense, the irrigation must supply the plant's physiological demand, because in conditions of water stress, the fig tree can suffer from severe stress [8,9], impairing nutrient absorption and causing physiological [4,10], productive, and qualitative damage to the plant [7,11,12].

Potassium (K) plays a key role in vegetative growth [13], production, and fruit quality [14,15]. Furthermore, in sufficient quantity in plants, K is an important mitigant of the deleterious effects of water stress due to its contribution to the prevention of oxidative stress, osmotic regulation, protein synthesis, and photosynthesis [16,17]. However, under water deficit conditions, K uptake is reduced, drastically reducing photosynthesis and productivity, causing leaf senescence and increasing the synthesis of reactive oxygen species (ROS) responsible for oxidative stress [18,19].

Thus, finding a balance between the ideal irrigation blade and potassium doses that mitigate the deleterious effects on plants and increases fruit productivity and quality under semiarid conditions is a key factor for efficient production. Controlling biotic and abiotic stress and accurately estimating water demand are essential for the sustainable management of water resources in fig trees. Therefore, the objective was to evaluate the effects of irrigation levels and potassium doses on the production and quality of fig fruits cultivated in semiarid climatic conditions.

2. Materials and Methods

2.1. Characterization of the Experimental Area

The experiment was carried out in the municipality of Mossoró, in the west region of the state of Rio Grande do Norte, Brazil (5°11′15″ S, 37°20′39″ W, 18 m above the sea level, flat relief). The climate of the region is 'BShw' according to the Köppen classification [20], with a 673.9 mm average annual rainfall and a 27.4 °C average annual temperature, featuring two well-defined seasons: dry and hot summer (from June to January) and dry winter (from February to May).

During the experiment, temperature, minimum and maximum air relative humidity (Figure 1A,B), solar radiation and rainfall (Figure 1C), and average wind speed (Figure 1D) were collected from the automatic weather station (EMA) of UFERSA.

2.2. Cultivation Conditions

Fig plants from the 'Roxo de Valinhos' cultivar, 5 years old and spaced 2.0 m × 1.5 m apart, were evaluated during two production cycles: the first from September 2018 to February 2019 and the second from August 2019 to February 2020. The plants were pruned on 25 September 2018 in the first cycle (18/19) and on August 10, 2019 in the second (19/20). The productive branches were pruned to 5 cm long, leaving two to five vegetative buds. At 15 days after pruning, the budding branches were thinned so that the plants remained with only ten productive branches each. During the first 30 days, all plants received the same irrigation depth (100% ETc) with the aim of inducing sprouts to develop equally. Afterwards, the plants received the different irrigation depths as treatments.

After production pruning, each plant was fertilized with 200 g of phosphorus and 160 g of nitrogen, split into three applications. Monoammonium phosphate (10% N, 46% P_2O_5) was used as phosphorus source, while urea (46% N) was used as nitrogen source. In both production cycles, fertilizers were applied under the canopy of the trees and incorporated superficially into the soil with the aid of a shovel [21]. In addition, 10 kg of organic compost with previously determined chemical characteristics was applied, as recommended by [12] (Table 1).

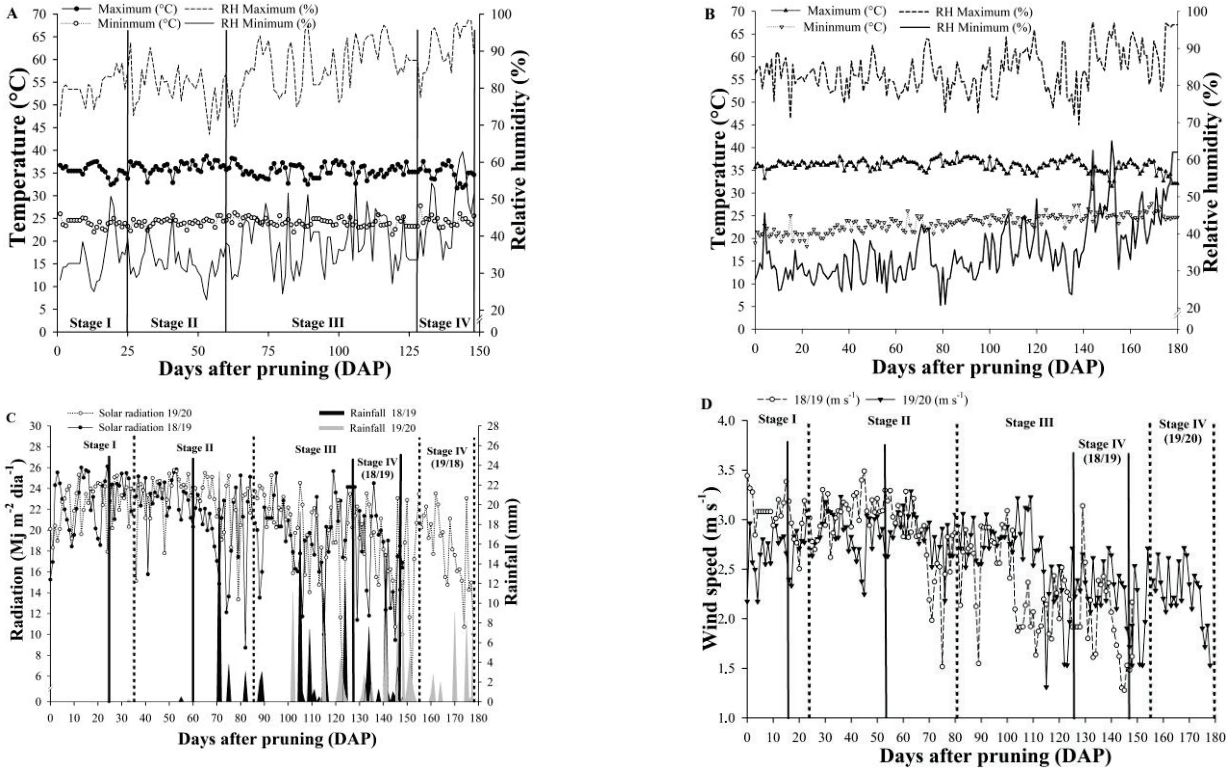

Figure 1. Climatic data collected during the experimental period (from 2018/2019 to 2019/2020). Temperature and relative humidity (18/19—(**A**); 19/20—(**B**)), global solar radiation and rainfall (**C**), and average wind speed (**D**) under semiarid conditions. Stage I—sprouting/initiation of new leaves; Stage II—start of effective full cover/inflorescence development; Stage III—effective full cover/beginning of fruit harvest; Stage IV—end of harvest.

Table 1. Analysis of the organic source used in fertilizing plants.

Samples	pH	EC	OM	P	K^+	Na^+	Ca^{2+}	Mg^{2+}	Al^{3+}	(H + Al)	SB	CTC	V	PET
	(Substrate)	dS m^{-1}	g kg^{-1}	Mg dm^3			cmolc dm^3						%	
Organic compost	7.24	3.26	38.17	522.275	433.61	3716.9	0	0	0	0	17.28	17.28	100	93.58

Electric conductivity (EC); organic matter (OM); phosphorus (P); potassium (K^+); sodium (Na^+) extractor mehlich-1; calcium (Ca^{2+}); magnesium (Mg^{2+}); aluminum (Al^{3+}) extraidos com KCl 1 mol L^{-1}; potential acidity (H + Al); sum of bases (SB); cationic exchange capacity (CTC); base saturation (V); percentage of exchangeable sodium (PET).

2.3. Experimental Design

The experimental design used was randomized blocks in a split-plot arrangement, with three blocks and two plants per experimental unit. The plots corresponded to the irrigation levels: 50, 75, 100, and 125% crop evapotranspiration (ETc). The potassium doses were applied in the subplots: 0, 60, 120, and 240 g plant^{-1}. At last, the sub-subplot corresponded to the crop years (2018/19 and 2019/20). Potassium chloride (60% K_2O) was used as the potassium source, being split into three applications every 20 days. The application and incorporation were performed according to [21].

The application of the irrigation levels was performed through an automatic microsprinkler irrigation system, using emitters with an average flow rate of 31 L h^{-1}, determined in the experiment, based on the estimation of the crop evapotranspiration (ETc). Due to low rainfall, irrigation was applied daily. The ETc and the reference evapotranspiration (ETo) were estimated by the standard FAO Penman–Monteith method [22]. The same irrigation blades were applied to the same plants in the two cultivation cycles. Due to the

long drought period in the region, the crop management, such as pruning and soil water storage replacement, was performed again.

The estimation of the crop coefficients (Kc) by the FAO method (Allen et al., 1998) used the basal crop coefficients (Kcb) of each plant growth stage. Stage I—sprouting/initiation of new leaves; Stage II—start of effective full cover/inflorescence development; Stage III—effective full cover/beginning of fruit harvest; stage IV—end of harvest. The irrigation time was then calculated for the treatment with 100% ETc, using the 94.5% irrigation efficiency determined in the field and a 2% leaching fraction, with plants spaced 2 m × 1.5 m apart (Table 2). Irrigation efficiency was calculated according to [23], considering it equal to the average of the application uniformity coefficient (AUC), Christiansen's uniformity coefficient (CUC), and statistical uniformity coefficient (SUE), which were tested using some microsprinklers in each irrigation level. The leaching fraction was only considered for this experiment, considering other research carried out in the region.

Table 2. Irrigation level applied—Li (mm) and crop coefficient—Kc in each growth stage and for each crop year (2018/2019 and 2019/2020).

Years/	Li (ETc%)	Stage/Total Days *					
		Stage I 25/33	**Stage II 35/59**	**Stage III 68/63**	**Stage IV 20/23**	**Total mm**	**Average mm Day^{-1}**
18/19	50	23.96	71.55	224.03	52.58	372.12	2.51
19/20		33.37	101.34	188	67.72	390.43	2.19
18/19	75	35.95	107.32	336.05	78.87	558.19	3.77
19/20		50.06	152.01	282	101.58	585.65	3.29
18/19	100	47.93	143.09	448.06	105.16	744.24	5.02
19/20		66.74	202.68	376.01	135.44	780.87	4.39
18/19	125	59.91	178.86	560.08	131.45	930.298	6.28
19/20		83.43	253.34	470.01	169.31	976.09	5.48
Kc 18/19		0.73	0.89	1.00	0.67	----------	
Kc 19/20		0.75	0.88	1.03	0.99		

* Total days at each stage (18–19/19–20).

2.4. Characteristics Evaluated

Fruits were harvested three times a week when they reached the physiological maturation stage (Stage III) suitable for in natura consumption [1]. Fruit weight was measured on a digital analytical scale (±0.01 g). The number of marketable fruits (MF) and yield of marketable fruits (MY) (t ha^{-1}) were quantified. When the production of fruits intended for commercialization drastically reduced, turning the harvest economically unfeasible, the remaining green fruits (destined for the industry) were harvested and counted to determine the number of green fruits (IF). In addition, the total number of fruits (TF) and total yield (green and ripe fruits) were determined as t ha^{-1}. Marketable fruits (mature stage) are destined for fresh consumption (mature stage), while green fruits are intended for industry, for instance, to produce figs in syrup (green and semimature stages).

Irrigation water-use efficiency—IWUE (t ha^{-1} mm) and water-use efficiency—WUE (t ha^{-1} mm) were calculated according to [24,25]:

$$\text{IWUE} = \left(\frac{E_y}{I_r}\right) * 100 \quad (1)$$

$$\text{WUE} = \left(\frac{E_y}{E_{Tc}}\right) * 100 \quad (2)$$

where E_y is the economical yield (t ha^{-1}), I_r is the amount of applied irrigation water (mm), and E_{Tc} is the evapotranspiration (mm). However, in our calculation, total yield was used for E_y.

2.5. Fruit Quality

To evaluate fruit quality, only the mature fruits intended for trade (in natura) were collected. Ten fruits were evaluated per plant to determine the average fruit length (FL), fruit diameter (FD), and fruit mass (FM), totaling twenty fruits per plot. The fruits were measured with a digital caliper (±0.01 mm). The average fruit mass was determined with an analytical balance, and the results were expressed in grams (±0.01 g).

Color space and fruit firmness were determined using ten fruits per plot. Peel color was determined with a Chroma Meter–400/410 colorimeter (Minolta Corp., Osaka, Japan), by performing one reading on each side of the fruit. The lightness (L*), saturation (C), and hue angle (°hue) were also evaluated. Fruit firmness was determined using a digital texture analyzer manufactured by Stable MicroSystems®, model TA.XTExpress/TA.XT2icon, equipped with a 5 mm diameter probe. Two readings were performed on each side of the fruit, and the results were expressed in newtons (N).

Twelve fruits were evaluated per plot to determine the fruit physicochemical characteristics. The soluble solids (SS) were determined directly in the homogenized pulp juice using a digital refractometer (model PR–100, Palette, Atago Co., Ltd., Tokyo, Japan), with the results expressed in °Brix [26].

The titratable acidity (TA) was determined by volumetric titration using 1 g of pulp transferred to a 125 mL Erlenmeyer flask with 50 mL of water. Subsequently, titration was performed with a previously standardized NaOH 0.1 M solution until pH reached 8.1, with the results expressed in g 100 g^{-1} pulp of citric acid [26]. The SS/TA ratio was determined by relating the values of soluble solids and titratable acidity.

The potential of hydrogen (pH) was estimated using a potentiometer with automatic temperature adjustment (Model mPA-210 Tecnal®, Ourinhos, Brazil), previously calibrated with buffer solutions at pH 7.0 and pH 4.0 [26]. The data were expressed in actual pH values.

Vitamin C was estimated by titration with Tilman's solution (DCPIP-2,6-dichlorophenolindophenol at 0.02%), using 1 g of sample diluted in a 100 mL volumetric flask with 0.5% oxalic acid, according to the methodology proposed by [27], with the results expressed in mg of ascorbic acid 100 g^{-1} pulp.

2.6. Statistical Analysis

The data obtained were subjected to the Shapiro–Wilk normality test and the test of homogeneity of variances according to Bartlett, and, if within the standards for normality and homogeneity, they were subjected to analysis of variance by the F-test (p = 0.05). The quantitative data were subjected to regression analysis, while the qualitative data were subjected to the least-significant difference test (LSD) (**p** = 0.05). All analyses were performed using the statistical software R, version. 4.0.2 [28].

3. Results

3.1. Climatic Influence

The maximum and minimum temperatures and humidity showed small variations during the crop growth period. The greatest discrepancies between climatic data in the period close to the same developmental stages were observed at 121 and 122 DAP, with differences of 4.31 °C and 4.83 °C from 2018/19 to 2019/20 (Figure 1A,B).

The solar radiation values showed greater reductions in the winter months, given the increase in cloudiness during this period. The most significant reductions were recorded in the first cycle (18/19) (Figure 1B). The total monthly rainfall values were higher in the first cycle, with 35.31, 57.40, and 33.53 mm from December 2018 to February 2019 (Figure 1B). The average wind speed observed during the fruit production period did not damage the fruits. A reduction in the wind speed was observed precisely when the fruits were under development and maturation, with a more significant reduction in the first cycle (18/19) (Figure 1D).

During the production period, the first crop year (18/19) showed lower average and total values for crop evapotranspiration (ETc—Stages I and IV) and reference evapotranspi-

ration (ETo—Stages III and IV) compared to the second crop season (19/20) (Figure 2A,B). The climatic effects influenced the irrigation levels (Li) applied, and although the second crop year (19/20) had higher Li values applied, the first crop year (18/19) showed higher average values, with stage III constituting the period with the highest water requirement by the plants (Table 2).

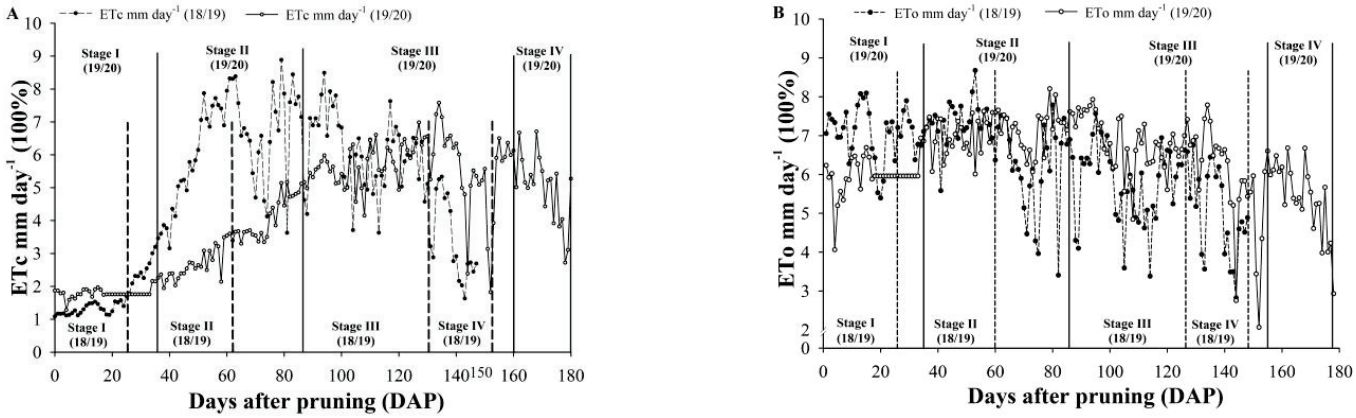

Figure 2. Standard crop evapotranspiration (**A**) (ETc 100% mm day^{-1}) and reference evapotranspiration (**B**) (ETo 100% mm day^{-1}) in the days after pruning, under semiarid climatic conditions, in the 2018/2019 and 2019/2020 crop years. Stage I—sprouting/initiation of new leaves; Stage II—start of effective full cover/inflorescence development; Stage III—effective full cover/beginning of fruit harvest; stage IV—end of harvest.

3.2. Production and Water Efficiency

The marketable yield (MY), the total yield (TY), the number of marketable fruits (MF), and the total number of fruits (TF) were influenced by the irrigation levels applied (Li) in the two crop years (18/19 and 19/20) ($p < 0.001$). As for the number of green fruits (GF) per plant, this variable was only influenced by the Li applied ($p < 0.01$). There was no significant effect for potassium doses ($p > 0.05$).

For the MY (Figure 3A) and TY (Figure 3B), the first crop year (18/19) showed linear increases with the increase in the Li, reaching yield values of 17.53 and 33.52 t ha^{-1} at 125% ETc, respectively. In the second year (19/20), the highest mean values for MY and TY (7.99 and 15.85 t ha^{-1}) were obtained at the Li of 95.16% and 102% ETc, respectively (Figure 3A,B). Among the Li values, there was a significant difference only at 125% ETc, for which the first year (18/19) resulted in an MY value 75.01% higher than the second year (19/20) ($p < 0.001$).

The first crop year (18/19) linearly influenced the MF, resulting, with the water deficit, in the lowest values. In the second year (19/20), for the same variable, the highest mean (61.60 fruits) was obtained at the Li of 94.89% ETc (Figure 3C). On the other hand, there was a greater number of green fruits (GF) (91.50 fruits) at the Li of 98.42% ETc (Figure 3D). For the TF, in the first and second years (18/19), the highest total numbers of fruits (169.69 and 162.69 fruits) were obtained at the Li of 125% and 95.13% ETc, respectively (Figure 3E).

The irrigation levels influenced the water-use efficiency (WUE) and the irrigation water-use efficiency (IWUE) in the two crop years ($p < 0.05$). In the first year (18/19), the highest values for WUE (2.14 t ha^{-1} mm) and IWUE (1.88 t ha^{-1} mm) were obtained at the Li of 125% ETc, resulting in the highest fig yields (Figure 4A,B).

There was a quadratic regression response in the second year (19/20), with means of 16 ton ha^{-1} mm for the WUE at the Li of 88.54% ETc and 0.99 ton ha^{-1} mm for the IWUE at the Li of 86.96% ETc. For the WUE, the first crop year obtained a 42.60% efficiency compared to the second year at the Li of 75% ETc ($p < 0.05$), and 78.04% at the Li of 125% ETc ($p < 0.001$).

Among the irrigation levels, there was a 21.02% yield reduction for the Li of 75% and 125% ETc, and only 2.75% for the Li of 75% and 100% ETc. The Li of 50% and 100% ETc

were not influenced between crop years ($p > 0.05$) (Figure 4A). For the IWUE, there was a difference only for the Li of 125% ETc, with the first crop year (18/19) being 76.17% superior to the second (19/20) ($p < 0.001$) (Figure 4B).

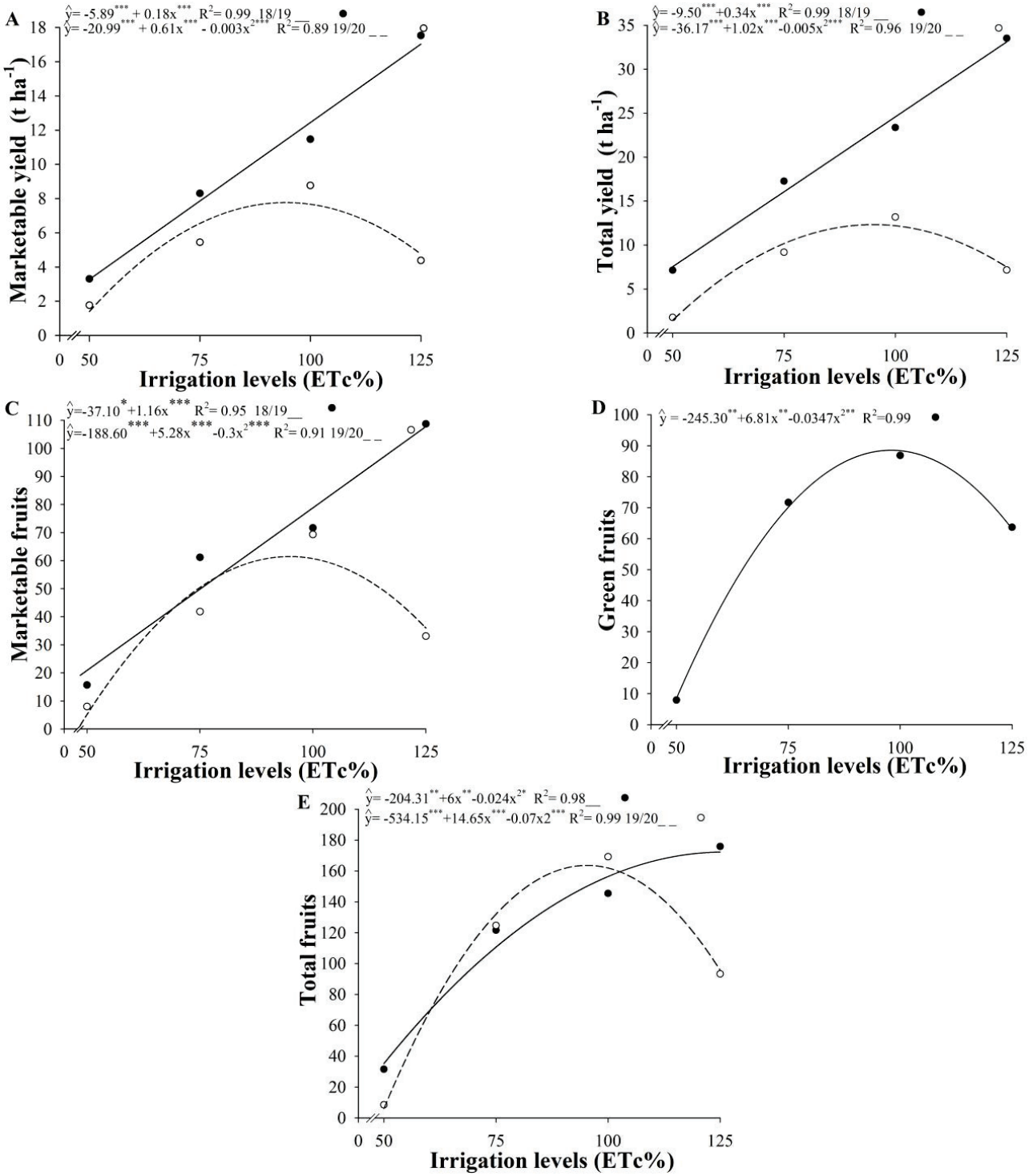

Figure 3. Marketable yield (**A**) and total yield (**B**)—ton ha^{-1}, and number of marketable fruits (**C**), green fruits (**D**), and total fruits (**E**) of fig plants grown under semiarid climatic conditions in the 2018/2019 and 2019/2020 crop years. * Significant ($p < 0.05$); ** ($p < 0.01$); *** ($p < 0.001$).

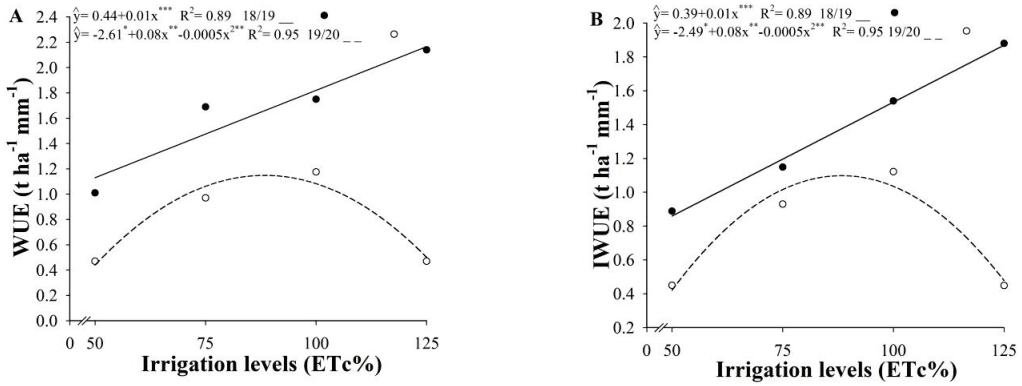

Figure 4. Water-use efficiency (WUE) (**A**) and irrigation water-use efficiency (IWUE) (**B**) of fig plants grown under semiarid climatic conditions in the 2018/2019 and 2019/2020 crop years. * Significant ($p < 0.05$); ** ($p < 0.01$); *** ($p < 0.001$).

3.3. Fruit Physical Characteristics

Fruit length (FL) was influenced by the Li and potassium doses in the two production years ($p < 0.001$). In the first year (18/19), the plants without potassium fertilization (0 g K plant^{-1}) and those fertilized with 60 and 120 g K plant^{-1} presented average fruit length (FL) values of 42.99, 42.19, and 41.70 mm at the Li of 104%, 104.55%, and 97.88% ETc, respectively (Figure 5A). In the second year (19/20), the plants fertilized with 60 and 120 g K plant^{-1} presented average FL values of 40.40 and 40.02 mm at the Li of 85.19% and 98.70% ETc, respectively. However, the regression response was negative in the plants without potassium (0 g K plant^{-1}), with a decrease occurring in the FL with the increase in the Li up to 92.07% ETc, with an average of 35.35 mm (Figure 5B).

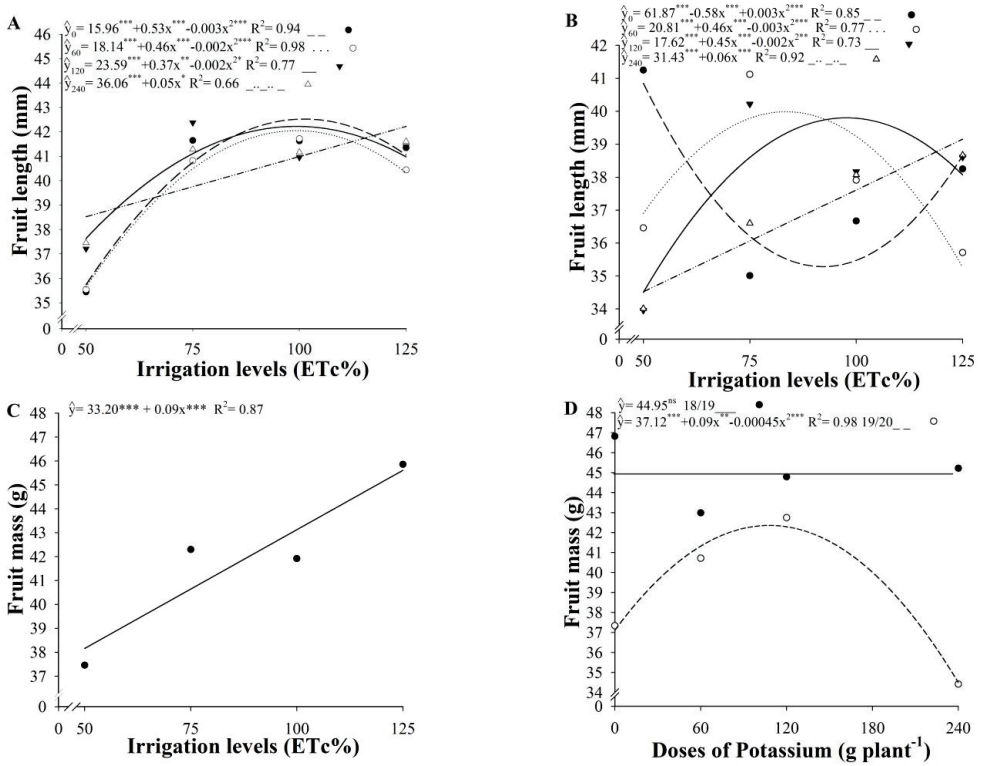

Figure 5. Fruit length ((**A**)—18/19 and (**B**)—19/20) and average fruit mass as a function of irrigation levels—Li (**C**) and potassium doses (**D**) in fig plants grown under semiarid climatic conditions in the 2018/2019 and 2019/2020 crop years. ^{ns} Not significant ($p > 0.05$); * Significant ($p < 0.05$); ** ($p < 0.01$); *** ($p < 0.001$).

There was an 18.51% reduction in the Li (19.36 mm) from the first to the second year with the application of 60 g K plant^{-1}, with a 6.02% loss in FL (1.78 mm). When 120 g K plant^{-1} was applied, there was only a 0.83% increase in the Li (0.81 mm) in the second year (19/20), with a 4.02% reduction in the FL (1.67 mm). For the plants fertilized with 240 g K plant^{-1}, there was a growing linear behavior with the increase in the irrigation levels applied in the first (18/19) and second crop years (19/20) (Figure 5A,B).

The irrigation levels influenced the fruit mass (FM) ($p > 0.01$) and the potassium doses in the two crop years ($p < 0.05$). There were linear increases in FM with the increase in the Li values up to 125% ETc (Figure 5C). For the potassium doses, the fruits from the first year (18/19) were larger than those produced in the second year ($p < 0.05$), but there was no significant reduction between them, thus being statistically equal. The second year, however (19/20), provided the highest average fruit mass (42.35 g) at the dose of 107.93 g K plant^{-1}, after which the FM was reduced at higher K doses (Figure 5D).

For the variables related to the color space of fruits, the irrigation levels influenced fruit lightness (L*) in the second year (19/20), presenting the lowest mean value for this variable (29.14 L*) at the Li of 82.87 ETc% (Figure 6A). The hue angle (°Hue) obtained the highest means in the fruits of the plants subjected to the highest water deficit, possibly characterizing fruits at an earlier maturation stage, closer to a green-yellowish color (Figure 6B).

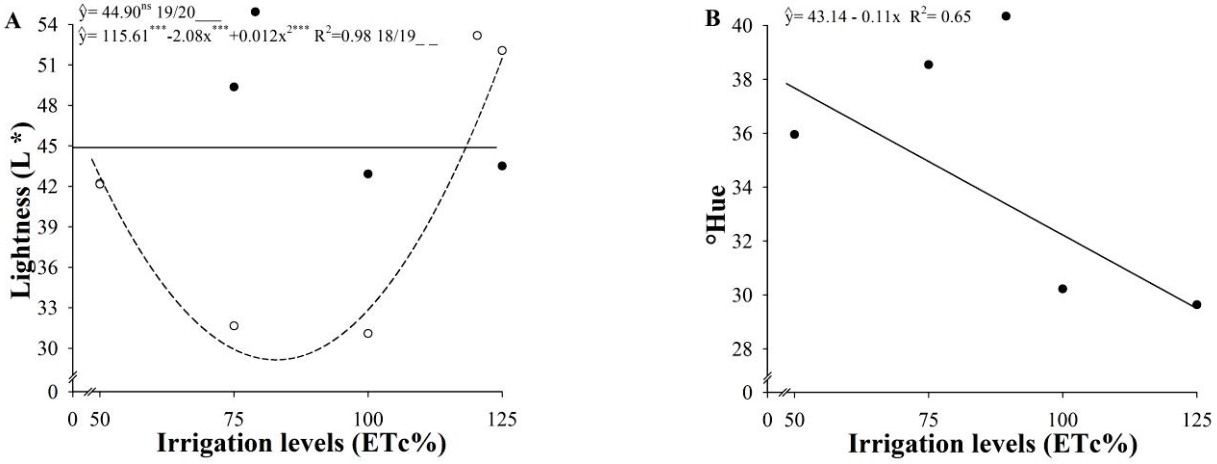

Figure 6. Lightness (L*) (**A**) and hue angle (°Hue) (**B**) of fruits as a function of the irrigation levels in fig plants grown under semiarid climatic conditions in the 2018/2019 and 2019/2020 crop years. ^{ns} Not significant ($p > 0.05$); *** ($p < 0.001$).

Fruit firmness (FF) was influenced by the irrigation levels and potassium doses in the two production years ($p < 0.01$). In the first year (18/19), the Li increase in the plants fertilized with 60 g K plant^{-1} caused a significant reduction in FF (2.08 N) up to the Li of 105% ETc, with further increases in FF occurring at higher Li values. In the plants without potassium (0 g K plant^{-1}), the firmest fruits (4.52 N) were obtained at the Li of 75.34% ETc, with reductions occurring in FF at lower Li values (water deficit), as well as at higher Li values up to 97.50% ETc, which resulted in the lowest result for FF (4.22 N). There were increases in FF at higher Li values (Figure 7A).

In the second year (19/20), the increase in the irrigation levels in the plants fertilized with 60 and 240 g K plant^{-1} caused reductions in FF up to the Li of 95.51% (2.82 N) and 92.50% (3.58 N), respectively, with further increases in FF occurring at higher Li values (Figure 7B). For the plants without potassium application (0 g plant^{-1}), there was a growing linear response of FF with the increase in the Li (ETc%). This response can be associated with the organic fertilization provided to the plants in both cycles (18/19 and 19/20). For the plants fertilized with 120 g K plant^{-1}, there were maximum increases in FF (4.36 N)

by applying irrigation levels up to 103.75% ETc, with reductions in FF at higher Li values (Figure 7B).

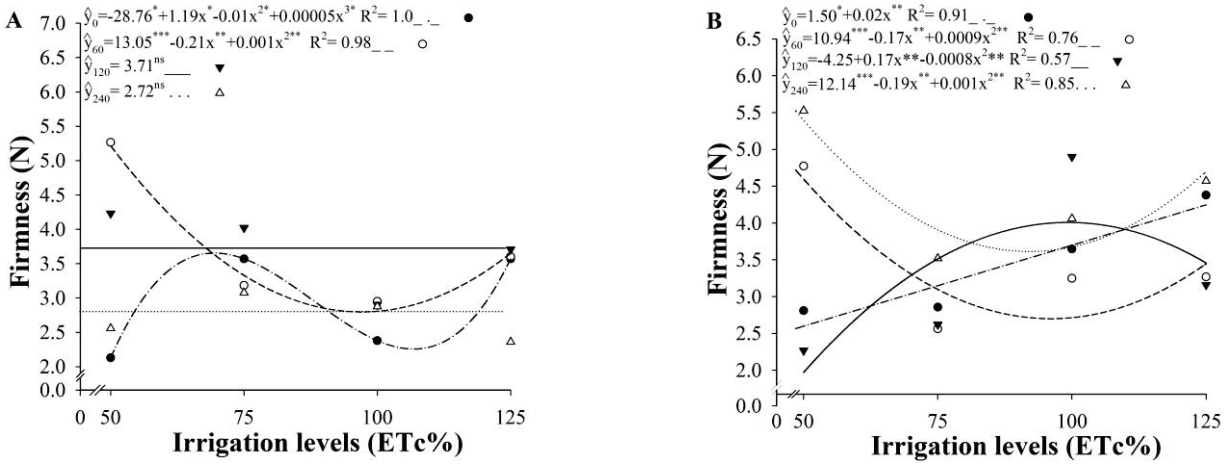

Figure 7. Firmness of fig fruits produced in the 2018/2019 (**A**) and 2019/2020 (**B**) crop years as a function of irrigation levels and potassium doses under semiarid conditions in the 2018/2019 and 2019/2020 crop years. * Significant ($p < 0.05$); ** Significant ($p < 0.01$); *** Significant ($p < 0.001$); ^{ns} Not significant ($p > 0.05$).

3.4. Fruit Physicochemical Characteristics

The contents of soluble solids (SS), titratable acidity (TA), potential of hydrogen (pH), and ratio (SS/TA) of the fig fruits were influenced by the irrigation levels (Li) and potassium doses in both production years ($p < 0.001$). The fruit vitamin C content, in turn, was only influenced by the Li.

In the first year (18/19), the plants without fertilization (0 g plant^{-1}) remained statistically equal, not being affected by water deficit or excess ($p > 0.05$). The SS content increased linearly with the increase in the Li (ETc%) in the plants fertilized with 60 g K plant^{-1}. For the plants fertilized with 120 and 240 g K plant^{-1}, the lowest SS contents were obtained with water deficit below the irrigation levels of 70.51% (10.69 °Brix) and 71.85% ETc (9.27 °Brix), while the highest SS contents were obtained with the increase in the Li up to 111.31% (14.42 °Brix) and 99.09% ETc (10.06 °Brix), respectively, with reductions in the SS contents at higher Li values (Figure 8A).

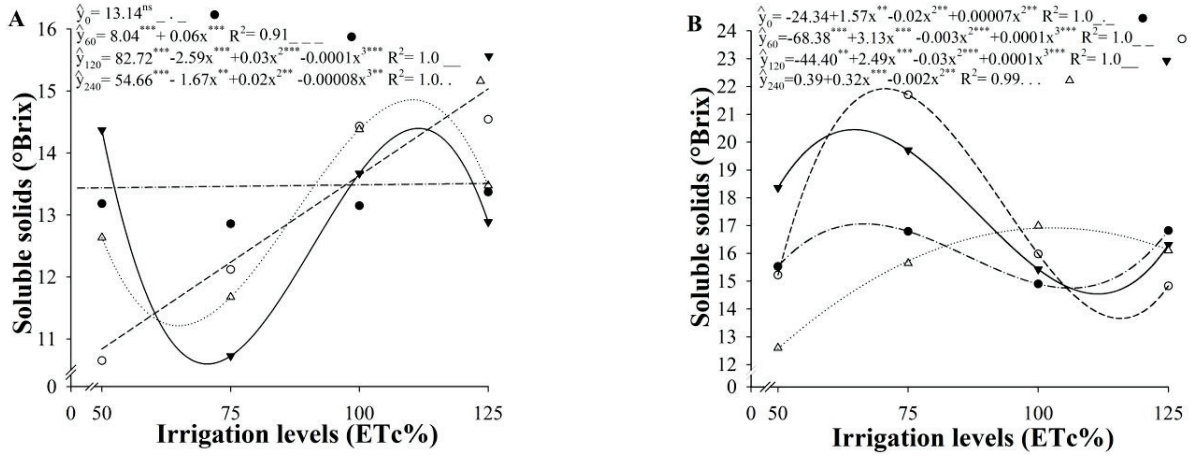

Figure 8. Soluble solids of fig fruits produced in the 2018/2019 (**A**) and 2019/2020 (**B**) production cycles as a function of irrigation levels and potassium doses under semiarid conditions in the 2018/2019 and 2019/2020 crop years. ** Significant ($p < 0.01$); *** Significant ($p < 0.001$); ^{ns} Not significant ($p > 0.05$).

In the second year (19/20), the highest SS contents were obtained at the Li of 63.84% (16.69 °Brix), 69.70% (20.38 °Brix), and 63.54% (20.28 °Brix) in the plants without fertilization (0 g K plant^{-1}) and in the plants fertilized with 60 and 120 g K plant^{-1}, respectively. There was a reduction in the SS contents at lower Li values (water deficit) and at Li values up to 117.1% (11.39 °Brix), 124.75% (10.37 °Brix), and 118.30% ETc (11.25 °Brix) for the doses of 0, 60, and 120 g K plant^{-1}, respectively. For the plants fertilized with 240 g K plant^{-1}, the highest SS content was obtained at the Li of 101.91% ETc, with 16.70 °Brix (Figure 8B).

In the first year (18/19), the TA at the Li values of 88.24%, 66.88%, and 89.29% ETc resulted in 0.19, 0.22, and 0.18 g of citric acid in the fruits grown with 0, 60, and 120 g K plant^{-1}, respectively. In the plants fertilized with 240 g K plant^{-1}, there was a growing linear increase in the TA of fruits with the increase in the Li values (Figure 9A). In the second year (19/20), the lowest TA value (0.16 g of citric acid) was obtained at the Li of 88.64% ETc for the plants without potassium fertilization (0 g K plant^{-1}) (Figure 9B). When applying 60 g K plant^{-1}, the lowest values appeared between the Li of 33.33% ETc, which resulted in 0.49 g of citric acid, and the Li of 100% ETc, with 0.64 g of citric acid.

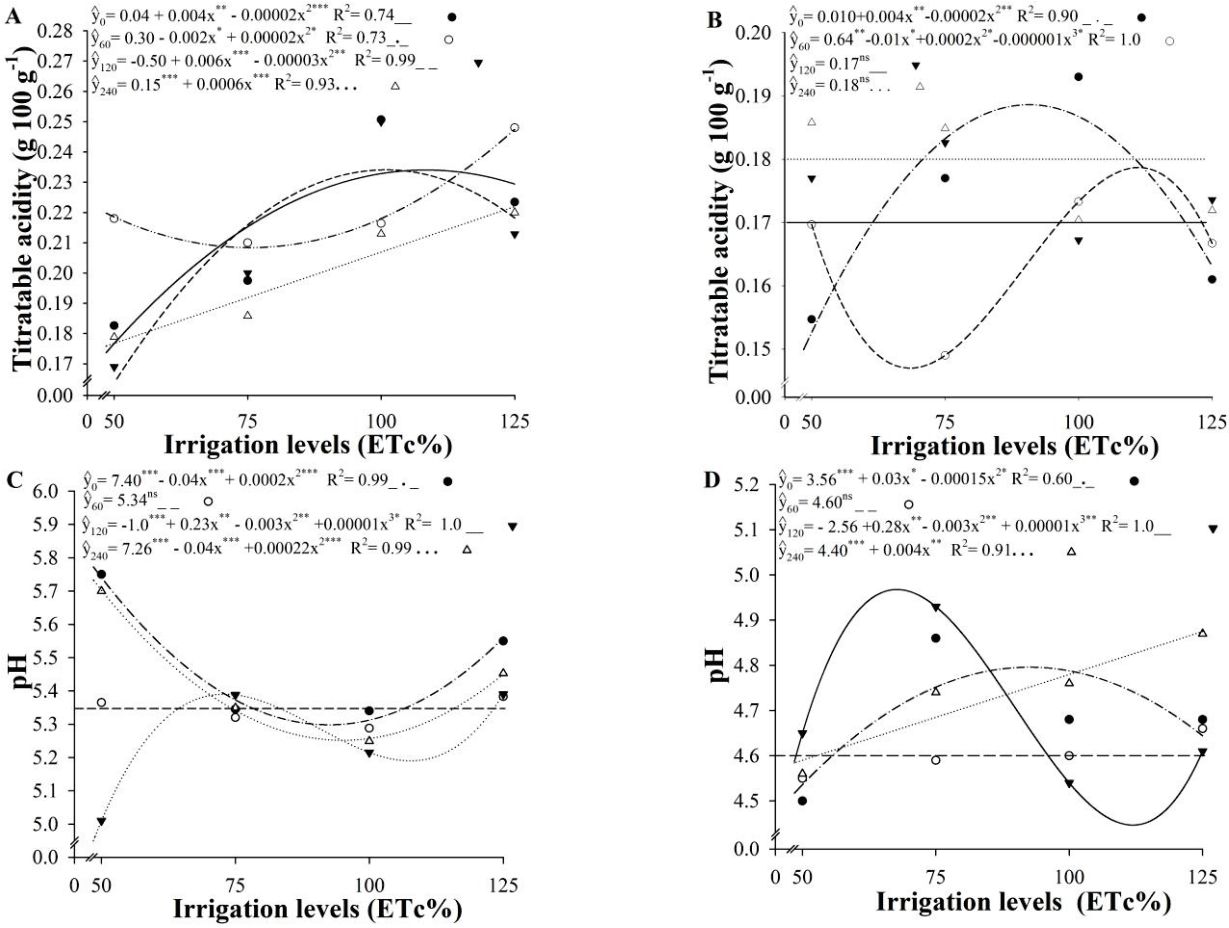

Figure 9. Titratable acidity of fig fruits in the 2018/2019 (**A**) and 2019/2020 (**B**) crop cycles, and pH of fig fruits in the 2018/2019 (**C**) and 2019/2020 (**D**) crop cycles as a function of irrigation levels and potassium doses under semiarid conditions in the 2018/2019 and 2019/2020 crop years. * Significant ($p < 0.05$); ** Significant ($p < 0.01$); *** Significant ($p < 0.001$); ^{ns} Not significant ($p > 0.05$).

Fruit pH showed no significant effect of the irrigation levels for the plants fertilized with 60 g K plant^{-1} in both years (18/20 and 19/20). In the absence or at the maximum K dose (0 and 240 g K plant^{-1}), the water deficit provided the highest fruit pH contents, with decreases in this variable (5.40 and 5.44) with the increase in the irrigation levels up to 100% and 90.91% ETc, respectively, further increasing at higher Li values (ETc%). The

fruits of plants fertilized with 120 g K plant^{-1} obtained a pH 5.09 at the Li of 73.33% ETc. The reduction (water deficit) or increase in the irrigation levels up to 100% ETc decreased the fruit pH (5.00). There were, however, increases in the fruit pH at higher Li values (Figure 9C).

In the second year (19/20), the plants without fertilization (0 g K plant^{-1}) showed the highest fruit pH value (4.80) at the Li of 92.76% ETc. The plants fertilized with 120 g K plant^{-1} showed the highest fruit pH (4.92) at the Li of 66.01% ETc, with a decrease occurring in this variable with the increase in water deficit and with the increase in the Li up to 117.32% ETc, which resulted in the lowest pH value (4.10) (Figure 9D). Fruit pH increased linearly with the increase in the Li (ETc%) in the plants fertilized with 240 g K plant^{-1} (Figure 9D).

For SS/TA ratio in the first crop year (18/19), the water deficit resulted in higher SS/TA values for the fruits of the plants fertilized with 120 g K plant^{-1}, reducing when the irrigation levels were increased up to 103.93%, which resulted in the lowest SS/TA ratio value (40.33) (Figure 10A).

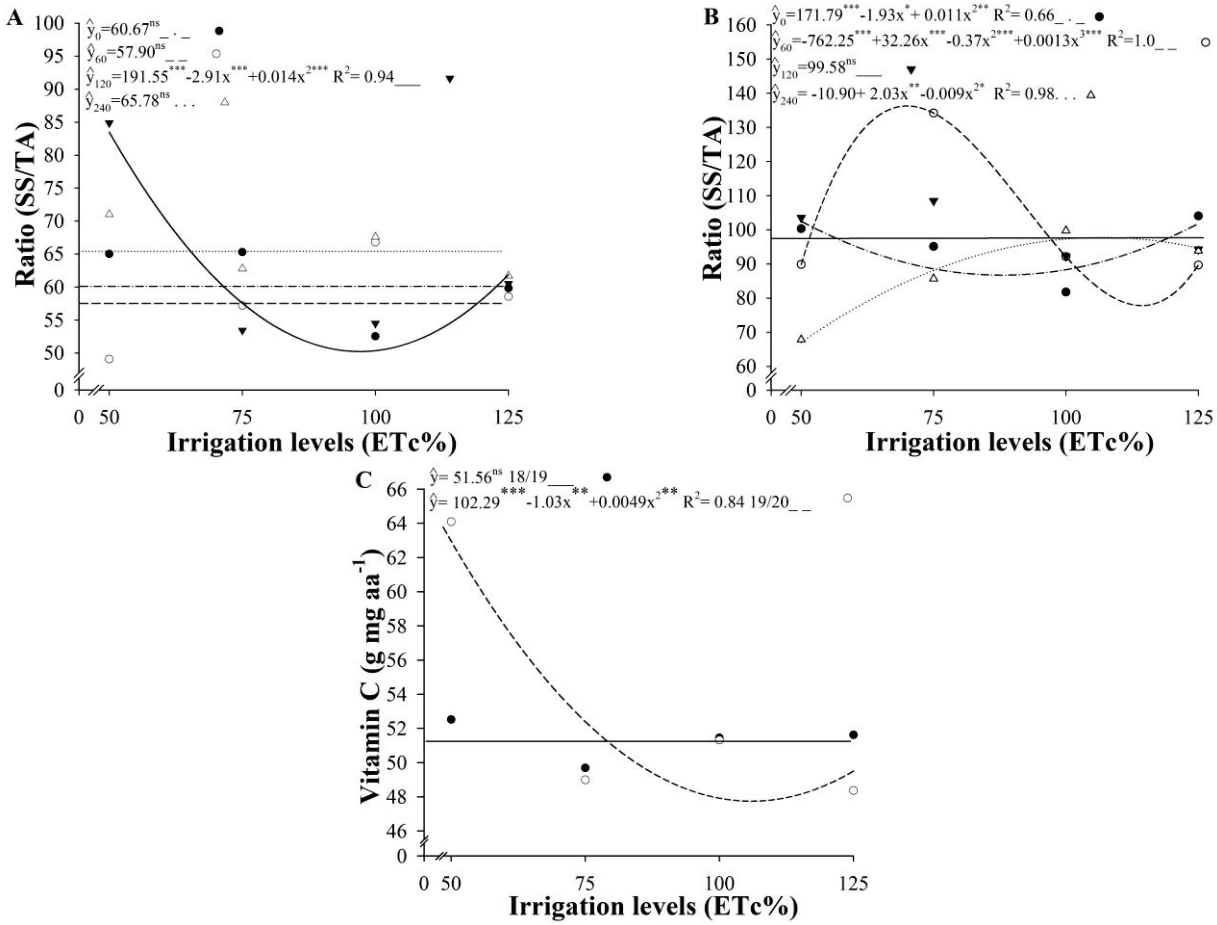

Figure 10. SS/TA ratio ((**A**)—2018/2019; (**B**)—2019/2020) and vitamin C (**C**) of fig fruits as a function of irrigation levels under semiarid conditions. * Significant ($p < 0.05$); ** Significant ($p < 0.01$); *** Significant ($p < 0.001$); ^{ns} Not significant ($p > 0.05$). Means of 2 crop years (2018/2019 and 2019/2020).

In the second year (19/20), the highest SS/TA values (87.13 and 103.57) were obtained at the Li of 87.93% and 112.78% ETc for the plants fertilized with 0 and 240 g K plant^{-1}, respectively (Figure 10B). The plants fertilized with 60 g K plant^{-1} showed the highest SS/TA values at the Li of 67.87% ETc (129.31), reducing the SS/TA values with increasing Li values up to 121.87% ETc, which resulted in the lowest value for the SS/TA ratio (26.99).

For the fruit vitamin C content, the first year (18/19) showed no statistical difference, with statistically equal means at the irrigation levels applied. For the second year (19/20), the highest vitamin C contents were obtained with plants subjected to a water deficit. The increase in the Li up to 105.93% ETc reduced the fruit vitamin C content (47.71 g mg of ascorbic acid 100 g^{-1} pulp), further increasing at higher Li values (Figure 10C).

4. Discussion

Solar radiation significantly influences plants during the production years, affecting the crop energy balance. The reflection of the incident solar radiation is associated with plant yield by photosynthesis, transpiration, flowering, and maturation. Daily observations regarding variations in soil moisture and water flow and climatic variation observations can provide essential elements to quantify the water balance components and estimate the actual crop evapotranspiration [29].

Under ideal management conditions, the plants did not show severe damages due to high temperatures for being a fruit species native to arid regions, featuring young leaves adapted to conditions of high radiation and temperature, and developing specific morpho-physiological characteristics to withstand the tensions mentioned above [30]. However, under water deficit conditions (50% ETc), the crop entered a rest period, maintaining only its physiological conditions for survival.

Water deficit reduces plant growth and productivity, although it improves some fruit quality attributes, such as increased antioxidant and sugar content [31], as we observed in our study. Such reductions caused by water stress were greater when low K was available to plants, causing drastic leaf dropping and decreasing MY and TY and increasing the content of soluble sugars and vitamin C. Similar results were observed by [32] in *Nicotiana rustica*.

Plants respond differently depending on the stress level: under mild water stress or water stress of limited duration, 'stress avoidance' mechanisms are induced, including stomatal closure and increased root/shoot ratio [4]. Under severe stress or after a long-term stress, in contrast, 'dehydration avoidance' mechanisms, such as osmolytes accumulation and cell wall stiffening, are induced [6].

The low yield is directly correlated with the number of fruits. The higher the water deficit imposed on the plants, the lower the fruit quality and yield. The more water provided to the plants, the higher the WUE and IWUE values in the first year, although reducing in the second year (19/20), which confirms the sensitivity of the plants subjected to water deficiency and water excess.

Lower WUE values possibly occur when soil evapotranspiration is high compared to the crop evapotranspiration, therefore not supplying the plant with the proper water requirement of the crop [33]. When faced with severe water stress, plants reduce the leaf area, close their stomata, and undergo leaf senescence, resulting in phenological responses that save water, possibly for survival in later periods [34].

The results showed that both water deficit and water excess, in a cumulative manner, caused fruit length reduction and that the irrigation level estimated by the FAO method [22] was highly precise in determining the water requirement of the plant. This limitation in the final fruit size may be related to the photosynthetic limitations of the plant faced with water deficit, which could cause reductions in the absorption and translocation of assimilates to the fruits. The effect of water deficit on fruit reduction has also been observed for the fig crop [7], for an extra early peach cultivar [35], and for highbush blueberries [36].

Likewise, water excess in the soil causes anaerobic stress to the roots, a condition that suppresses root activity, reduces root growth, and decreases nutrient and water absorption due to low transpiration. However, the plants fertilized with 240 g K $plant^{-1}$ showed a linear increase in fruit length at high irrigation levels. This linear behavior may be associated with the high K content in the soil solution, allowing absorption by mass flow, which may not have occurred at the lowest doses due to K depletion in the soil solution, with absorption occurring by diffusion instead [37]. The greater fruit mass obtained at

the high K dose may be related to the effect of abiotic stress, considering that the climatic conditions of study are extreme, which may require an increased content of this nutrient.

The plants subjected to the highest water deficit condition (50% ETc) showed a considerable delay in fruit harvest: almost 30 days in the first crop year (18/19) and 20 days of difference in the second (19/20). Fruit harvest becomes a problem for the fig crop under water deficit (50% ETc): although all harvest aspects were analyzed, the fruits produced by plants subjected to water stress showed a dull green color (higher hue angle value), which was confirmed by the fruit color analysis (L* and h°), and may indicate a semimature maturation stage, considering that water stress strongly influences the fruit maturation process [38]. Moderate stress usually acts by providing improvements in fruit maturation, as noted in the results, while severe water stress (50% ETc) acts by delaying the process.

Although the plants fertilized with potassium presented reduced FF with the increase in the irrigation levels, satisfactory firmness values were still verified in the fruits, especially in the second year. Similar results with expressive responses only in the second year were reported by [39].

The reduction in the SS concentration in the fruits of plants under excessive irrigation levels (125% ETc) may be related to a dilution effect [36,40]. On the other hand, there was no effect of the irrigation levels on the SS, TA, SS/TA ratio, and firmness of fig fruits from cultivars subjected to irrigation deficit regulated at 50 and 100% ETc [41]. The increase in SS in the plants subjected to water deficit may be caused by an active osmotic adjustment in the fruits, which favors the increase in the content of solutes [39].

What may explain the high vitamin C content in the second cycle (19/20) is the effect of aerobic metabolism in plants on the generation of reactive oxygen species (ROS). The overproduction of ROS may be a response to water stress (drought), and plants regulate the expression of antioxidant enzymes to maintain ROS homeostasis, ensuring uninterrupted metabolism [5]. Antioxidants possess greater potential according to their ability to provide bioactive substances that neutralize ROS and remaining free radicals by oxidative stress [42–44]. When there is an excessive production of ROS under stress conditions, there is also membrane, DNA, and protein damage, in addition to lipid peroxidation [45], with the production of small hydrocarbon fragments, which may react with thiobarbituric acid to form colored products called TBARS [46].

5. Conclusions

Considering what was observed, water deficit significantly reduces the production characteristics of plants, as well as irrigation water levels equal to or greater than 100% ETc applied cumulatively throughout the years of cultivation. Thus, irrigation water levels between 85.19% and 95.16% ETc are the most recommended to obtain greater water efficiency for the crop and produce quality fruits. It was observed that a higher water deficit leads to increases in the SS and vitamin C contents in the fruits. Potassium influenced the reduction in water stress in the fig plants, providing reductions in the irrigation levels applied, especially in the second year, without compromising the fruit properties. The dose of 107.93 g K plant^{-1} provides fruits with a higher average mass.

Author Contributions: Conceptualization, E.A.M. and V.B.F.; methodology, E.A.M. and V.B.F.; software, E.A.M.; validation, E.A.M., V.M. and V.B.F.; formal analysis, E.A.M.; investigation, E.A.M., L.M.O., M.F.M., T.H.S.I., A.D.M.A. and E.S.F.; resources, E.A.M., L.M.O., M.F.M., T.H.S.I., A.D.M.A. and E.S.F.; data curation, E.A.M. and E.S.F.; writing—original draft preparation, E.A.M., F.R.A.F., L.F.M.M. and M.F.M.; writing—review and editing, P.C.C. and V.M.; visualization, E.A.C.; supervision, V.M.; project administration, V.M.; funding acquisition, V.M. All authors have read and agreed to the published version of the manuscript.

Funding: This research was funded by the Coordenação de Aperfeiçoamento de Pessoal de Nível Superior.

Institutional Review Board Statement: Not applicable.

Data Availability Statement: The data presented in this study are available in the article.

Acknowledgments: The authors thank the Higher Education Personnel Improvement Coordination (CAPES) for their scholarships and the Federal Rural University of the Semi-arid for the infrastructure.

Conflicts of Interest: The authors declare no conflict of interest.

References

1. Silva, F.S.O.; Pereira, E.C.; Mendonça, V.; da Silva, R.M.; Alves, A.A. Phenology and Yield of the "Roxo de Valinhos" Fig Cultivar in Western Potiguar. *Rev. Caatinga* **2017**, *30*, 802–810. [CrossRef]
2. Moursi, H.; Kim, D.; Kaluarachchi, J.J. A Probabilistic Assessment of Agricultural Water Scarcity in a Semi-Arid and Snowmelt-Dominated River Basin under Climate Change. *Agric. Water Manag.* **2017**, *193*, 142–152. [CrossRef]
3. Bayer, A.; Ruter, J.; van Iersel, M.W. Elongation of Hibiscus Acetosella under Well-Watered and Drought-Stressed Conditions. *HortScience* **2016**, *51*, 1384–1388. [CrossRef]
4. Abdolahipour, M.; Kamgar-Haghighi, A.A.; Sepaskhah, A.R.; Zand-Parsa, S.; Honar, T.; Razzaghi, F. Time and Amount of Supplemental Irrigation at Different Distances from Tree Trunks Influence on Morphological Characteristics and Physiological Responses of Rainfed Fig Trees under Drought Conditions. *Sci. Hortic.* **2019**, *253*, 241–254. [CrossRef]
5. Wang, X.; Cai, X.; Xu, C.; Wang, Q.; Dai, S. Drought-Responsive Mechanisms in Plant Leaves Revealed by Proteomics. *Int. J. Mol. Sci.* **2016**, *17*, 1706. [CrossRef] [PubMed]
6. Darwish, A.D.; El-Berry, I.; Moursy, F.S.; Hagagg, L.F. Detecting Drought Tolerance of Fig (*Ficus carica*, L.) Cultivars Depending on Vegetative Growth and Peroxidase Activity. *Int. J. ChemTech Res.* **2015**, *8*, 1520–1532.
7. Trevisan, P.V.; Menegaes, J.F.; Fronza, D.; Nishijima, T. Produtividade Da Cultura Da Figueira (*Ficus carica* L.) Submetida a Diferentes Estratégias de Irrigação Por Gotejamento. *Acta Iguazu* **2016**, *5*, 49–60.
8. Gholami, M.; Rahemi, M.; Kholdebarin, B.; Rastegar, S. Biochemical Responses in Leaves of Four Fig Cultivars Subjected to Water Stress and Recovery. *Sci. Hortic.* **2012**, *148*, 109–117. [CrossRef]
9. Gholami, M.; Rahemi, M.; Rastegar, S. Use of Rapid Screening Methods for Detecting Drought Tolerant Cultivars of Fig (*Ficus carica* L.). *Sci. Hortic.* **2012**, *143*, 7–14. [CrossRef]
10. Abdolahipour, M.; Kamgar-Haghighi, A.A.; Sepaskhah, A.R. Time and Amount of Supplemental Irrigation at Different Distances from Tree Trunks Influence on Soil Water Distribution, Evaporation and Evapotranspiration in Rainfed Fig Orchards. *Agric. Water Manag.* **2018**, *203*, 322–332. [CrossRef]
11. Bagheri, E.; Sepaskhah, A.R. Rain-Fed Fig Yield as Affected by Rainfall Distribution. *Theor. Appl. Climatol.* **2013**, *117*, 433–439. [CrossRef]
12. Souza, A.P.; Silva, A.C.; Leonel, S.; Souza, M.E.; Tanaka, A.A. Evapotranspiração e Eficiência Do Uso Da Água No Primeiro Ciclo Produtivo Da Figueira "Roxo de Valinhos" Submetida a Cobertura Morta. Available online: http://www.seer.ufu.br/index.php/biosciencejournal/article/view/14076 (accessed on 4 July 2020).
13. Kanai, S.; Moghaieb, R.E.; El-Shemy, H.A.; Panigrahi, R.; Mohapatra, P.K.; Ito, J.; Nguyen, N.T.; Saneoka, H.; Fujita, K. Potassium Deficiency Affects Water Status and Photosynthetic Rate of the Vegetative Sink in Green House Tomato Prior to Its Effects on Source Activity. *Plant Sci.* **2011**, *180*, 368–374. [CrossRef]
14. Caretto, S.; Parente, A.; Serio, F.; Santamaria, P. Influence of Potassium and Genotype on Vitamin E Content and Reducing Sugar of Tomato Fruits. *HortScience* **2008**, *43*, 2048–2051. [CrossRef]
15. Daoud, B.; Pawelzik, E.; Naumann, M. Different Potassium Fertilization Levels Influence Water-Use Efficiency, Yield, and Fruit Quality Attributes of Cocktail Tomato—A Comparative Study of Deficient-to-Excessive Supply. *Sci. Hortic.* **2020**, *272*, 109562. [CrossRef]
16. Hawkesford, M.; Horst, W.; Kichey, T.; Lambers, H.; Schjoerring, J.; Møller, I.S.; White, P. Functions of Macronutrients. *Marschner's Miner. Nutr. High. Plants* **2012**, *1*, 135–189. [CrossRef]
17. White, P.J.; Karley, A.J. Potassium. *Plant Cell Monogr.* **2010**, *17*, 199–224. [CrossRef]
18. Cakmak, I. The Role of Potassium in Alleviating Detrimental Effects of Abiotic Stresses in Plants. *J. Plant Nutr. Soil Sci.* **2005**, *168*, 521–530. [CrossRef]
19. Rostami, A.A.; Rahemi, M. Screening Drought Tolerance in Caprifig Varieties in Accordance to Responses of Antioxidant Enzymes. *World Appl. Sci. J.* **2013**, *21*, 1213–1219. [CrossRef]
20. Peel, M.C.; Finlayson, B.L.; McMahon, T.A. Updated World Map of the Köppen-Geiger Climate Classification. *Hydrol. Earth Syst. Sci.* **2007**, *11*, 1633–1644. [CrossRef]
21. Leonel, S.; Reis, L.L. Potassium Fertilization on Fruits Orchards: A Study Case from Brazil. In *Soil Fertility*; InTech: London, UK, 2012.
22. Allen, R.G.; Pereira, L.S.; Raes, D.; Smith, M. *Crop Evapotranspiration-Guidelines for Computing Crop Water Requirements-FAO Irrigation and Drainage Paper 56*; FAO—Food and Agriculture Organization of the United Nations: Rome, Italy, 1998.
23. Merriam, J.L.; Keller, J. *Farm Irrigation System Evaluation: A Guide for Management*, 3rd ed.; Utah State University: Logan, UT, USA, 1978.
24. Howell, T.A.; Cuenca, R.H.; Solomon, K.H. Crop Yield Response. In *Management of Farm Irrigation Systems*; Hoffman, G.J., Howell, T.A., Solomon, K.H., Eds.; ASAE: St. Joseph, MI, USA, 1990; pp. 93–122.

25. Kanber, R.; Yazar, A.; Köksal, H.; Oguzer, V. Evapotranspiration of Grapefruit in the Eastern Mediterranean Region of Turkey. *Sci. Hortic.* **1992**, *52*, 53–62. [CrossRef]
26. AOAC. *Official Methods of Analysis of AOAC International*, 19th ed.; AOAC International: Gaithersburg, MD, USA, 2012; ISBN 0935584838 9780935584837.
27. Strohecker, R.; Henning, H.M. *Análises de vitaminas: Métodos comprovados*; Editora Paz Montalvo: Madrid, Spanish, 1967; 428p.
28. R Core Team. *R: A Language and Environment for Statistical Computing*; R Foundation for Statistical Computing: Vienna, Austria, 2020.
29. Souza, A.P.; Pereira, J.B.A.; da Silva, L.D.B.; Guerra, J.G.M.; de Carvalho, D.F. Evapotranspiração, Coeficientes de Cultivo e Eficiência Do Uso Da Água Da Cultura Do Pimentão Em Diferentes Sistemas de Cultivo. *Acta Sci. Agron.* **2011**, *33*, 15–22. [CrossRef]
30. González-Rodríguez, A.M.; Peters, J. Strategies of Leaf Expansion in *Ficus Carica* under Semiarid Conditions. *Plant Biol.* **2010**, *12*, 469–474. [CrossRef]
31. Ripoll, J.; Urban, L.; Brunel, B.; Bertin, N. Water Deficit Effects on Tomato Quality Depend on Fruit Developmental Stage and Genotype. *J. Plant Physiol.* **2016**, *190*, 26–35. [CrossRef]
32. Bahrami-Rad, S.; Hajiboland, R. Effect of Potassium Application in Drought-Stressed Tobacco (*Nicotiana rustica* L.) Plants: Comparison of Root with Foliar Application. *Ann. Agric. Sci.* **2017**, *62*, 121–130. [CrossRef]
33. Ertek, A.; Şensoy, S.; Gedik, İ.; Küçükyumuk, C. Irrigation Scheduling Based on Pan Evaporation Values for Cucumber (*Cucumis sativus* L.) Grown under Field Conditions. *Agric. Water Manag.* **2006**, *81*, 159–172. [CrossRef]
34. Chirinéa, C.F.; Pasqual, M.; de Araujo, A.G.; Pereira, A.R.; de Castro, E.M. Aclimatização e Anatomia Foliar de Plântulas de Figo Micropropagadas. *Rev. Bras. Frutic.* **2012**, *34*, 1180–1188. [CrossRef]
35. Alcobendas, R.; Mirás-Avalos, J.M.; Alarcón, J.J.; Pedrero, F.; Nicolás, E. Combined Effects of Irrigation, Crop Load and Fruit Position on Size, Color and Firmness of Fruits in an Extra-Early Cultivar of Peach. *Sci. Hortic.* **2012**, *142*, 128–135. [CrossRef]
36. Ehret, D.L.; Frey, B.; Forge, T.; Helmer, T.; Bryla, D.R. Effects of Drip Irrigation Configuration and Rate on Yield and Fruit Quality of Young Highbush Blueberry Plants. *HortScience* **2012**, *47*, 414–421. [CrossRef]
37. Oliveira, R.H.; Rosolem, C.A.; Trigueiro, R.M. Importance of Mass Flow and Diffusion on the Potassium Supply to Cotton Plants as Affected by Soil Water and Potassium. *Rev. Bras. Cienc. do Solo* **2004**, *28*, 439–445. [CrossRef]
38. Lopez, G.; Behboudian, M.H.; Vallverdu, X.; Mata, M.; Girona, J.; Marsal, J. Mitigation of Severe Water Stress by Fruit Thinning in "O'Henry" Peach: Implications for Fruit Quality. *Sci. Hortic.* **2010**, *125*, 294–300. [CrossRef]
39. Lobos, T.E.; Retamales, J.B.; Ortega-Farías, S.; Hanson, E.J.; López-Olivari, R.; Mora, M.L. Pre-Harvest Regulated Deficit Irrigation Management Effects on Post-Harvest Quality and Condition of V. Corymbosum Fruits Cv. Brigitta. *Sci. Hortic.* **2016**, *207*, 152–159. [CrossRef]
40. Lu, J.; Shao, G.; Cui, J.; Wang, X.; Keabetswe, L. Yield, Fruit Quality and Water Use Efficiency of Tomato for Processing under Regulated Deficit Irrigation: A Meta-Analysis. *Agric. Water Manag.* **2019**, *222*, 301–312. [CrossRef]
41. Kong, M.; Lampinen, B.; Shackel, K.; Crisosto, C.H. Fruit Skin Side Cracking and Ostiole-End Splitting Shorten Postharvest Life in Fresh Figs (*Ficus carica* L.), but Are Reduced by Deficit Irrigation. *Postharvest Biol. Technol.* **2013**, *85*, 154–161. [CrossRef]
42. Zhang, Y.J.; Gan, R.Y.; Li, S.; Zhou, Y.; Li, A.N.; Xu, D.P.; Li, H.B.; Kitts, D.D. Antioxidant Phytochemicals for the Prevention and Treatment of Chronic Diseases. *Molecules* **2015**, *20*, 21138–21156. [CrossRef] [PubMed]
43. Huan, C.; Jiang, L.; An, X.; Yu, M.; Xu, Y.; Ma, R.; Yu, Z. Potential Role of Reactive Oxygen Species and Antioxidant Genes in the Regulation of Peach Fruit Development and Ripening. *Plant Physiol. Biochem.* **2016**, *104*, 294–303. [CrossRef]
44. Oliveira, A.B.; Almeida Lopes, M.M.; Moura, C.F.H.; Siqueira Oliveira, L.; Souza, K.O.; Filho, E.G.; Urban, L.; de Miranda, M.R.A. Effects of Organic vs. Conventional Farming Systems on Quality and Antioxidant Metabolism of Passion Fruit during Maturation. *Sci. Hortic.* **2017**, *222*, 84–89. [CrossRef]
45. Johnson, H.E.; Broadhurst, D.; Goodacre, R.; Smith, A.R. Metabolic Fingerprinting of Salt-Stressed Tomatoes. *Phytochemistry* **2003**, *62*, 919–928. [CrossRef]
46. Larkindale, J.; Knight, M.R. Protection against Heat Stress-Induced Oxidative Damage in Arabidopsis Involves Calcium, Abscisic Acid, Ethylene, and Salicylic Acid. *Plant Physiol.* **2002**, *128*, 682–695. [CrossRef]

agriculture

MDPI

Brief Report

Variability in Stomatal Adaptation to Drought among Grapevine Cultivars: Genotype-Dependent Responses

Luca Nerva [1,†], Walter Chitarra [1,†], Gianni Fila [2], Lorenzo Lovat [1] and Federica Gaiotti [1,*]

[1] Research Centre for Viticulture and Enology, Council for Agricultural Research and Economics (CREA-VE), Via XXVIII Aprile 26, 31015 Conegliano, Italy; luca.nerva@crea.gov.it (L.N.); walter.chitarra@crea.gov.it (W.C.); lorenzo.lovat@crea.gov.it (L.L.)

[2] Research Centre Agriculture and Environment, Council for Agricultural Research and Economics, Sericulture Laboratory, Via Leonardo Eulero 6a, 35143 Padova, Italy

* Correspondence: federica.gaiotti@crea.gov.it

† These authors contributed equally to this work.

Abstract: Leaf stomata are the primary determinants of the plant water relations. Physiological adaptations of stomata in response to water stress have been extensively reported for grapevine. On the contrary, little is known about how the plasticity in stomatal anatomical features may affect their adaptability to drought conditions. In this study, we investigated, at the molecular and anatomical level, the effect of water stress on the stomatal anatomical features of four grapevine varieties extensively cultivated in the north of Italy. Potted plants of Garganega, Glera, Moscato giallo, and Merlot varieties were subjected to a 12–13 day period of water restriction during two consecutive seasons. Stomatal density and size were investigated in newly developed young leaves, 7 days after tip separation, following the occurrence of a water stress event. Furthermore, the gene expression of three key stomagenesis genes (*VvEPFL9*, *VvEPF1,* and *VvEPF2*) was analysed. The response of stomatal anatomical features to drought varied among the studied varieties. Moscato and Glera showed an increase in stomatal density and a decrease in stomatal size. On the contrary, Merlot displayed a reduction in stomatal number, while Garganega remained unchanged in terms of these values. Transcript levels of *VvEPFL9* were overall in agreement with stomatal densities measured in the four varieties, showing an up-regulation when drought induced an increase in stomatal density or a down-regulation when the stomatal number decreased. The wide variability in stomatal response observed in the four varieties under study suggests that anatomical changes in stomatal characteristics are genotype dependent. These variations contribute to the intra-specific variability in grapevine's response to water stress.

Keywords: *Vitis vinifera*; water stress; stomata; stomagenesis

1. Introduction

Drought stress poses a major threat to grapevine production and quality worldwide and is predicted to increase in intensity as a consequence of the ongoing climate change [1]. In view of this, the identification of strategies that can counteract the effects of climate is crucial to maintain the economic sustainability of viticulture in the near future. This requires a comprehensive knowledge of the mechanisms underlying grapevine drought responses and the definition of phenotypic, physiological, or molecular traits that can be used to identify stress-tolerant genotypes.

Leaf stomata, the minute apertures found mainly in the epidermis of leaves, are major determinants of the plant water stress response. Rapid changes in leaf stomatal conductance and photosynthesis in response to water stress have been extensively reported for grapevine and several other crops [2–4]. The regulation of water consumption by stomatal control plays a key role in determining the genotype adaptability to limited water conditions and has been shown to vary greatly among grapevine varieties and clones [5–7].

Leaf morphoanatomy also takes part in determining the genotype adaptability to drought conditions. Among leaf features, stomatal density and size on the leaf epidermis are key anatomical drivers in determining the transpiration rate [8]. Plants can adjust stomatal development to optimise gas exchange in response to water stress [8]. These anatomical adaptations to drought have been shown to vary greatly by species, cultivar, and the level of stress. In response to water limitation, stomatal density was reported to increase in wheat [9], olive [10], apricot [11], and sugarcane [12], and it was often coupled with a reduction in stomatal size [10,11,13].

In grapevine, stomatal density and size have been reported to vary in response to several environmental factors, including temperature and CO_2 levels [14], wind [15], and water availability [16–18]. Palliotti et al. [16] found that the Sangiovese variety exhibited a notable rise in stomatal count and a decrease in stomatal dimensions during periods of drought. Theodorou et al. [17] reported a similar behaviour for Grenache and Xinomavro varieties. However, in the same study, opposite results (reduced stomatal density and increased size) were observed in Agiorgitiko and Syrah. Overall, these studies concur that grapevine can regulate stomatal development on new leaves in response to water limitation. Variability in the response of stomatal density and size across cultivars suggests a variety-dependent adaptation response.

The molecular processes regulating stomatal development in response to environmental signals in plants, including grapevines, remain poorly understood, limiting our knowledge of how vines (and woody crops in general) may sense environmental constraints and change stomatal development to adapt to protracted water deficits [8,19,20] and references therein. In the model plant Arabidopsis, stomata development is under the control of a complex molecular network, which is regulated by a signalling pathway involving three key regulators, i.e., the epidermal patterning factors EPF1, EPF2, and EPFL9 (also known as STOMAGEN). EPF1 and EPF2 are negative regulators of stomatal density, whereas EPFL9 promotes stomata development [20–22]. The latter was recently functionally characterized in edited grapevine plants of the "Sugraone" variety, demonstrating its role in stomatal density determination [23]. Until now, no study has investigated the gene expression patterns of *VvEPFL9* and other putative genes associated with stomagenesis in grapevine plants under varying water availability. Furthermore, it is unclear whether immature leaves possess the ability to detect water deficit both at the biochemical level (such as responses mediated by the abscisic acid—ABA hormone) and at the molecular level, by activating gene pathways in response to drought (such as ABA-responsive genes like dehydrin (DH), a well-recognized marker of drought in plants, including grapevines) [24–26]. These data could enhance our understanding of the molecular pathways involved in stomatal development under drought conditions.

Glera, Garganega, Moscato giallo, and Merlot are four varieties widely cultivated in the north of Italy [27]. In a recent study, we analysed the physiological responses to water stress of these cultivars and revealed differences in their water-use strategy [28]. For instance, a more typical near-isohydric behaviour was found for Moscato, and a near-anisohydric one for Garganega, Glera, and Merlot.

In this study, we examined the impact of water limitation on the stomatal characteristics of young leaves (7 days after tip separation) of Garganega, Glera, Merlot, and Moscato varieties, to determine whether the variation in stomatal density and size could serve as an adaptive mechanism enabling tolerance to extended periods of water stress conditions. Moreover, to gain deeper insights into stomatal adaptations to water deficit in the selected varieties, we investigated the gene expression patterns of three pivotal genes (*VvEPFL9*, *VvEPF1*, and *VvEPF2*) that regulate stomatal development. These genes are homologous to those previously characterized in Arabidopsis. In summary, the objective of this study is to enhance our comprehension of the morpho-anatomical mechanisms contributing to varietal differences in water stress tolerance. Additionally, the study aims to elucidate the molecular regulation of stomagenesis in newly developed grapevine leaves exposed to water limitation.

2. Materials and Methods

2.1. Plant Material and Experimental Design

In this study, the plant material and experimental design were consistent with those employed in our recent study, which focused on comparative ecophysiological responses among various grapevine cultivars [28]. Briefly, four-year-old *V. vinifera* L. potted plants of Garganega, Glera, Merlot, and Moscato giallo, grafted onto Kober 5BB rootstock, were selected for this experiment. Glera is a white variety grown in the Friuli and Veneto Regions and is used to produce the recognized Prosecco wine. Garganega is a white variety mainly grown in the provinces of Verona and Vicenza and is used to produce the Soave wines. Moscato giallo belongs to the Moscato family and is cultivated mostly in the Colli Euganei area to produce the Moscato Fior d'Arancio wine. All three of these varieties are characterised by good vigour and productivity. Merlot is a well-known international variety cultivated worldwide.

The vines were grown in open air at the experimental farm of the Research Centre for Viticulture and Enology (CREA-VE) in Susegana (45°51′ N–12°15′ E), Italy, in 80 L plastic pots filled with a sand–peat–clay mixture (50–35–15% in volume) and covered with plastic waterproof sheets. Vines were positioned in rows at a spacing of 1 m and pruned to one single cane that is 14–15 nodes in length. Shoot thinning was performed in spring to standardize the number of shoots to 14–15 for all plants. Ten vines per cultivar were randomly selected and initially maintained well watered at field capacity. At the beginning of the experiment (start of veraison, BBCH 81 stage) [29], the vines of each cultivar were divided into two groups of five plants and assigned to the following treatments: well-watered vines (WW) received 100% of the total daily water requirement and water-stressed vines (WS) received 30% of the total daily water requirement. Daily water consumption was monitored through continuously weighing two reference potted vines with Laumas Elettronica ISC scales connected to a D1 Flex log 1.9 datalogger (Tecnopenta, Teolo, PD, Italy).

Plant water status during the experiment was monitored by measuring the midday stem water potential (Ψ_{stem}) with a Scholander pressure chamber. Stem data recorded in the two years of study are available in Gaiotti et al. (2023) [28] and are summarised in Figure S1. Water restriction was applied for 12 days in 2017 and 13 days in 2018, until vines reached severe water stress, defined as $\Psi_{stem} \leq 1.3$ MPa [30,31]. Thereafter, all vines were rehydrated by applying 100% of the total daily water usage. For the profiling of stomagenesis target genes by the means of qPCR, unfolded leaves were collected at the end of water stress imposition, immediately before the rewatering phase, from WS plants and WW ones used as controls. For stomatal density and size measurements, the experiment was concluded one week after the re-watering, when samples of young leaves were collected from WW and WS vines for the analysis of stomatal characteristics. All samples for stomatal density and gene expression analysis were collected from shoots bearing one single cluster.

Weather conditions were monitored using the local CREA-VE weather station coupled to Watch Dog 1400 datalogger (Spectrum Technologies, Bridgend, UK). Mean temperature during the trial ranged between 27 and 28 °C in the two study seasons. Mean air humidity and irradiance during the experiment were 60.7% and 22.6 MJ/m^{-2} day^{-1}, respectively.

2.2. Stomatal Density in Developing Leaves

To explore the stomatal developmental changes induced by water limitation in the four varieties, stomatal density and length were measured in young leaves collected from WW and WS plants. Leaves developed from shoot tips that had experienced water stress during the period of water restriction were sampled one week after re-watering. From each variety, a young leaf with an at least 40 mm long main vein was collected from the tip of each vine's main stem (n = 5, randomly selected leaves per treatment for each variety). The impression method was used to determine leaf stomatal density, expressed as the number of stomata per unit leaf area, and the stomata length, defined as the length in micrometres between the junctions of the guard cells at each end of the stoma. In detail, clear nail

polish was applied to three different areas of the abaxial epidermis of each leaf avoiding the midvein and allowed to dry as previously reported [32]. According to Düring (1990) [2], stomata are uniformly distributed across the abaxial epidermis; thus, the selection of areas for stomatal counting was considered irrelevant. The nail polish was then removed using transparent tape and transferred onto a microscope glass slide. Images were captured for each film strip using an optical microscope system equipped with a built-in camera (microscope Leica DM750, Camera Leica ICC50HD, lens HIPLAN 20X/04, software Leica Application Suite ver. 4.4.0, Leica, Wetzlar, Germany). Stomatal density and length were counted on a standard area (655 × 491 μm) for each strip.

2.3. RNA Isolation and RT-qPCR Analysis of Target Genes Involved in Stomatal Development

In order to explore the effect of water stress on the expression of genes involved in stomatal development, during the second year of the experiment (2018), shoot tips containing unfolded leaves were collected from WW and WS plants on the final day of water stress imposition. For each treatment and cultivar, three shoot tips (independent biological replicates) from three independent plants were collected and promptly frozen at −80 °C for subsequent gene expression analysis. Total RNA was isolated from the unfolded lyophilized leaf samples using the SpectrumTM Total RNA Kit (Sigma-Aldrich, St. Louis, MO, USA) following manufacturer's instructions. RNA concentration of the extracted samples was quantified using the NanoDropTM (Thermo Fisher Scientific, Waltham, MA, USA). DNAse treatment and cDNA synthesis was performed as previously reported starting from 1 μg of total RNA [33]. The absence of genomic DNA contamination was checked before cDNA synthesis with qPCR using ubiquitin (*VvUBI*) specific primers of grapevine. RT-qPCR reactions were carried out in a final volume of 10 μL containing 5 μL of SYBR® Green Master Mix (Bio-Rad Laboratories, Inc., Hercules, CA, USA), 5 μM specific primers, and 1:10 of diluted cDNA. Reactions were run in the CFX 96 apparatus (Bio-Rad Laboratories, Inc.) using the following program: 10 min preincubation at 95 °C, followed by 40 cycles of 15 s at 95 °C, and 30 s at 60 °C. Each amplification was followed by melting curve analysis (60–94 °C) with a heating rate of 0.5 °C every 15 s. All reactions were performed with at least two technical replicates for three biological replicates. Transcripts expression levels were normalized to the geometric mean of the ubiquitin (*VvUBI*) and actin (*VvACT*) transcripts and calculated with the $2^{-\Delta Ct}$ method using CFX Maestro software v. 2.3 (Bio-Rad Laboratories, Inc.). Oligonucleotide sequences are listed in Table S1 [25,26,34].

2.4. Statistical Analysis

The significance of differences between WS and WW treatments for stomatal characteristics and gene expression was assessed using Student's *t*-test. The tests were performed using the software Statistica 7.0 (StatSoft Inc., Tulsa, OK, USA).

3. Results

3.1. Stomatal Density and Size in Developing Leaves

Densities observed in the four varieties under WW conditions ranged between 130 and 230 stomata/mm^2 in the two study years (Figure 1A–D). Changes induced by water limitation were different among the cultivars under study. Moscato and Glera responded similarly, with an increase in stomatal density and a decrease in stomatal size in WS plants relative to WW plants. Although the differences in Moscato stomatal density were significant only during the second season of the study, the results were consistent in both years, with a similar increase of 22–23% in WS vines compared to WW ones. Merlot is the variety that exhibited the lowest stomatal density (between 130 and 160 stomata/mm^2 under WW conditions), and displayed the opposite response as WS plants showed a decrease in the stomatal number relative to WW plants, while the stomatal size remained unchanged. The stomatal characteristics of Garganega were not significantly affected by water restriction over the two years of the experiment. Figure S2 displays comparative images of the stomata of the four varieties under study in the WW and WS conditions.

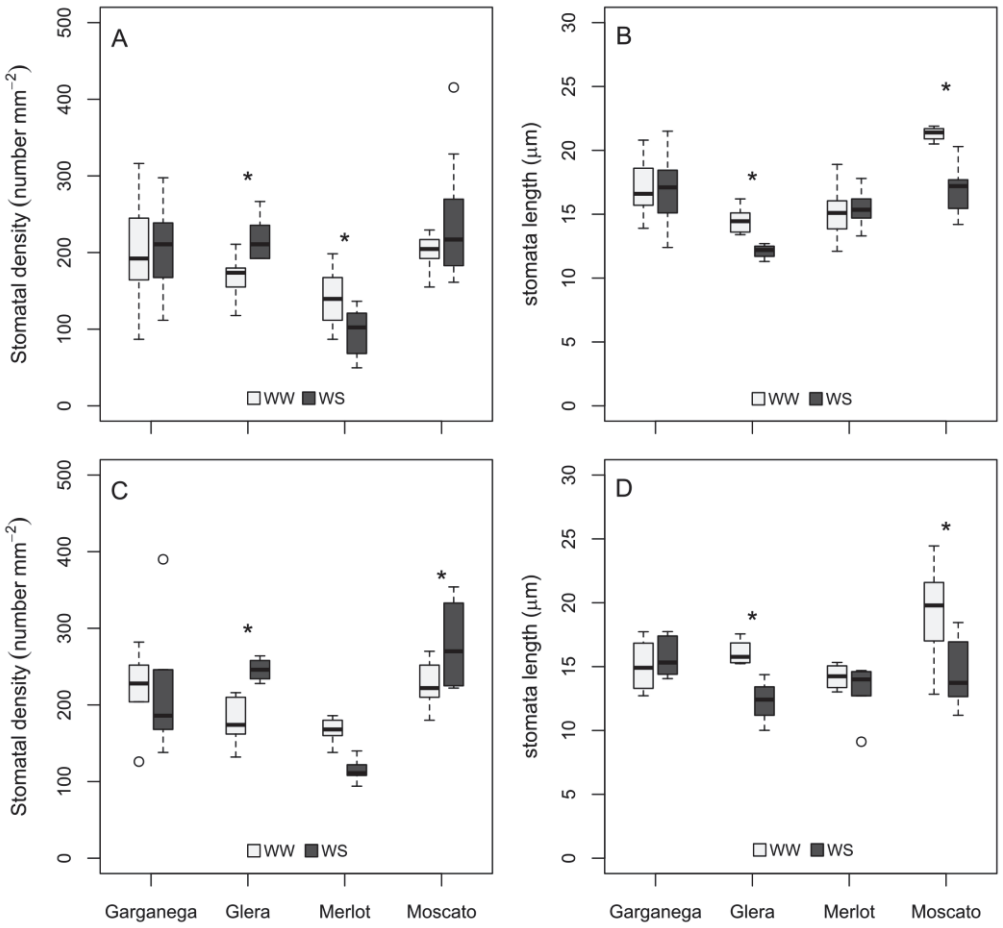

Figure 1. Box plot for stomatal density and stomata length measured in young leaves (7 days after tip separation) of well-watered (WW) and water-stressed (WS) treatments of Garganega, Glera, Merlot, and Moscato varieties. Analysis were performed in 2017 (**A**,**B**) and 2018 (**C**,**D**) on leaf samples collected one week after rewatering. The lines that delimit the bottom and the top of the boxes are the 25th and 75th percentiles, respectively. The 10th and 90th percentiles are indicated by whiskers. Outlayers are indicated by dots. For each variety, asterisks indicate a significant difference between WS and WW treatments according to *t*-test analysis ($p \leq 0.05$).

3.2. Expression of Target Genes Involved in Water Stress Sensing and Stomagenesis in Developing Leaves

To better understand how newly forming leaves sense water constraints and modulate their stomatal development in the four varieties under study, the expression of a dehydrin (*VvDH*) and three key genes related to stomatal development were examined using RT-qPCR, i.e., *VvEPFL9* that competes with *VvEPF1* and *VvEPF2* for receptor binding and thus promotes stomatal development. It is worth noting that developing leaves could perceive water stress, as evidenced by a significant *VvDH* up-regulation in all WS conditions (Figure 2A) across all varieties. Upon WS, *VvEPFL9* transcripts levels increased in Moscato and Glera, although only in Glera this trend was statistically significant (Figure 2B). In contrast, transcript levels for this gene decreased in Merlot exposed to WS.

Under water stress, the negative regulator *VvEPF1* responded differently in Merlot and Glera, being up-regulated in the former and down-regulated in the latter (Figure 2C). The transcript levels of this gene did not vary significantly in Moscato and Garganega. Under WS condition, the gene expression of *VvEPF2* was suppressed in all four varieties (Figure 2D).

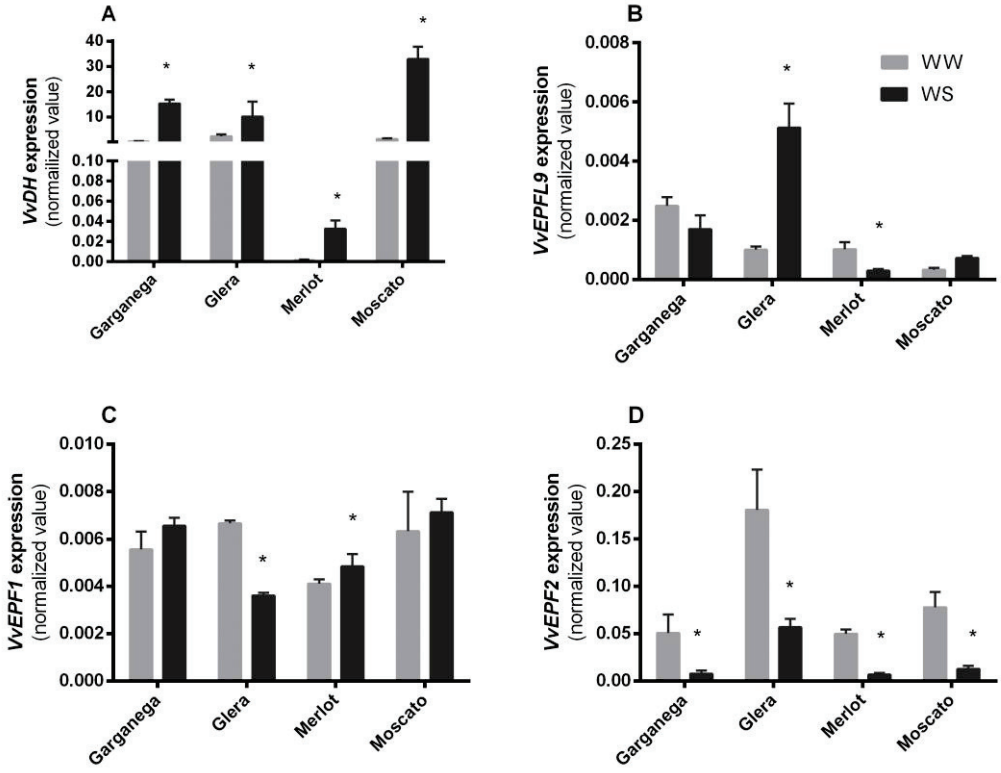

Figure 2. Expression changes of water-stress- and stomagenesis-related genes in unfolded leaves collected on the last day of water restriction in 2018 from WW (grey bars) and WS (black bars) treatments of the four varieties: (**A**) *VvDH*; (**B**) *VvEPFL9*; (**C**) *VvEPF1*; and (**D**) *VvEPF2*. For each cultivar. asterisks indicate significant differences between treatments as attested by student *t*-test ($p \leq 0.05$).

4. Discussion

Grapevine has demonstrated the ability to modulate leaf stomatal development, adjusting stomata density and size to better cope with prolonged water stress [16,17]. As no information regarding this adaptive strategy has been previously reported for Glera, Garganega, Moscato, or Merlot, we analysed their stomatal characteristics in young leaves (7 days after tip separation) developed under different water availability conditions.

The response of stomatal anatomical features to drought was not consistent among the studied varieties, with some exhibiting an increase, while others demonstrating a decrease or no changes in their values. This wide range of responses suggests that morpho-anatomical changes in stomatal characteristics are genotype-dependent and can contribute to the intra-specific variability in the response to water stress observed in grapevine. When the four cultivars were compared, Moscato and Glera responded similarly, with a rise in stomatal density and a decrease in stomatal size in newly formed leaves over the drought stress imposition. A comparable response to water stress has been extensively reported in various crops as a water deficit adaptation [11,13,35,36]. According to these studies, a higher stomatal density allows for the maintenance or improvement of CO_2 external supply, whereas small stomata are reported to provide a quicker adjustment of aperture response [35,37]. Merlot WS, unlike Glera and Moscato, exhibited a decrease in stomatal density as previously found in Argiorgitiko and Shyrah varieties under water stress [17]. Despite the fact that this adjustment has been documented less frequently in response to water stress, studies on transgenic plants with reduced stomatal density revealed that this modification can improve Water Use Efficiency (WUE) and drought tolerance in several species, including grapevine [23,38–40].

Our results indicated that adjustments in stomatal anatomical features were not related to the varietal water use strategy. In fact, similar changes in density and size were observed for Glera that displays a near-anisohydric behaviour and Moscato that displays a near-isohydric behaviour. On the contrary, opposite adjustments in stomatal characteristics were observed in Merlot and Glera, despite the common anisohydric water use strategy of these varieties [28].

To better understand the stomatal adaptations to water deficit in the cultivars under study, we analysed the gene expression of a dehydrin (*VvDH*) and of three key genes (*VvEPFL9*, *VvEPF1*, and *VvEPF2*) controlling stomatal development, homologues to those characterized in Arabidopsis. As, in Arabidopsis, stomata formation is determined in the early stages of leaf development, when the epidermal cells of leaf primordia either differentiate into pavement cells or into meristemoid mother cell that initiate the stomata lineage [41,42], gene expression analysis was performed on unfolded leaves collected from the main shoot tips of WW and WS treatments. Apexes analogous to those collected for gene analysis were allowed to develop over the subsequent week. Stomatal density measurements were conducted on the young leaves developed from these structures. The dehydrin gene (*VvDH*) has been generally regarded as a drought perception marker, since its expression has been shown to be induced by water stress in grapevine [25,43]. *VvDH* expression analysis demonstrated that unfolded leaves could perceive water stress, as attested by the considerable up-regulation of this gene in all WS-exposed cultivars. Although *VvEPFL9* has been shown to promote stomatal development [21–23], no prior studies have looked into its regulation in developing leaves in grapevines exposed to water restriction. The transcript levels of *VvEPFL9* were overall in agreement with stomata densities on young leaves in the four varieties, showing an up-regulation when drought induced an increase in stomatal density (in WS Glera and WS Moscato) and a down-regulation when the stomatal number decreased (in WS Merlot).

In model plants, *VvEPF1* and *VvEPF2* genes have been shown to act as negative regulators of *VvEPFL9*, thus negatively regulating stomatal density [8,21]. The relation between the expression of these genes and stomatal density was not clear in all varieties. *VvEPF1*, as a negative regulator of stomagenesis, was expected to be down-regulated in Glera and Moscato varieties in which water stress induced an increase in stomatal density. Surprisingly, the comparison of the transcript levels of WS and WW plants revealed that only Glera exhibited a lower level of expression. Merlot was the only variety in which drought induced an up-regulation of *VvEPF1*, and this result supports, at the molecular level, the decrease in stomatal density observed in WS Merlot plants. The function of *VvEPF2* is similar to that of *VvEPF1*, but EPF2 acts as a negative regulator of stomatal development slightly earlier than EPF1 [22]. Even though stomatal density responses to water stress varied among cultivars, the expression of the *VvEPF2* gene was down-regulated in all four WS plants.

Overall, the expression analysis of *VvEPFL9* showed a trend similar to that observed for stomatal density, also confirming the putative role of this gene in promoting stomagenesis in grapevine as recently demonstrated in the "Sugraone" grape variety [23]. Additionally, results indicate that *VvEPF1* and *VvEPF2* may act antagonistically to *VvEPFL9*. Nonetheless, the up- or down-regulation of a single gene among those mentioned above could not entirely account for the observed alterations in stomatal density. This suggests that stomatal development is probably controlled by the combined effects of all the analysed genes and potentially by other unidentified components that require further exploration.

5. Conclusions

The findings of this study, both at the anatomical and molecular levels, confirm that water stress can influence the stomatal development in young leaves (7 days after tip separation). This adaptive response potentially equips the plant for enhanced drought tolerance for future drought events. The wide variability in stomatal responses observed in the four varieties under study reinforces the idea that adjustments in stomatal anatomical

features represent a genotype-dependent mechanism of adaptation to prolonged water stress rather than a strategy common to all grapevine cultivars.

This short report clearly illustrates the substantial impact of drought on stomagenesis. However, our data do not permit an assessment of the functional significance of the observed variations in stomatal traits. This limitation arises from the unsuitability of young leaves for physiological measurements, given their known lack of full photosynthetic activity. Future studies should address this aspect, planning long-term drought experiments to analyse if changes induced in stomata density and size in mature leaves imply improved grapevine physiological performances.

Supplementary Materials: The following supporting information can be downloaded at: https://www.mdpi.com/article/10.3390/agriculture13122186/s1, Table S1: List of the oligonucleotides used in the study; Figure S1: Midday stem water potential (Ψ_{stem}) measured in well-watered (A) and water stress treatments (B) of the four varieties under study during the experiment. Each point is the average of measurements taken on five individual plants over 2 seasons (2017–2018). This figure summarises the data published in extended form in Gaiotti et al. (2023), [28]; Figure S2: Comparative images of the stomata of the four varieties under study under well-watered (WW) and water stress (WS) conditions. Photomicrographies are taken from nail polish impressions of the abaxial leaf surface of young leaves (7 days after tip separations).

Author Contributions: Conceptualization, L.N., W.C. and F.G.; methodology, L.N., W.C. and F.G.; investigation, L.N., W.C. and F.G.; data curation, L.L., G.F., L.N., W.C. and F.G.; writing—original draft preparation, L.N., W.C. and F.G.; writing—review and editing, L.L. and G.F.; visualization, L.L. and G.F. All authors have read and agreed to the published version of the manuscript.

Funding: This research received no external funding.

Data Availability Statement: The data that support the findings of this study are available from the corresponding author upon reasonable request.

Conflicts of Interest: The authors declare no conflict of interest.

References

1. Spinoni, J.; Naumann, G.; Vogt, J.; Barbosa, P. *Meteorological Droughts in Europe: Events and Impacts: Past Trends and Future Projection*; European Union: Luxembourg, 2016.
2. Düring, H. Stomatal Adaptation of Leaves to Drought. *Vitis* **1990**, *29*, 366–370.
3. Chaves, M.M. Effects of Water Deficits on Carbon Assimilation. *J. Exp. Bot.* **1998**, *42*, 16. [CrossRef]
4. Galmés, J.; Ochogavía, J.M.; Gago, J.; Roldán, E.J.; Cifre, J.; Conesa, M.À. Leaf Responses to Drought Stress in Mediterranean Accessions of Solanum Lycopersicum: Anatomical Adaptations in Relation to Gas Exchange Parameters. *Plant Cell Environ.* **2013**, *36*, 920–935. [CrossRef] [PubMed]
5. Bota, J.; Tomás, M.; Flexas, J.; Medrano, H.; Escalona, J.M. Differences among Grapevine Cultivars in Their Stomatal Behavior and Water Use Efficiency under Progressive Water Stress. *Agric. Water Manag.* **2016**, *164*, 91–99. [CrossRef]
6. Tortosa, I.; Escalona, J.M.; Bota, J.; Tomás, M.; Hernández, E.; Escudero, E.G.; Medrano, H. Exploring the Genetic Variability in Water Use Efficiency: Evaluation of Inter and Intra Cultivar Genetic Diversity in Grapevines. *Plant Sci.* **2016**, *251*, 35–43. [CrossRef]
7. Levin, A.D.; Williams, L.E.; Matthews, M.A. A Continuum of Stomatal Responses to Water Deficits among 17 Wine Grape Cultivars (*Vitis vinifera*). *Funct. Plant Biol.* **2019**, *47*, 11–25. [CrossRef]
8. Bertolino, L.T.; Caine, R.S.; Gray, J.E. Impact of Stomatal Density and Morphology on Water-Use Efficiency in a Changing World. *Front. Plant Sci.* **2019**, *10*, 225. [CrossRef]
9. Yang, H.M.; Wang, G.X. Leaf Stomatal Densities and Distribution in Triticum Aestivum under Drought and CO_2 Enrichment. *Chin. J. Plant Ecol.* **2001**, *25*, 312.
10. Ennajeh, M.; Vadel, A.M.; Cochard, H.; Khemira, H. Comparative Impacts of Water Stress on the Leaf Anatomy of a Drought-Resistant and a Drought-Sensitive Olive Cultivar. *J. Hortic. Sci. Biotechnol.* **2010**, *85*, 289–294. [CrossRef]
11. Laajimi, N.O.; Boussadia, O.; Skhiri, F.H.; Teixeira da Silva, J.A.; Rezgui, S.; Hellali, R. Anatomical Adaptations in Vegetative Structures of Apricot Tree (*Prunus armeniaca* L.) Cv. "Amor El Euch" Grown under Water Stress. *Fruit Veg. Cereal Sci. Biotechnol.* **2011**, *5*, 46–51.
12. Taratima, W.; Ritmaha, T.; Jongrungklang, N.; Maneerattanarungroj, P.; Kunpratum, N. Effect of Stress on the Leaf Anatomy of Sugarcane Cultivars with Different Drought Tolerance (*Saccharum officinarum*, Poaceae). *Rev. Biol. Trop.* **2020**, *68*, 1159–1170. [CrossRef]

13. Xu, Z.; Zhou, G. Responses of Leaf Stomatal Density to Water Status and Its Relationship with Photosynthesis in a Grass. *J. Exp. Bot.* **2008**, *59*, 3317–3325. [CrossRef] [PubMed]
14. Rogiers, S.Y.; Hardie, W.J.; Smith, J.P. Stomatal Density of Grapevine Leaves (*Vitis vinifera* L.) Responds to Soil Temperature and Atmospheric Carbon Dioxide. *Aust. J. Grape Wine Res.* **2011**, *17*, 147–152. [CrossRef]
15. Gokbayrak, Z.; Dardeniz, A.; Bal, M. Stomatal Density Adaptation of Grapevine to Windy Conditions. *Trakia J. Sci.* **2008**, *6*, 41–60.
16. Palliotti, A.; Silvestroni, O.; Petoumenou, D.; Vignaroli, S.; Berrios, J.G. Evaluation of Low-Energy Demand Adaptive Mechanisms in Sangiovese Grapevine during Drought. *OENO One* **2008**, *42*, 41–47. [CrossRef]
17. Theodorou, N.; Koundouras, S.; Zioziou, E.; Nikolaou, N. Responses of Leaf Stomatal Density and Anatomy to Water Deficit in Four Winegrape Cultivars (*Vitis vinifera* L.). In Proceedings of the 3rd Internetional Ampelos Symposyum, Santorini, Greece, 30–31 May 2013.
18. Montoro, A.; López-Urrea, R.; Fereres, E. Role of Stomata Density in the Water Use of Grapevines. *Acta Hortic.* **2016**, *1115*, 41–47. [CrossRef]
19. Driesen, E.; Van den Ende, W.; De Proft, M.; Saeys, W. Influence of environmental factors light, CO_2, temperature, and relative humidity on stomatal opening and development: A review. *Agronomy* **2020**, *10*, 1975. [CrossRef]
20. Herrmann, A.; Torii, K.U. Shouting out loud: Signaling modules in the regulation of stomatal development. *Plant Physiol.* **2021**, *185*, 765–780. [CrossRef]
21. Jewaria, P.K.; Hara, T.; Tanaka, H.; Kondo, T.; Betsuyaku, S.; Sawa, S.; Sakagami, Y.; Aimoto, S.; Kakimoto, T. Differential Effects of the Peptides Stomagen, EPF1 and EPF2 on Activation of MAP Kinase MPK6 and the SPCH Protein Level. *Plant Cell Physiol.* **2013**, *54*, 1253–1262. [CrossRef]
22. Zoulias, N.; Harrison, E.L.; Casson, S.A.; Gray, J.E. Molecular Control of Stomatal Development. *Biochem. Eng. J.* **2018**, *475*, 441–454. [CrossRef]
23. Clemens, M.; Faralli, M.; Lagreze, J.; Bontempo, L.; Piazza, S.; Varotto, C.; Malnoy, M.; Oechel, W.; Rizzoli, A.; Dalla Costa, L. *VvEPFL9-1* Knock-Out via CRISPR/Cas9 Reduces Stomatal Density in Grapevine. *Front. Plant Sci.* **2022**, *13*, 878001. [CrossRef] [PubMed]
24. Chater, C.C.; Oliver, J.; Casson, S.; Gray, J.E. Putting the brakes on: Abscisic acid as a central environmental regulator of stomatal development. *New Phytol.* **2014**, *202*, 376–391. [CrossRef] [PubMed]
25. Chitarra, W.; Balestrini, R.; Vitali, M.; Pagliarani, C.; Perrone, I.; Schubert, A.; Lovisolo, C. Gene Expression in Vessel-Associated Cells upon Xylem Embolism Repair in *Vitis vinifera* L. *Petioles. Planta* **2014**, *239*, 887–899. [CrossRef] [PubMed]
26. Pagliarani, C.; Moine, A.; Chitarra, W.; Nerva, L.; Catoni, M.; Tavazza, R.; Matić, S.; Vallino, M.; Secchi, F.; Noris, E. The C4 protein of tomato yellow leaf curl Sardinia virus primes drought tolerance in tomato through morphological adjustments. *Hortic. Res.* **2022**, *9*, uhac164. [CrossRef] [PubMed]
27. Scienza, A. *Atlante Geologico Dei Vini d'Italia: Vitigno, Suolo e Fattori Climatici*; Giunti: Firenze, Italy, 2015; ISBN 9788809883222.
28. Gaiotti, F.; Nerva, L.; Fila, G.; Lovat, L.; Belfiore, N.; Chitarra, W. Comparative effects of drought stress on leaf gas exchange, foliar ABA and leaf orientation in four grapevine cultivars grown in Northern Italy. *Physiol. Plant.* **2023**, *175*, e14063. [CrossRef]
29. Lorenz, D.H.; Eichhorn, K.W.; Bleiholder, H.; Klose, R.; Meier, U.; Weber, E. Growth Stages of the Grapevine: Phenological growth stages of the grapevine (*Vitis vinifera* L. ssp. *vinifera*) Codes and descriptions according to the extended BBCH scale. *Aust. J. Grape Wine Res.* **1995**, *1*, 100–103. [CrossRef]
30. Van Leeuwen, C.; Tregoat, O.; Choné, X.; Bois, B.; Pernet, D.; Gaudillère, J.P. Vine Water Status Is a Key Factor in Grape Ripening and Vintage Quality for Red Bordeaux Wine. How Can It Be Assessed for Vineyard Management Purposes. *J. Int. Sci. Vigne Vin.* **2009**, *43*, 121–134.
31. Miras-Avalos, J.M.; Araujo, E.S. Optimization of Vineyard Water Management: Challenges, Strategies, and Perspectives. *Water* **2021**, *13*, 746. [CrossRef]
32. Chitarra, W.; Pagliarani, C.; Maserti, B.; Lumini, E.; Siciliano, I.; Cascone, P.; Schubert, A.; Gambino, G.; Balestrini, R.; Guerrieri, E. Insights on the impact of arbuscular mycorrhizal symbiosis on tomato tolerance to water stress. *Plant Physiol.* **2016**, *171*, 1009–1023. [CrossRef]
33. Nerva, L.; Giudice, G.; Quiroga, G.; Belfiore, N.; Lovat, L.; Perria, R.; Volpe, M.G.; Moffa, L.; Sandrini, M.; Gaiotti, F.; et al. Mycorrhizal Symbiosis Balances Rootstock-Mediated Growth-Defence Tradeoffs. *Biol. Fertil. Soils* **2021**, *58*, 17–34. [CrossRef]
34. Chitarra, W.; Cuozzo, D.; Ferrandino, A.; Secchi, F.; Palmano, S.; Perrone, I.; Boccacci, P.; Pagliarani, C.; Gribaudo, I.; Mannini, F.; et al. Dissecting Interplays between *Vitis vinifera* L. and Grapevine Virus B (GVB) under Field Conditions. *Mol. Plant Pathol.* **2018**, *19*, 2651–2666. [CrossRef] [PubMed]
35. Franks, P.J.; Drake, P.L.; Beerling, D.J. Plasticity in Maximum Stomatal Conductance Constrained by Negative Correlation between Stomatal Size and Density: An Analysis Using Eucalyptus Globulus. *Plant. Cell Environ.* **2009**, *32*, 1737–1748. [CrossRef] [PubMed]
36. Bosabalidis, A.M.; Kofidis, G. Comparative Effects of Drought Stress on Leaf Anatomy of Two Olive Cultivars. *Plant Sci.* **2002**, *163*, 375–379. [CrossRef]
37. Lawson, T.; Vialet-Chabrand, S. Speedy Stomata, Photosynthesis and Plant Water Use Efficiency. *New Phytol.* **2019**, *221*, 93–98. [CrossRef]
38. Wang, C.; Liu, S.; Dong, Y.; Zhao, Y.; Geng, A.; Xia, X.; Yin, W. PdEPF1 Regulates Water-Use Efficiency and Drought Tolerance by Modulating Stomatal Density in Poplar. *Plant Biotechnol. J.* **2016**, *14*, 849–860. [CrossRef]

39. Hughes, J.; Hepworth, C.; Dutton, C.; Dunn, J.A.; Hunt, L.; Stephens, J.; Waugh, R.; Cameron, D.D.; Gray, J.E. Reducing Stomatal Density in Barley Improves Drought Tolerance without Impacting on Yield. *Plant Physiol.* **2017**, *174*, 776–787. [CrossRef]
40. Caine, R.S.; Yin, X.; Sloan, J.; Harrison, E.L.; Mohammed, U.; Fulton, T.; Biswal, A.K.; Dionora, J.; Chater, C.C.; Coe, R.A.; et al. Rice with Reduced Stomatal Density Conserves Water and Has Improved Drought Tolerance under Future Climate Conditions. *New Phytol.* **2019**, *221*, 371–384. [CrossRef] [PubMed]
41. Geisler, M.J.; Sack, F.D. Variable Timing of Developmental Progression in the Stomatal Pathway in Arabidopsis Cotyledons. *New Phytol.* **2002**, *153*, 469–476. [CrossRef] [PubMed]
42. Dow, G.J.; Bergmann, D.C. Patterning and Processes: How Stomatal Development Defines Physiological Potential. *Curr. Opin. Plant Biol.* **2014**, *21*, 67–74. [CrossRef]
43. Cramer, G.R.; Ergül, A.; Grimplet, J.; Tillett, R.L.; Tattersall, E.A.R.; Bohlman, M.C.; Vincent, D.; Sonderegger, J.; Evans, J.; Osborne, C.; et al. Water and Salinity Stress in Grapevines: Early and Late Changes in Transcript and Metabolite Profiles. *Funct. Integr. Genom.* **2007**, *7*, 111–134. [CrossRef]

MDPI AG
Grosspeteranlage 5
4052 Basel
Switzerland
Tel.: +41 61 683 77 34

Agriculture Editorial Office
E-mail: agriculture@mdpi.com
www.mdpi.com/journal/agriculture

Academic Open
Access Publishing

mdpi.com

ISBN 978-3-7258-4566-8